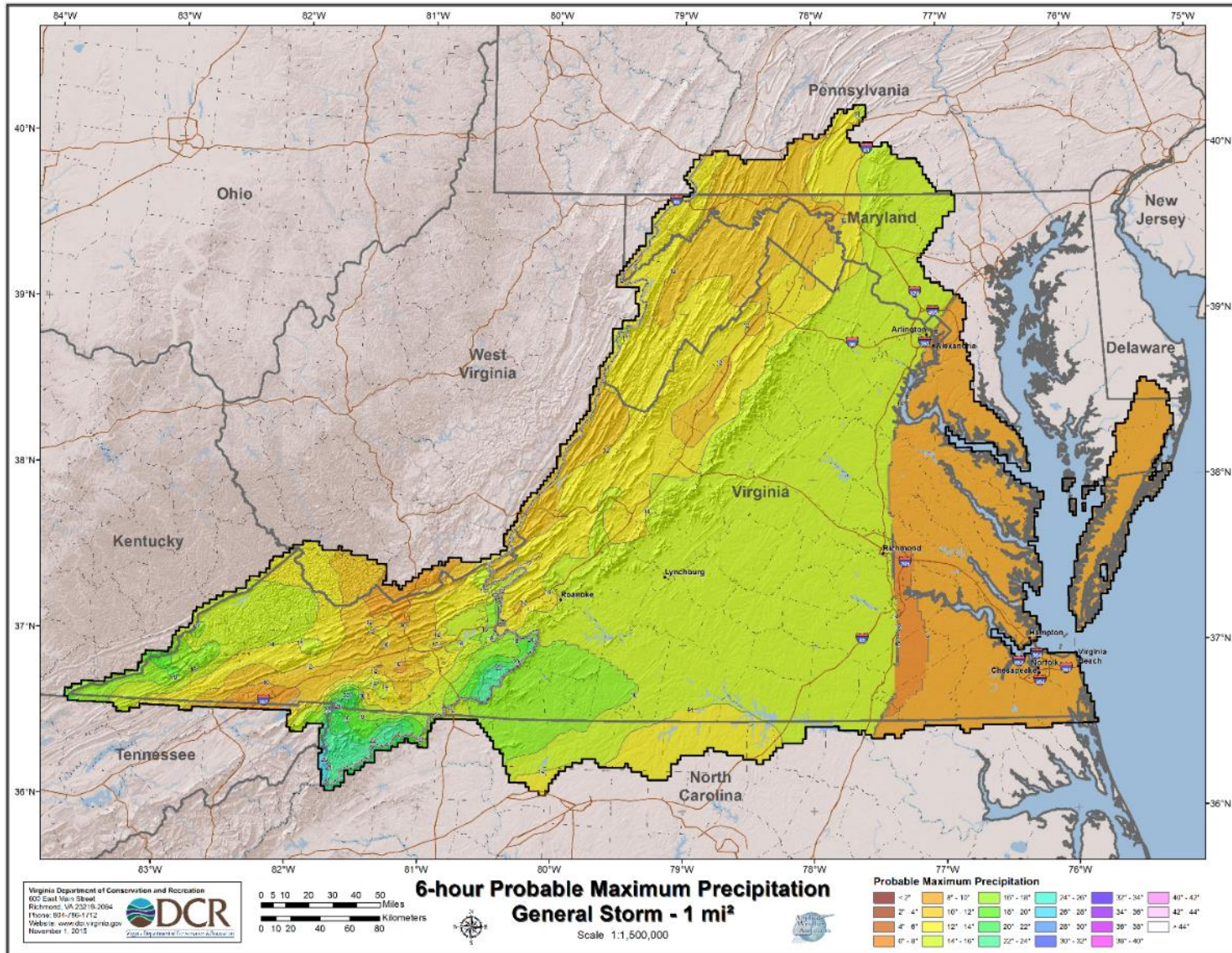
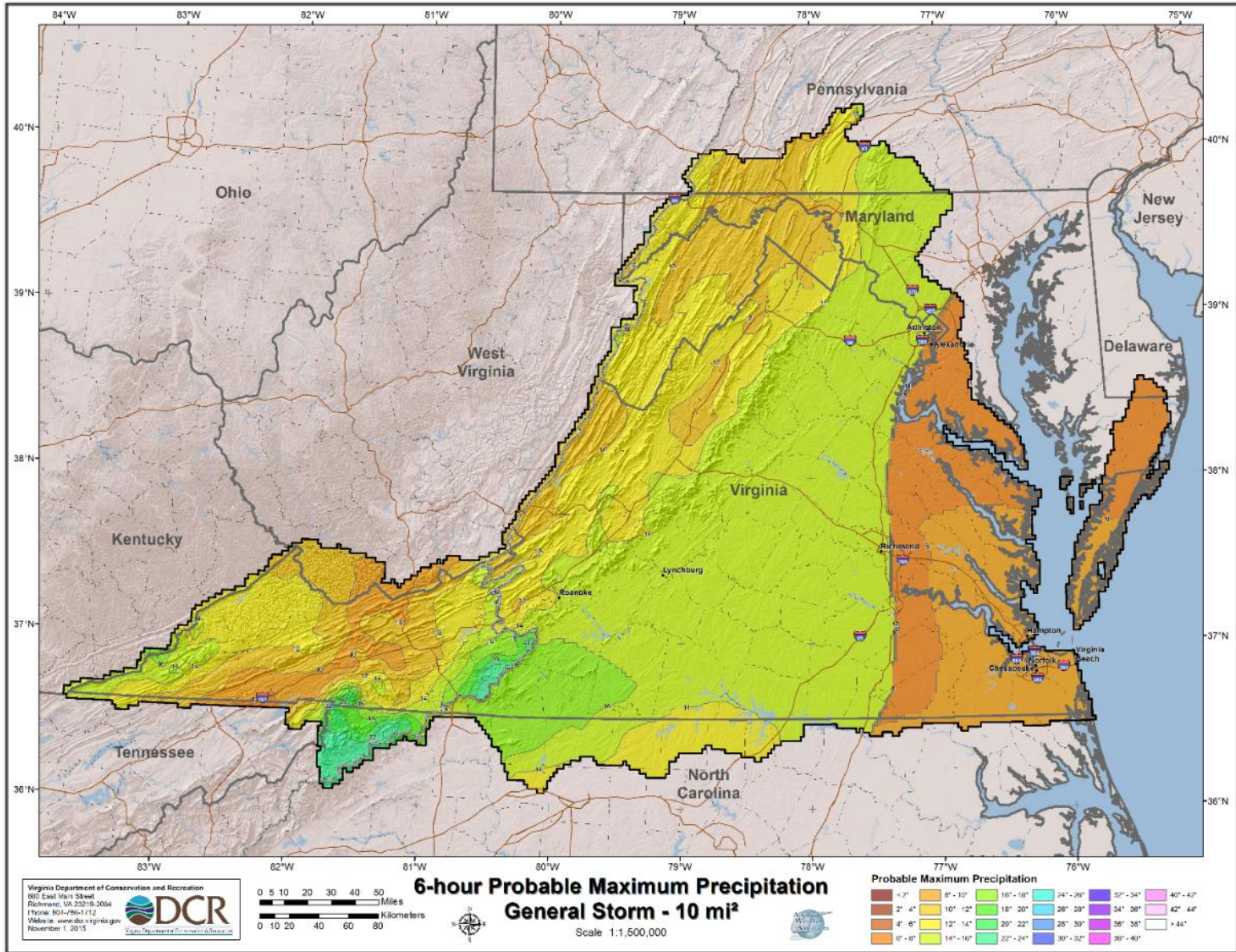


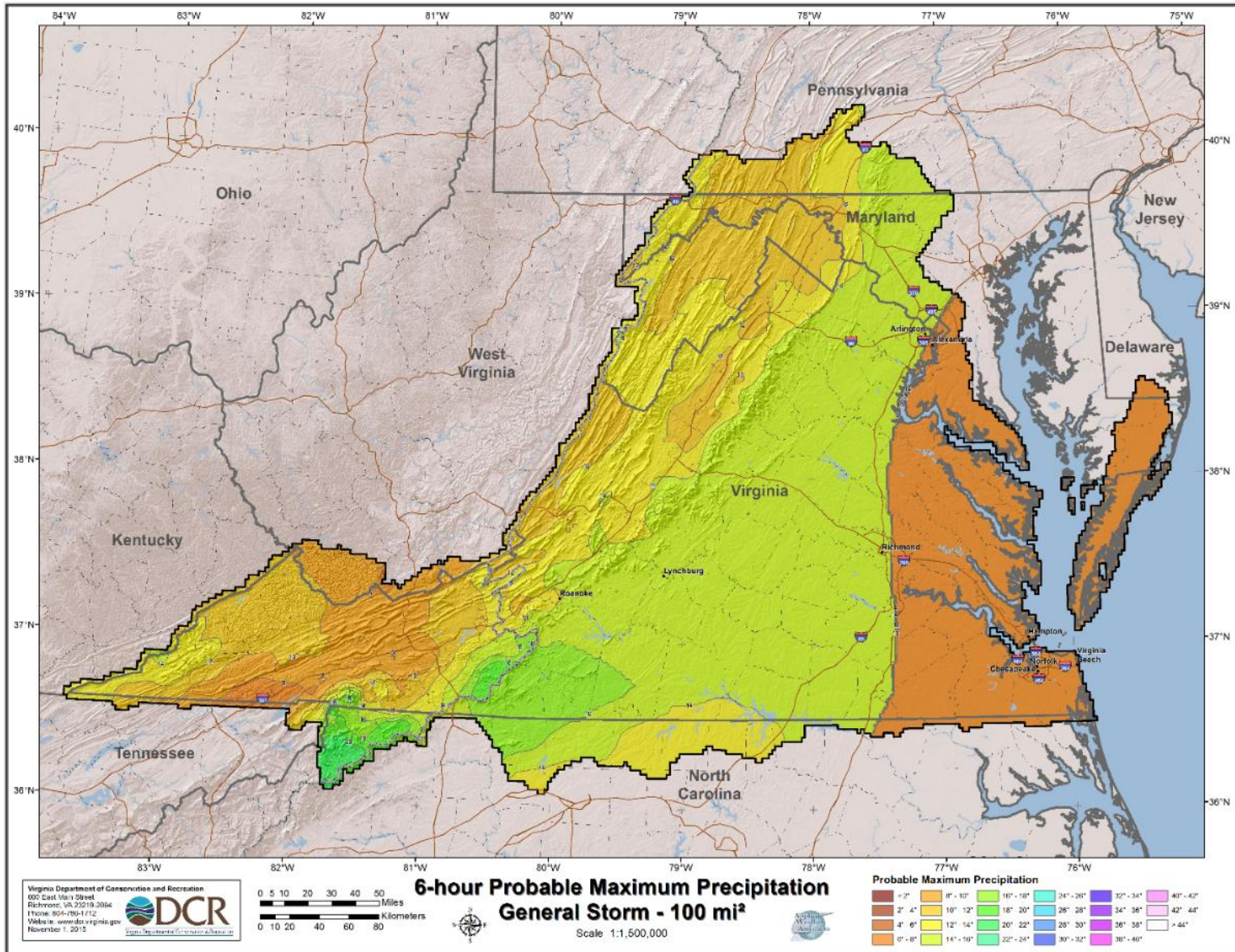
Appendix A

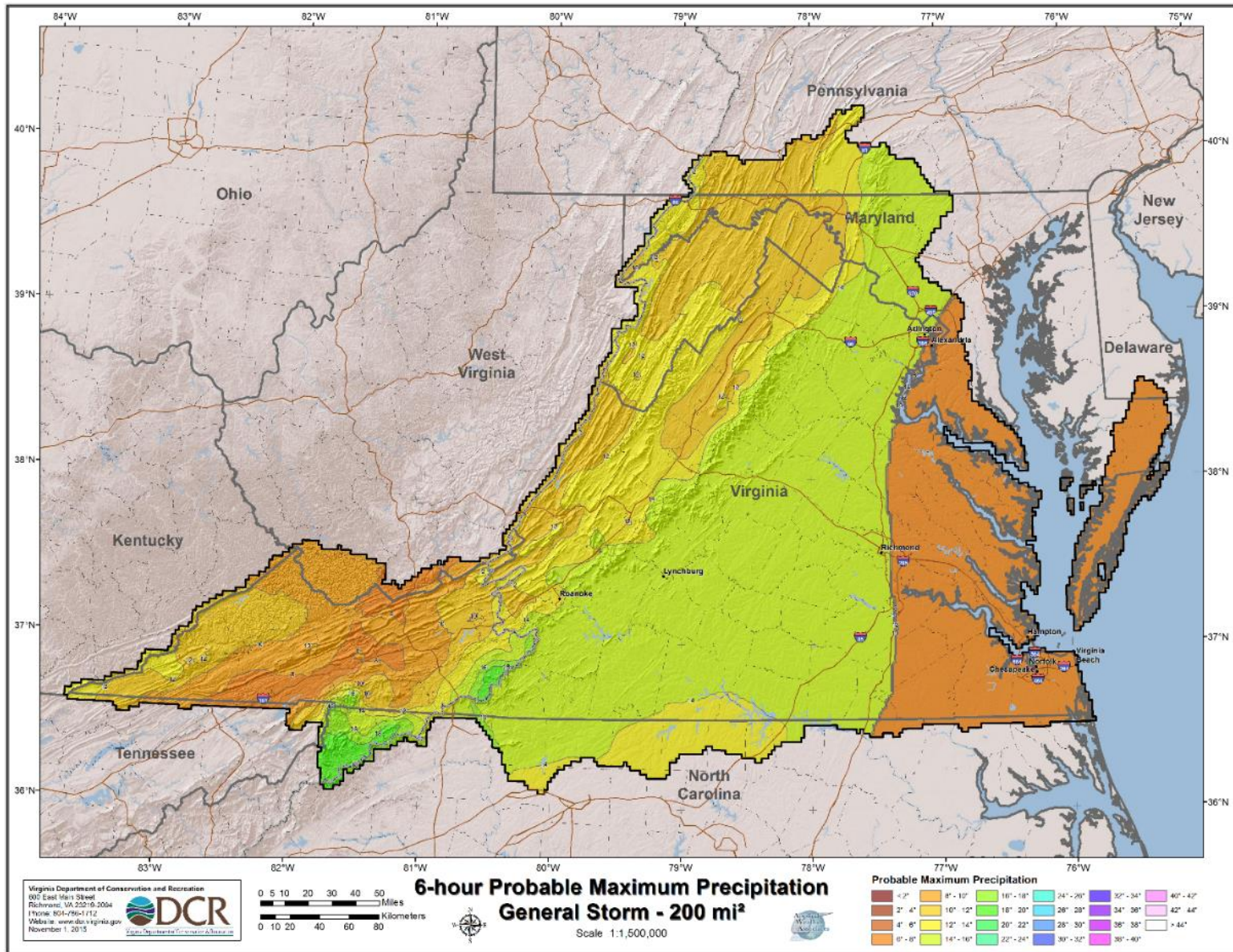
Virginia Probable Maximum Precipitation Maps

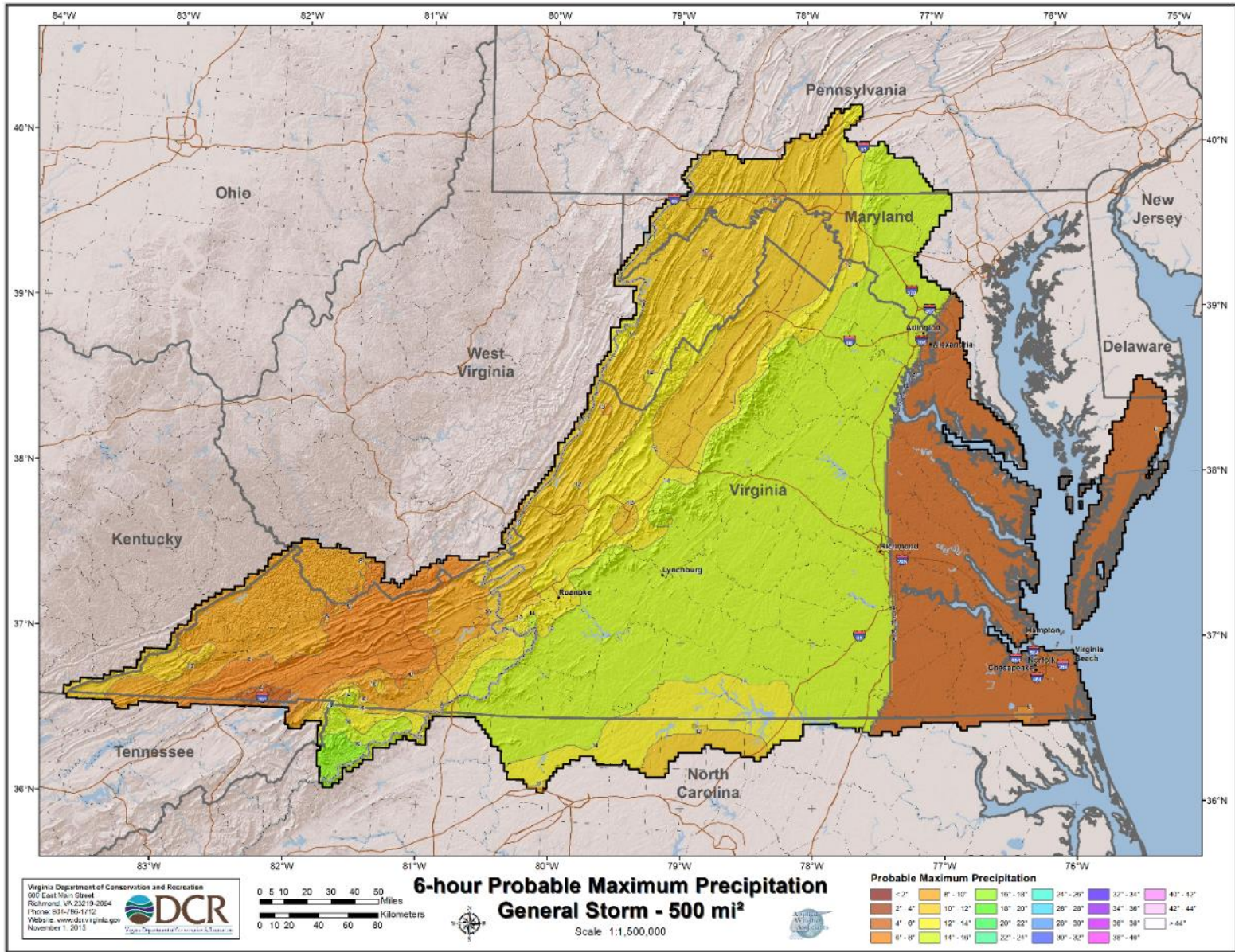
General Storm

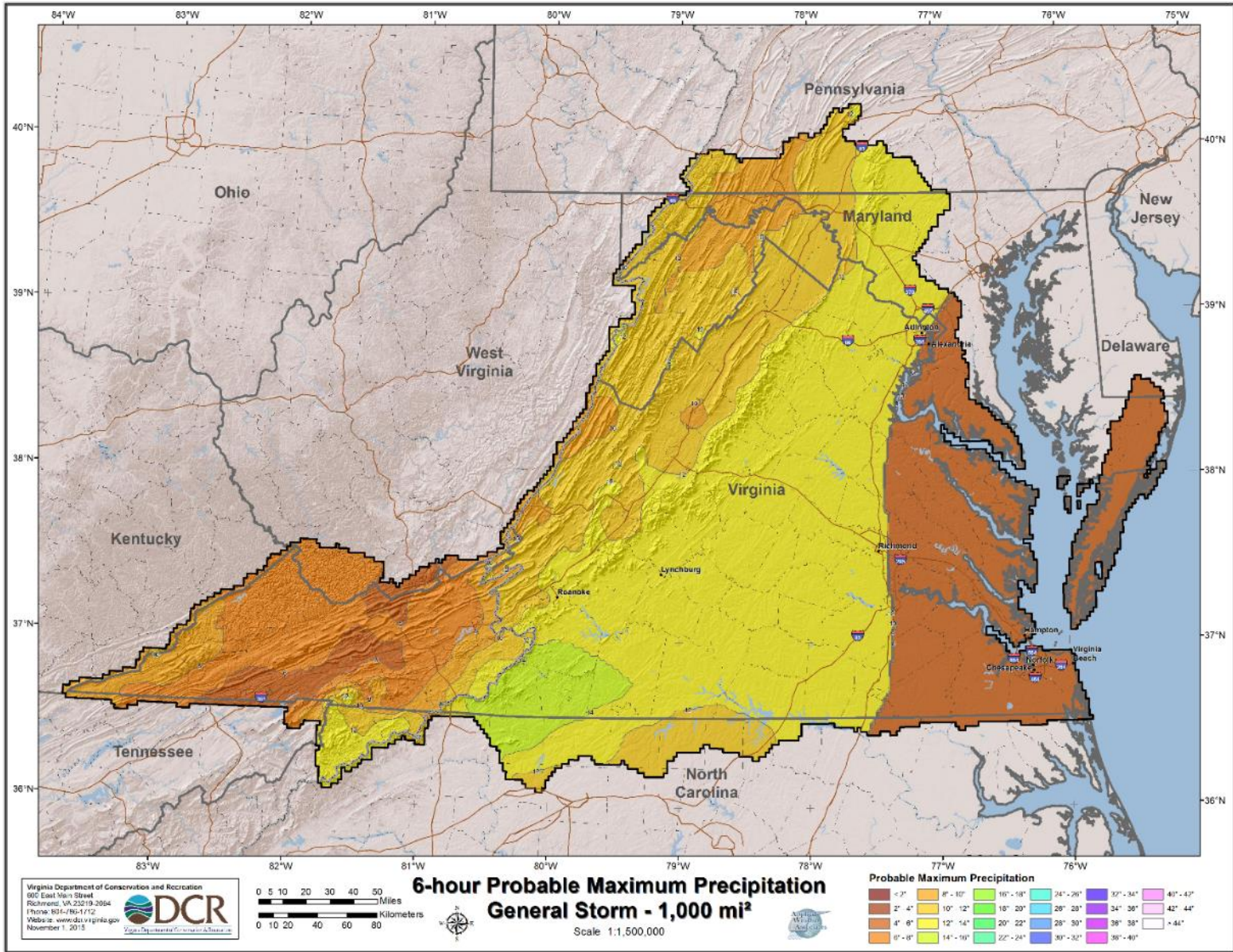


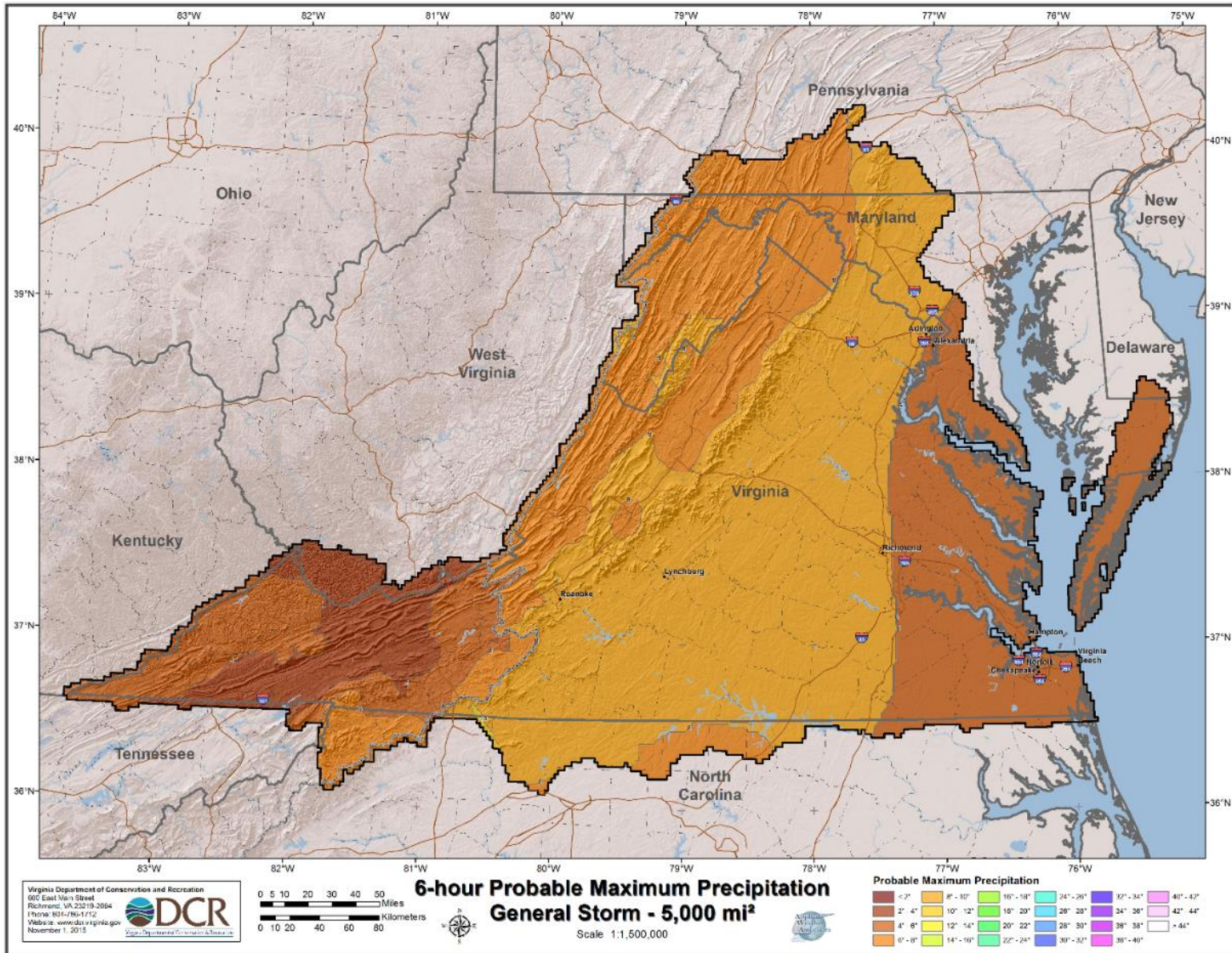


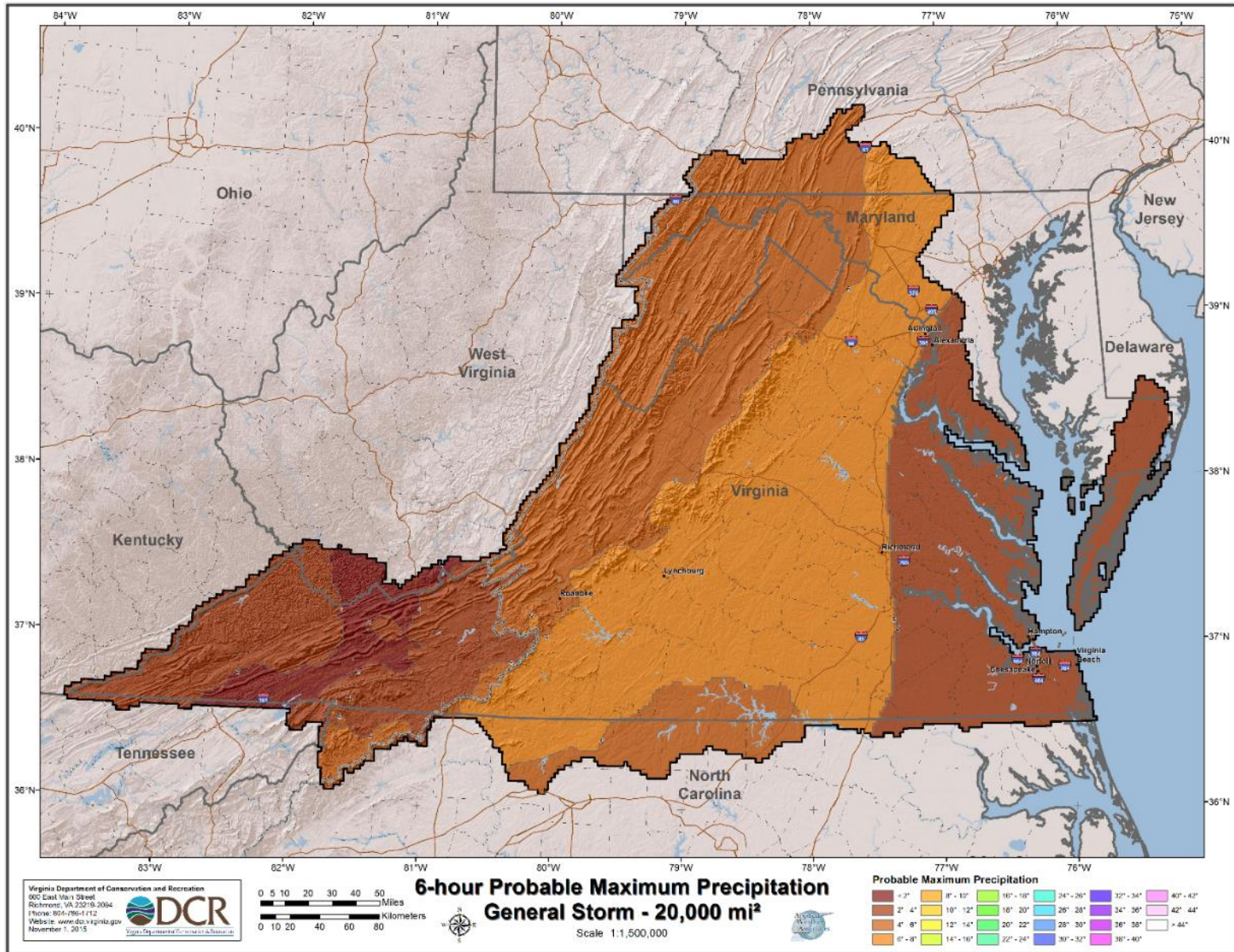


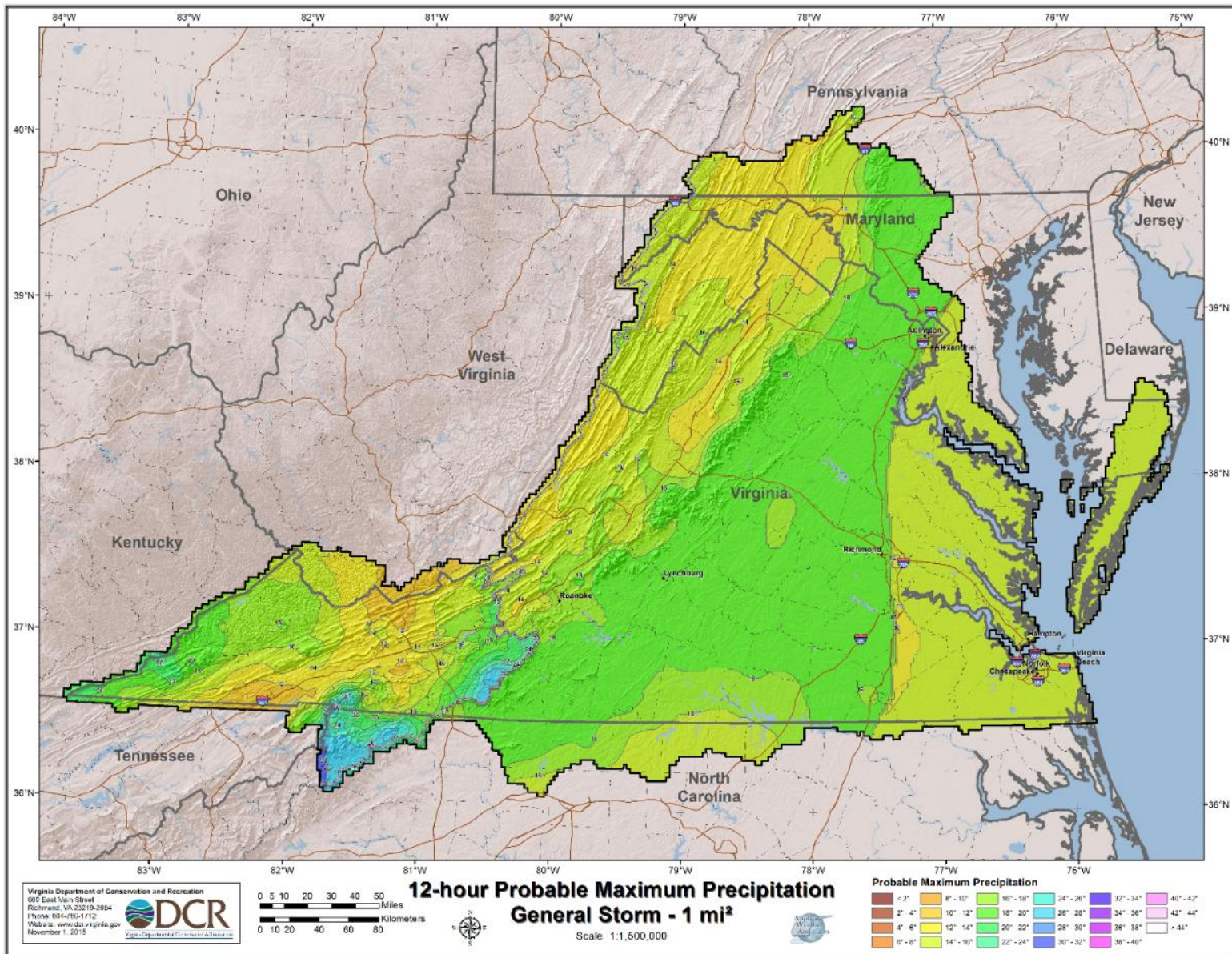


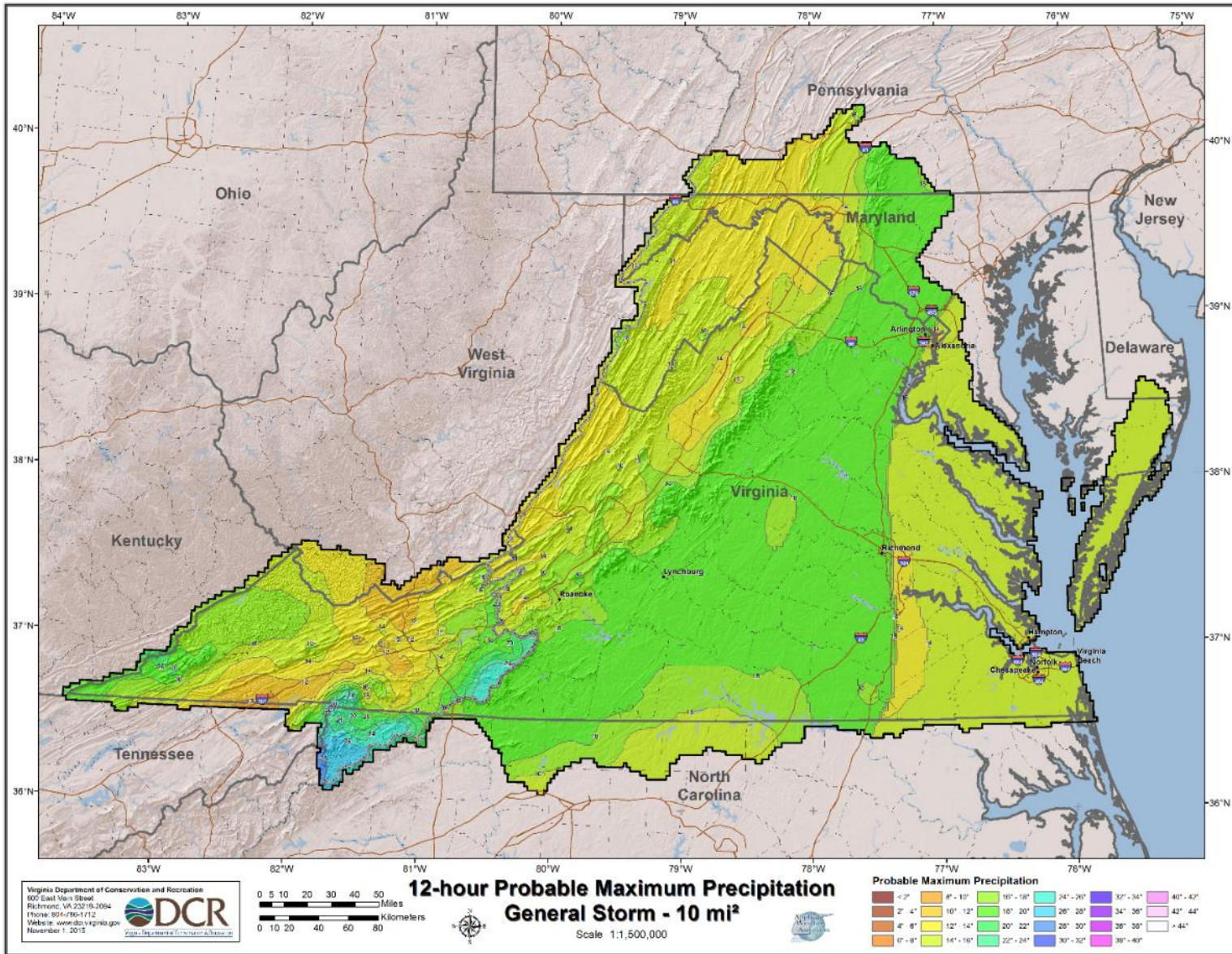


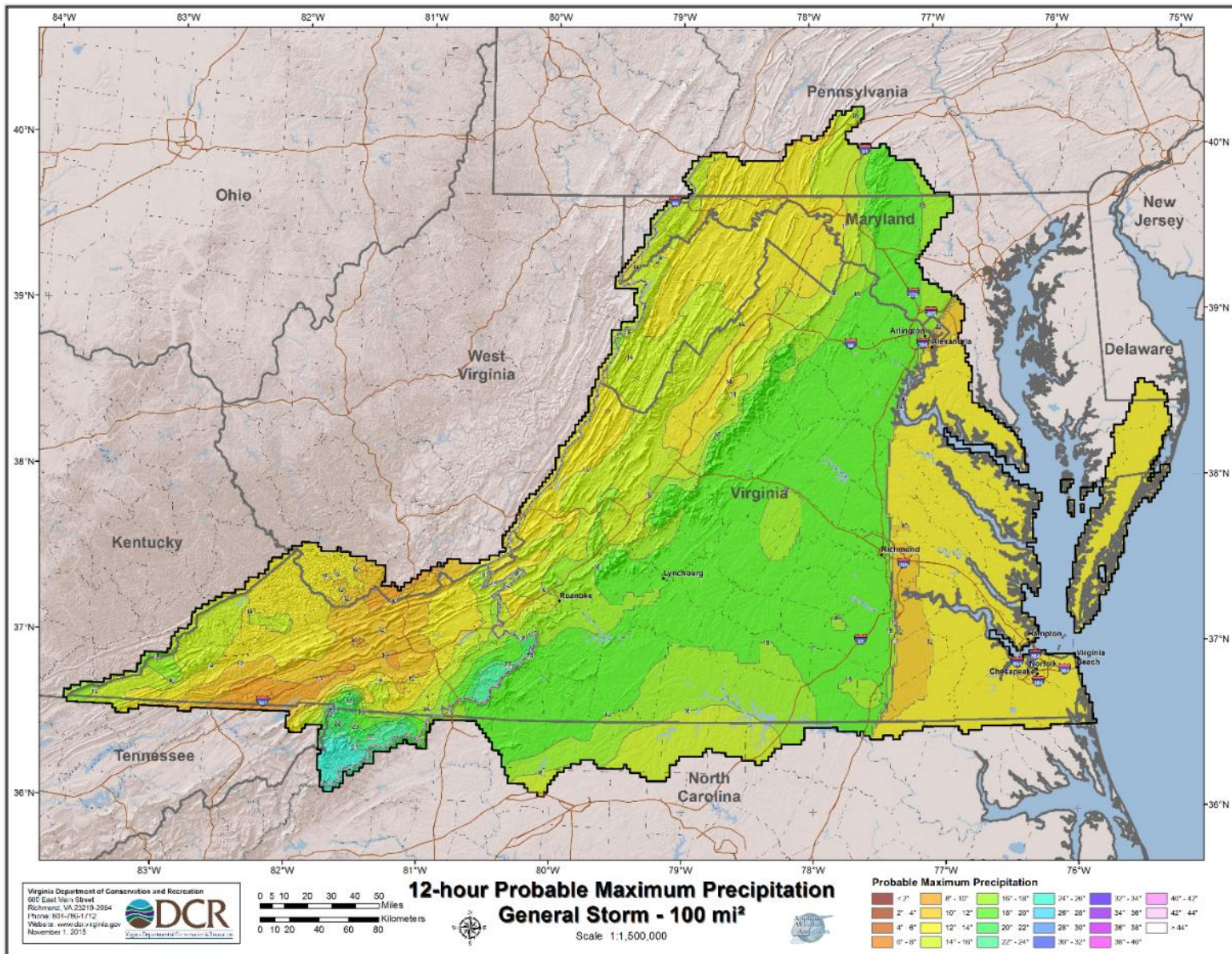


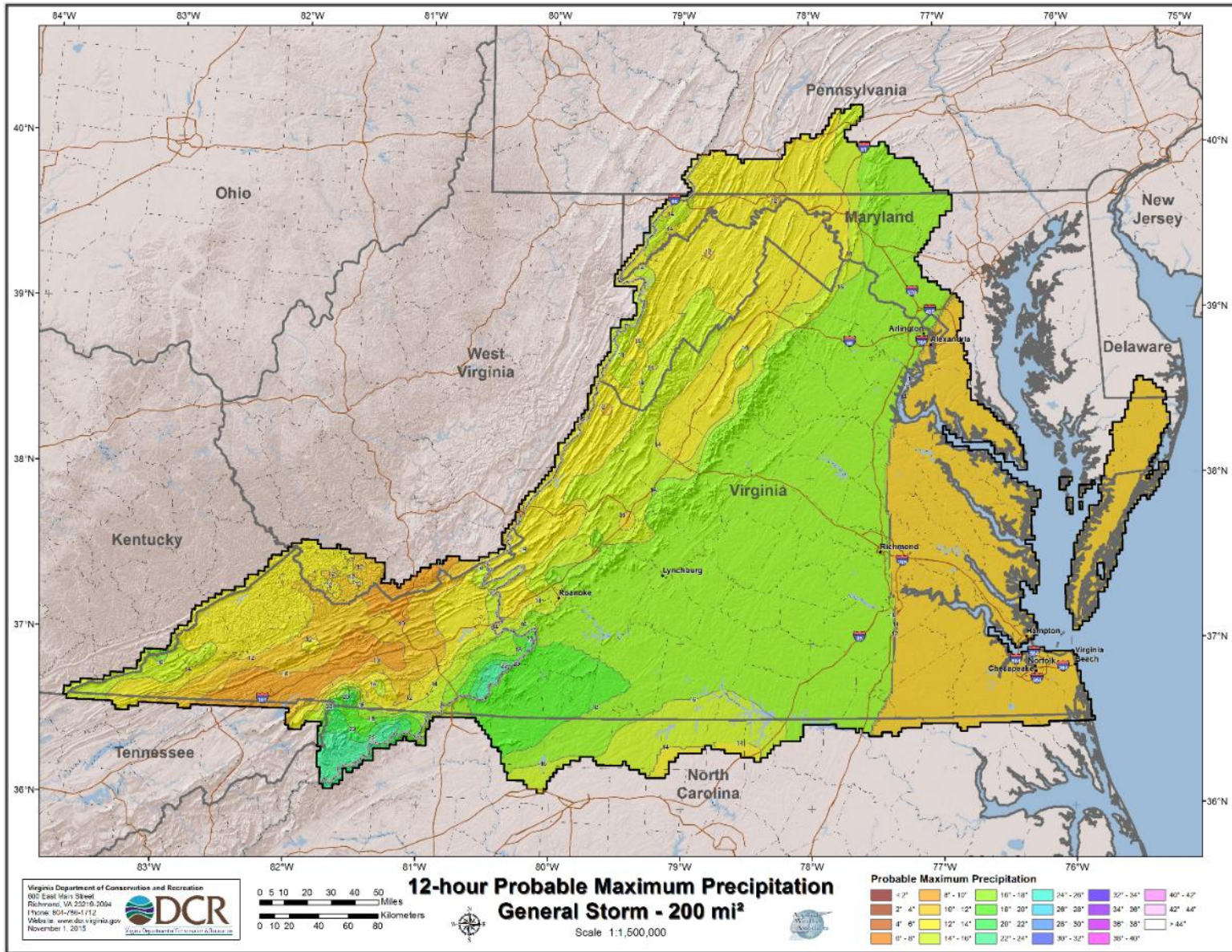


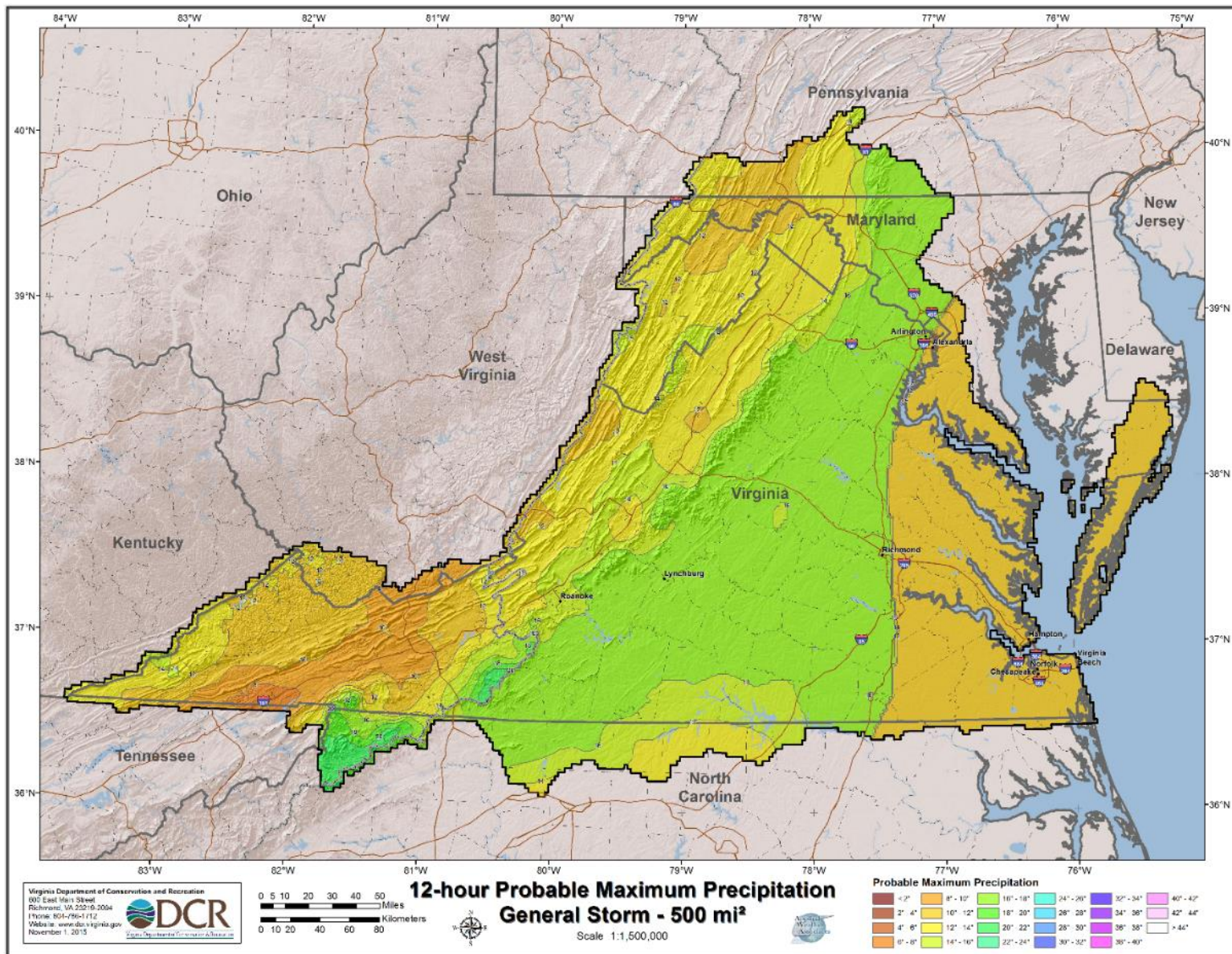


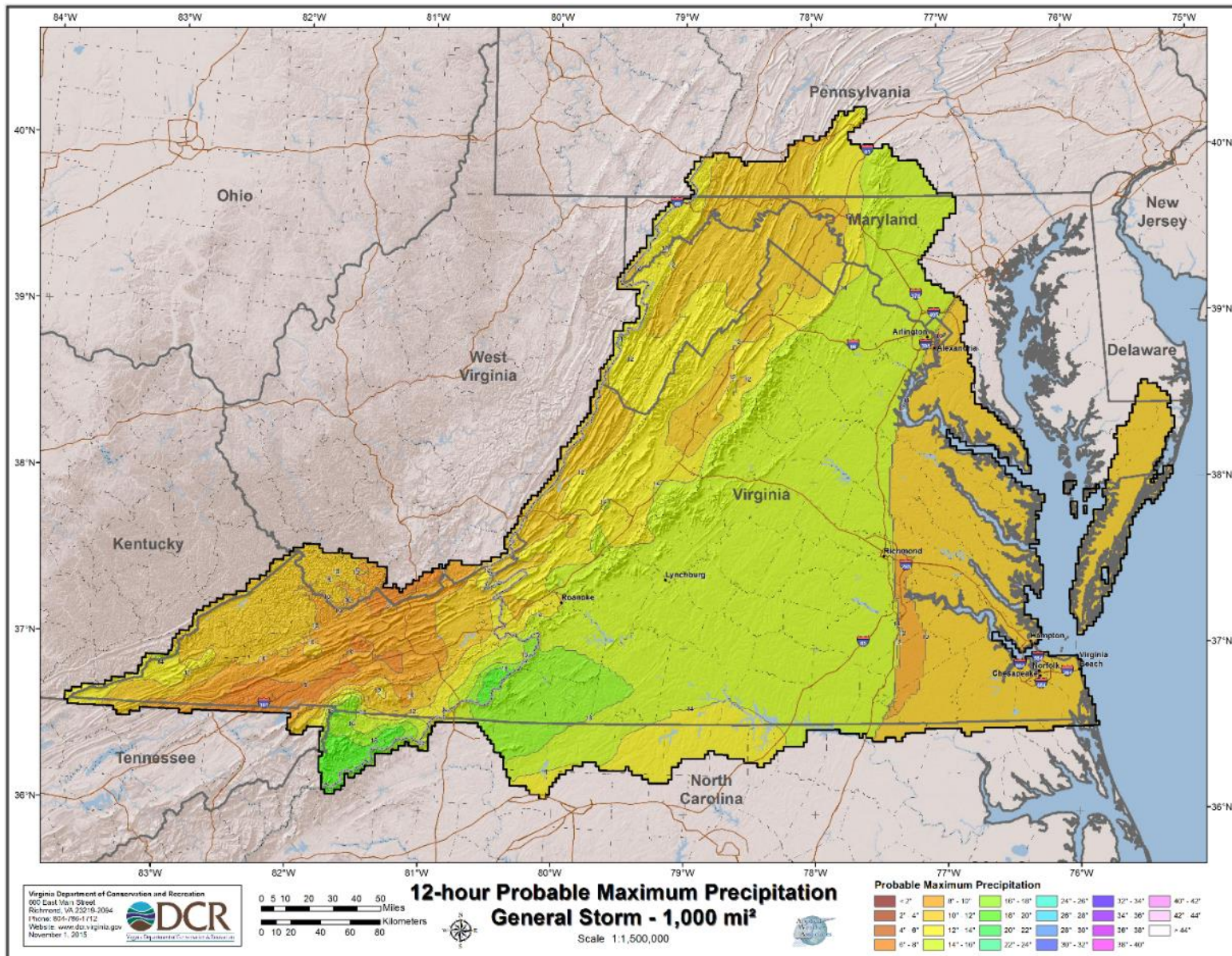


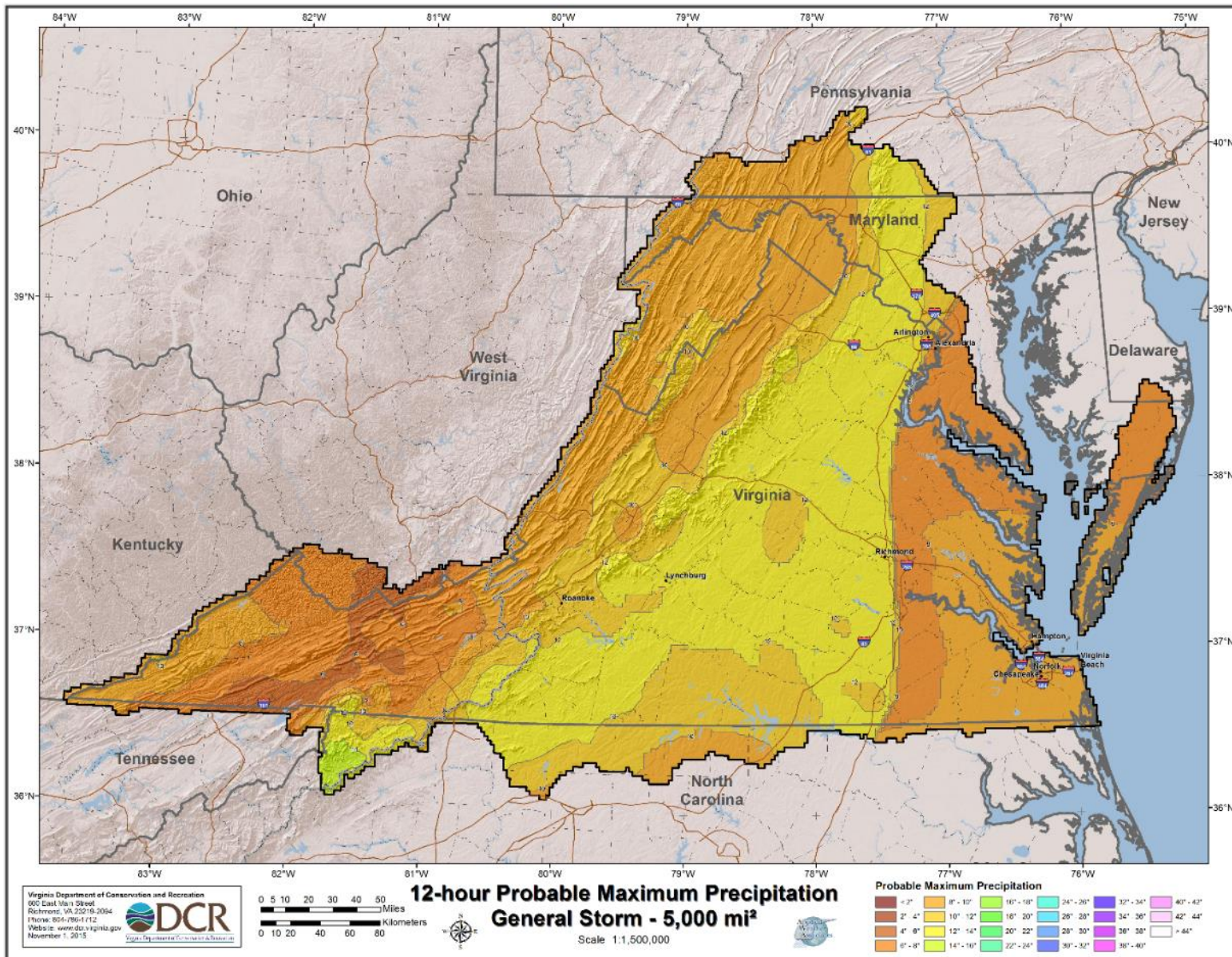


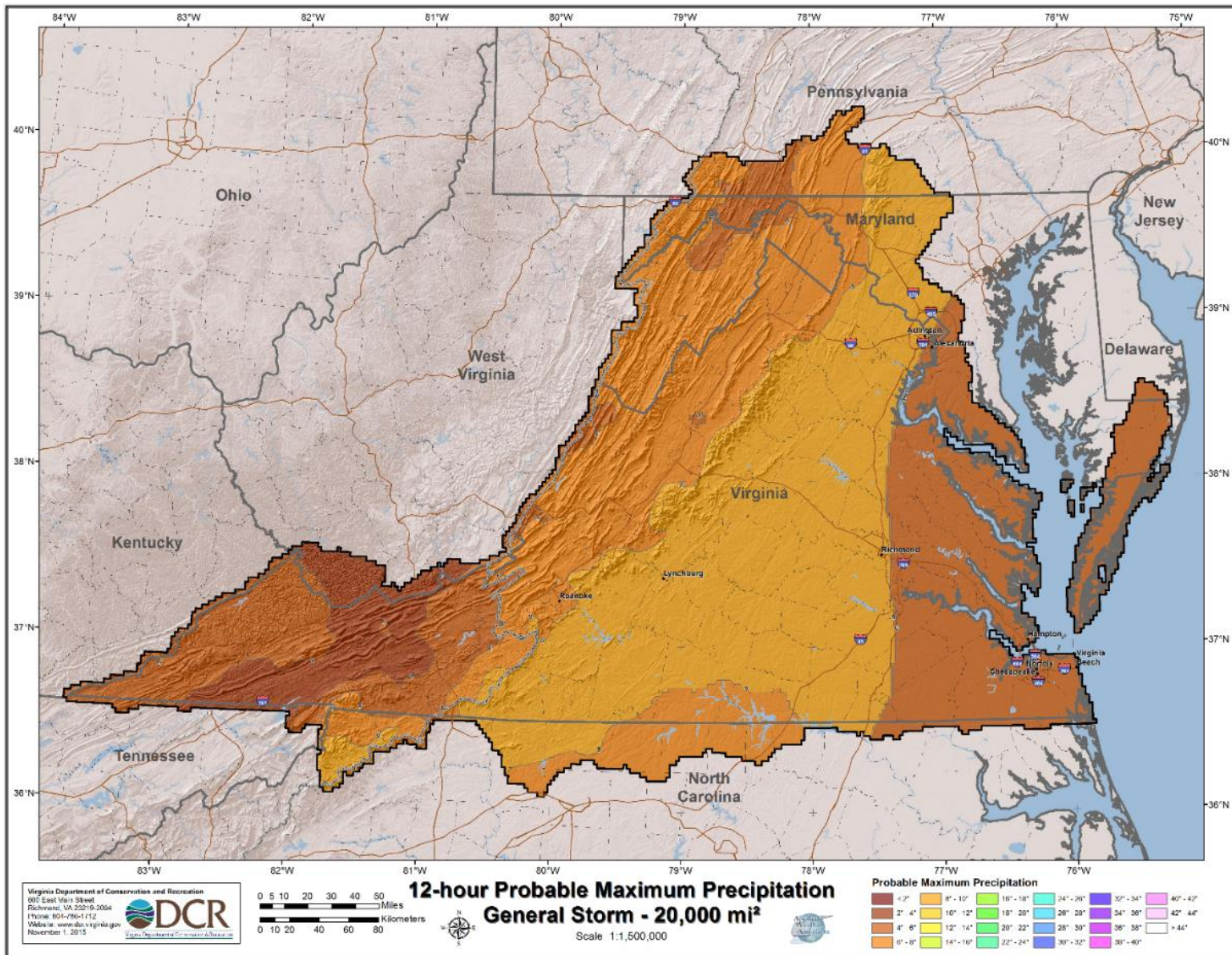


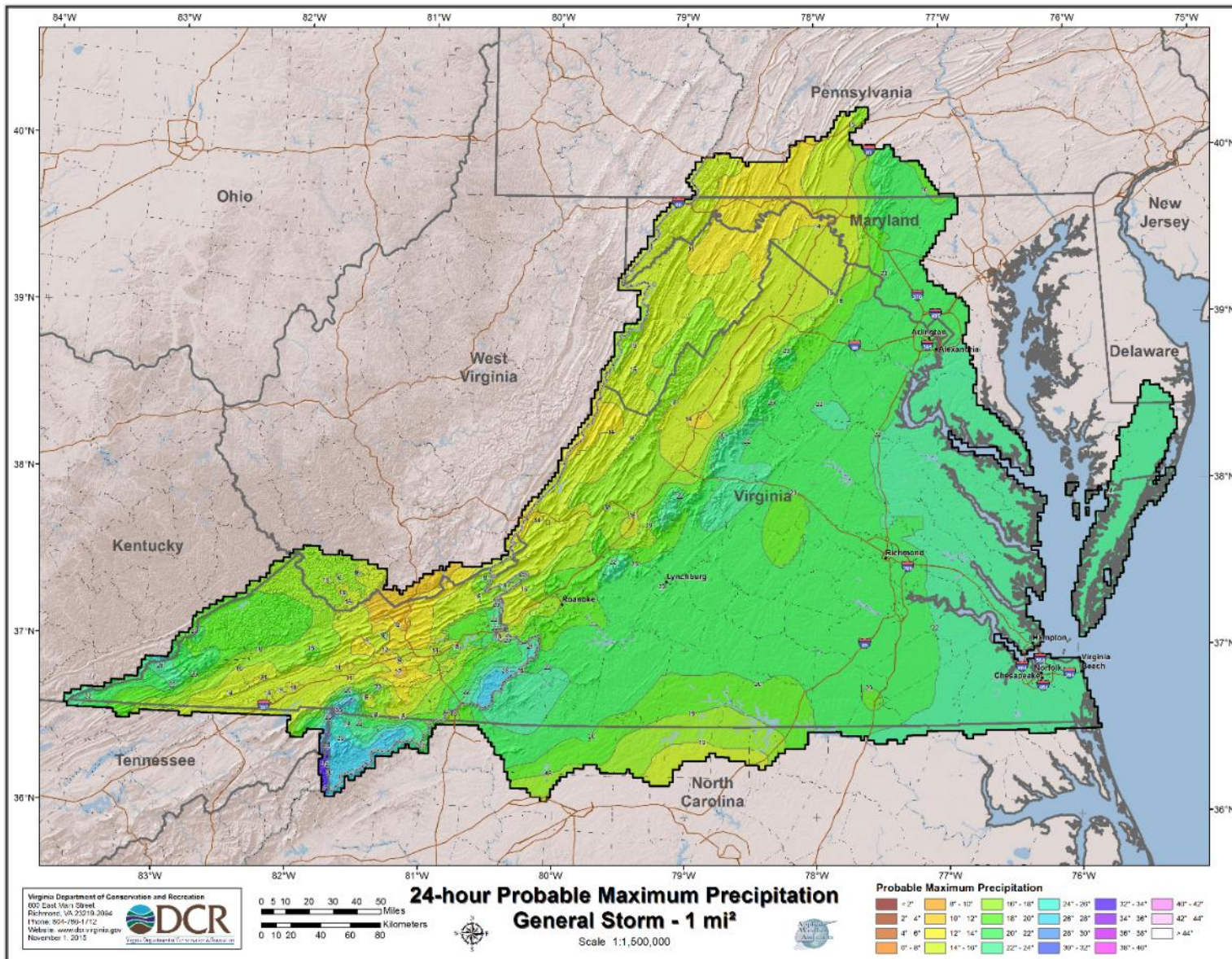


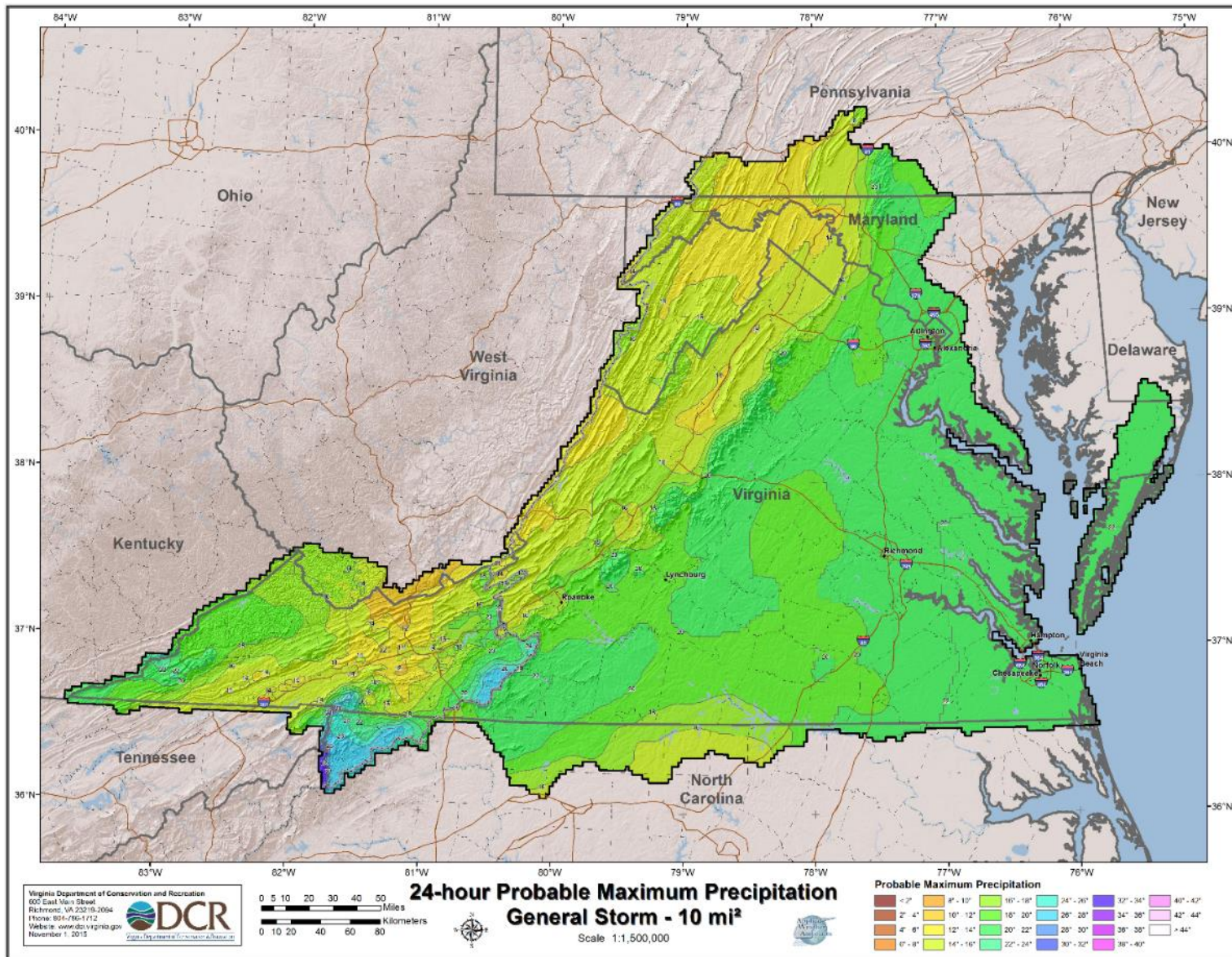


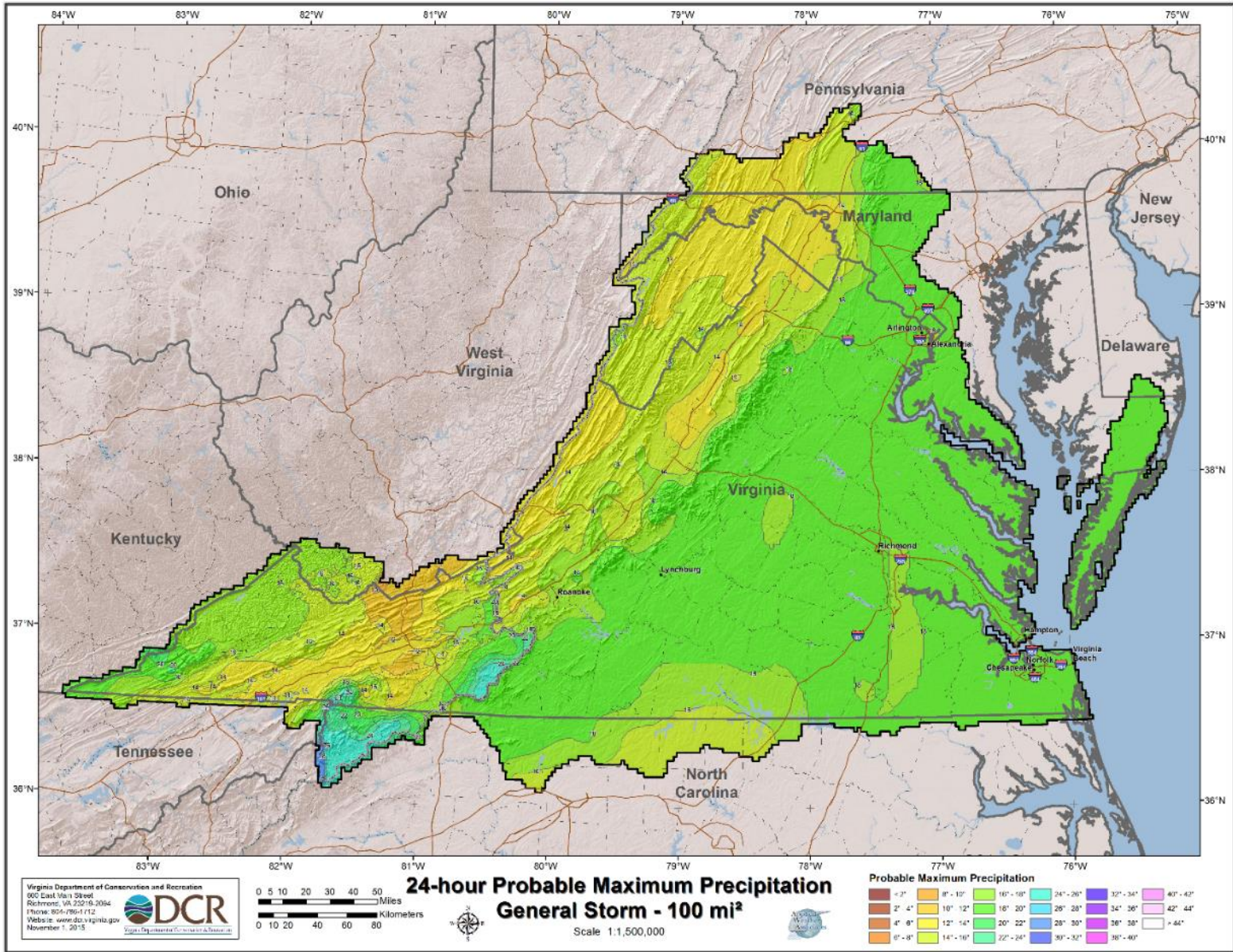


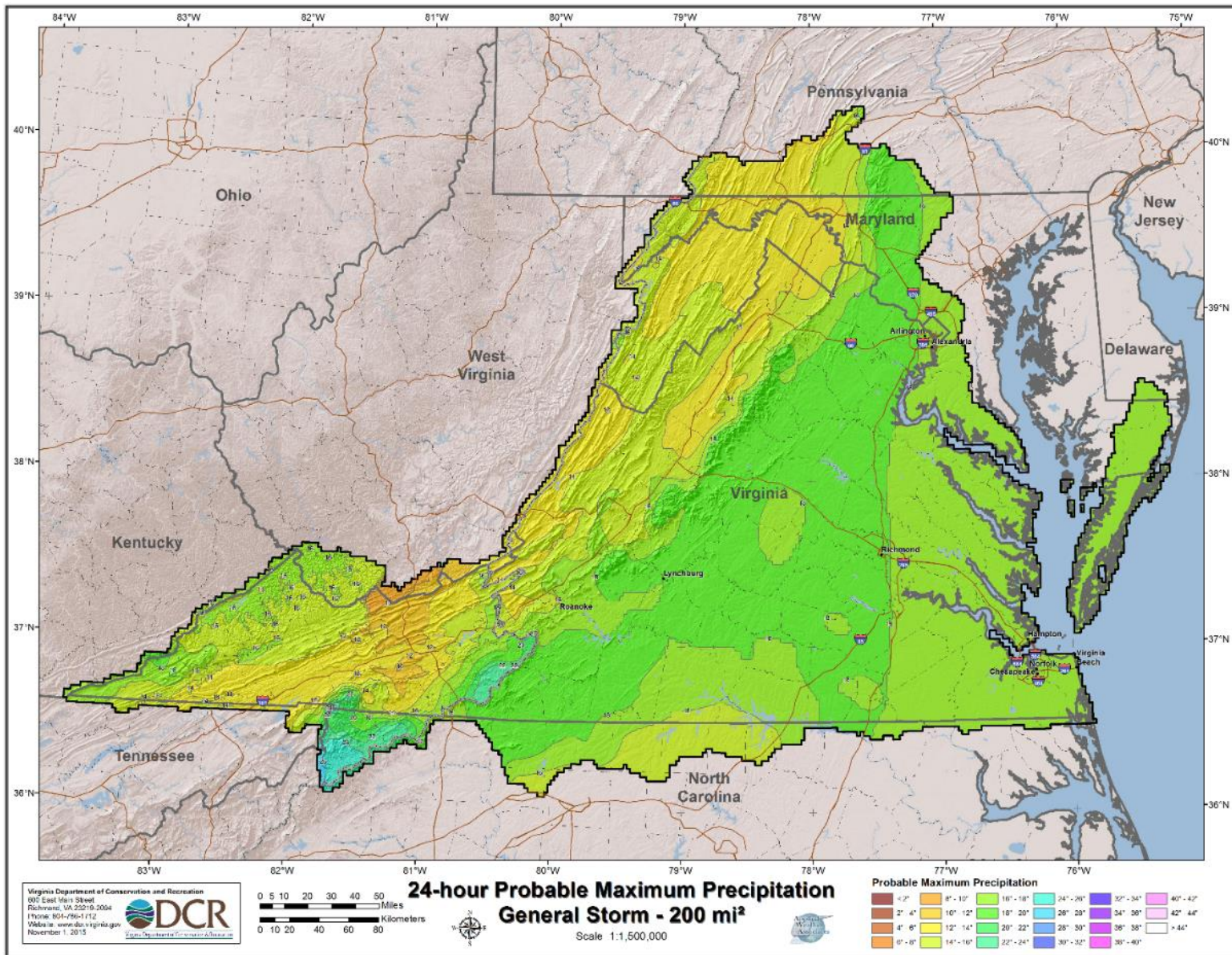


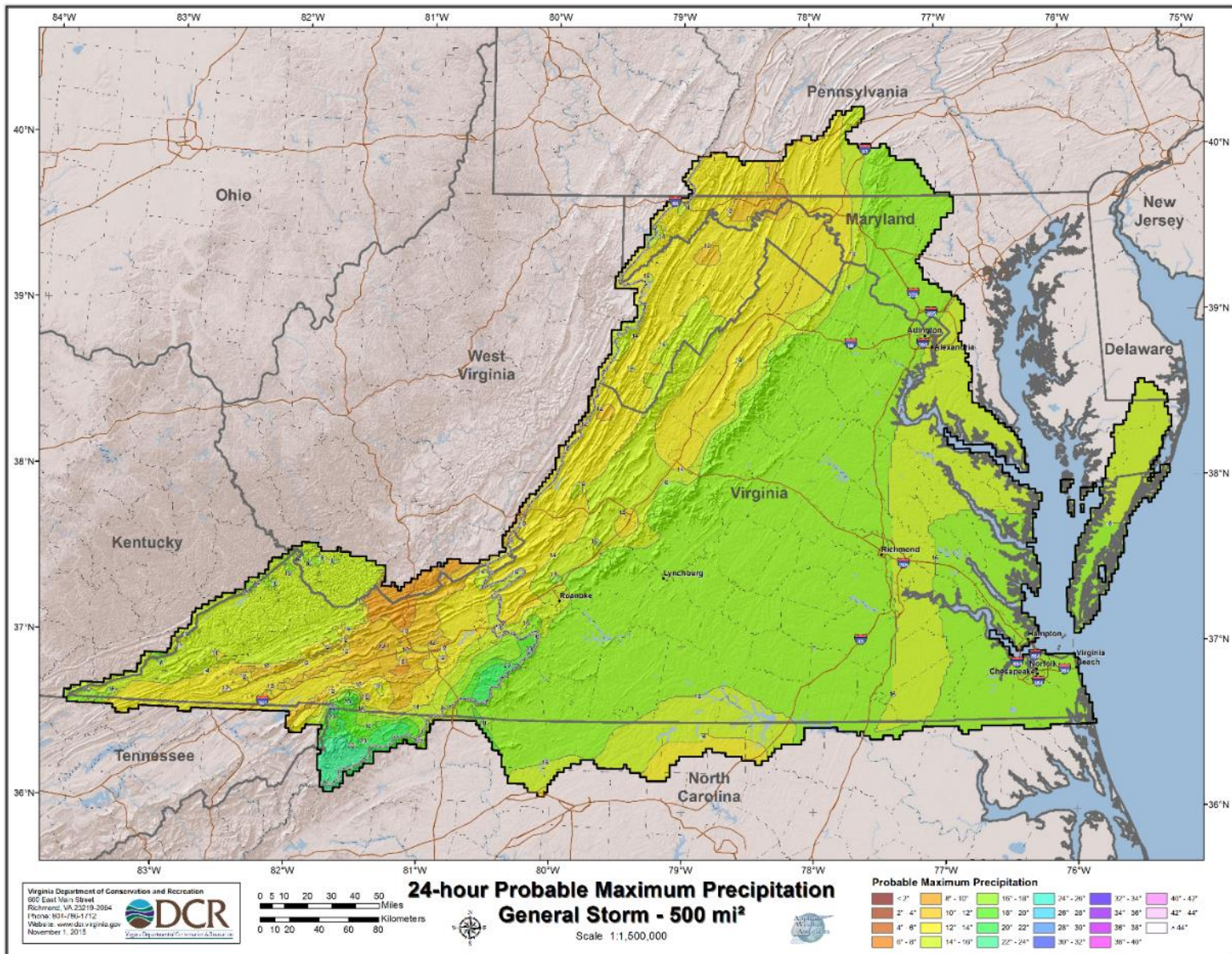


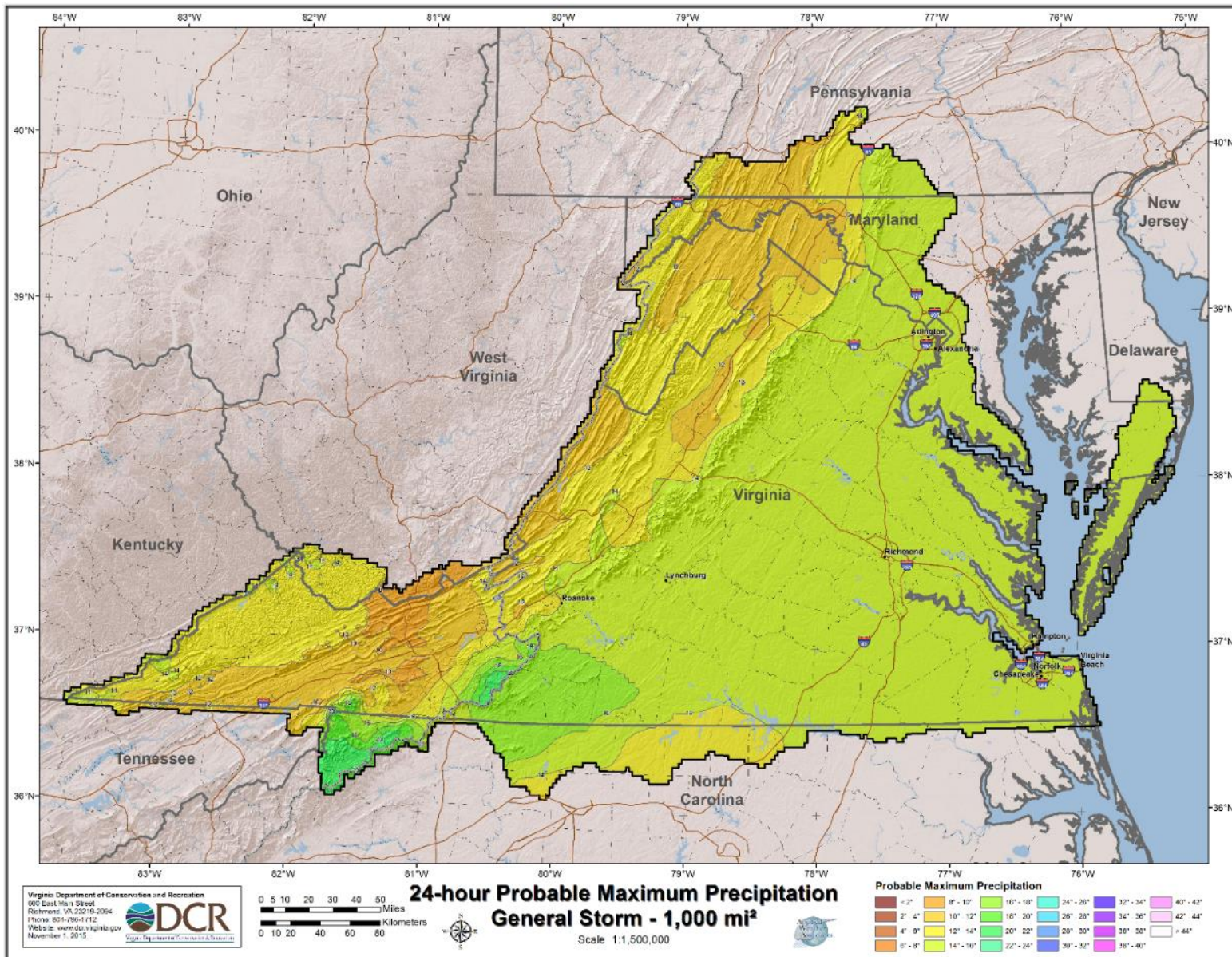


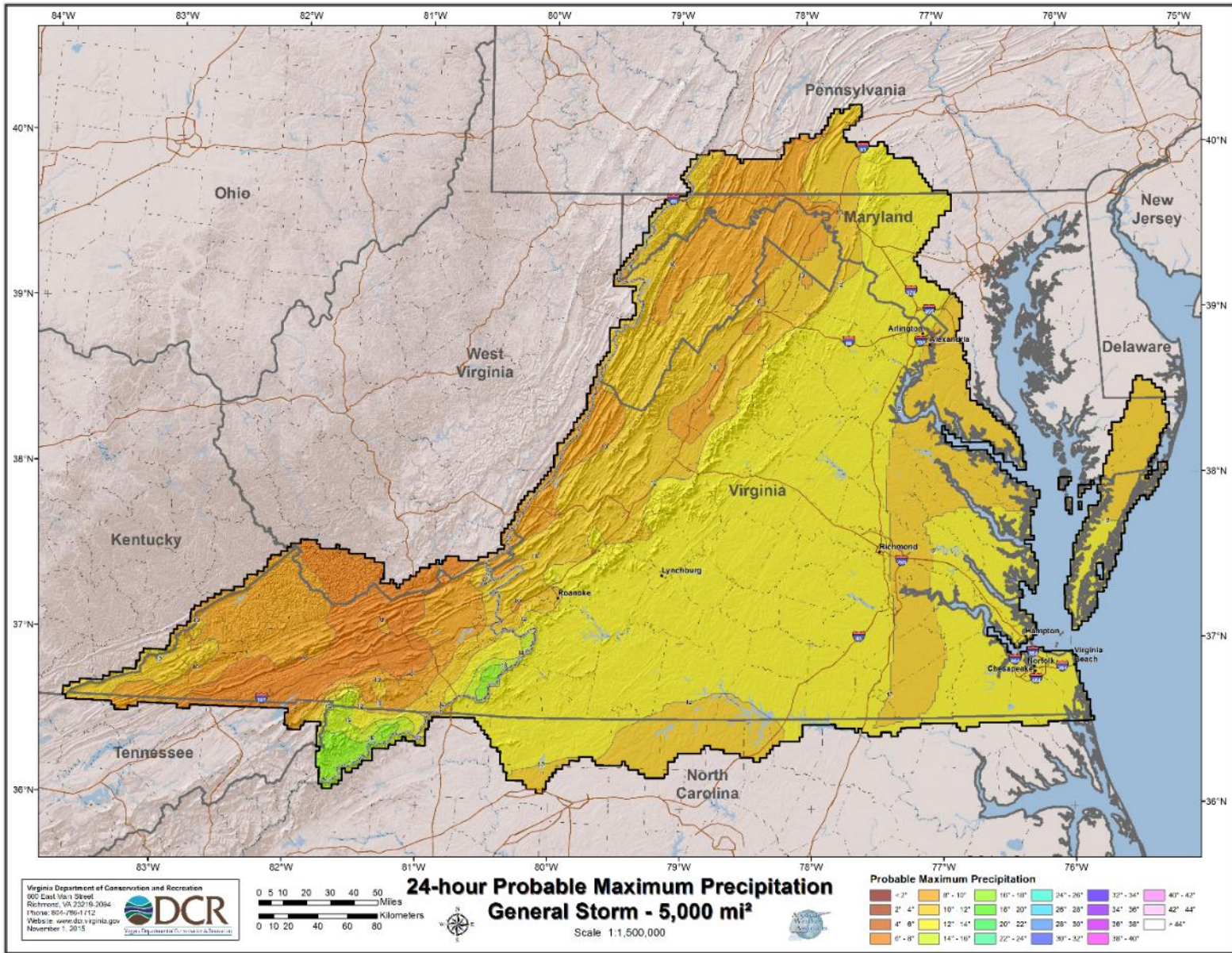


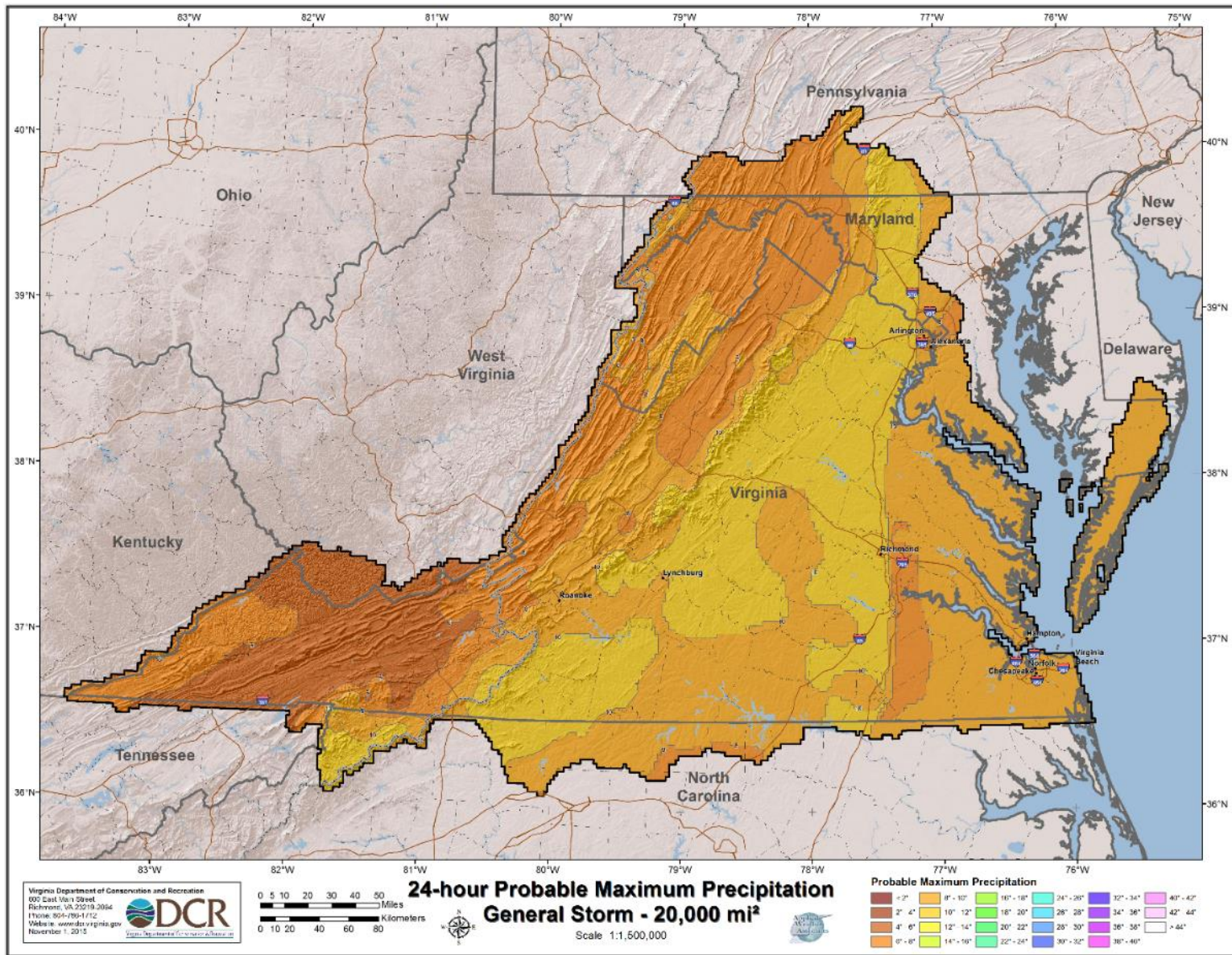


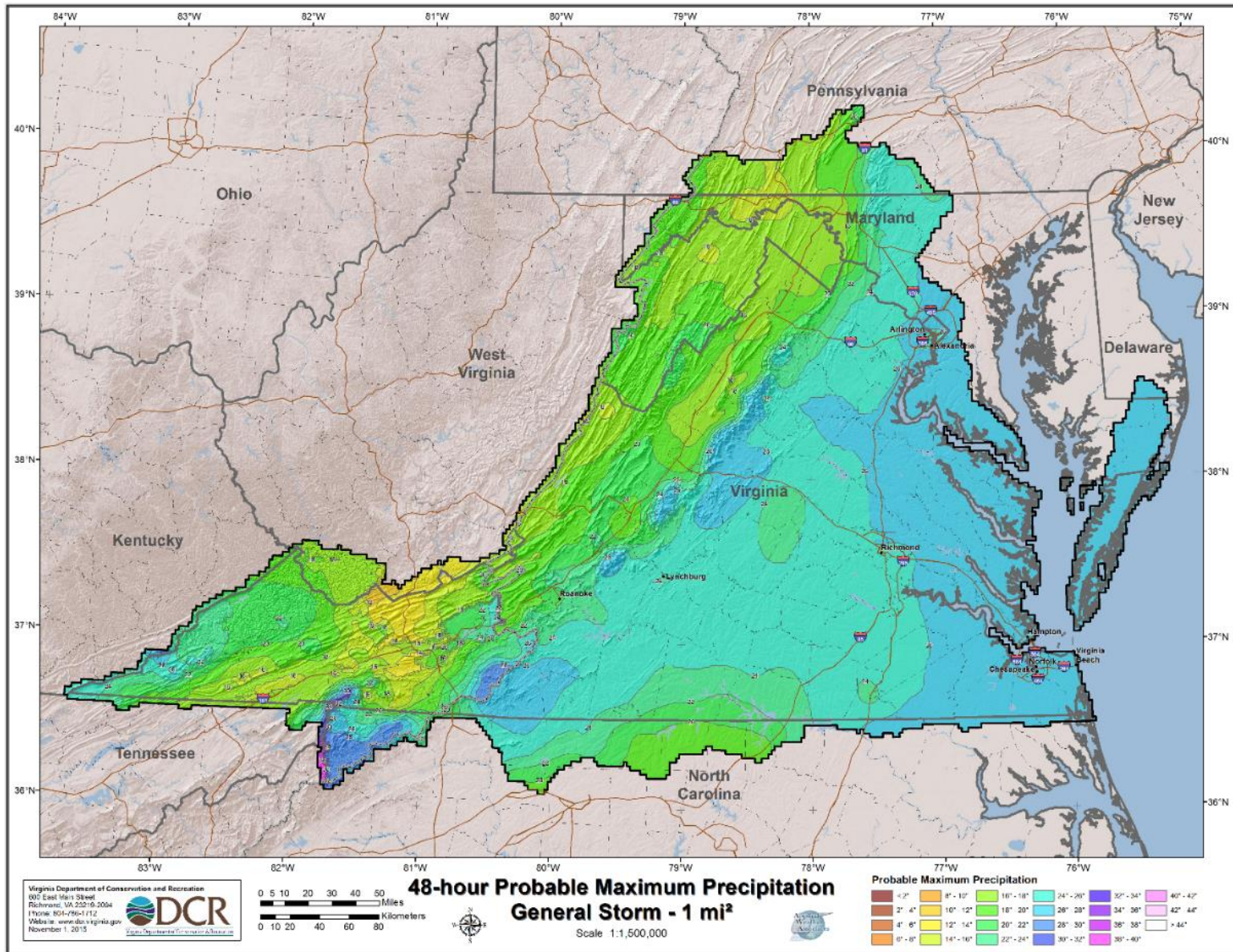


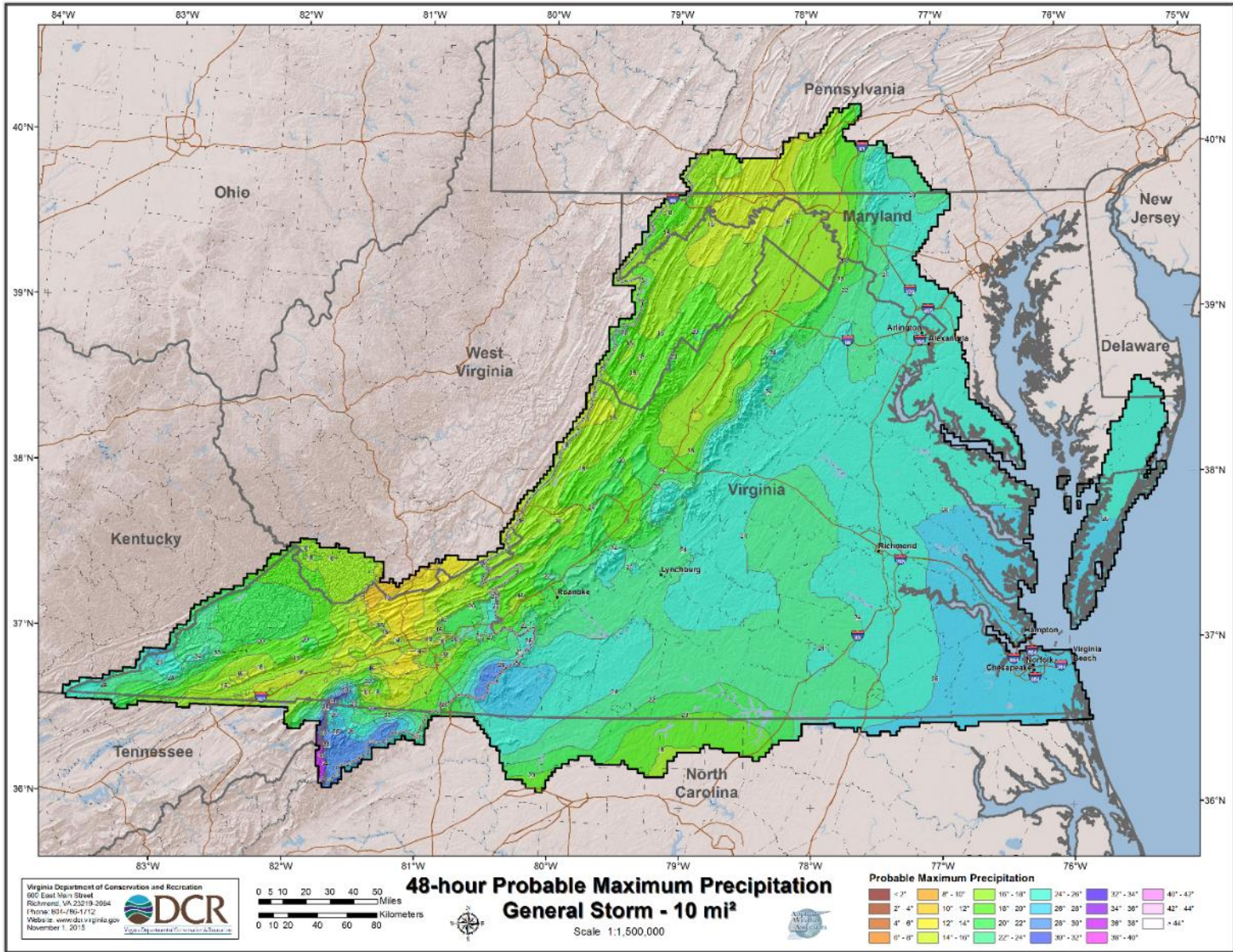


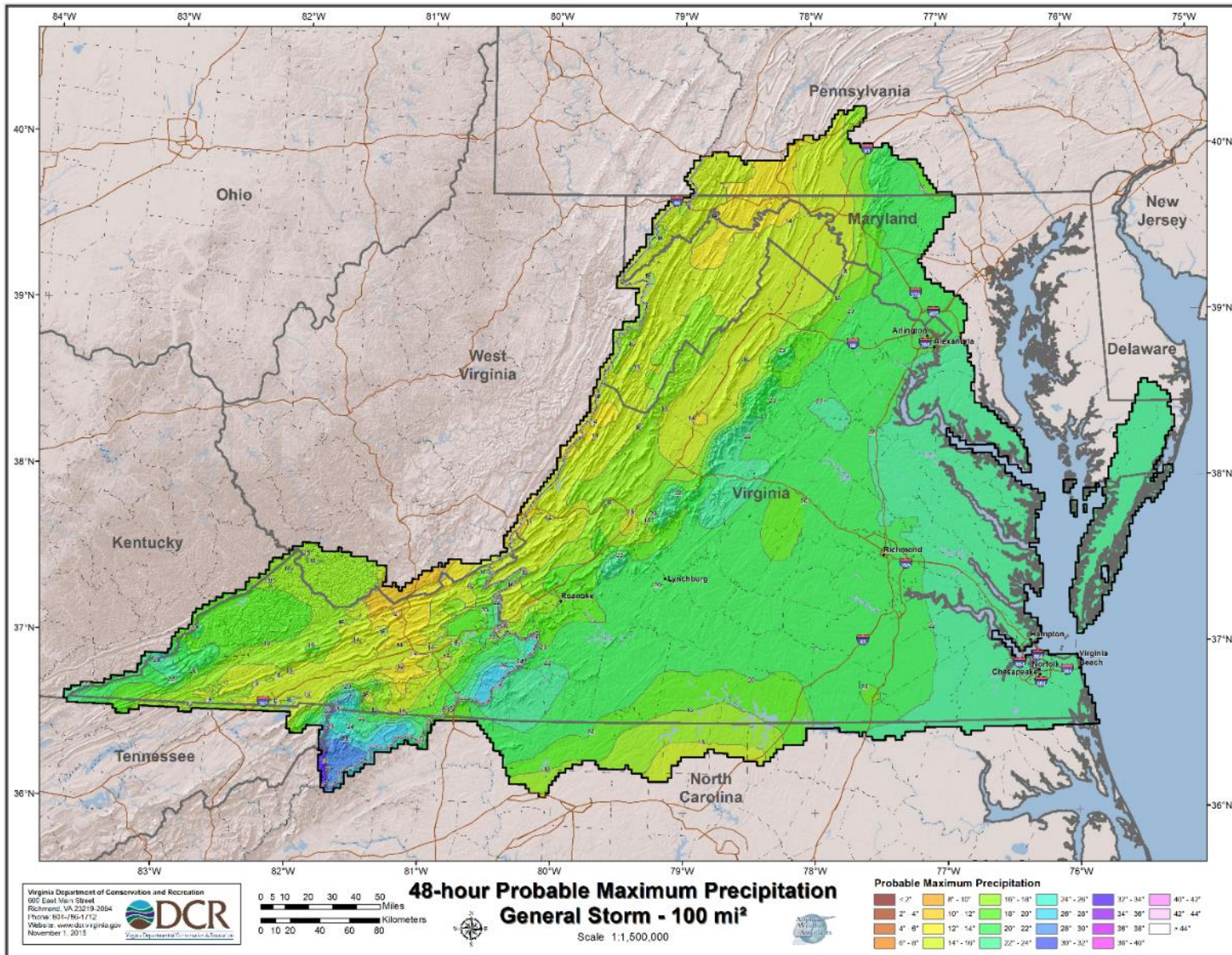


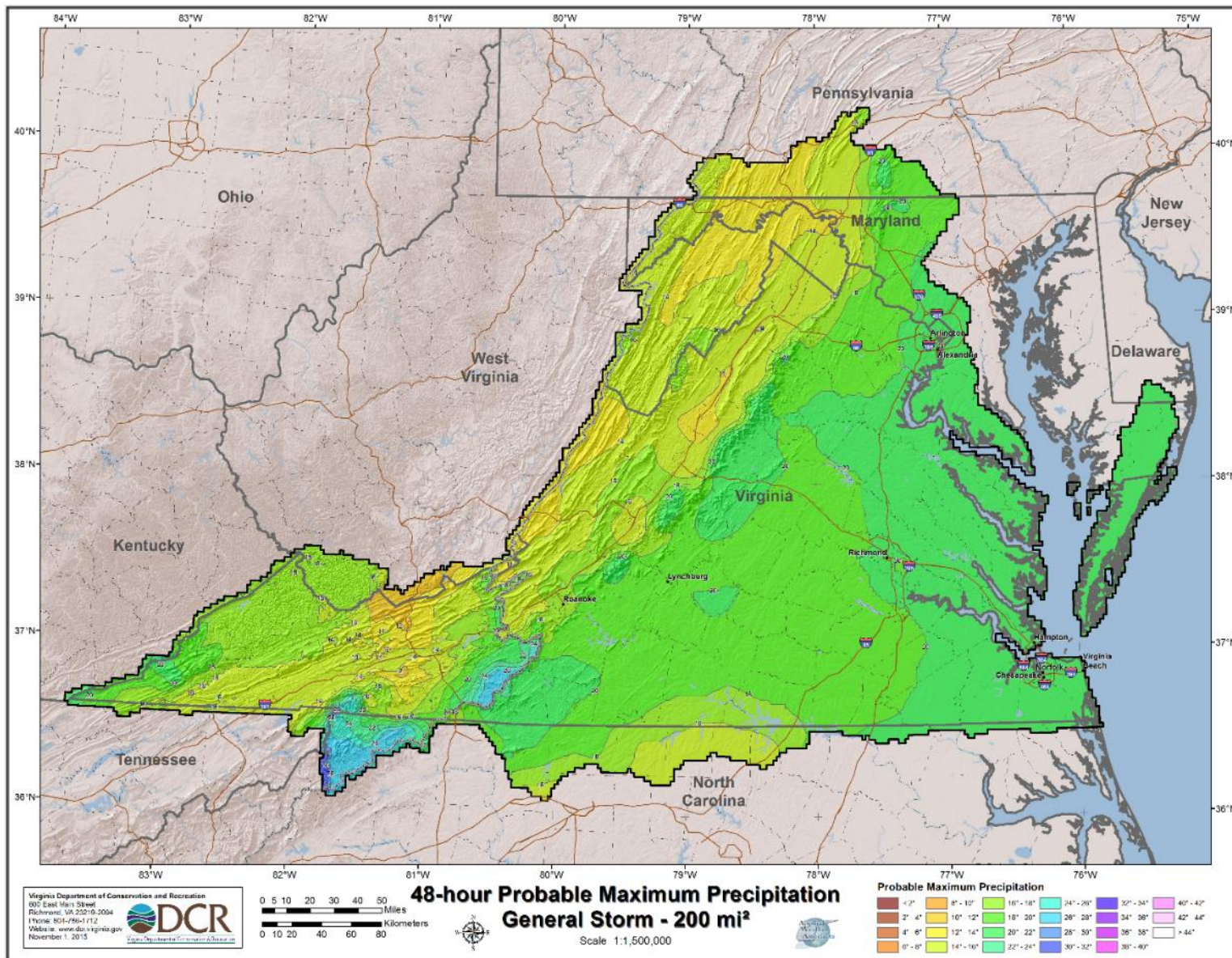


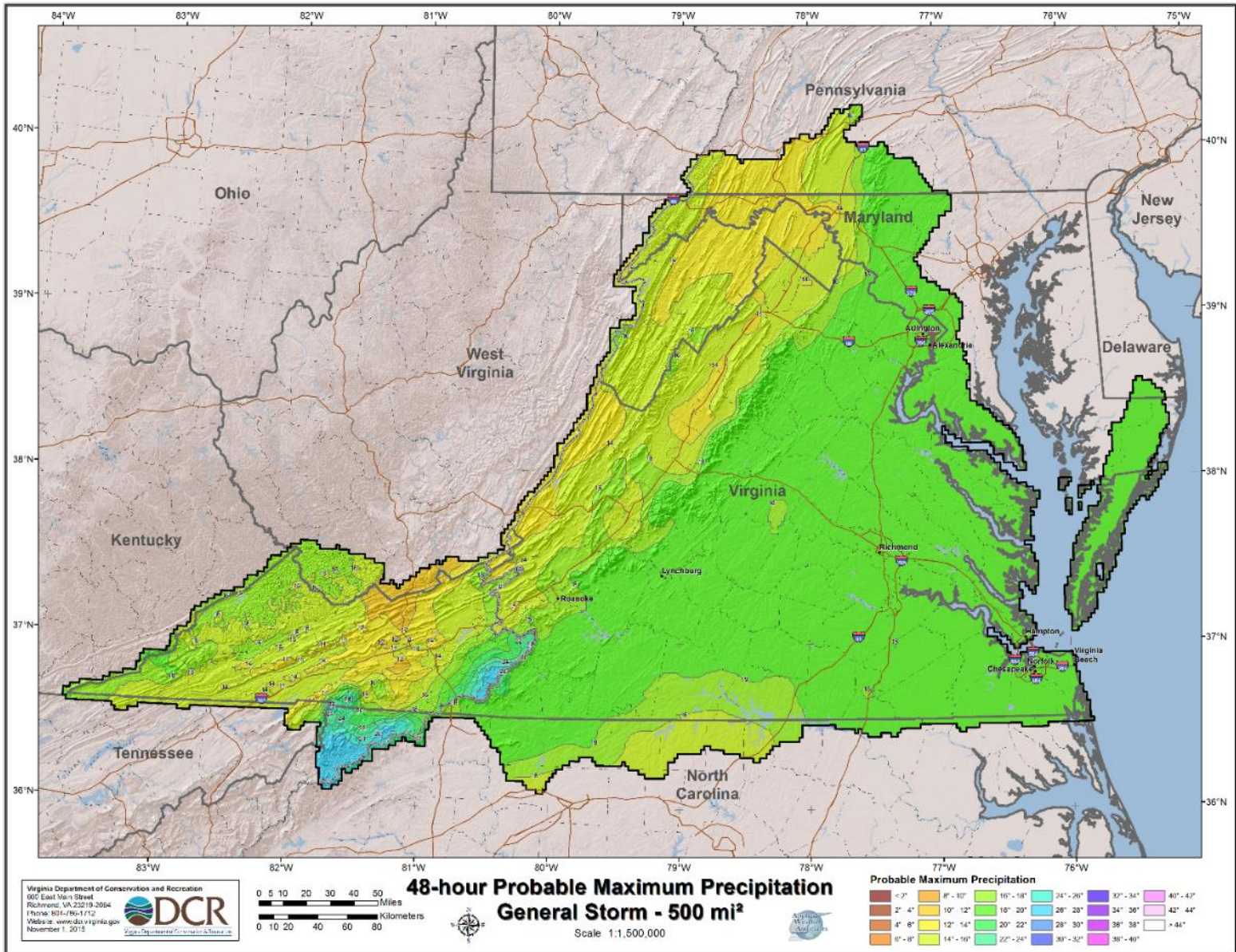


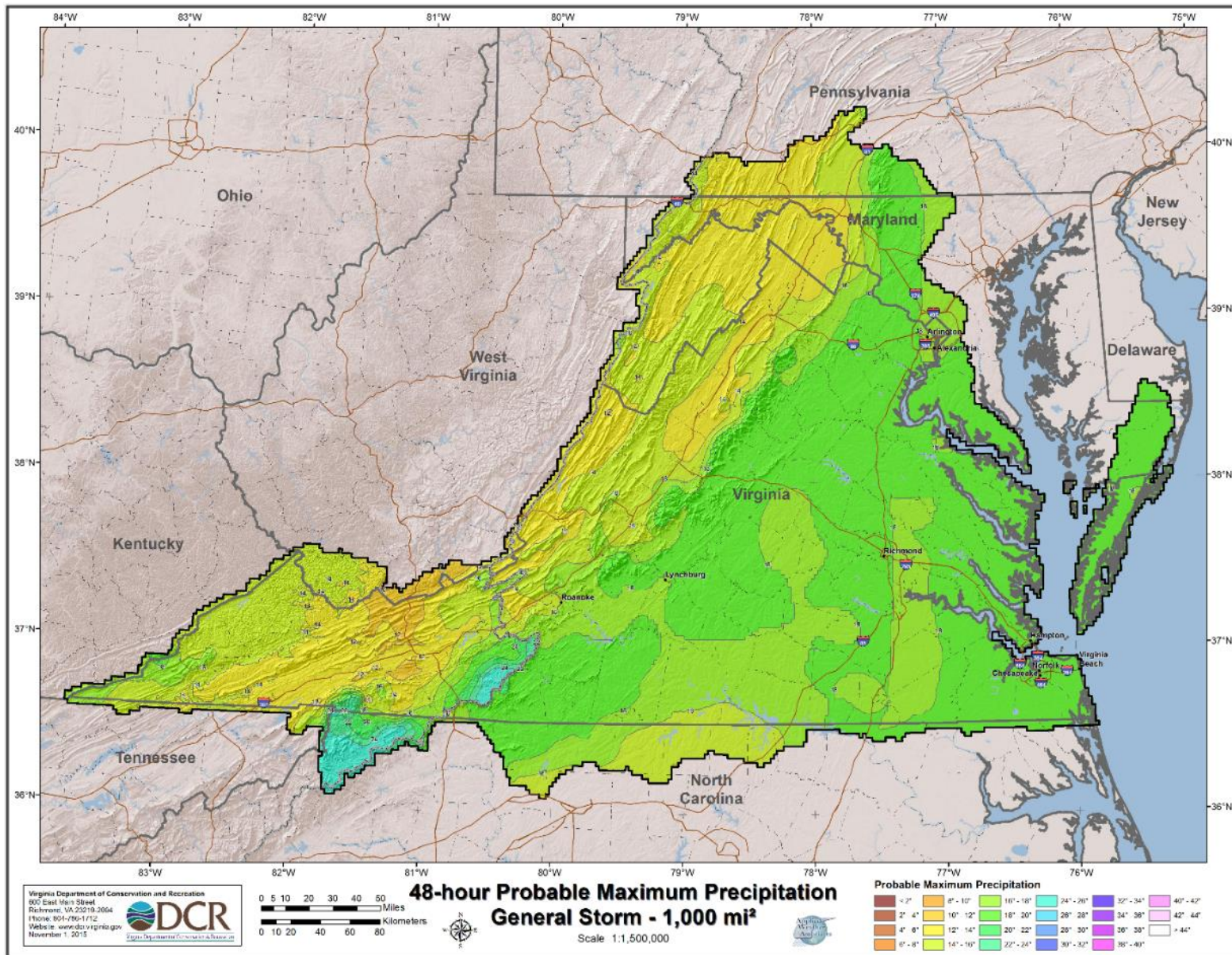


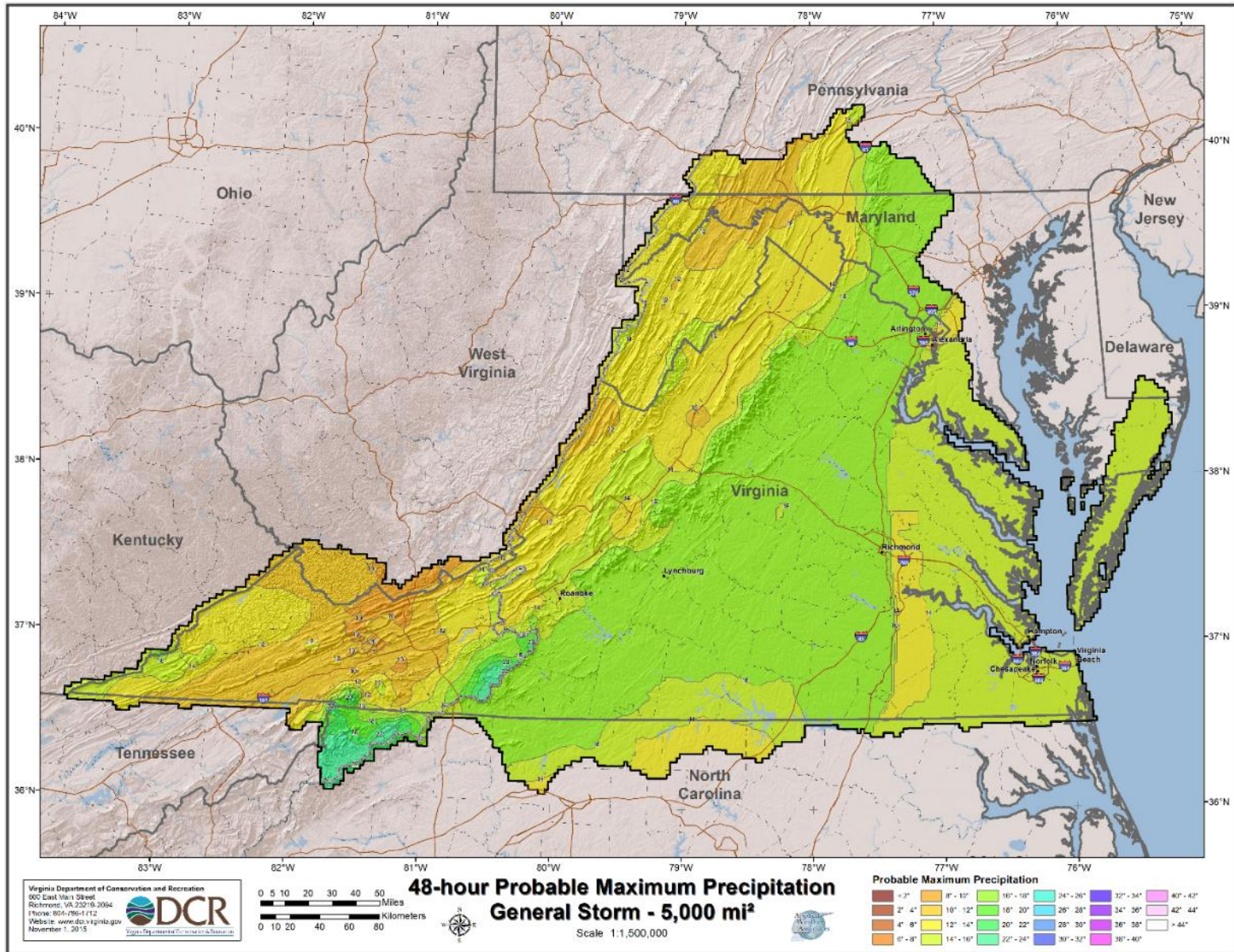


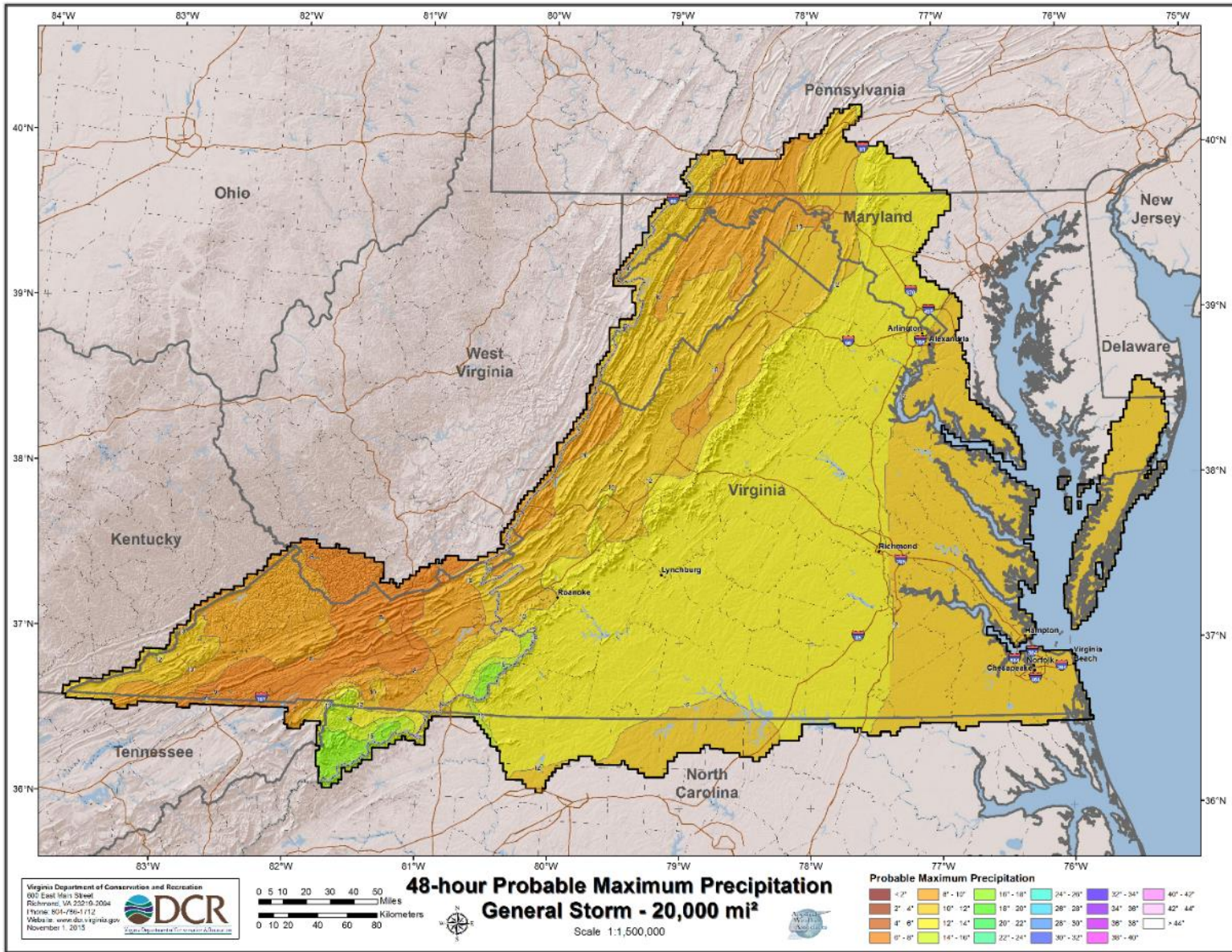


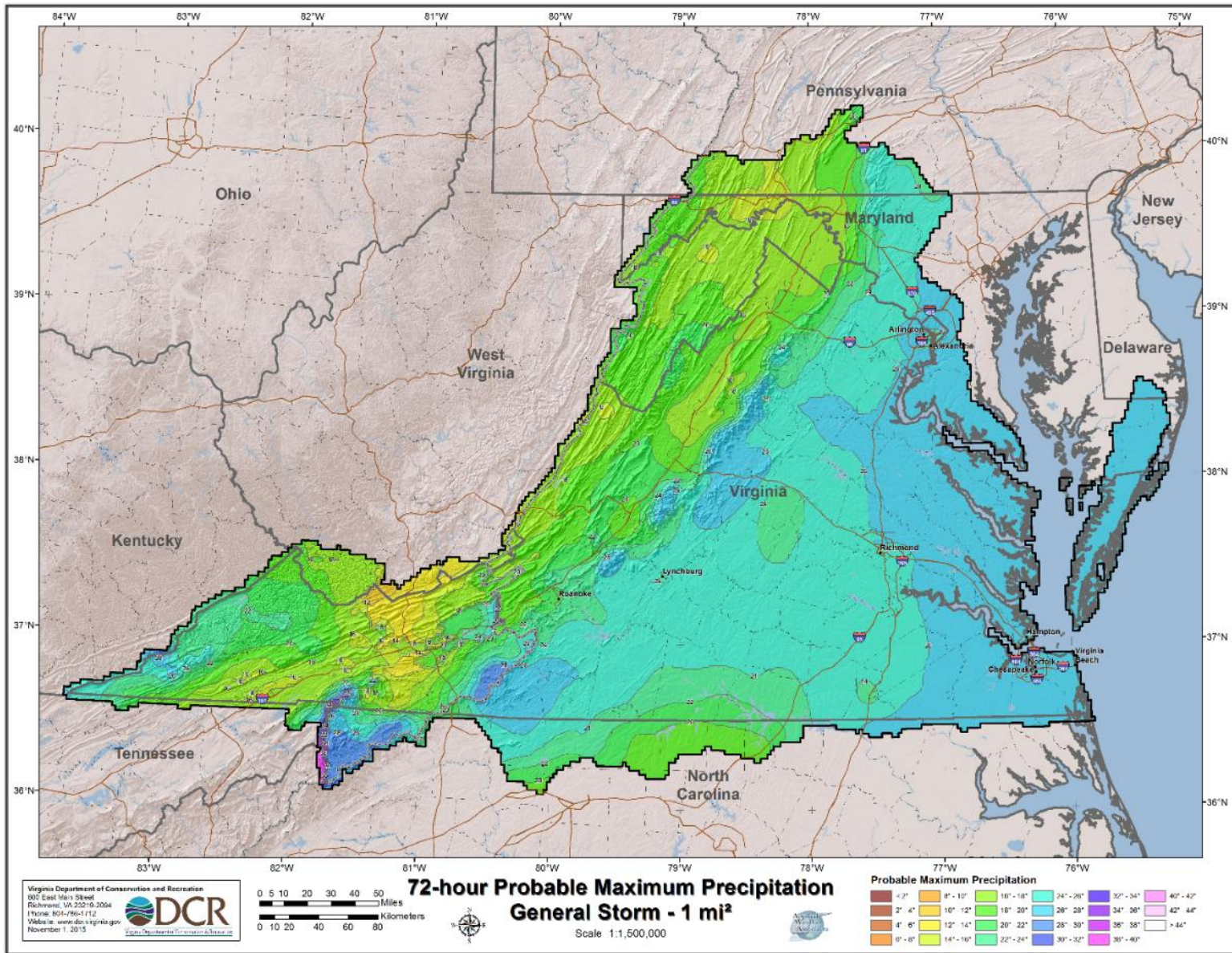


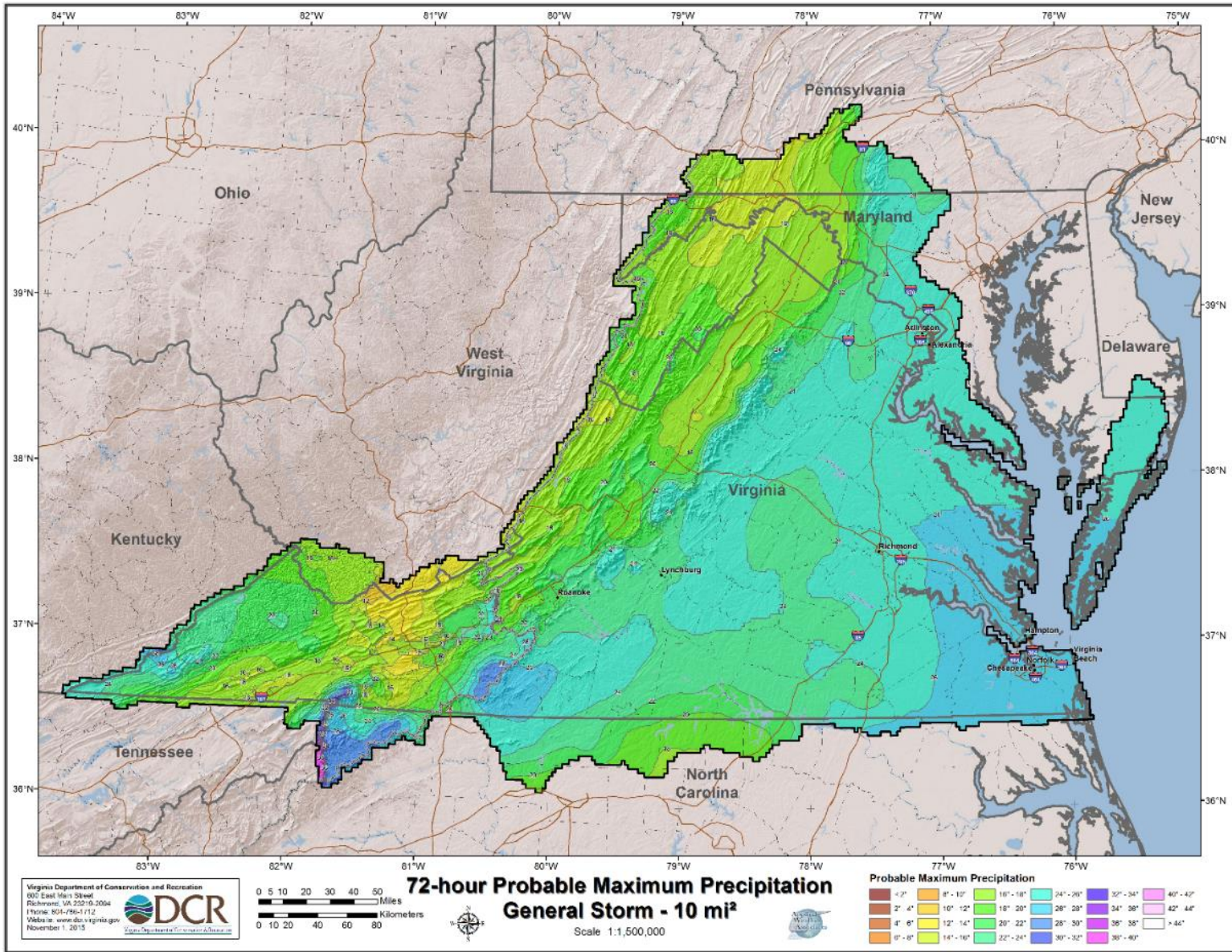


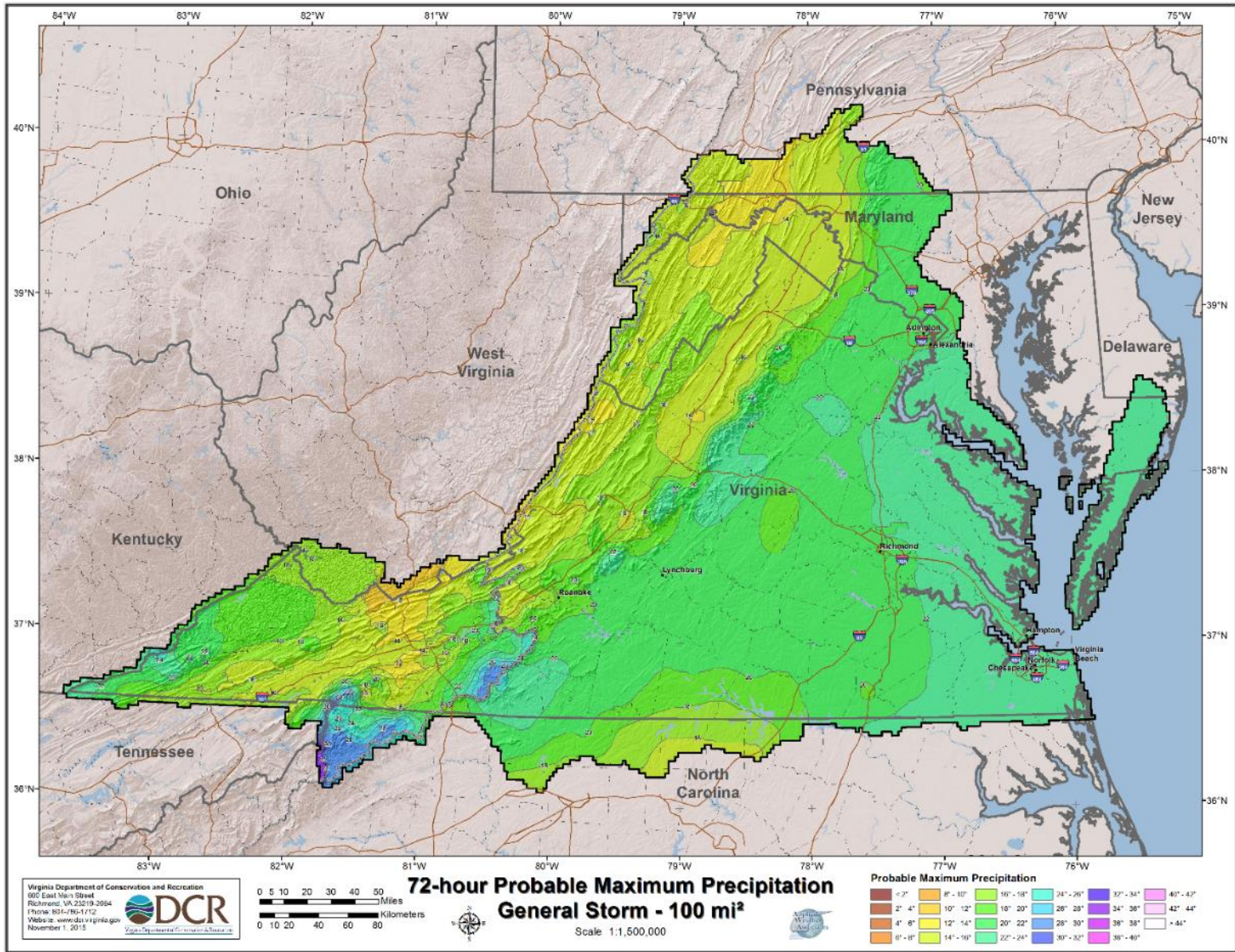


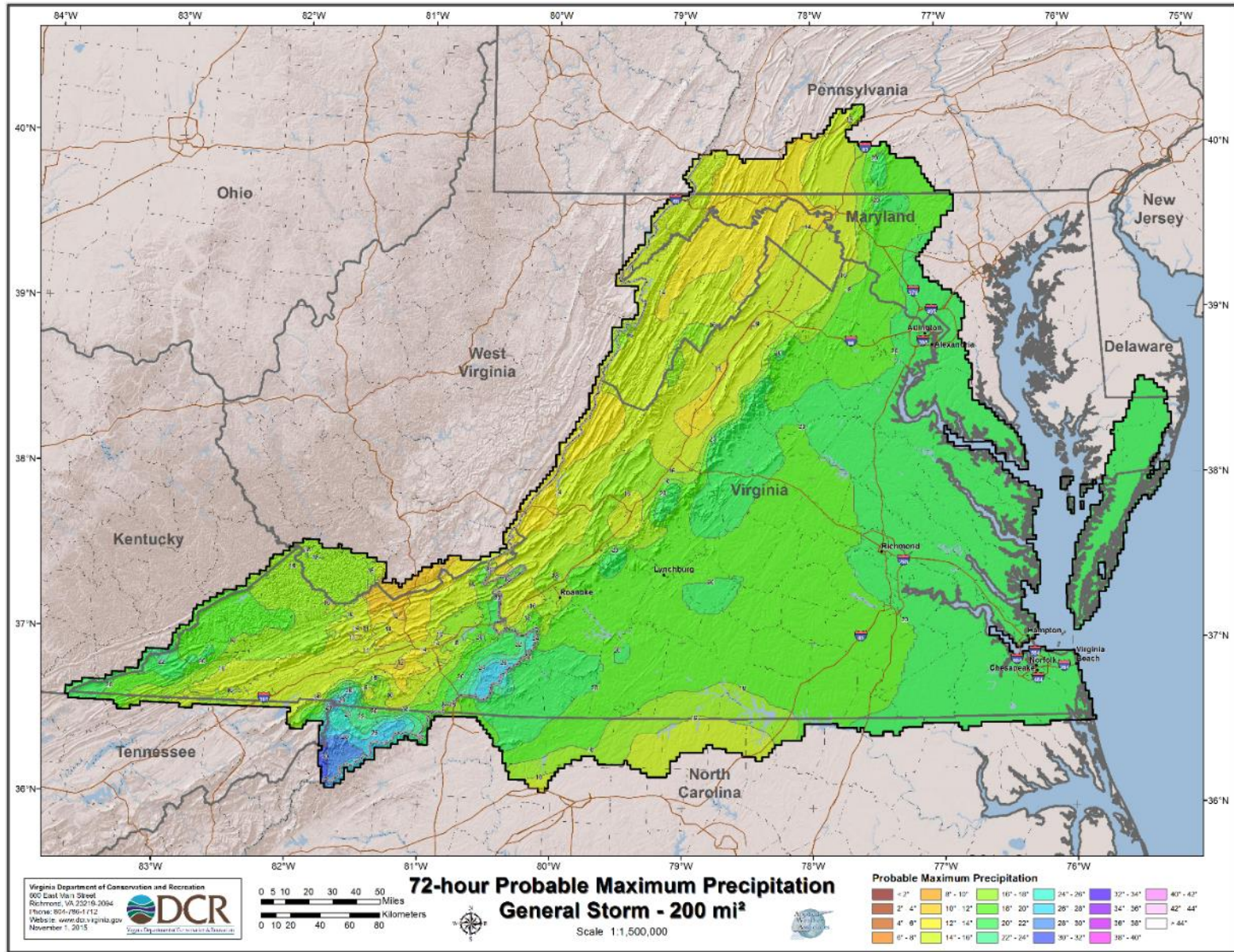


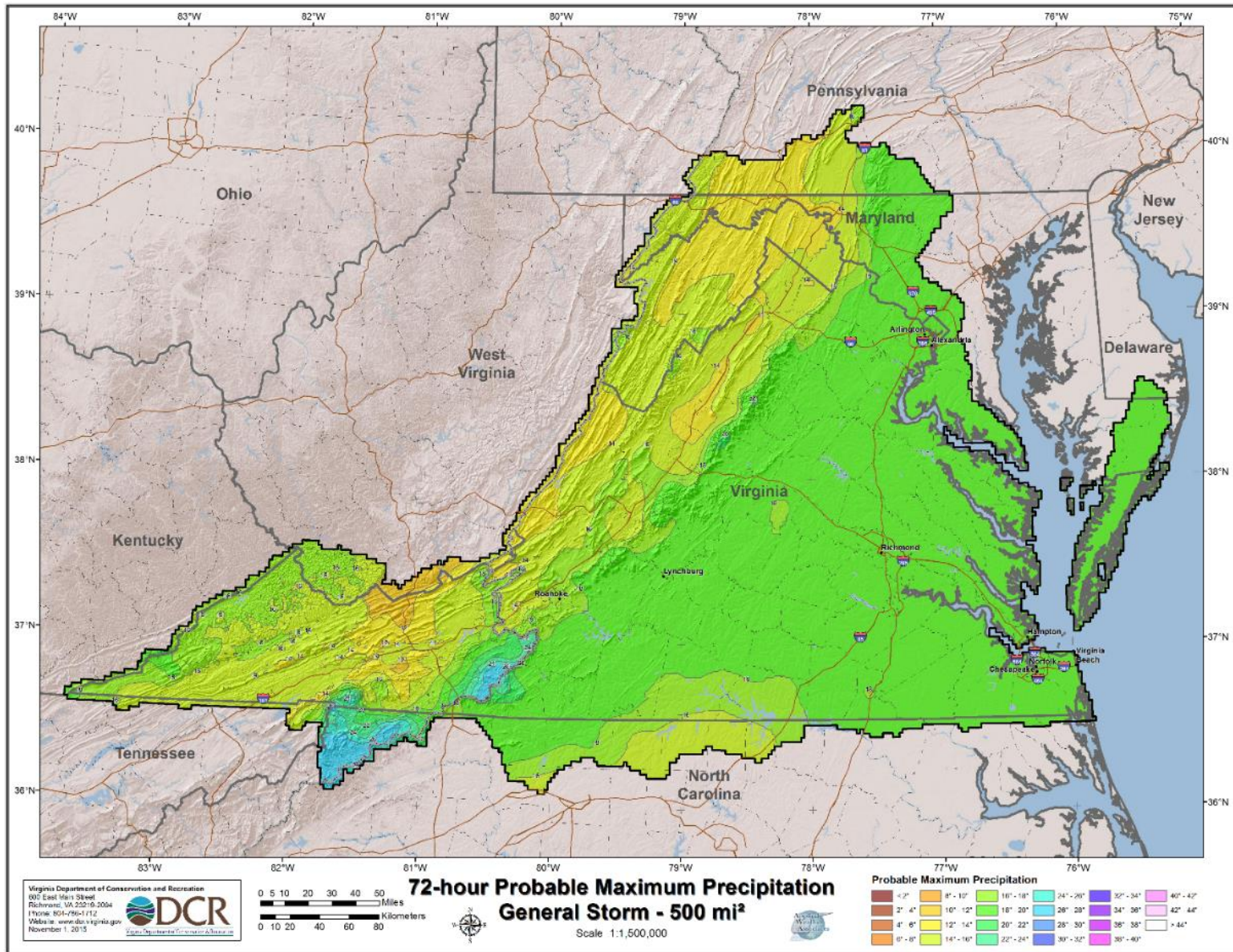


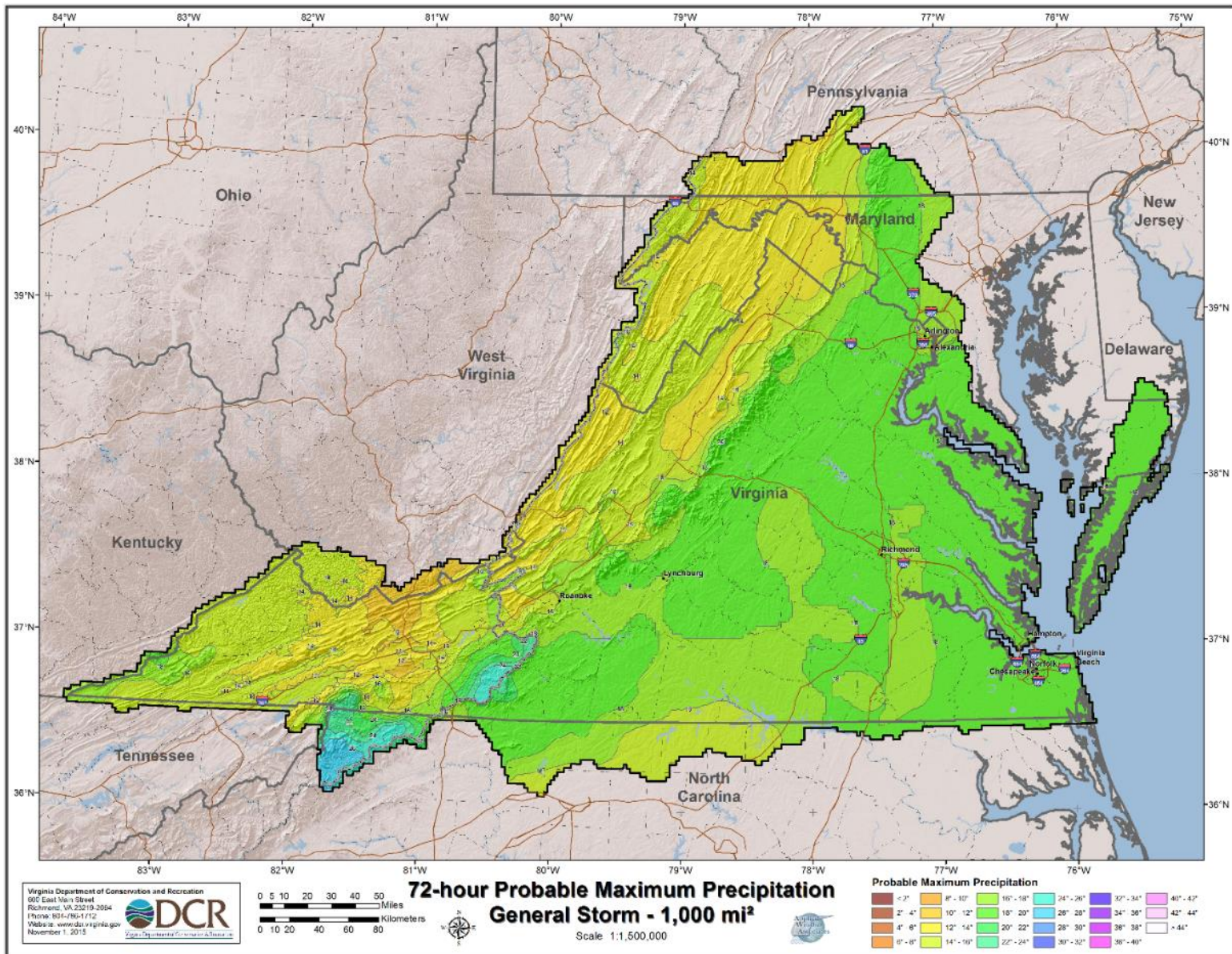


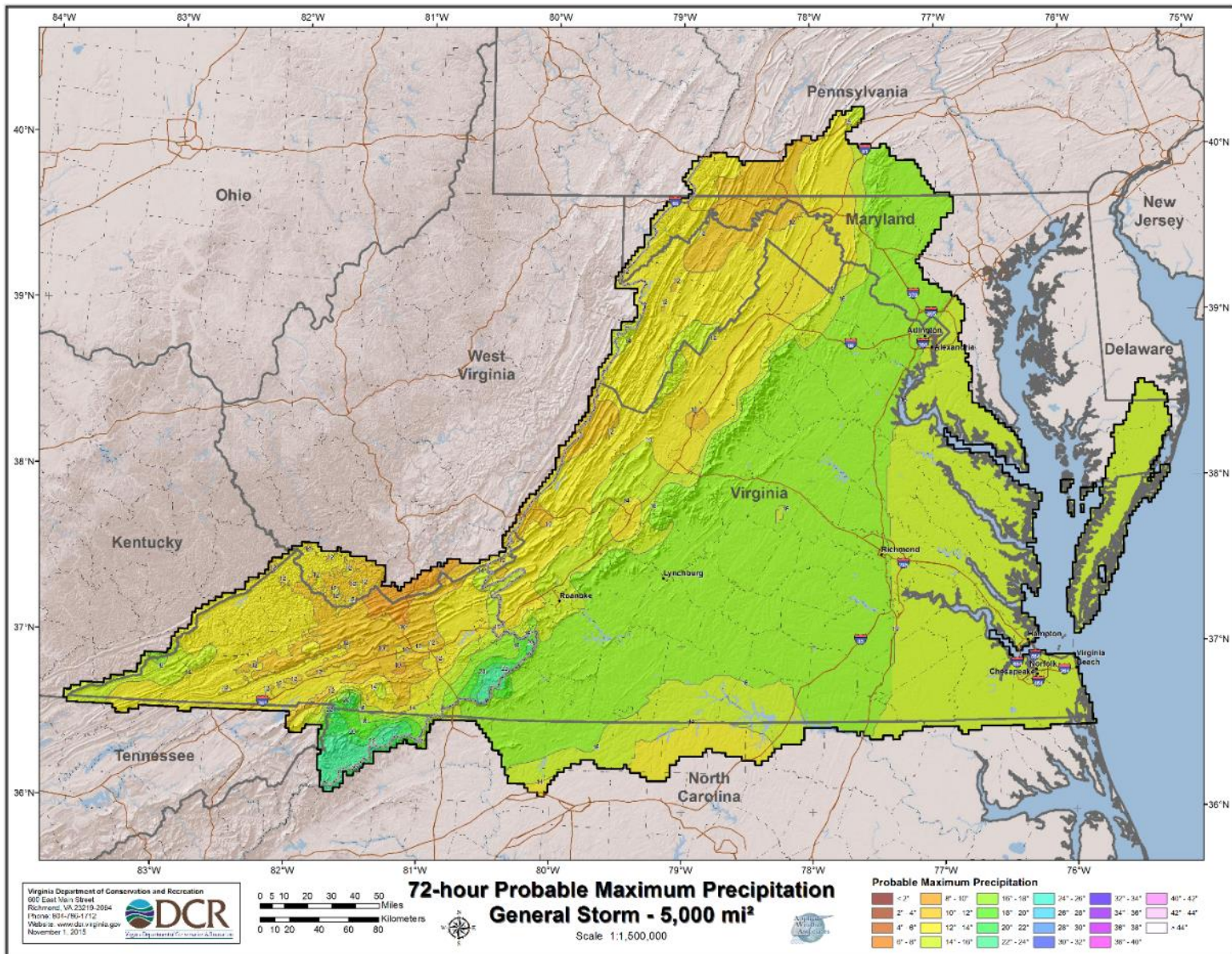


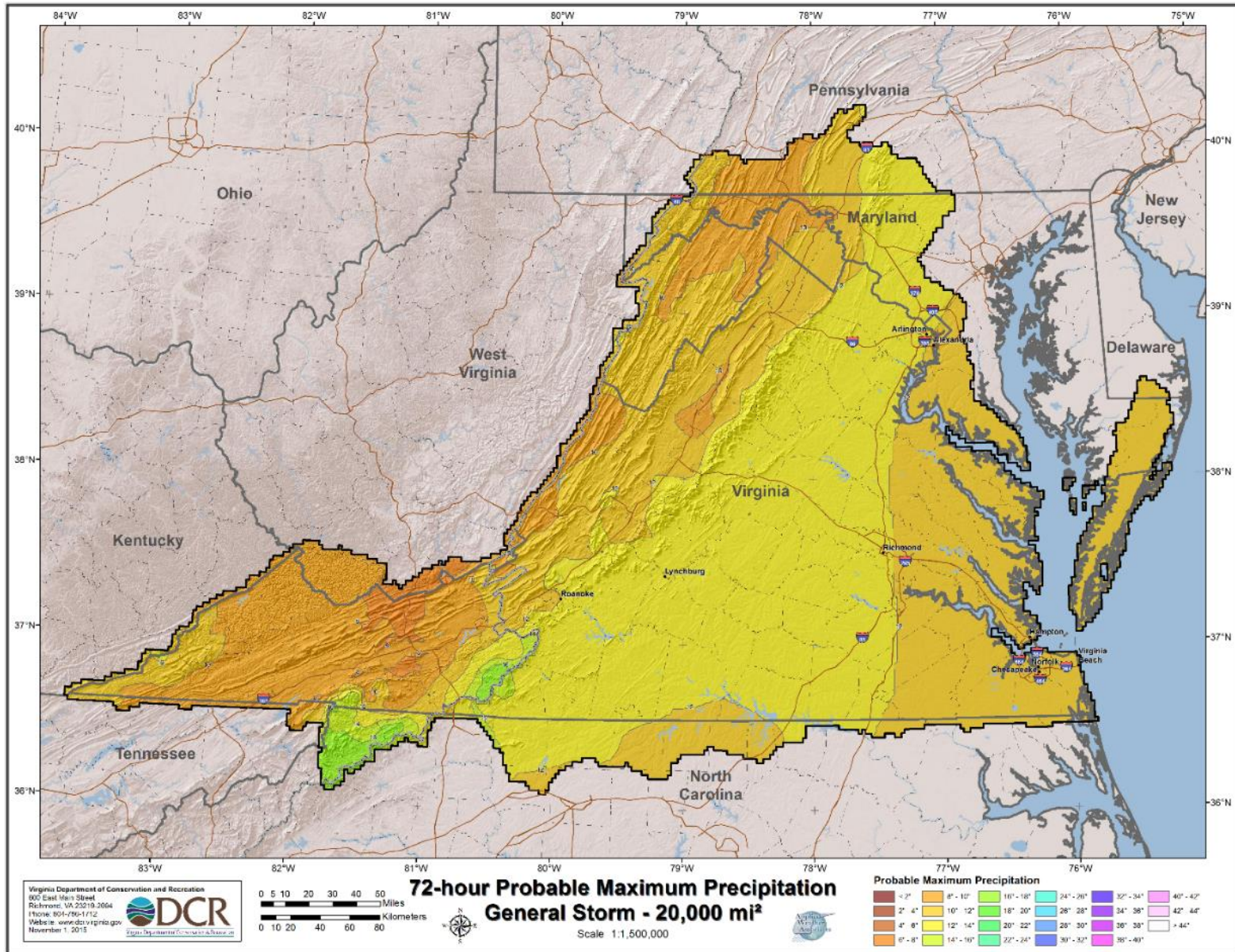




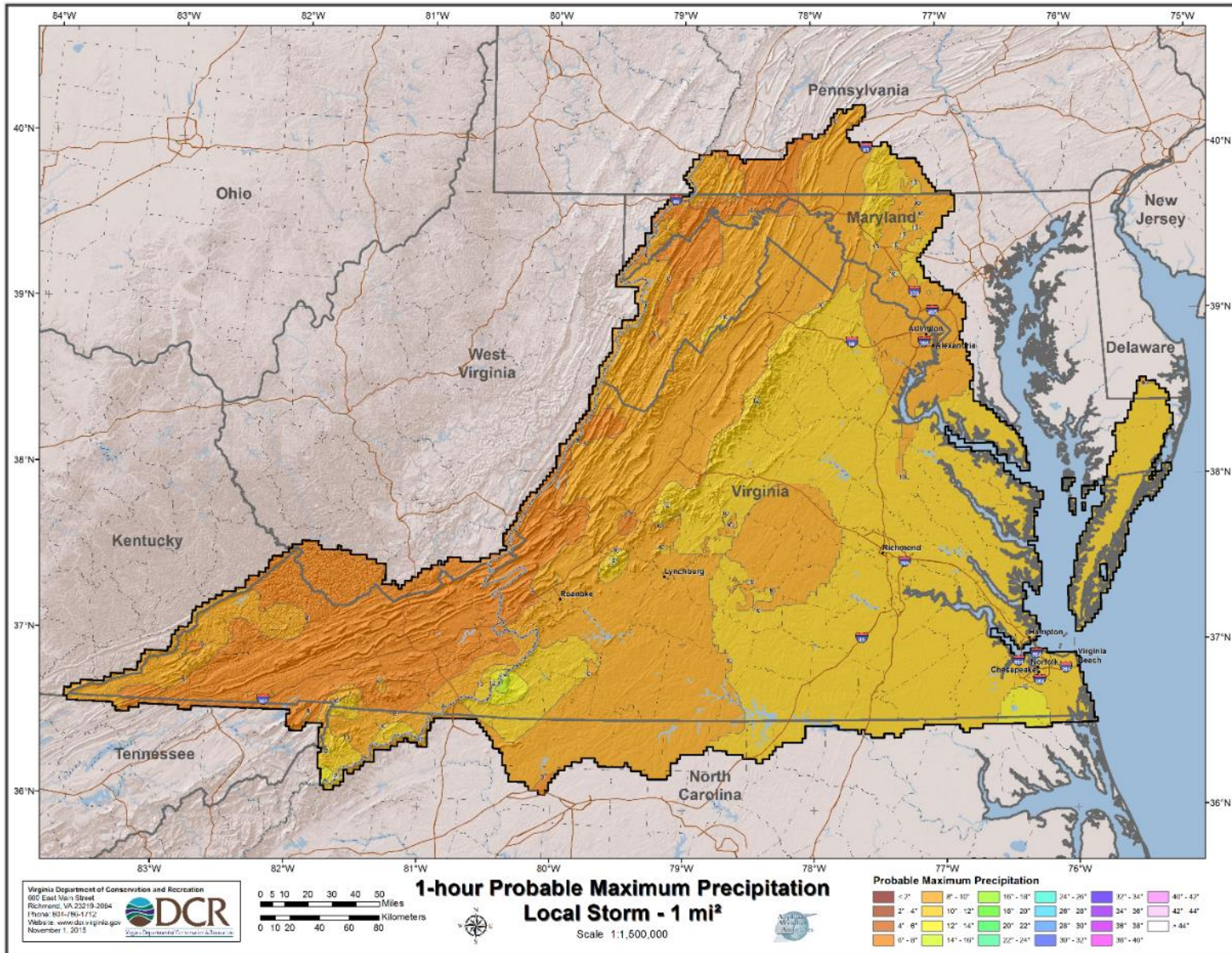


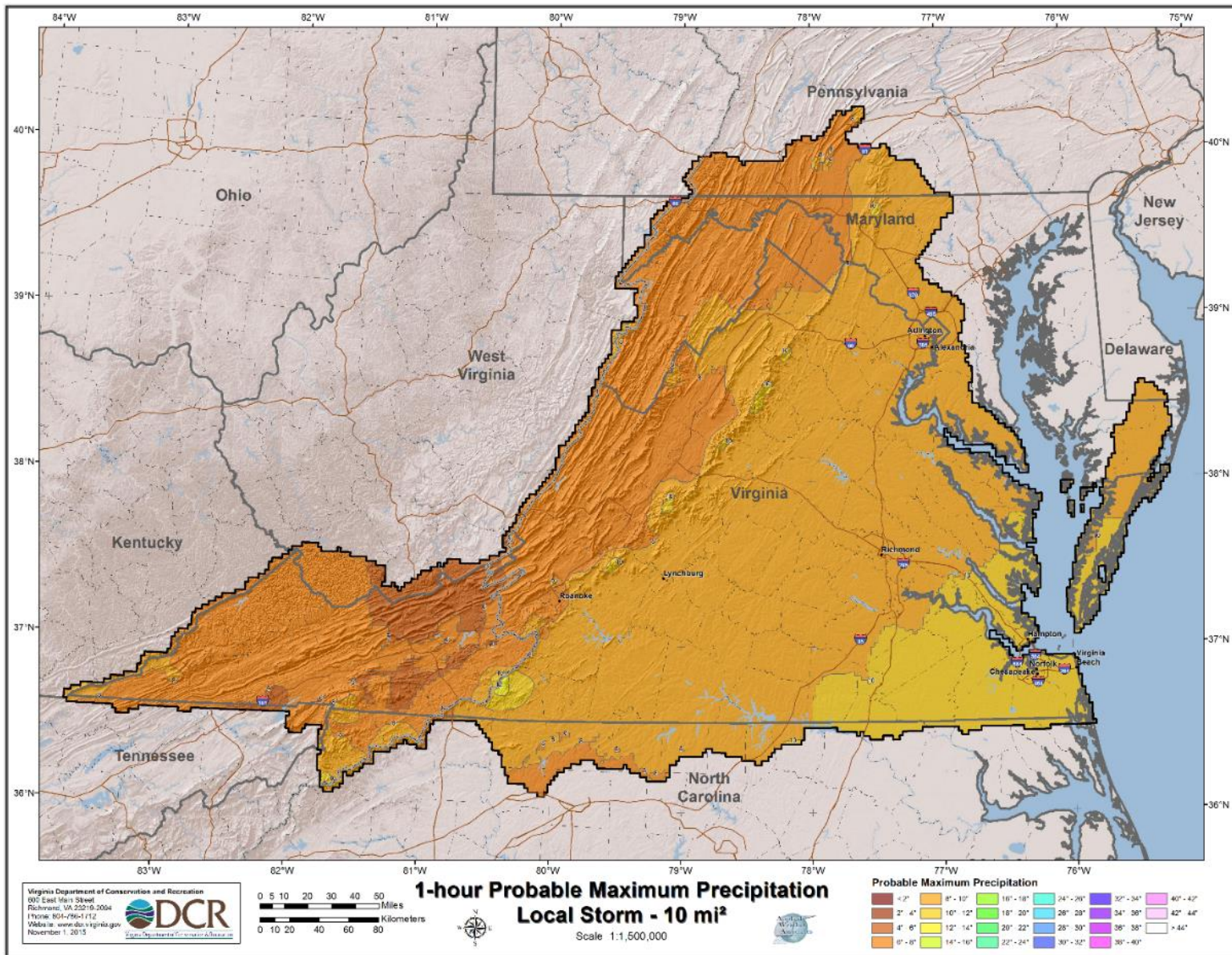


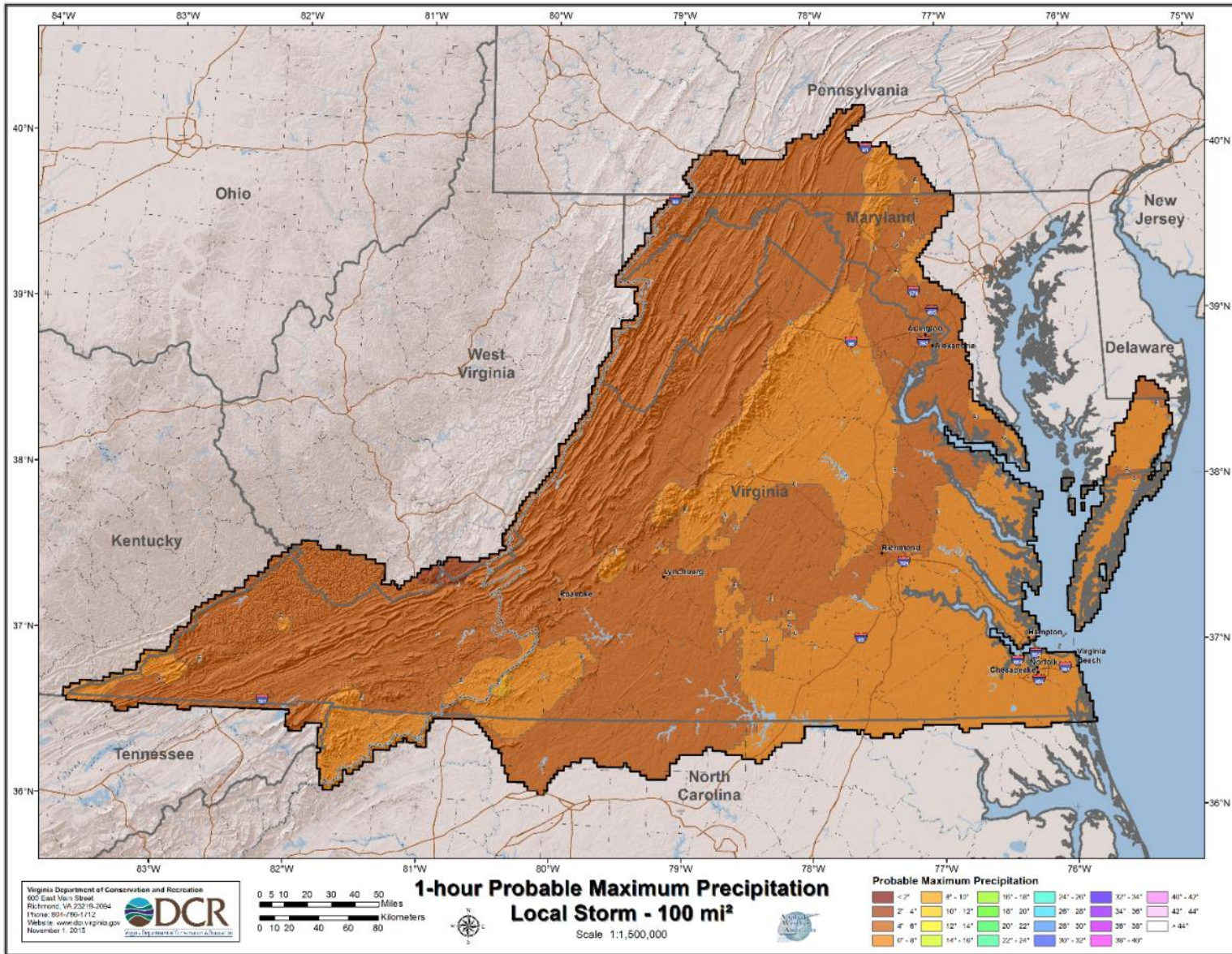


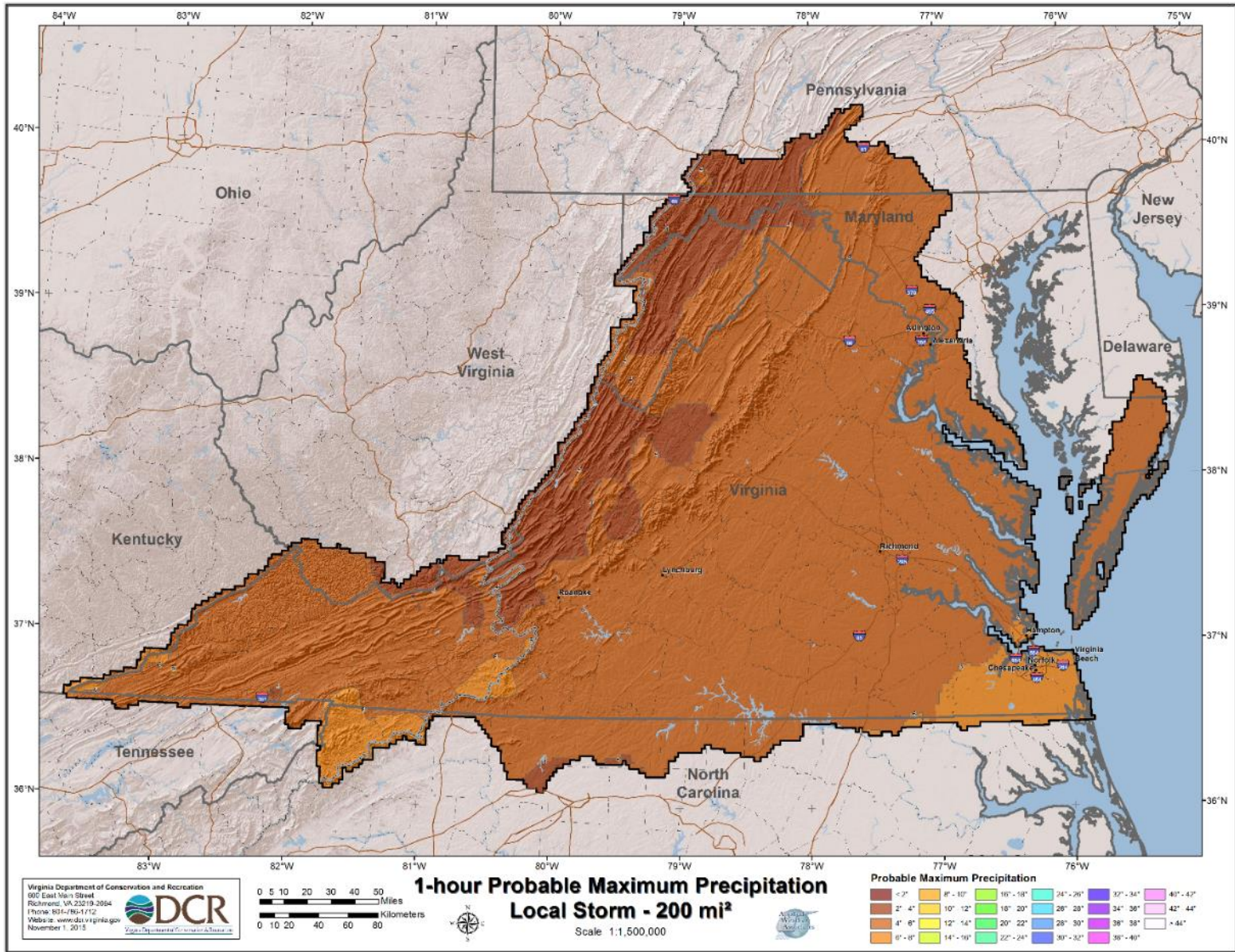


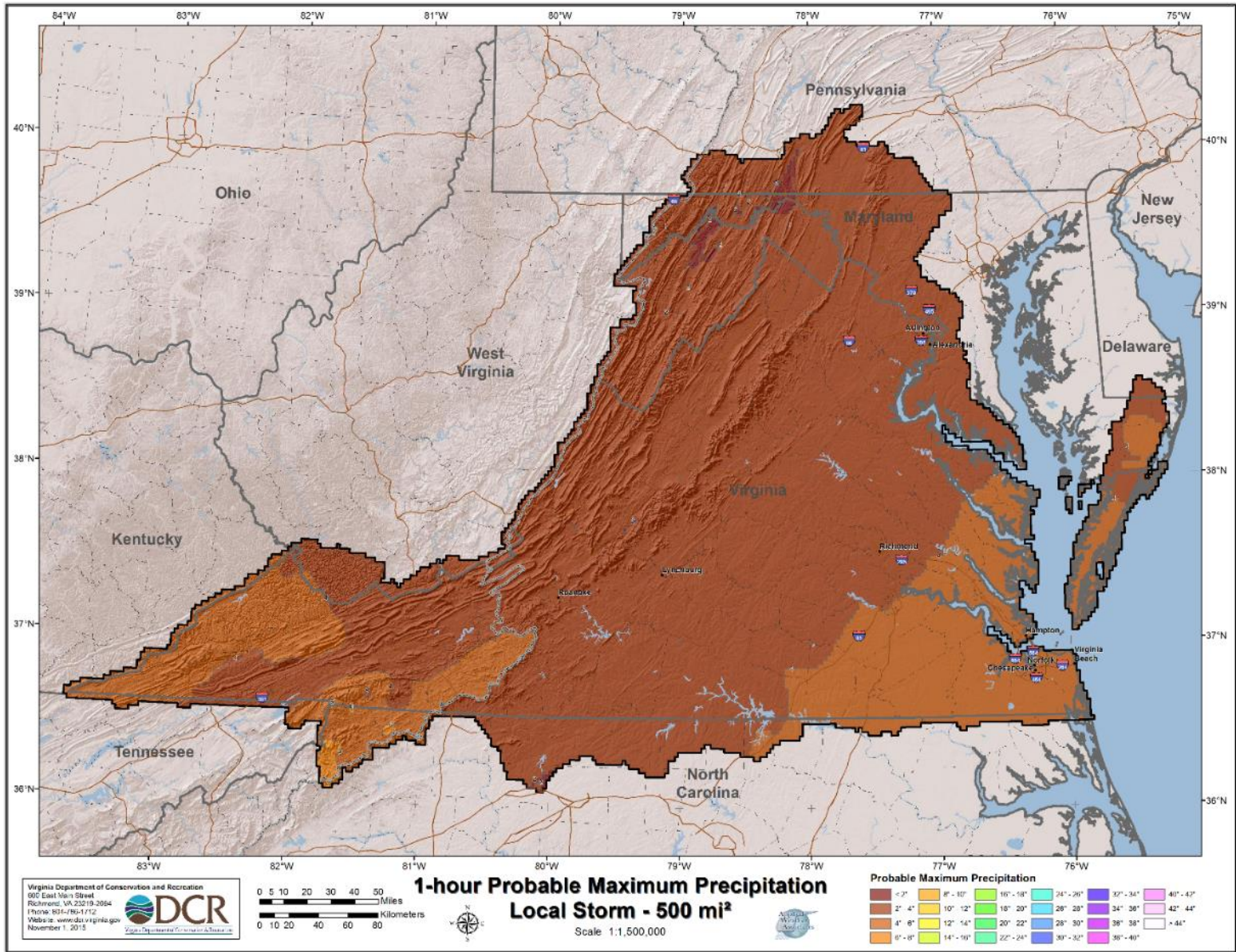
Local Storms

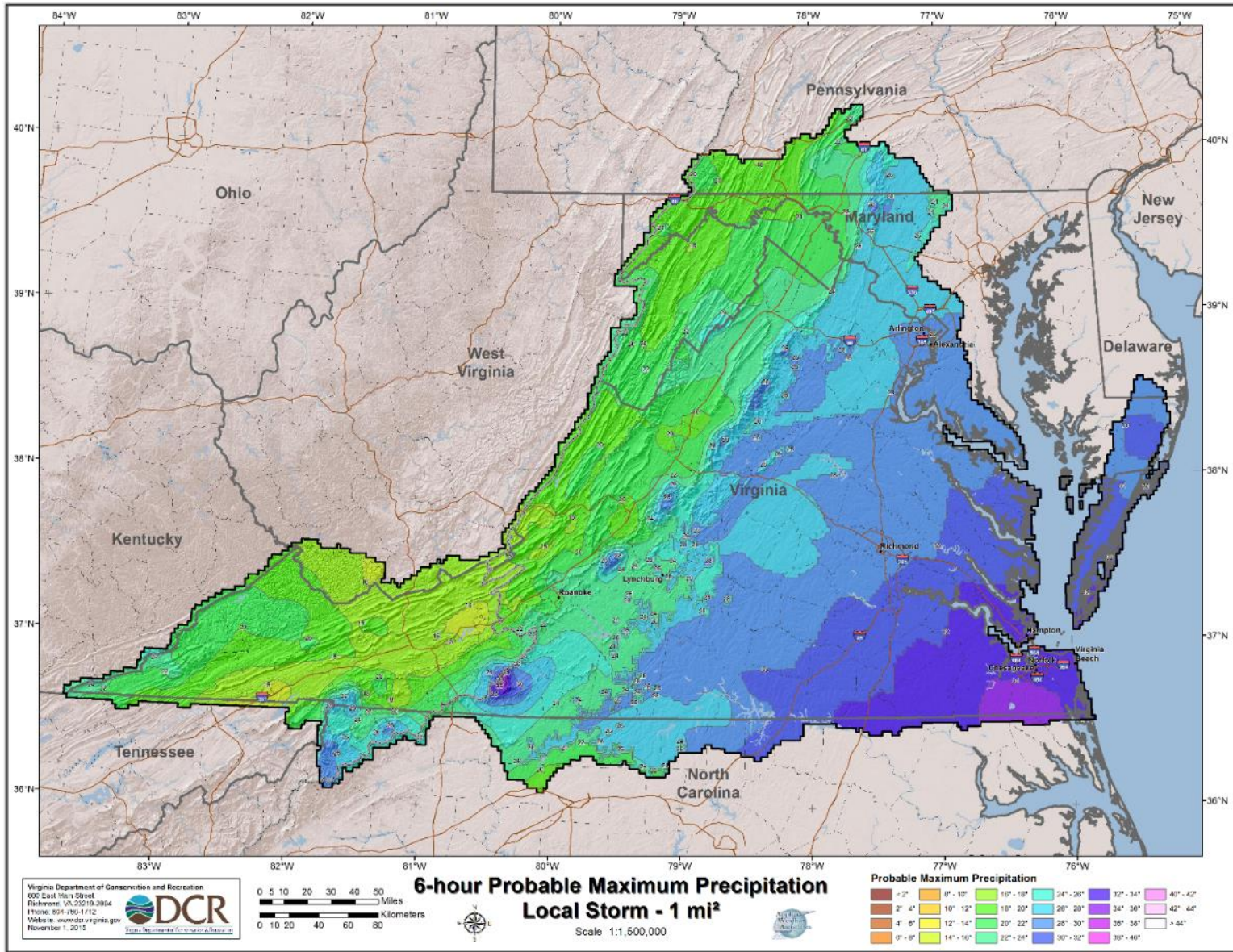


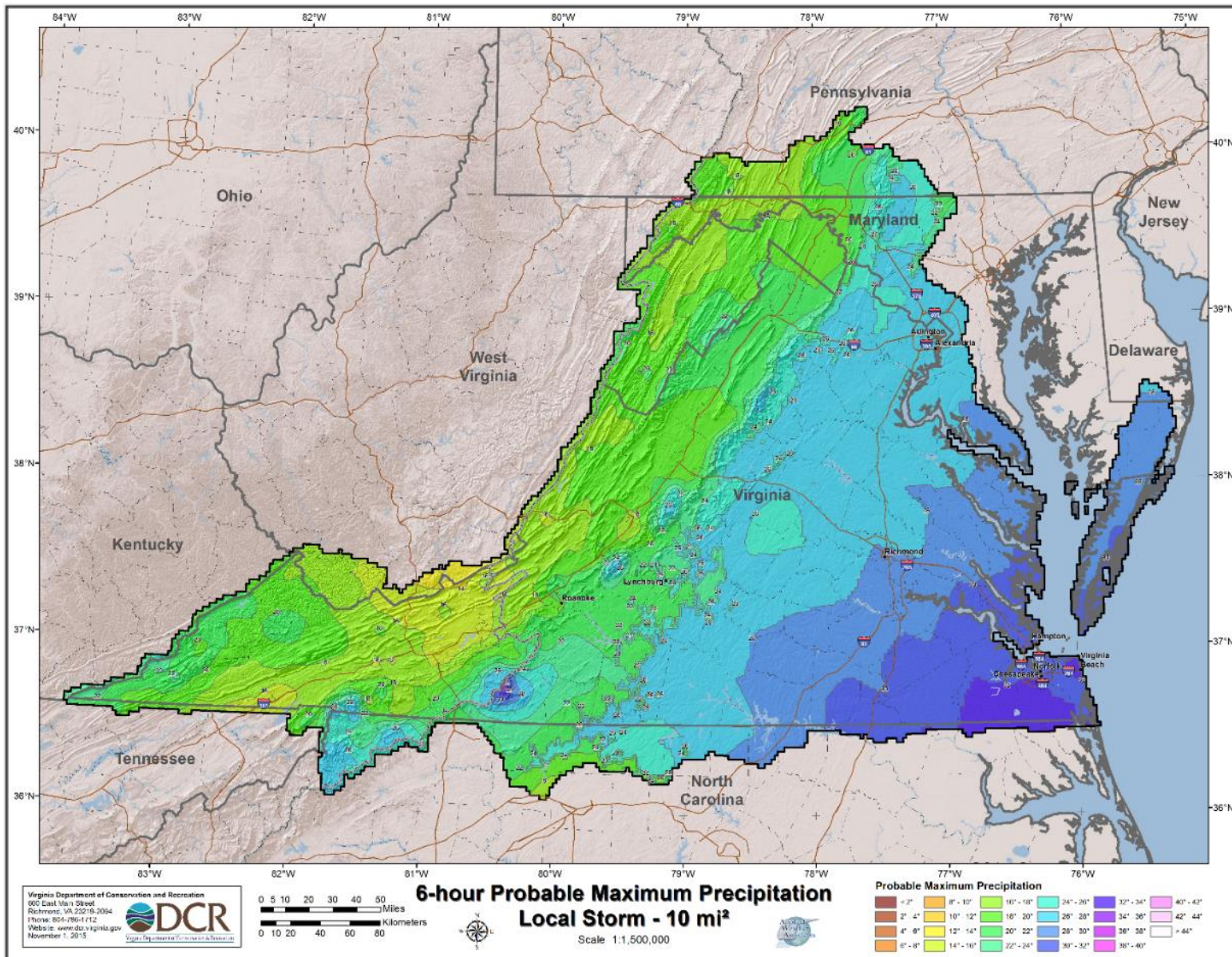


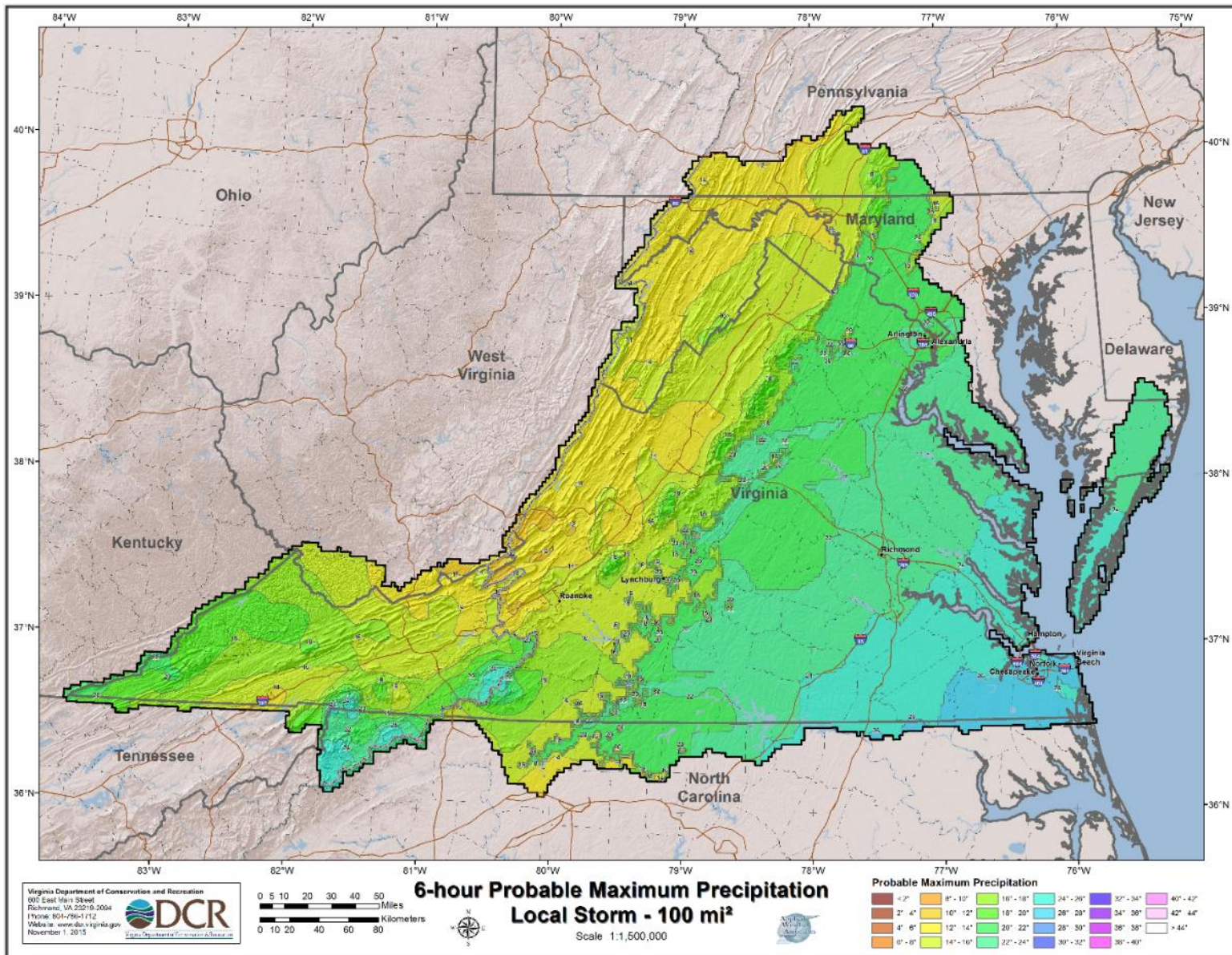


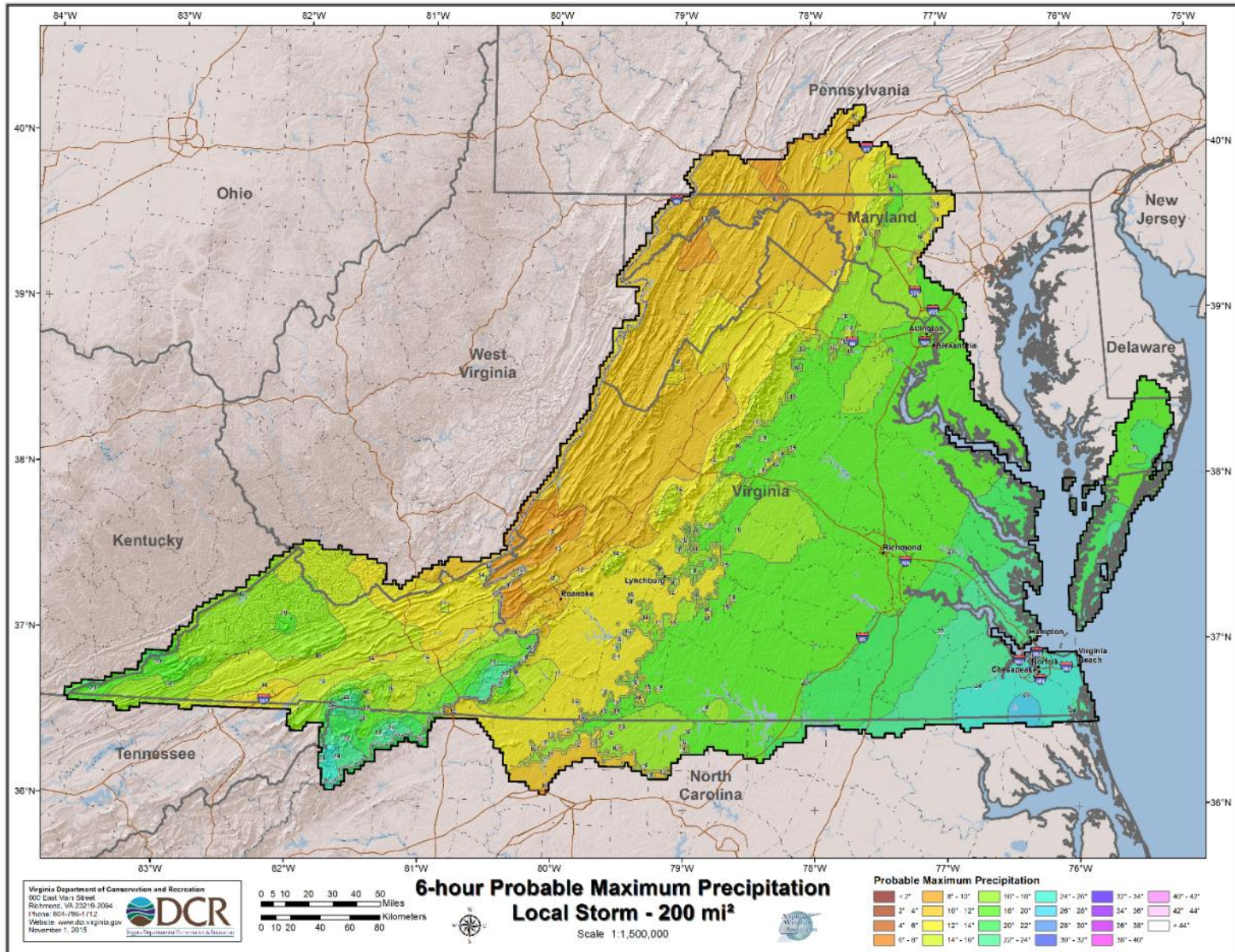


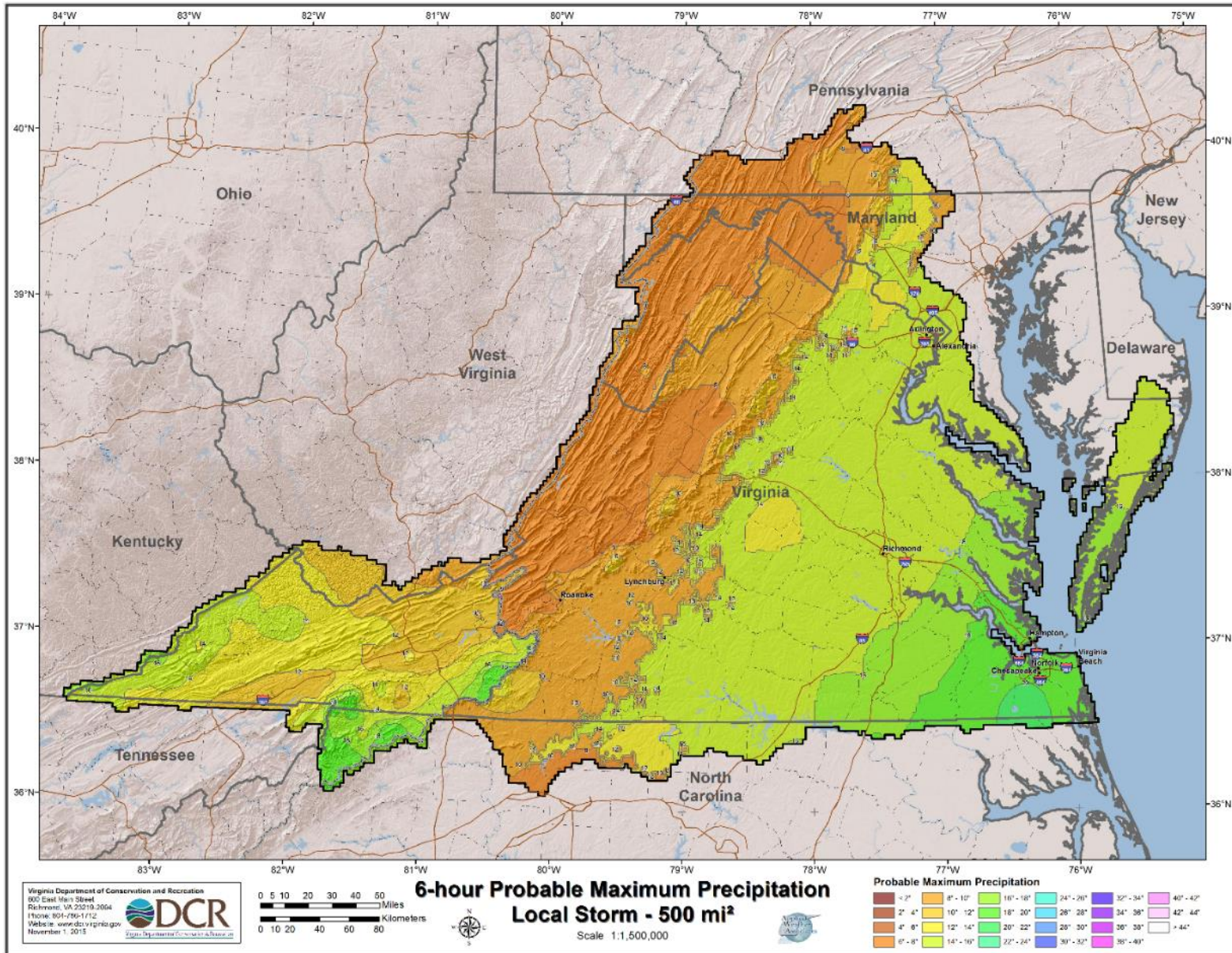


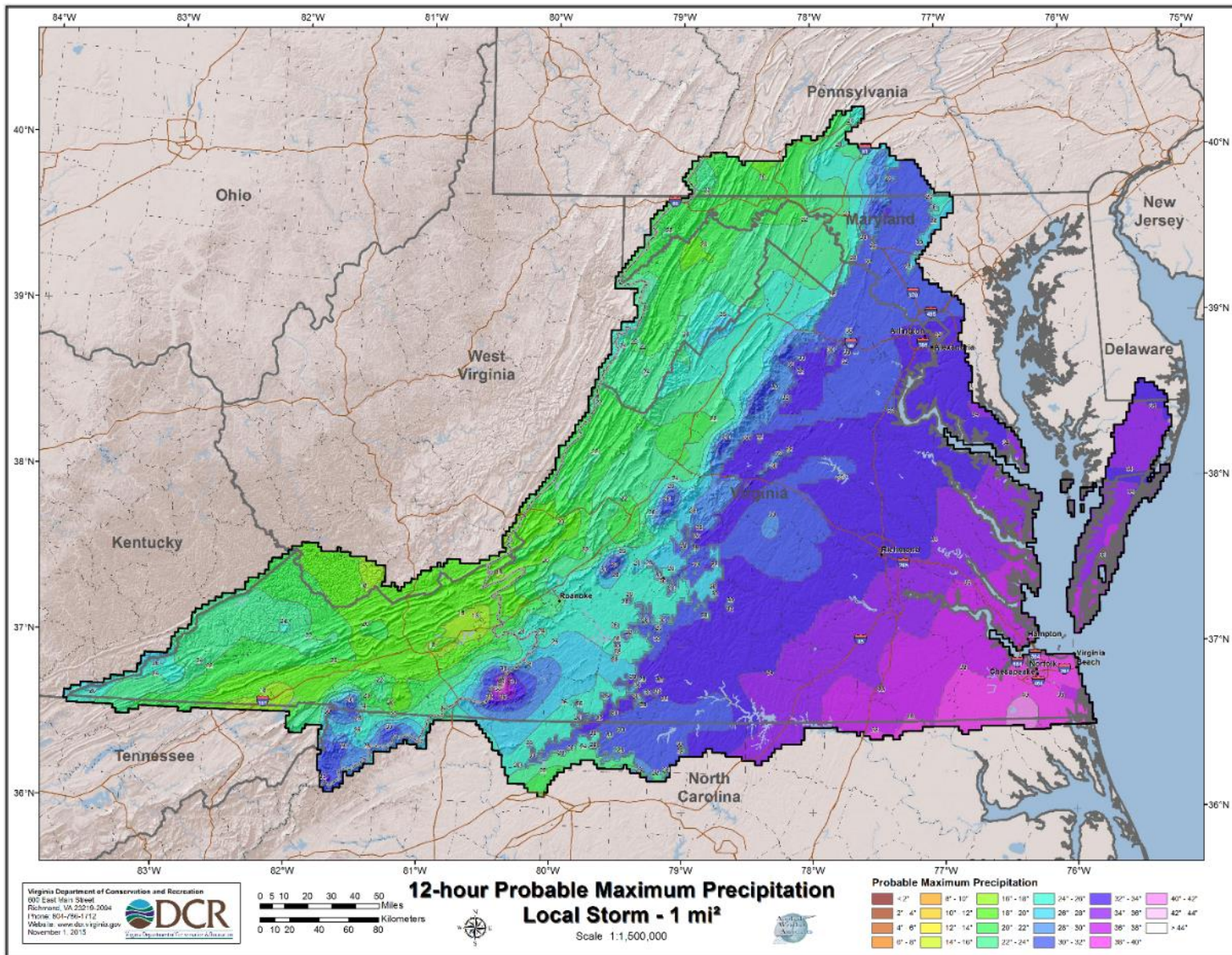


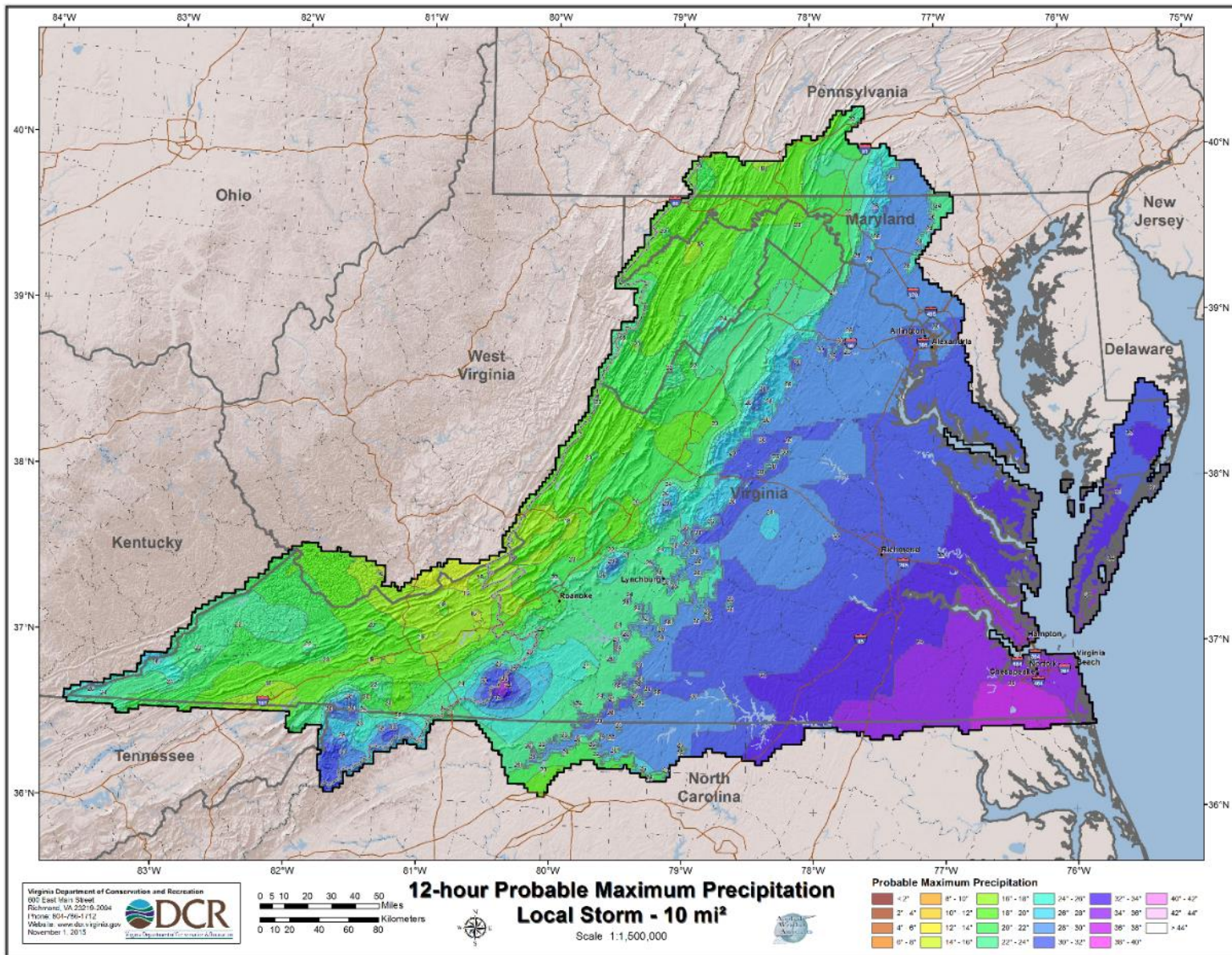


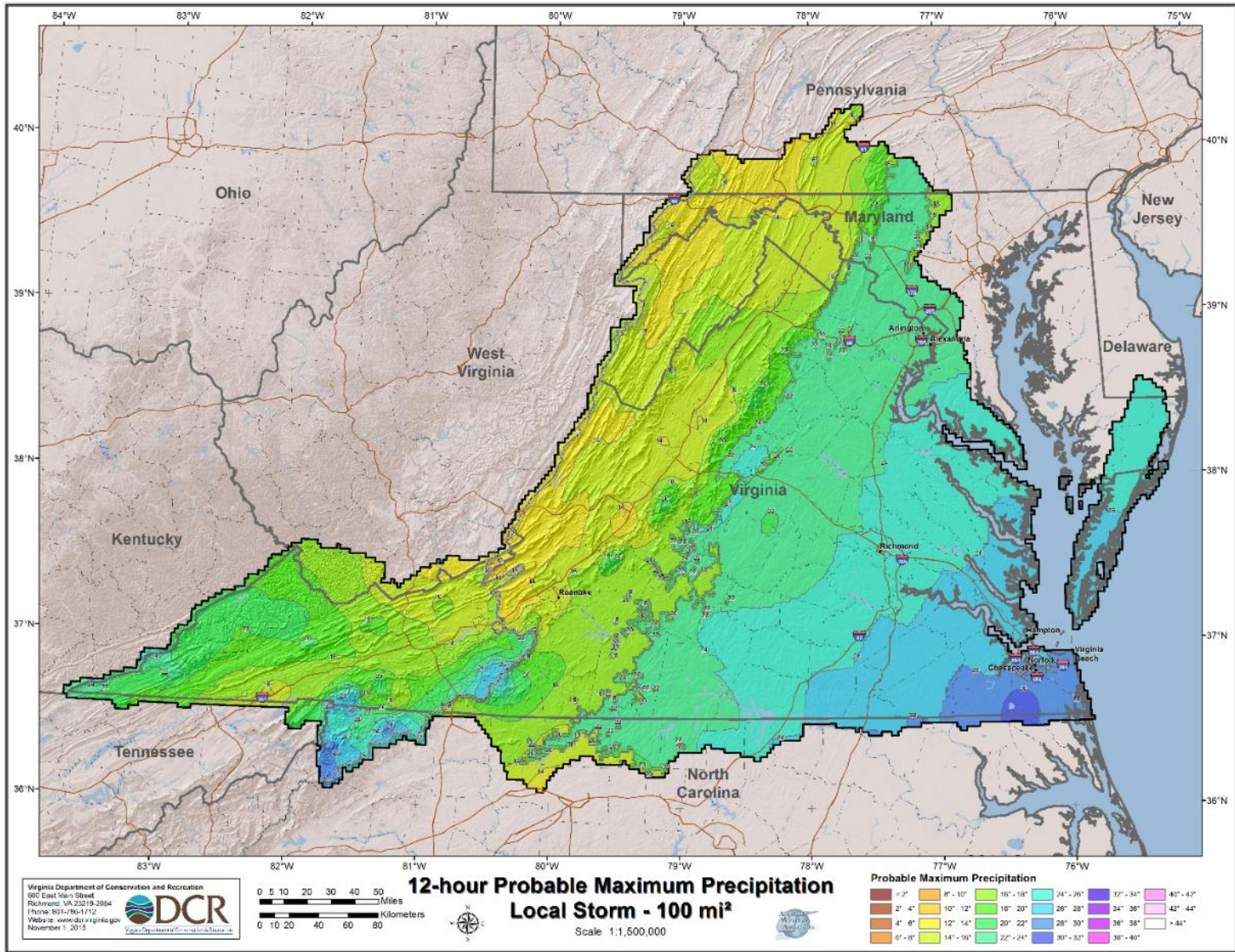


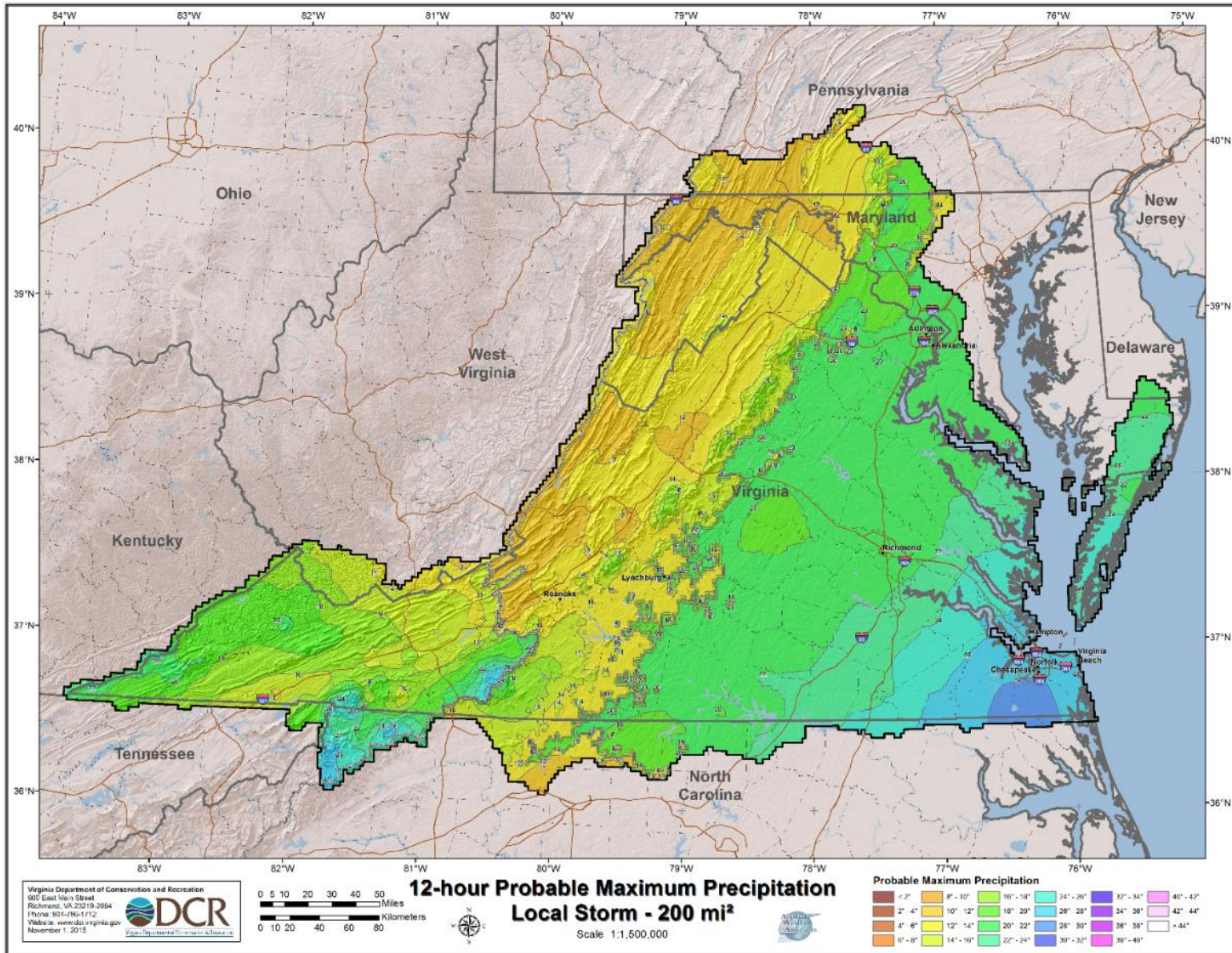


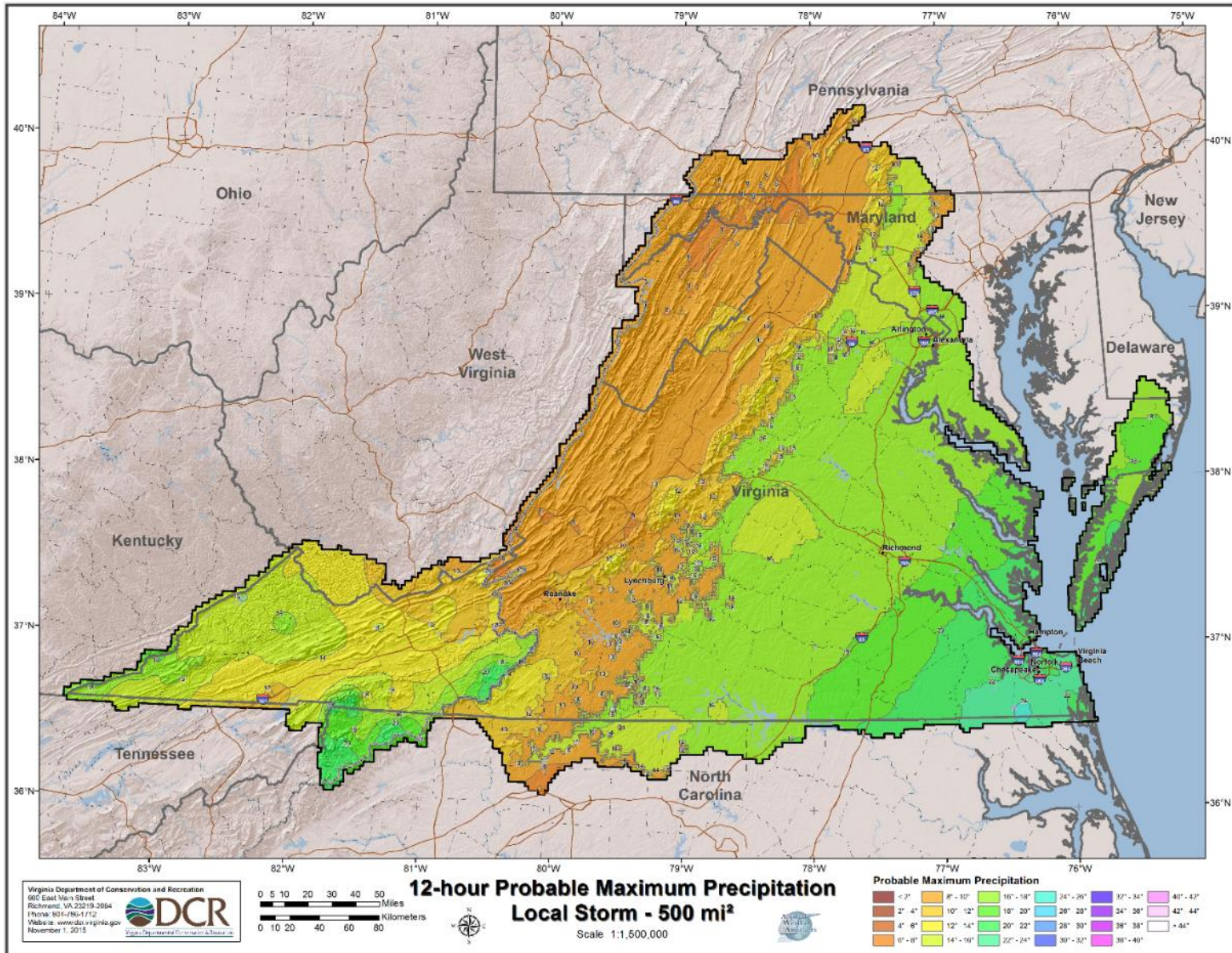


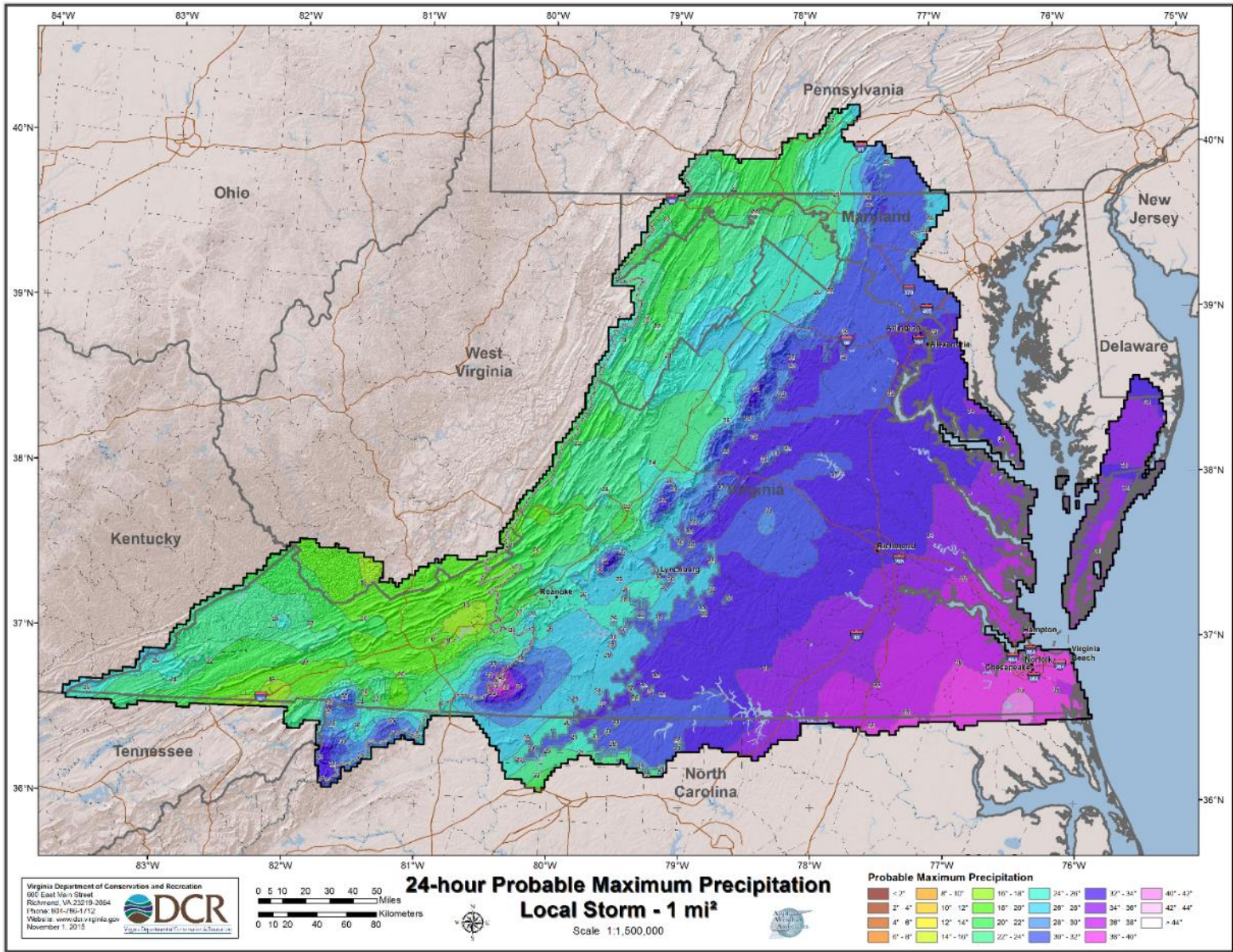


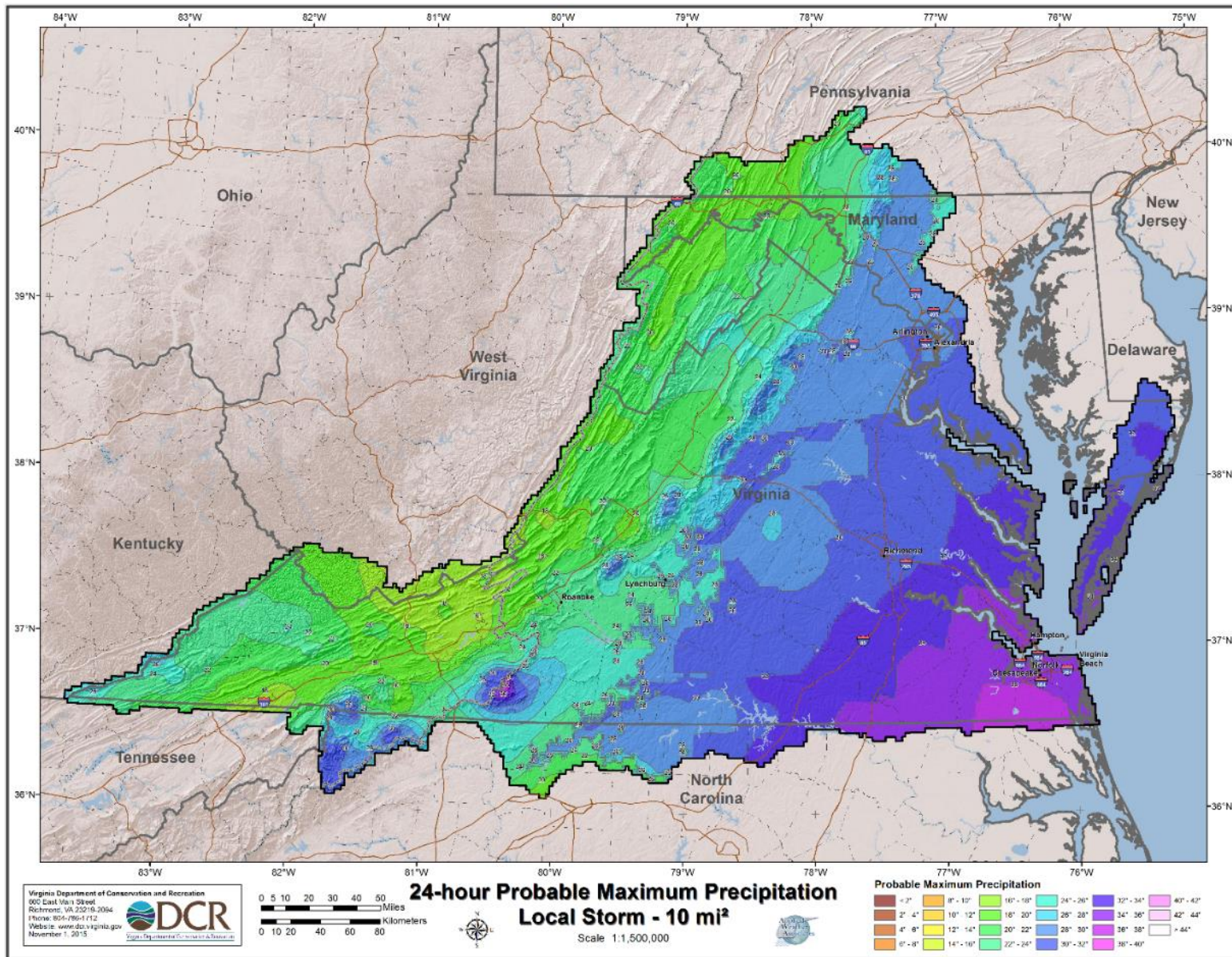


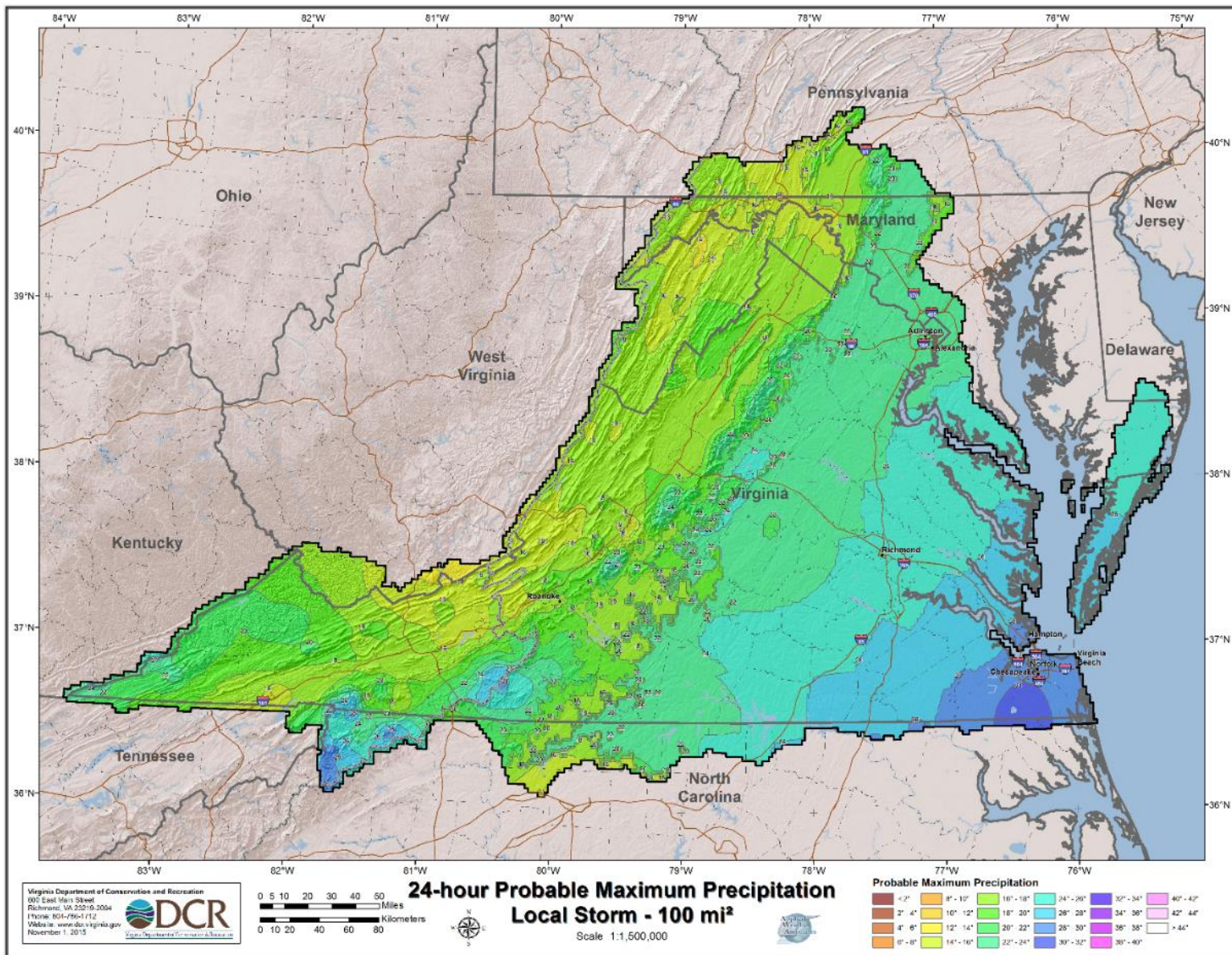


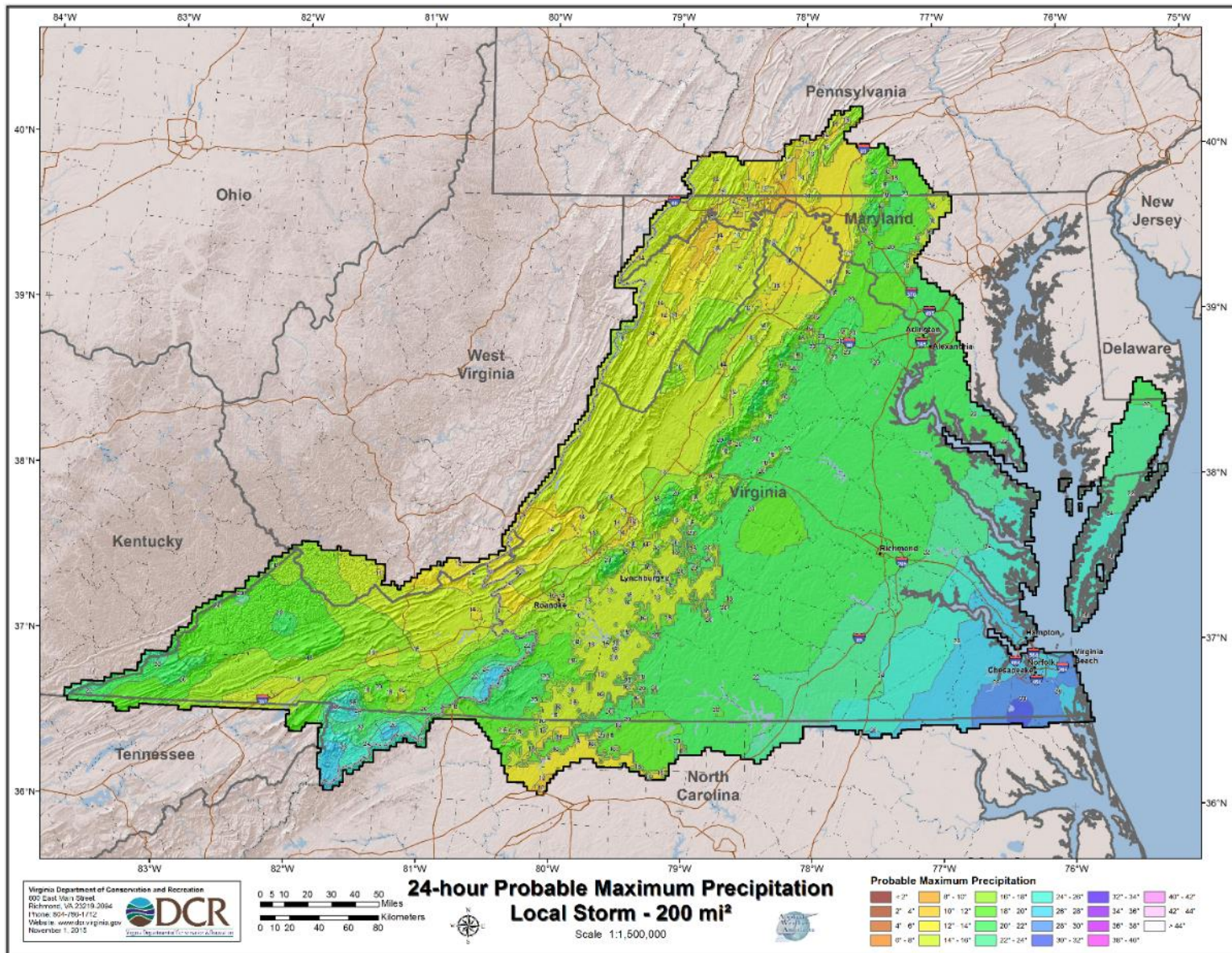


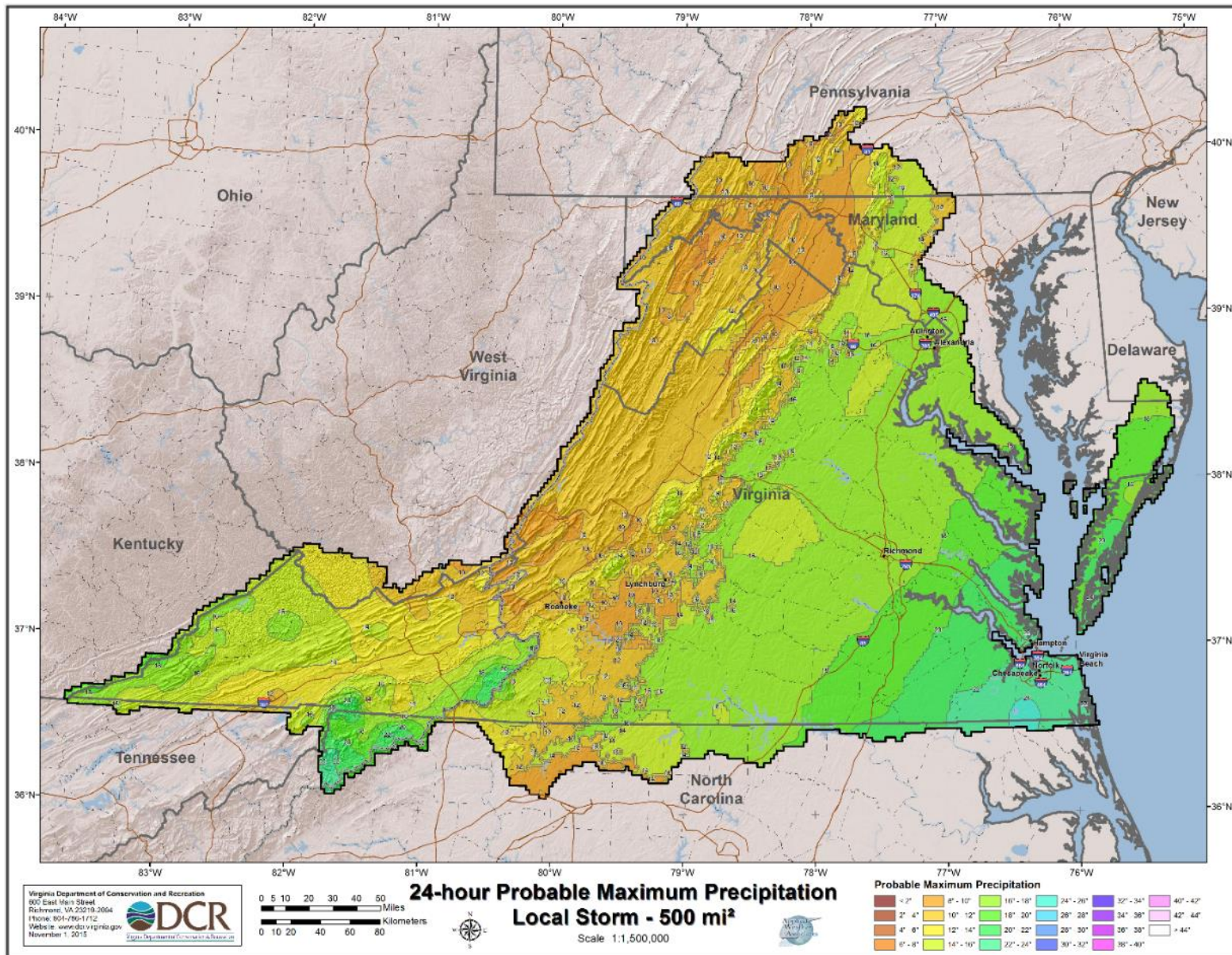




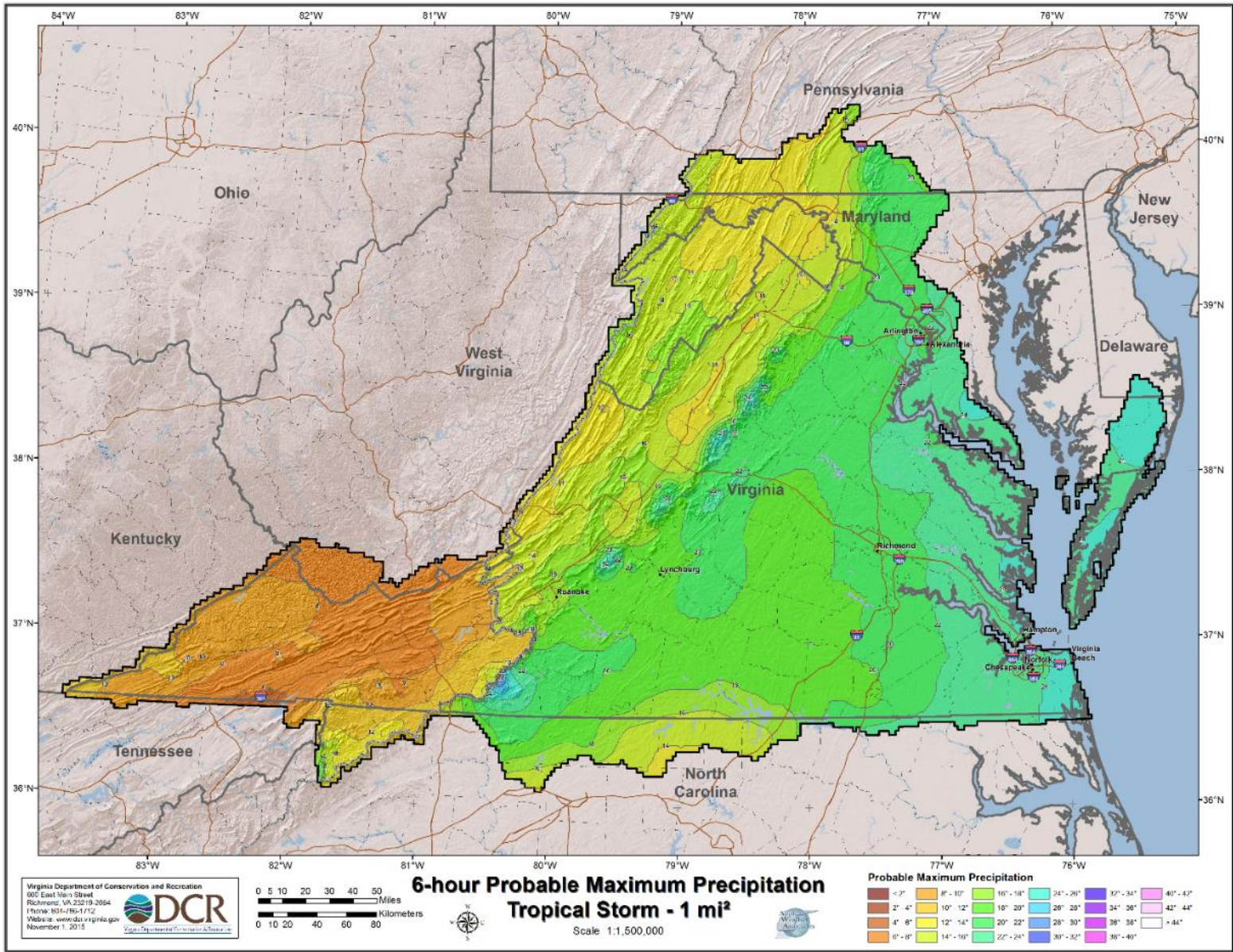


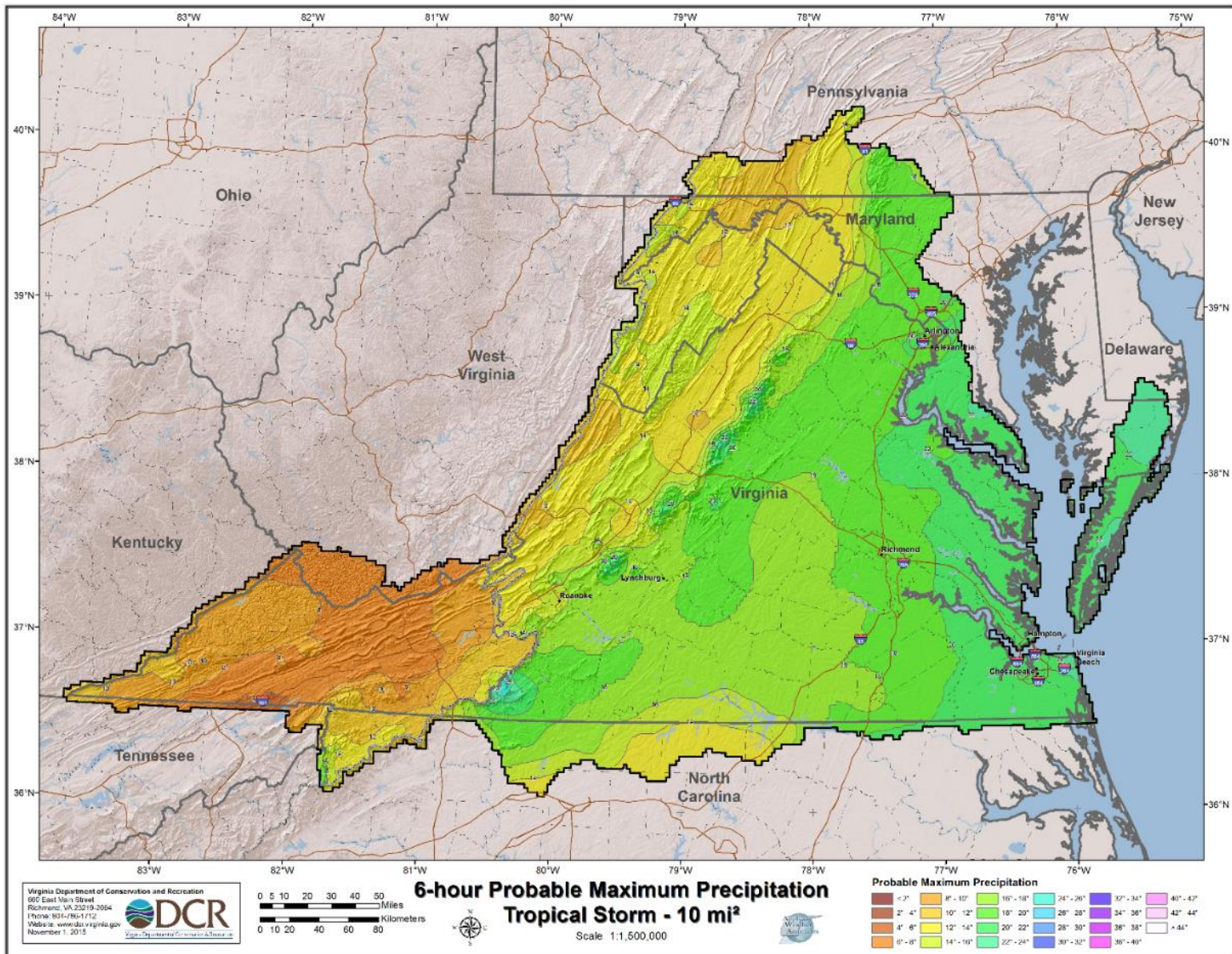


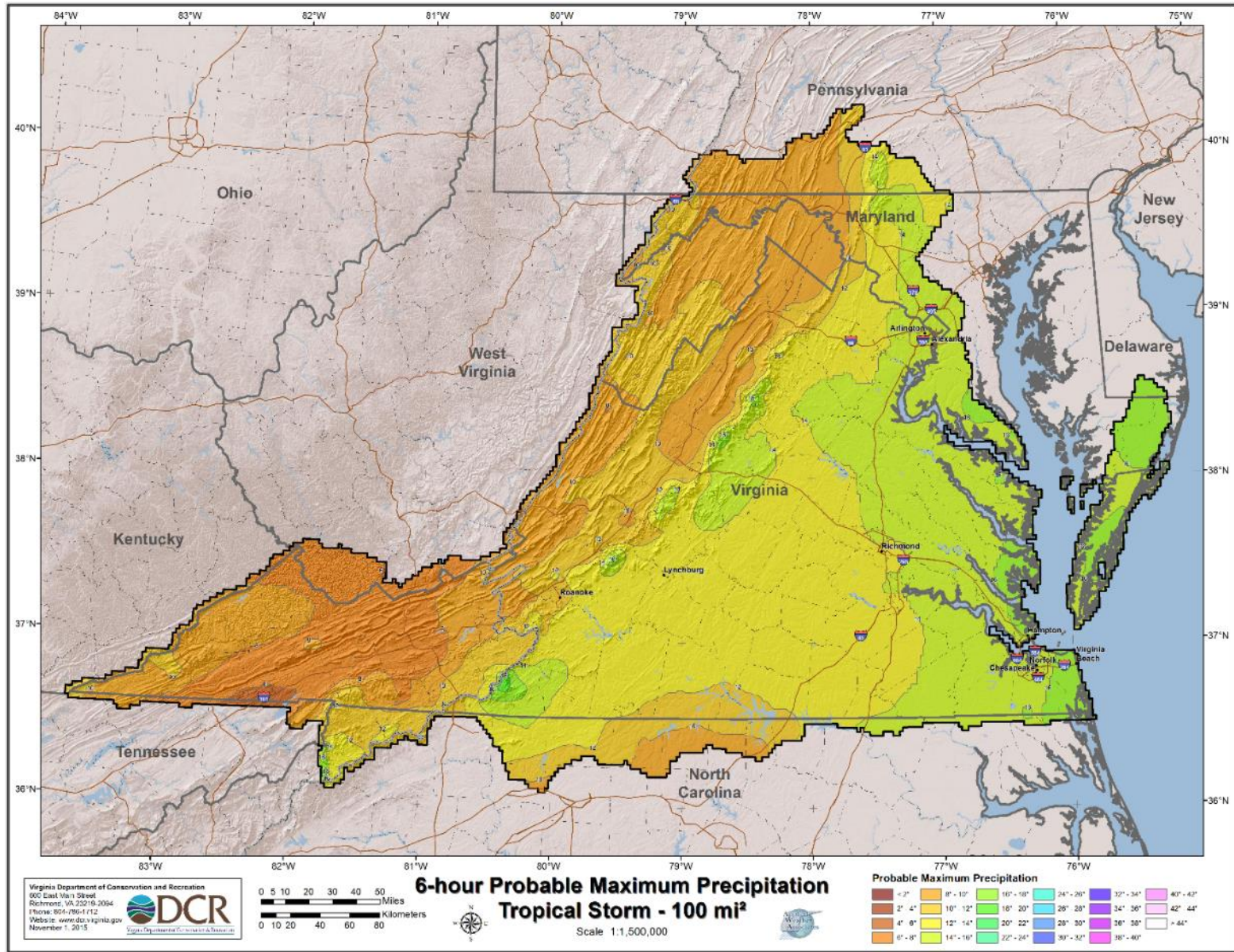


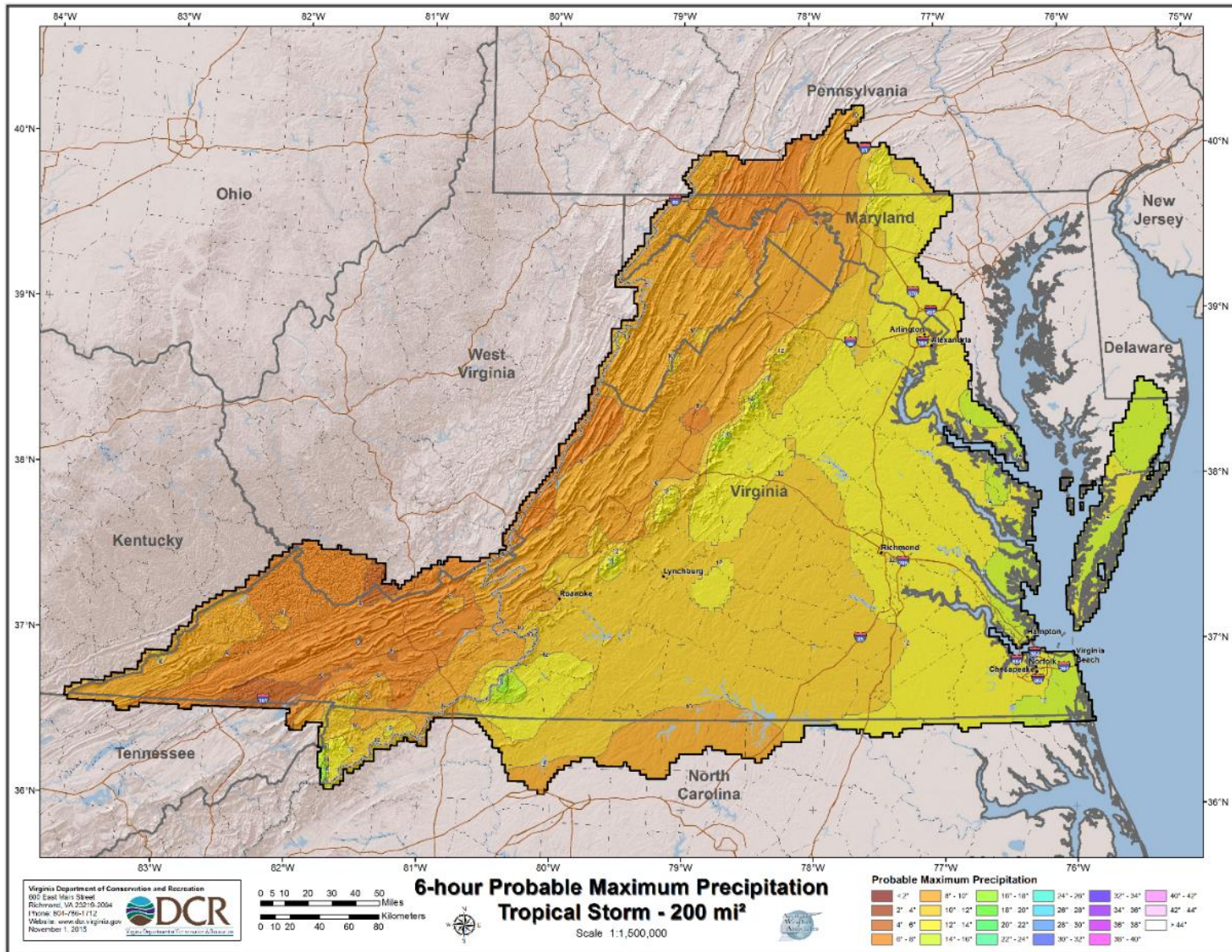


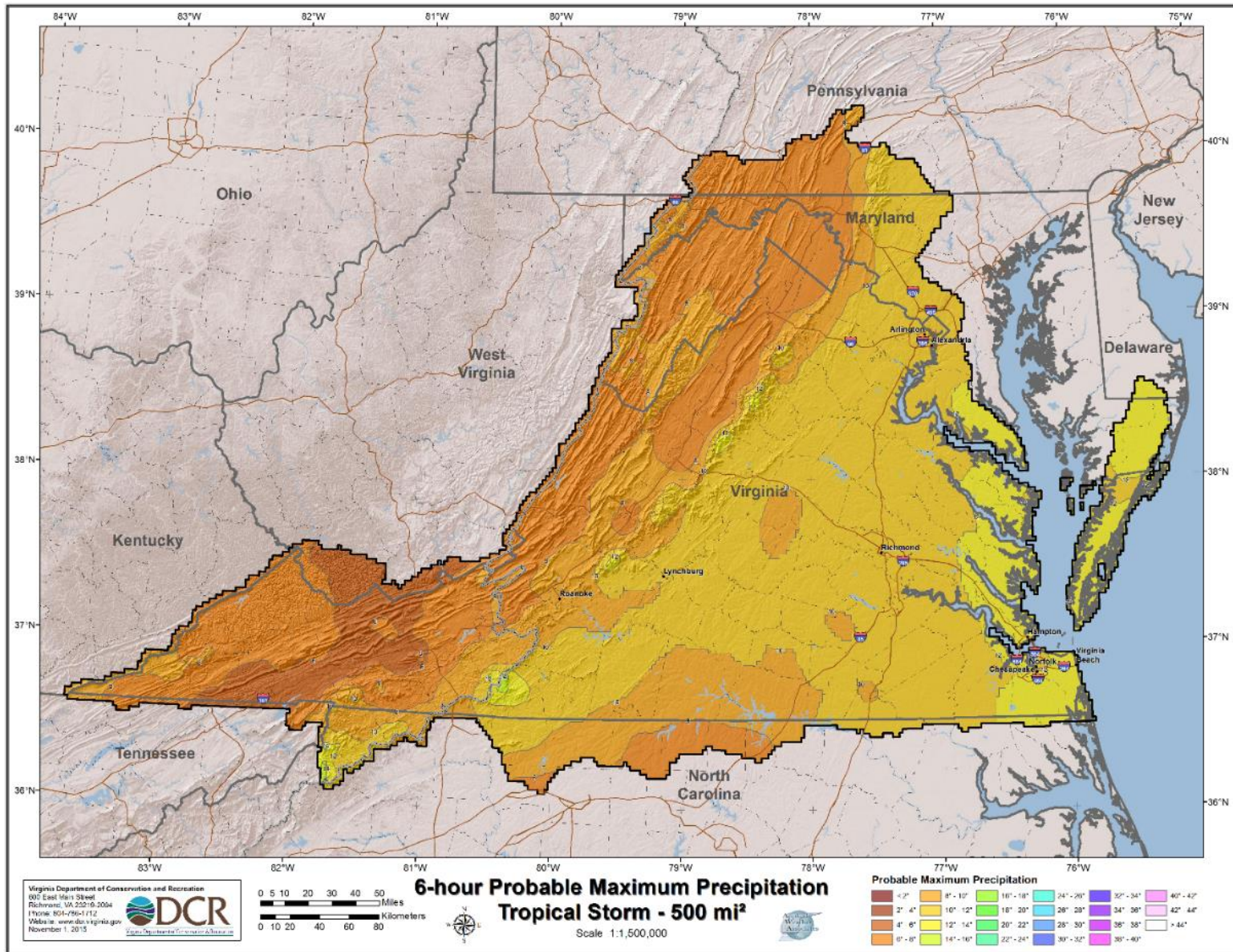
Tropical Storms

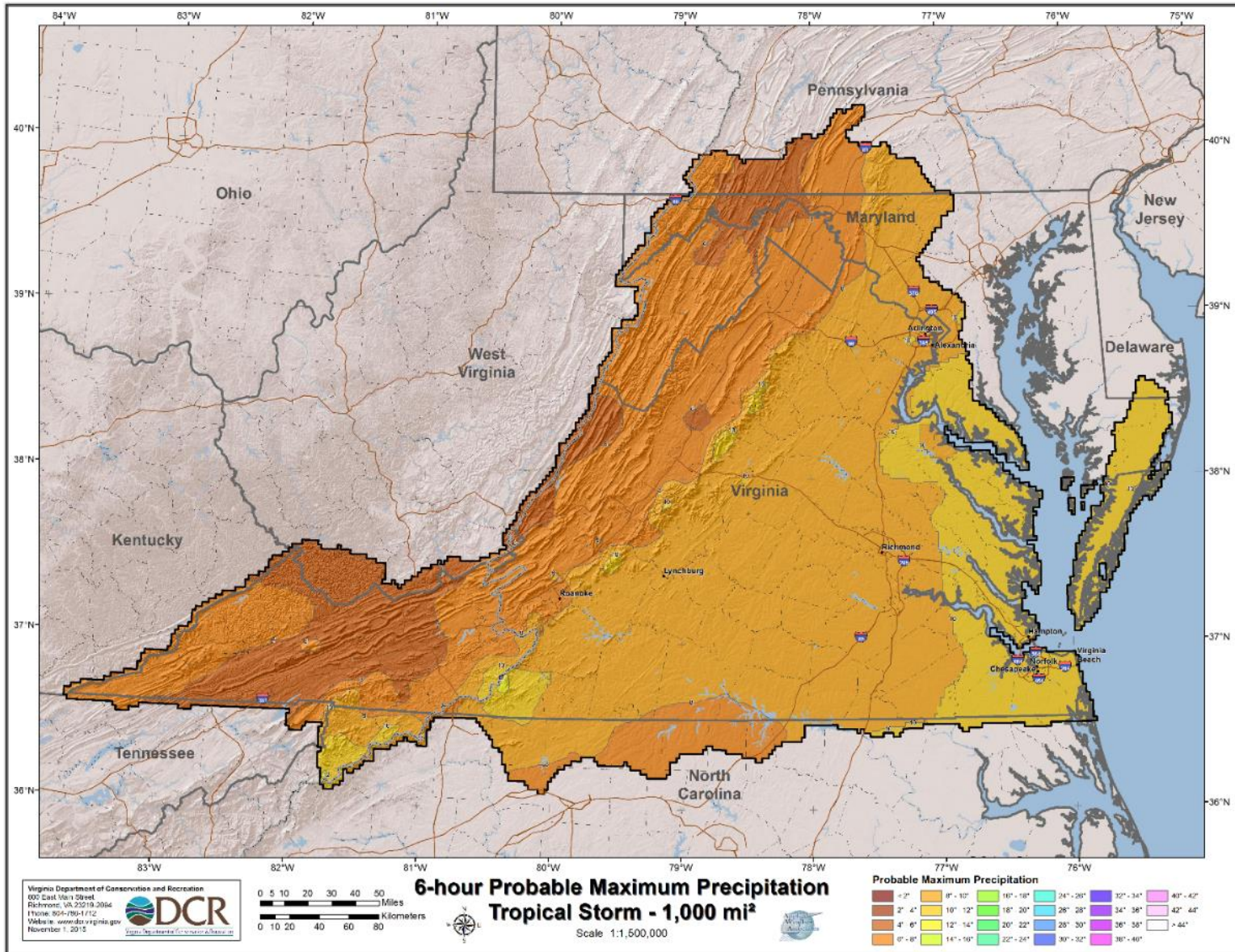


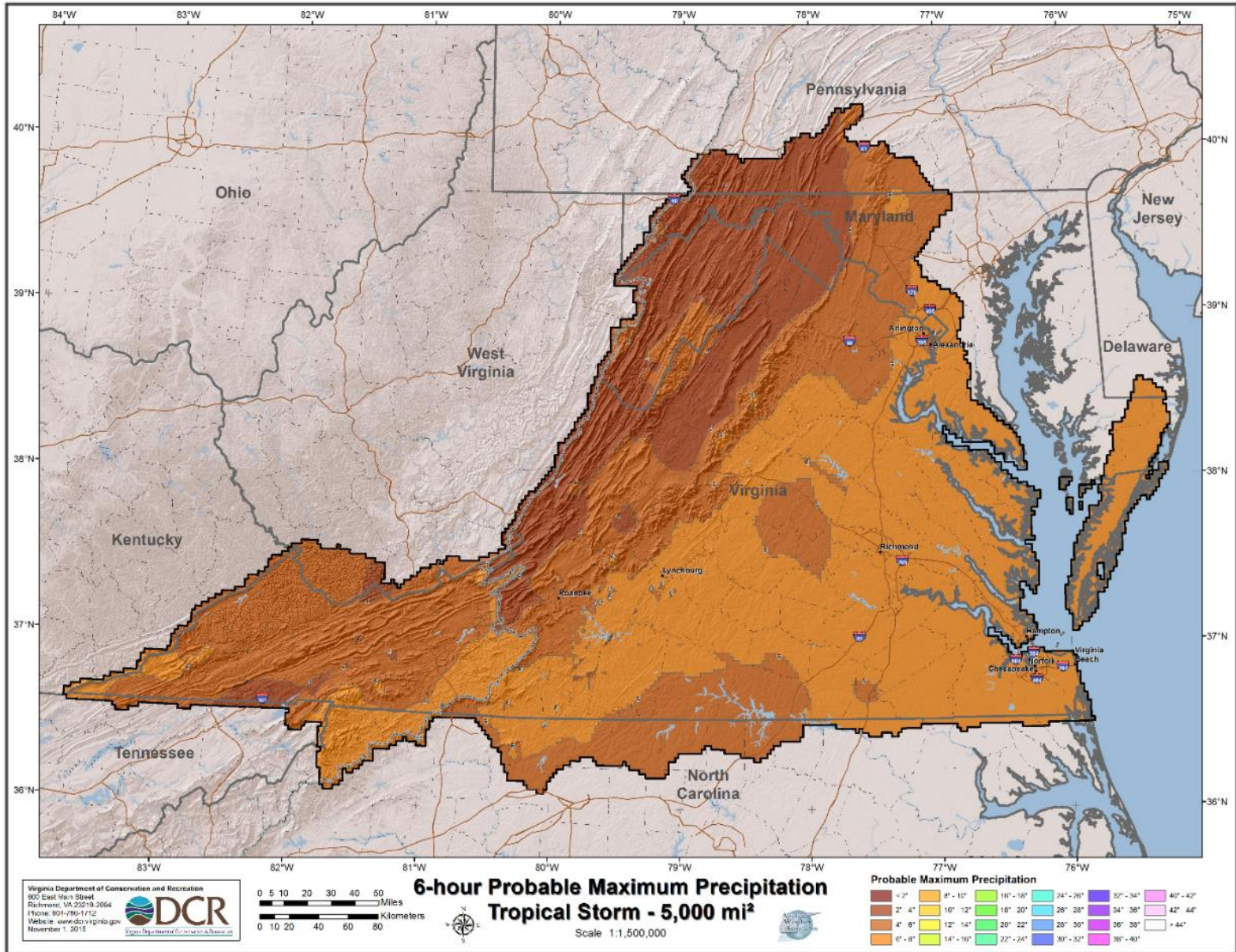


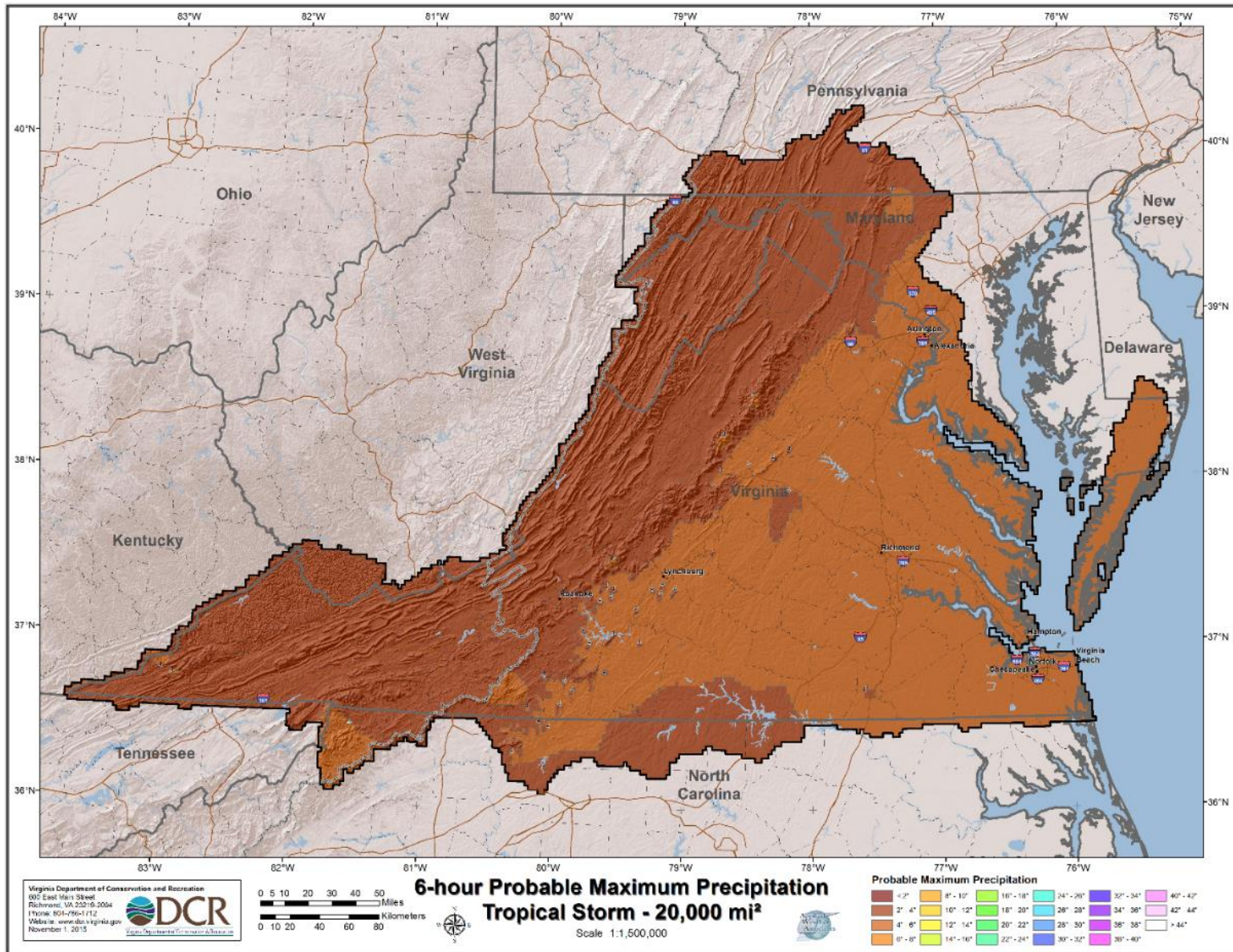


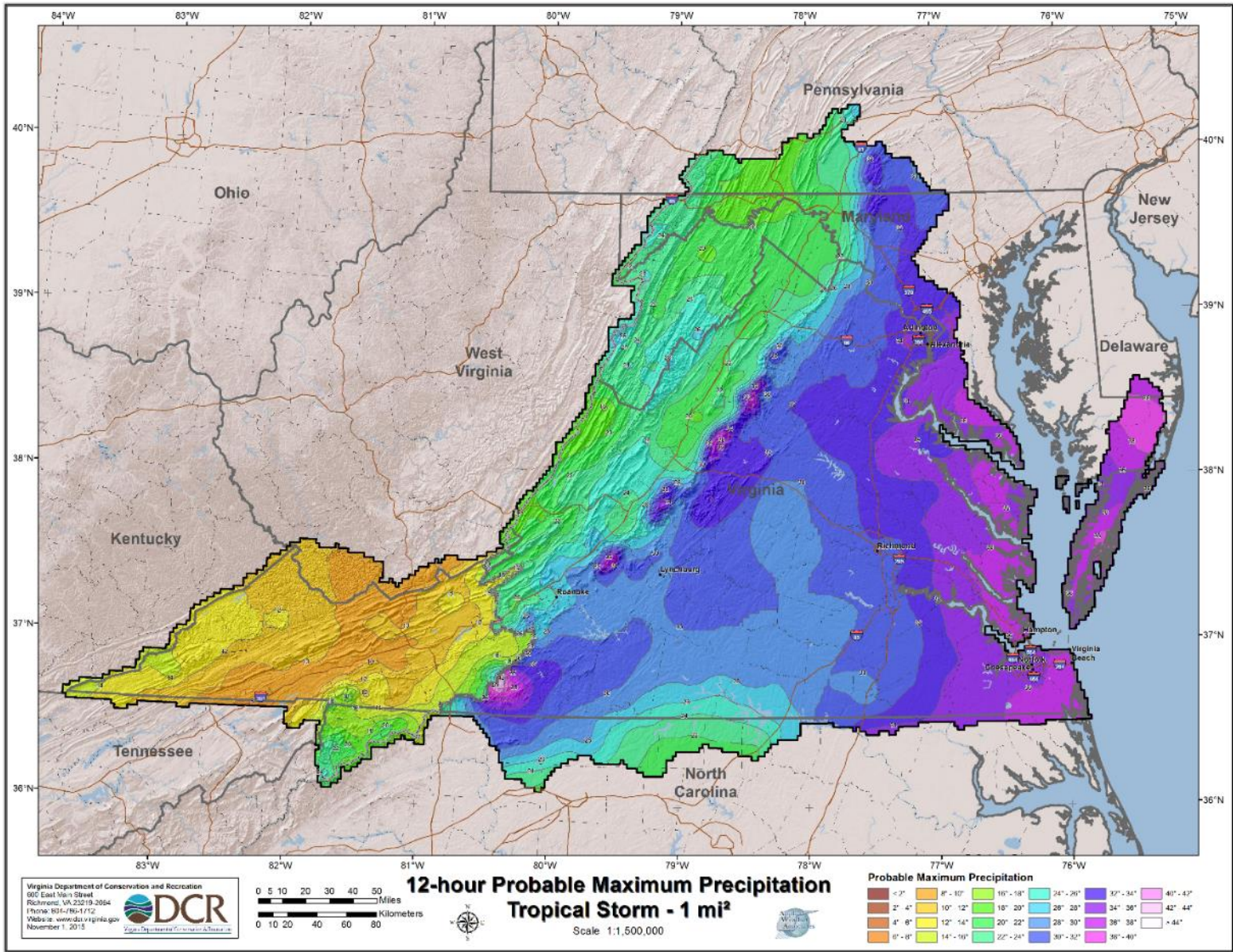


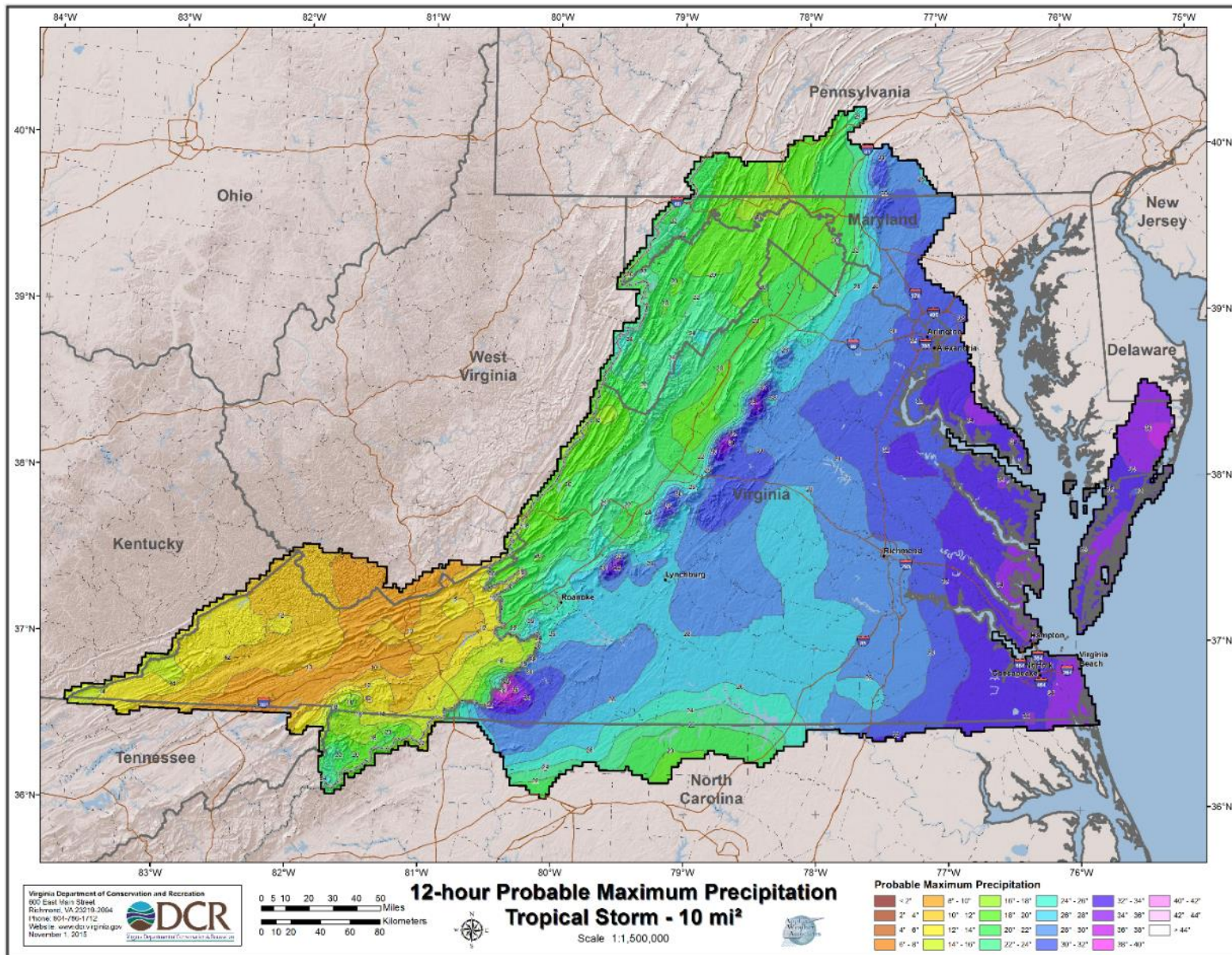


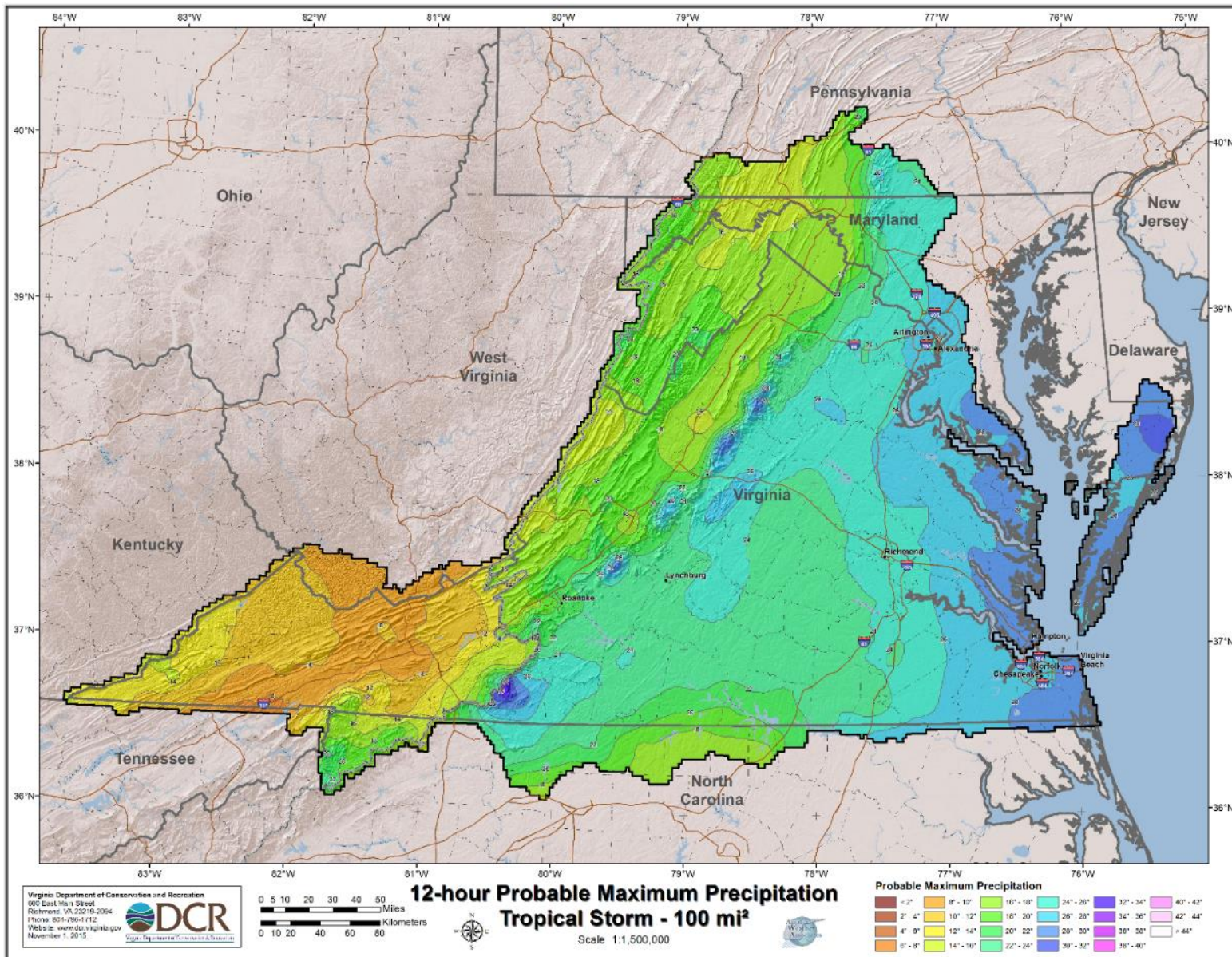


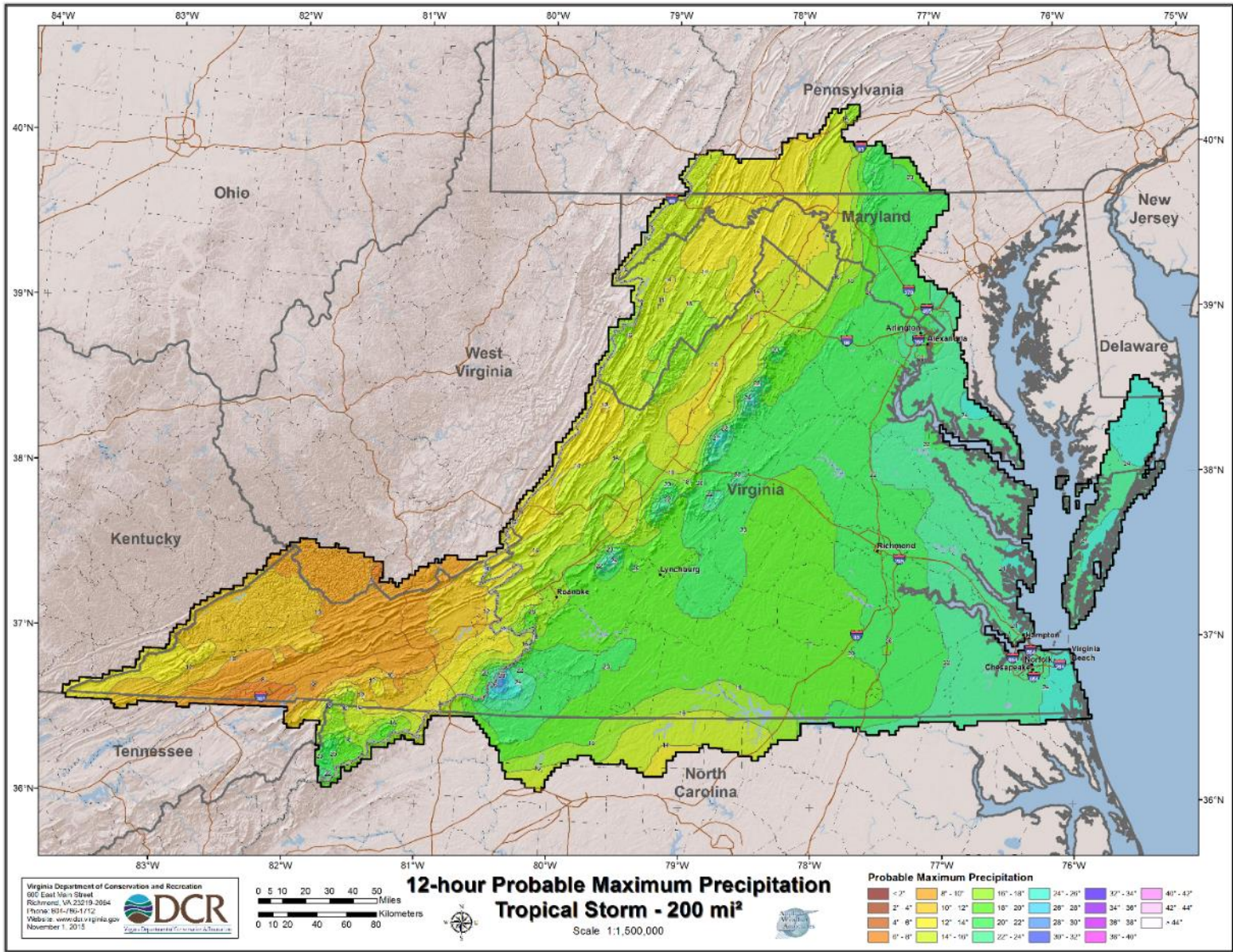


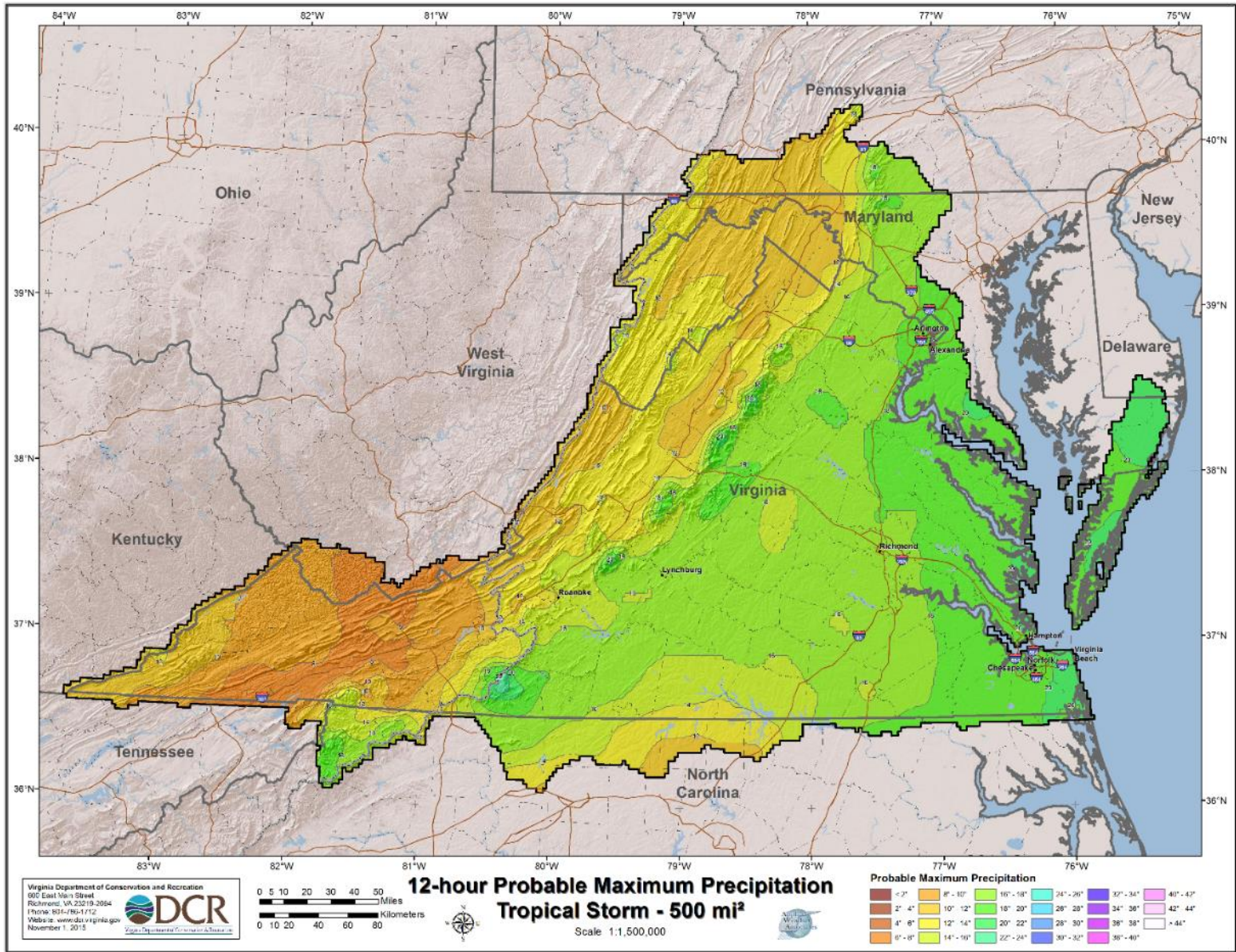


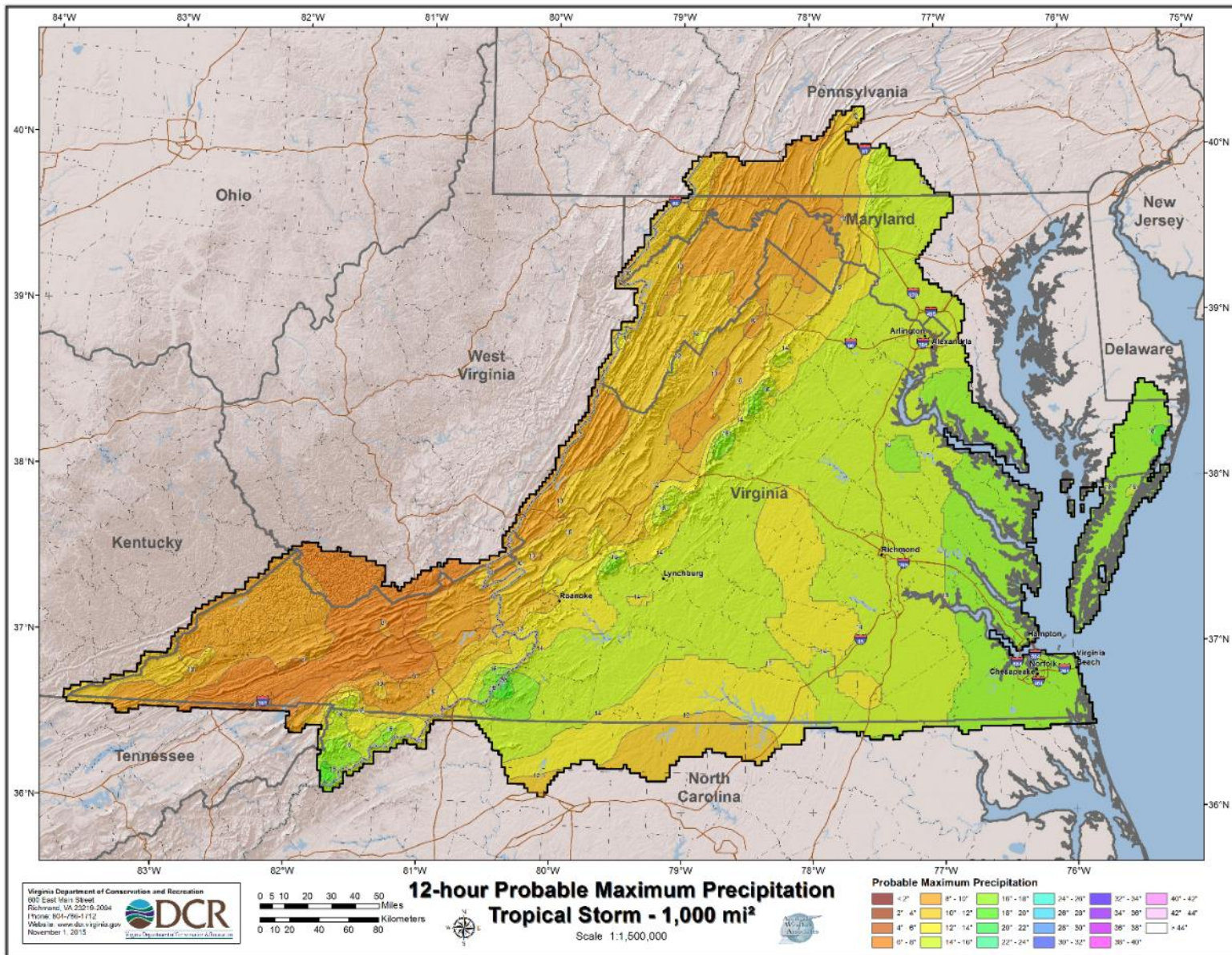


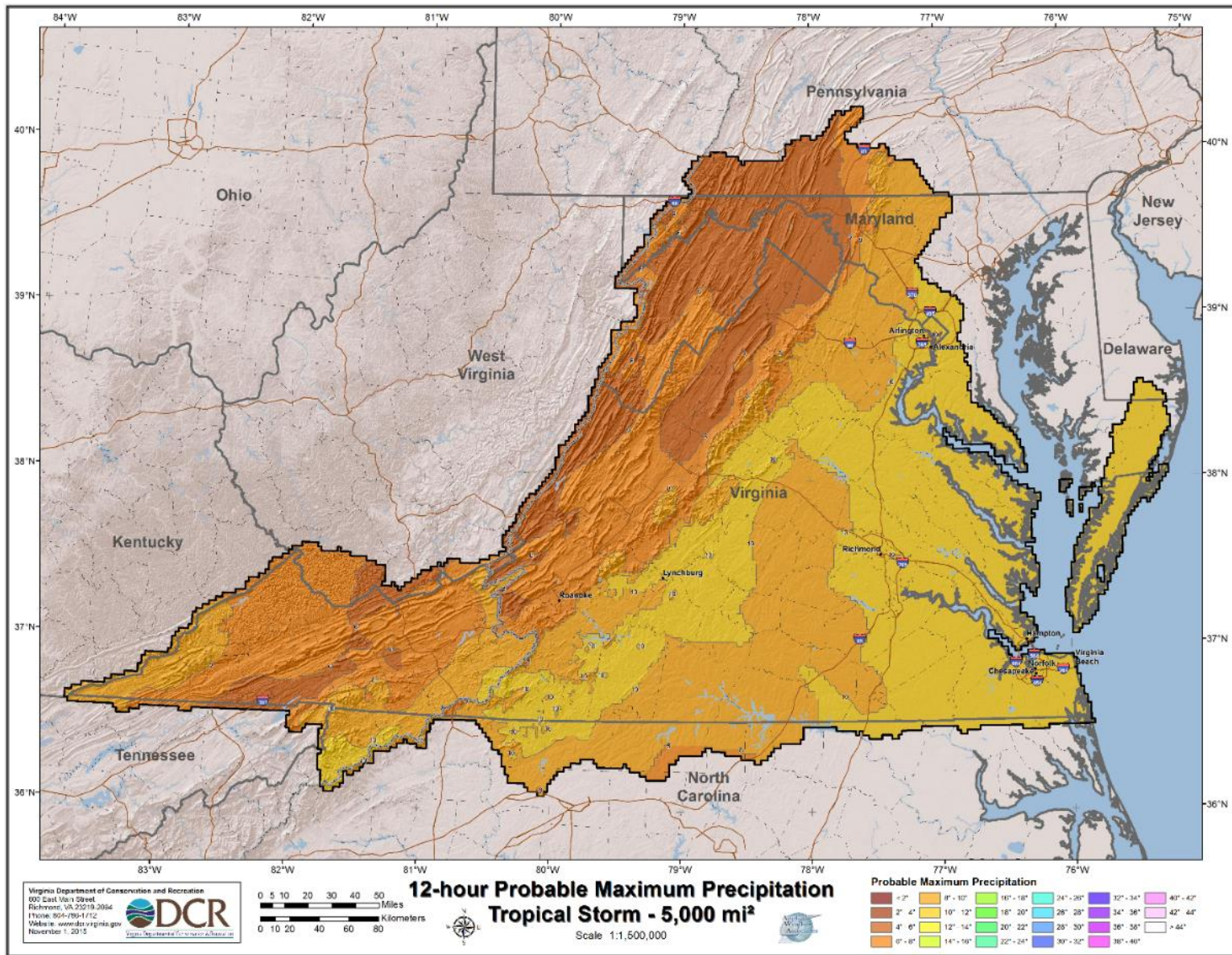


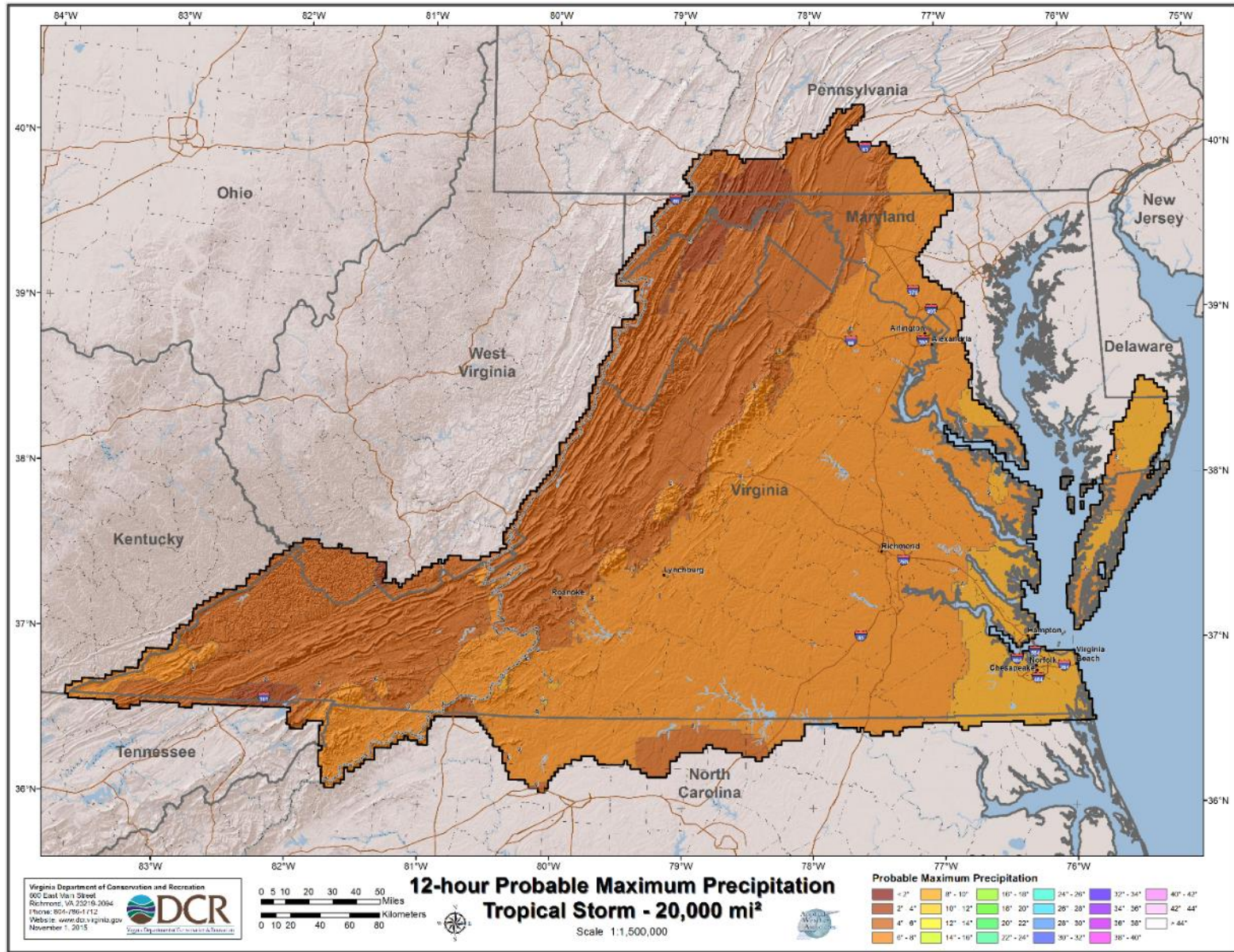


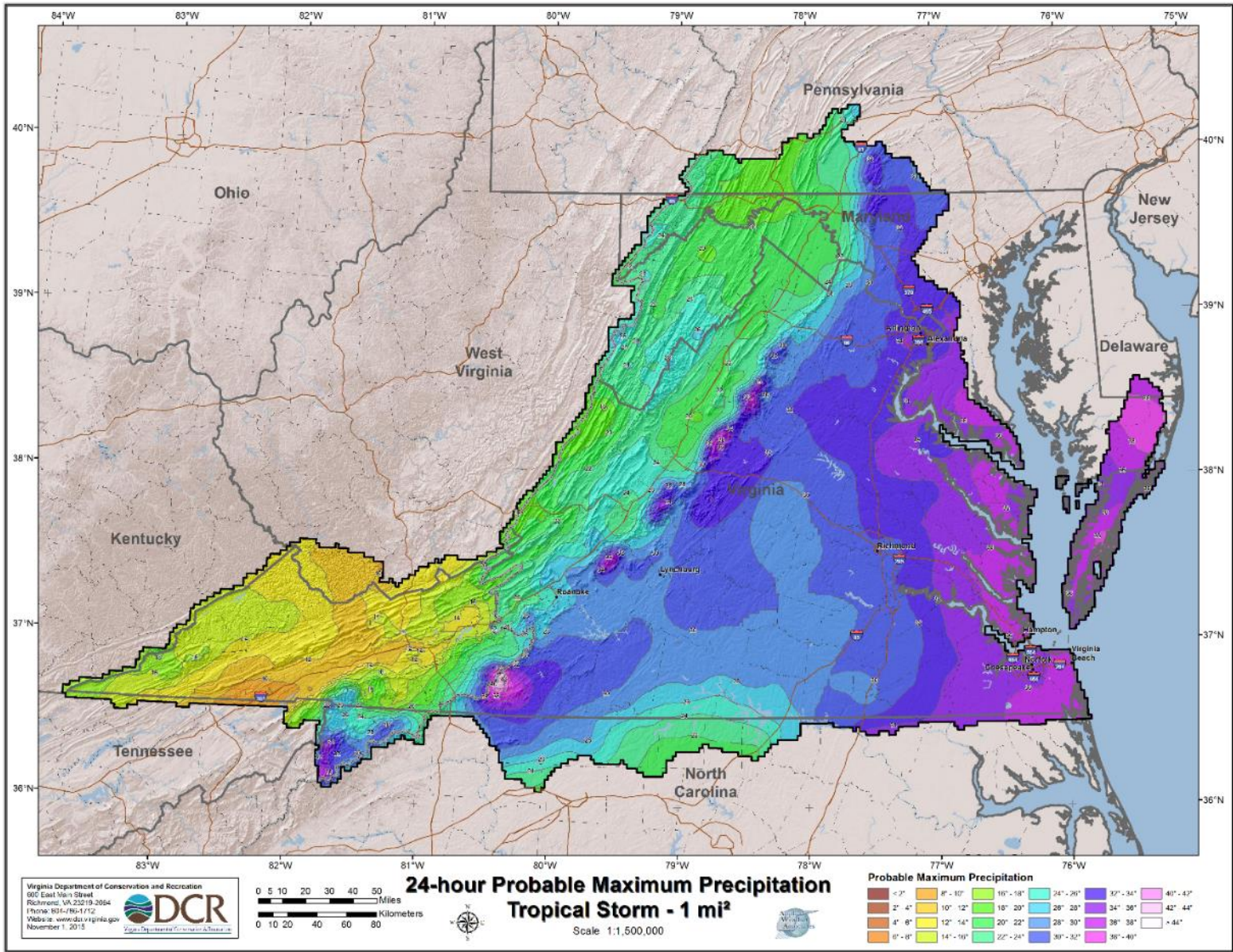


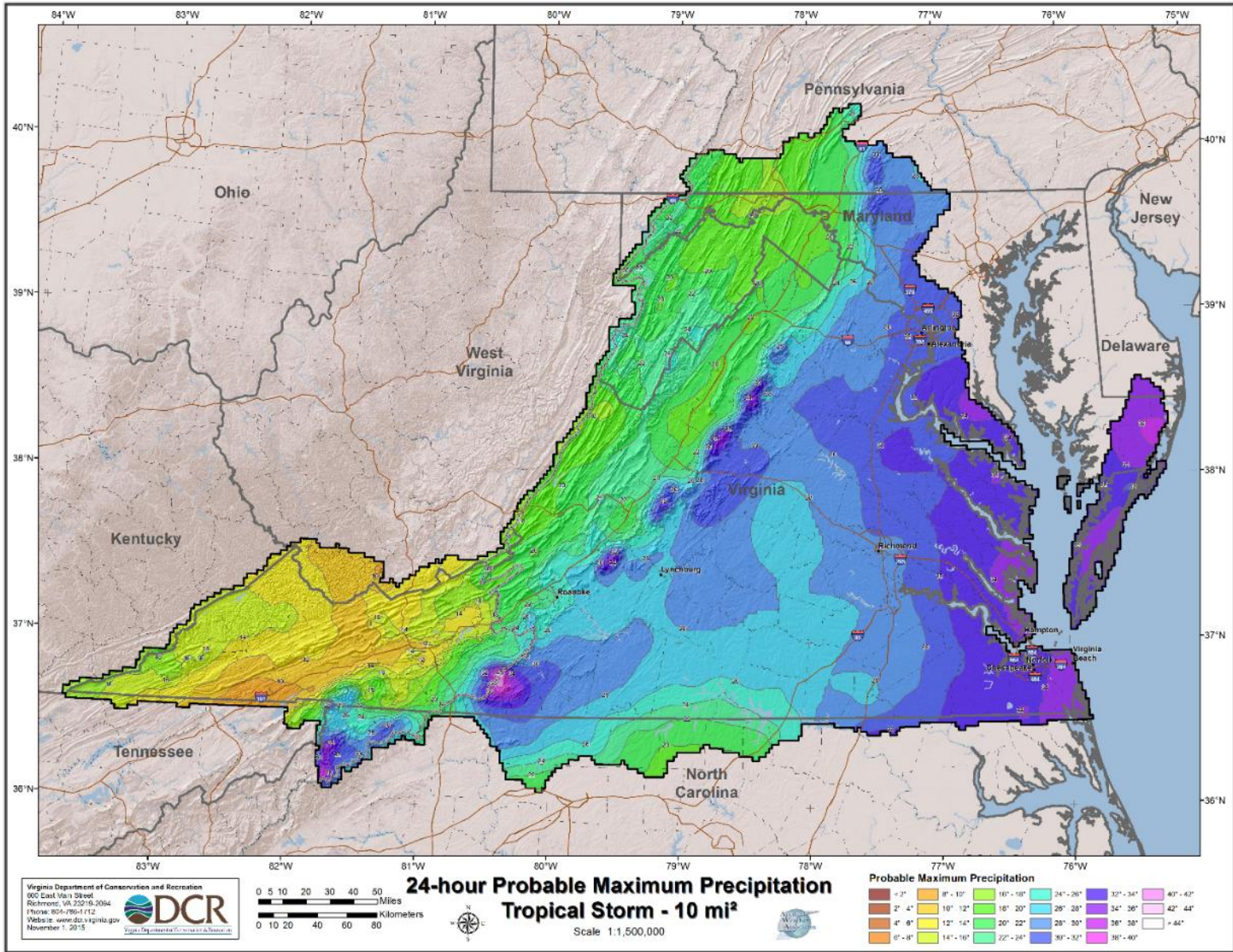


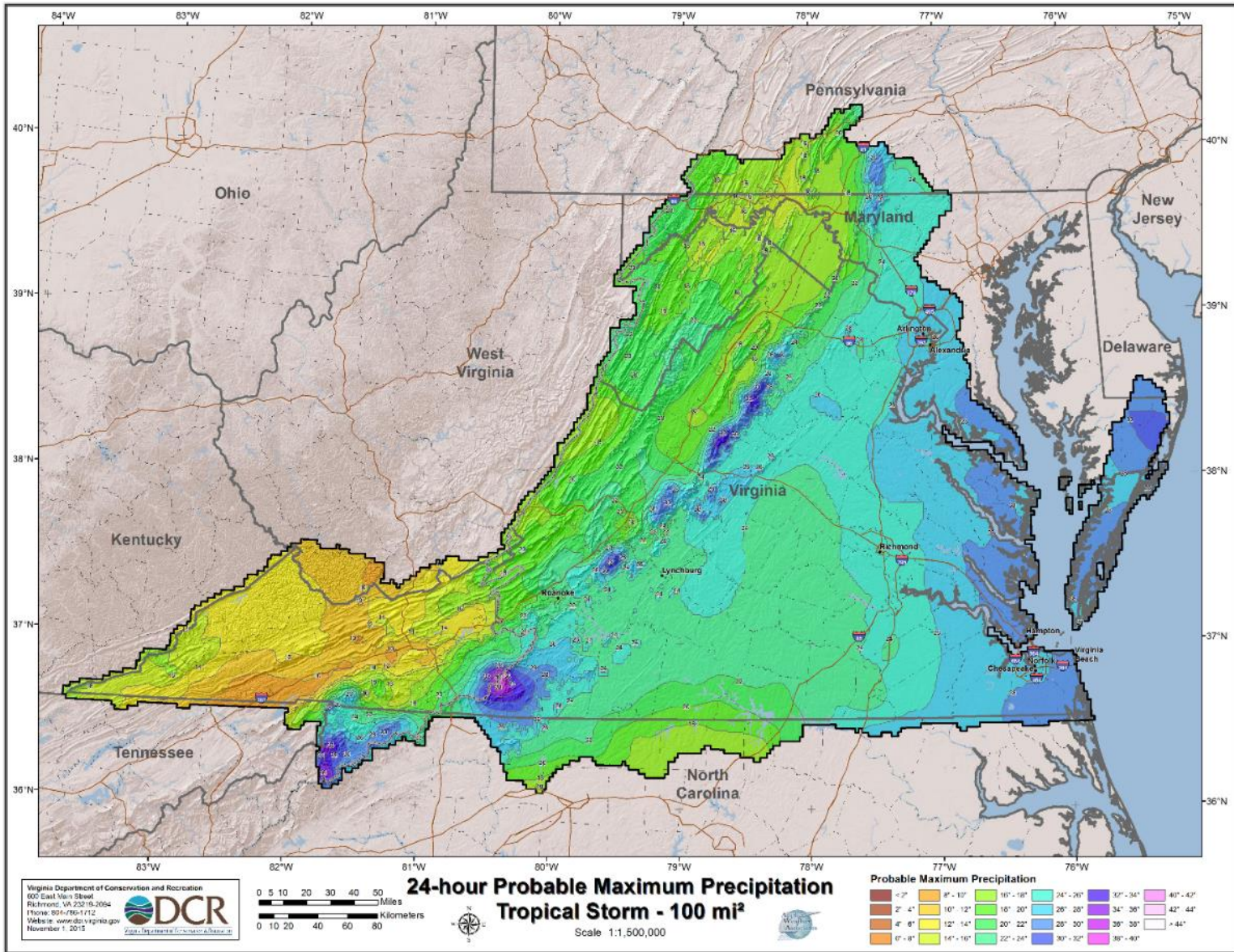


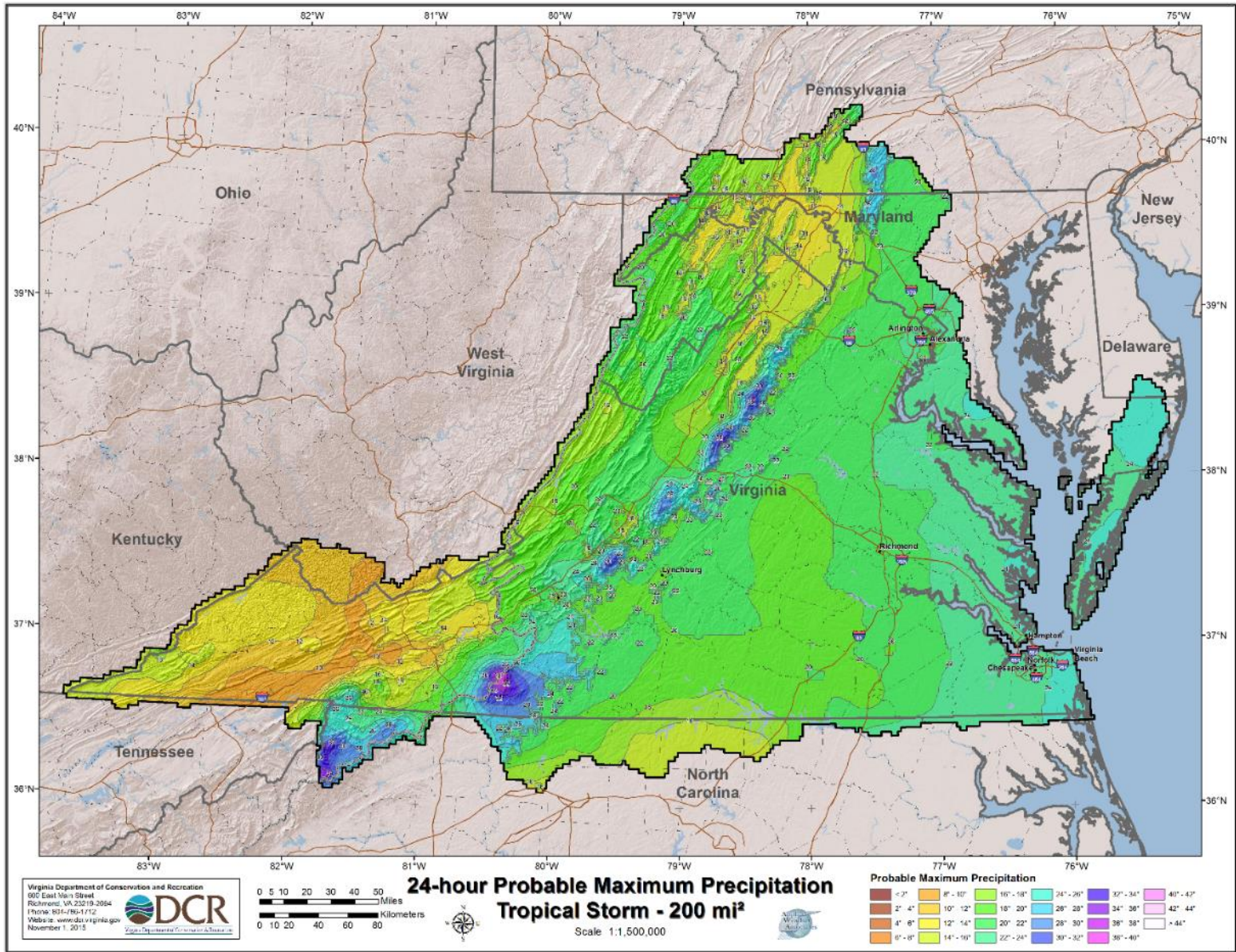


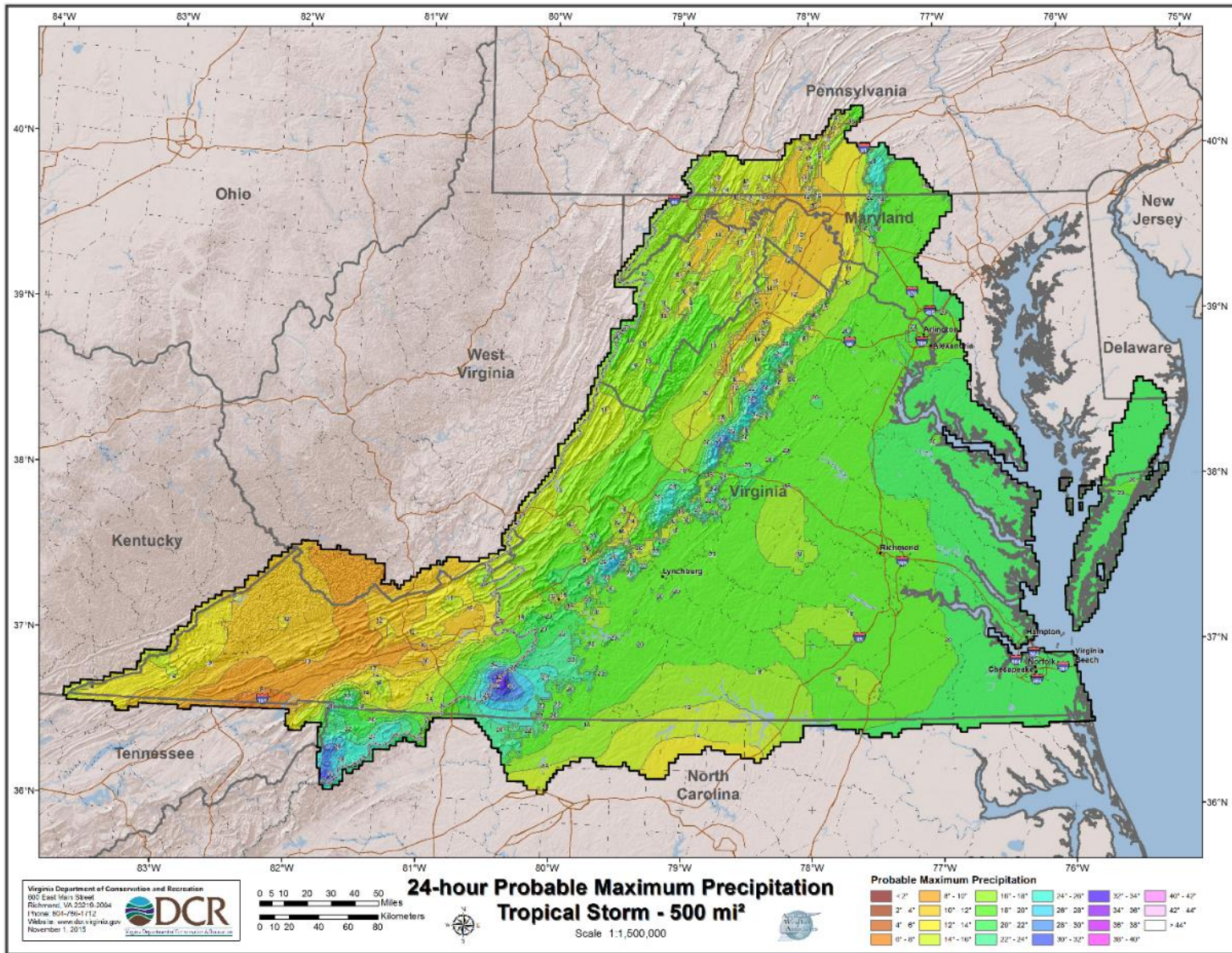


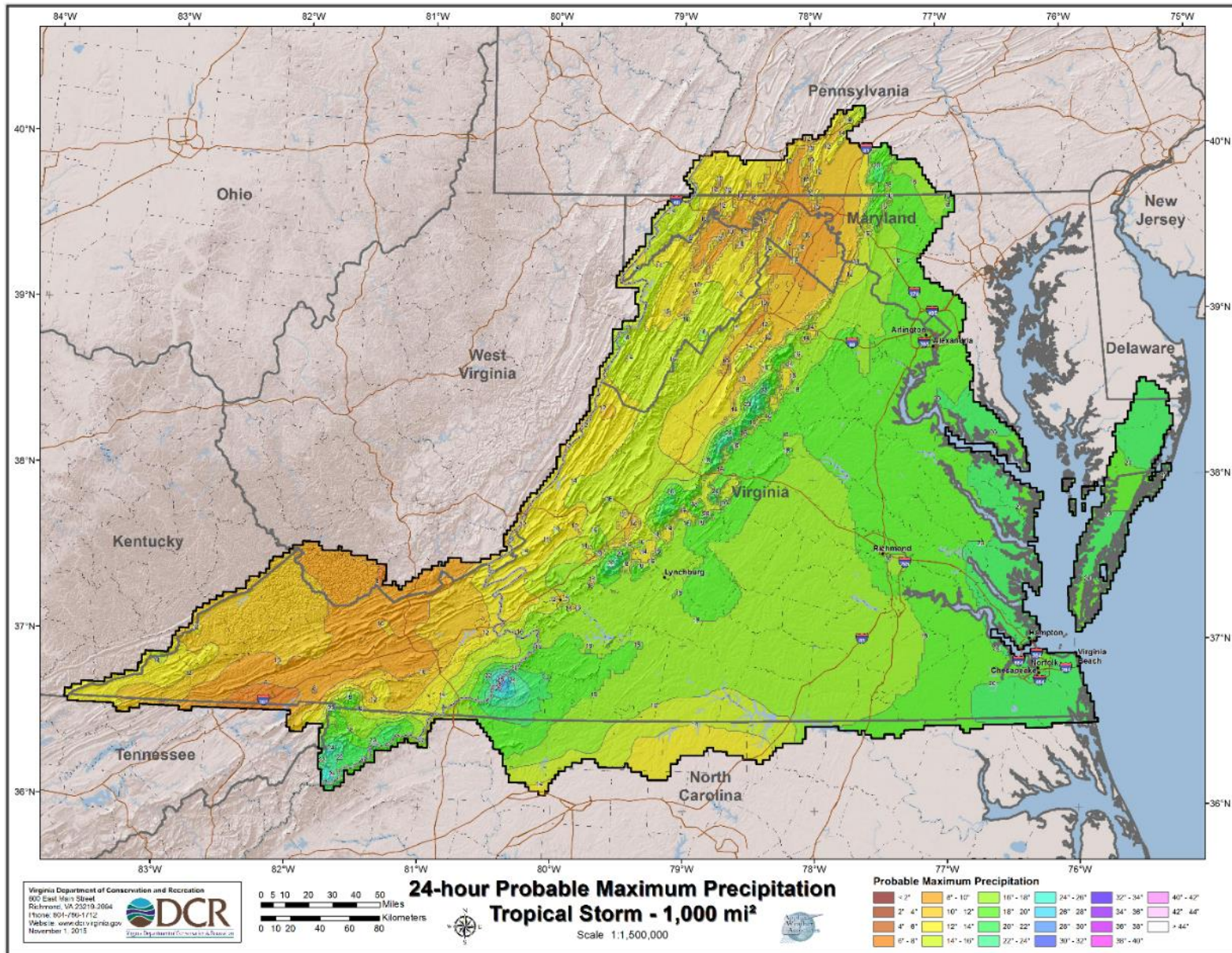


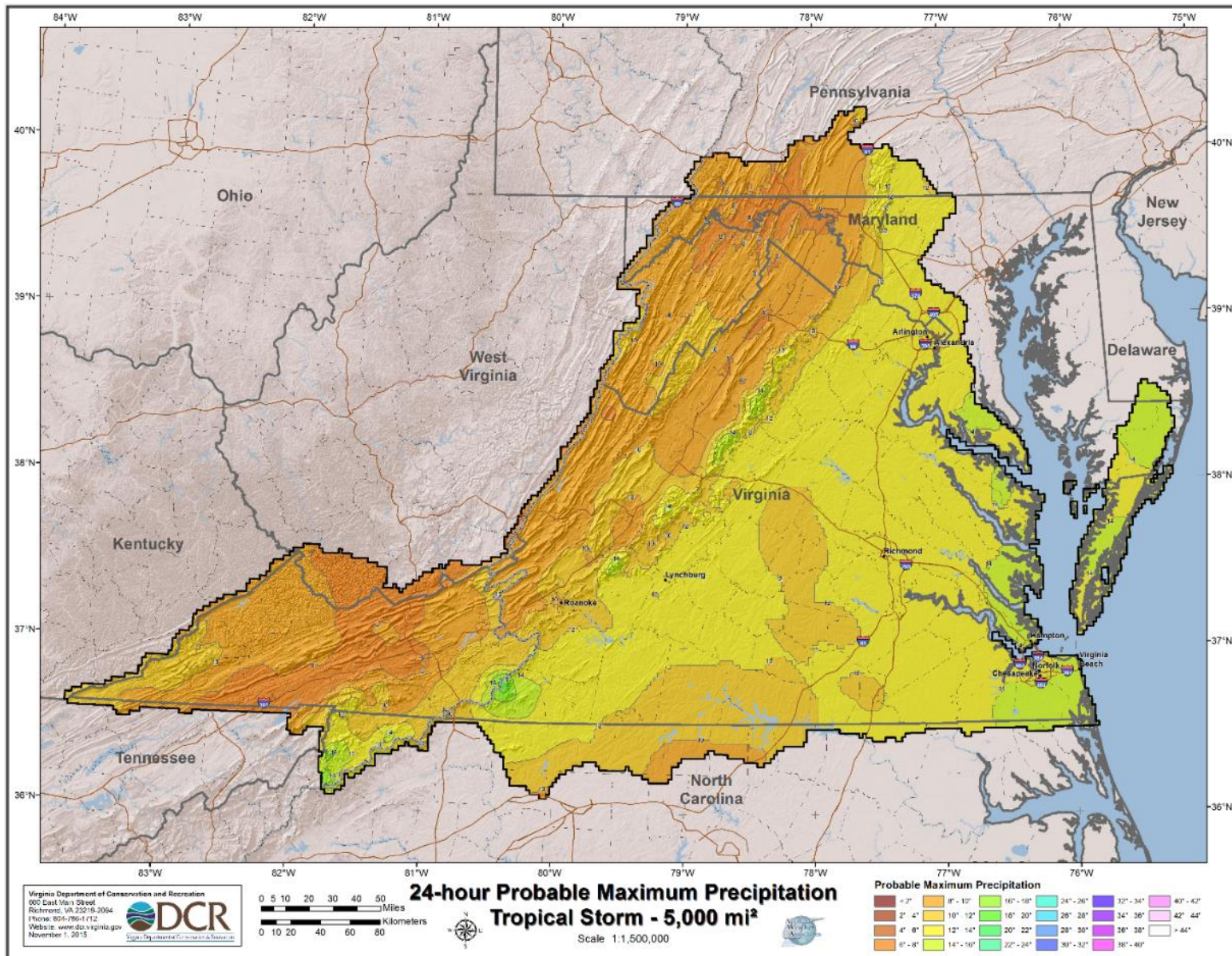


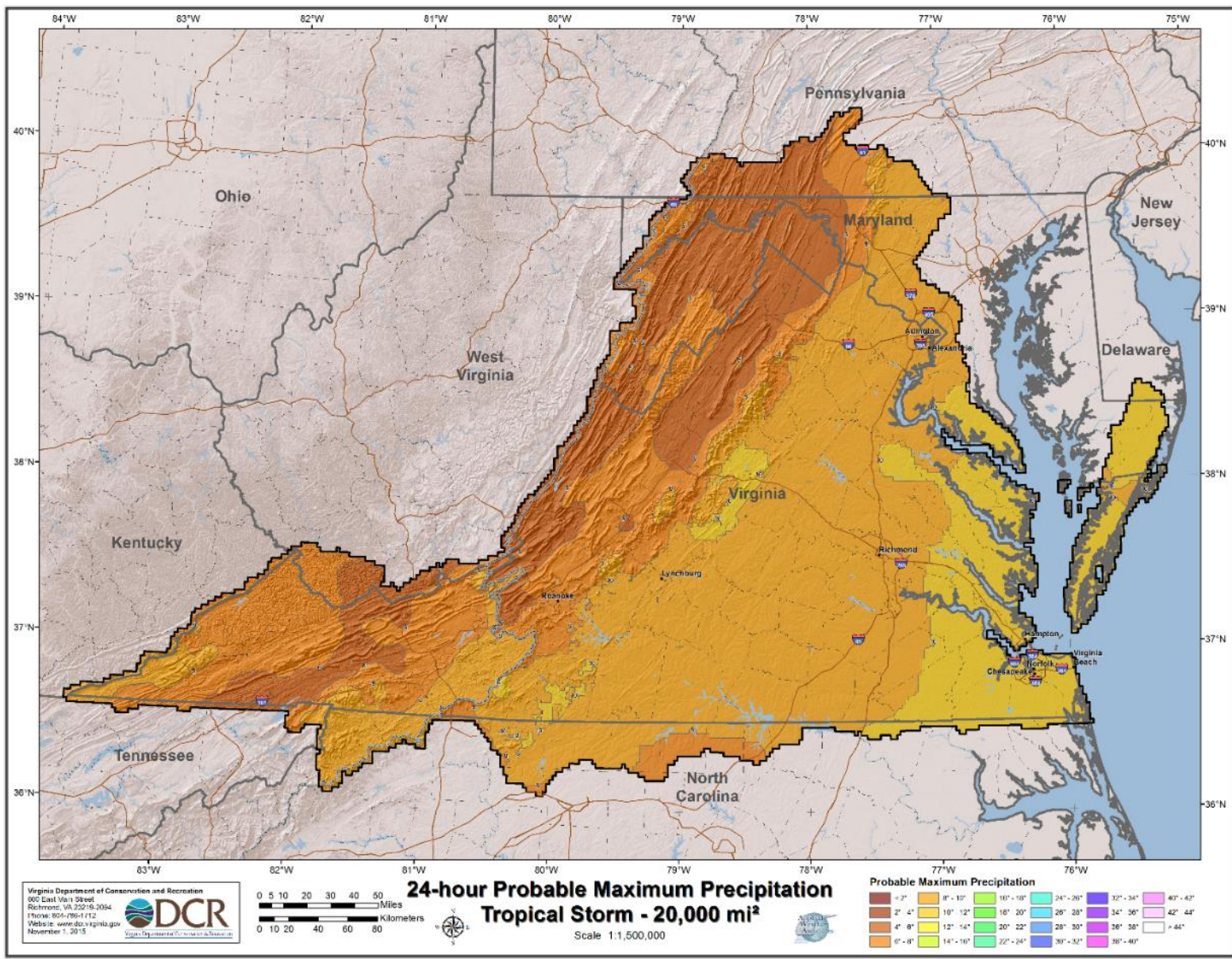


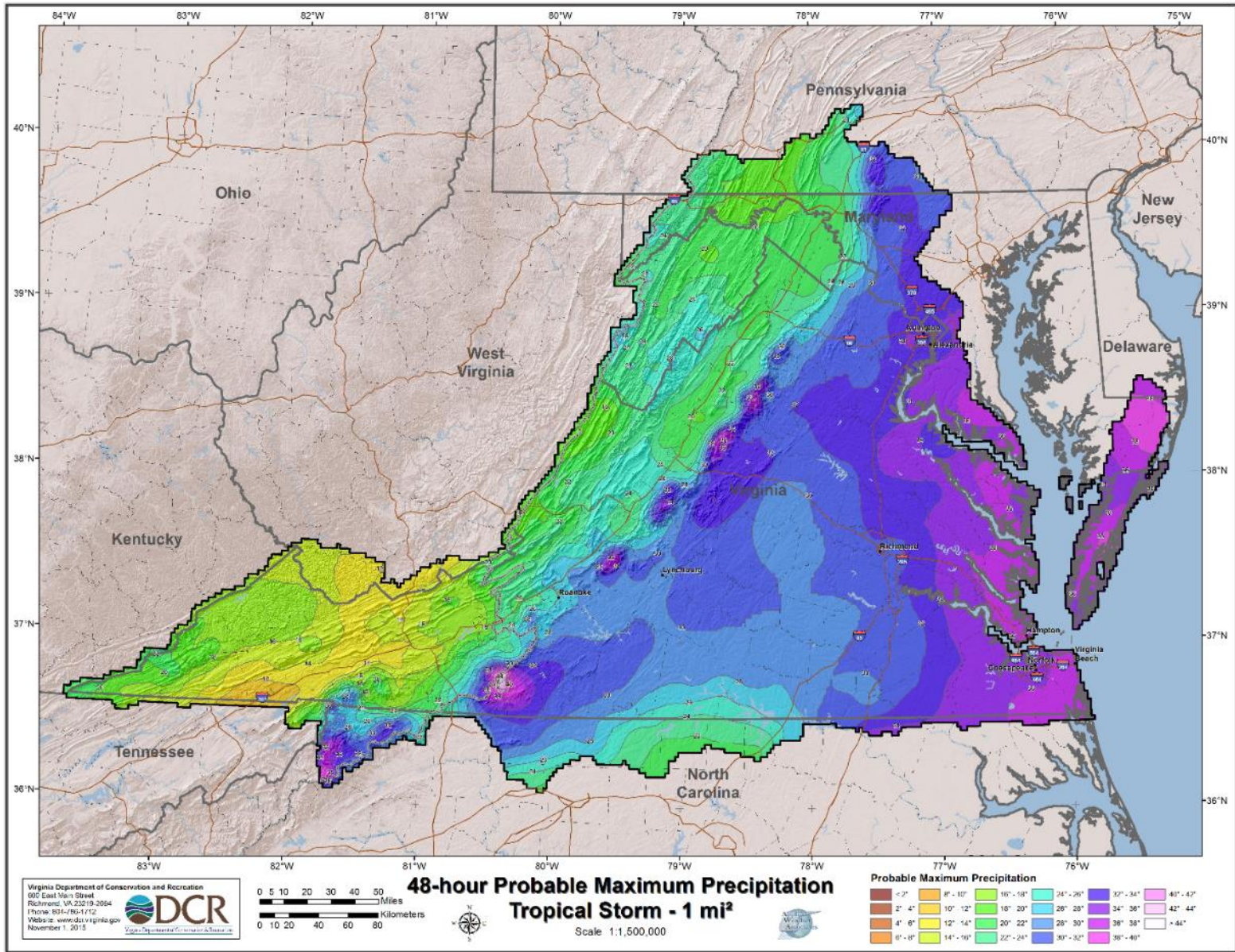


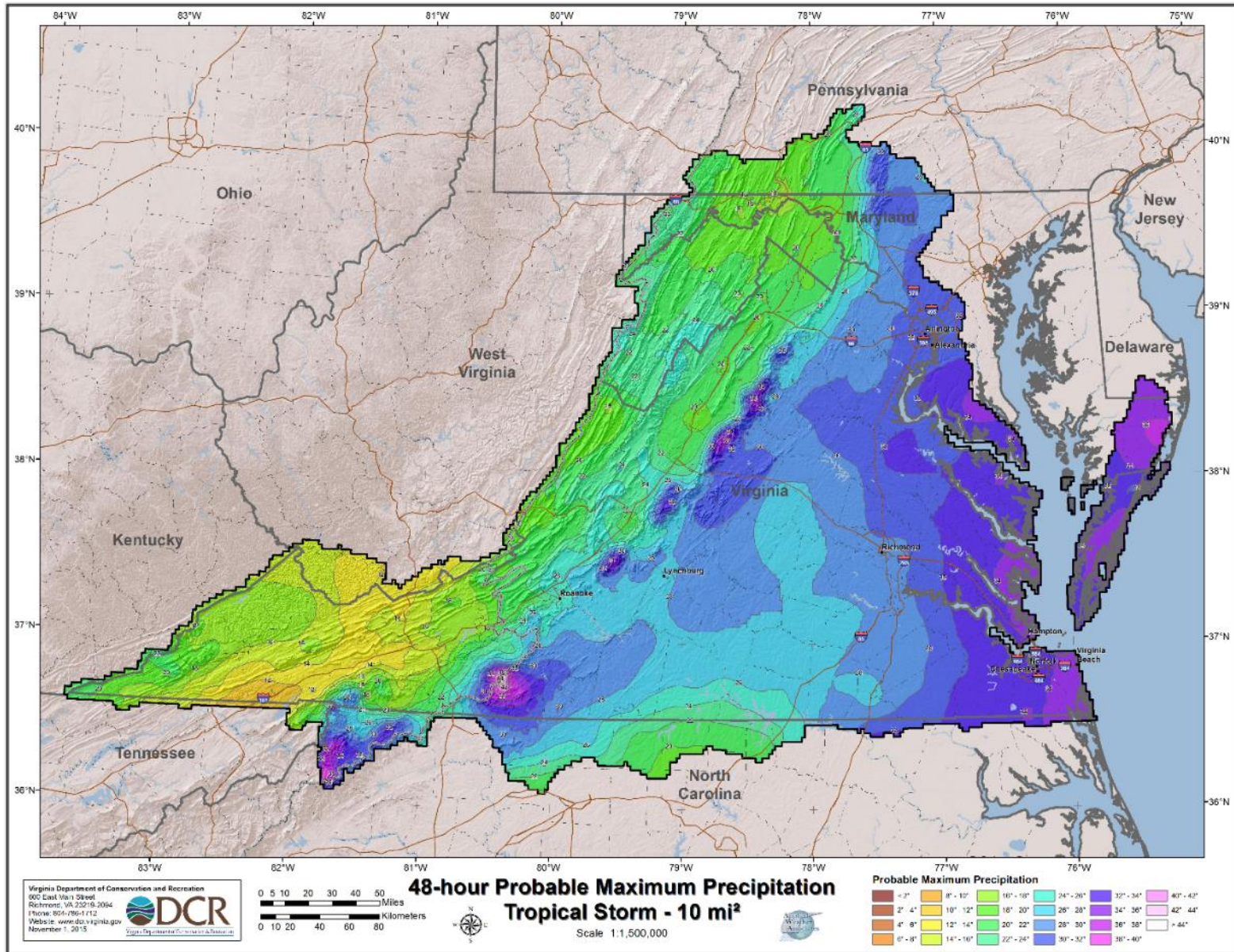


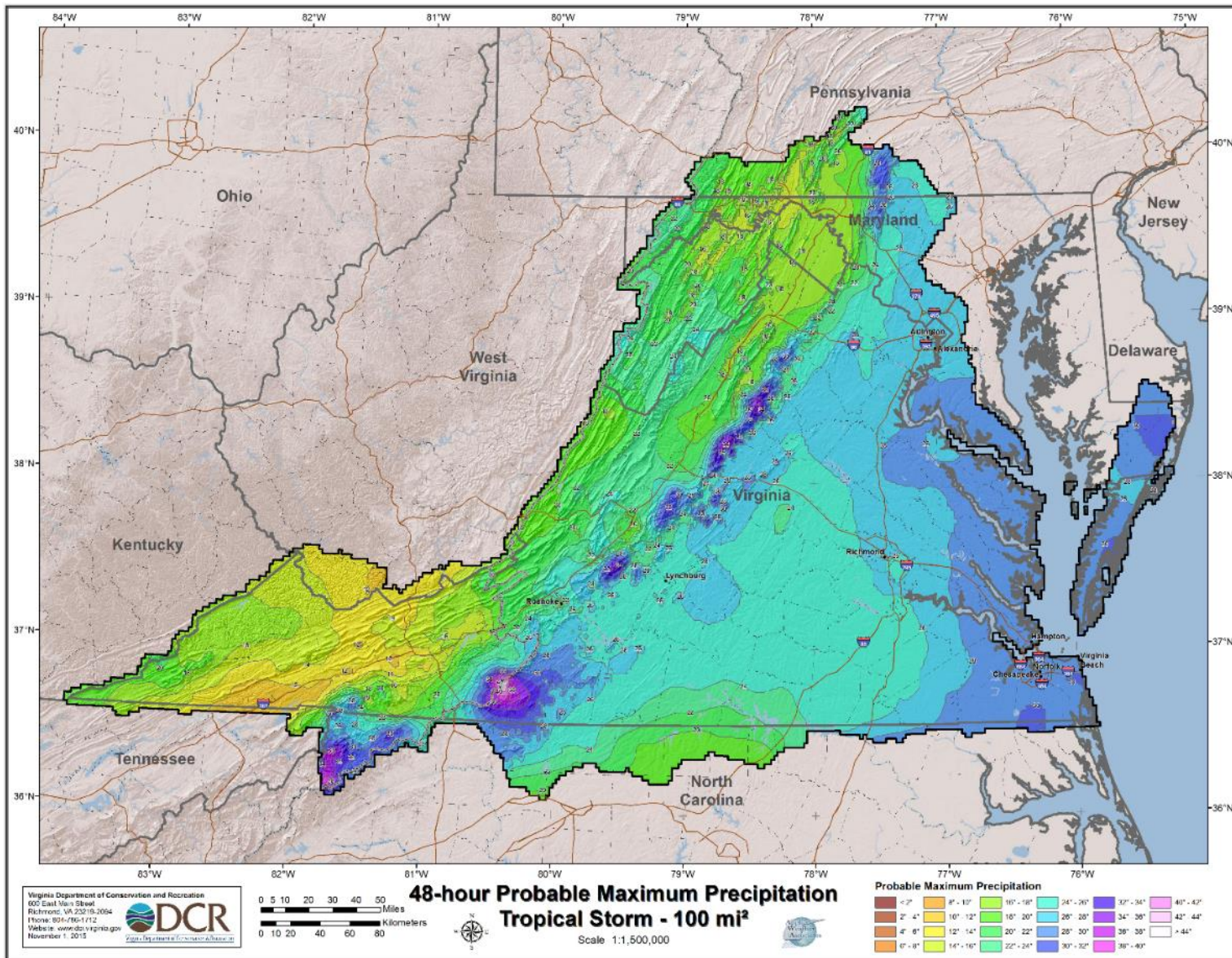


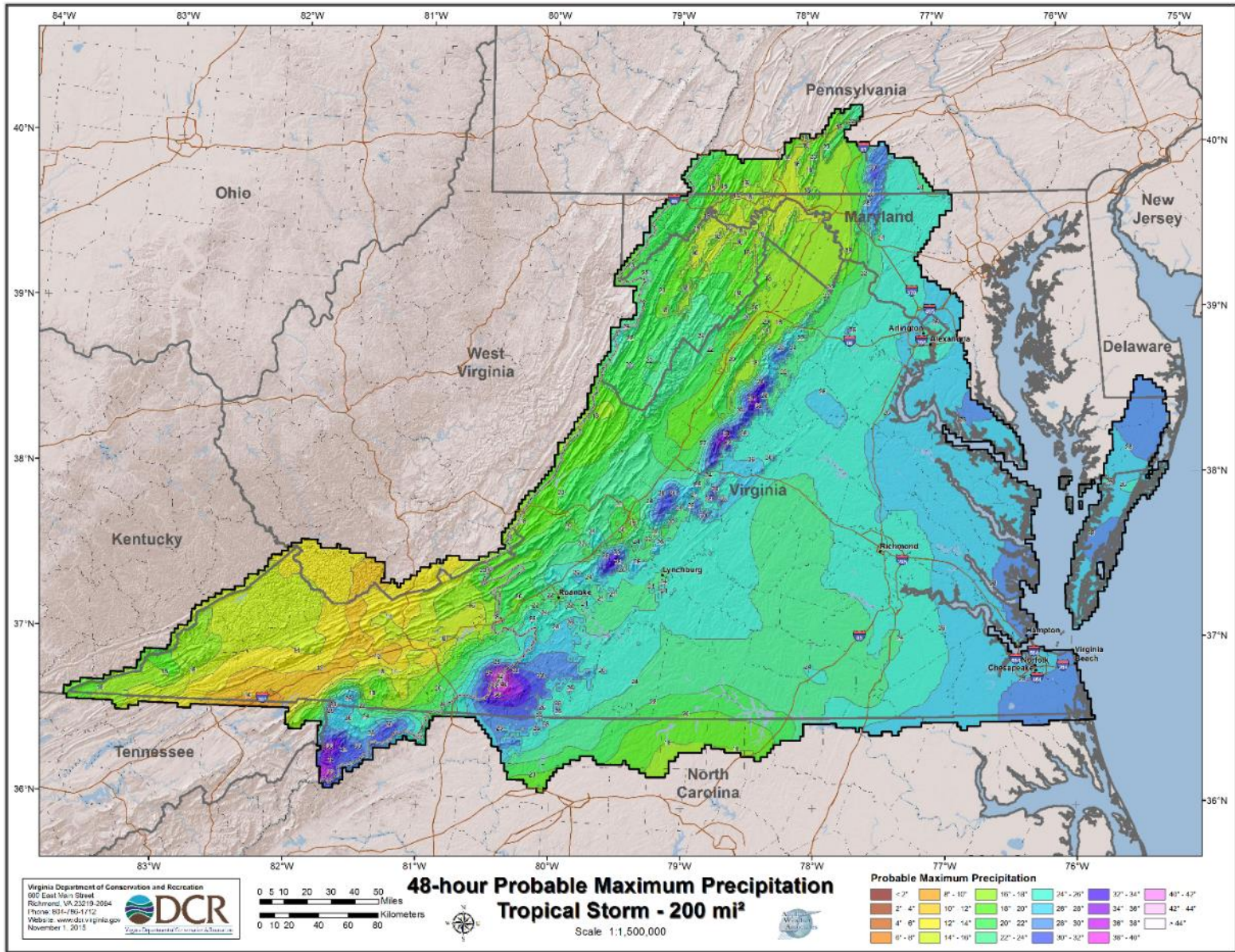


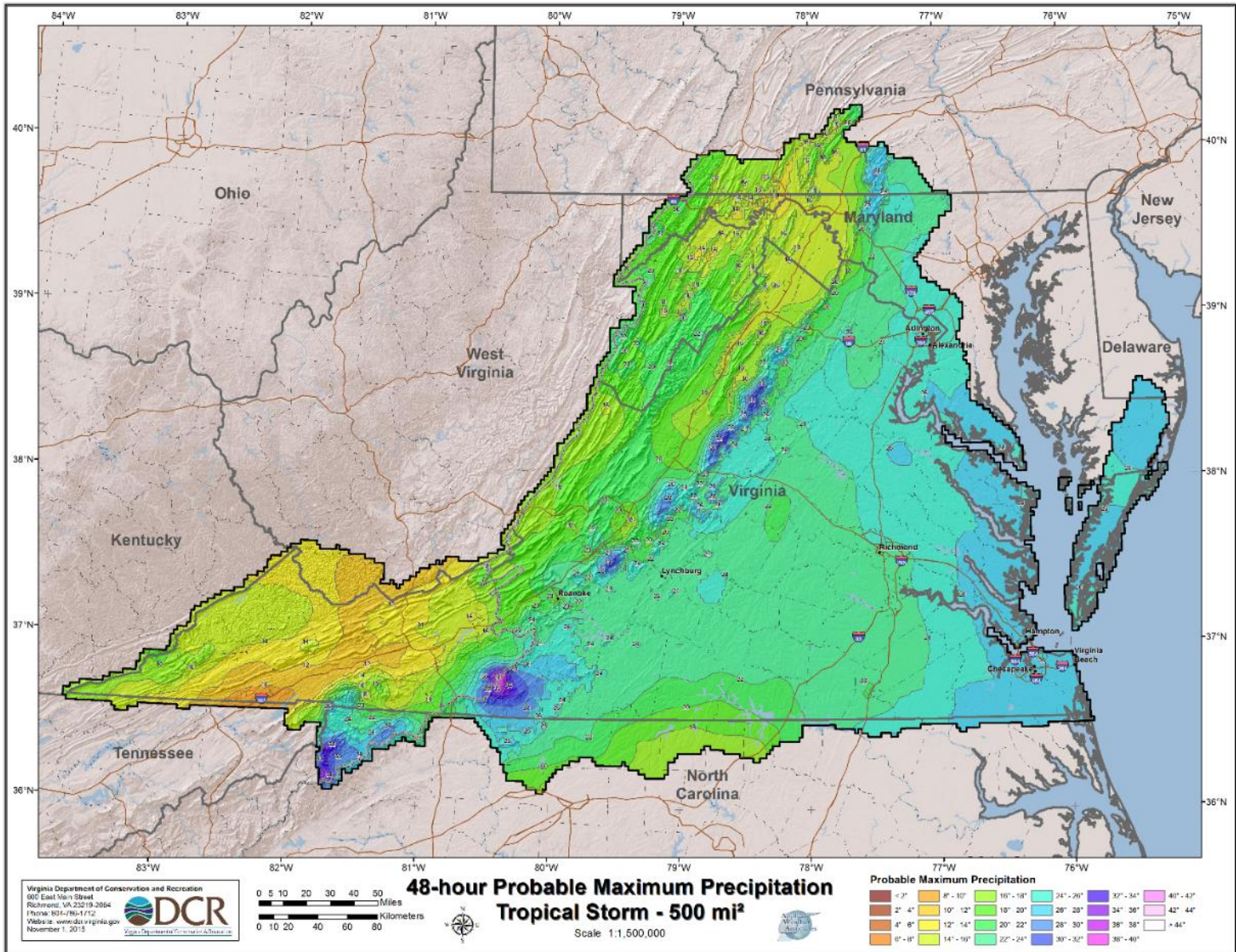


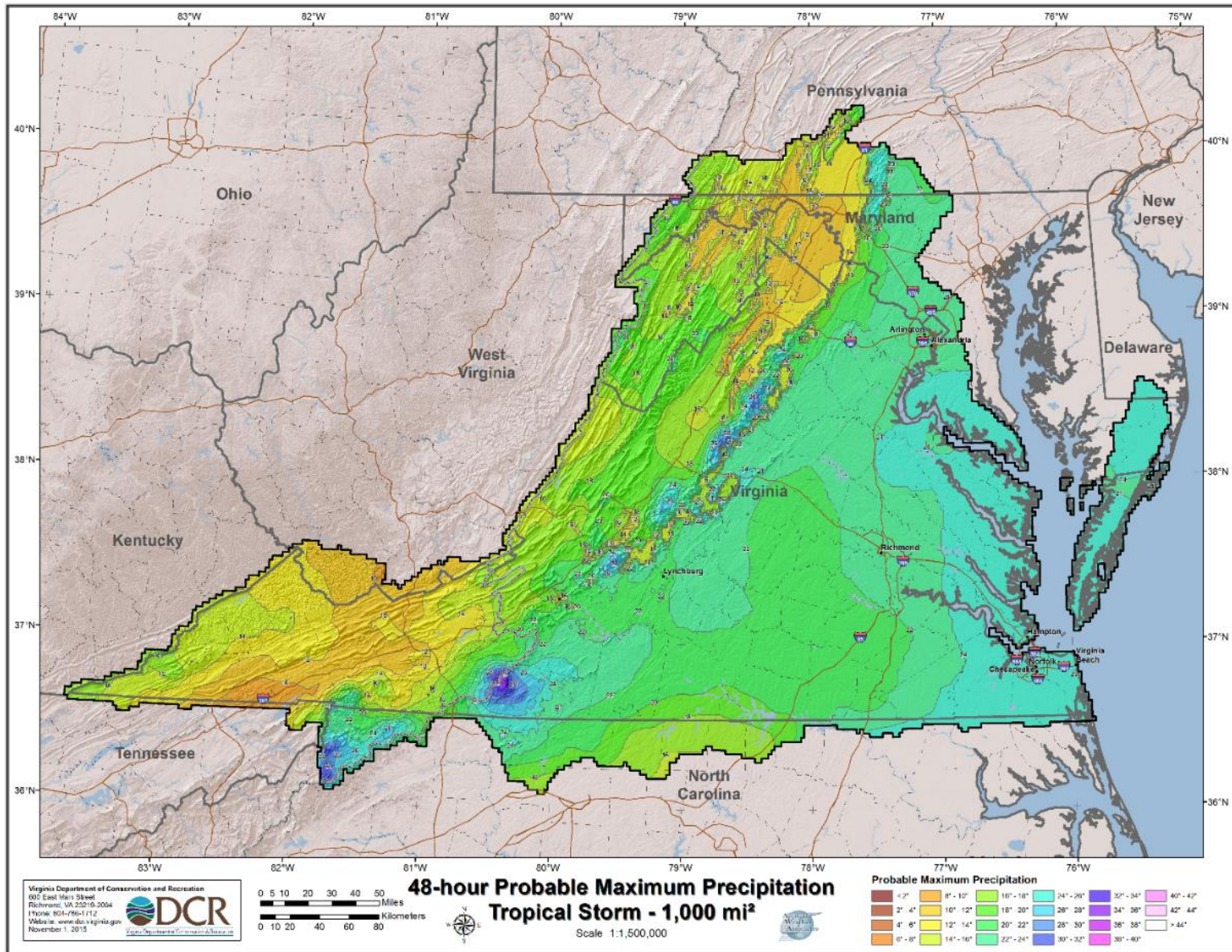


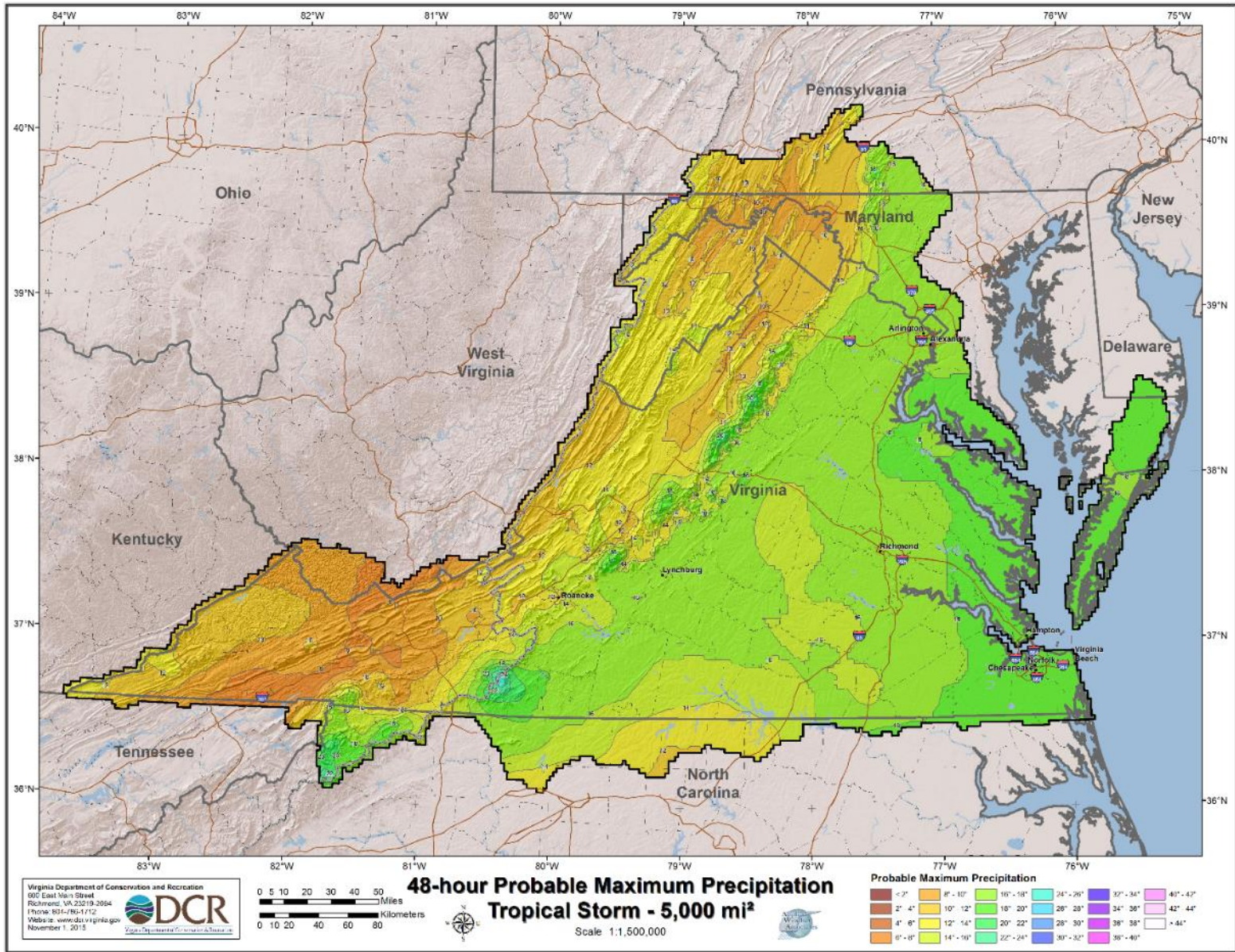


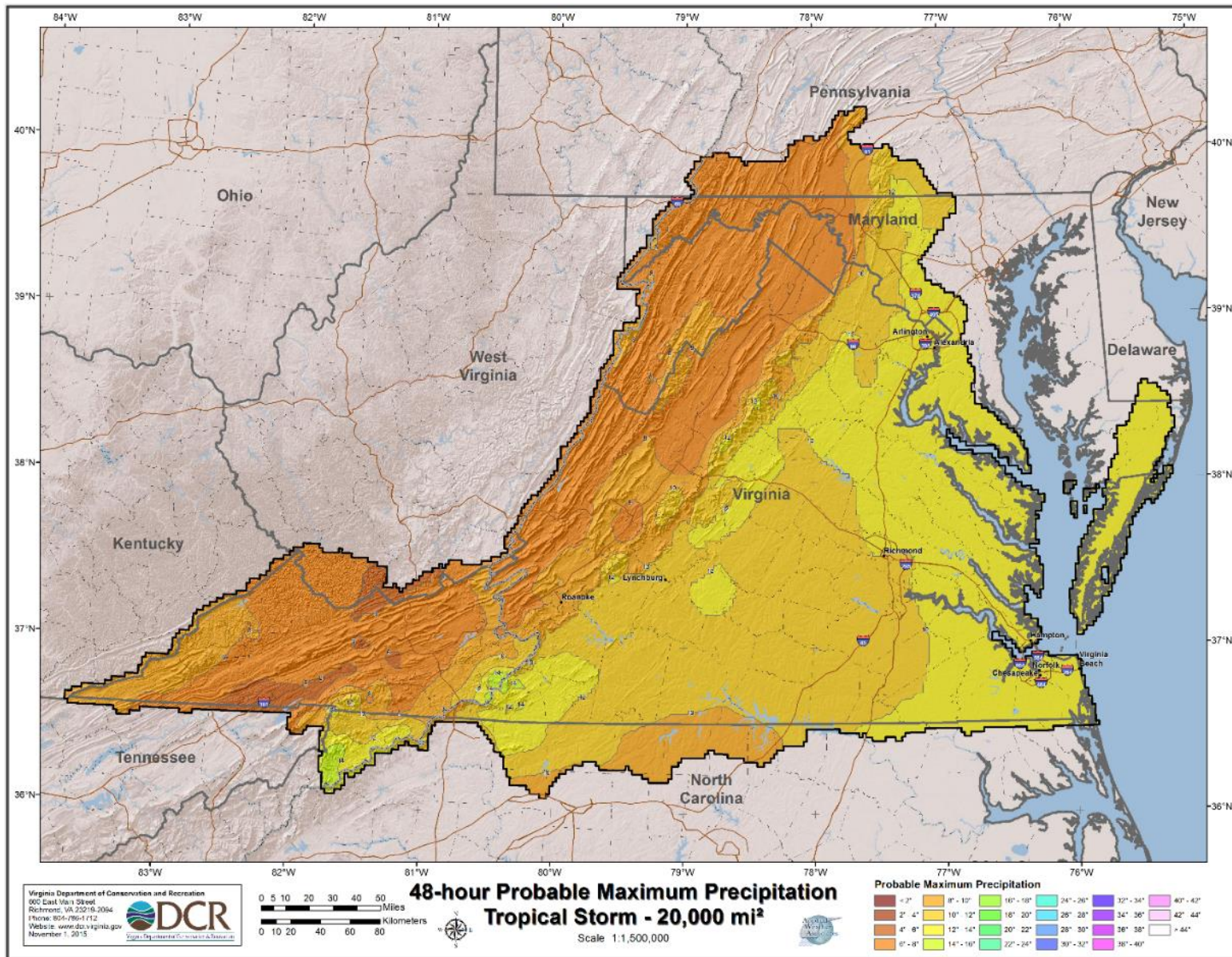


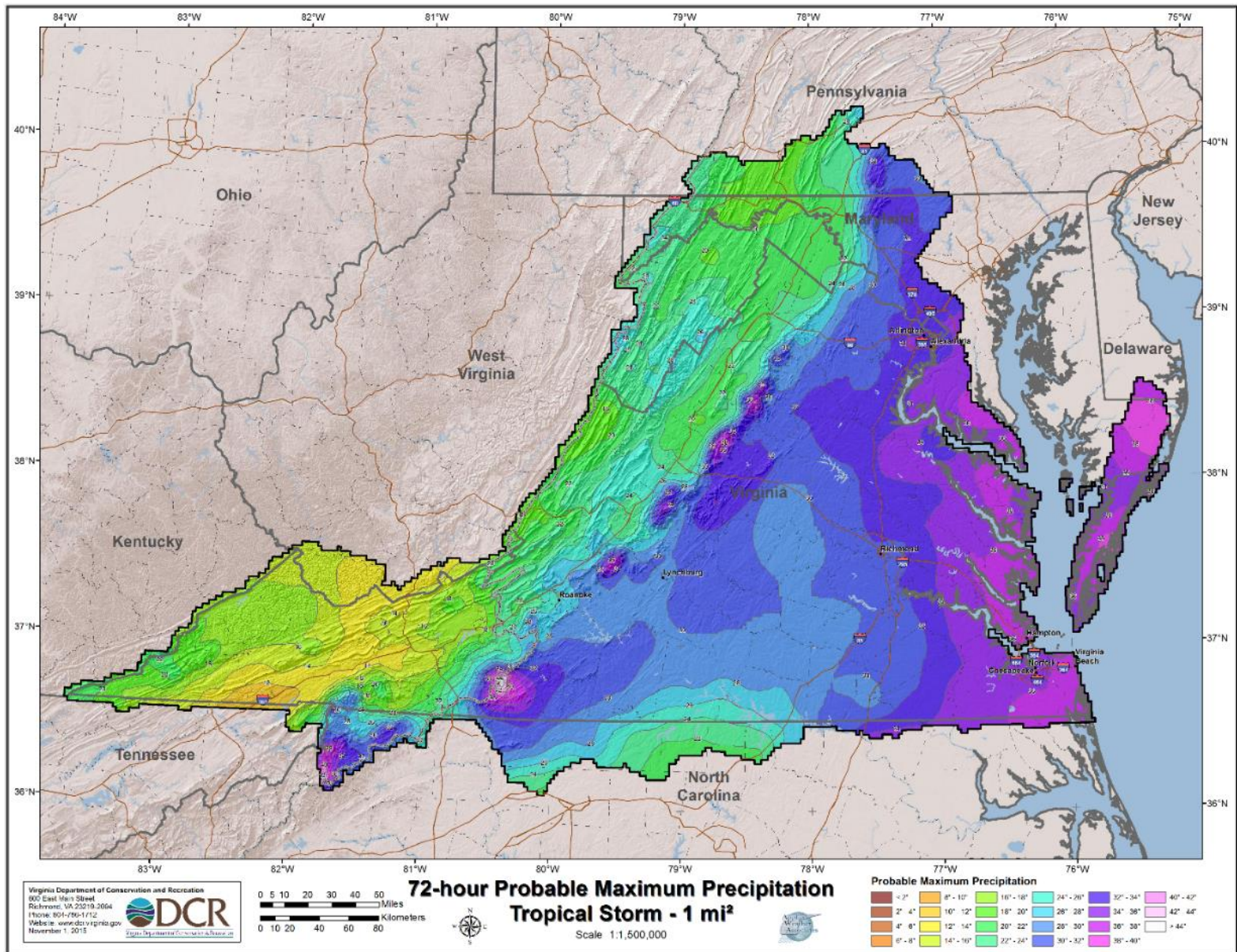


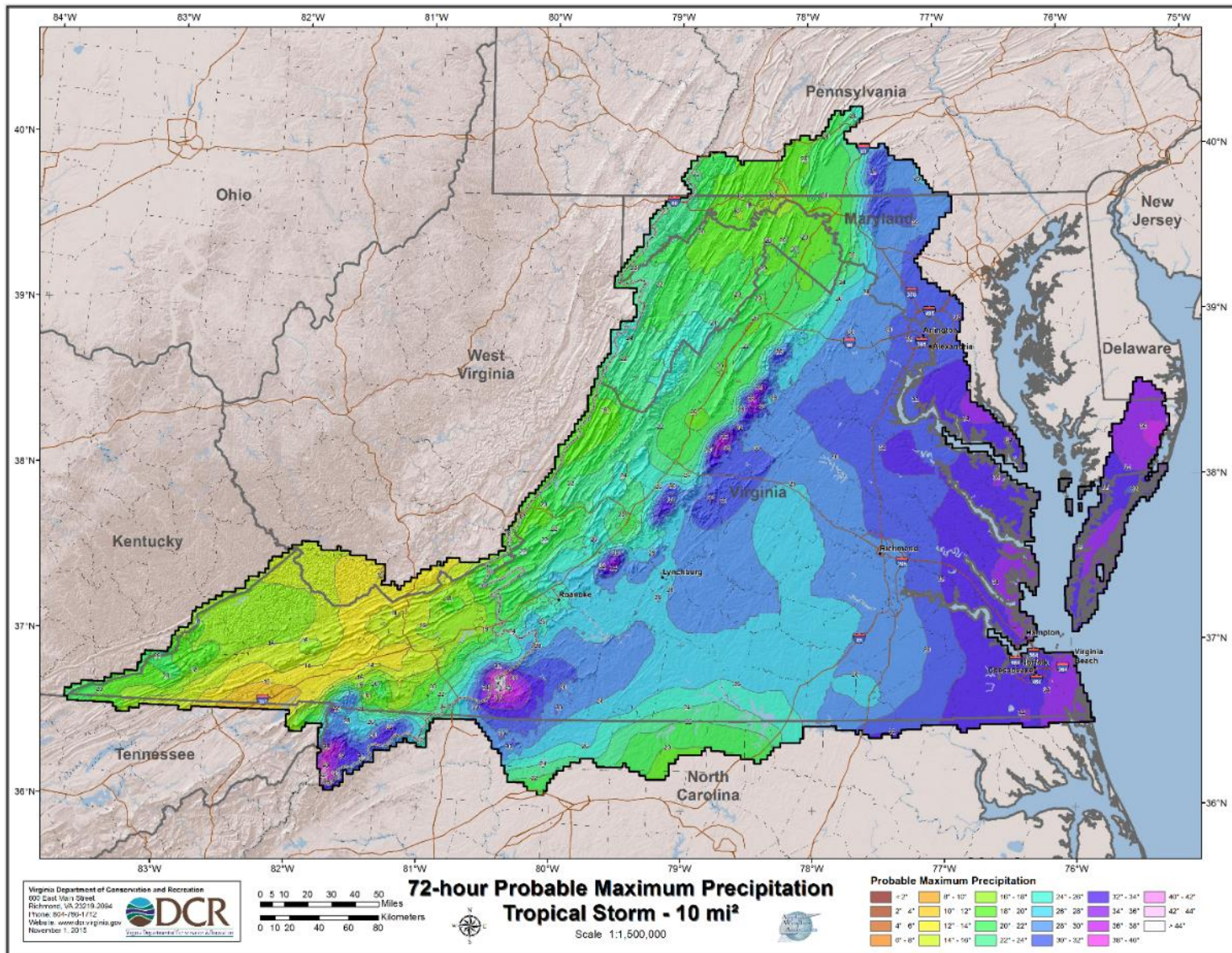


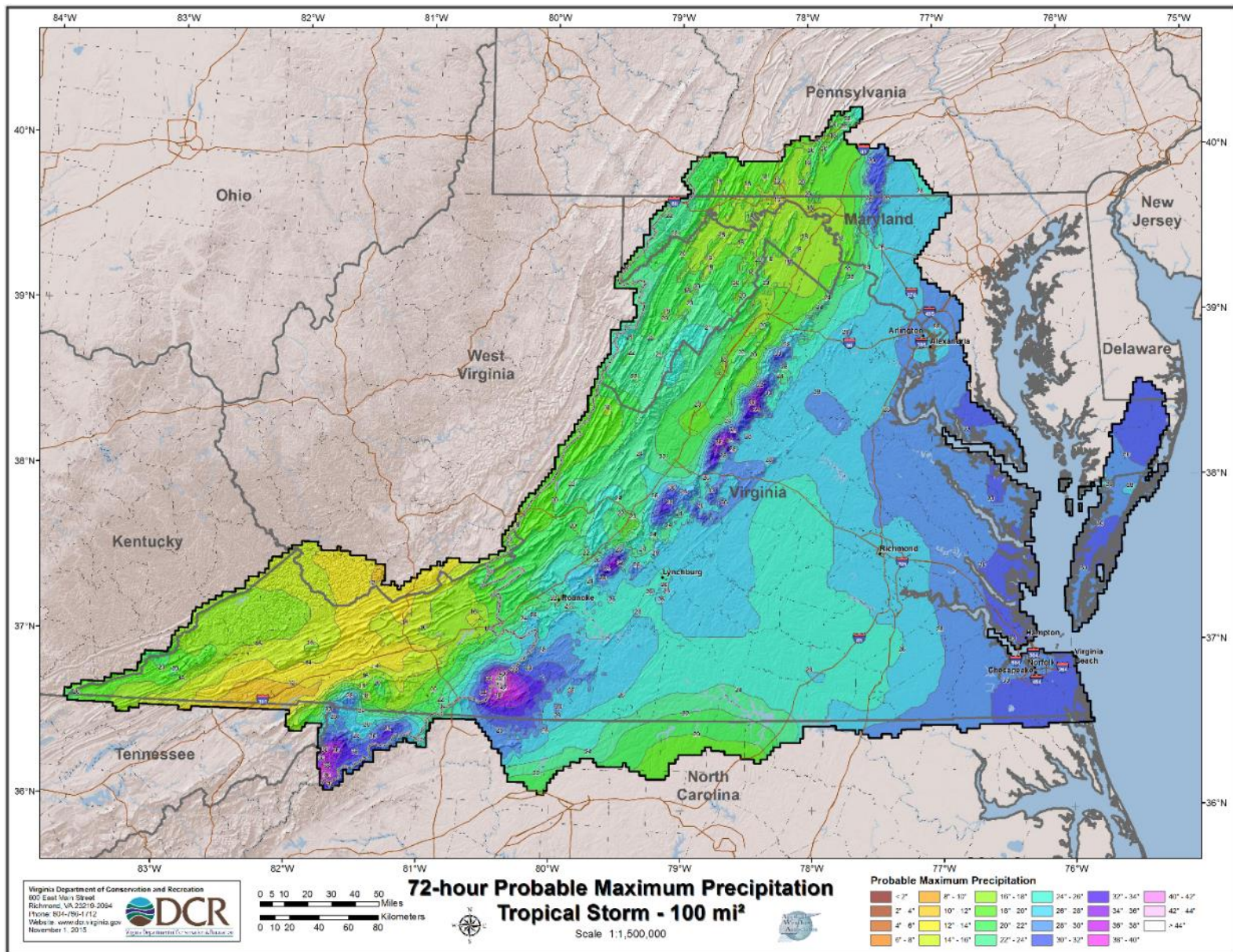


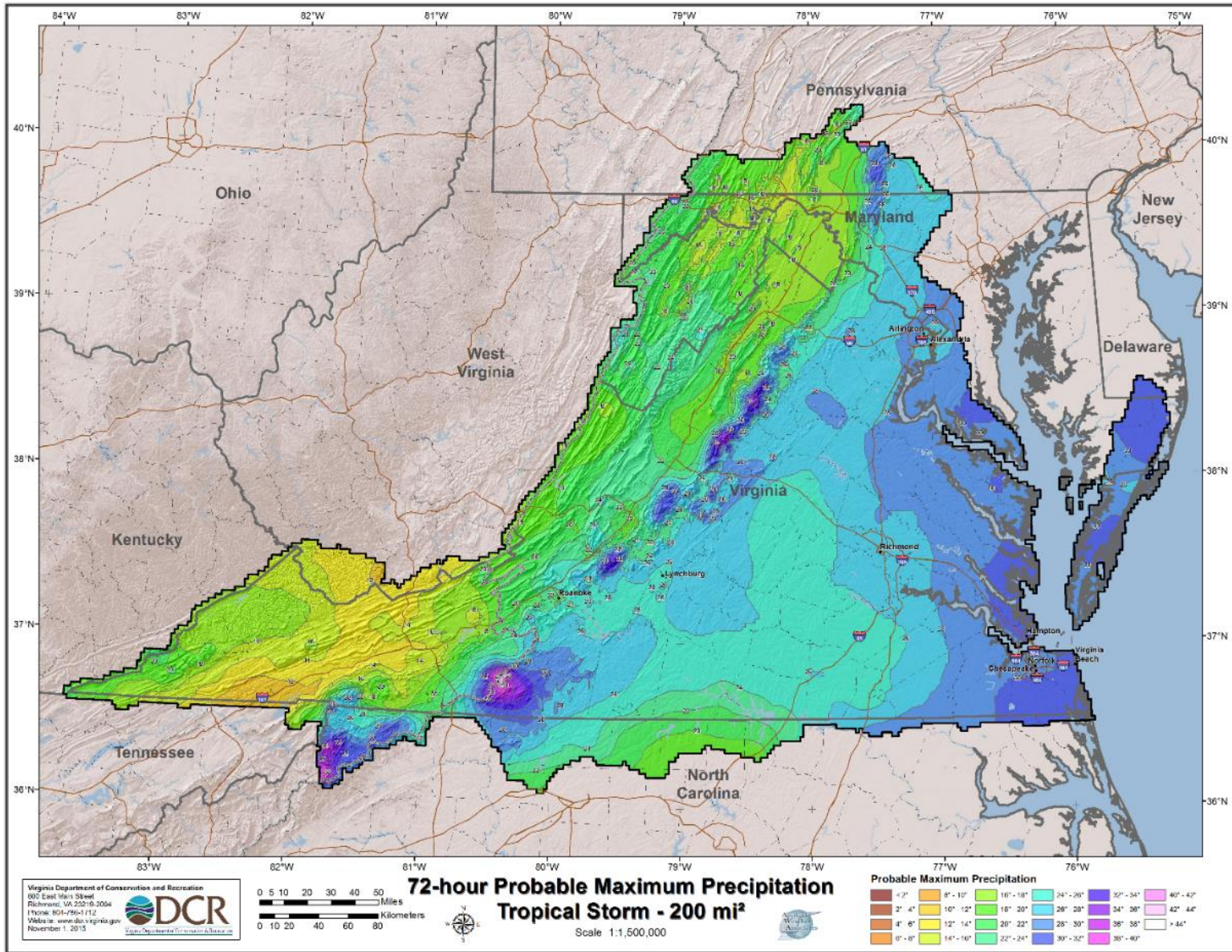


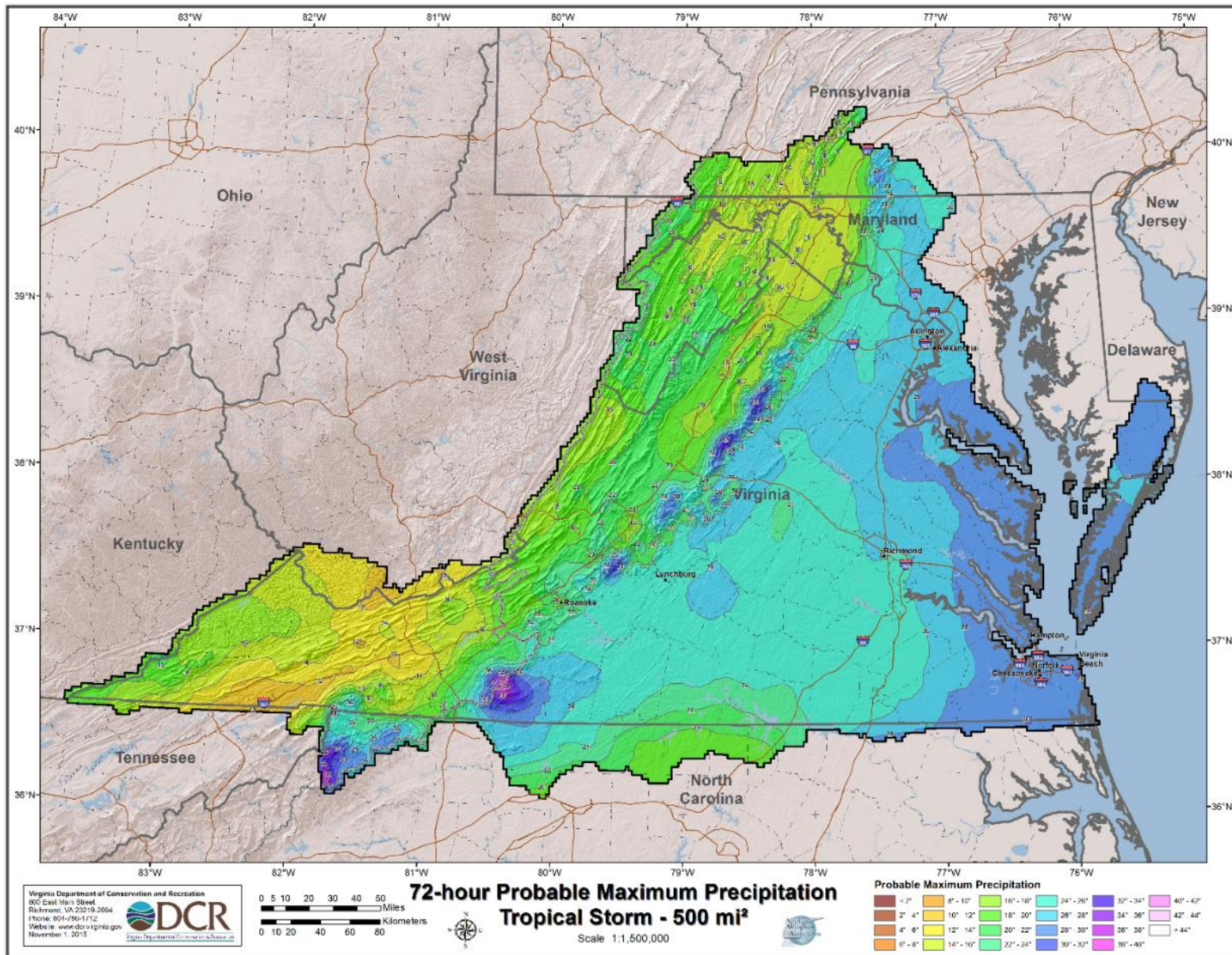


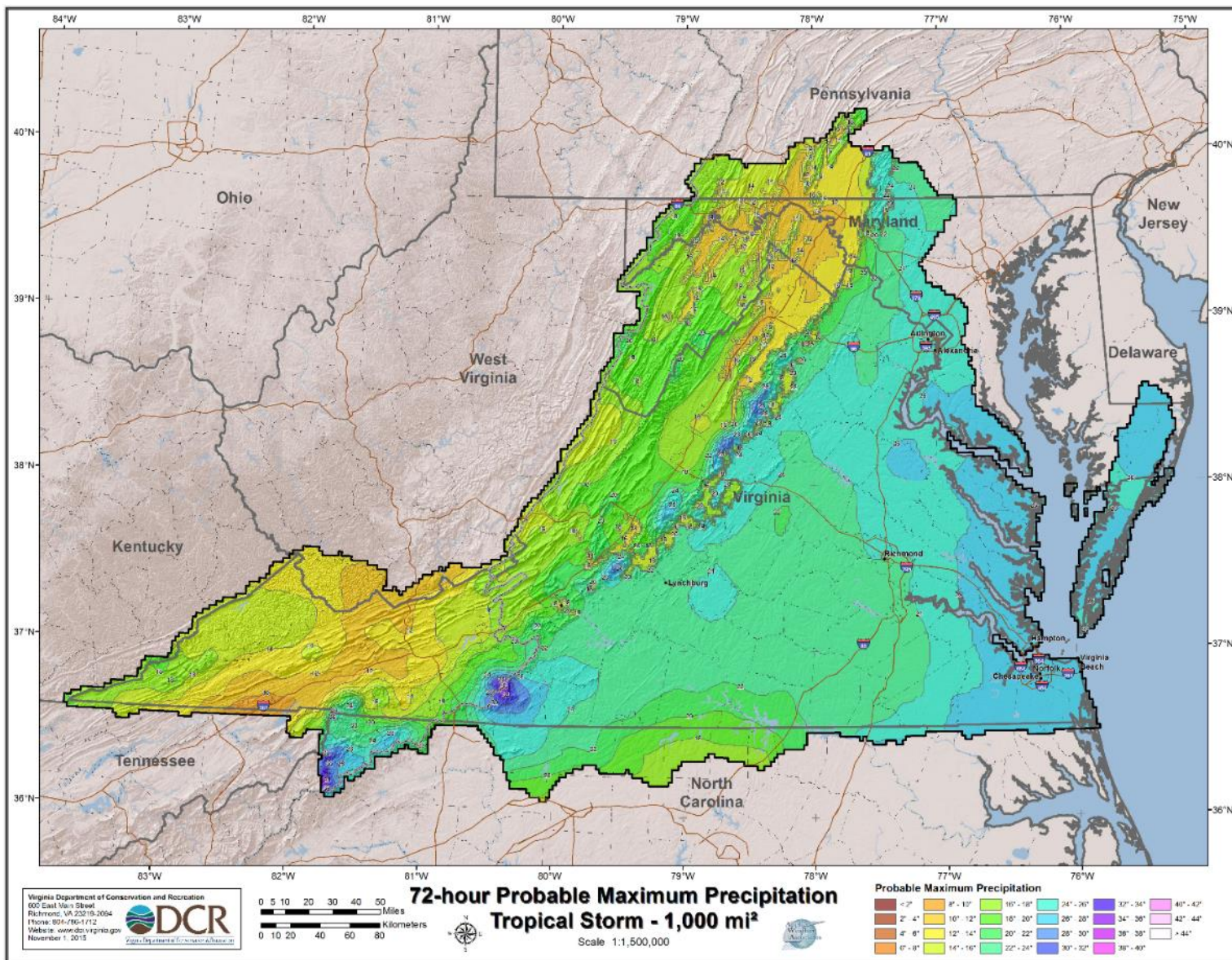


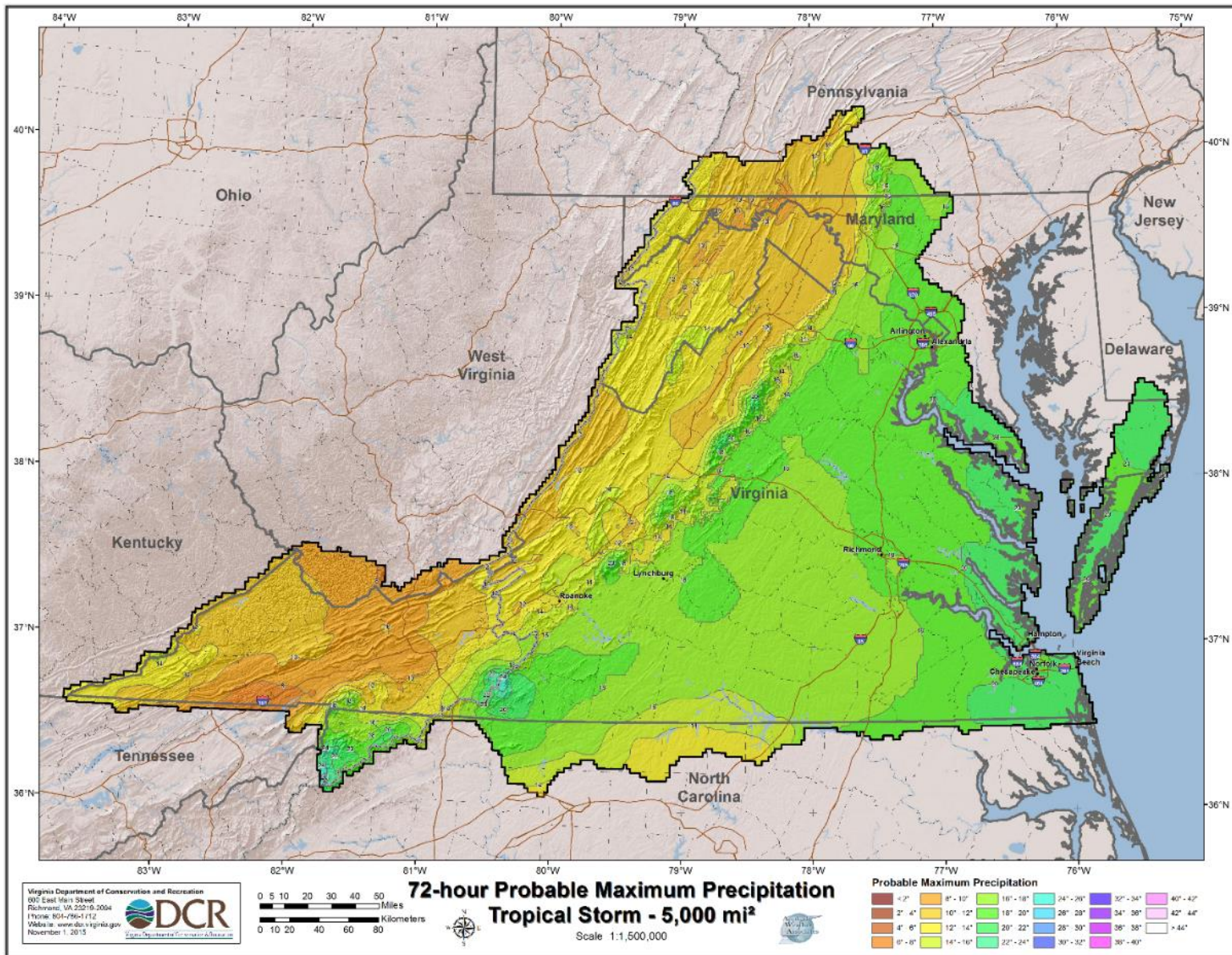


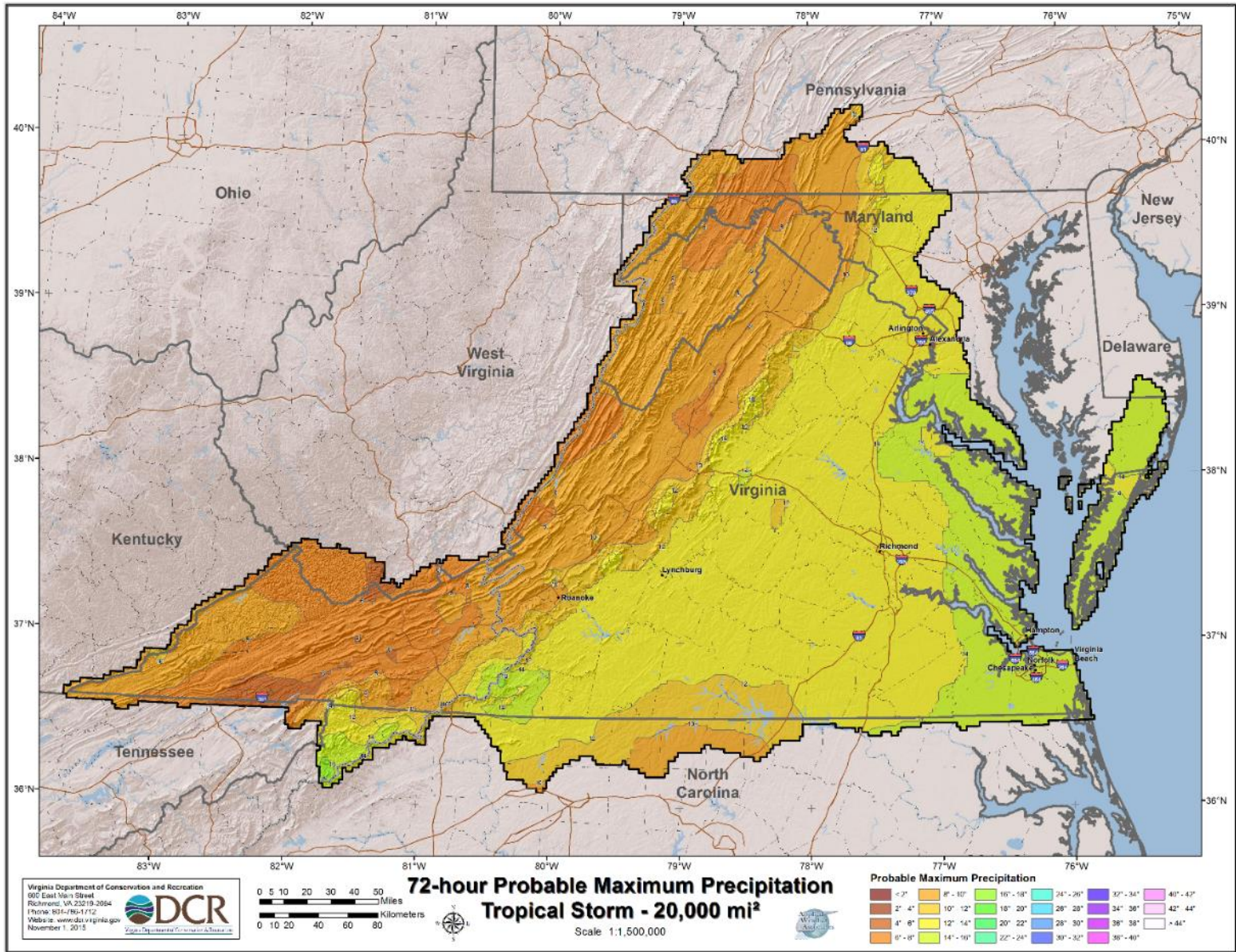










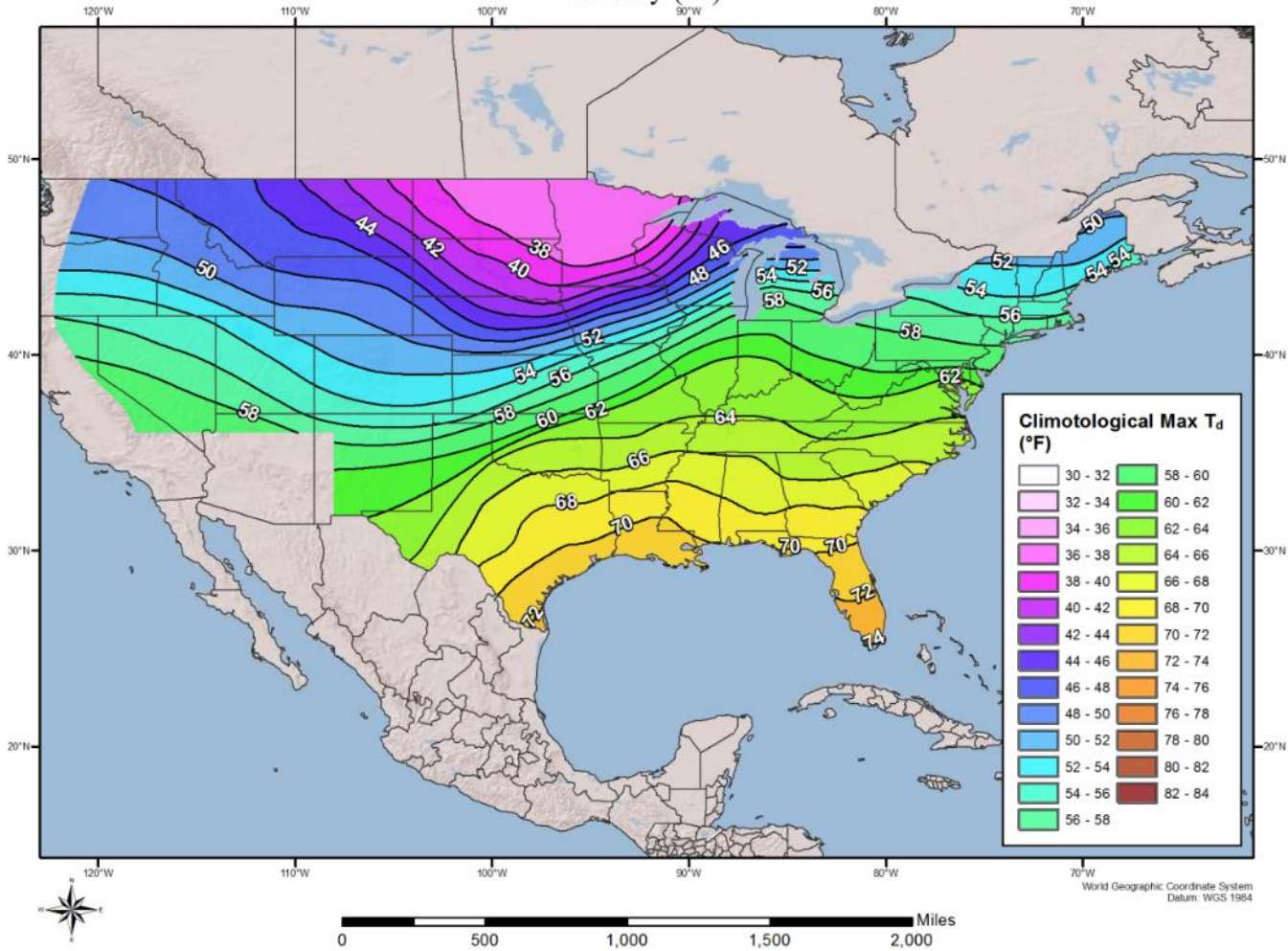


Appendix B

100-year Return Frequency Maximum Average Dew Point and SST Climatology Maps

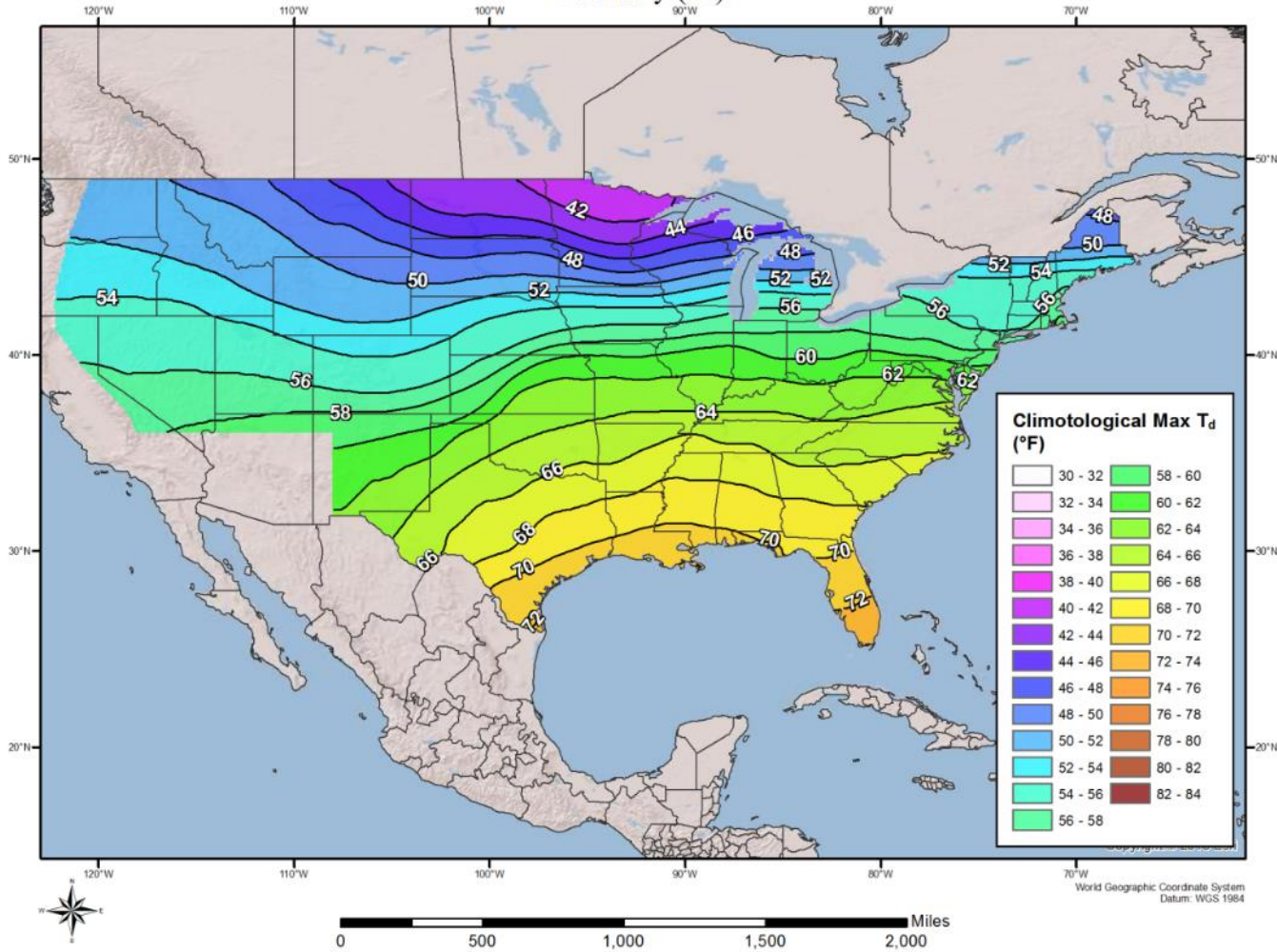
6-Hour, 100-year Recurrence Interval Dew Point Maps

6-hour Monthly Dew Point Climatology
January (°F)



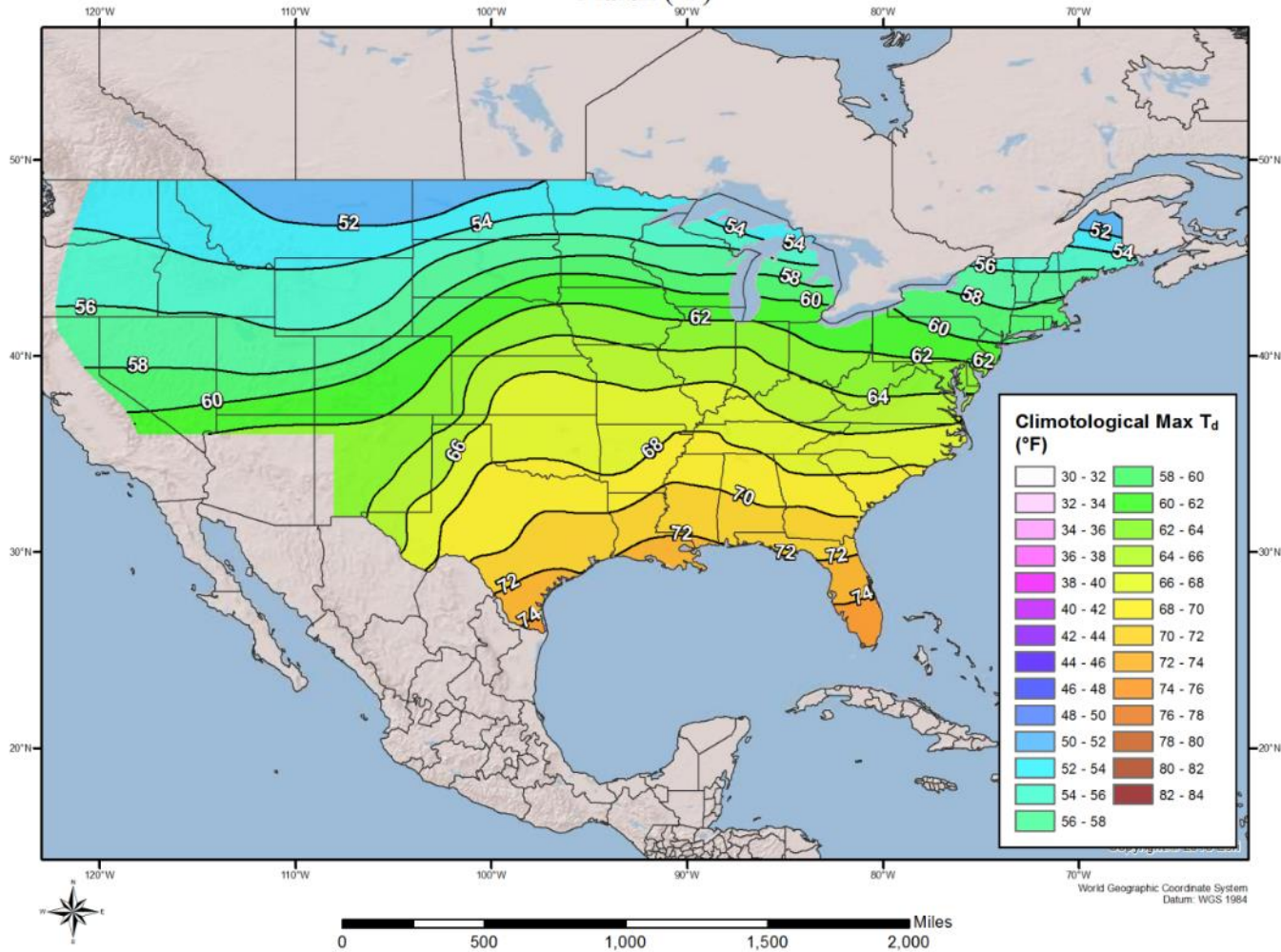
100-year Return Frequency 6-hour Maximum Dew Point Climatology - January

100-year Return Frequency 6-hour Maximum Dew Point Climatology
February (°F)



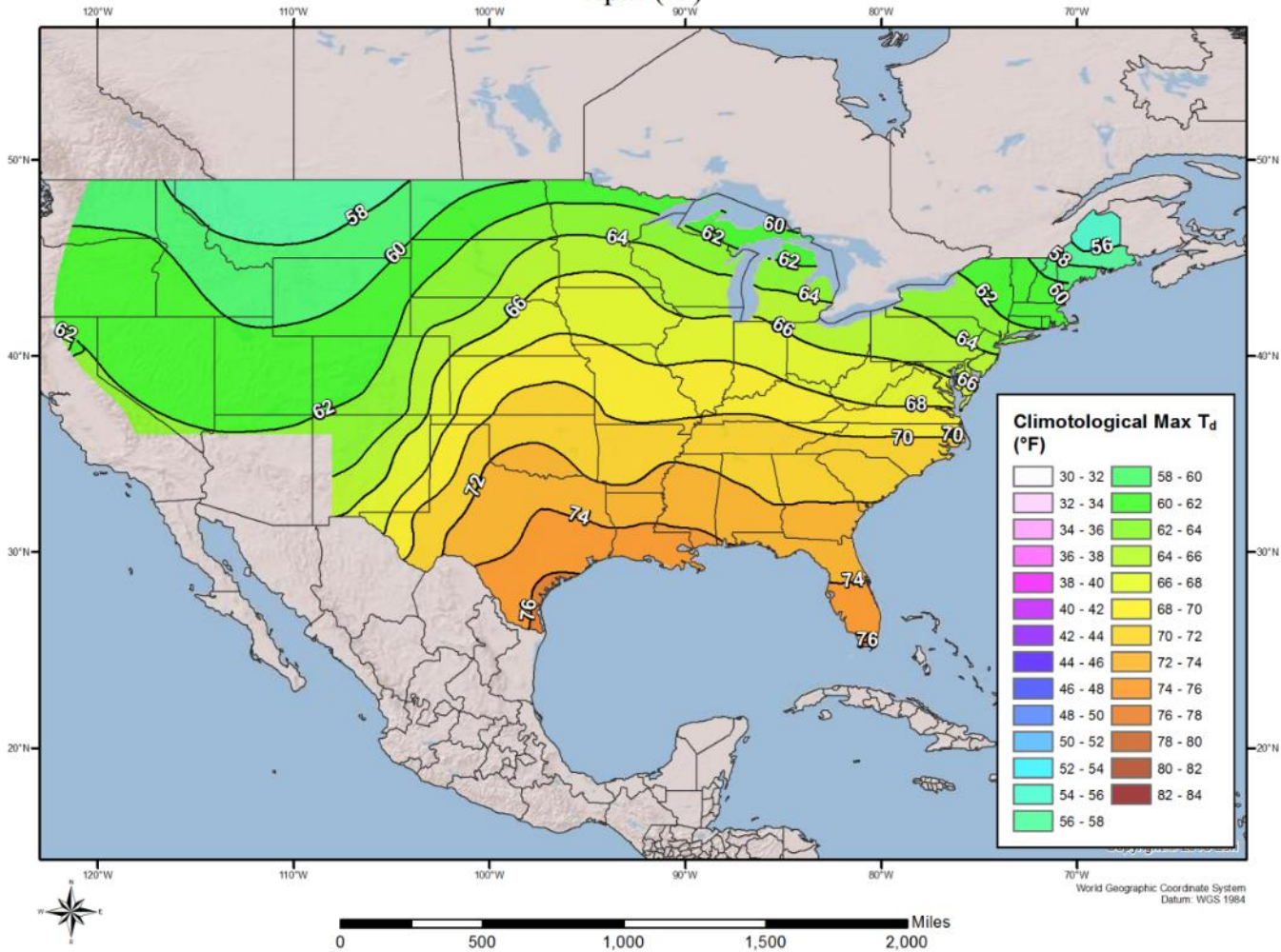
100-year Return Frequency 6-hour Maximum Dew Point Climatology - February

100-year Return Frequency 6-hour Maximum Dew Point Climatology
March (°F)



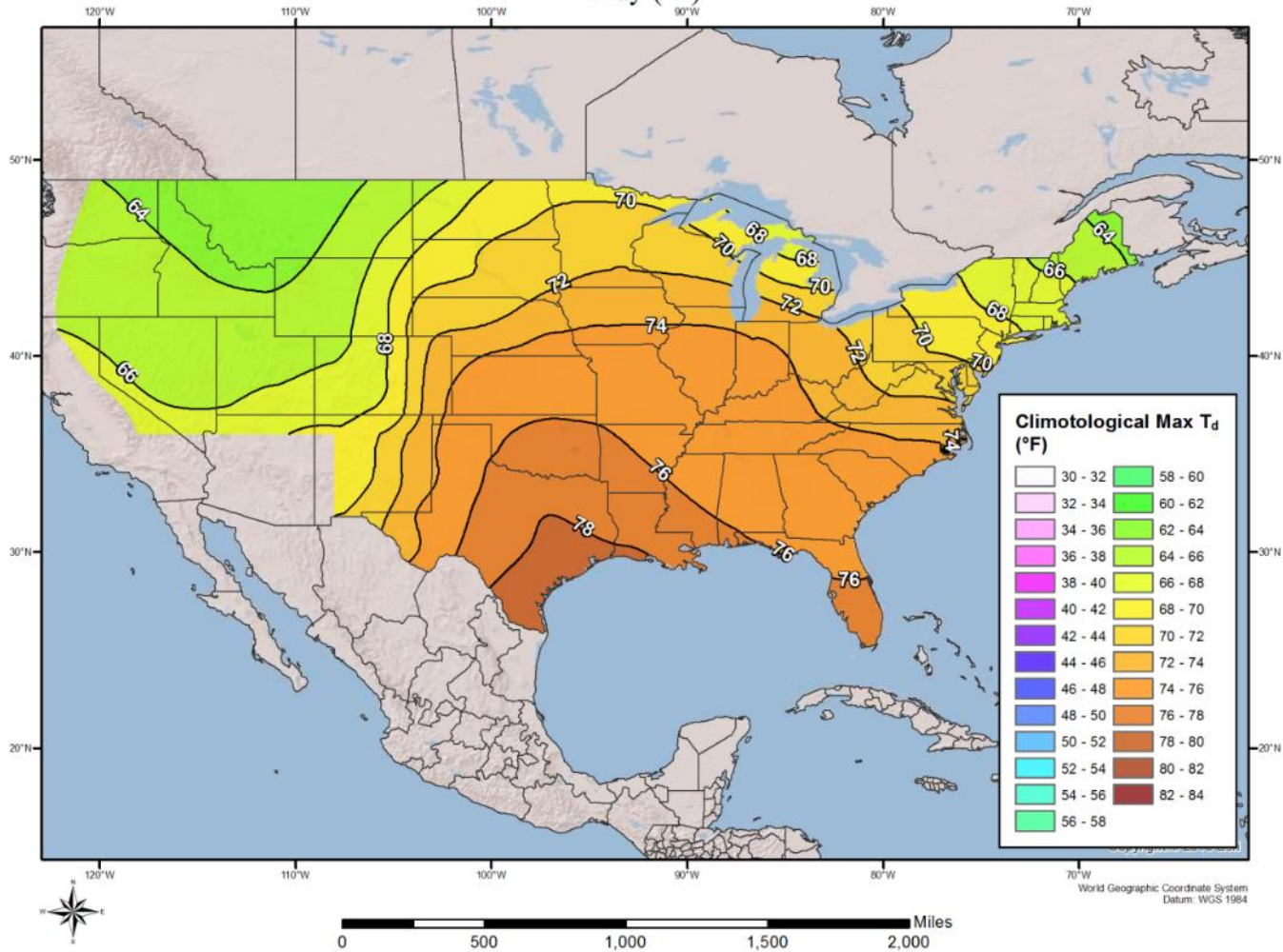
100-year Return Frequency 6-hour Maximum Dew Point Climatology - March

100-year Return Frequency 6-hour Maximum Dew Point Climatology
April (°F)



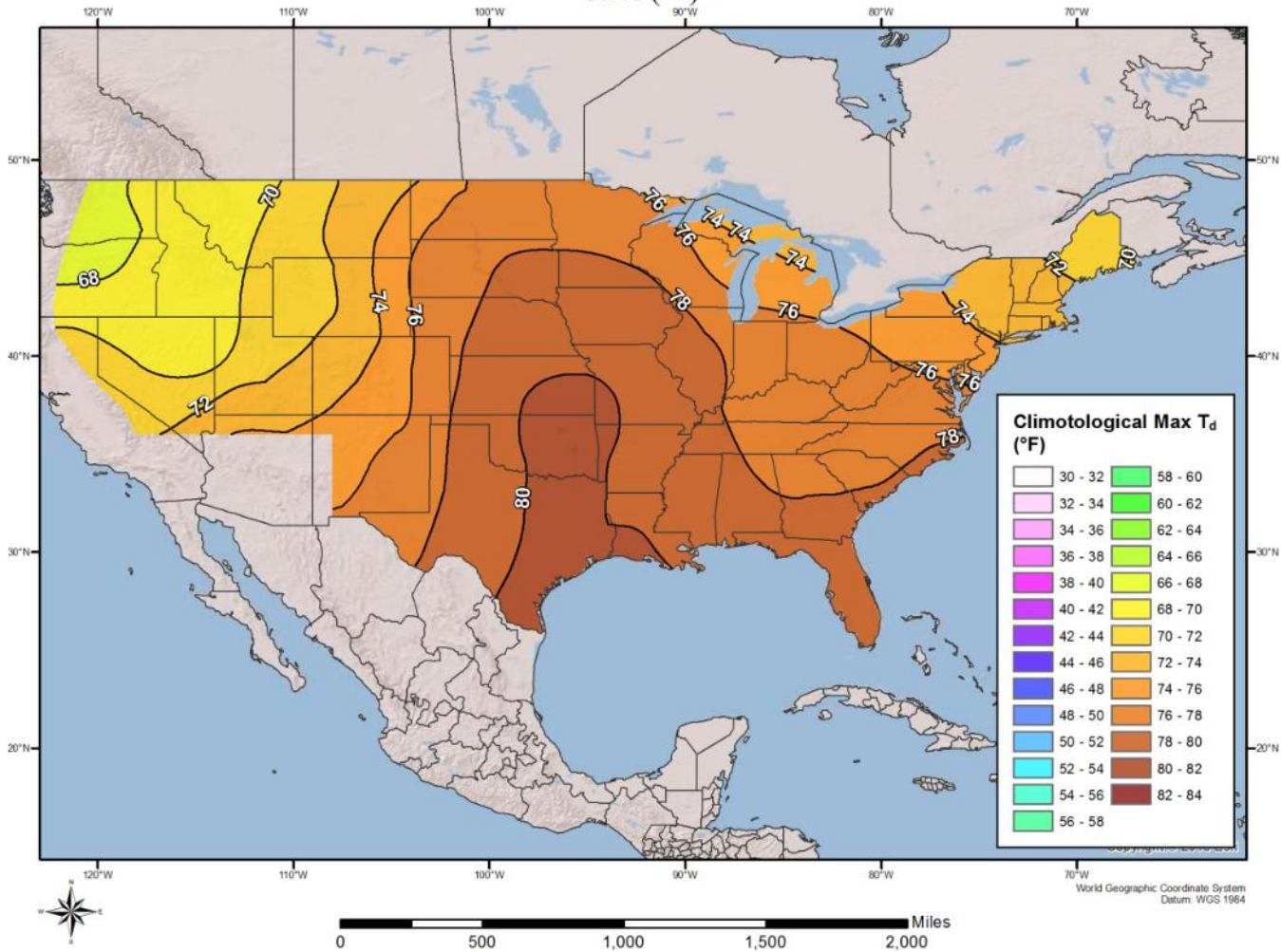
100-year Return Frequency 6-hour Maximum Dew Point Climatology - April

100-year Return Frequency 6-hour Maximum Dew Point Climatology
 May (°F)



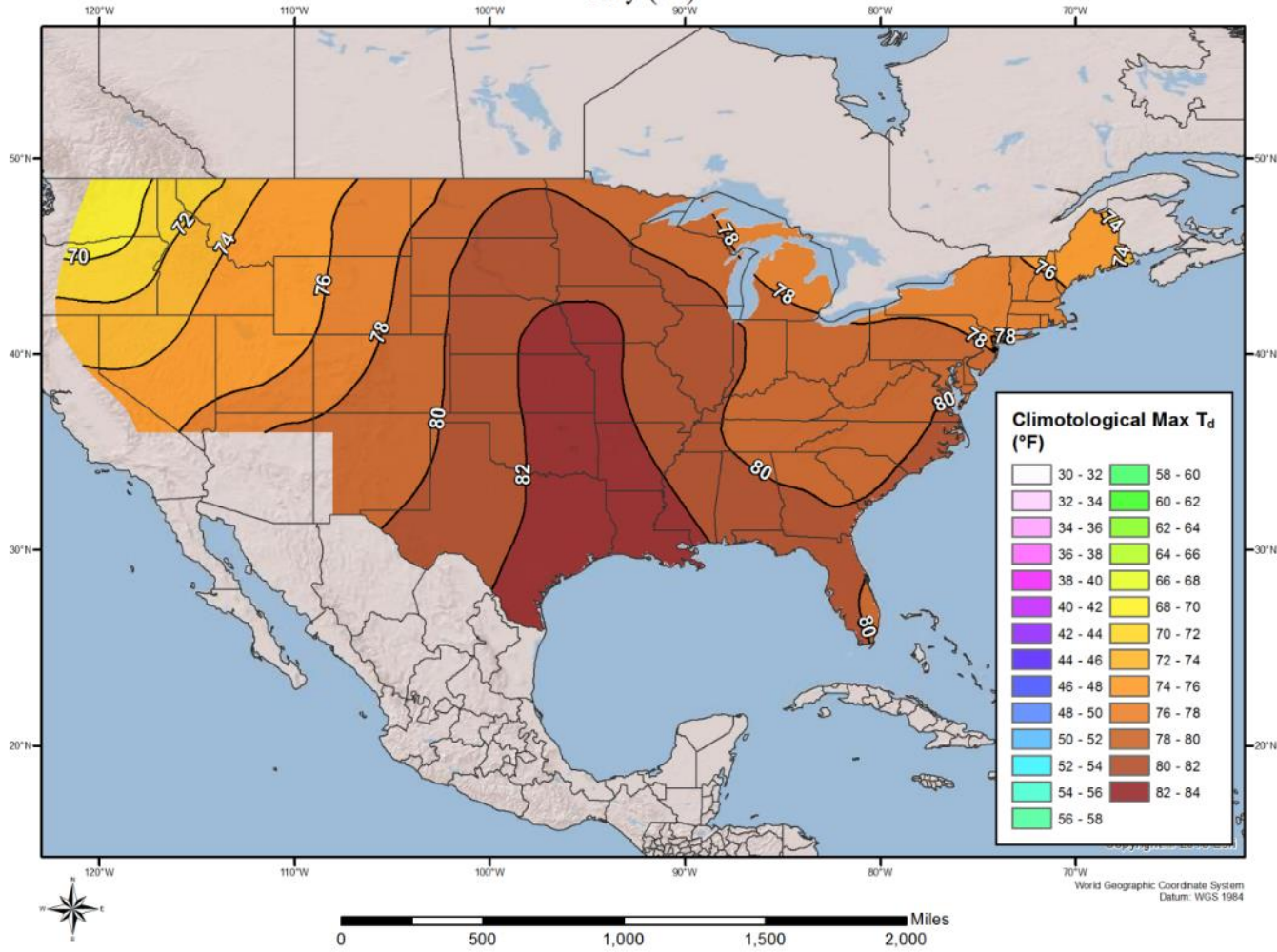
100-year Return Frequency 6-hour Maximum Dew Point Climatology - May

100-year Return Frequency 6-hour Maximum Dew Point Climatology
June (°F)



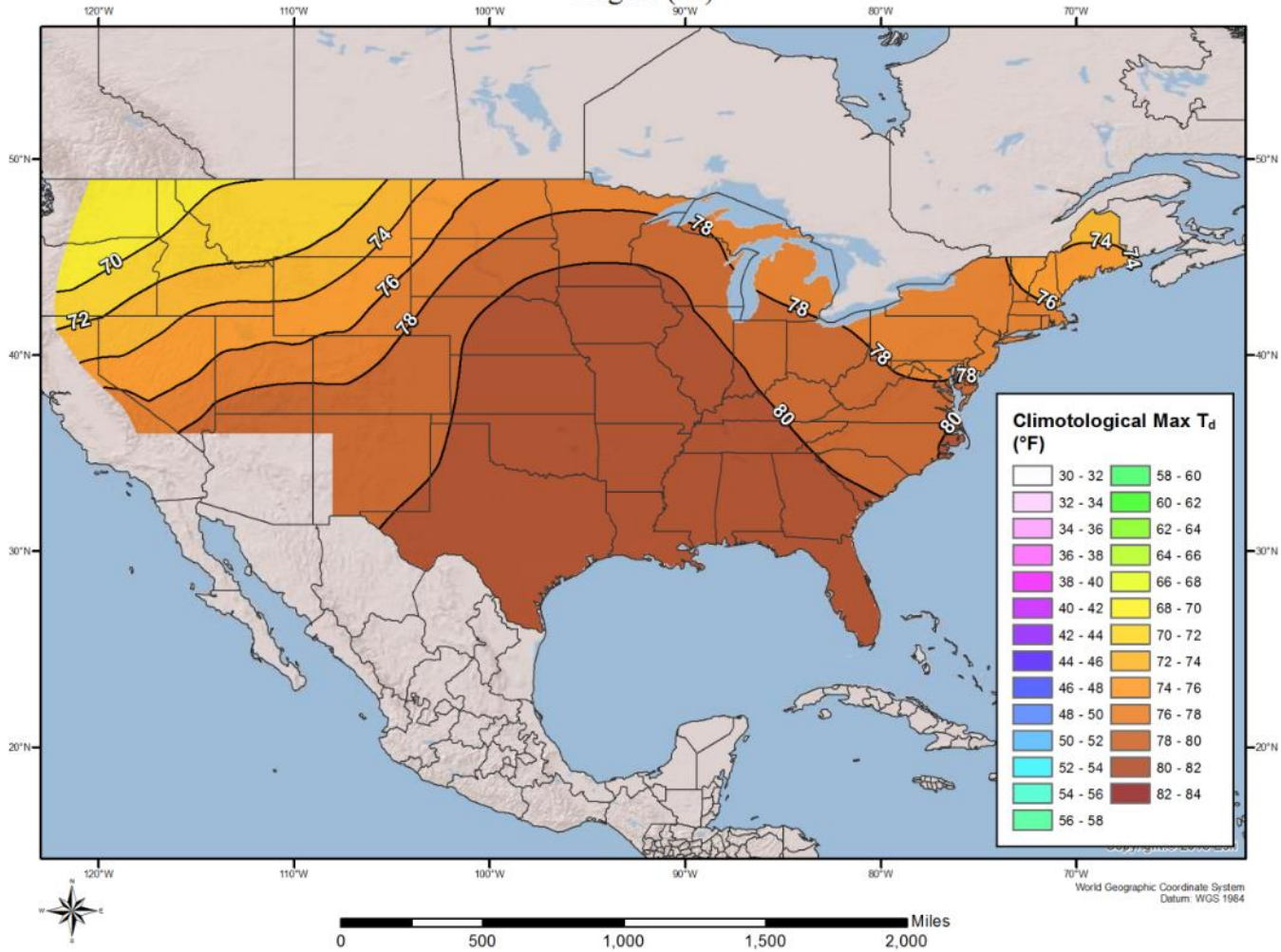
100-year Return Frequency 6-hour Maximum Dew Point Climatology - June

100-year Return Frequency 6-hour Maximum Dew Point Climatology
July (°F)



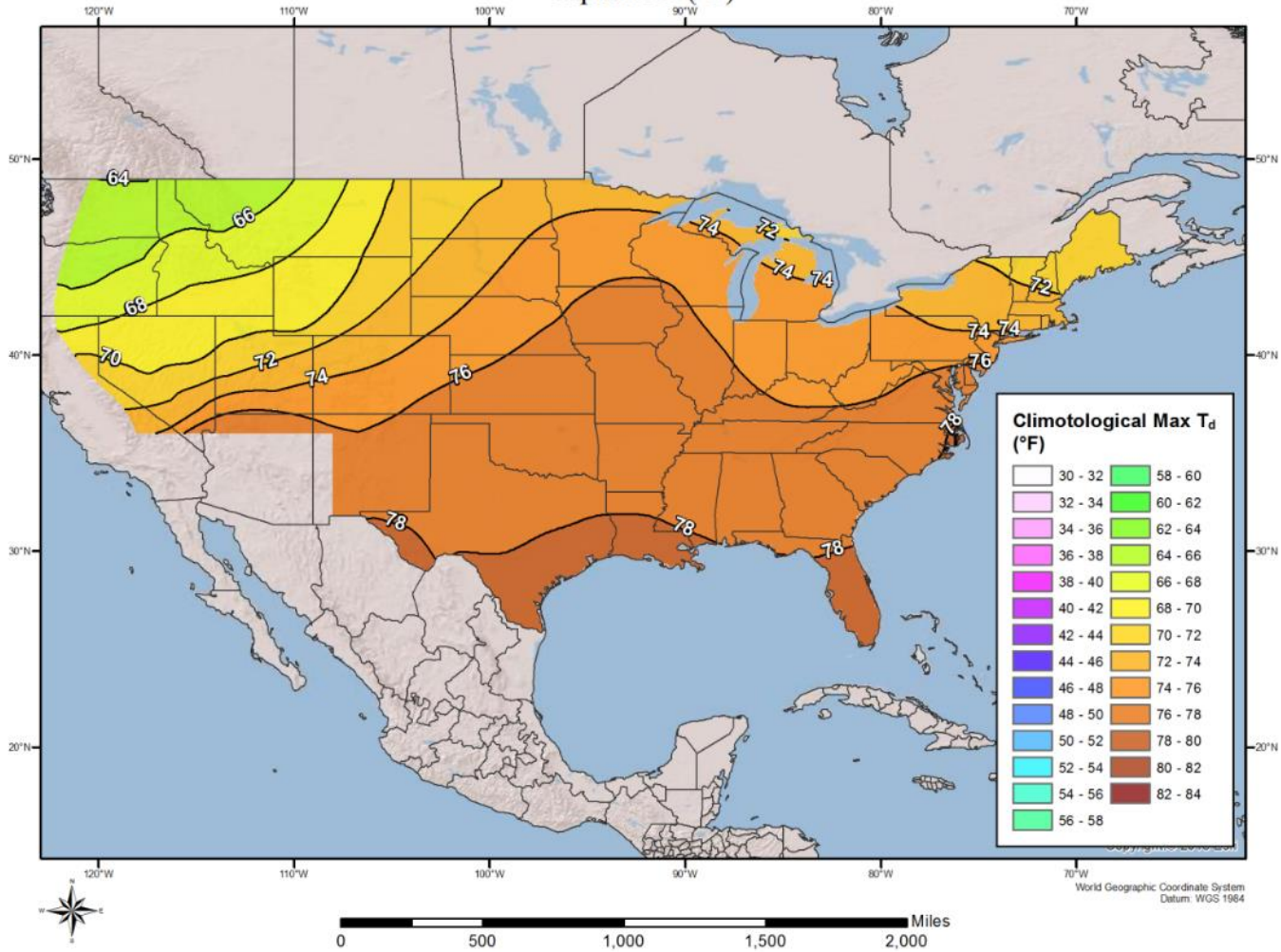
100-year Return Frequency 6-hour Maximum Dew Point Climatology - July

100-year Return Frequency 6-hour Maximum Dew Point Climatology
August (°F)



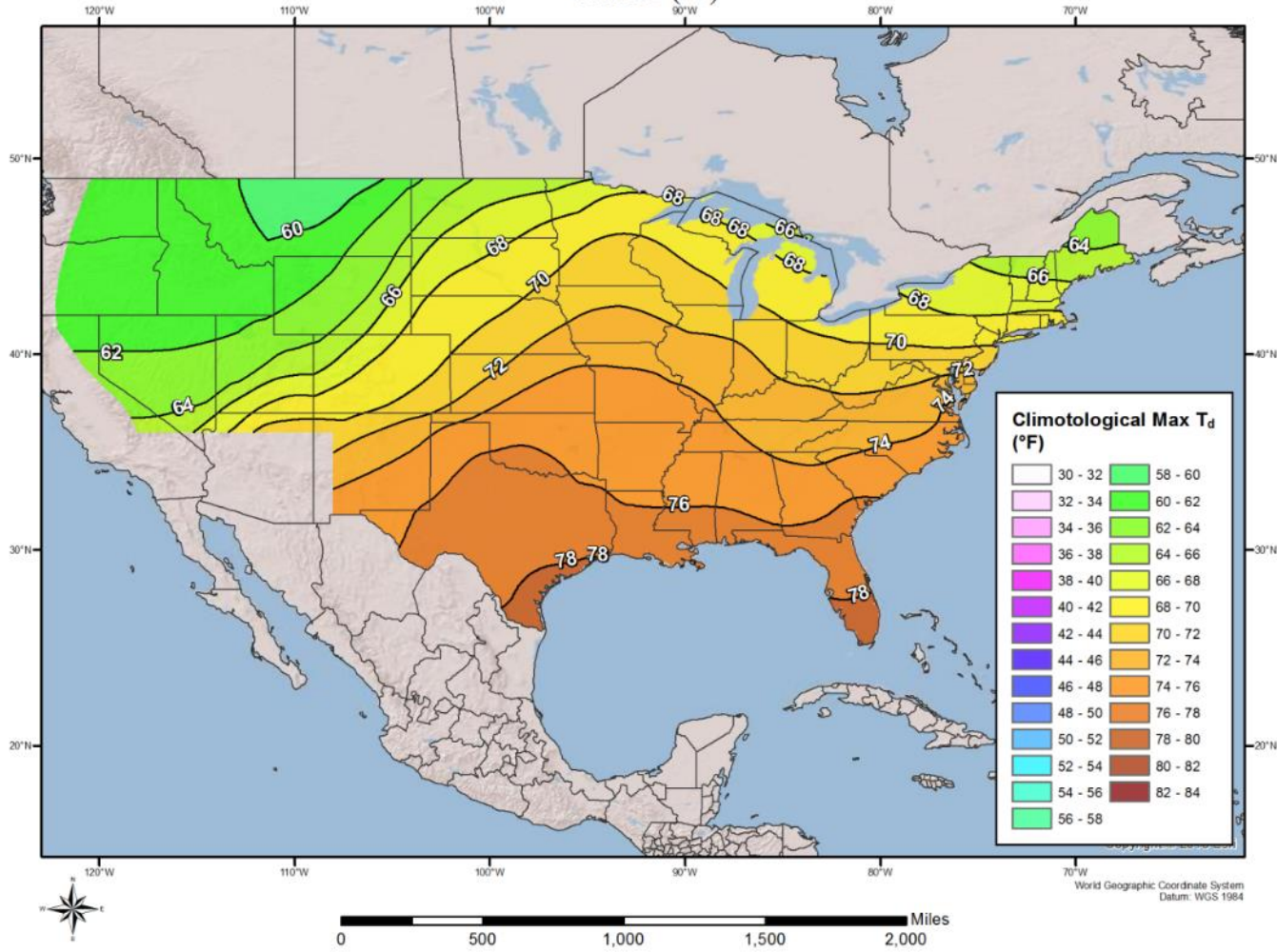
100-year Return Frequency 6-hour Maximum Dew Point Climatology - August

100-year Return Frequency 6-hour Maximum Dew Point Climatology
September (°F)



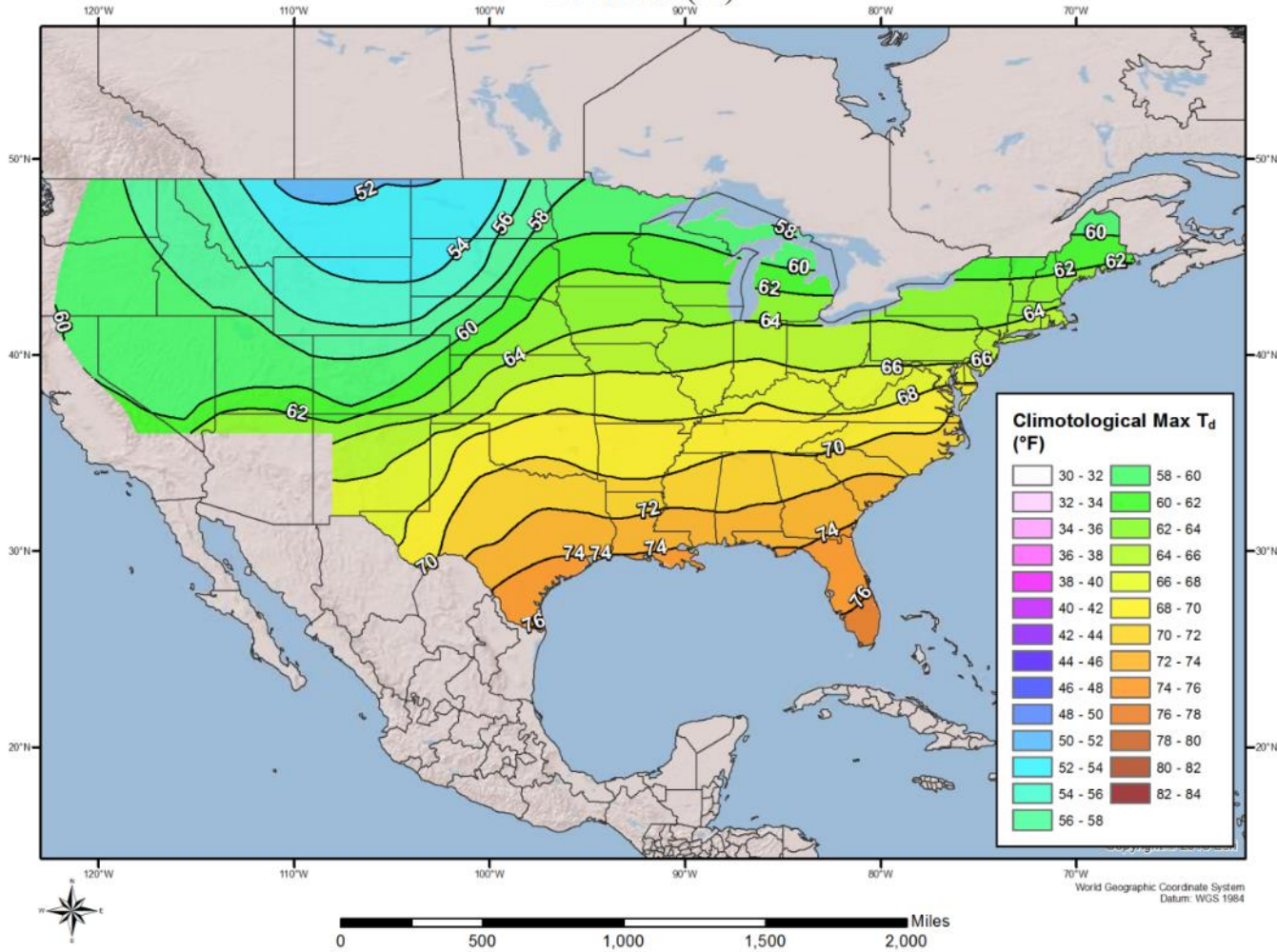
100-year Return Frequency 6-hour Maximum Dew Point Climatology - September

100-year Return Frequency 6-hour Maximum Dew Point Climatology
October (°F)



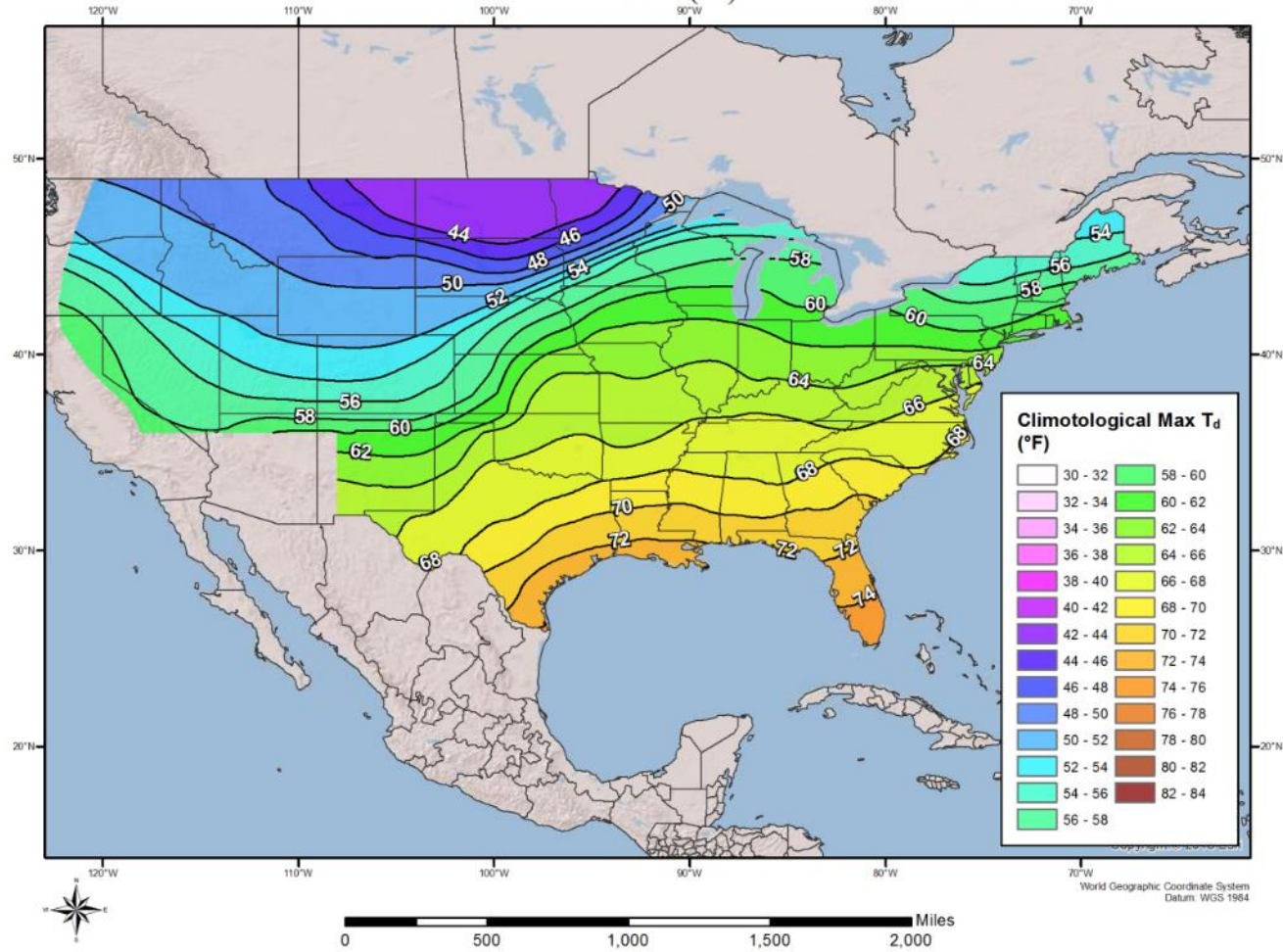
100-year Return Frequency 6-hour Maximum Dew Point Climatology - October

100-year Return Frequency 6-hour Maximum Dew Point Climatology
November (°F)



100-year Return Frequency 6-hour Maximum Dew Point Climatology - November

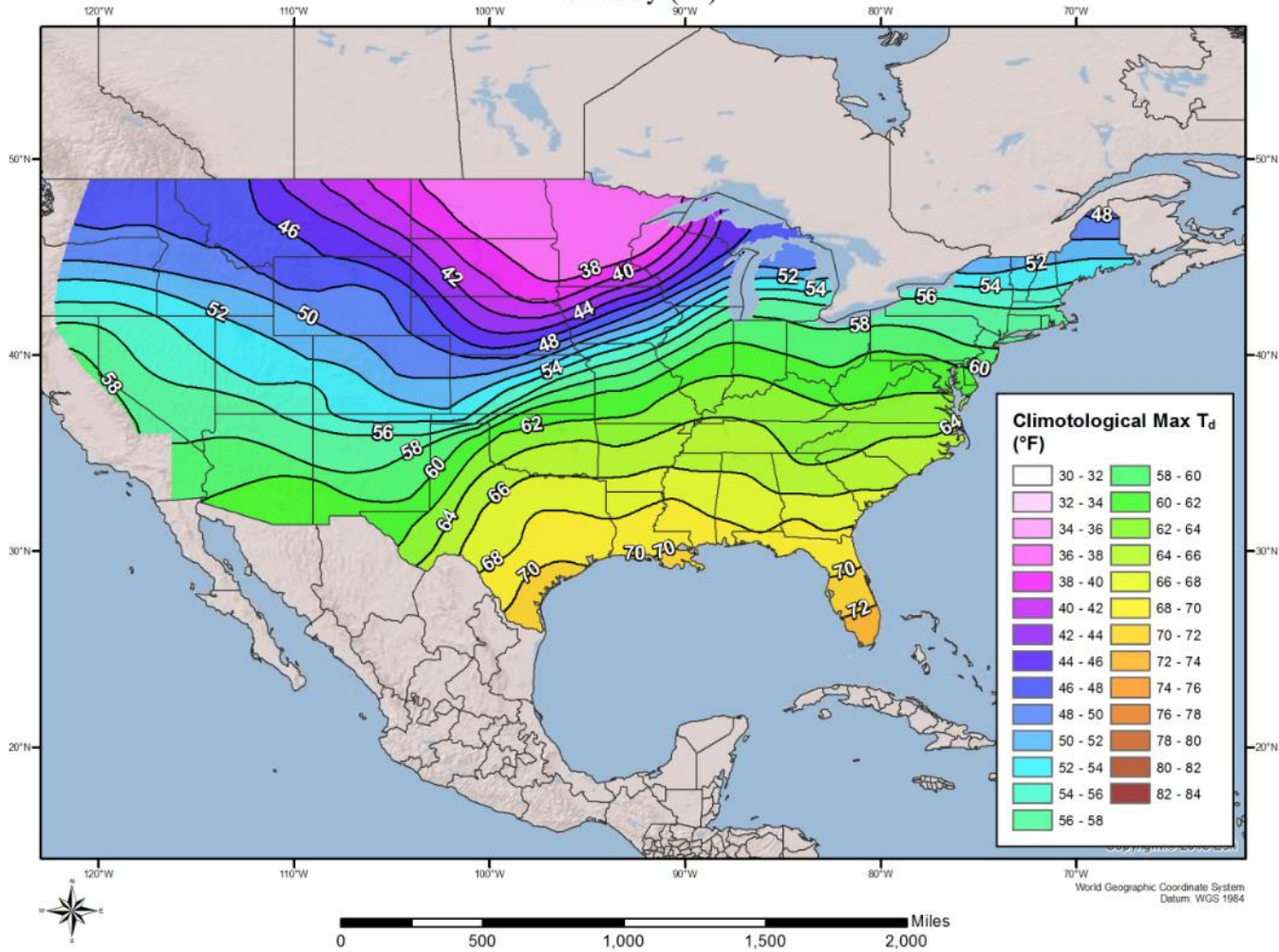
100-year Return Frequency 6-hour Maximum Dew Point Climatology
December (°F)



100-year Return Frequency 6-hour Maximum Dew Point Climatology - December

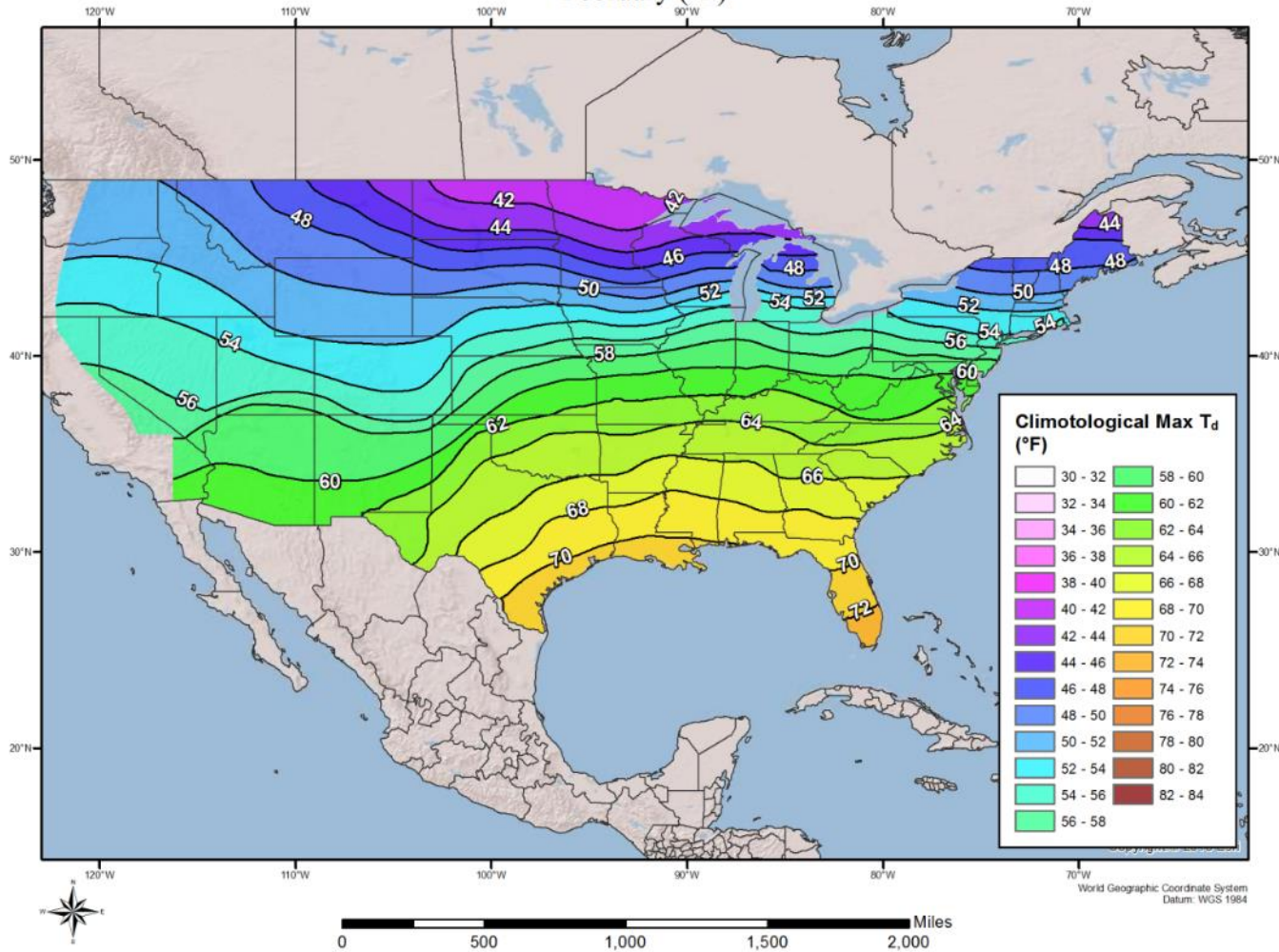
12-Hour, 100-year Dew Point Maps

100-year Return Frequency 12-hour Maximum Dew Point Climatology
January (°F)



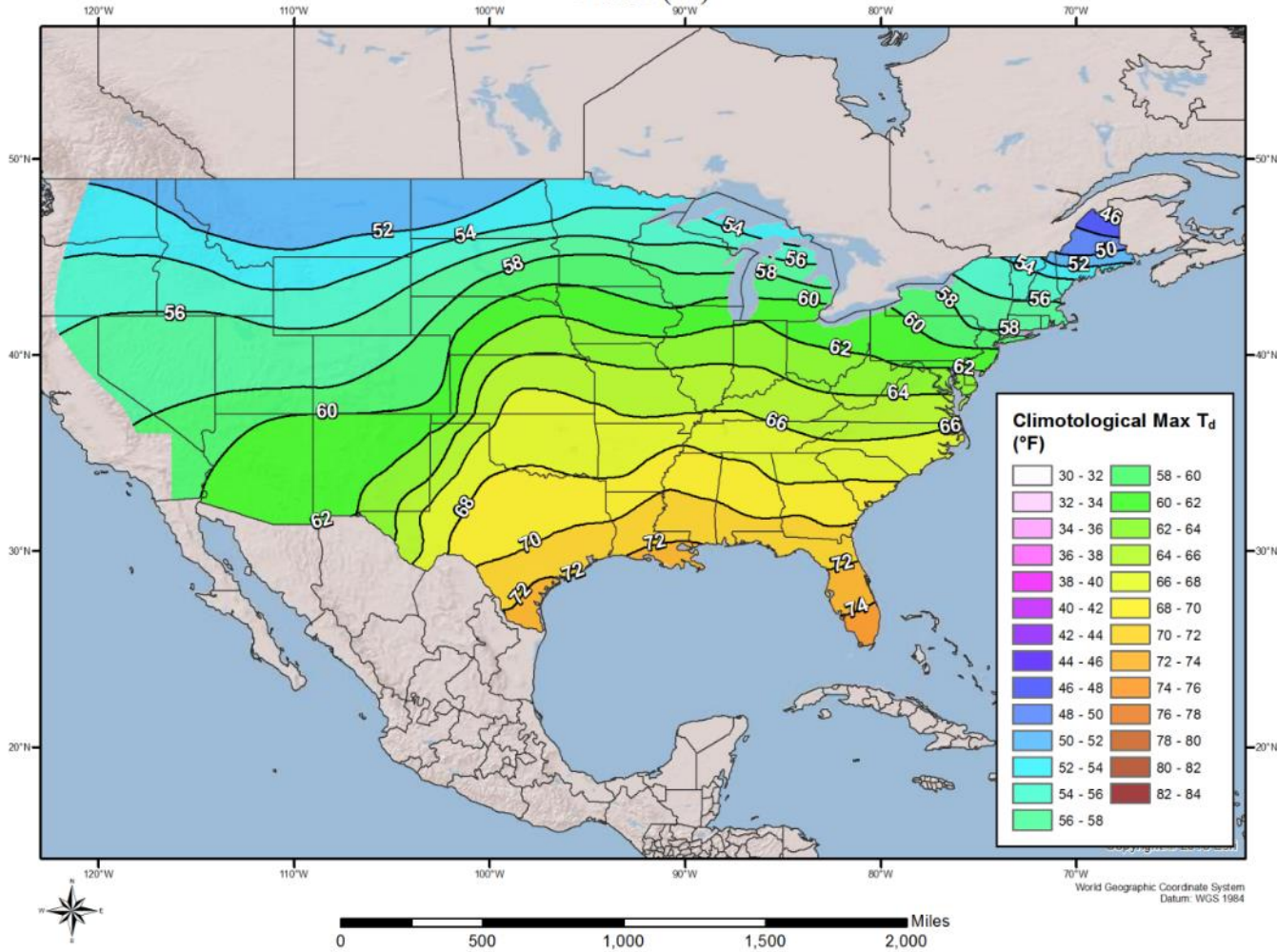
100-year Return Frequency 12-hour Maximum Dew Point Climatology - January

100-year Return Frequency 12-hour Maximum Dew Point Climatology
February (°F)



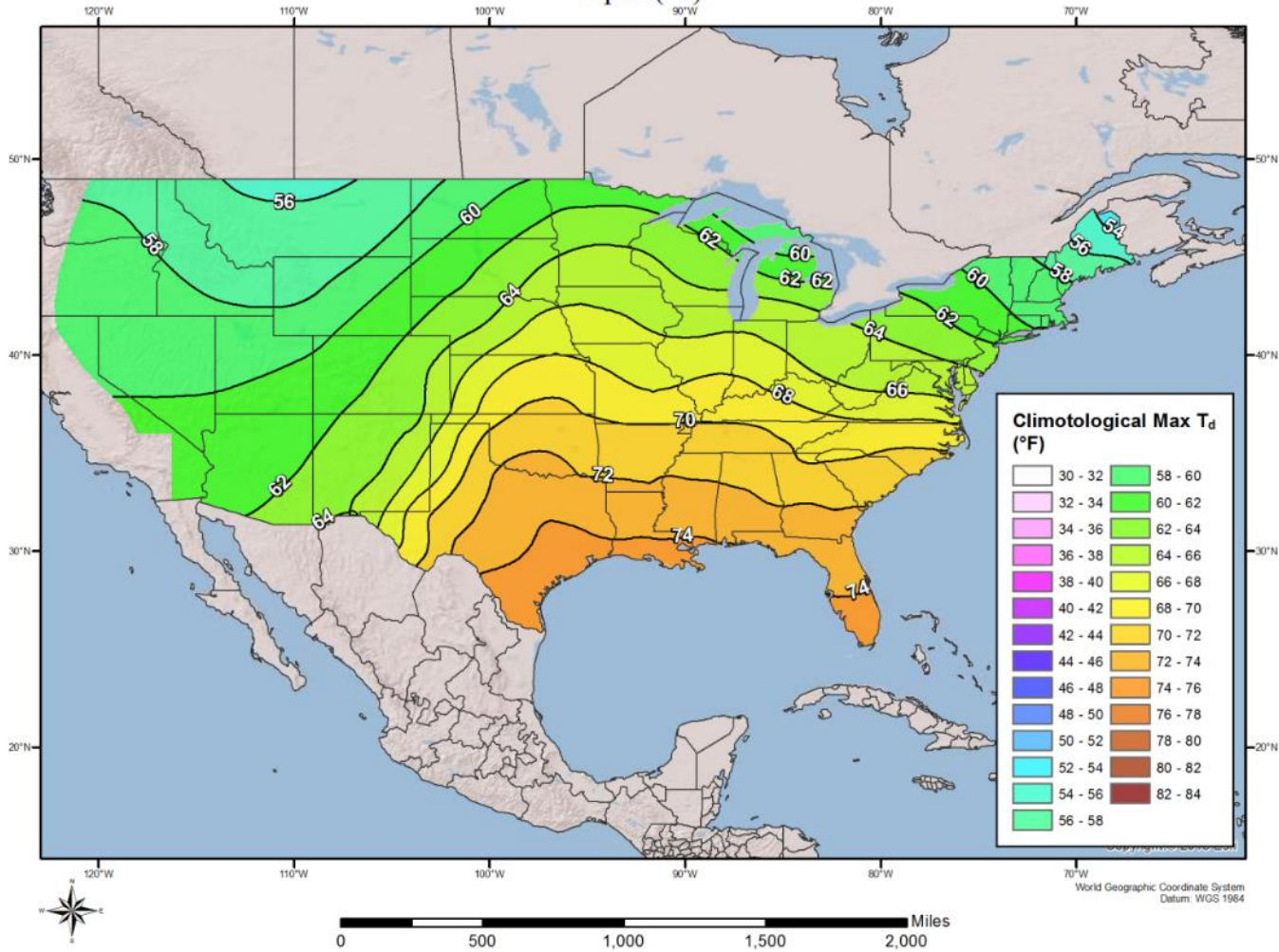
100-year Return Frequency 12-hour Maximum Dew Point Climatology - February

100-year Return Frequency 12-hour Maximum Dew Point Climatology
 March (°F)



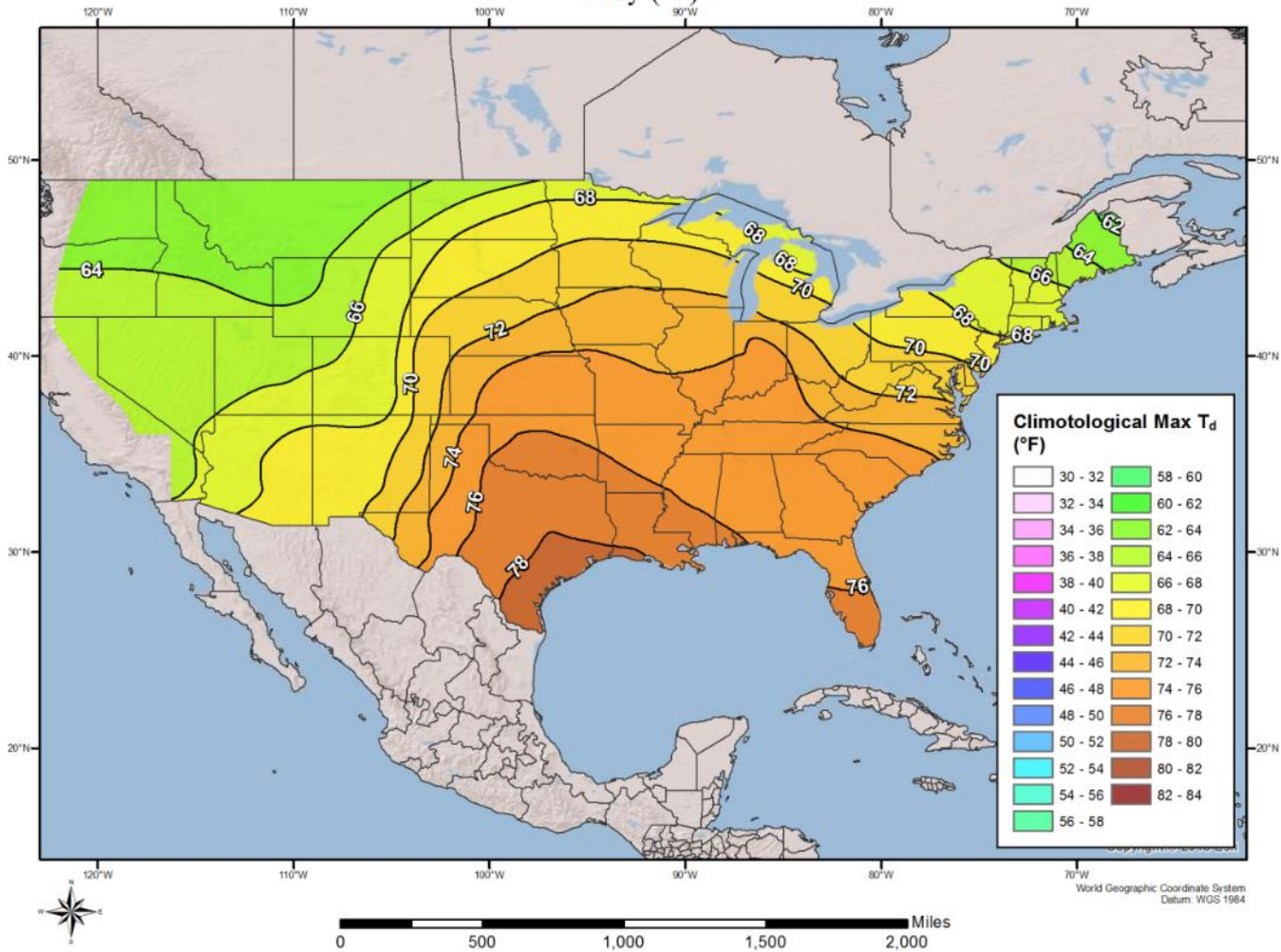
100-year Return Frequency 12-hour Maximum Dew Point Climatology - March

100-year Return Frequency 12-hour Maximum Dew Point Climatology
April (°F)



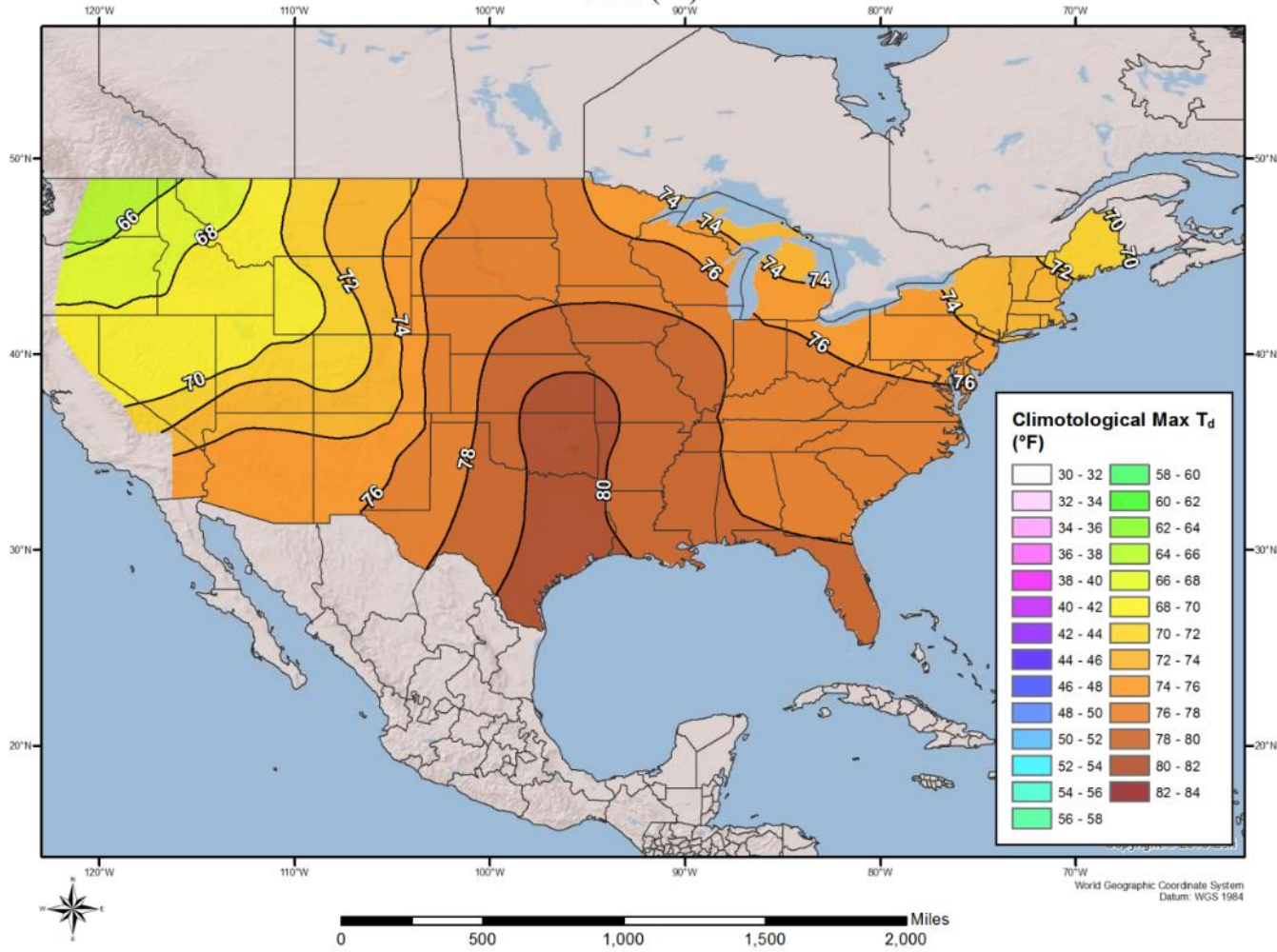
100-year Return Frequency 12-hour Maximum Dew Point Climatology - April

100-year Return Frequency 12-hour Maximum Dew Point Climatology
 May (°F)



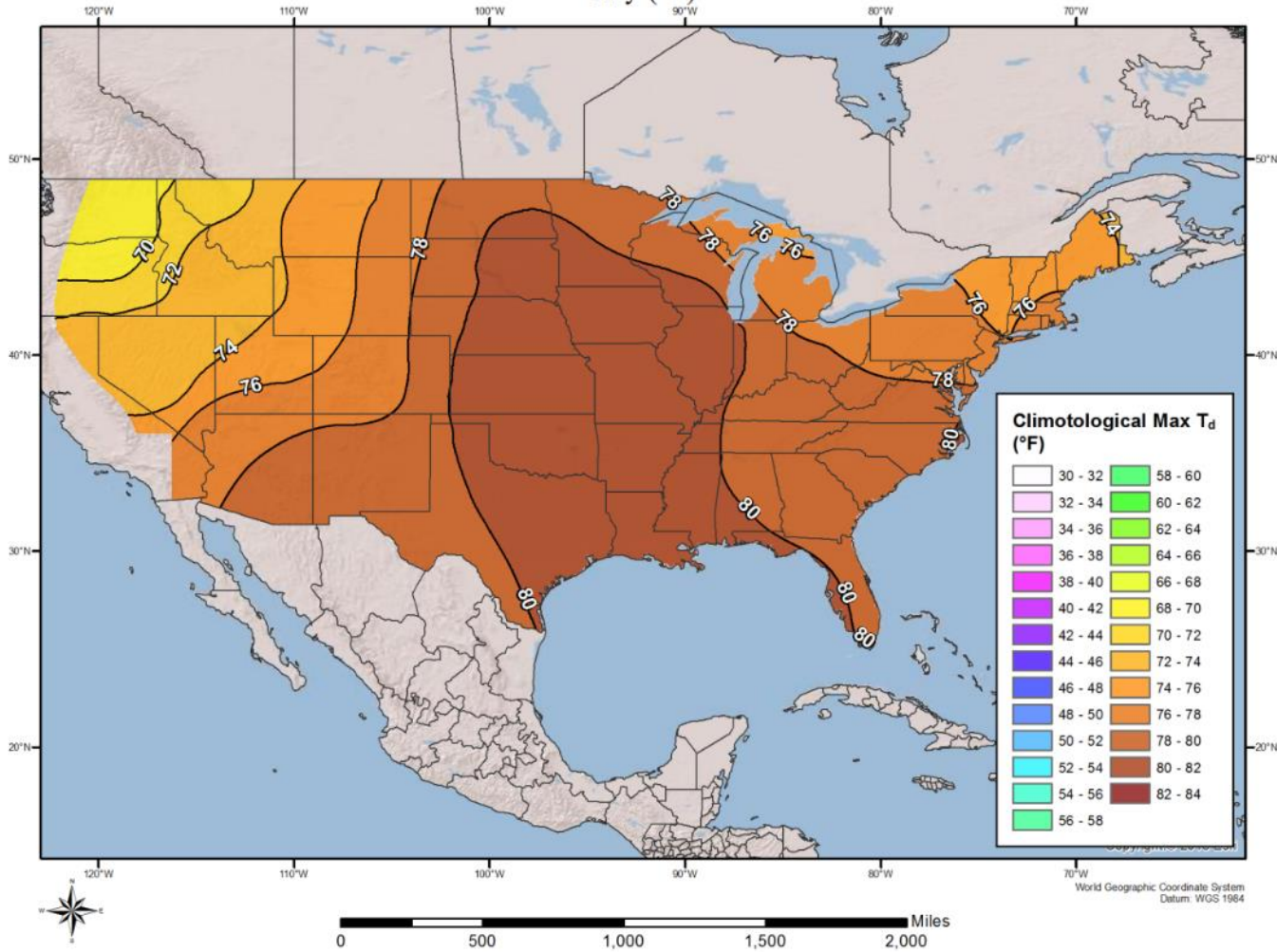
100-year Return Frequency 12-hour Maximum Dew Point Climatology - May

100-year Return Frequency 12-hour Maximum Dew Point Climatology
June (°F)



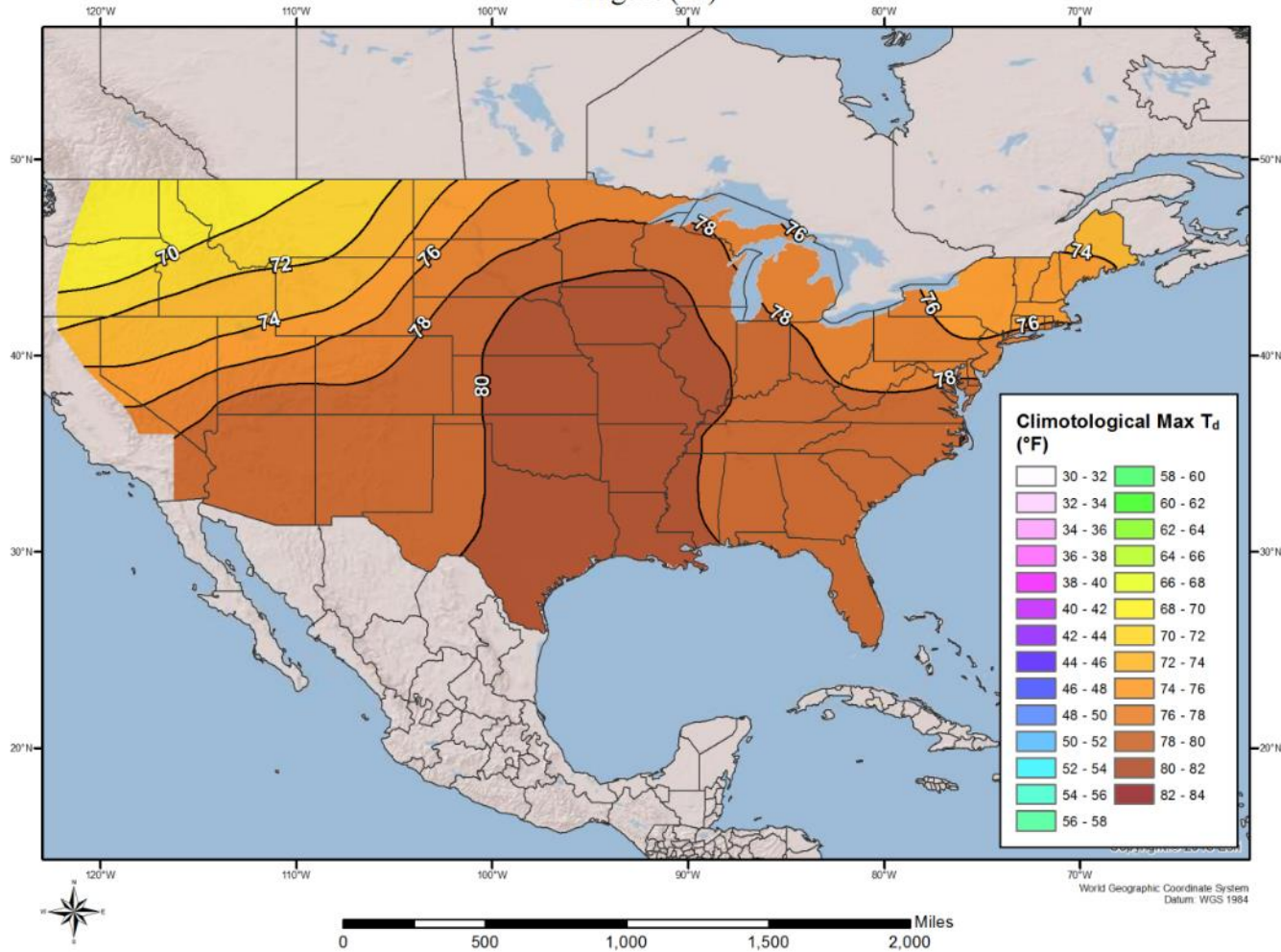
100-year Return Frequency 12-hour Maximum Dew Point Climatology - June

100-year Return Frequency 12-hour Maximum Dew Point Climatology
July (°F)



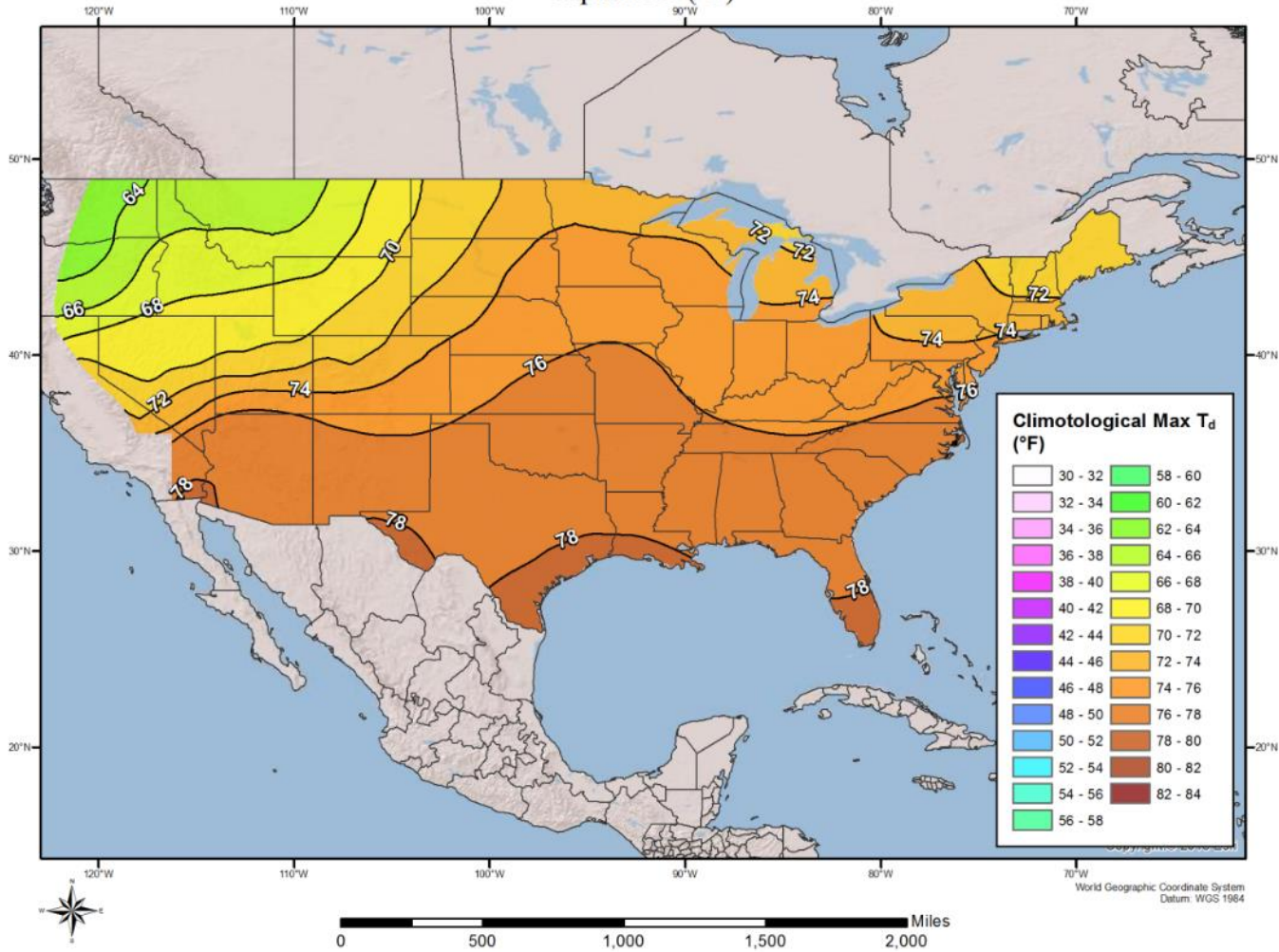
100-year Return Frequency 12-hour Maximum Dew Point Climatology - July

100-year Return Frequency 12-hour Maximum Dew Point Climatology
August (°F)



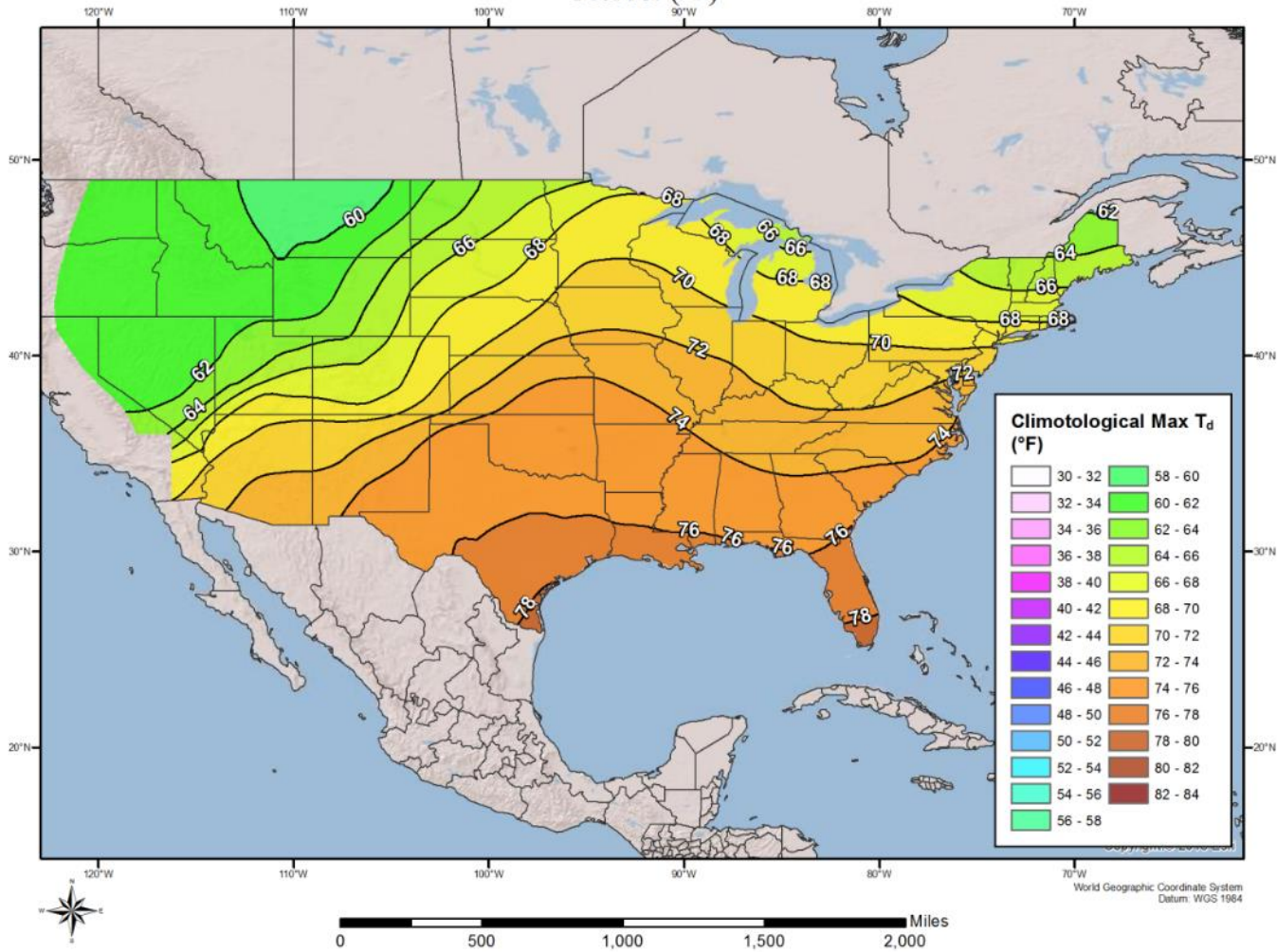
100-year Return Frequency 12-hour Maximum Dew Point Climatology - August

100-year Return Frequency 12-hour Maximum Dew Point Climatology
September (°F)



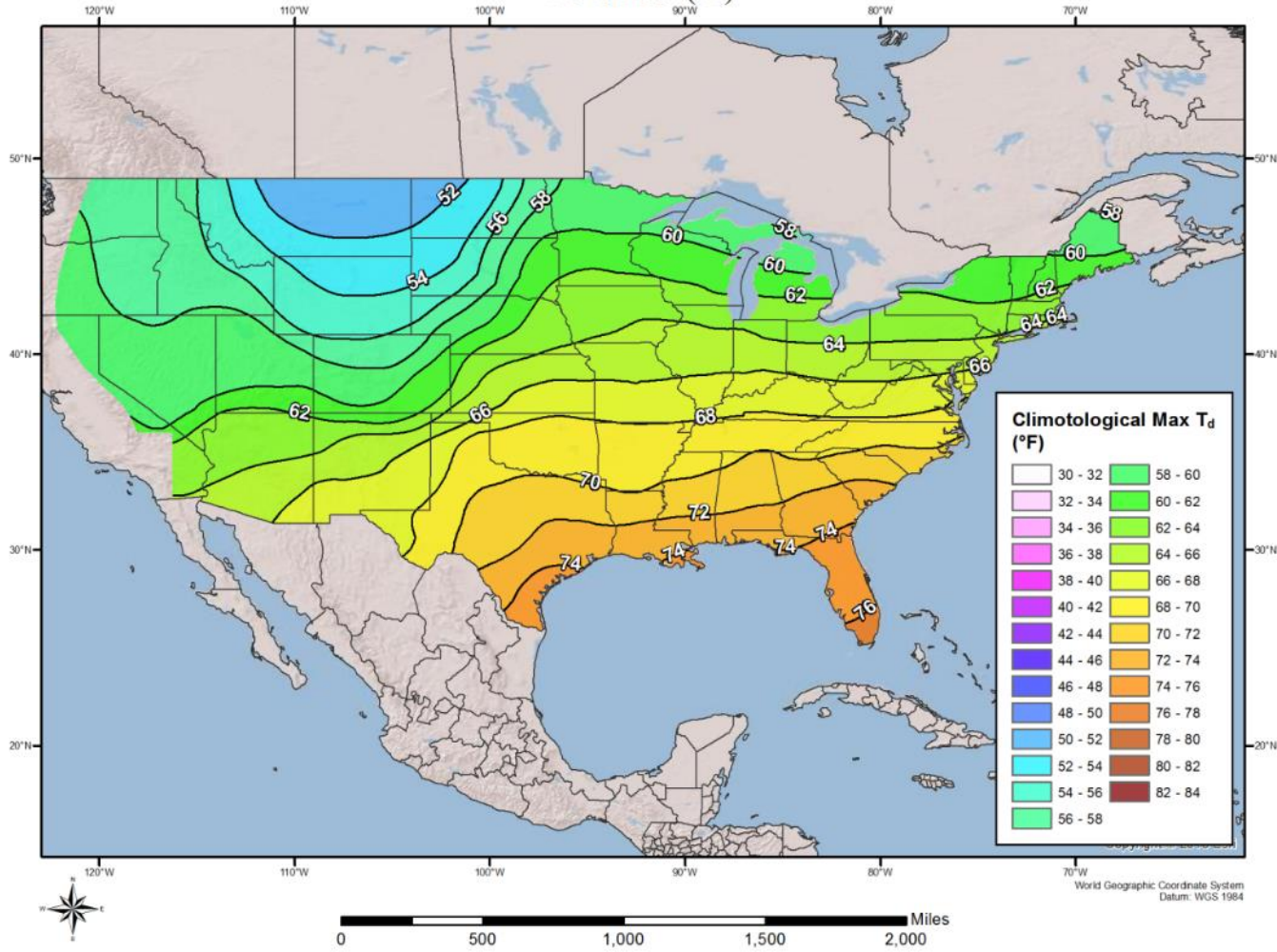
100-year Return Frequency 12-hour Maximum Dew Point Climatology - September

100-year Return Frequency 12-hour Maximum Dew Point Climatology
October (°F)



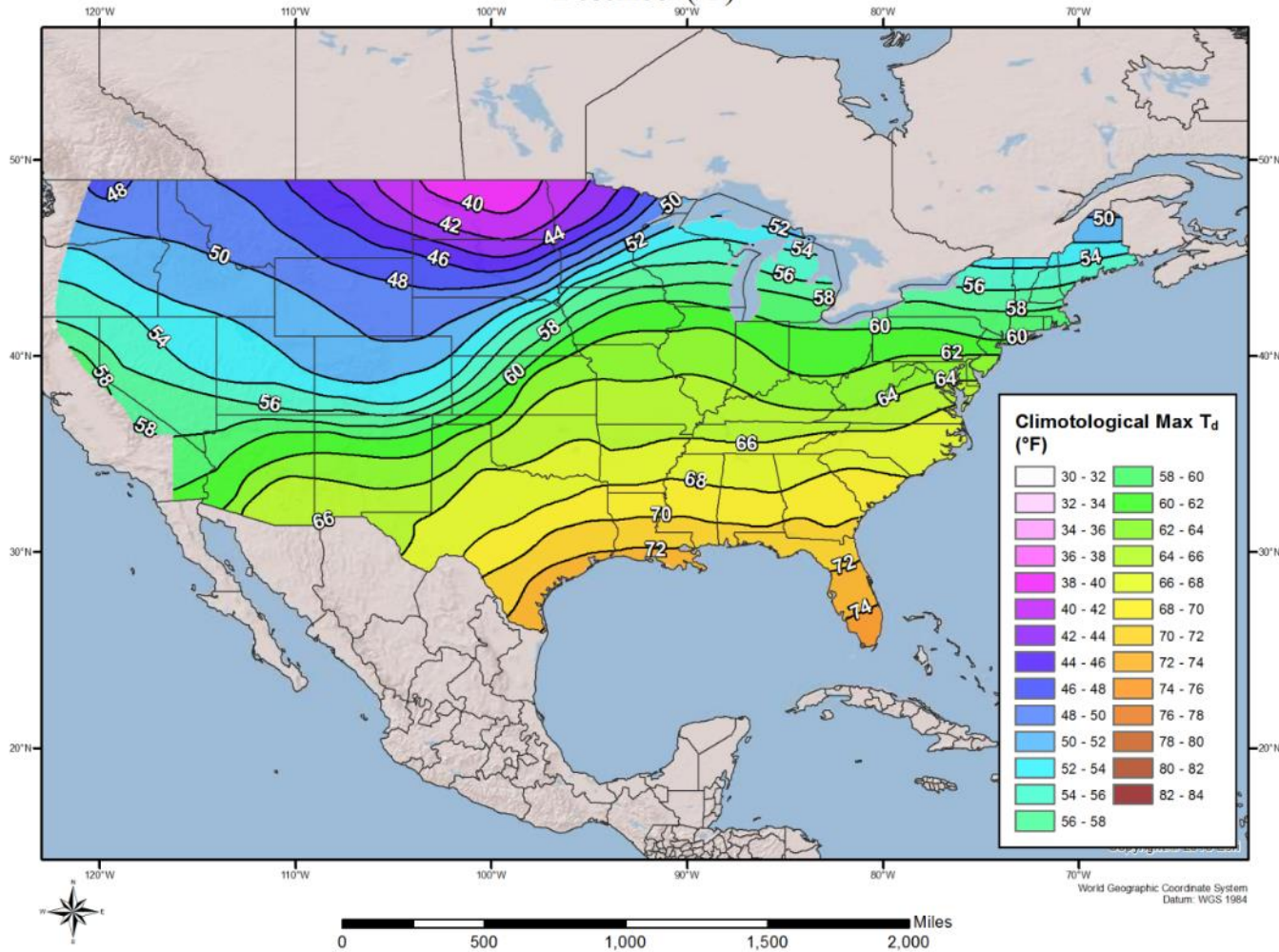
100-year Return Frequency 12-hour Maximum Dew Point Climatology - October

100-year Return Frequency 12-hour Maximum Dew Point Climatology
November (°F)



100-year Return Frequency 12-hour Maximum Dew Point Climatology - November

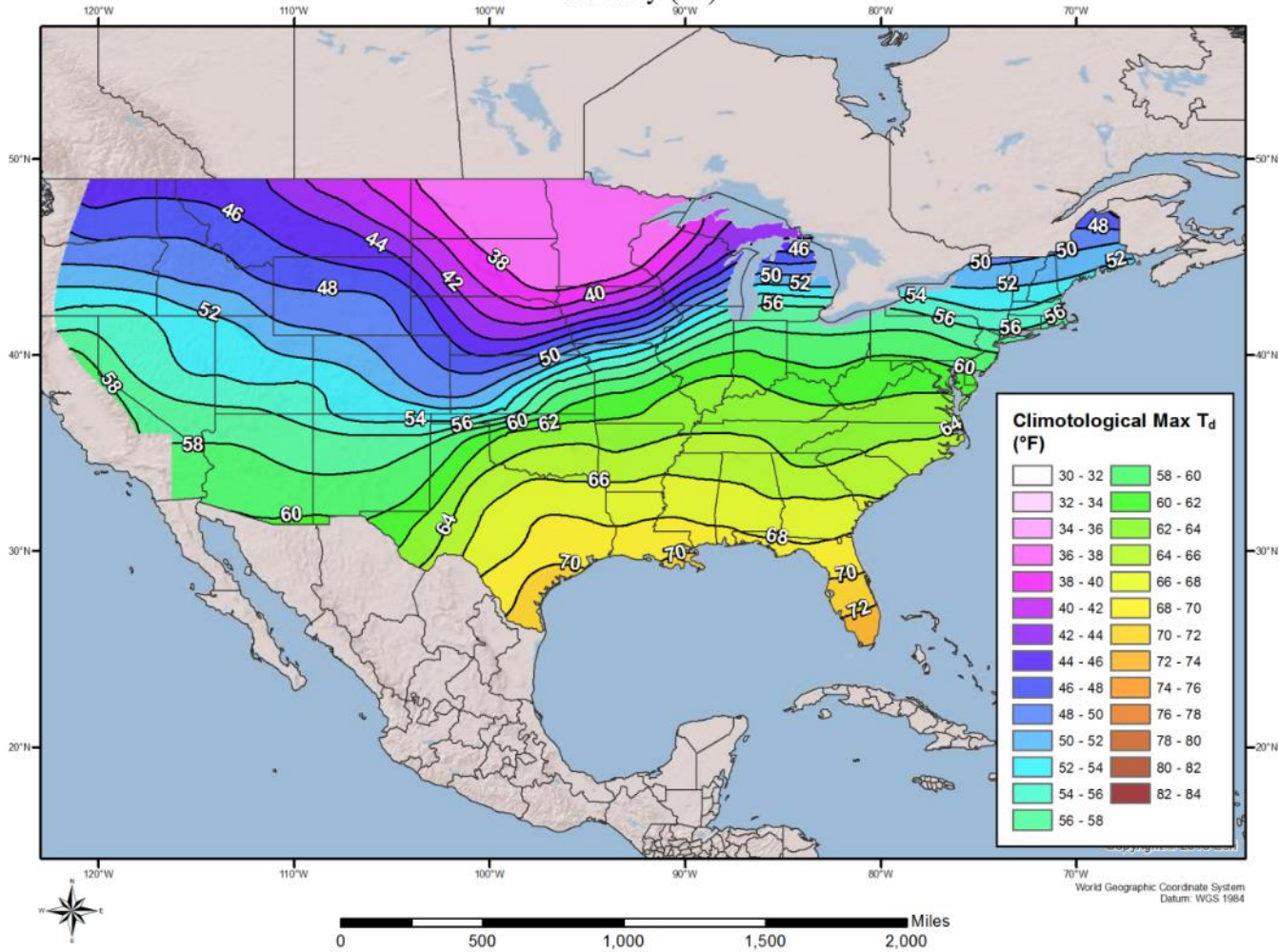
100-year Return Frequency 12-hour Maximum Dew Point Climatology December (°F)



100-year Return Frequency 12-hour Maximum Dew Point Climatology - December

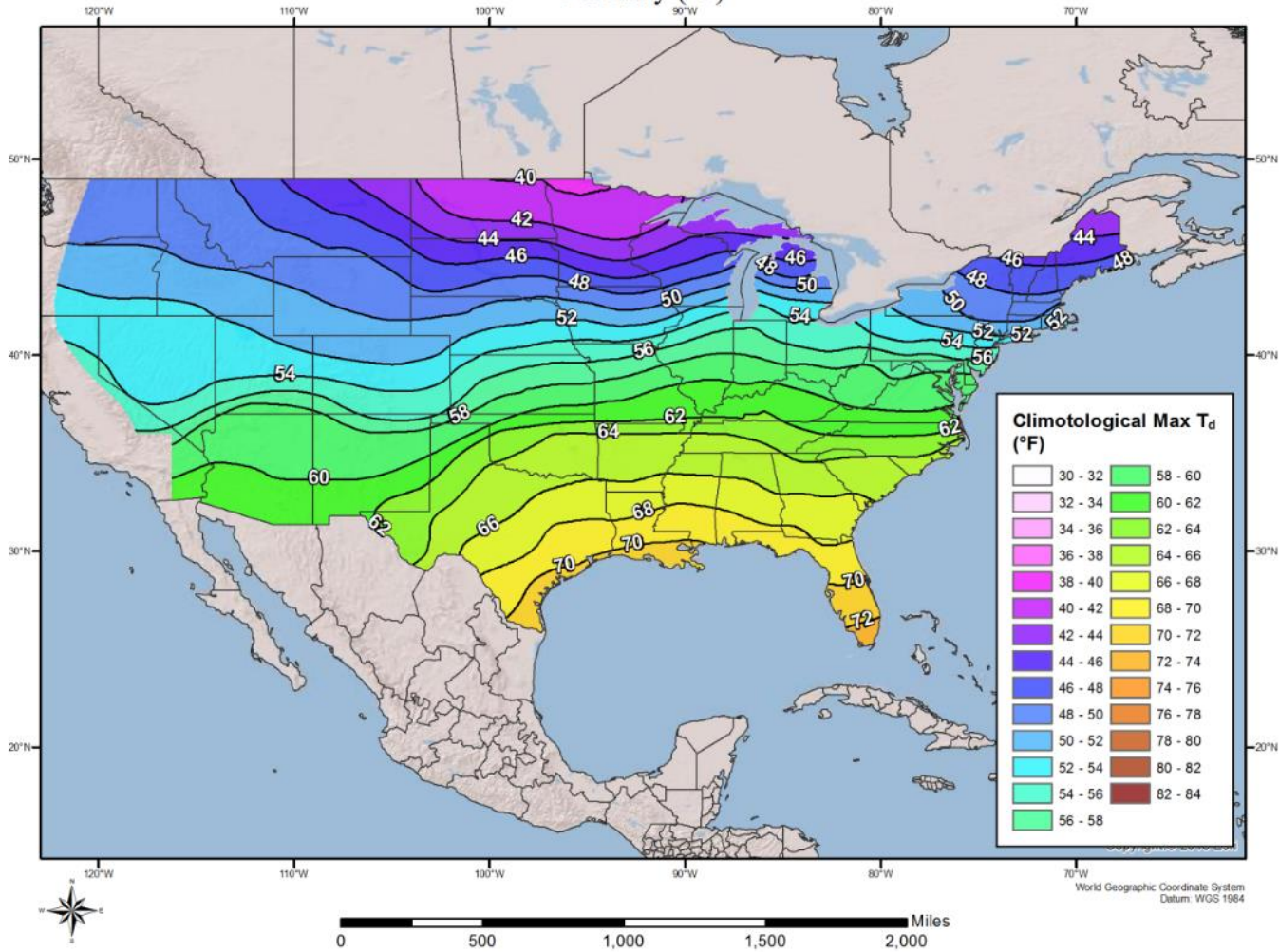
24-Hour, 100-year Dew Point Maps

100-year Return Frequency 24-hour Maximum Dew Point Climatology
January (°F)



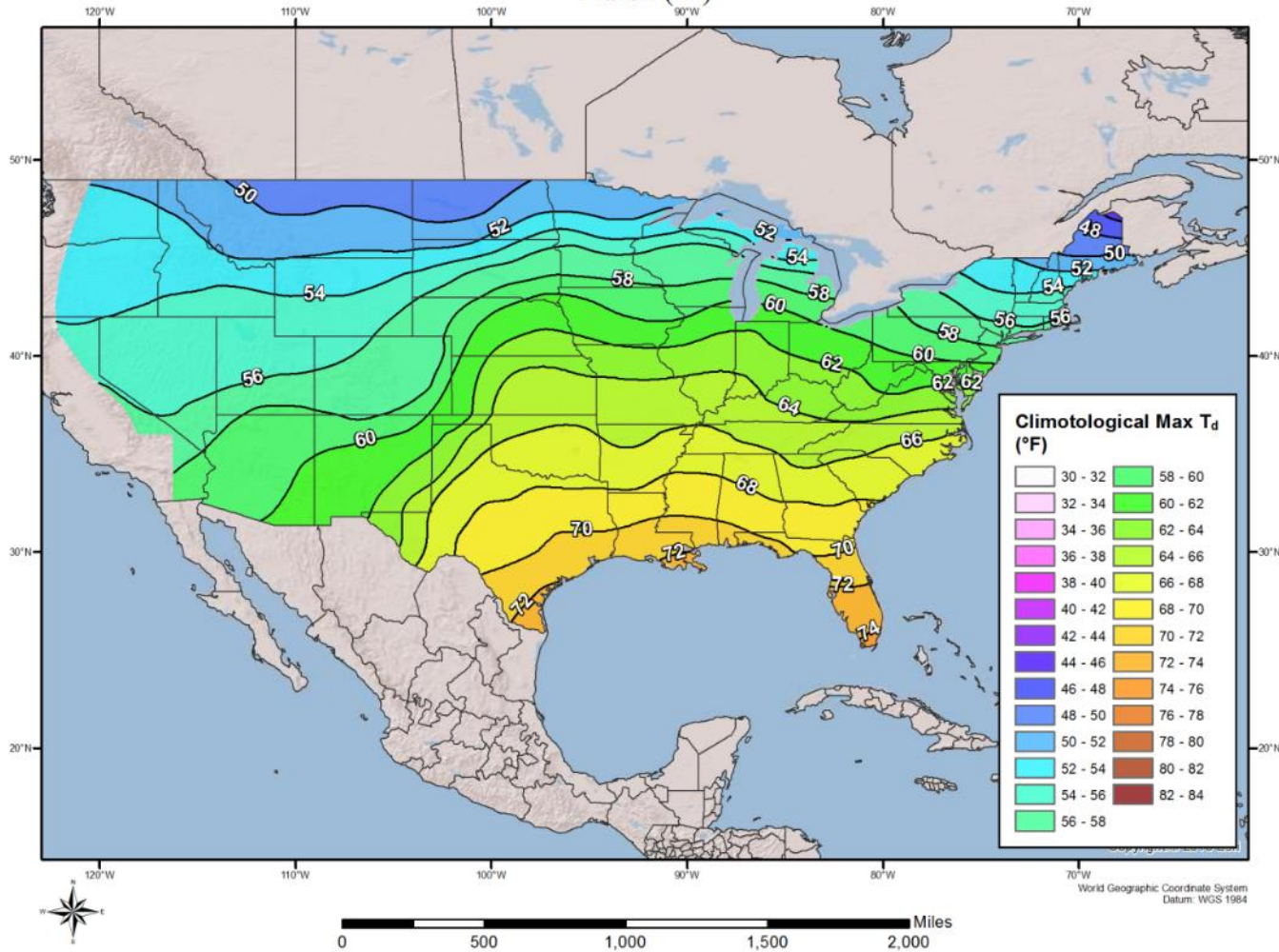
100-year Return Frequency 24-hour Maximum Dew Point Climatology - January

100-year Return Frequency 24-hour Maximum Dew Point Climatology
February (°F)



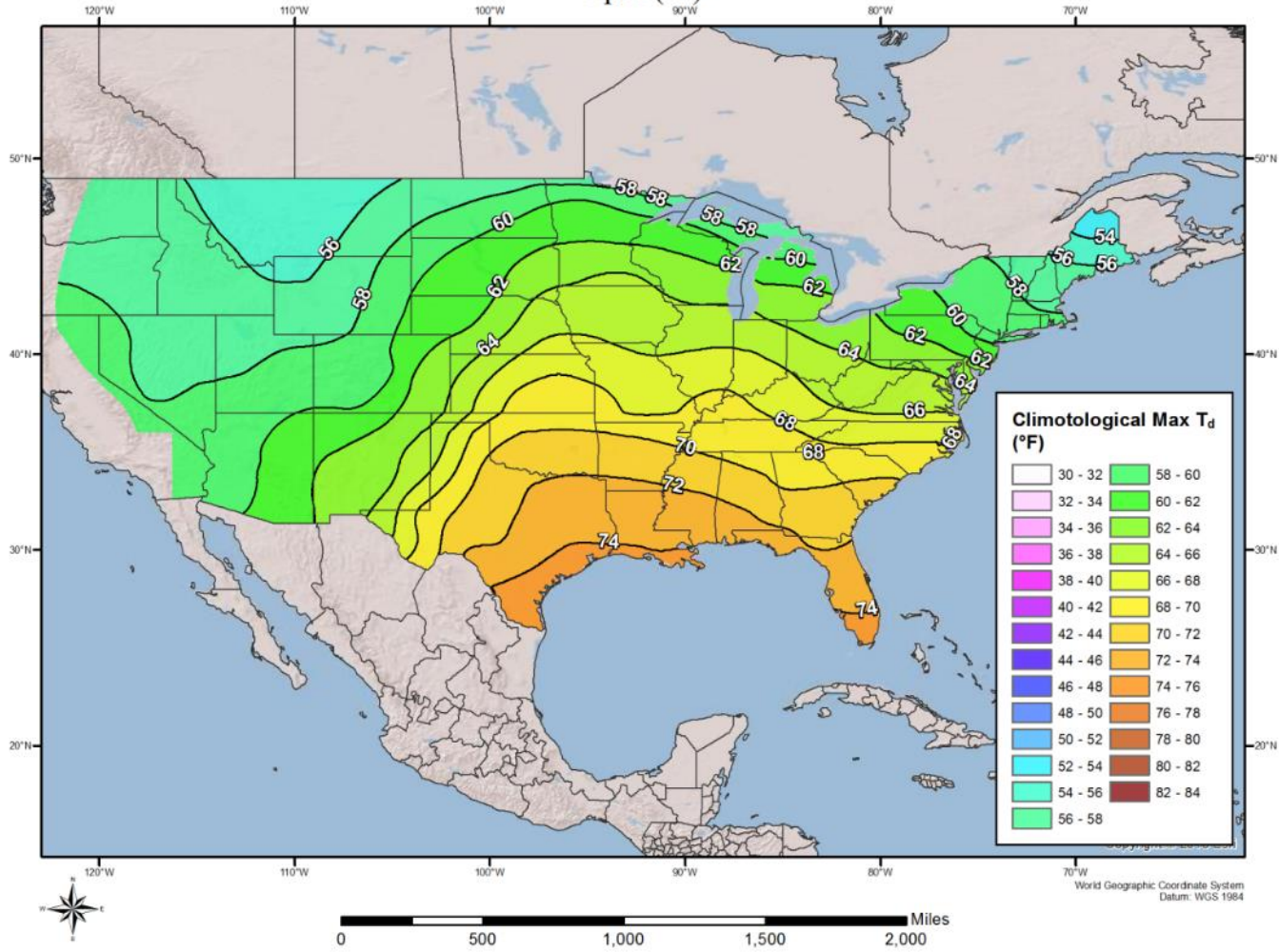
100-year Return Frequency 24-hour Maximum Dew Point Climatology - February

100-year Return Frequency 24-hour Maximum Dew Point Climatology
March (°F)



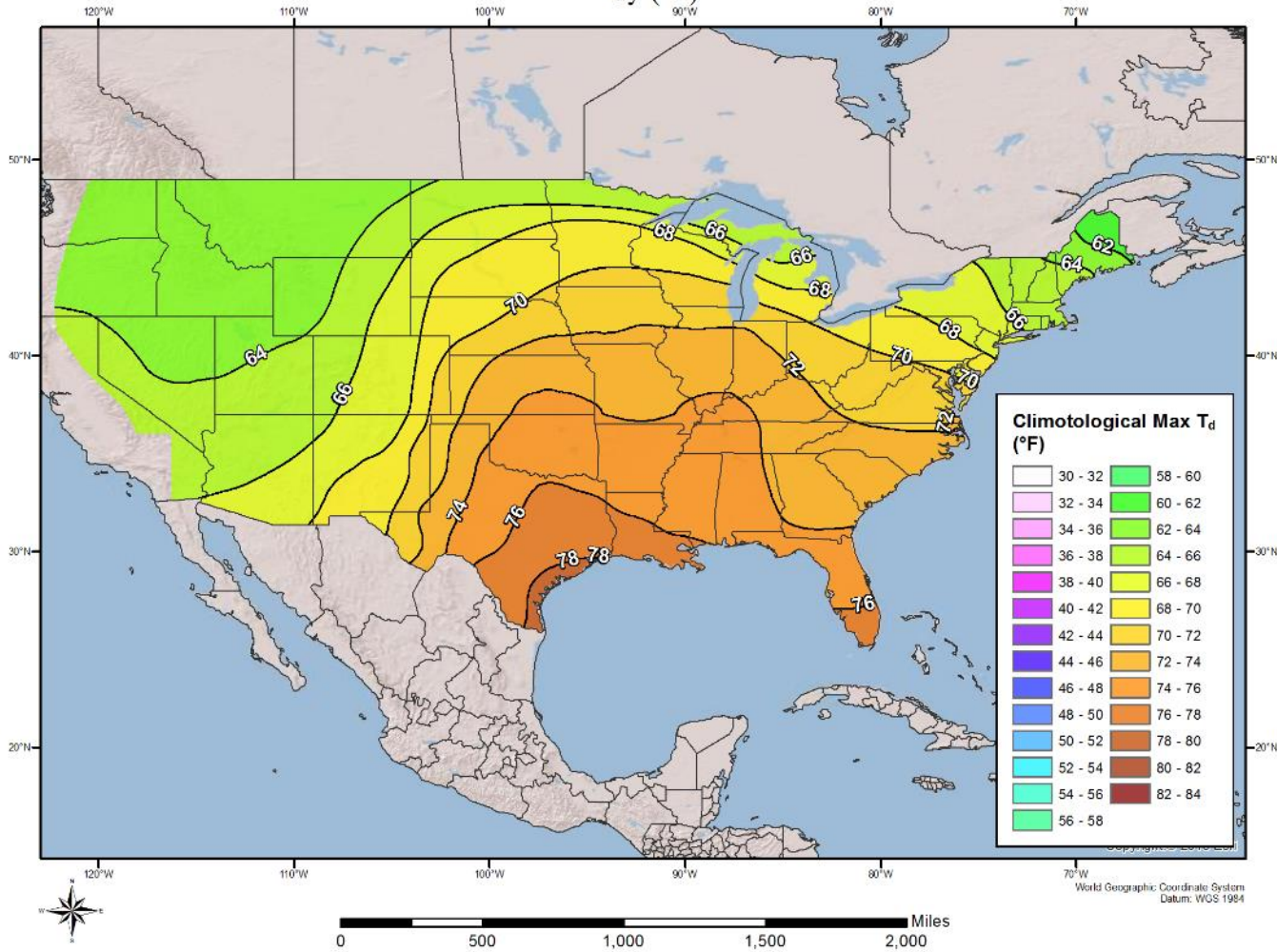
100-year Return Frequency 24-hour Maximum Dew Point Climatology - March

100-year Return Frequency 24-hour Maximum Dew Point Climatology
April (°F)



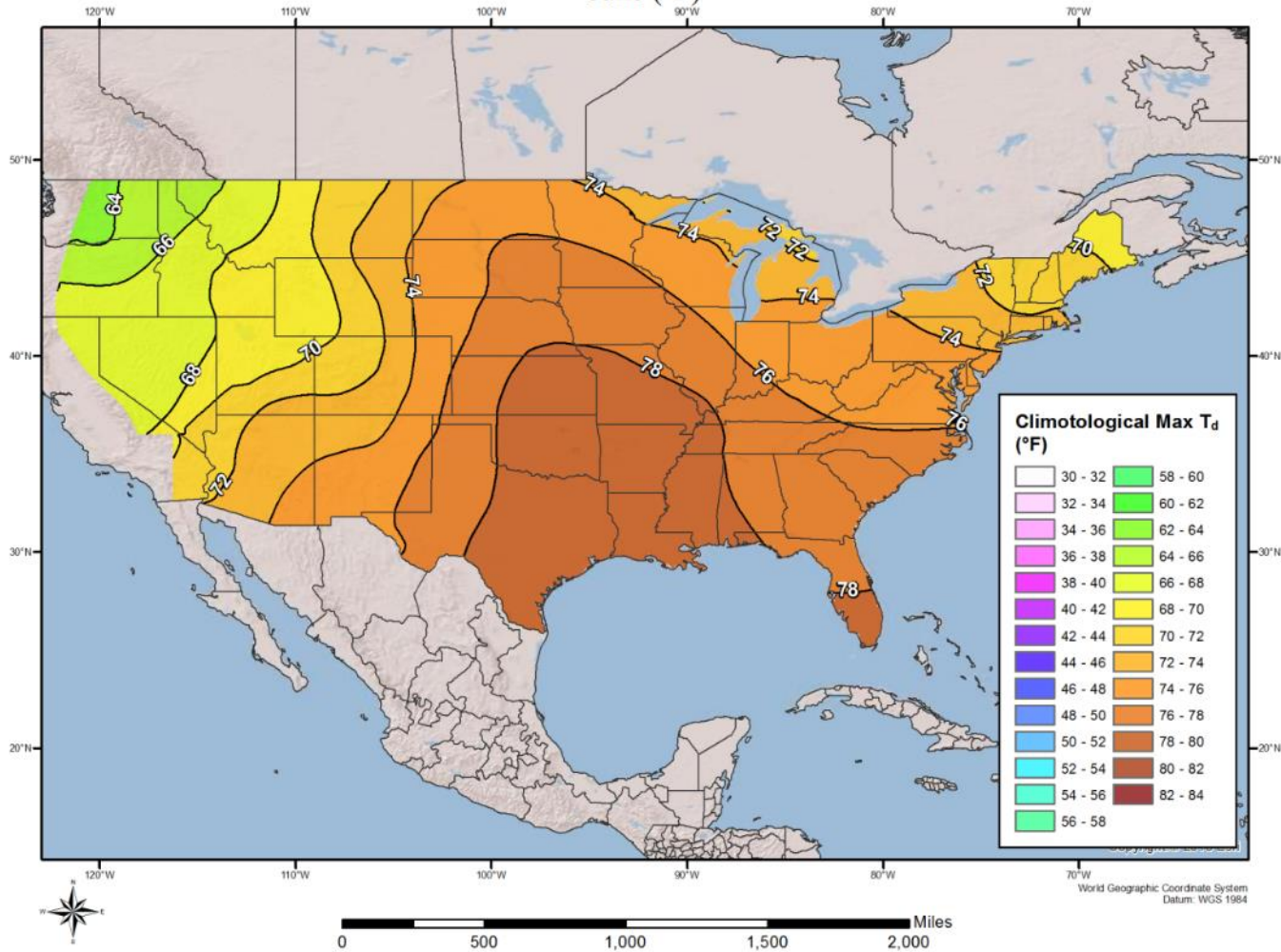
100-year Return Frequency 24-hour Maximum Dew Point Climatology - April

100-year Return Frequency 24-hour Maximum Dew Point Climatology
 May (°F)



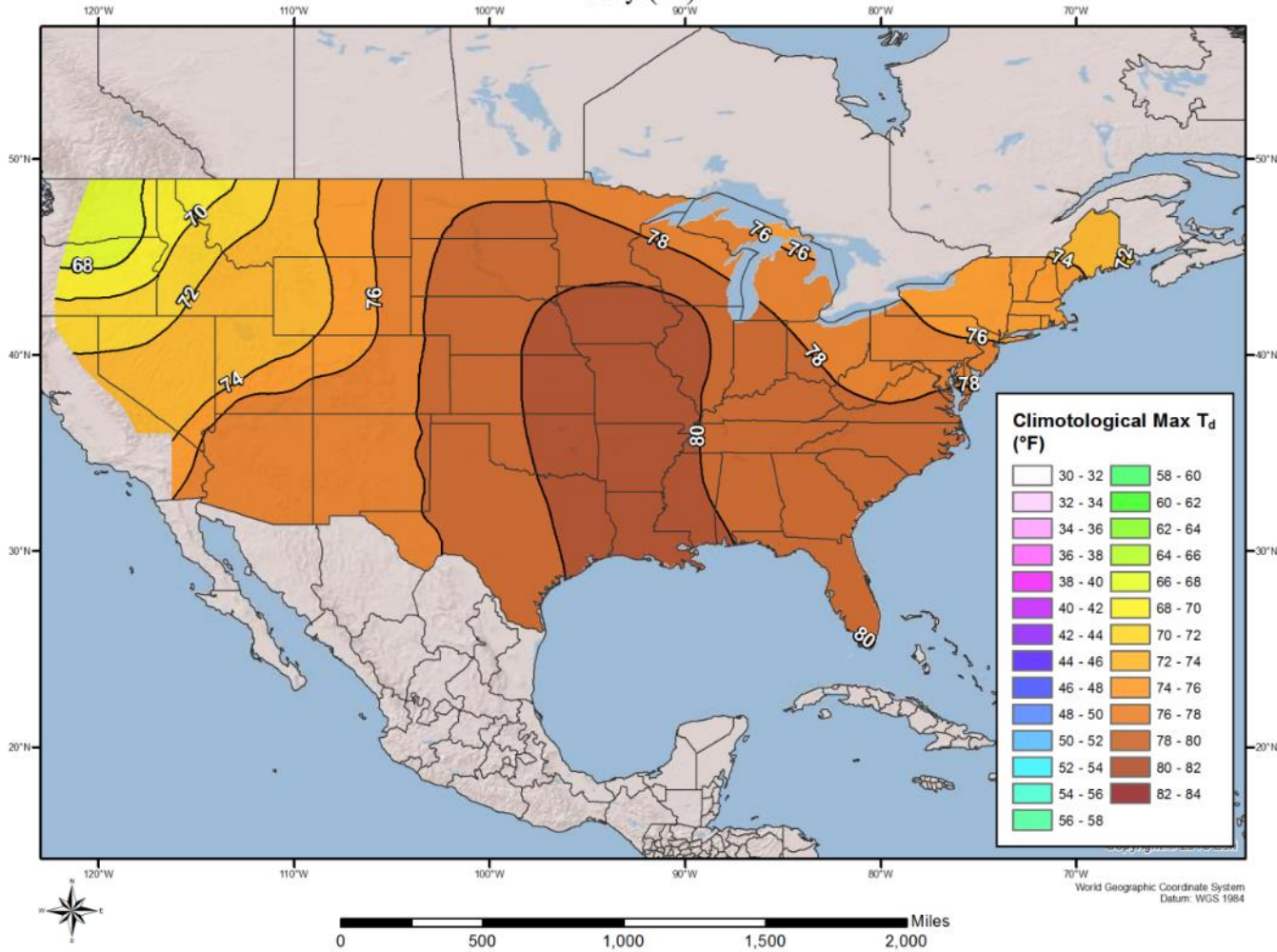
100-year Return Frequency 24-hour Maximum Dew Point Climatology - May

100-year Return Frequency 24-hour Maximum Dew Point Climatology
June (°F)



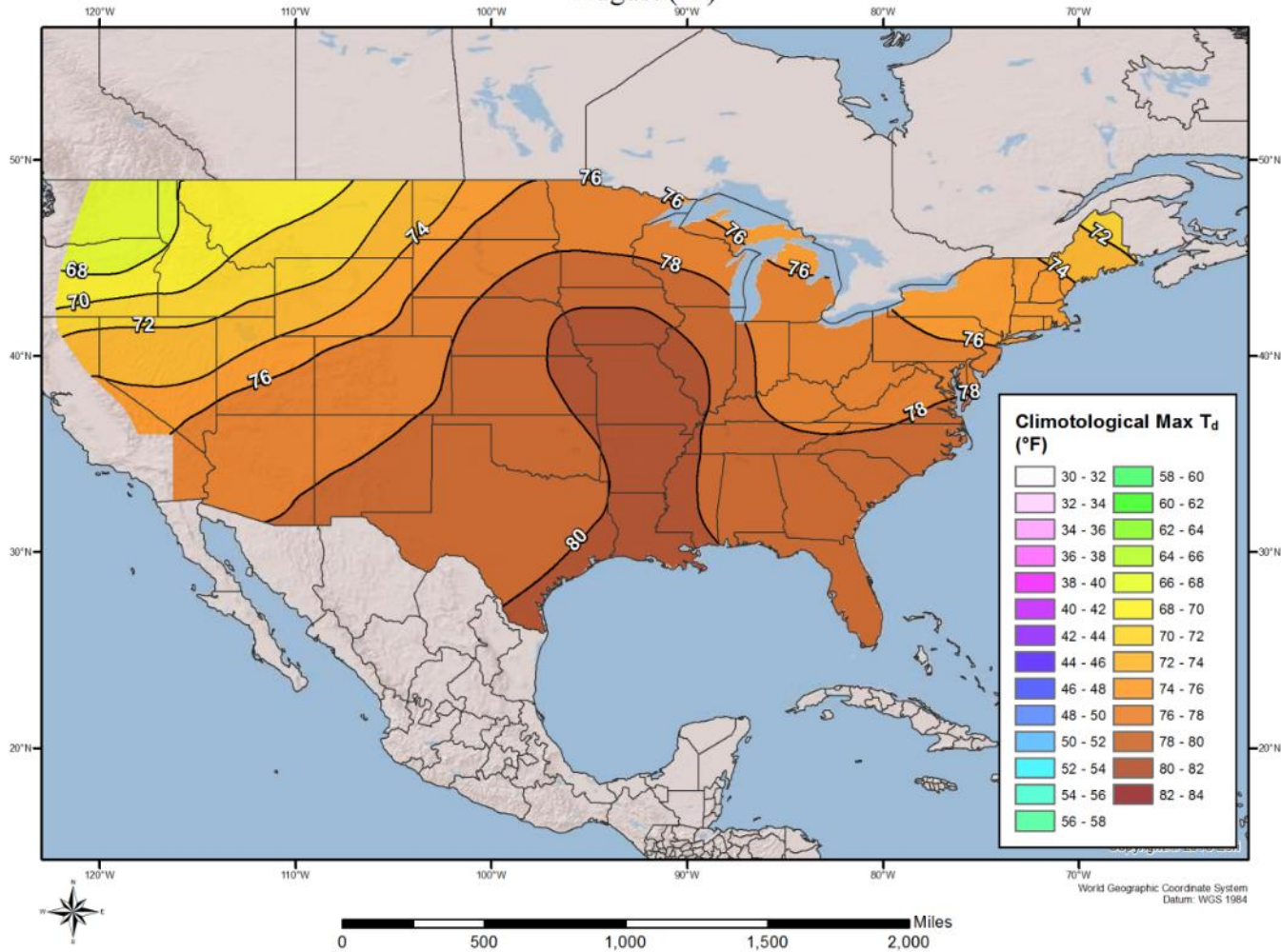
100-year Return Frequency 24-hour Maximum Dew Point Climatology - June

100-year Return Frequency 24-hour Maximum Dew Point Climatology
July (°F)



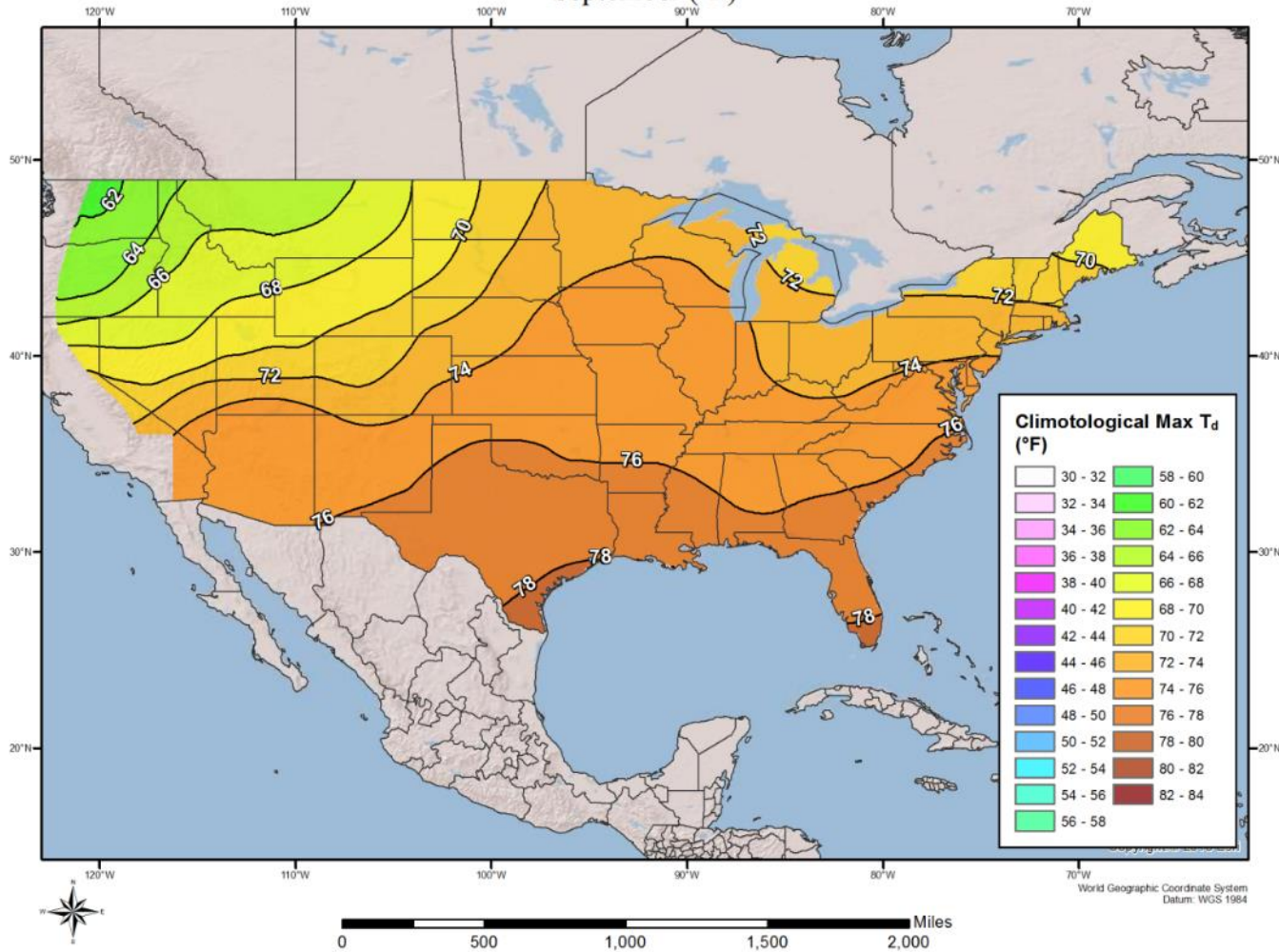
100-year Return Frequency 24-hour Maximum Dew Point Climatology - July

100-year Return Frequency 24-hour Maximum Dew Point Climatology
August (°F)



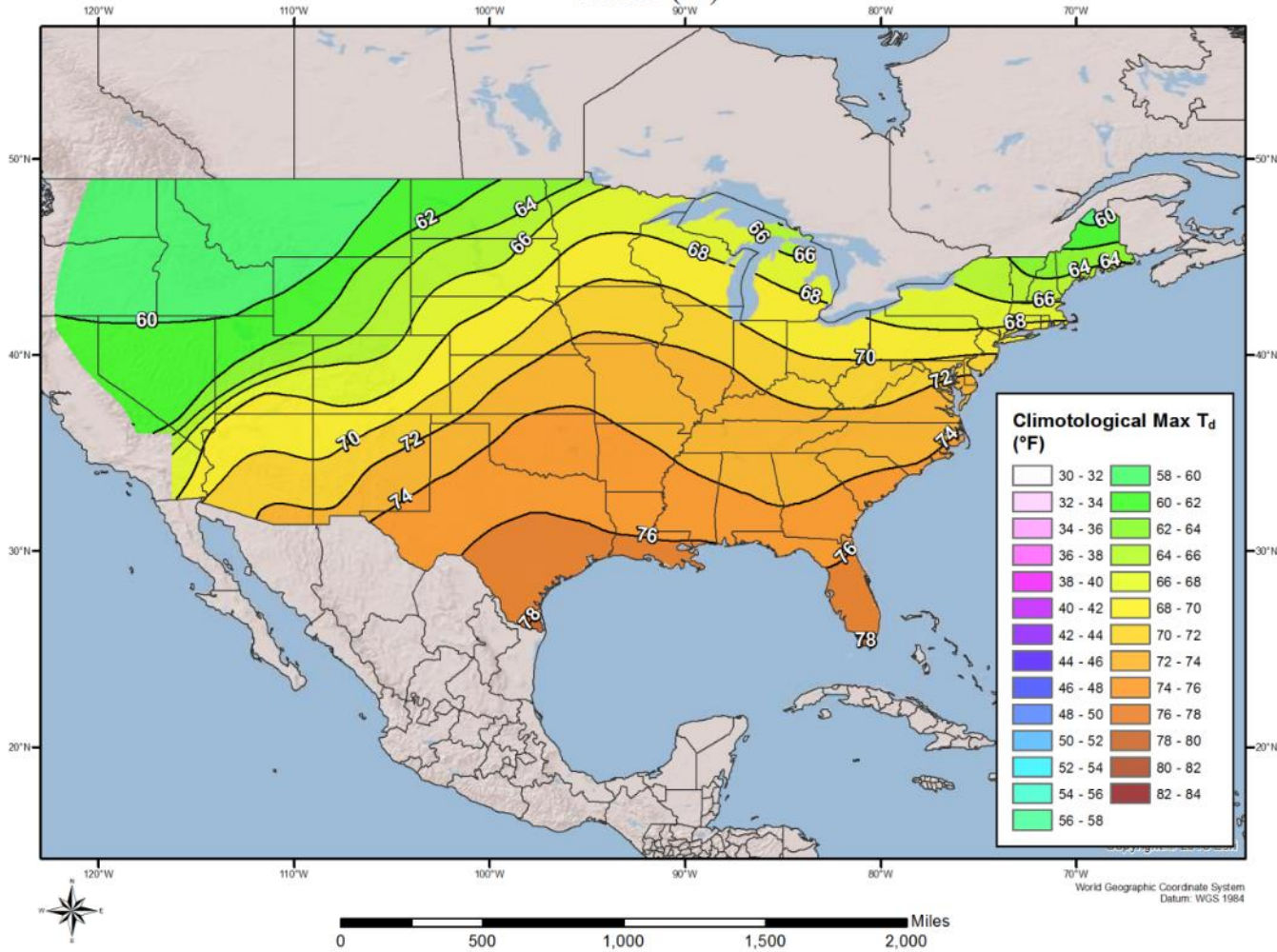
100-year Return Frequency 24-hour Maximum Dew Point Climatology - August

100-year Return Frequency 24-hour Maximum Dew Point Climatology
September (°F)



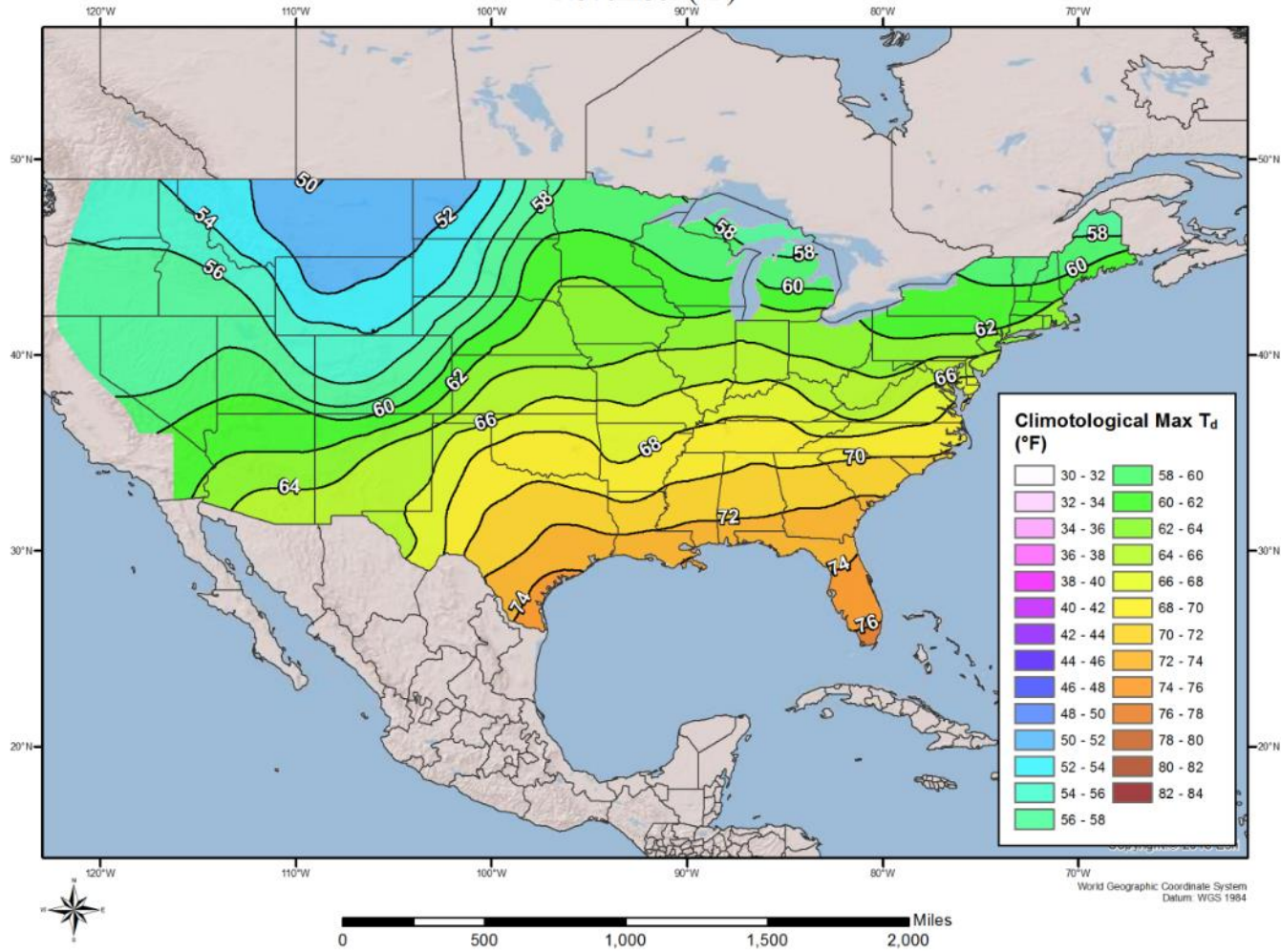
100-year Return Frequency 24-hour Maximum Dew Point Climatology - September

100-year Return Frequency 24-hour Maximum Dew Point Climatology
October (°F)



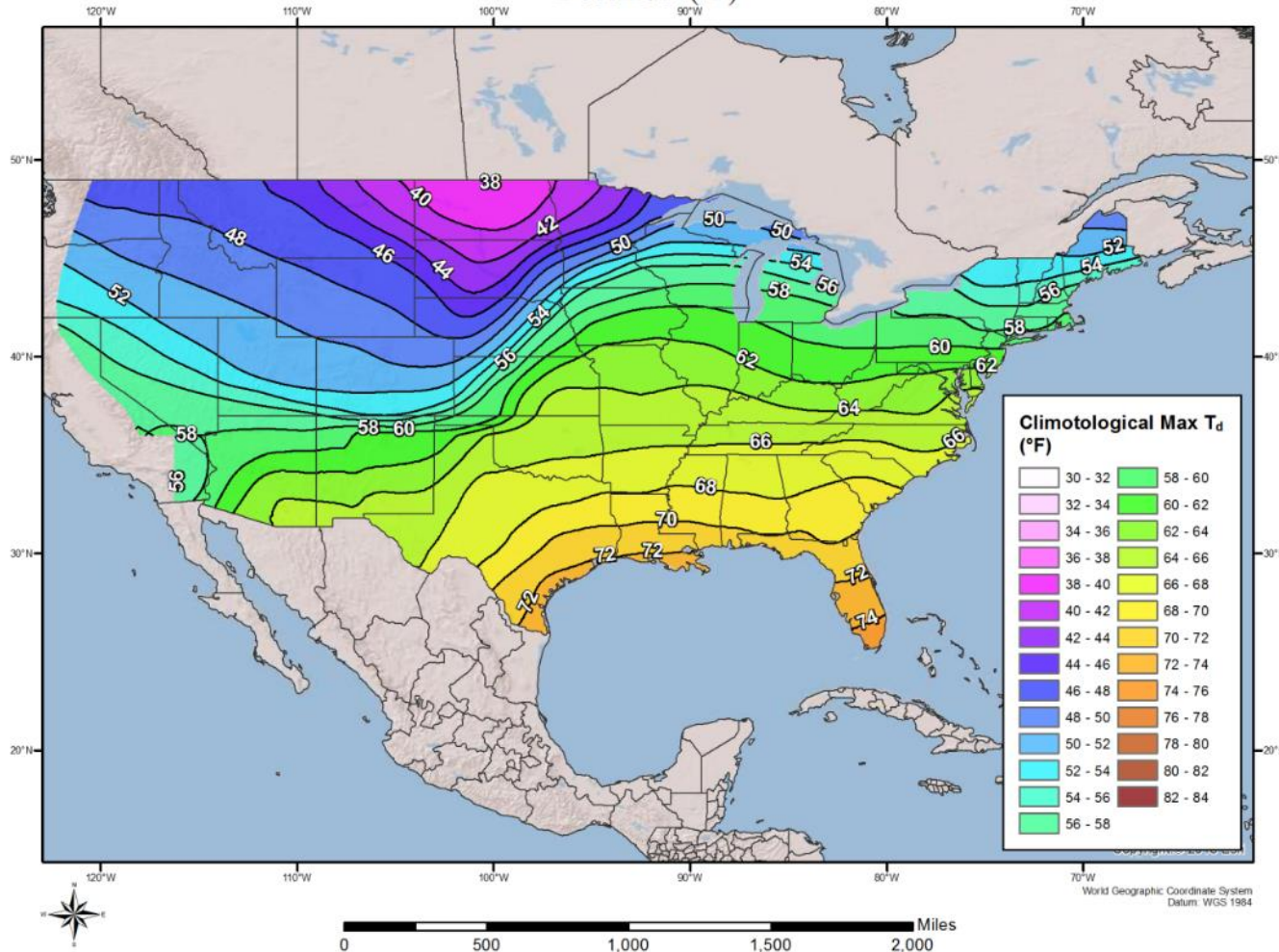
100-year Return Frequency 24-hour Maximum Dew Point Climatology - October

100-year Return Frequency 24-hour Maximum Dew Point Climatology
November (°F)



100-year Return Frequency 24-hour Maximum Dew Point Climatology - November

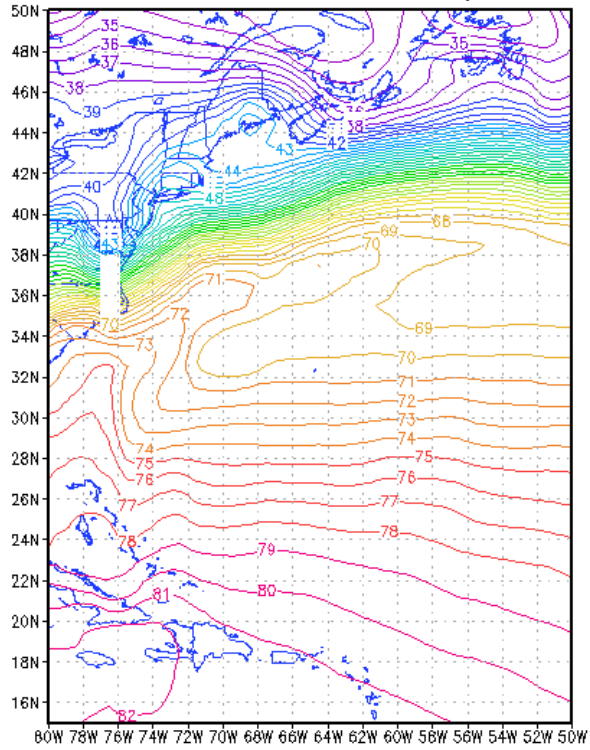
100-year Return Frequency 24-hour Maximum Dew Point Climatology
December (°F)



100-year Return Frequency 24-hour Maximum Dew Point Climatology - December

2-Sigma Sea Surface Temperature Maps

+2 sigma (1982-2010) Jan SST (DegF)
NOAA OI.v2 Sea Surface Temperature

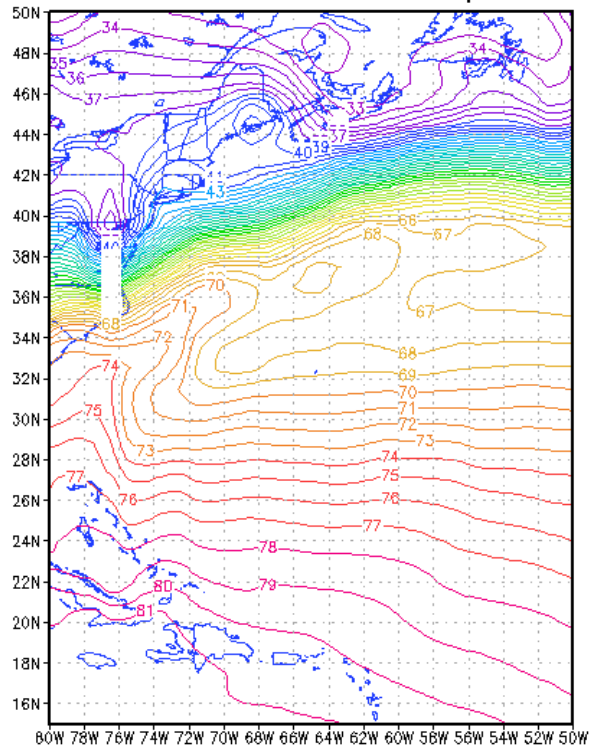


GrADS: COLA/IGES

2010-12-09-21:33

January +2 sigma SST climatology-western Atlantic Ocean

+2 sigma (1982-2010) Feb SST (DegF)
NOAA OI.v2 Sea Surface Temperature

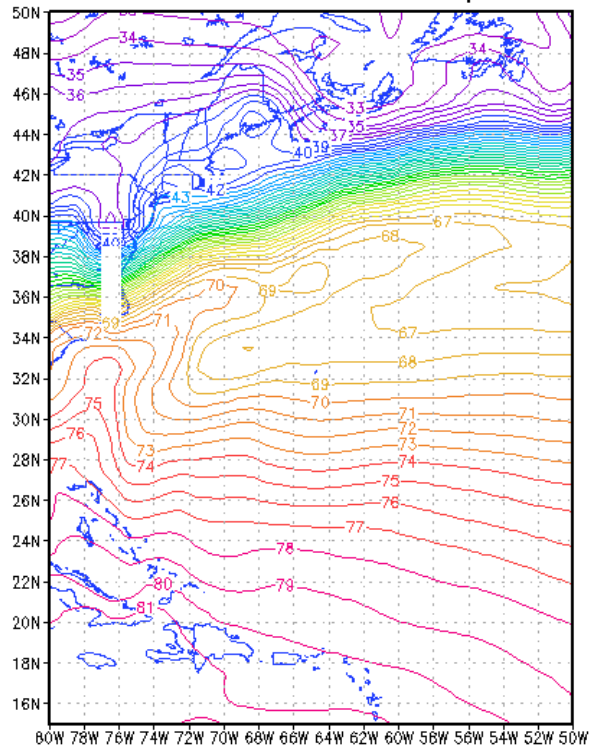


GrADS: COLA/IGES

2010-12-09-21:33

February +2 sigma SST climatology-western Atlantic Ocean

+2 sigma (1982-2010) Mar SST (DegF)
NOAA OI.v2 Sea Surface Temperature

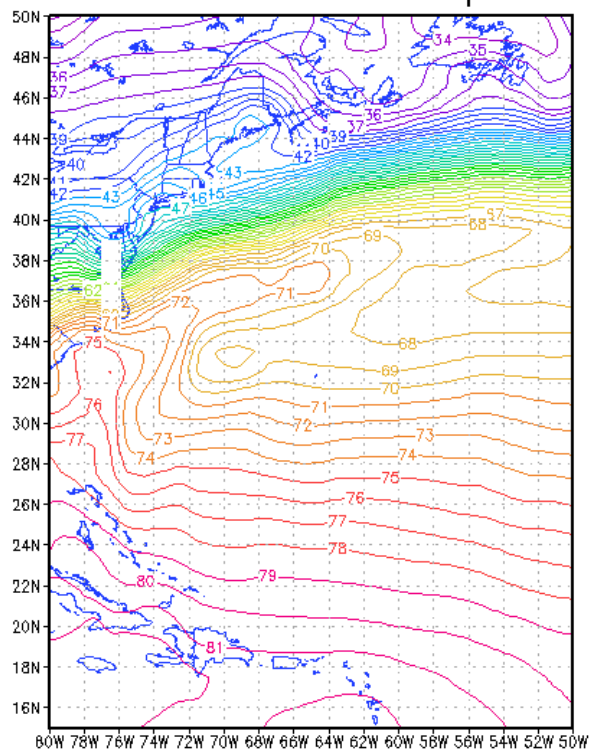


GrADS: COLA/IGES

2010-12-09-21:33

March +2 sigma SST climatology-western Atlantic Ocean

+2 sigma (1982–2010) Apr SST (DegF)
NOAA OI.v2 Sea Surface Temperature

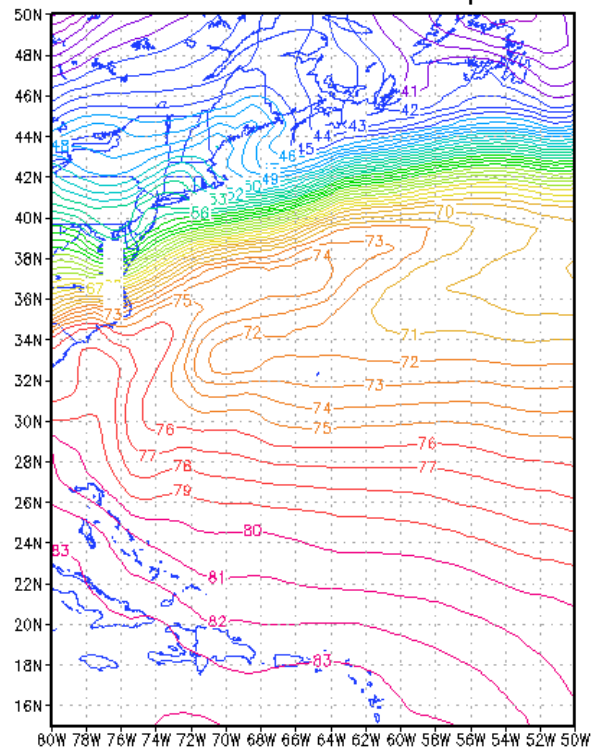


GrADS: COLA/IGES

2010-12-09-21:33

April +2 sigma SST climatology-western Atlantic Ocean

+2 sigma (1982-2010) May SST (DegF)
NOAA OI.v2 Sea Surface Temperature

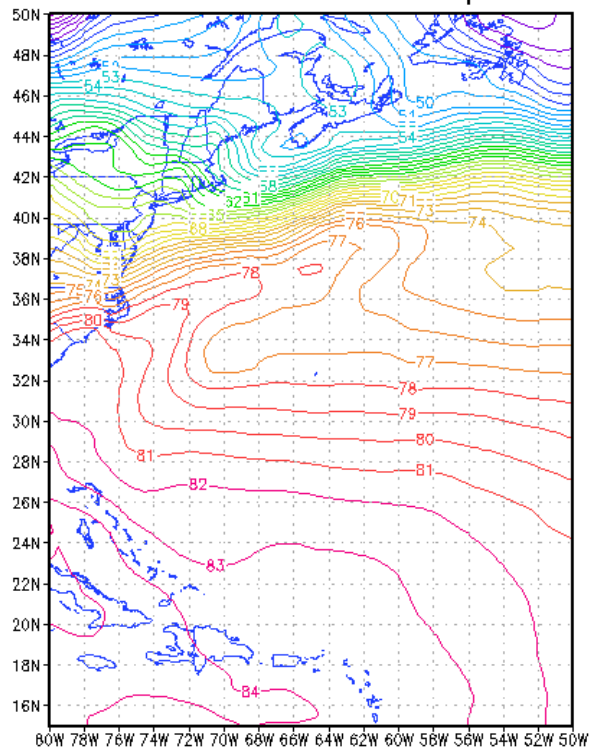


GrADS: COLA/IGES

2010-12-09-21:34

May +2 sigma SST climatology-western Atlantic Ocean

+2 sigma (1982–2010) Jun SST (DegF)
NOAA OI.v2 Sea Surface Temperature

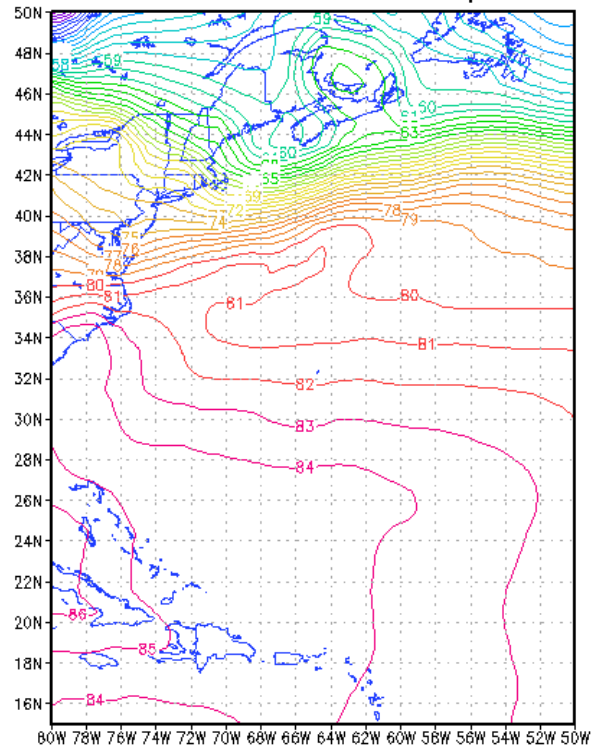


GrADS: COLA/IGES

2010-12-09-21:34

June +2 sigma SST climatology-western Atlantic Ocean

+2 sigma (1982-2010) Jul SST (DegF)
NOAA OI.v2 Sea Surface Temperature

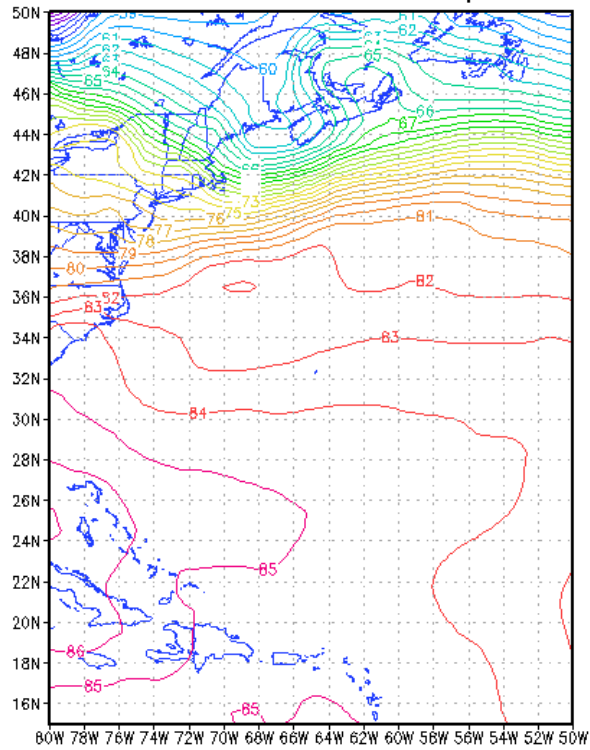


GrADS: COLA/IGES

2010-12-09-21:34

July +2 sigma SST climatology-western Atlantic Ocean

+2 sigma (1982-2010) Aug SST (DegF)
NOAA OI.v2 Sea Surface Temperature

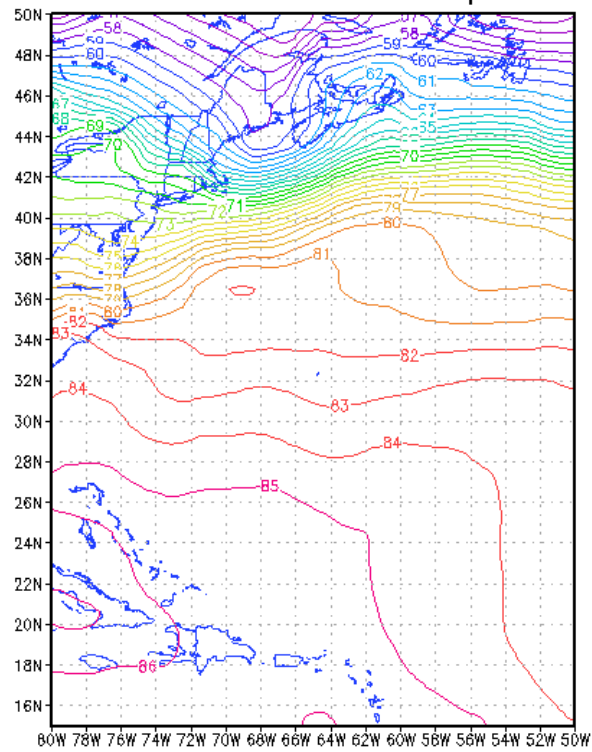


GrADS: COLA/IGES

2010-12-09-21:34

August +2 sigma SST climatology-western Atlantic Ocean

+2 sigma (1982-2010) Sep SST (DegF)
NOAA OI.v2 Sea Surface Temperature

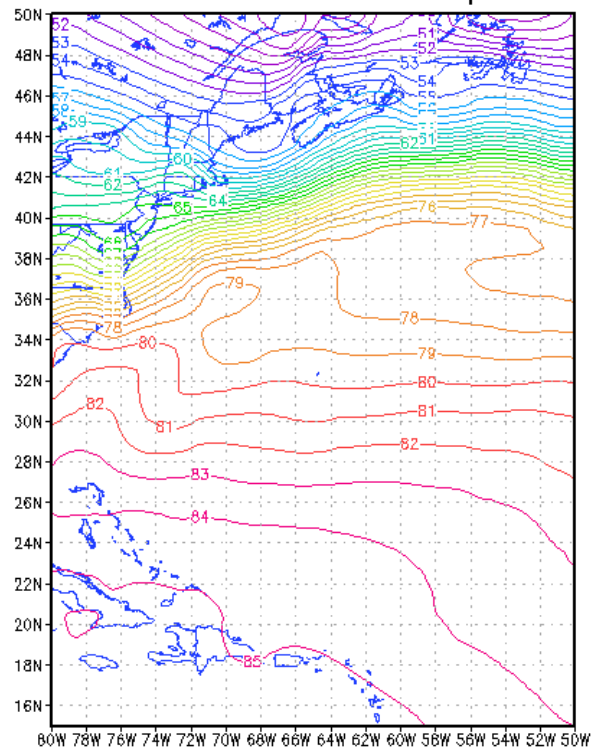


GrADS: COLA/IGES

2010-12-09-21:34

September +2 sigma SST climatology-western Atlantic Ocean

+2 sigma (1982-2010) Oct SST (DegF)
NOAA OI.v2 Sea Surface Temperature

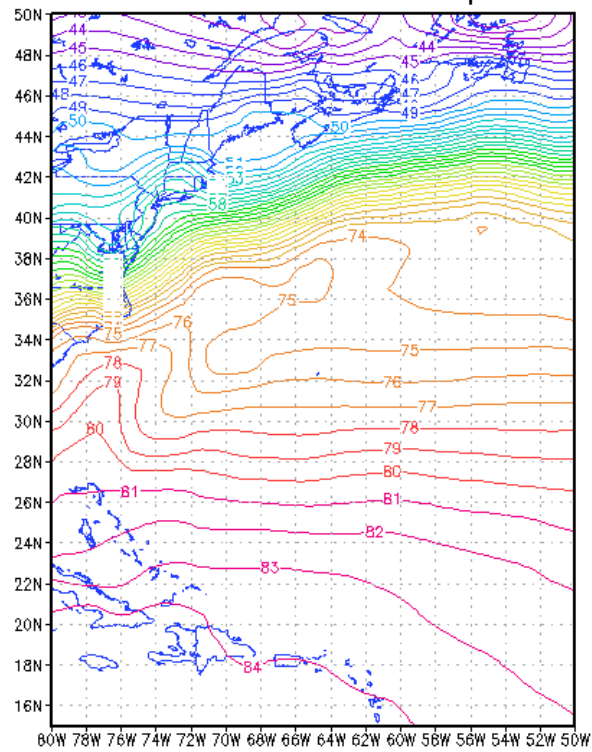


GrADS: COLA/IGES

2011-02-28-16:46

October +2 sigma SST climatology-western Atlantic Ocean

+2 sigma (1982-2010) Nov SST (DegF)
NOAA OI.v2 Sea Surface Temperature

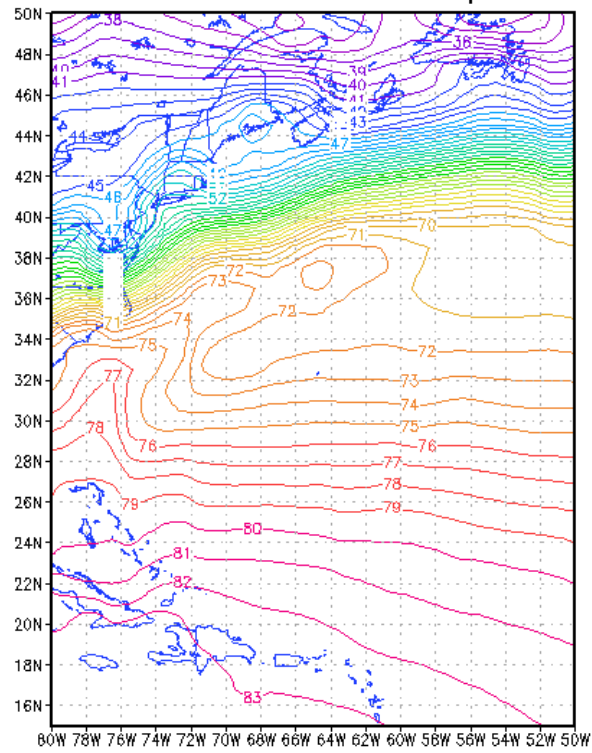


GrADS: COLA/IGES

2010-12-09-21:35

November +2 sigma SST climatology-western Atlantic Ocean

+2 sigma (1982-2010) Dec SST (DegF)
NOAA OI.v2 Sea Surface Temperature

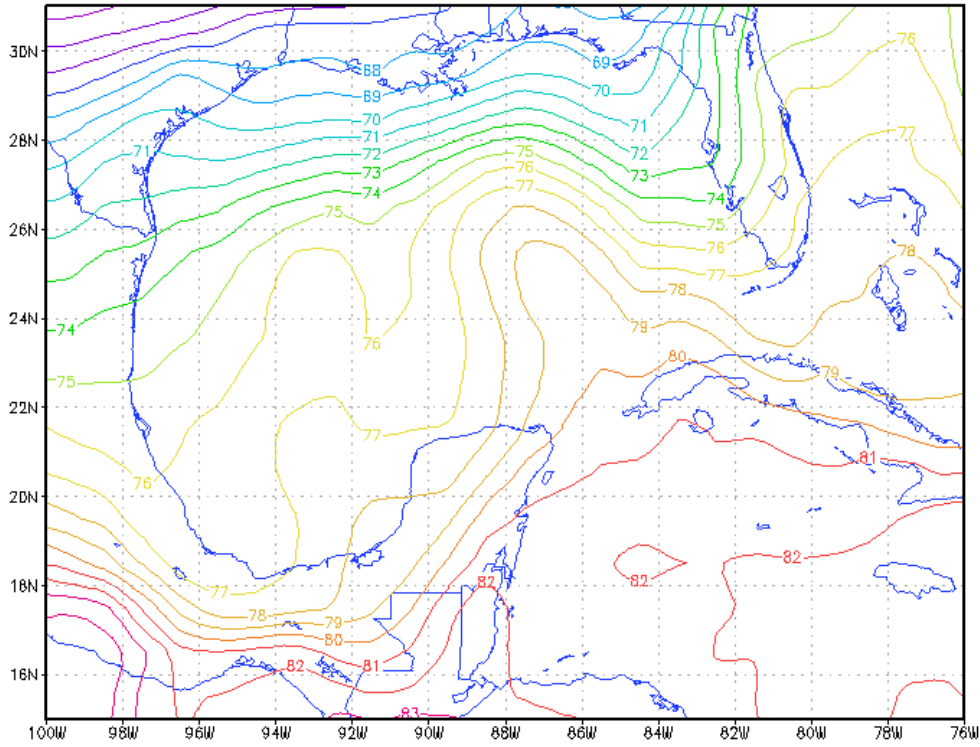


GrADS: COLA/IGES

2011-01-11-14:19

December +2 sigma SST climatology-western Atlantic Ocean

+2 sigma (1982-2008) Jan SST (DegF)
NOAA OI.v2 Sea Surface Temperature

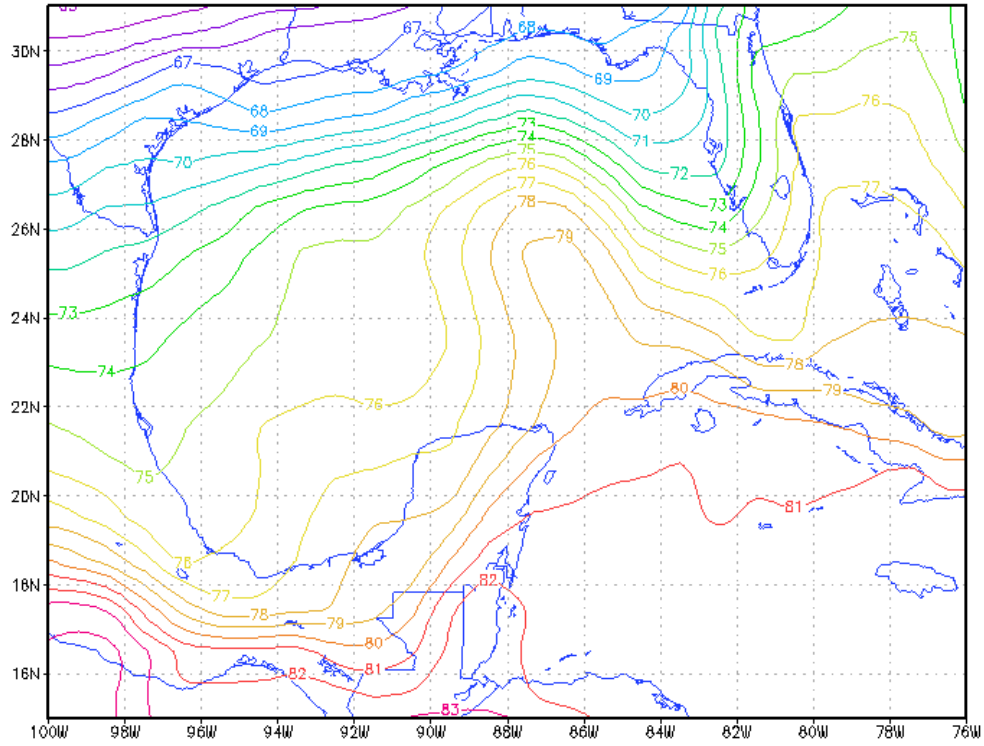


GrADS: COLA/IGES

2010-04-06-14:51

January +2 sigma SST climatology-Gulf of Mexico

+2 sigma (1982-2008) Feb SST (DegF)
NOAA OI.v2 Sea Surface Temperature

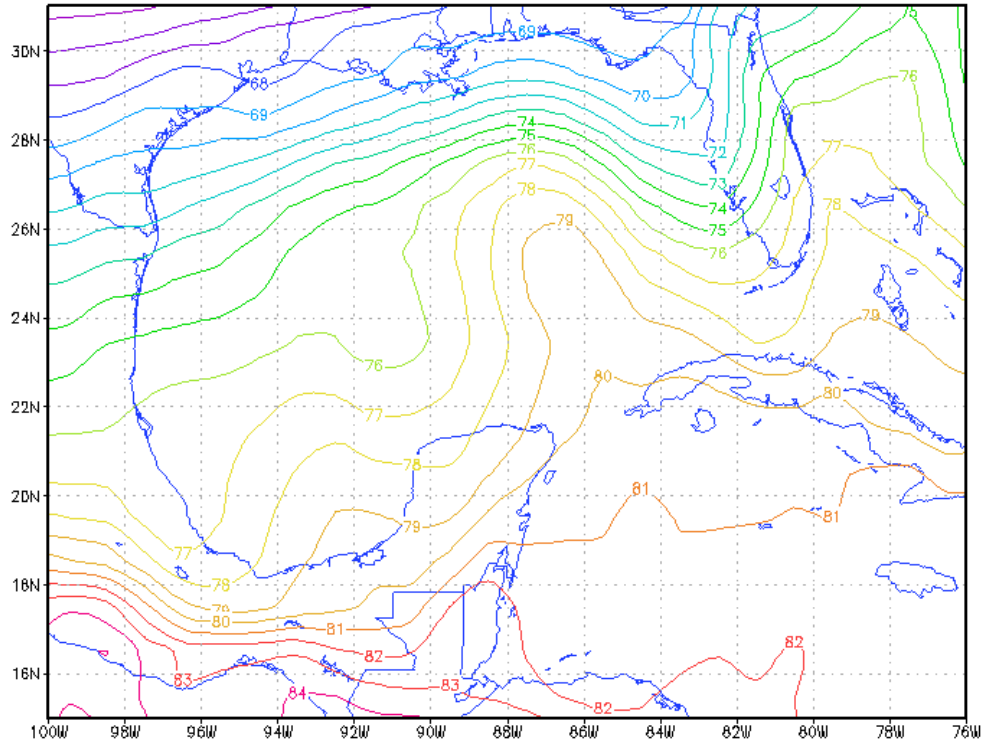


GrADS: COLA/IGES

2010-04-06-14:51

February +2 sigma SST climatology-Gulf of Mexico

+2 sigma (1982-2008) Mar SST (DegF)
NOAA OI.v2 Sea Surface Temperature

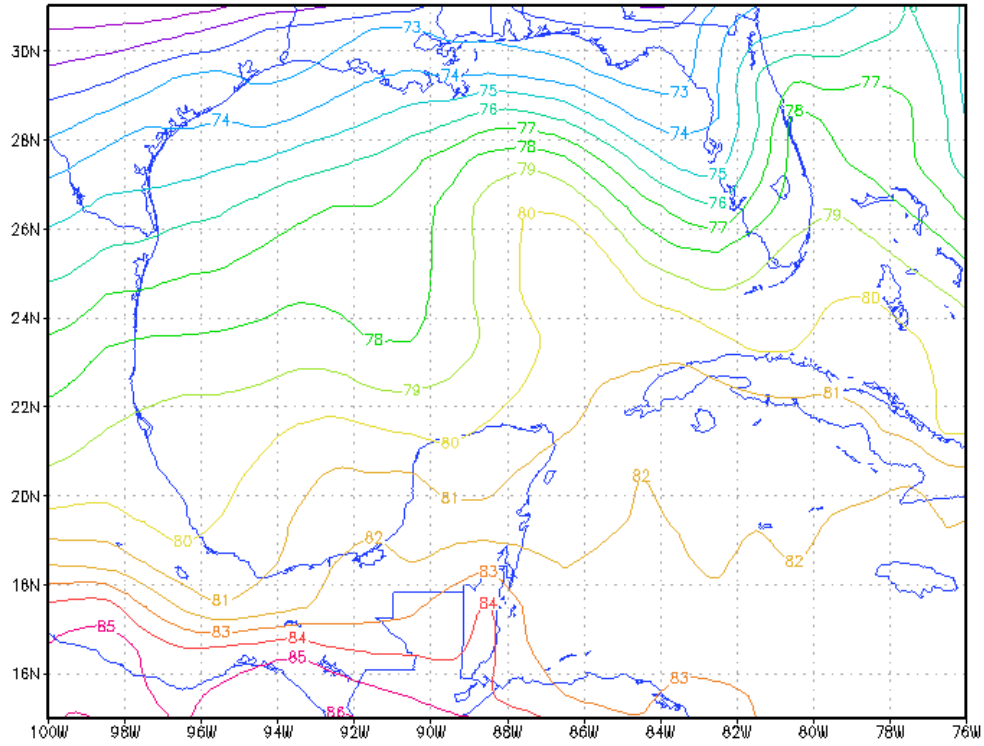


GrADS: COLA/IGES

2010-04-06-14:51

March +2 sigma SST climatology-Gulf of Mexico

+2 sigma (1982-2008) Apr SST (DegF)
NOAA OI.v2 Sea Surface Temperature

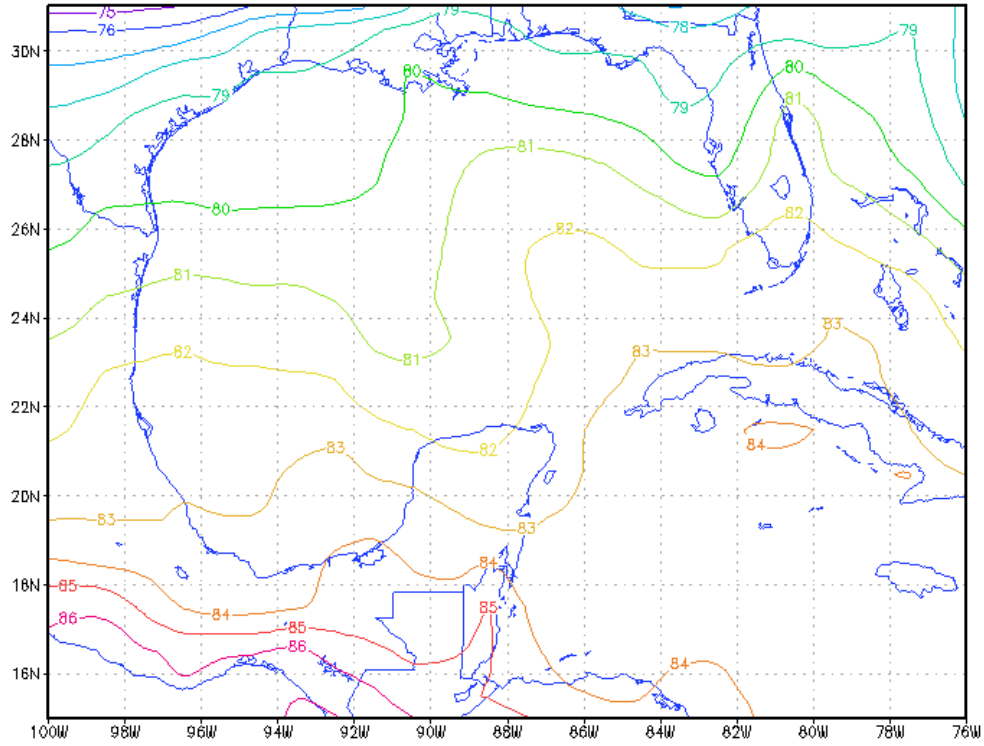


GrADS: COLA/IGES

2010-04-06-14:51

April +2 sigma SST climatology-Gulf of Mexico

+2 sigma (1982-2008) May SST (DegF)
NOAA OI.v2 Sea Surface Temperature

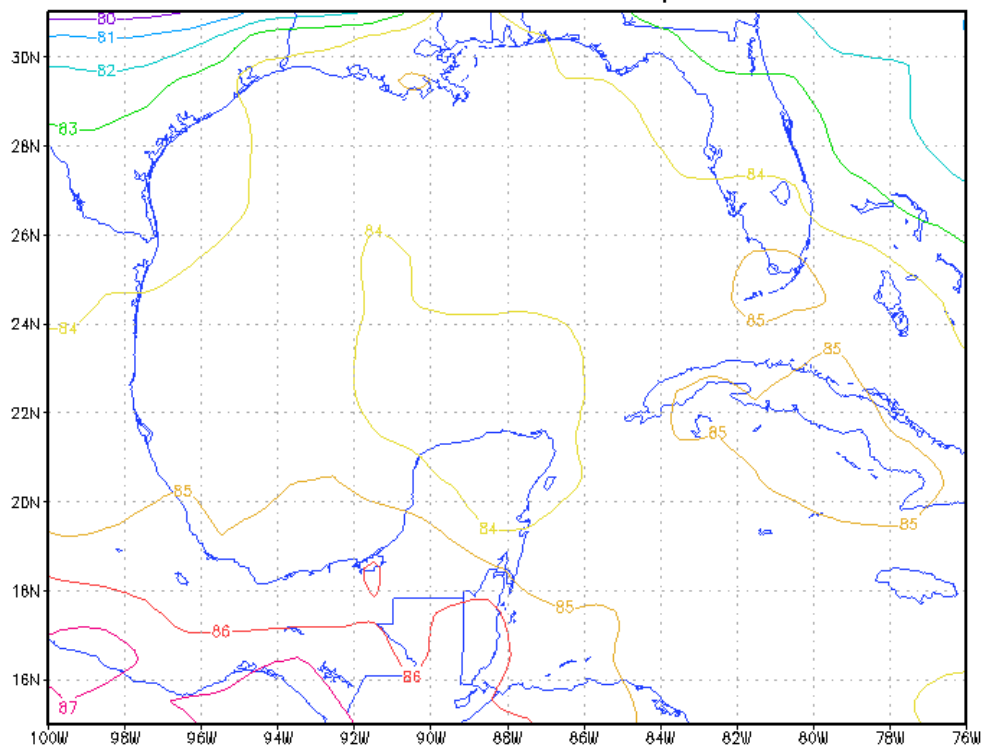


GrADS: COLA/IGES

2010-04-06-14:51

May +2 sigma SST climatology-Gulf of Mexico

+2 sigma (1982-2008) Jun SST (DegF)
NOAA OI.v2 Sea Surface Temperature

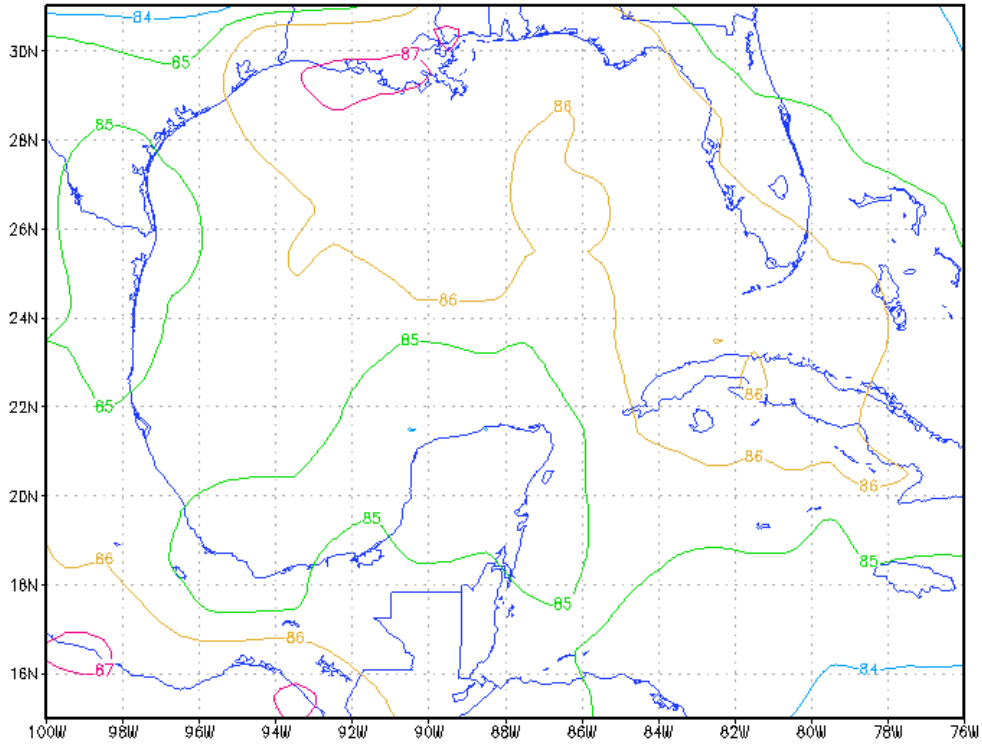


GrADS: COLA/IGES

2010-04-06-14:52

June +2 sigma SST climatology-Gulf of Mexico

+2 sigma (1982-2008) Jul SST (DegF)
NOAA OI.v2 Sea Surface Temperature

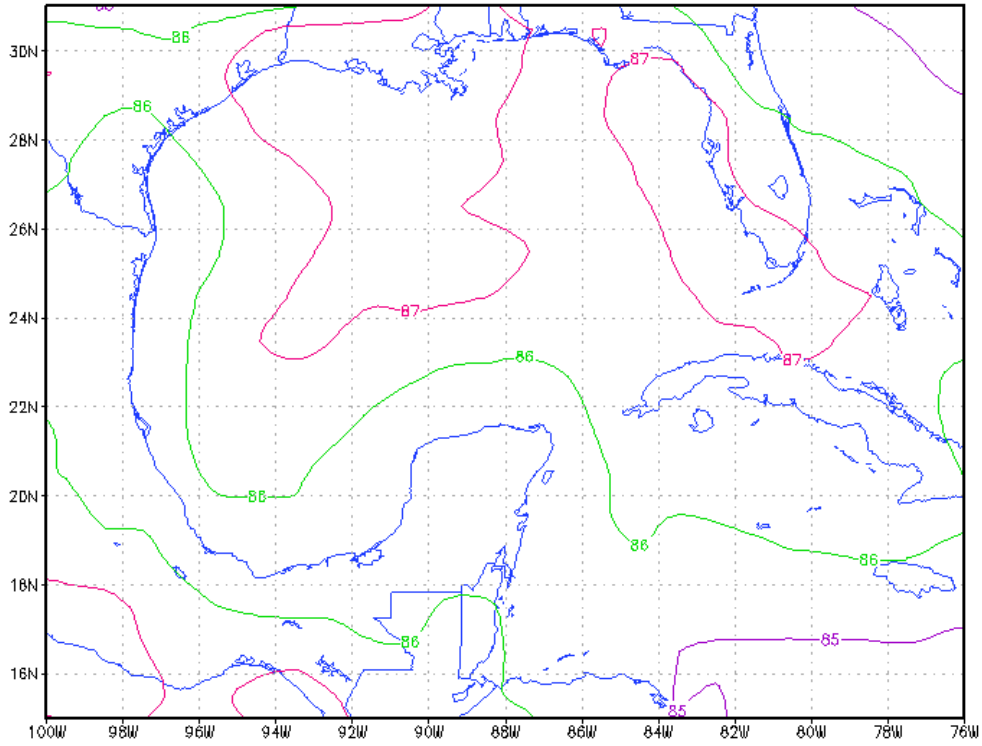


GrADS: COLA/IGES

2010-04-06-14:52

July +2 sigma SST climatology-Gulf of Mexico

+2 sigma (1982-2008) Aug SST (DegF)
NOAA OI.v2 Sea Surface Temperature

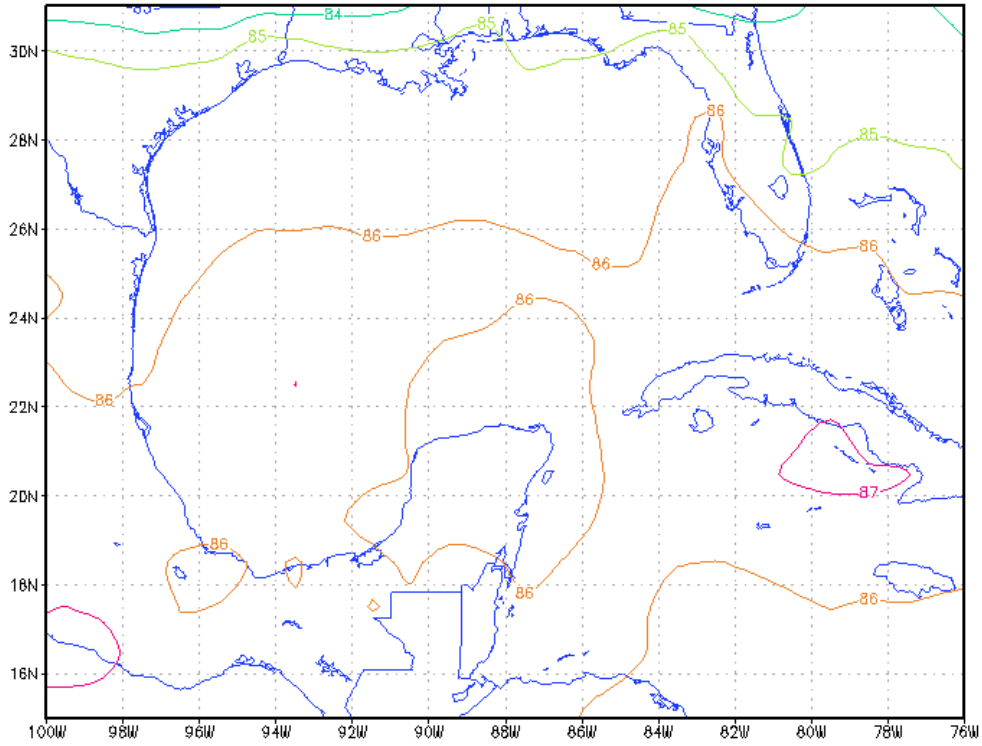


GrADS: COLA/IGES

2010-04-06-14:52

August +2 sigma SST climatology-Gulf of Mexico

+2 sigma (1982-2008) Sep SST (DegF)
NOAA OI.v2 Sea Surface Temperature

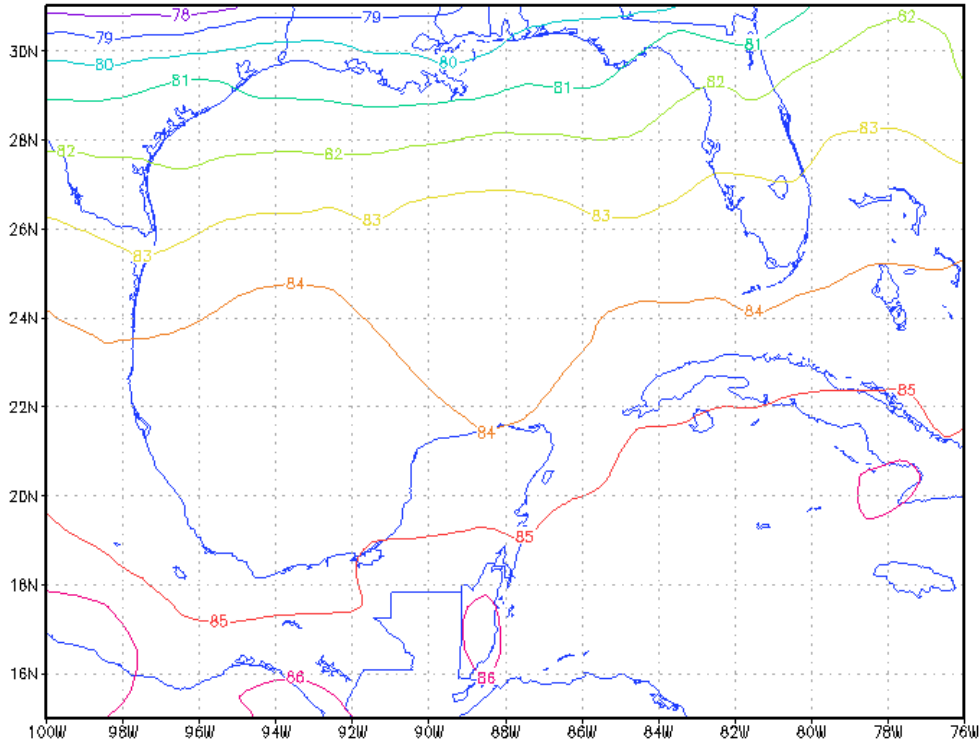


GrADS: COLA/IGES

2010-04-06-14:52

September +2 sigma SST climatology-Gulf of Mexico

+2 sigma (1982-2008) Oct SST (DegF)
NOAA OI.v2 Sea Surface Temperature

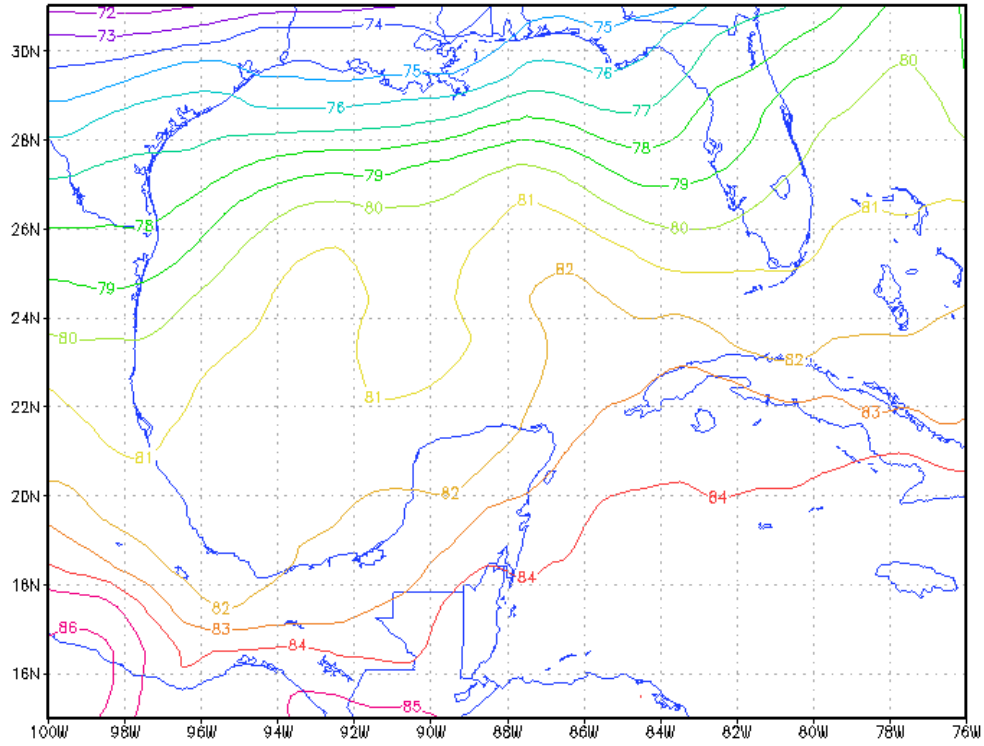


GrADS: COLA/IGES

2010-04-06-14:52

October +2 sigma SST climatology-Gulf of Mexico

+2 sigma (1982-2008) Nov SST (DegF)
NOAA OI.v2 Sea Surface Temperature

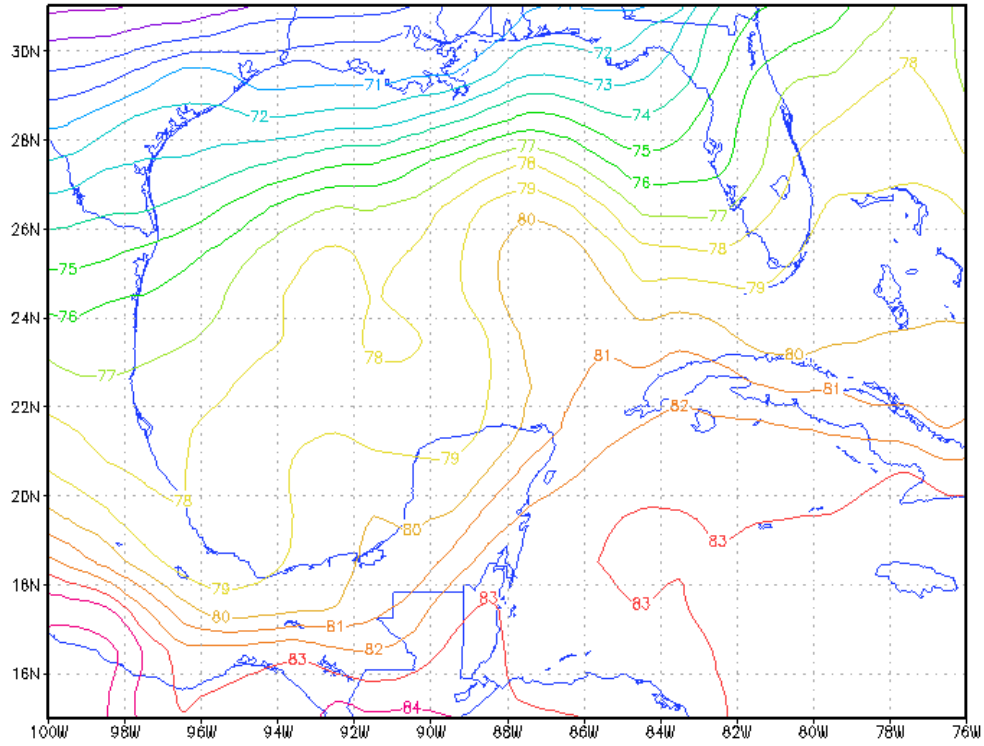


GrADS: COLA/IGES

2010-04-06-14:52

November +2 sigma SST climatology-Gulf of Mexico

+2 sigma (1982-2008) Dec SST (DegF)
NOAA OI.v2 Sea Surface Temperature



GrADS: COLA/IGES

2010-04-06-14:52

December +2 sigma SST climatology-Gulf of Mexico

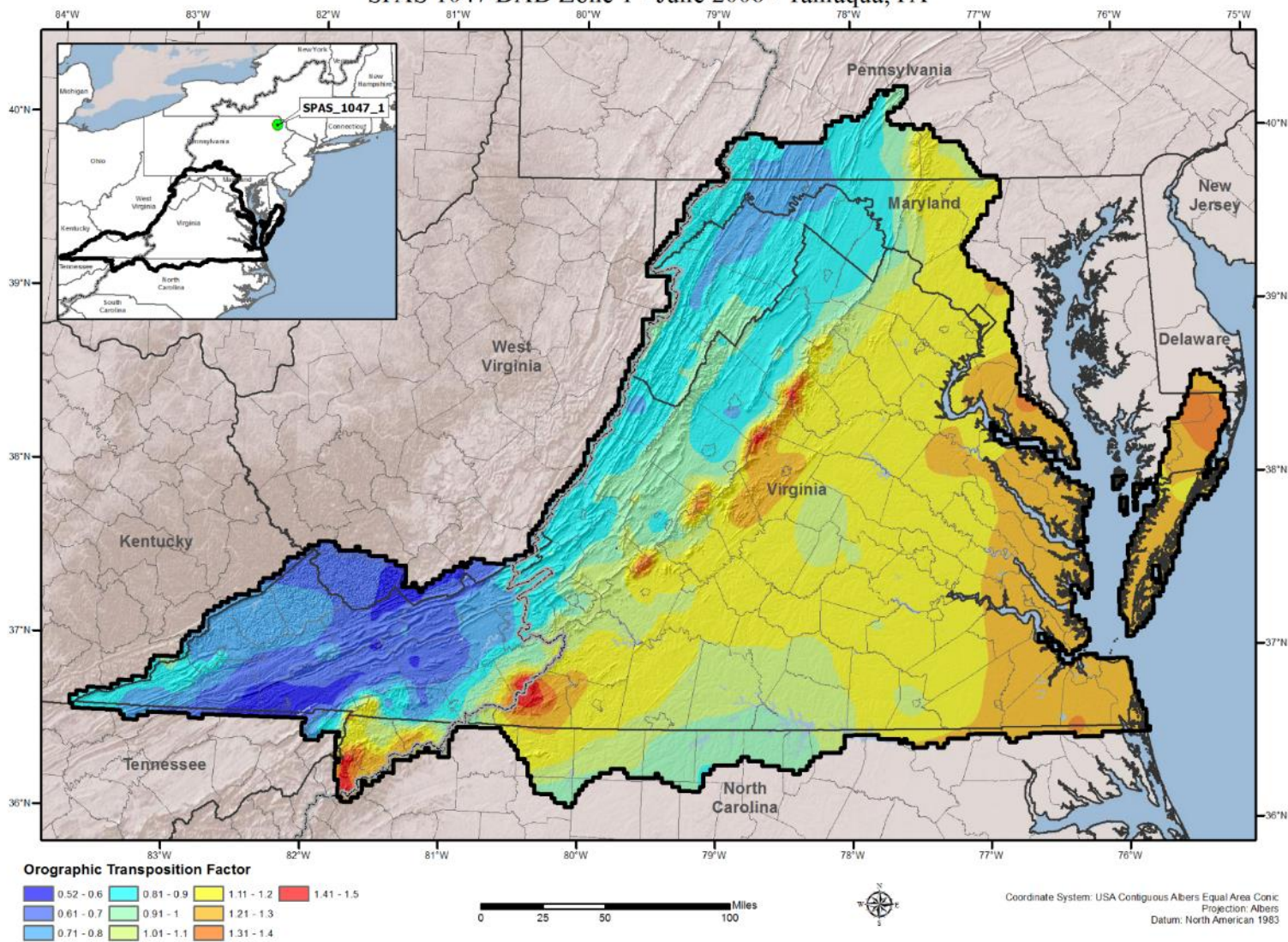
Appendix C

Orographic Transpositioning Factor (OTF) Maps

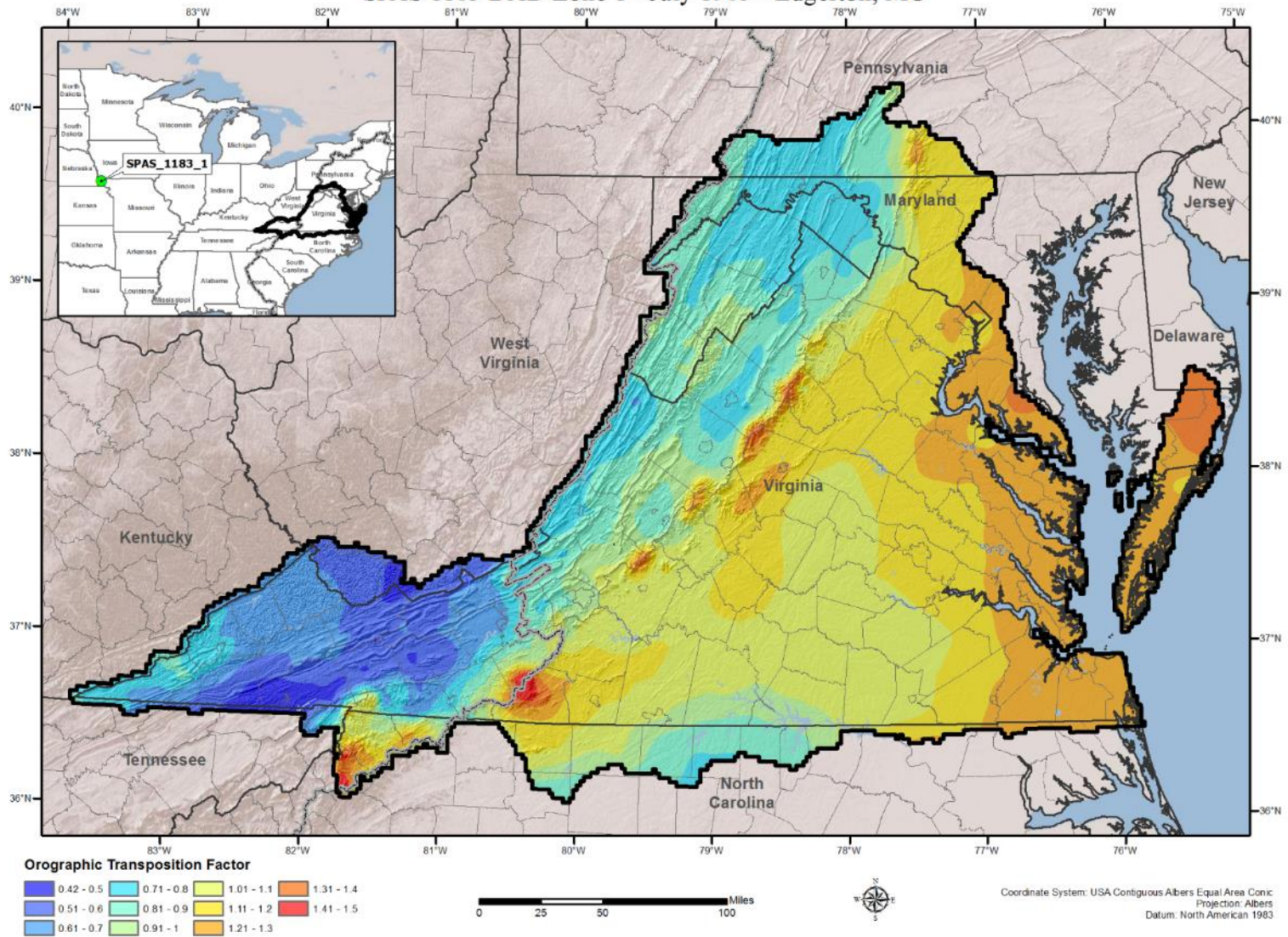
The following OTF maps represent the values as calculated at each grid point across the entire domain for each storm. For PMP calculation purposes, storms were limited to specific transposition locations and the OTF was only used for the grid points within those transposition regions during the PMP calculations. The OTF data as provided in this appendix helped to define and set those transposition limits through evaluation of the spatial variations and comparison of the values. A cap was also placed on OTF values greater than 1.50 or less than 0.50 in the calculation process.

General Storms

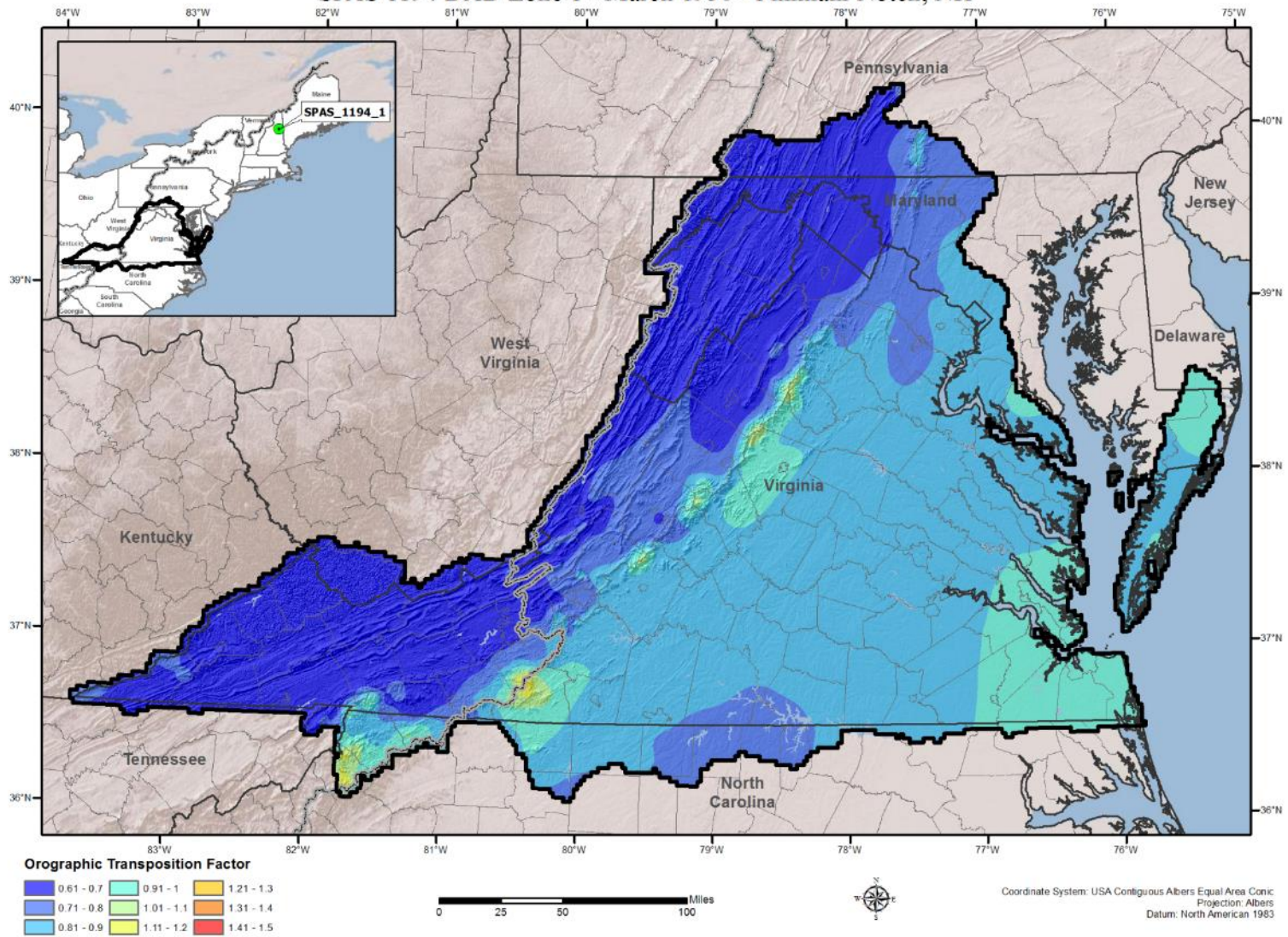
Orographic Transposition Factor (OTF) SPAS 1047 DAD Zone 1 - June 2006 - Tamaqua, PA



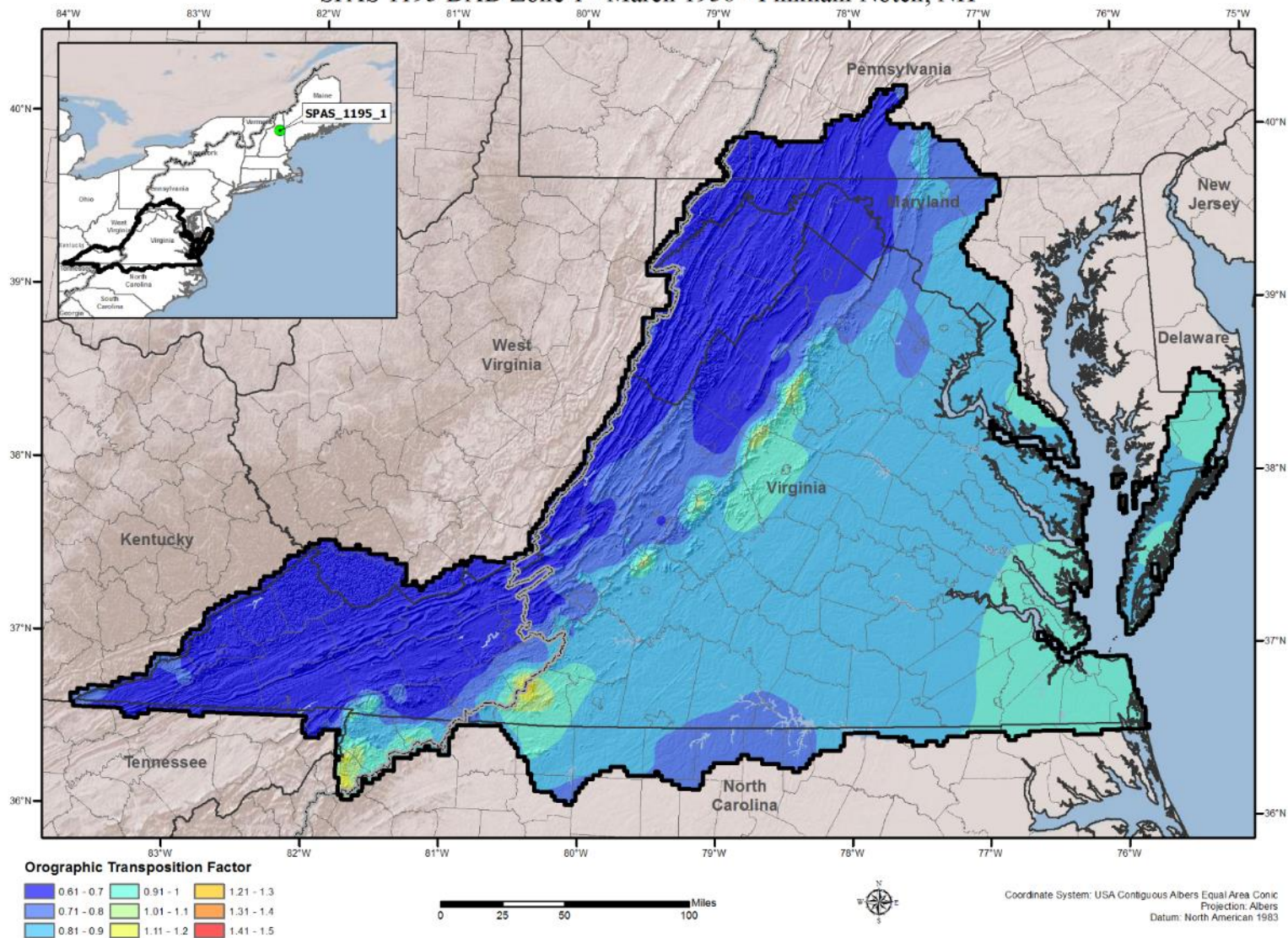
Orographic Transposition Factor (OTF)
 SPAS 1183 DAD Zone 1 - July 1965 - Edgerton, MO



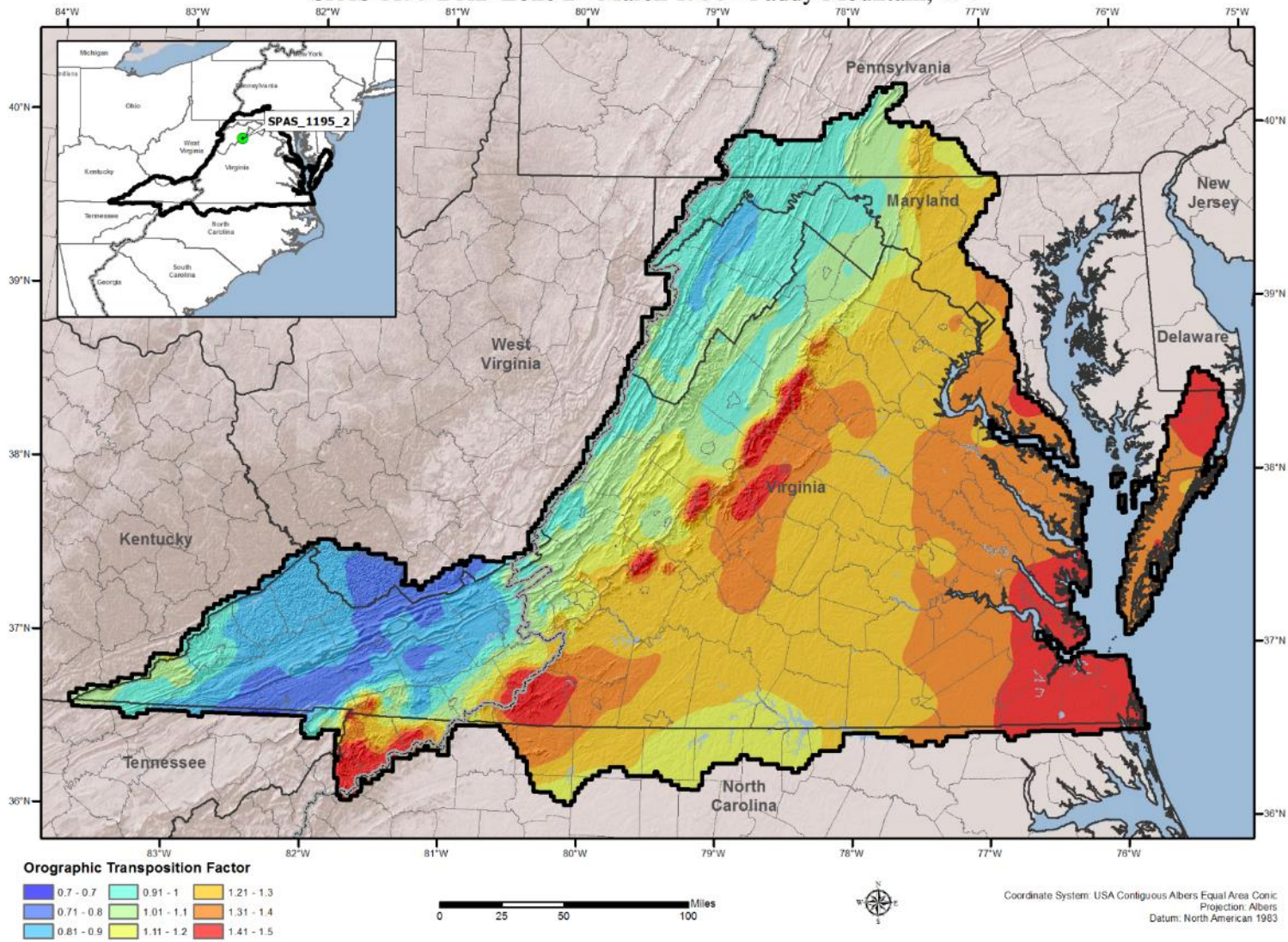
Orographic Transposition Factor (OTF)
 SPAS 1194 DAD Zone 1 - March 1936 - Pinkham Notch, NH



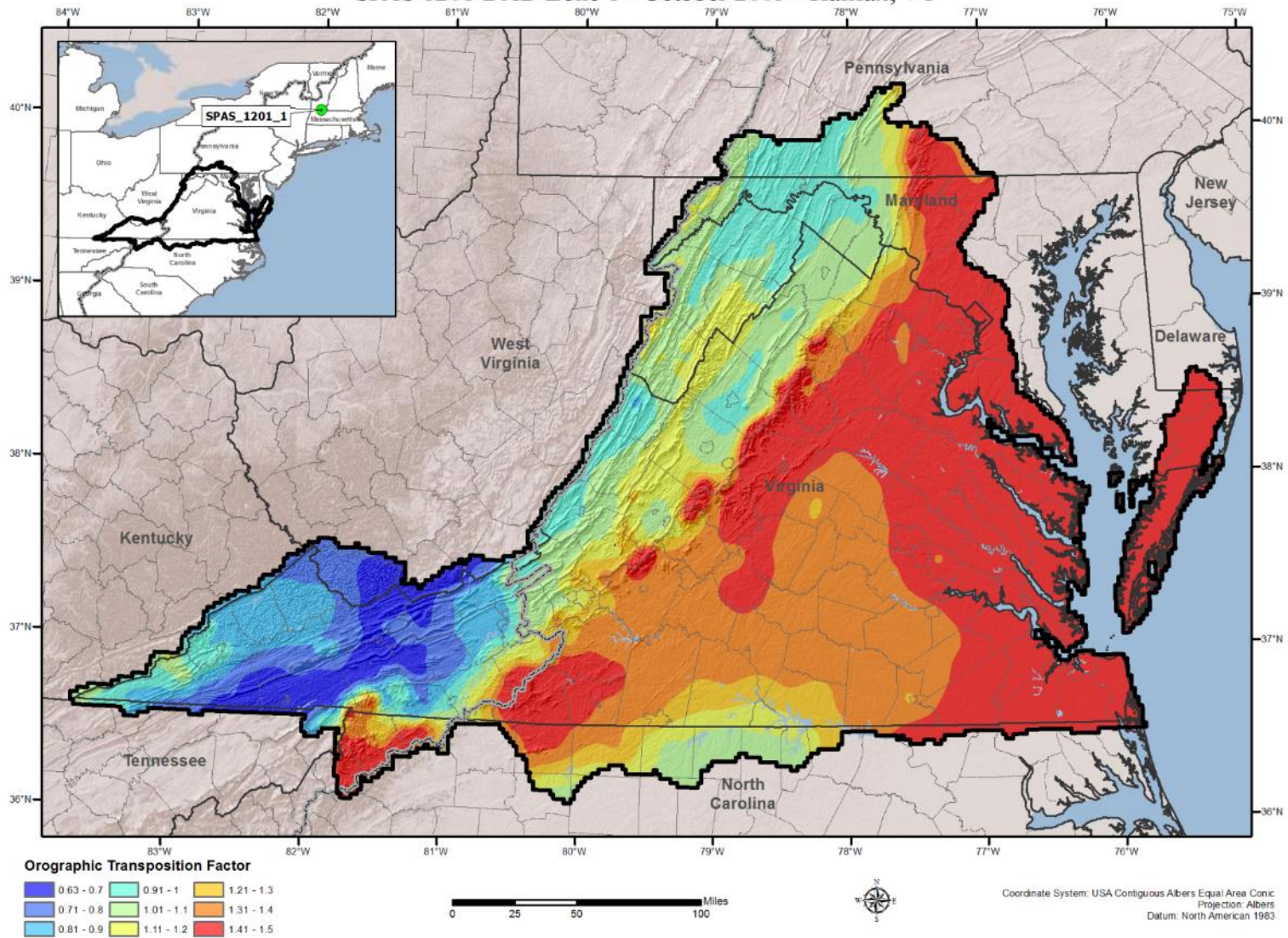
Orographic Transposition Factor (OTF)
 SPAS 1195 DAD Zone 1 - March 1936 - Pinkham Notch, NH



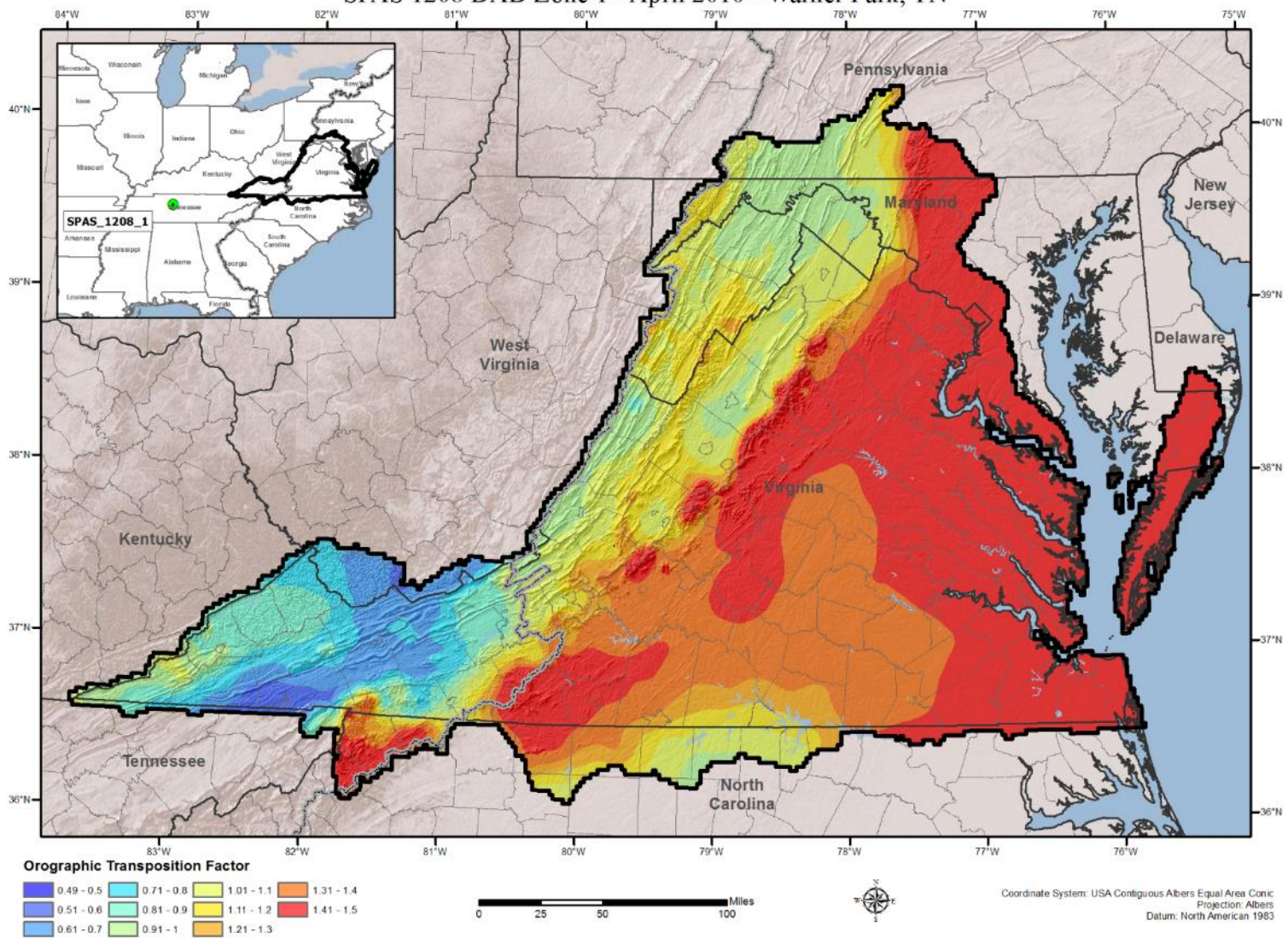
Orographic Transposition Factor (OTF)
 SPAS 1195 DAD Zone 2 - March 1936 - Paddy Mountain, WV



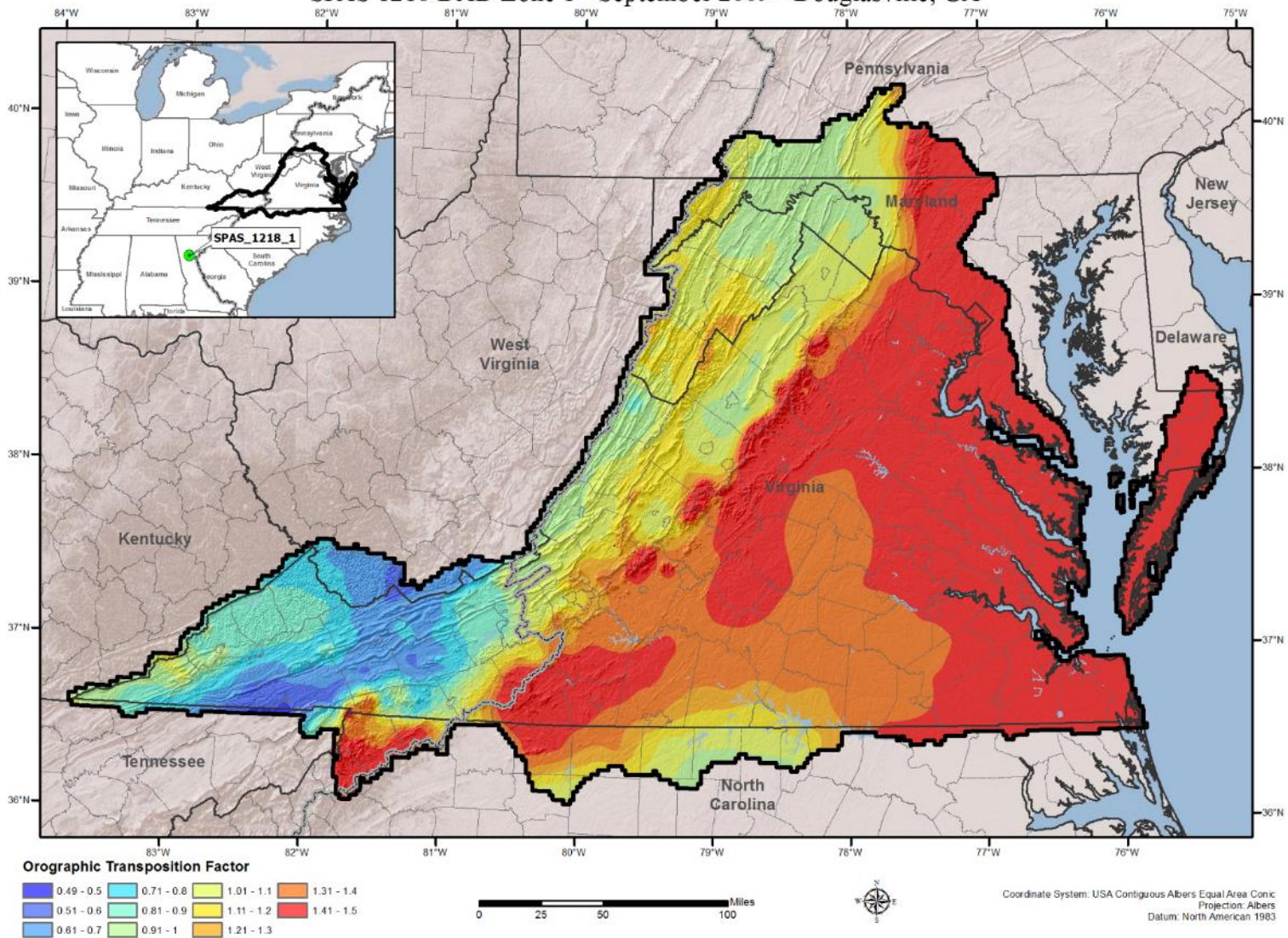
Orographic Transposition Factor (OTF) SPAS 1201 DAD Zone 1 - October 2005 - Halifax, VT



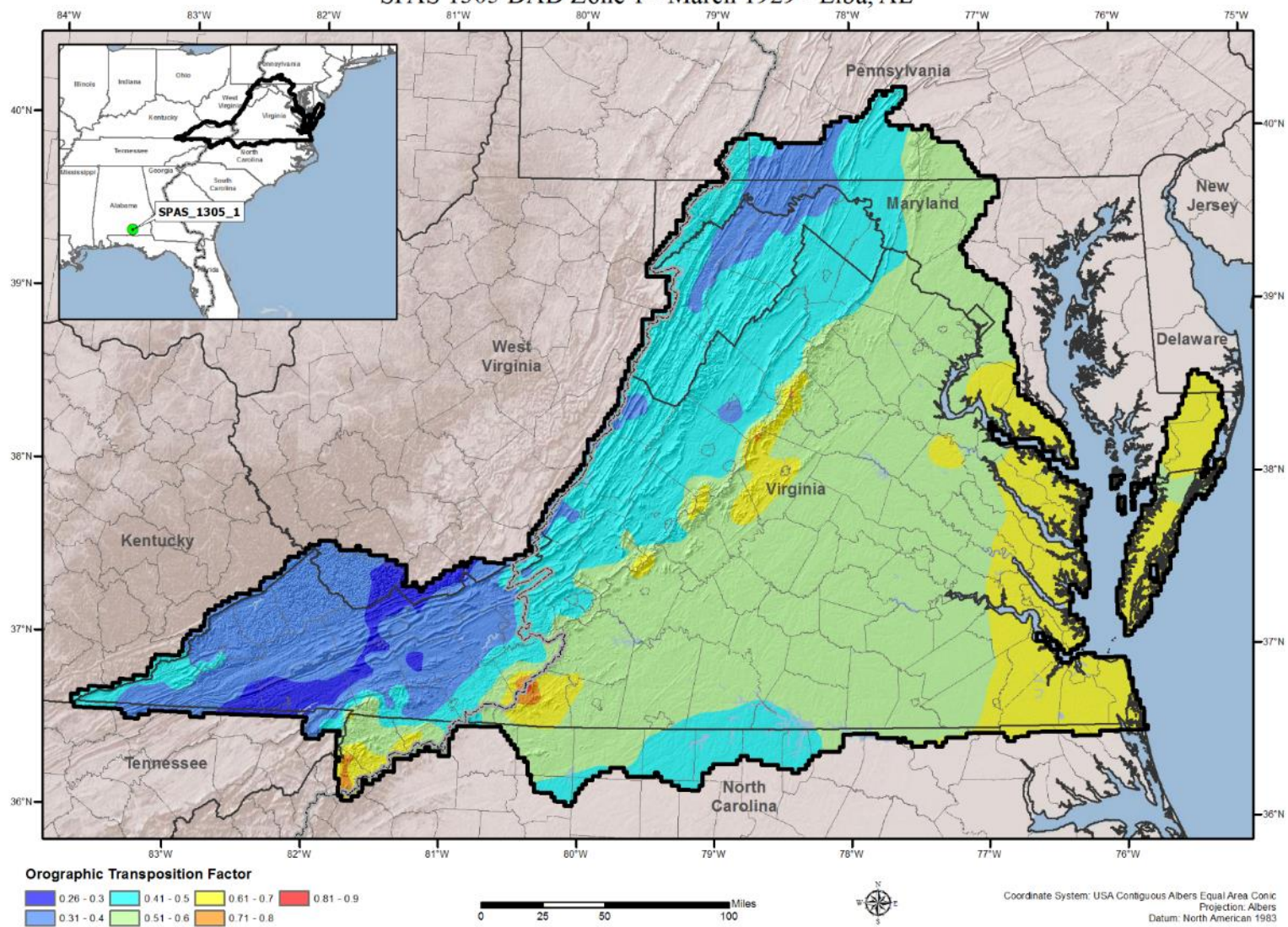
Orographic Transposition Factor (OTF) SPAS 1208 DAD Zone 1 - April 2010 - Warner Park, TN



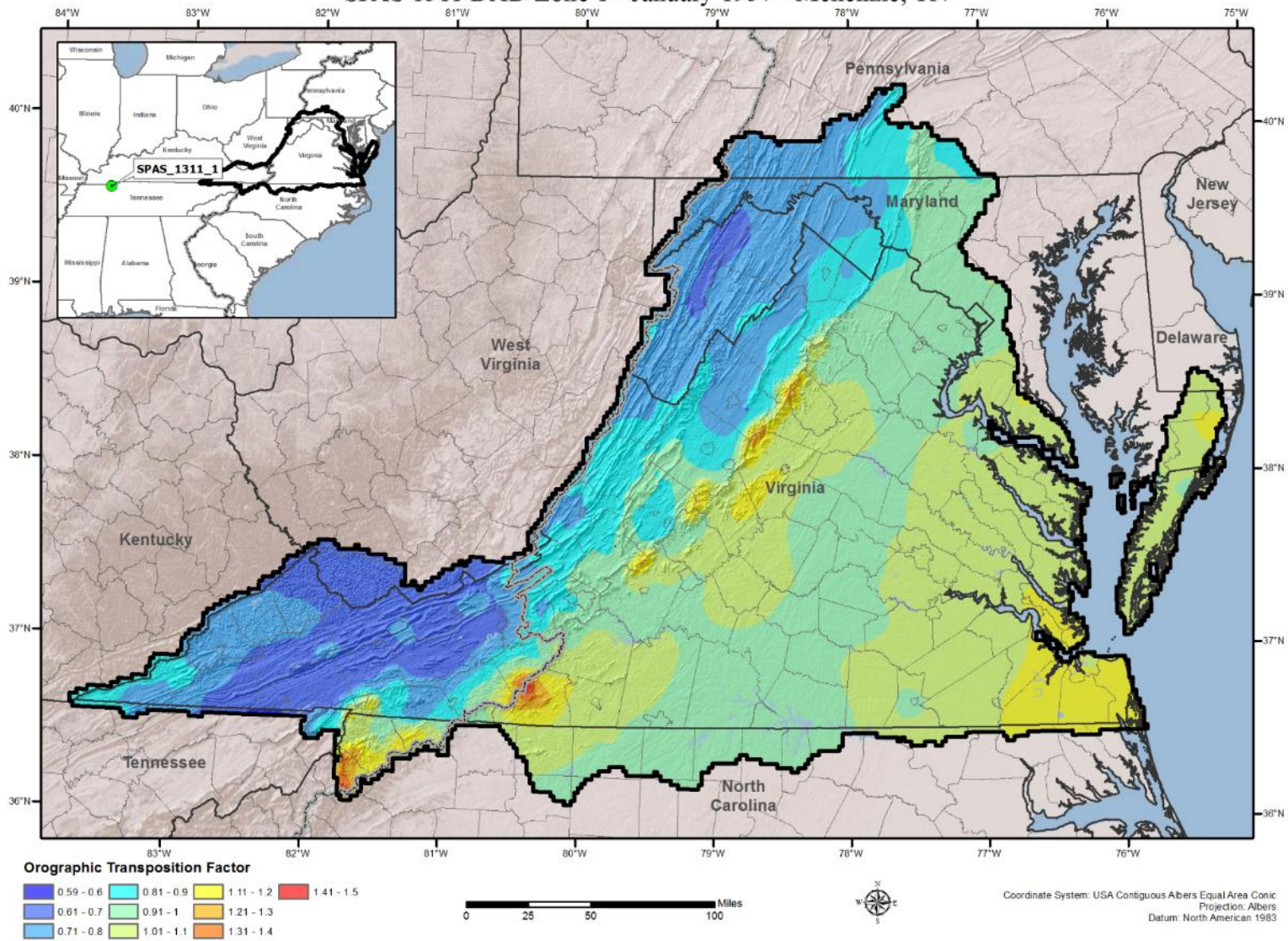
Orographic Transposition Factor (OTF)
 SPAS 1218 DAD Zone 1 - September 2009 - Douglasville, GA



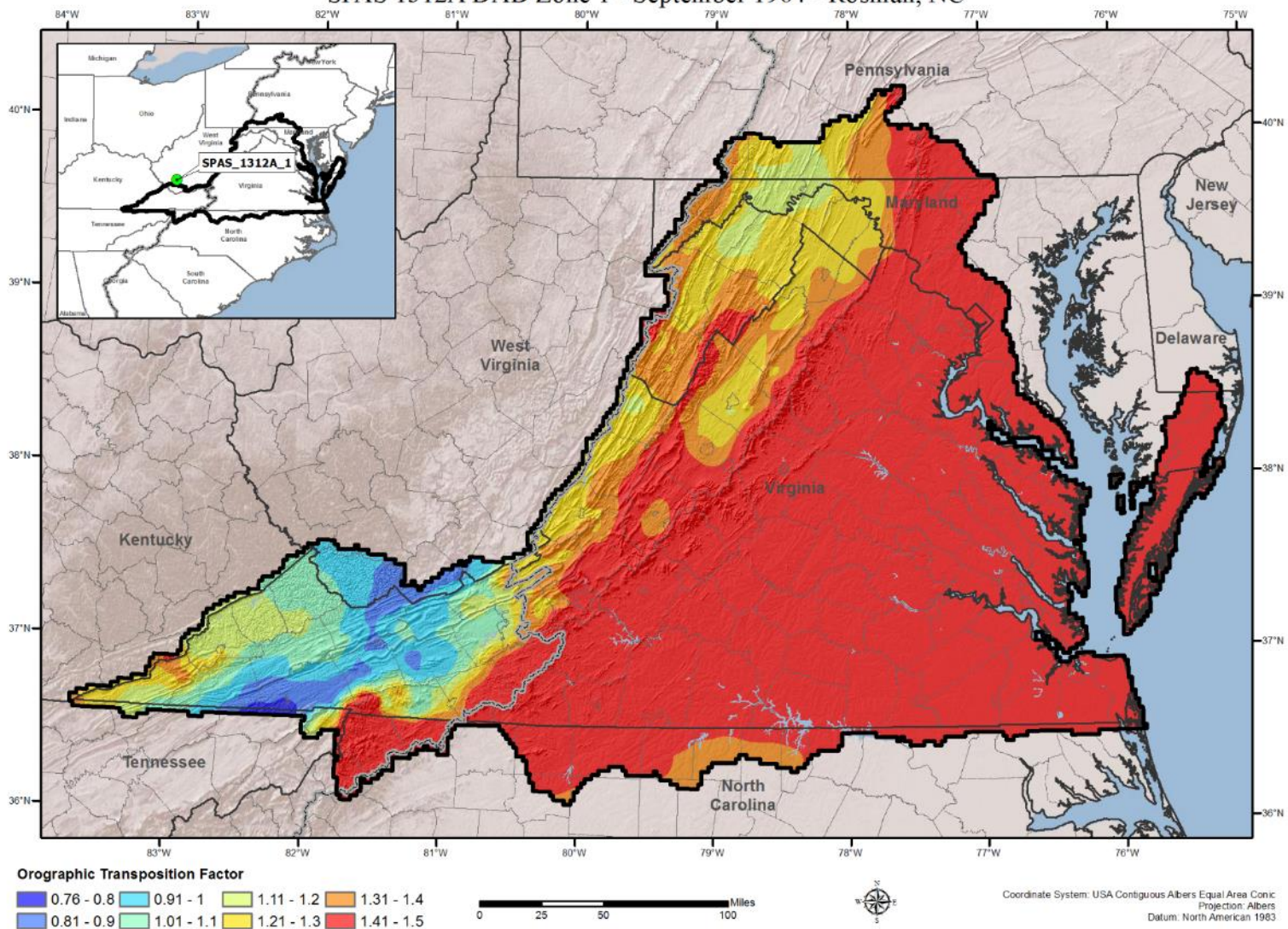
Orographic Transposition Factor (OTF)
 SPAS 1305 DAD Zone 1 - March 1929 - Elba, AL



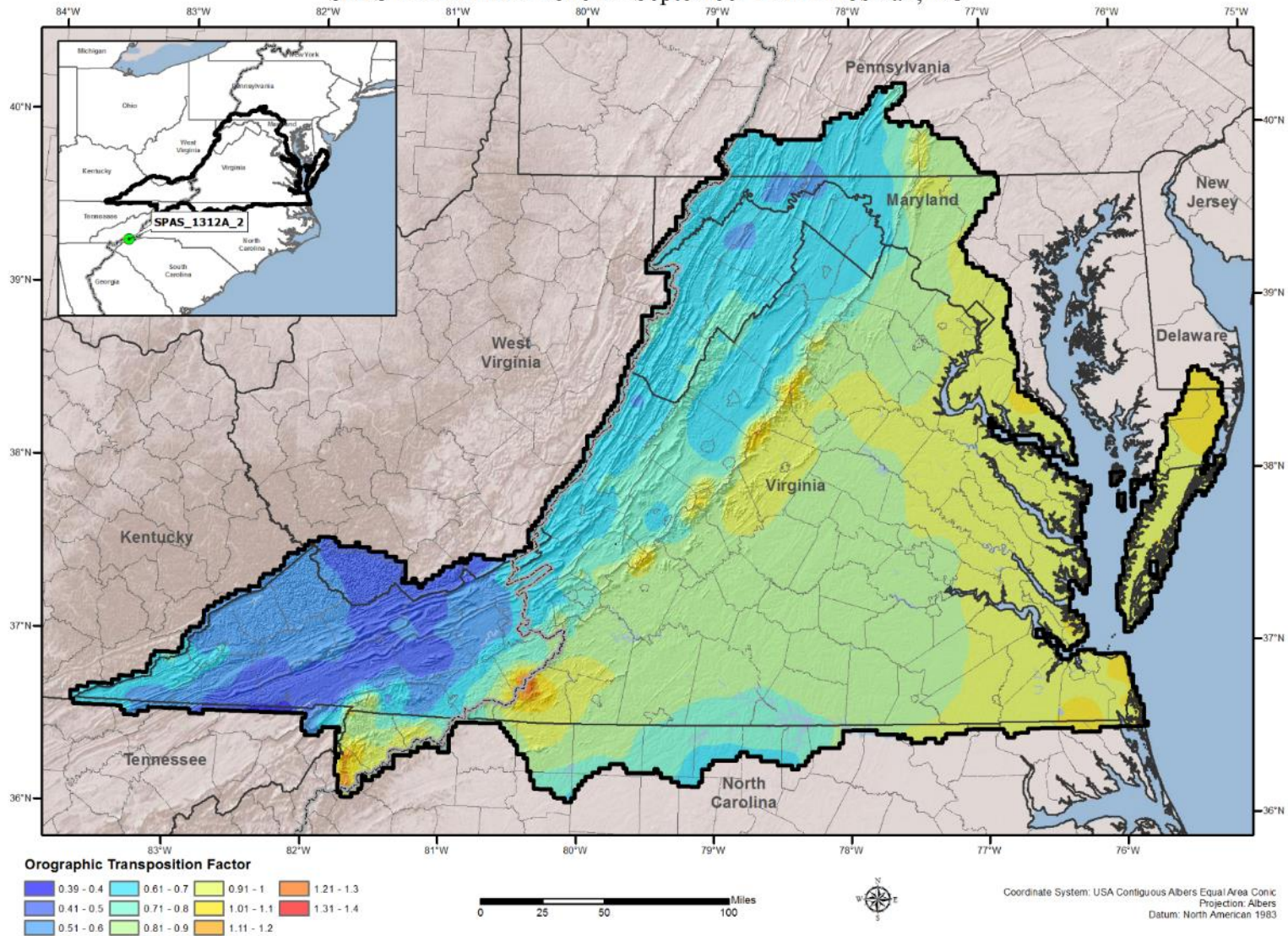
Orographic Transposition Factor (OTF)
 SPAS 1311 DAD Zone 1 - January 1937 - Mckenzie, TN



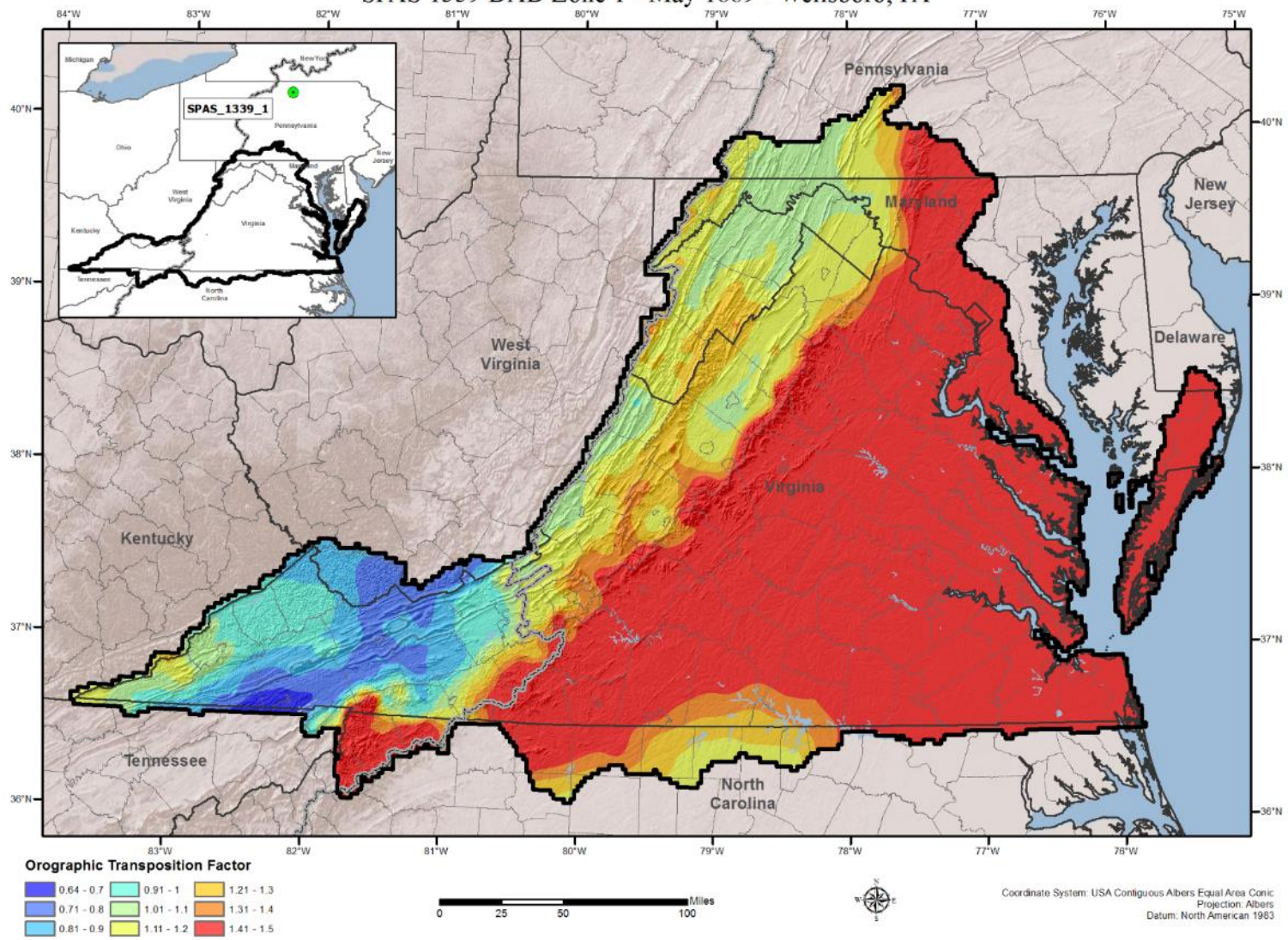
Orographic Transposition Factor (OTF) SPAS 1312A DAD Zone 1 - September 1964 - Rosman, NC



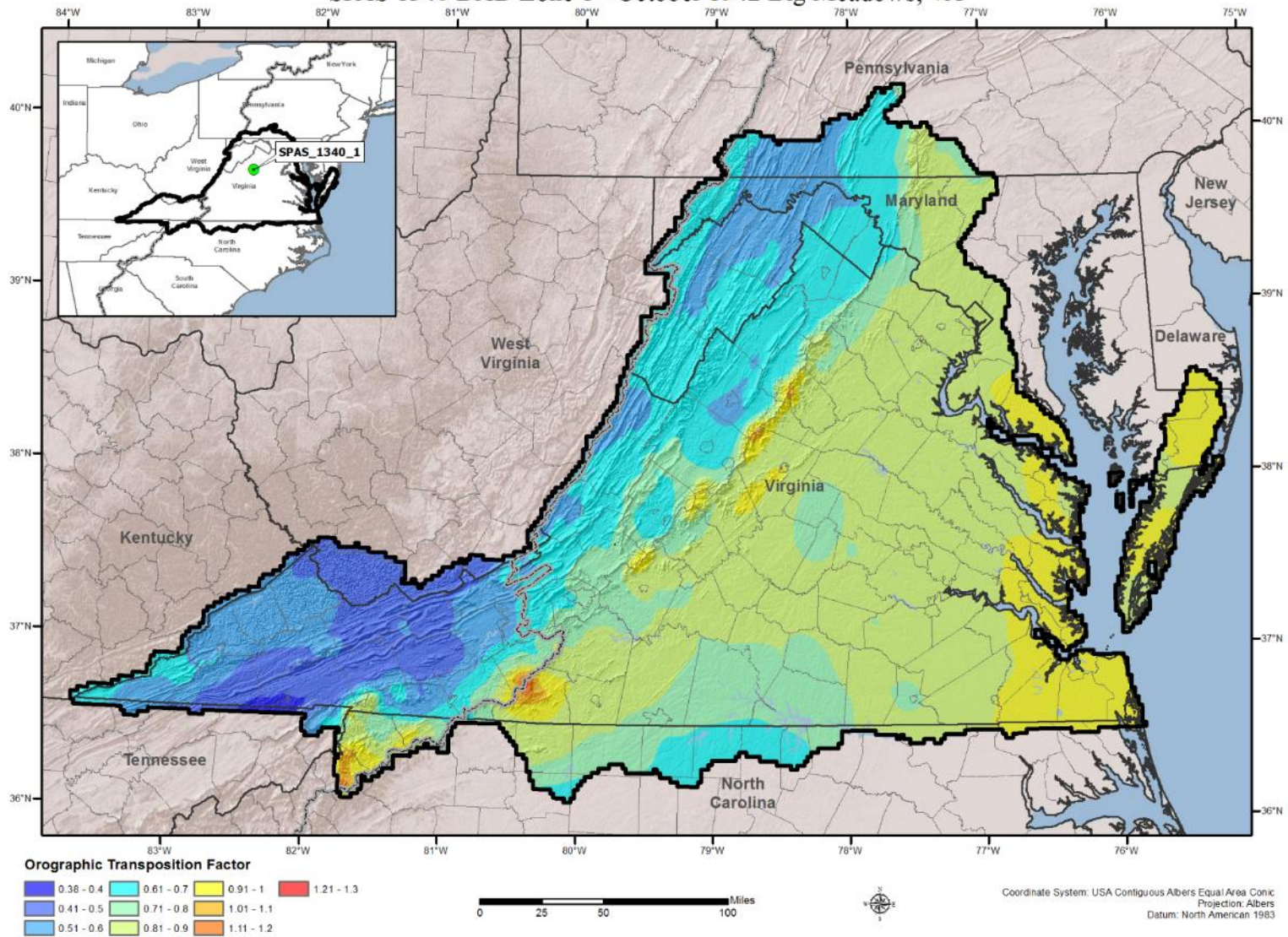
Orographic Transposition Factor (OTF)
 SPAS 1312A DAD Zone 2 - September 1964 - Rosman, NC



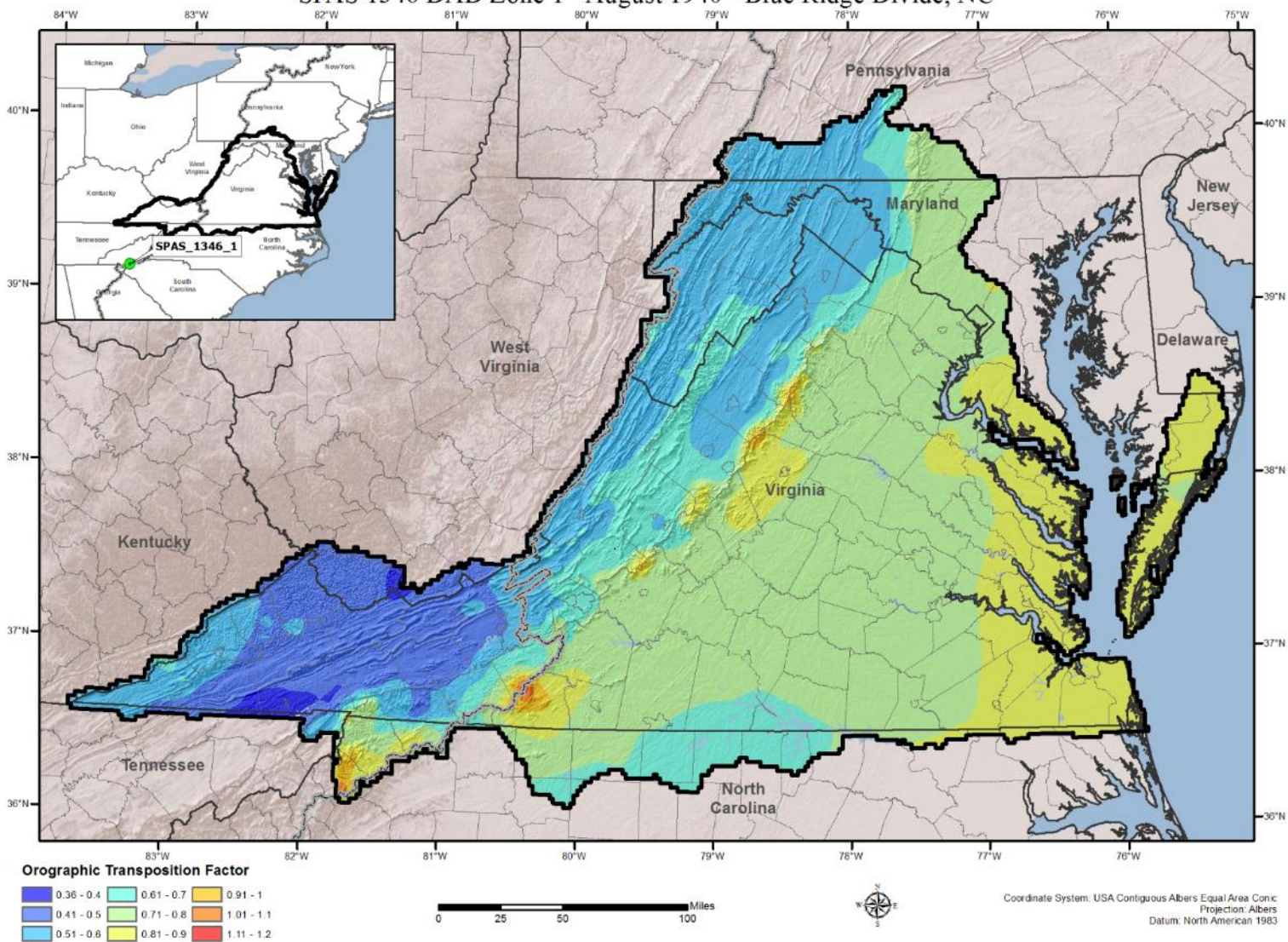
Orographic Transposition Factor (OTF) SPAS 1339 DAD Zone 1 - May 1889 - Wellsboro, PA



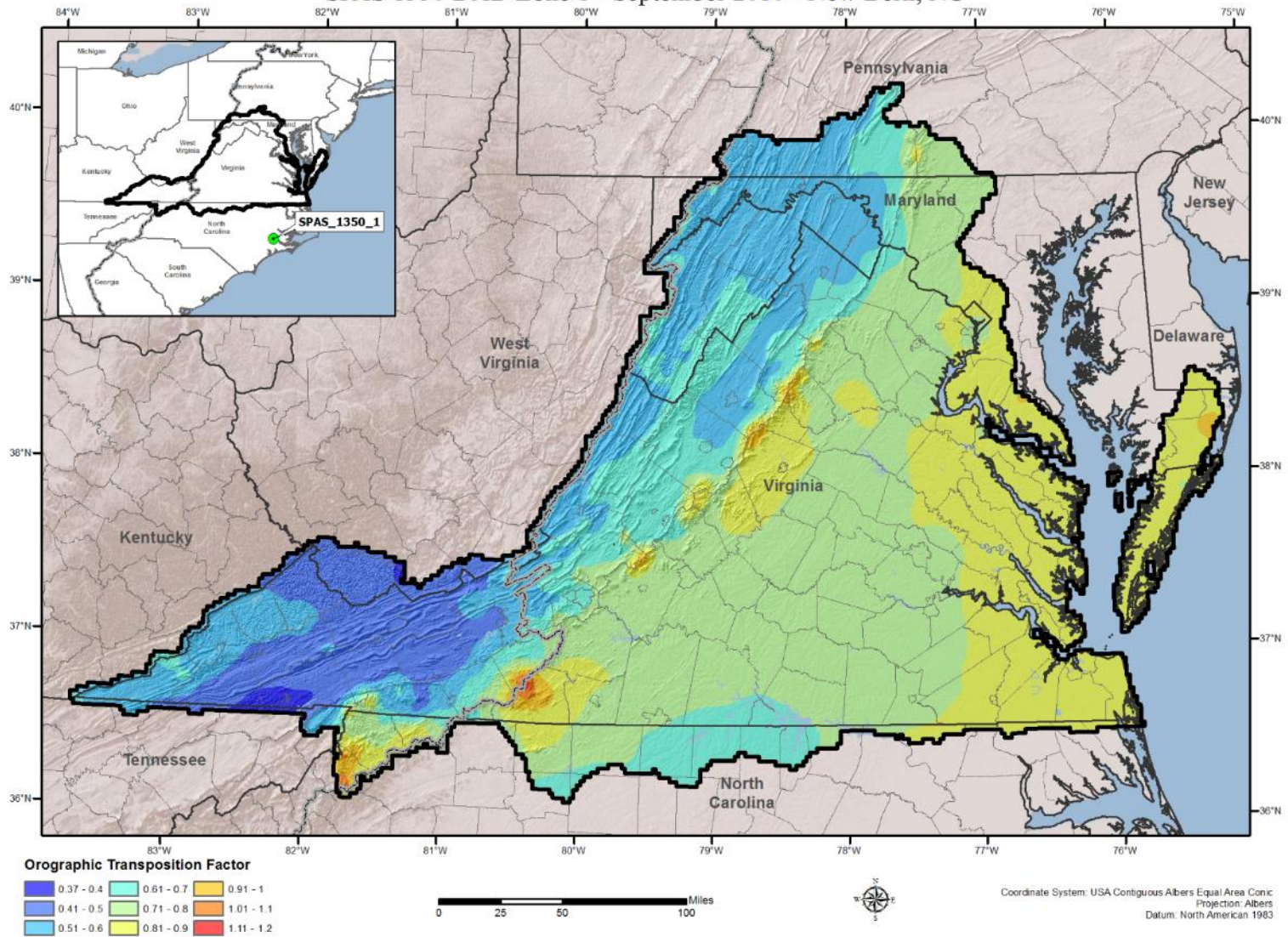
Orographic Transposition Factor (OTF)
 SPAS 1340 DAD Zone 1 - October 1942 Big Meadows, VA



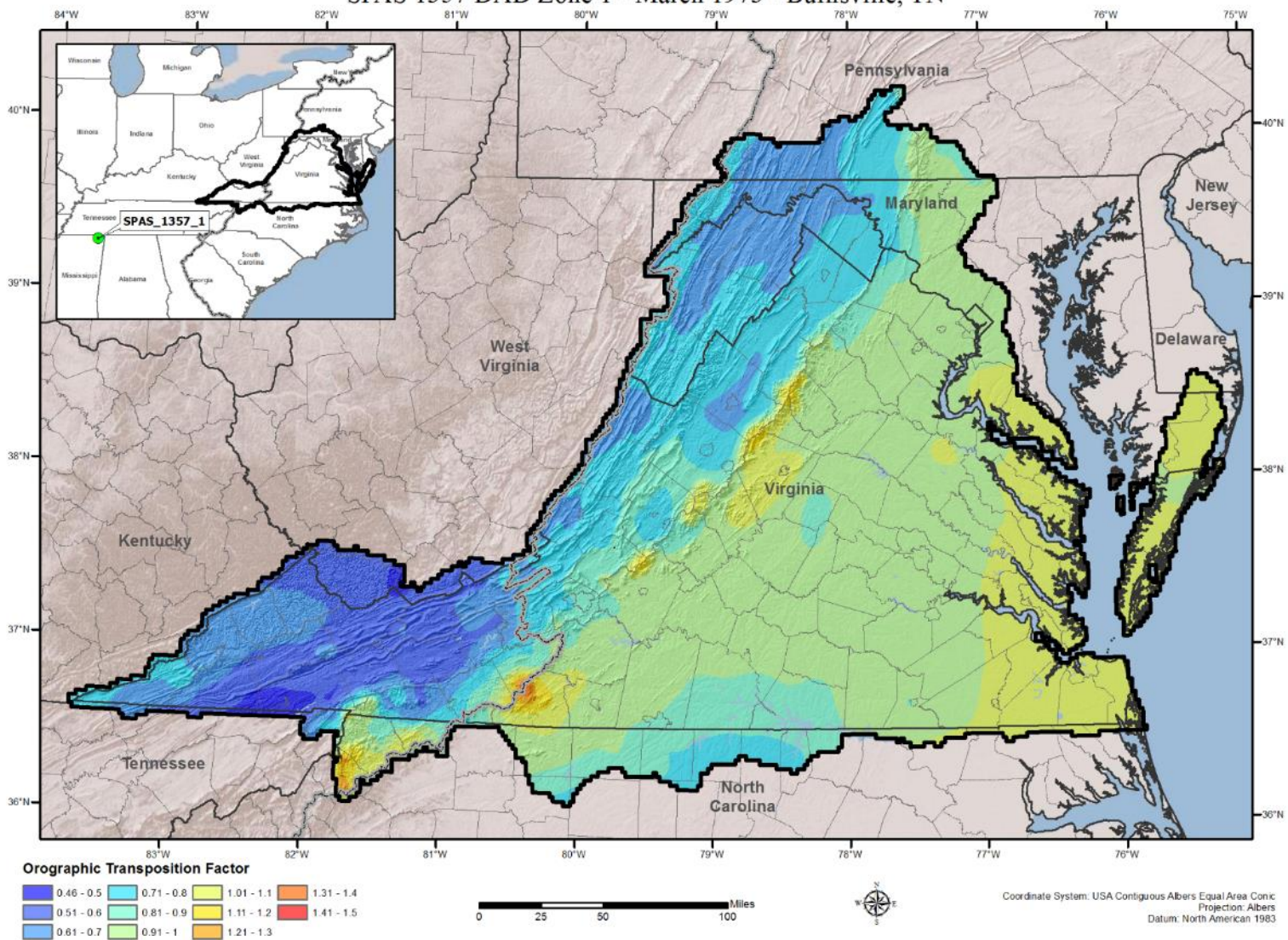
Orographic Transposition Factor (OTF) SPAS 1346 DAD Zone 1 - August 1940 - Blue Ridge Divide, NC



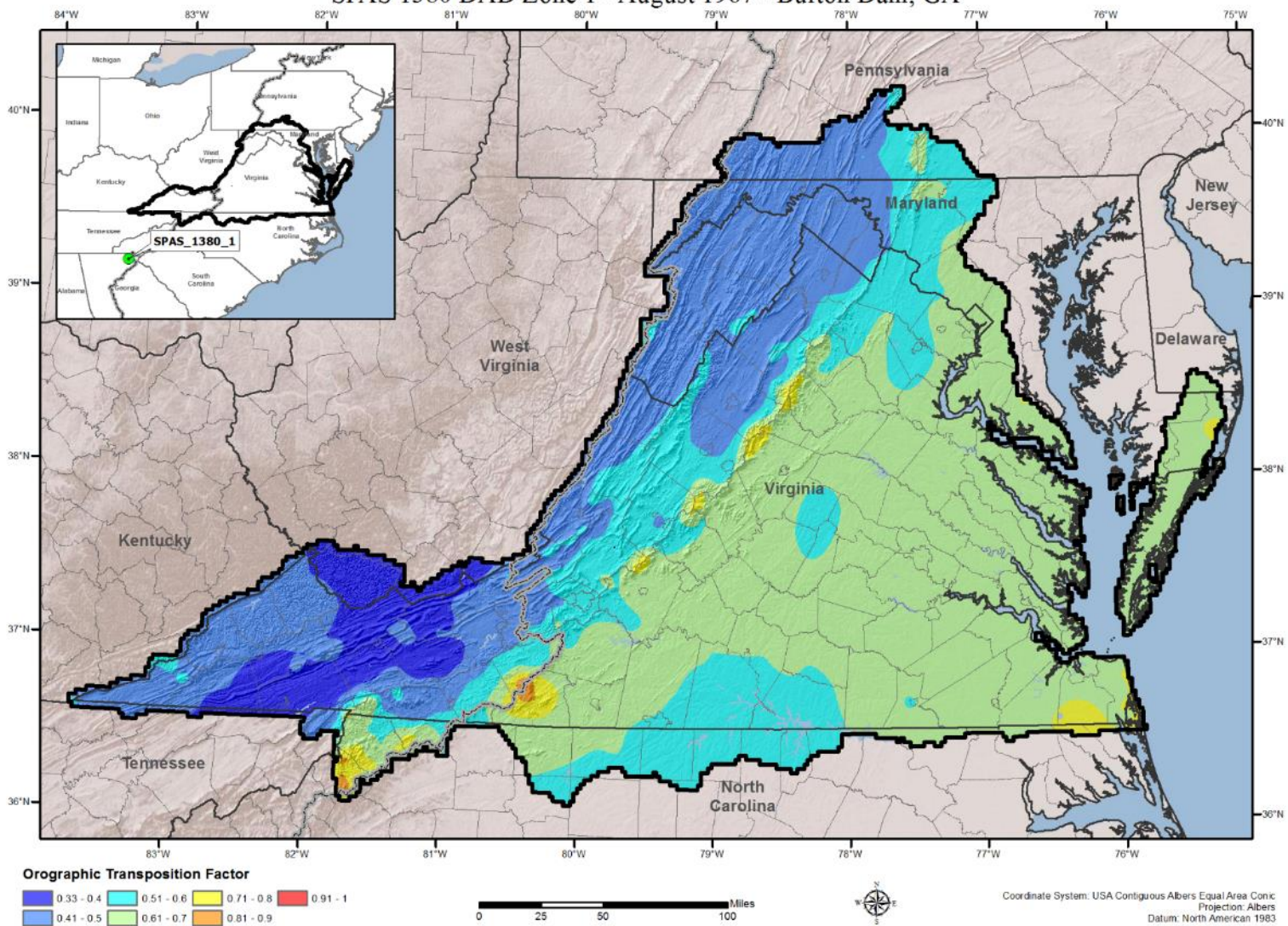
Orographic Transposition Factor (OTF)
 SPAS 1350 DAD Zone 1 - September 2010 - New Bern, NC



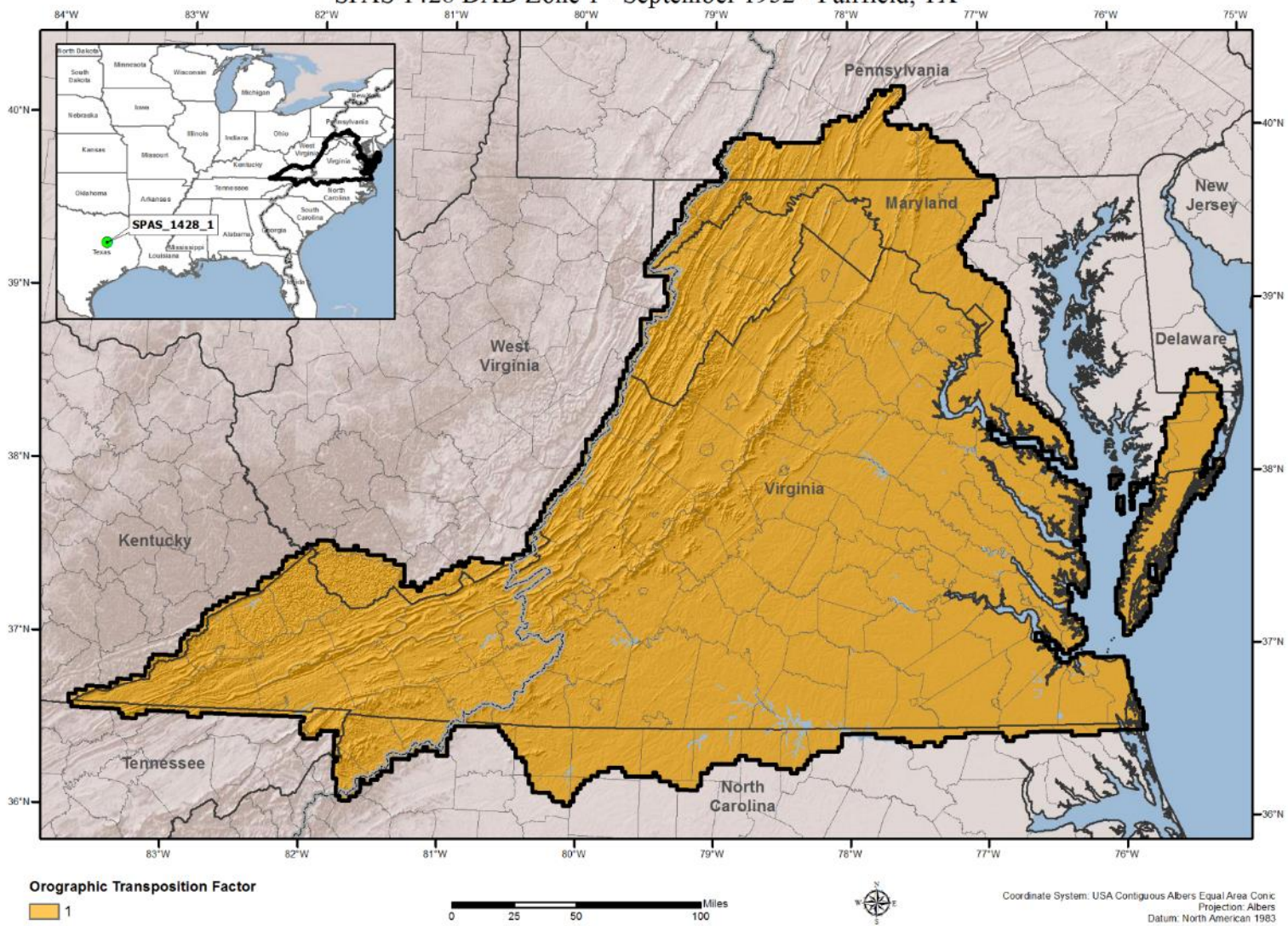
Orographic Transposition Factor (OTF) SPAS 1357 DAD Zone 1 - March 1973 - Burnsville, TN



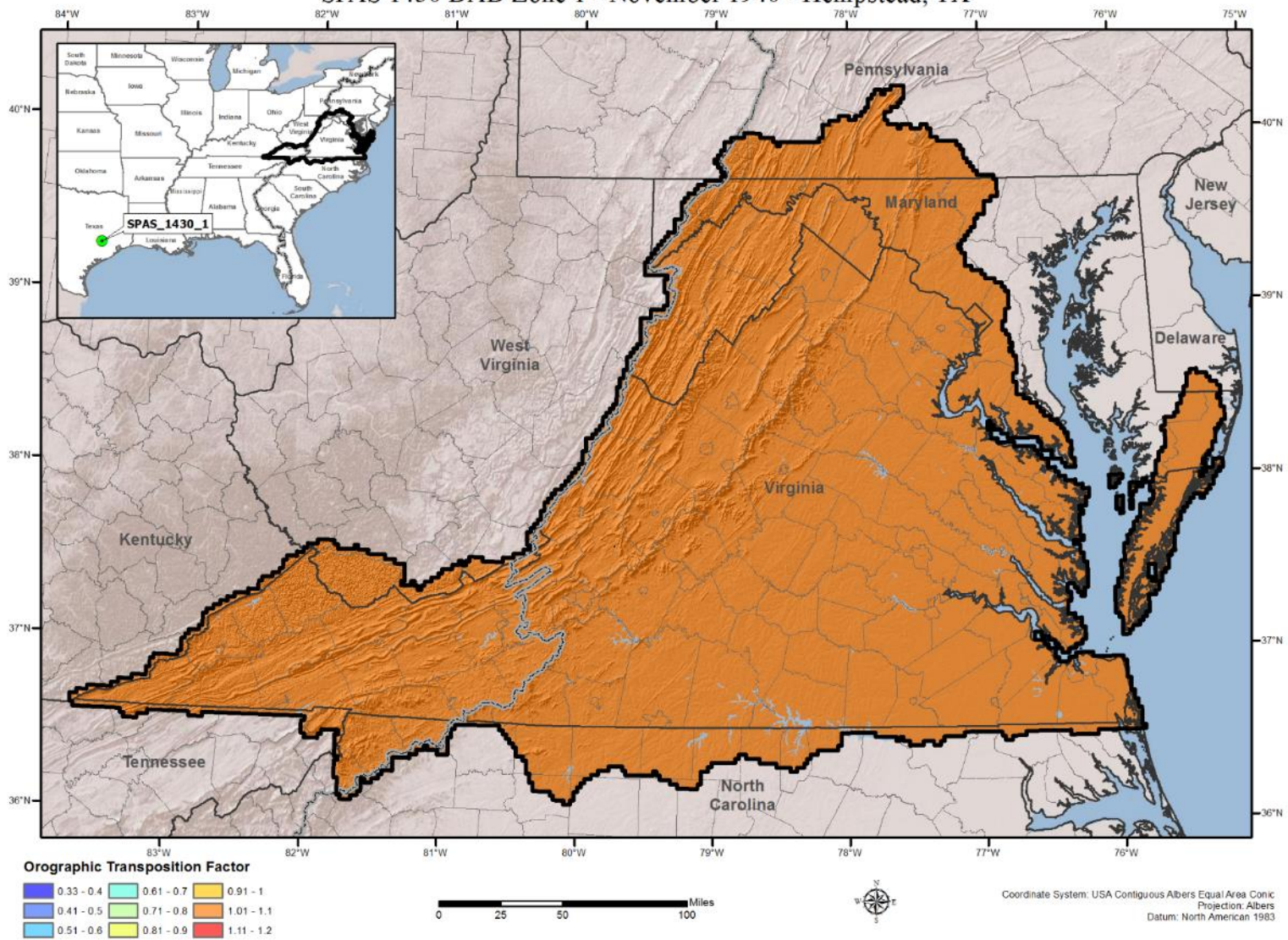
Orographic Transposition Factor (OTF)
 SPAS 1380 DAD Zone 1 - August 1967 - Burton Dam, GA



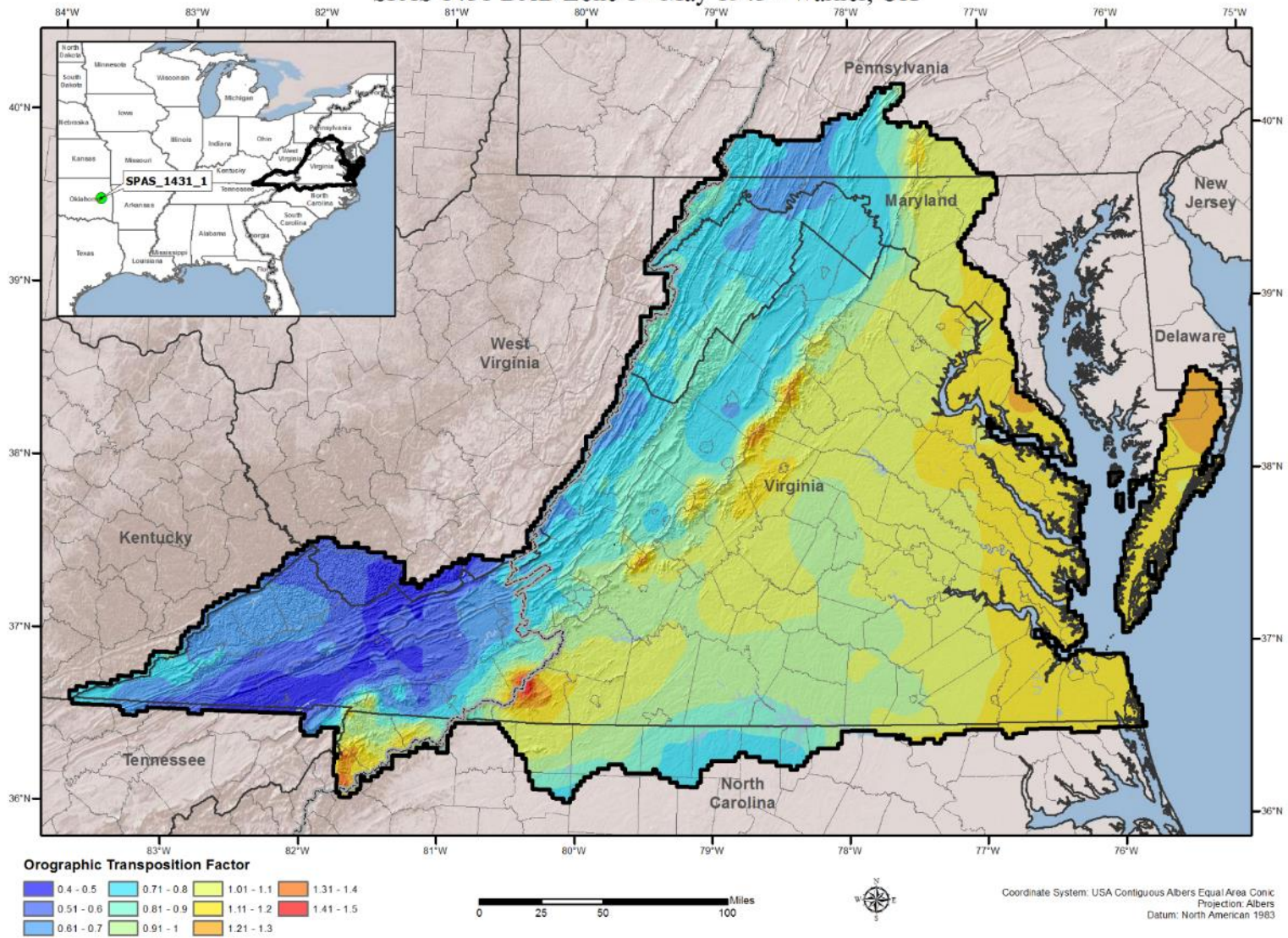
Orographic Transposition Factor (OTF)
SPAS 1428 DAD Zone 1 - September 1932 - Fairfield, TX



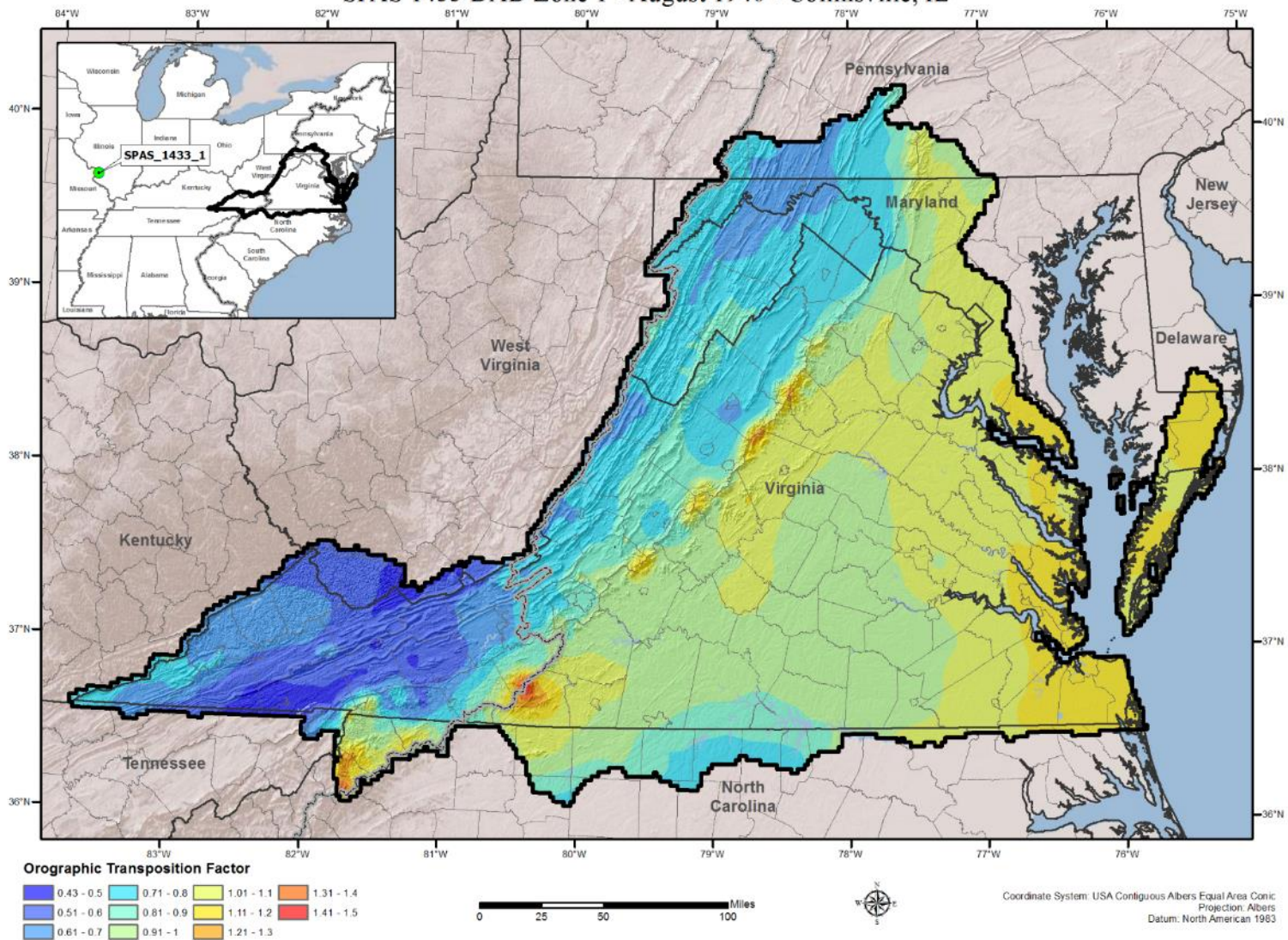
Orographic Transposition Factor (OTF) SPAS 1430 DAD Zone 1 - November 1940 - Hempstead, TX



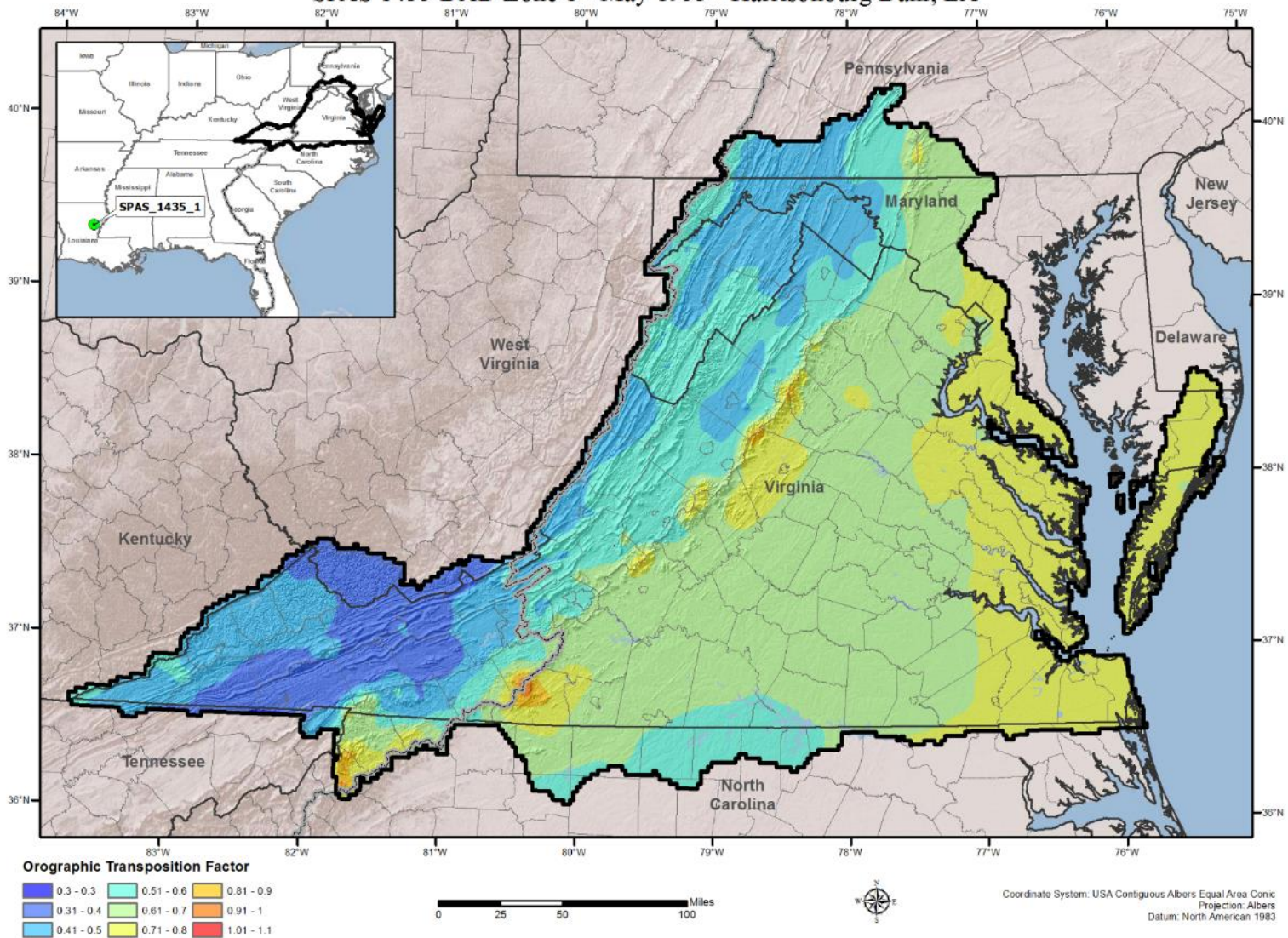
Orographic Transposition Factor (OTF)
 SPAS 1431 DAD Zone 1 - May 1943 - Warner, OK



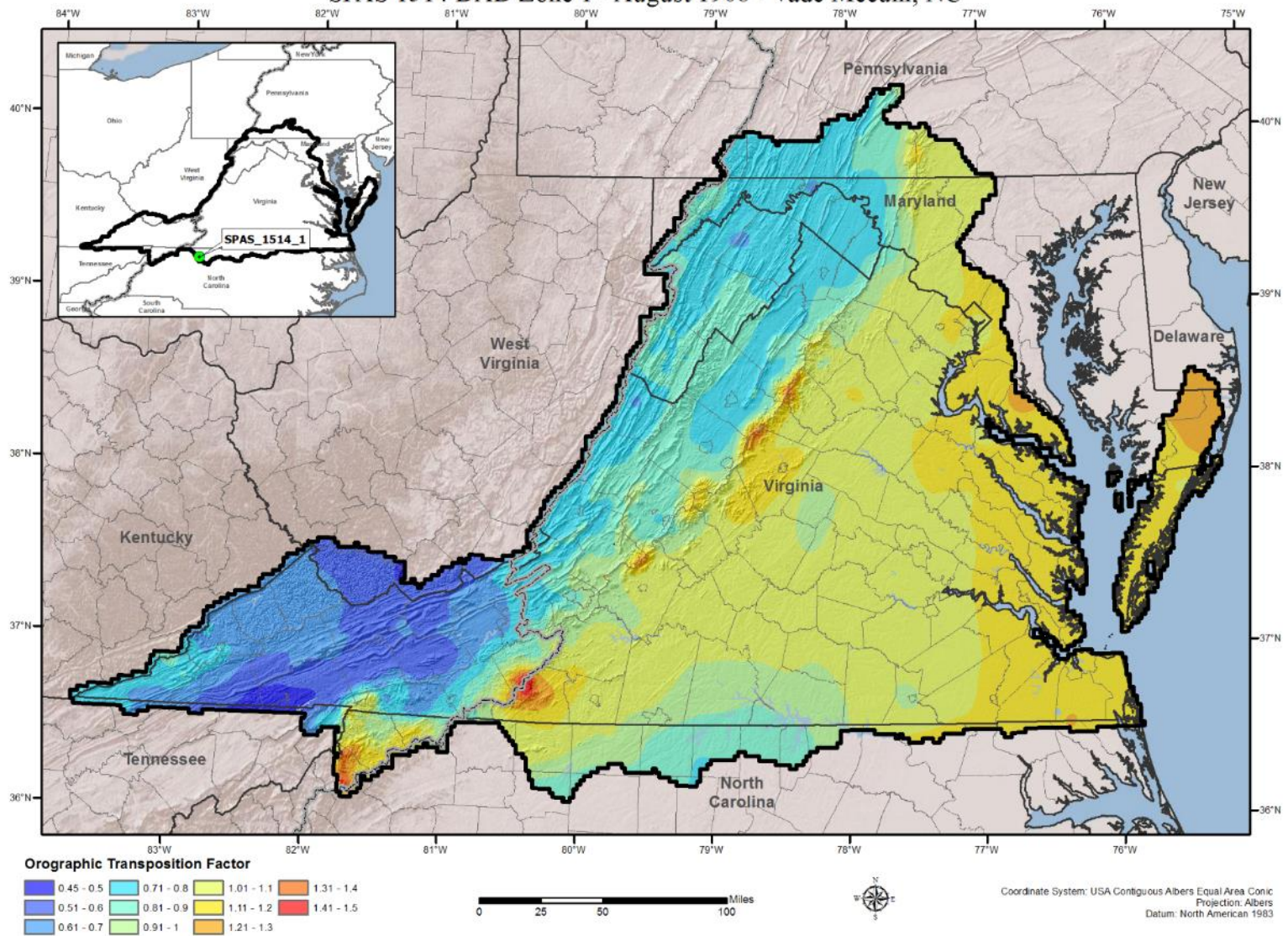
Orographic Transposition Factor (OTF)
 SPAS 1433 DAD Zone 1 - August 1946 - Collinsville, IL



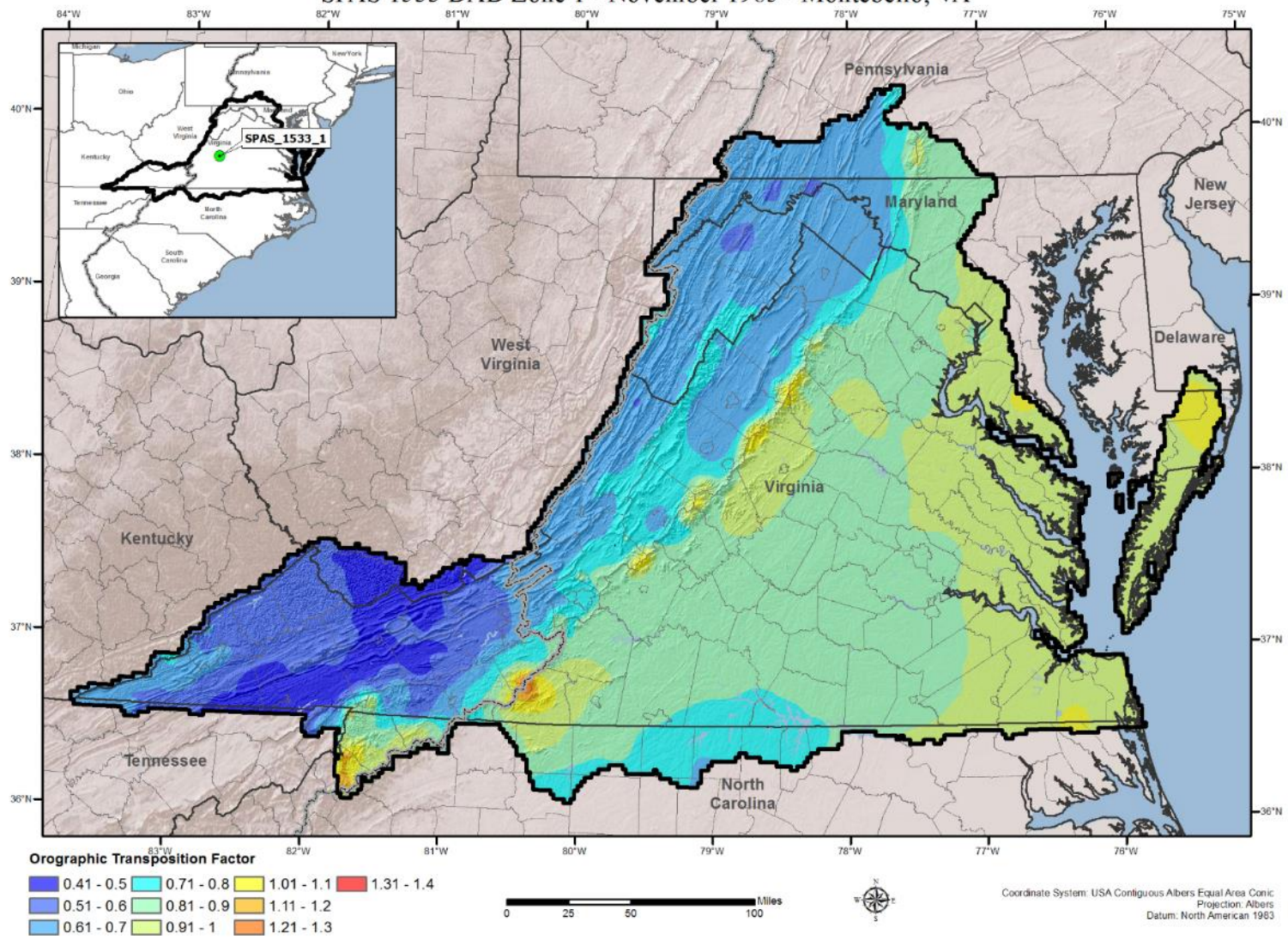
Orographic Transposition Factor (OTF)
 SPAS 1435 DAD Zone 1 - May 1953 - Harrisonburg Dam, LA



Orographic Transposition Factor (OTF) SPAS 1514 DAD Zone 1 - August 1908 - Vade Mecum, NC

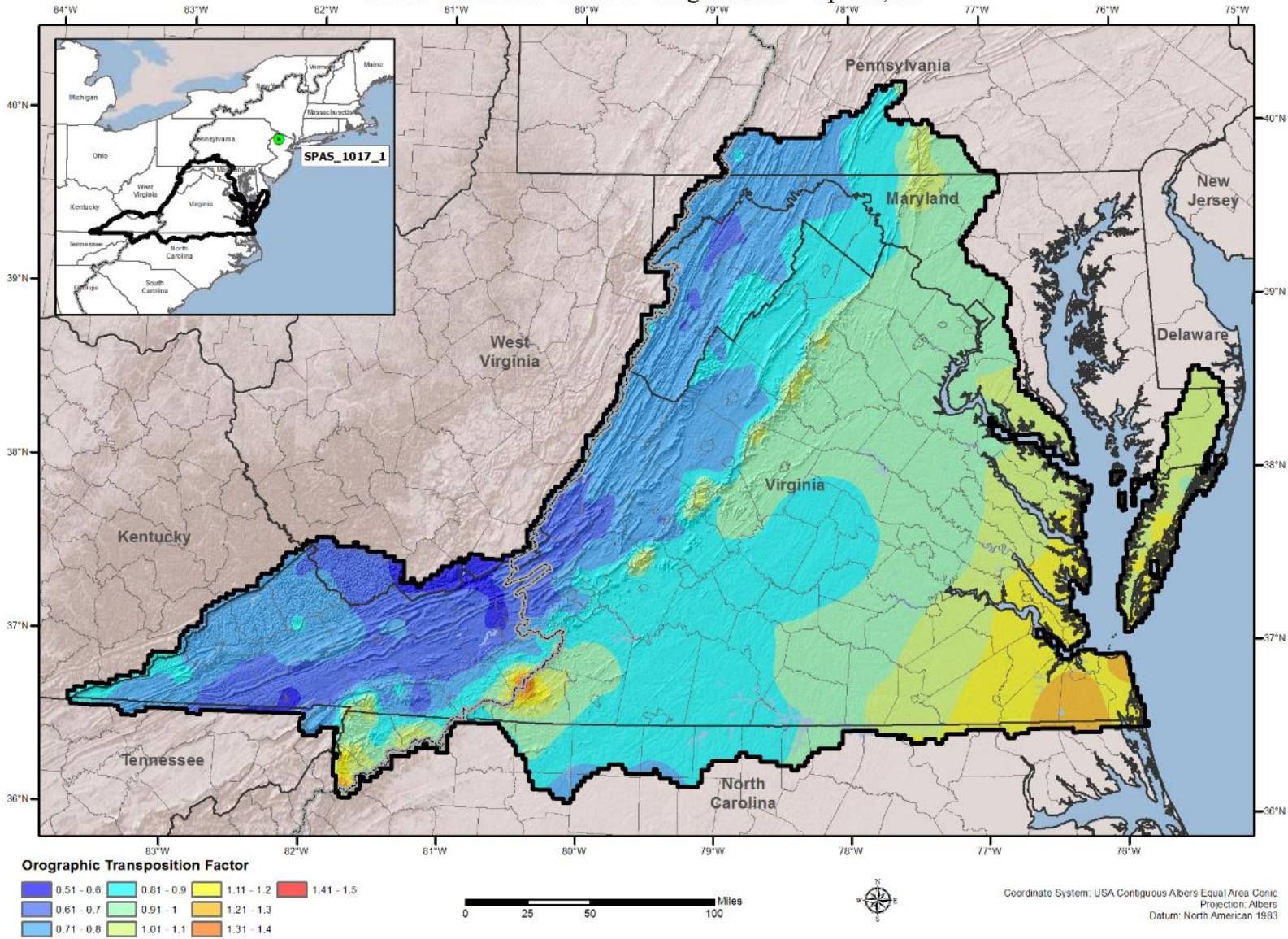


Orographic Transposition Factor (OTF)
 SPAS 1533 DAD Zone 1 - November 1985 - Montebello, VA

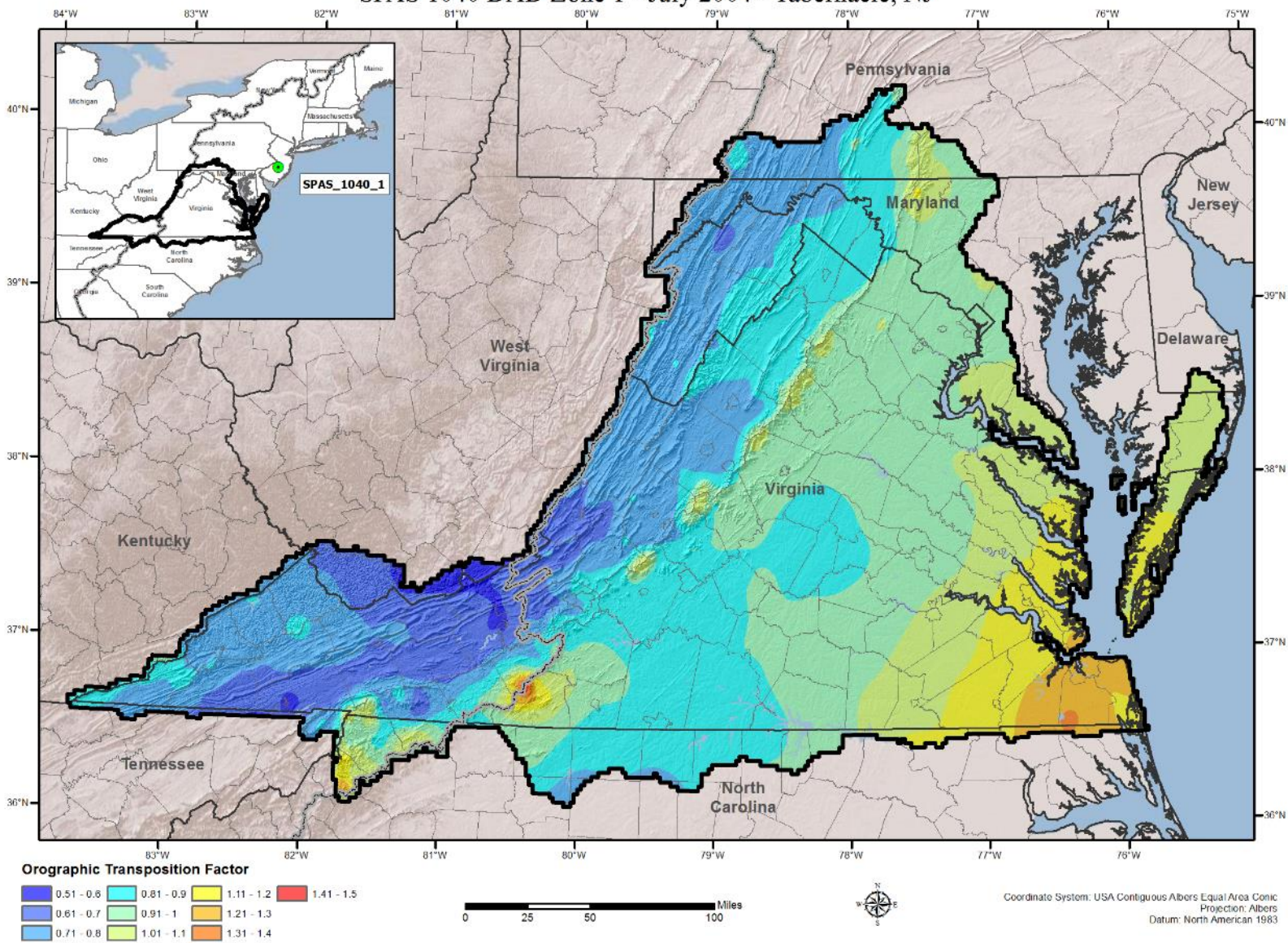


Local Storms

Orographic Transposition Factor (OTF) SPAS 1017 DAD Zone 1 - August 2000 - Sparta, NJ

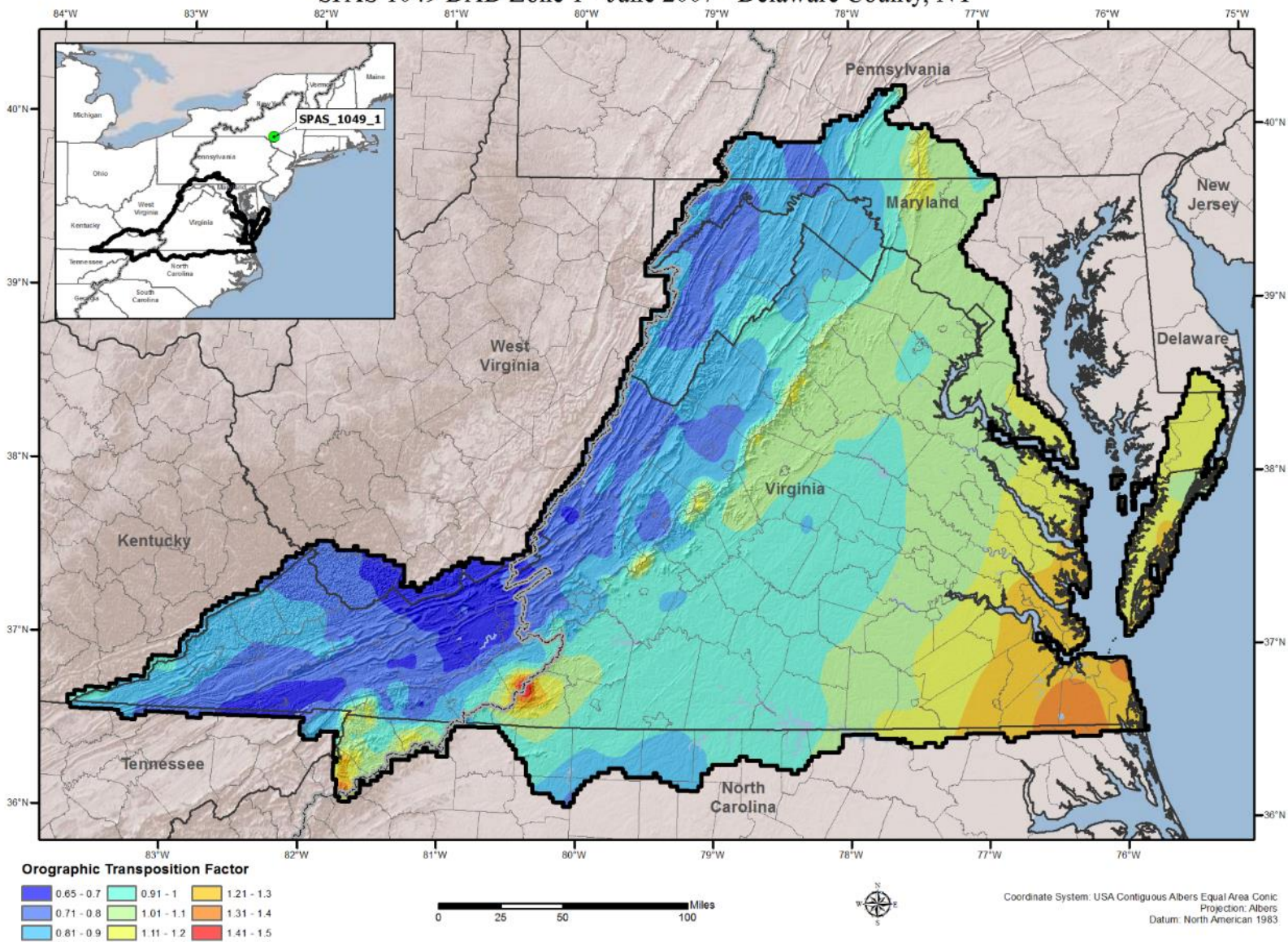


Orographic Transposition Factor (OTF) SPAS 1040 DAD Zone 1 - July 2004 - Tabernacle, NJ

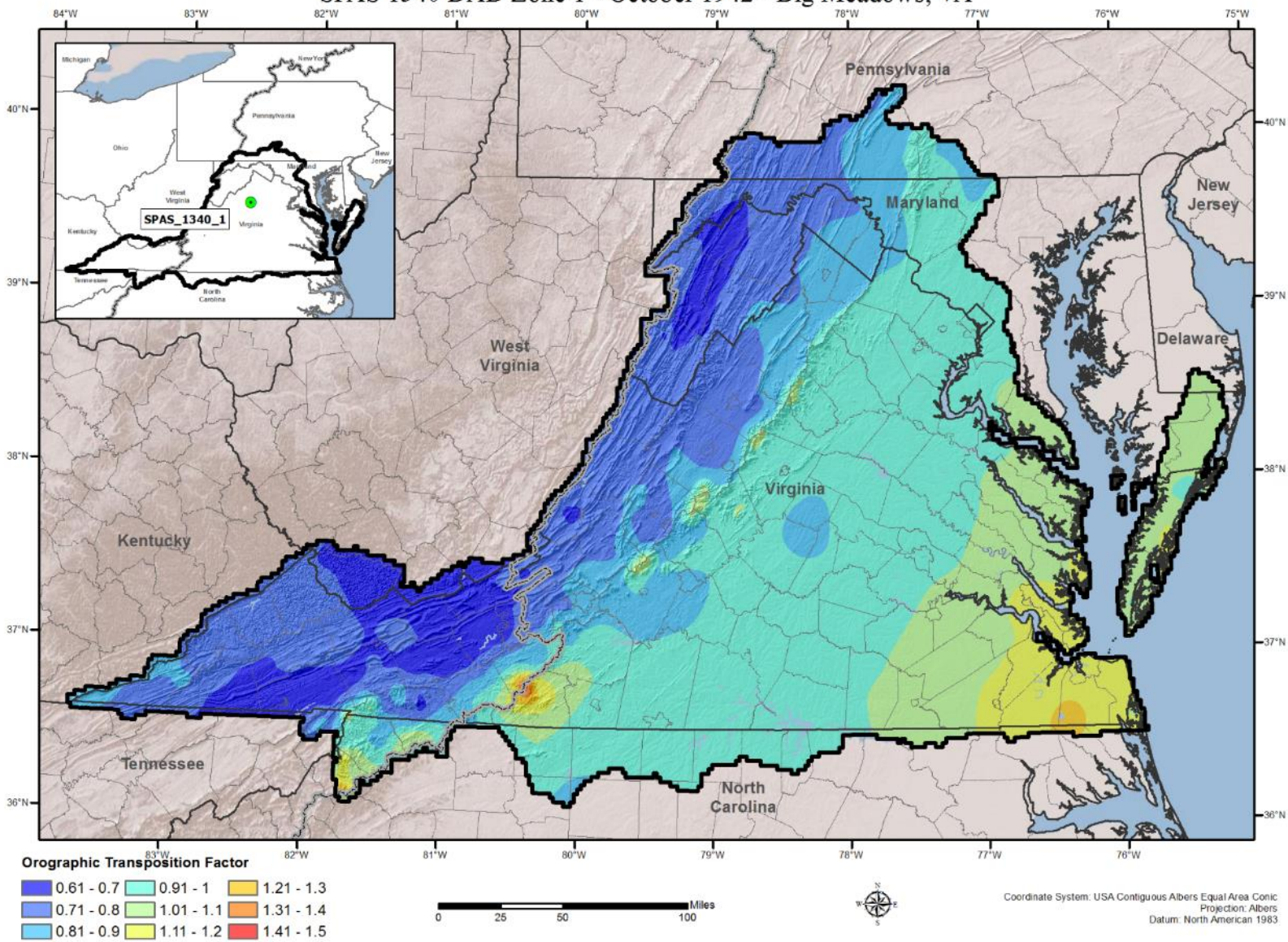


Orographic Transposition Factor (OTF)

SPAS 1049 DAD Zone 1 - June 2007 - Delaware County, NY

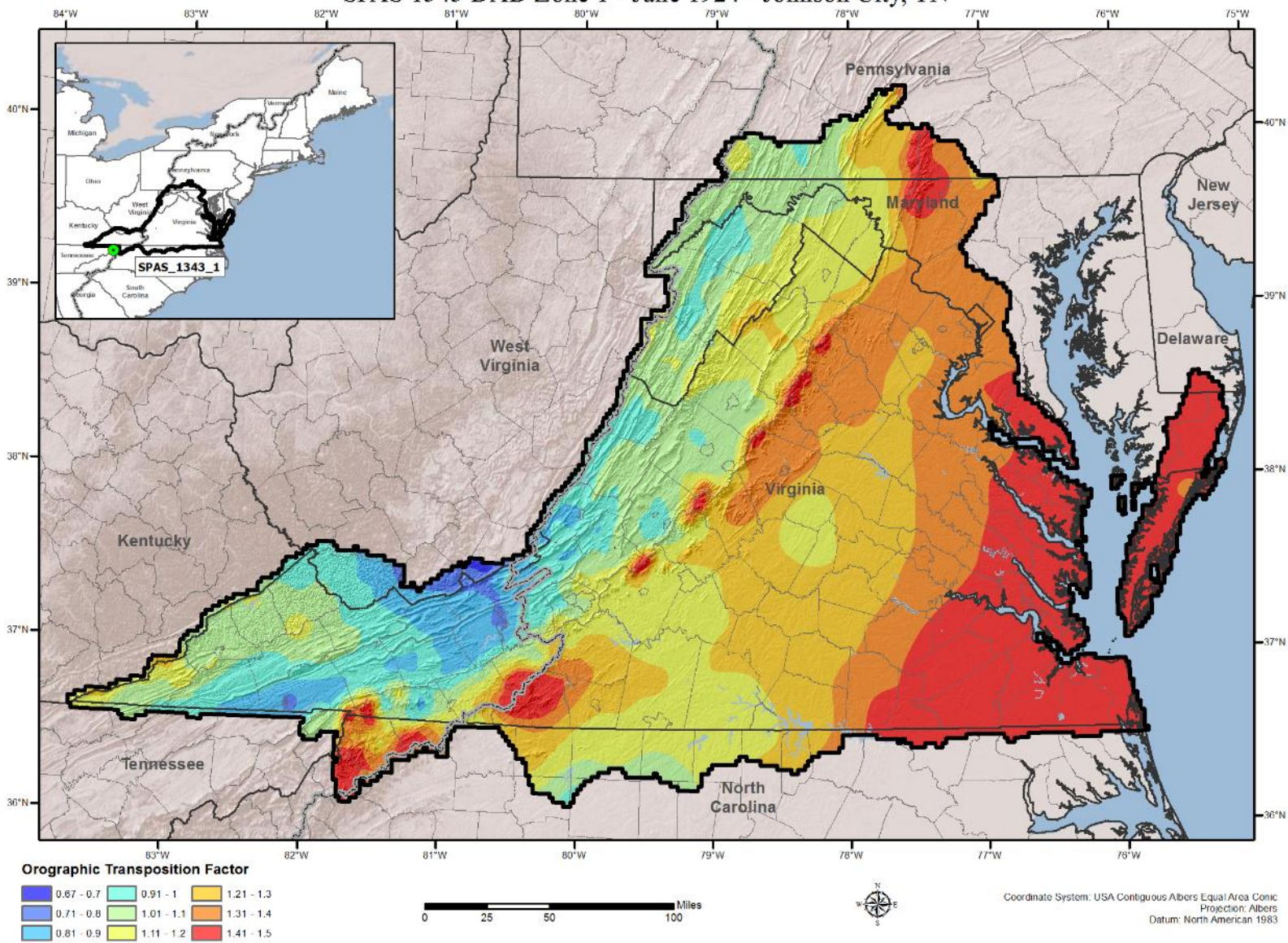


Orographic Transposition Factor (OTF) SPAS 1340 DAD Zone 1 - October 1942 - Big Meadows, VA

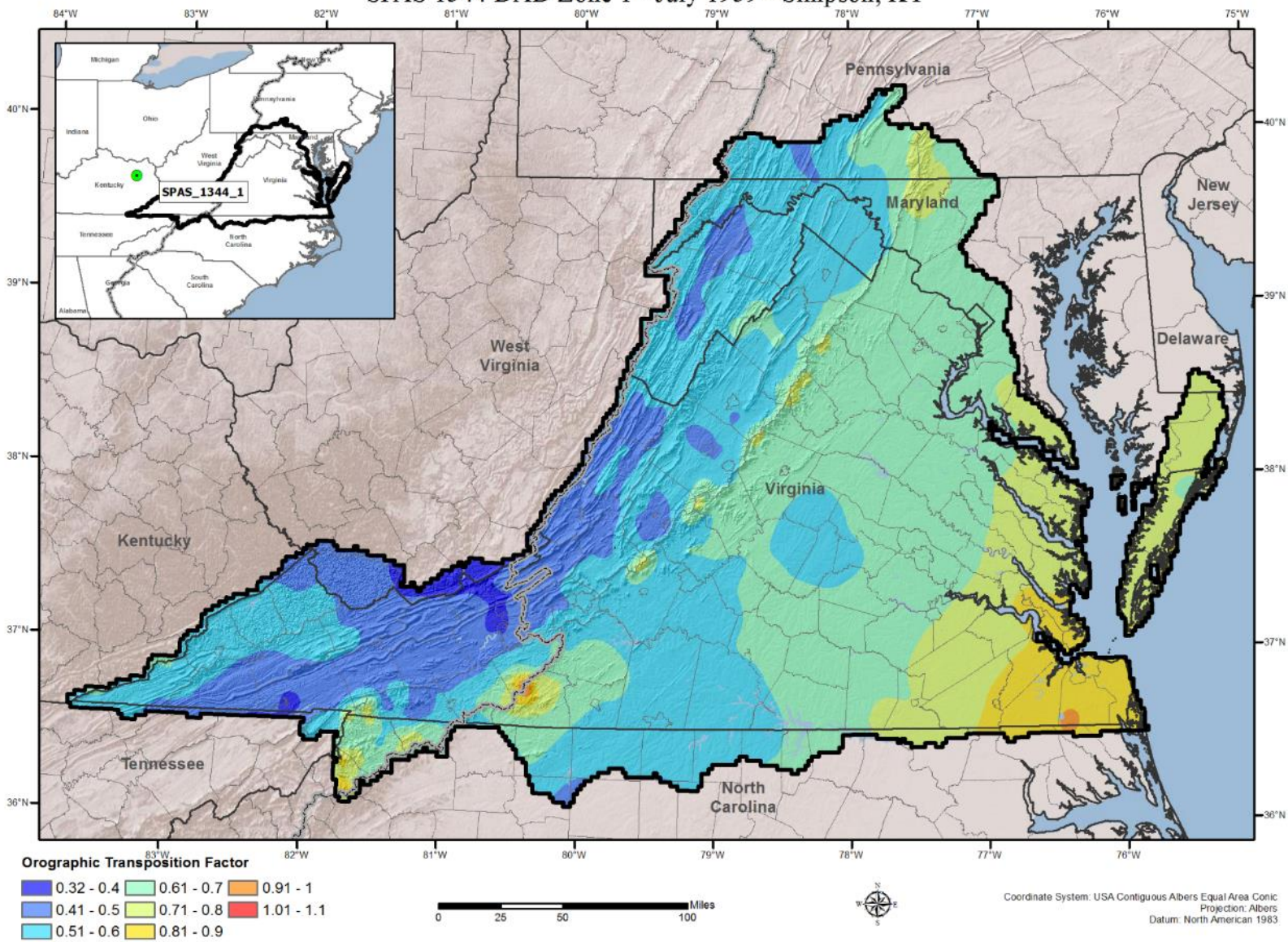


Orographic Transposition Factor (OTF)

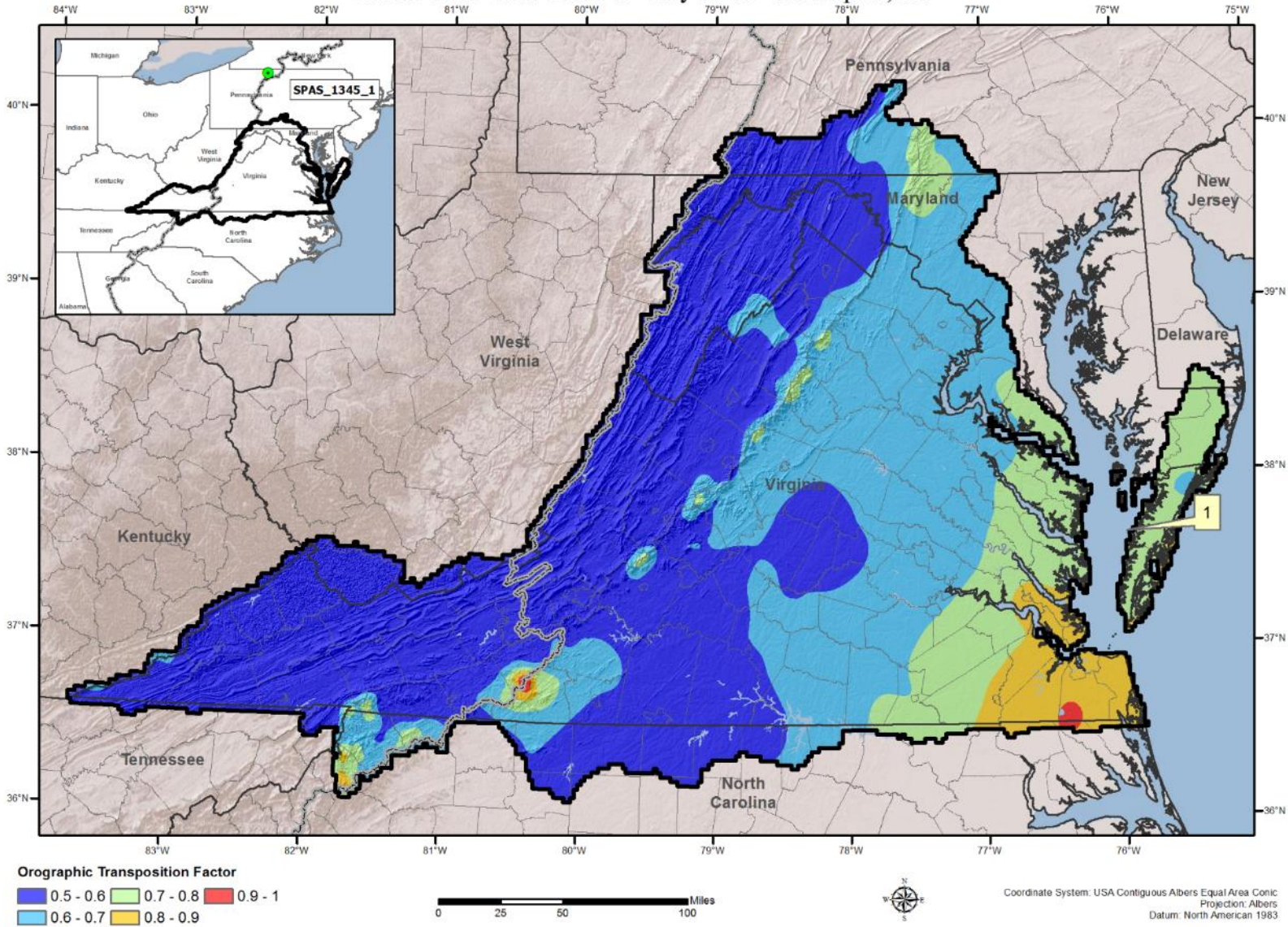
SPAS 1343 DAD Zone 1 - June 1924 - Johnson City, TN



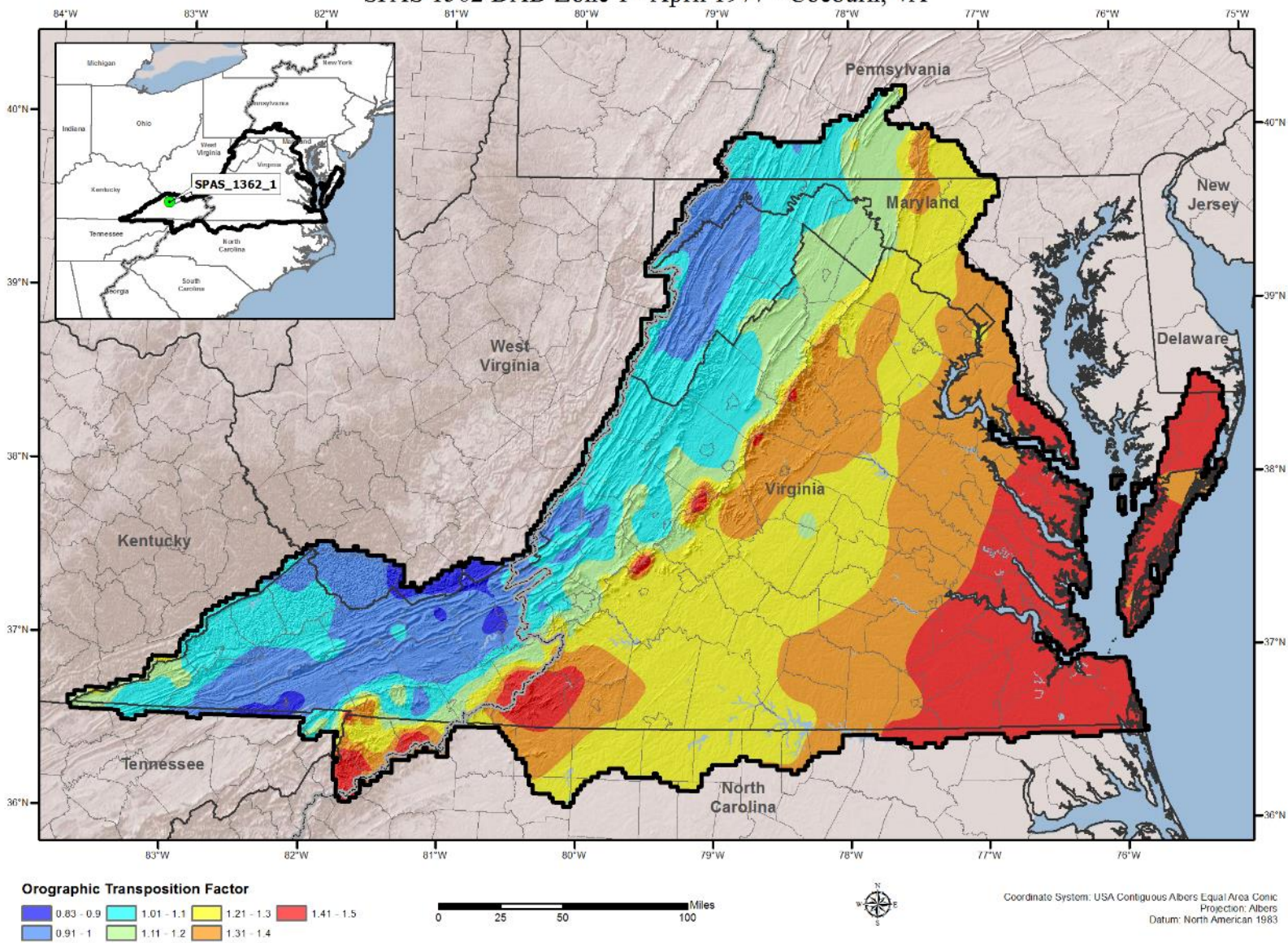
Orographic Transposition Factor (OTF) SPAS 1344 DAD Zone 1 - July 1939 - Simpson, KY



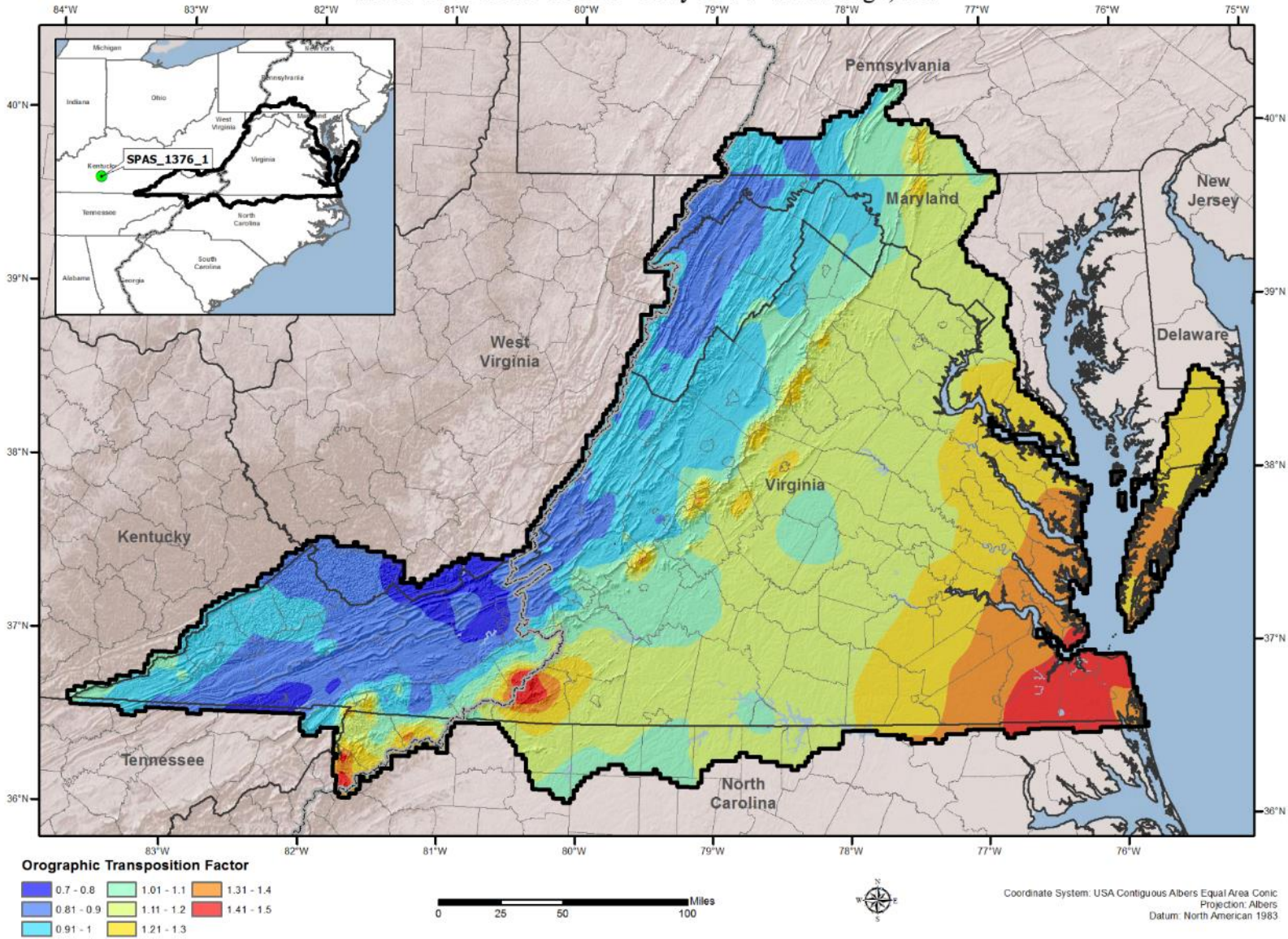
Orographic Transposition Factor (OTF) - Normalized to Max of 1
 SPAS 1345 DAD Zone 1 - July 1942 - Smethport, PA



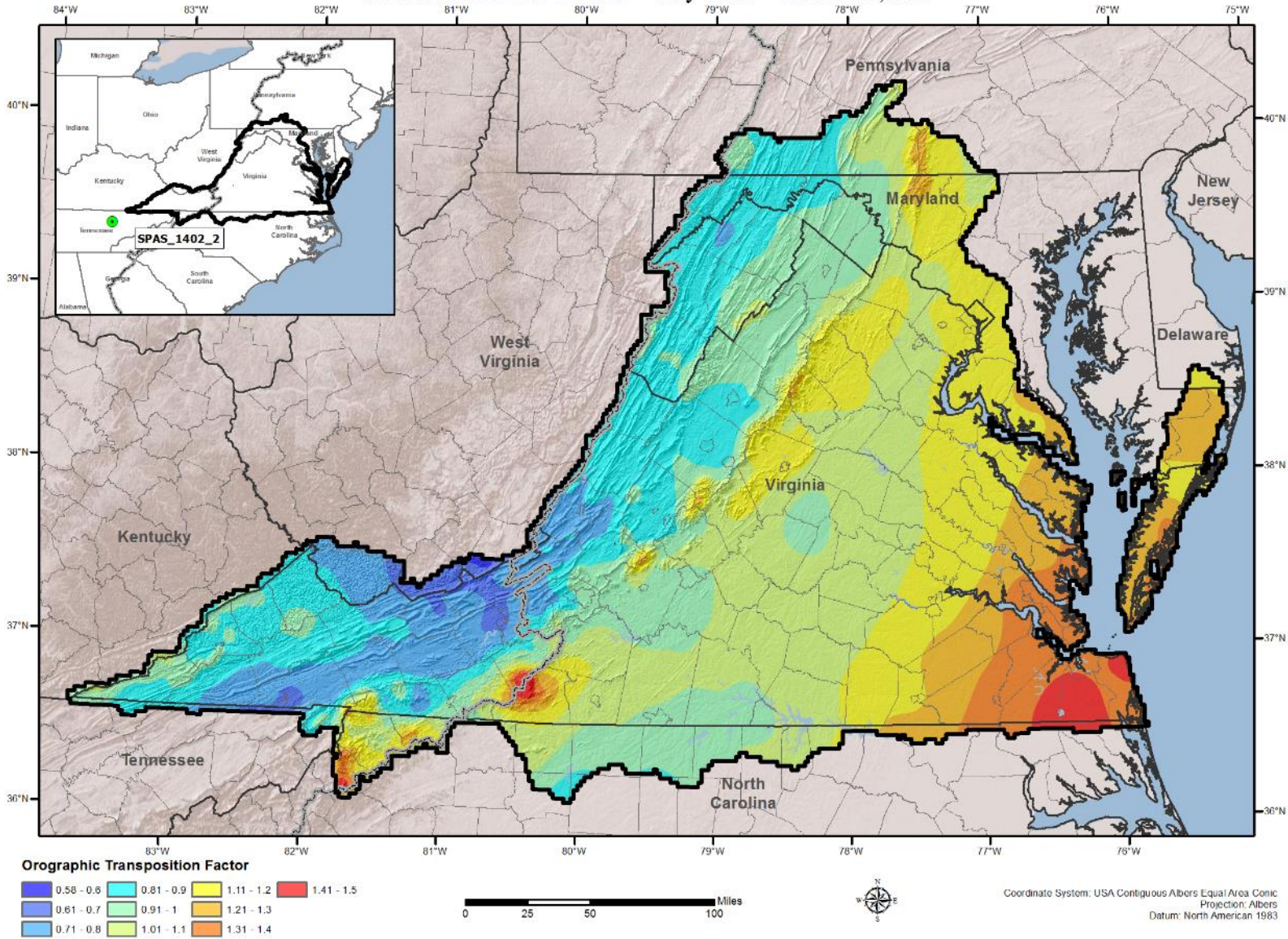
Orographic Transposition Factor (OTF) SPAS 1362 DAD Zone 1 - April 1977 - Coeburn, VA



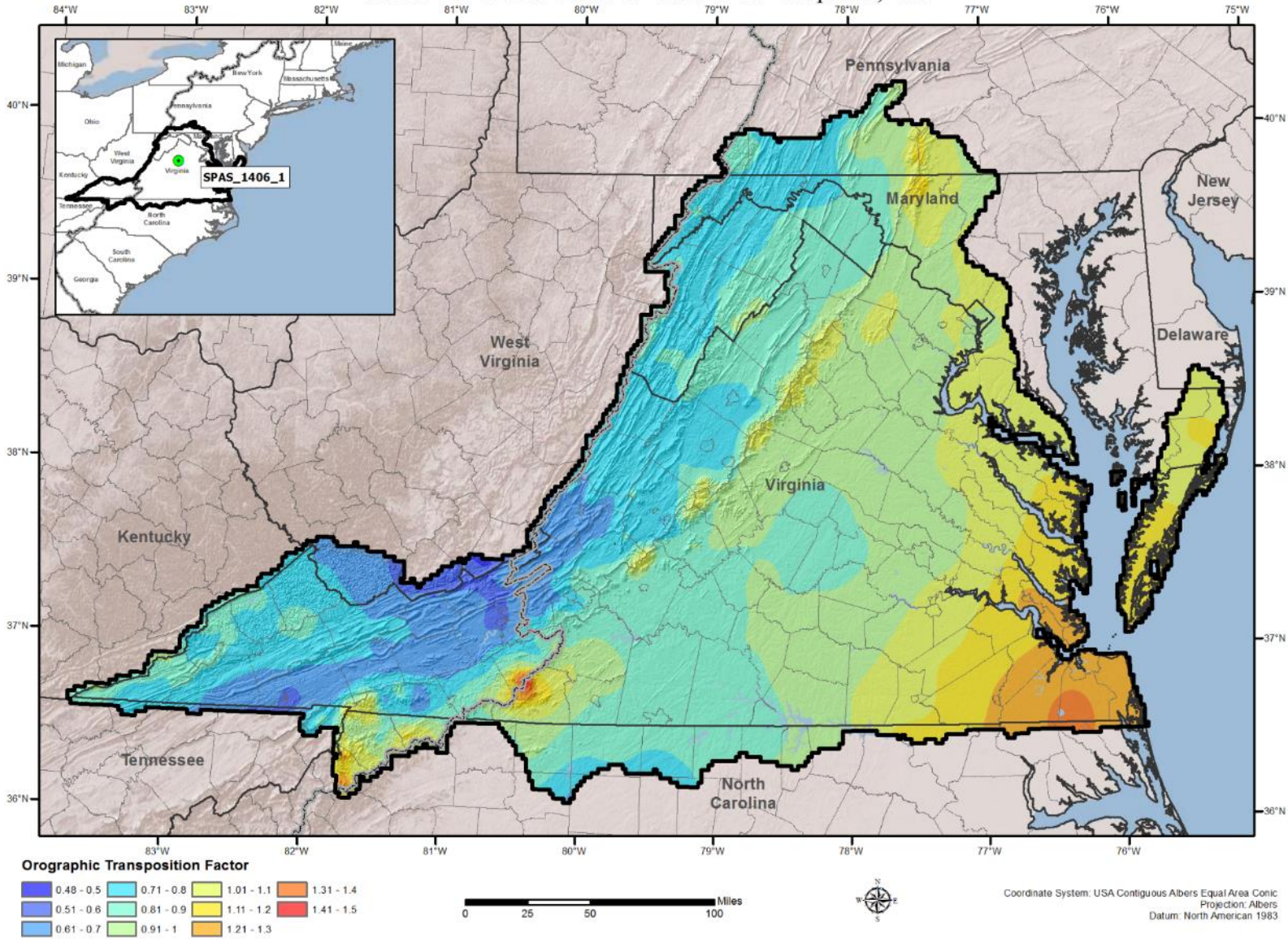
Orographic Transposition Factor (OTF) SPAS 1376 DAD Zone 1 - May 1984 - Dandridge, TN



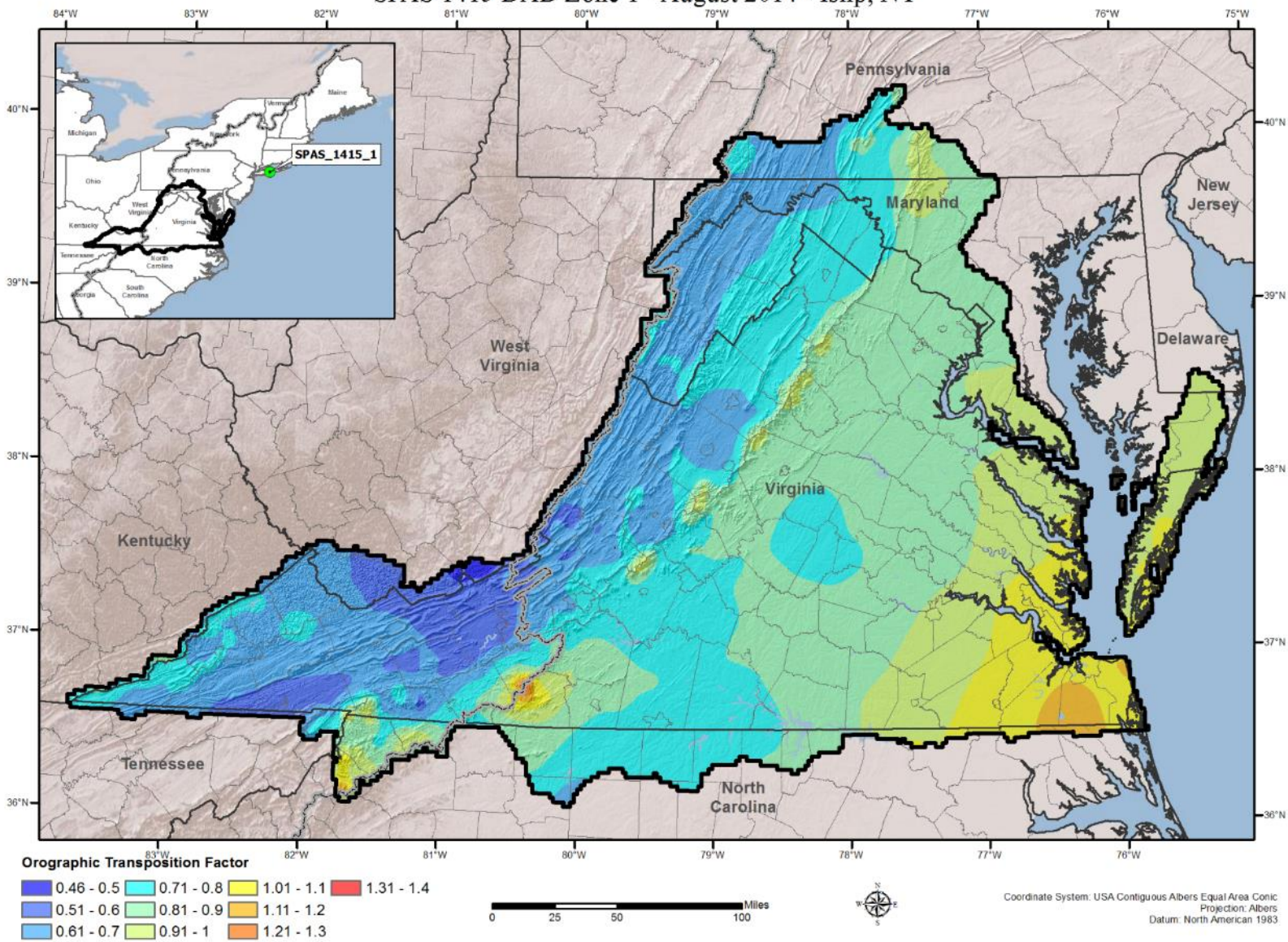
Orographic Transposition Factor (OTF) SPAS 1402 DAD Zone 2 - July 1965 - Rosedale, TN



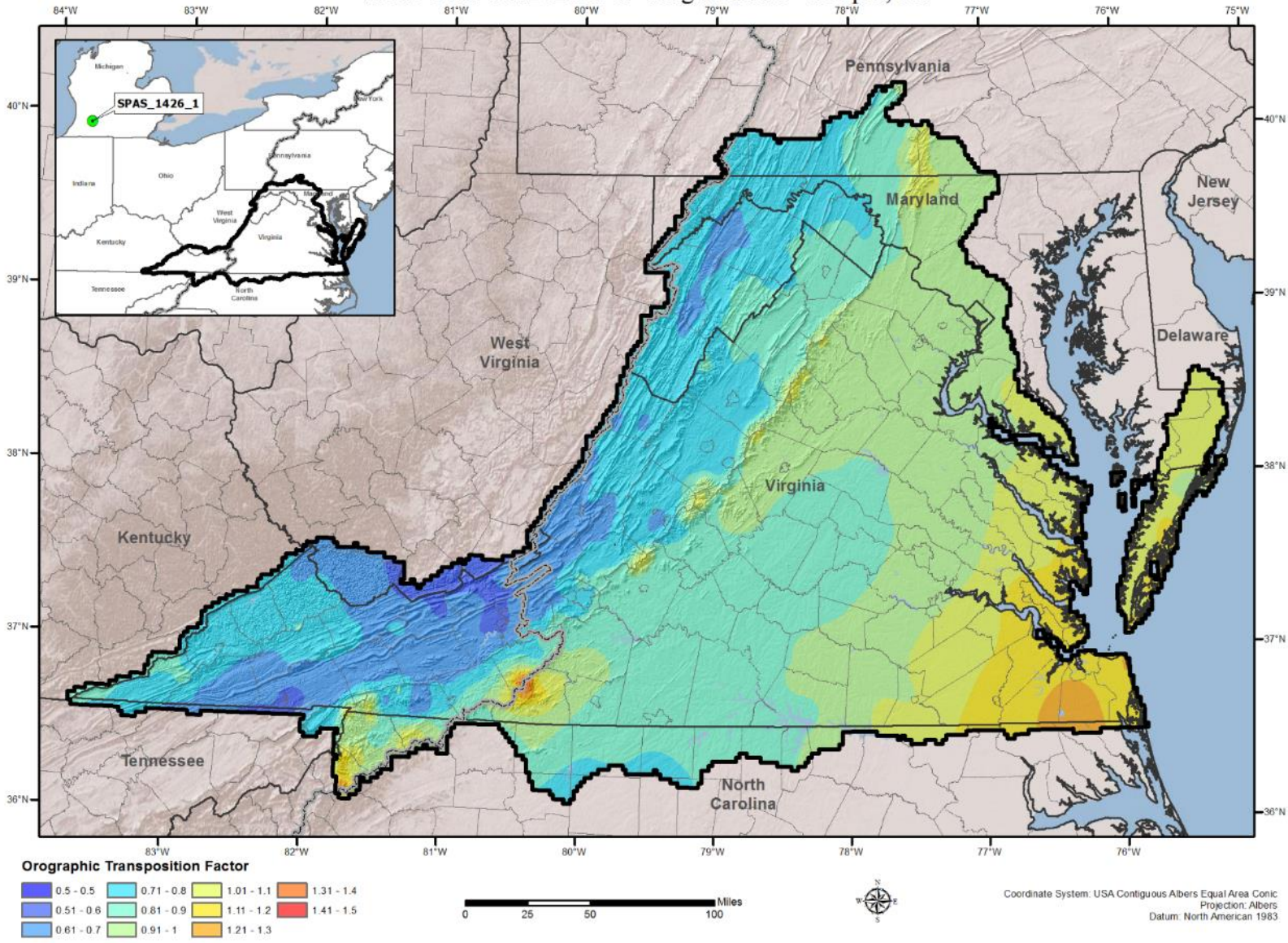
Orographic Transposition Factor (OTF) SPAS 1406 DAD Zone 1 - June 1995 - Rapidan, VA



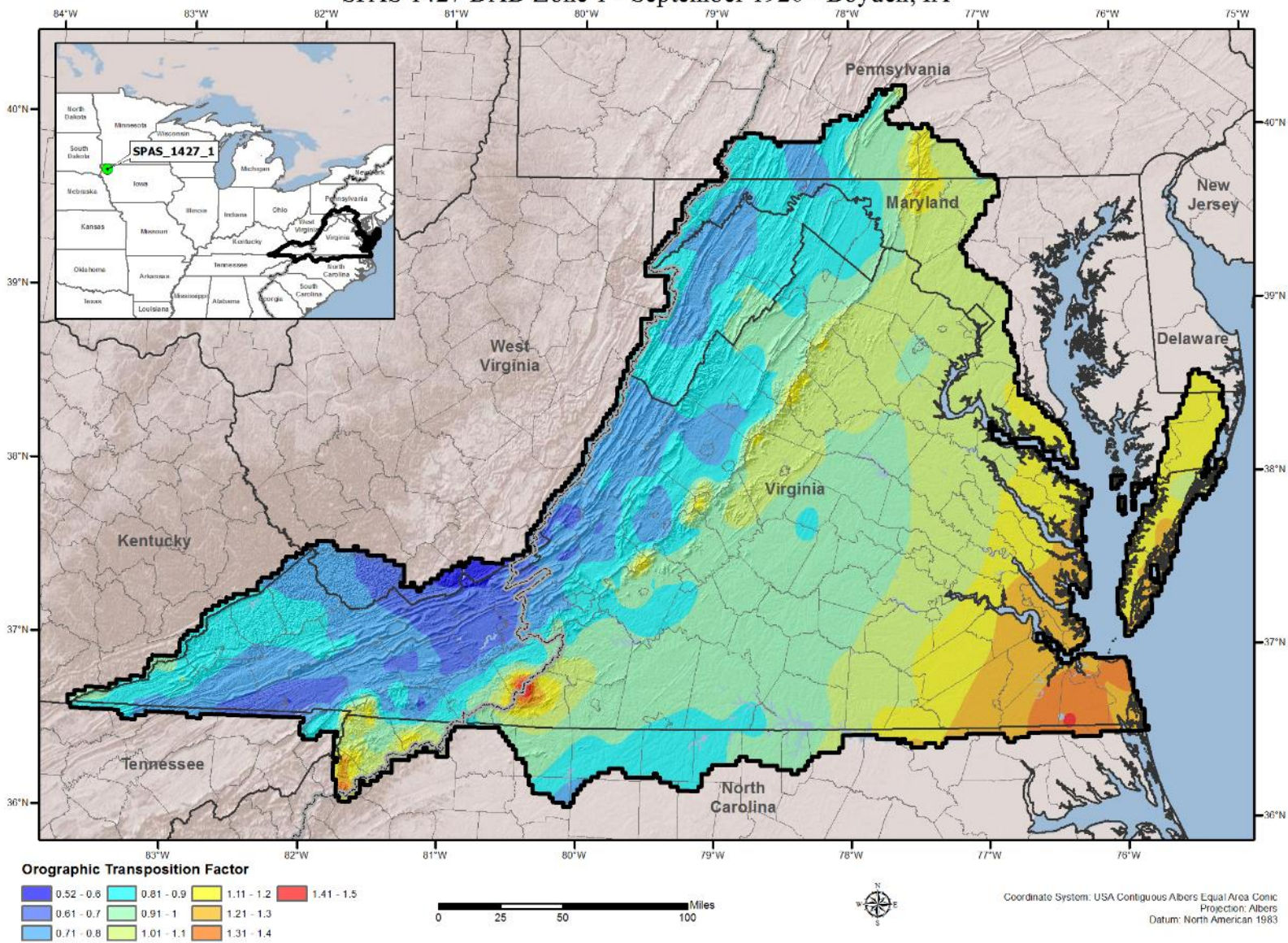
Orographic Transposition Factor (OTF) SPAS 1415 DAD Zone 1 - August 2014 - Islip, NY



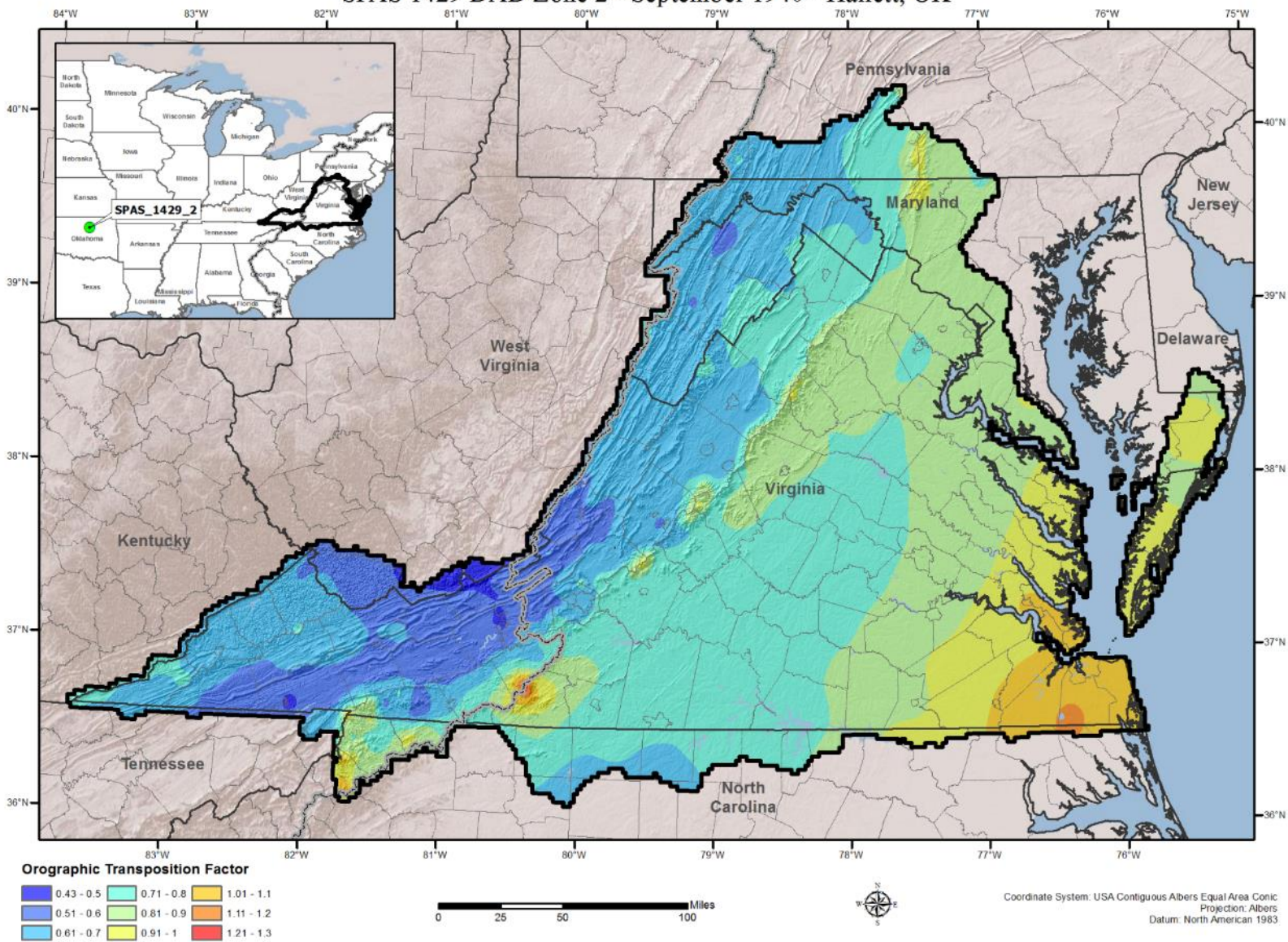
Orographic Transposition Factor (OTF) SPAS 1426 DAD Zone 1 - August 1914 - Cooper, MI



Orographic Transposition Factor (OTF) SPAS 1427 DAD Zone 1 - September 1926 - Boyden, IA

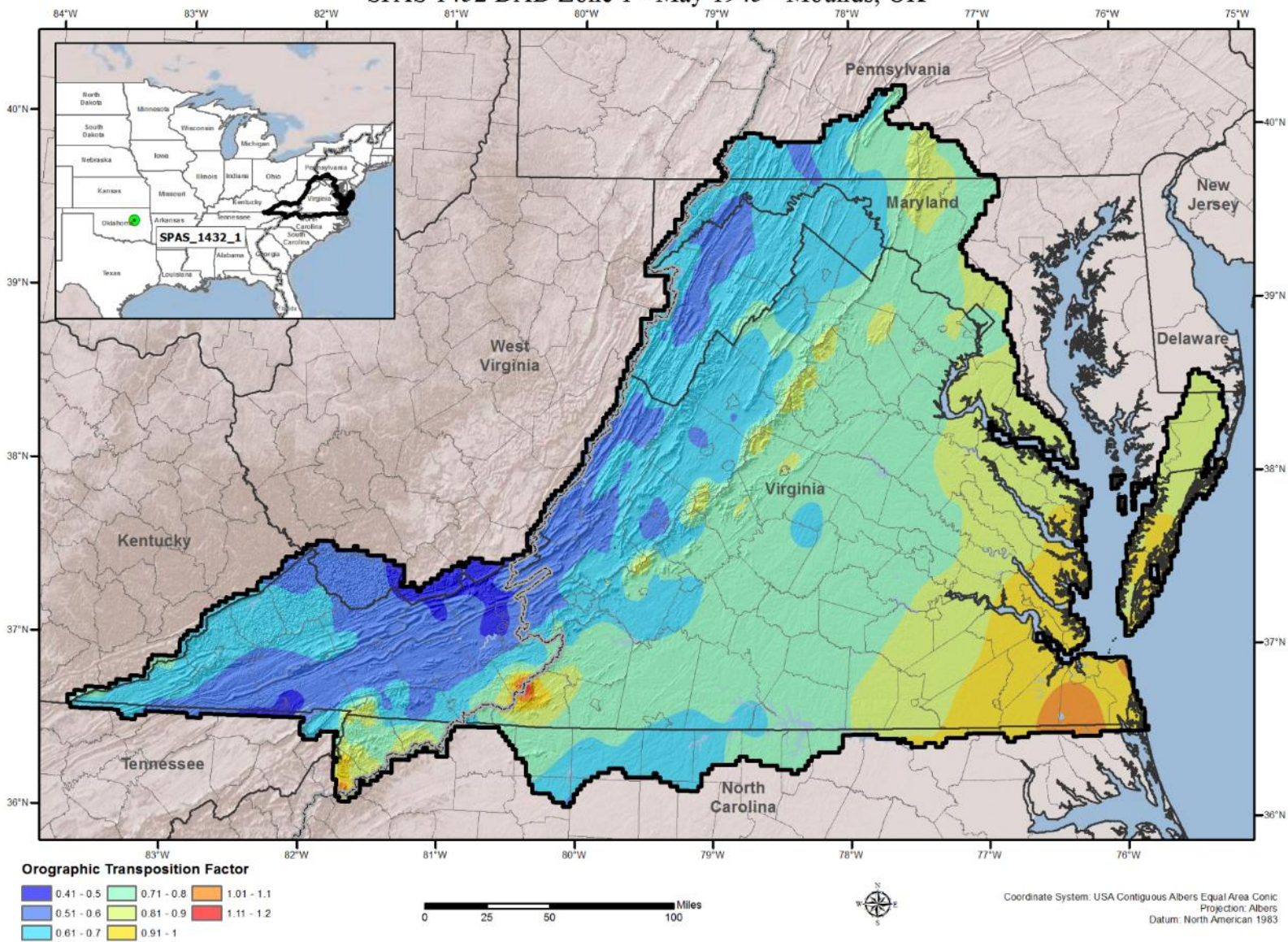


Orographic Transposition Factor (OTF) SPAS 1429 DAD Zone 2 - September 1940 - Hallett, OK

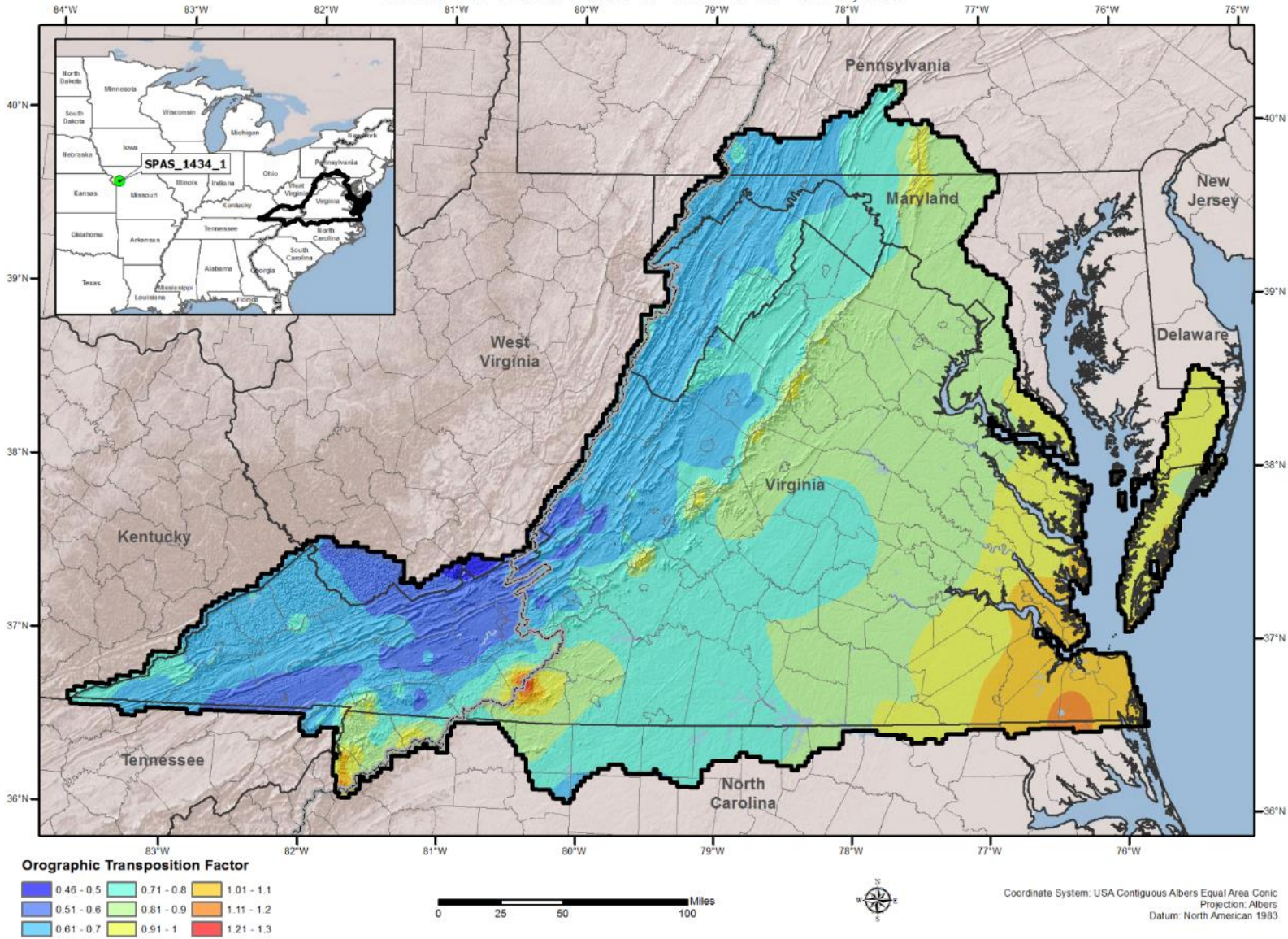


Orographic Transition Factor (OTF)

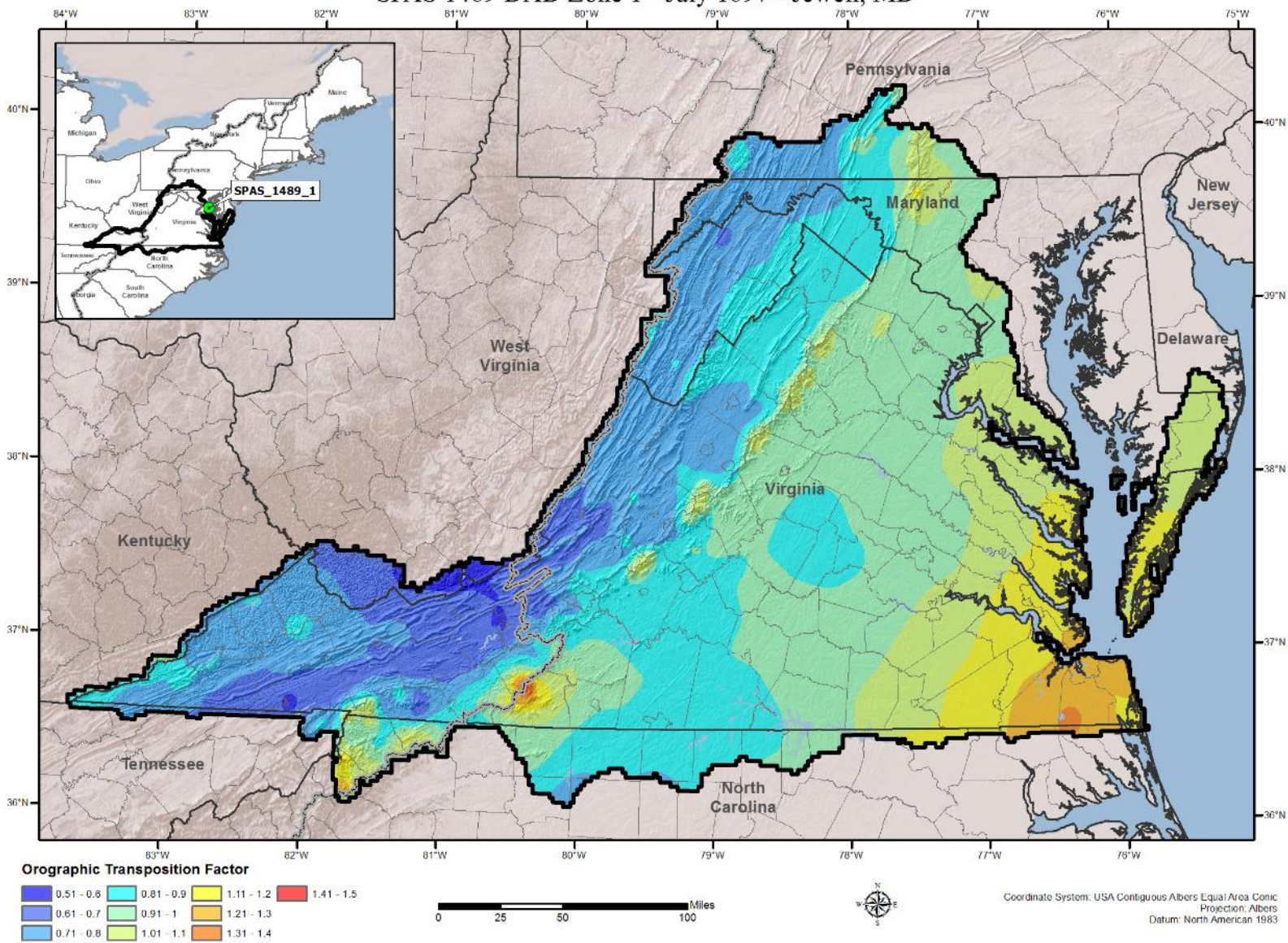
SPAS 1432 DAD Zone 1 - May 1943 - Mounds, OK



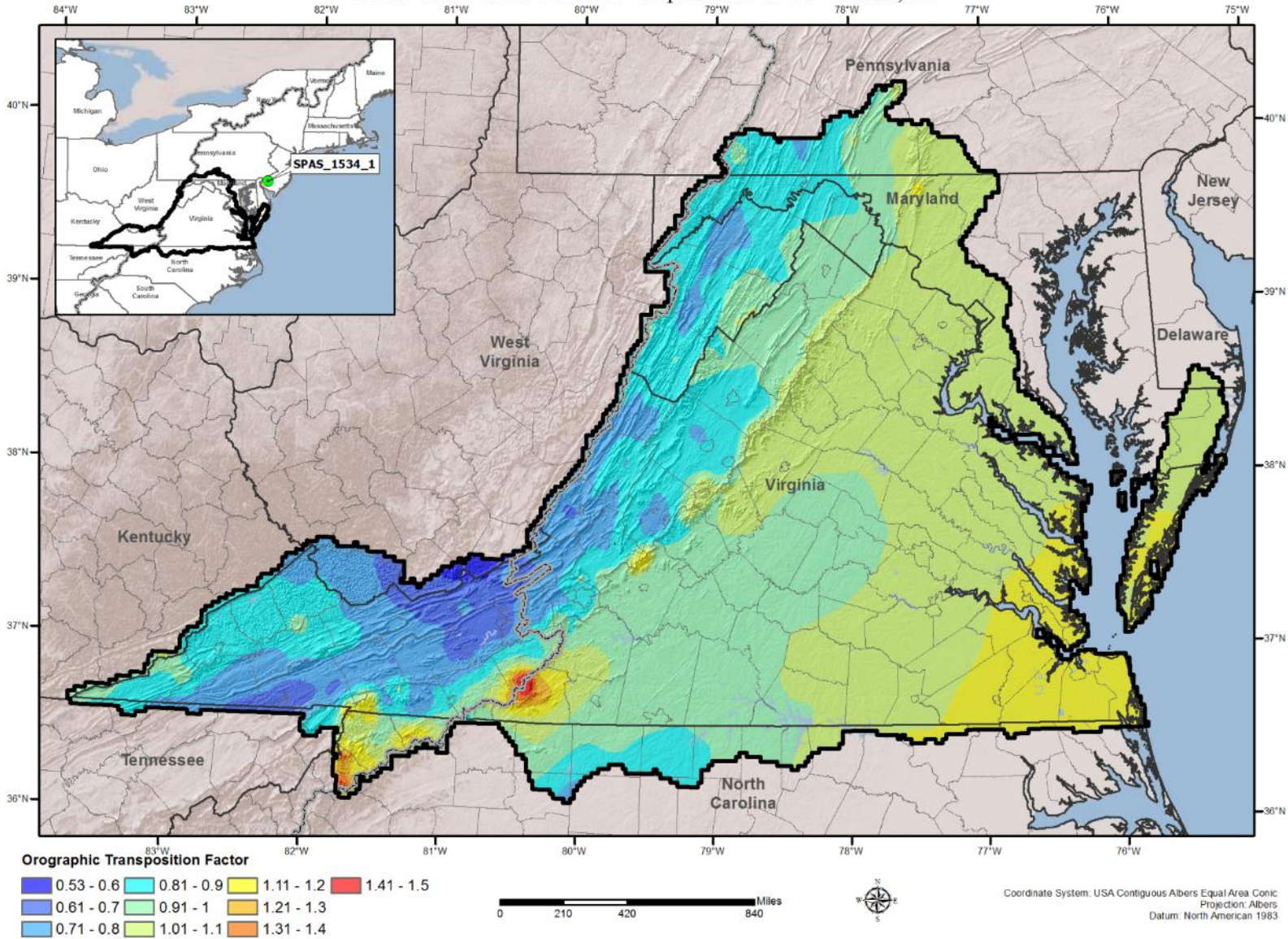
Orographic Transposition Factor (OTF)
 SPAS 1434 DAD Zone 1 - June 1947 - Holt, MO



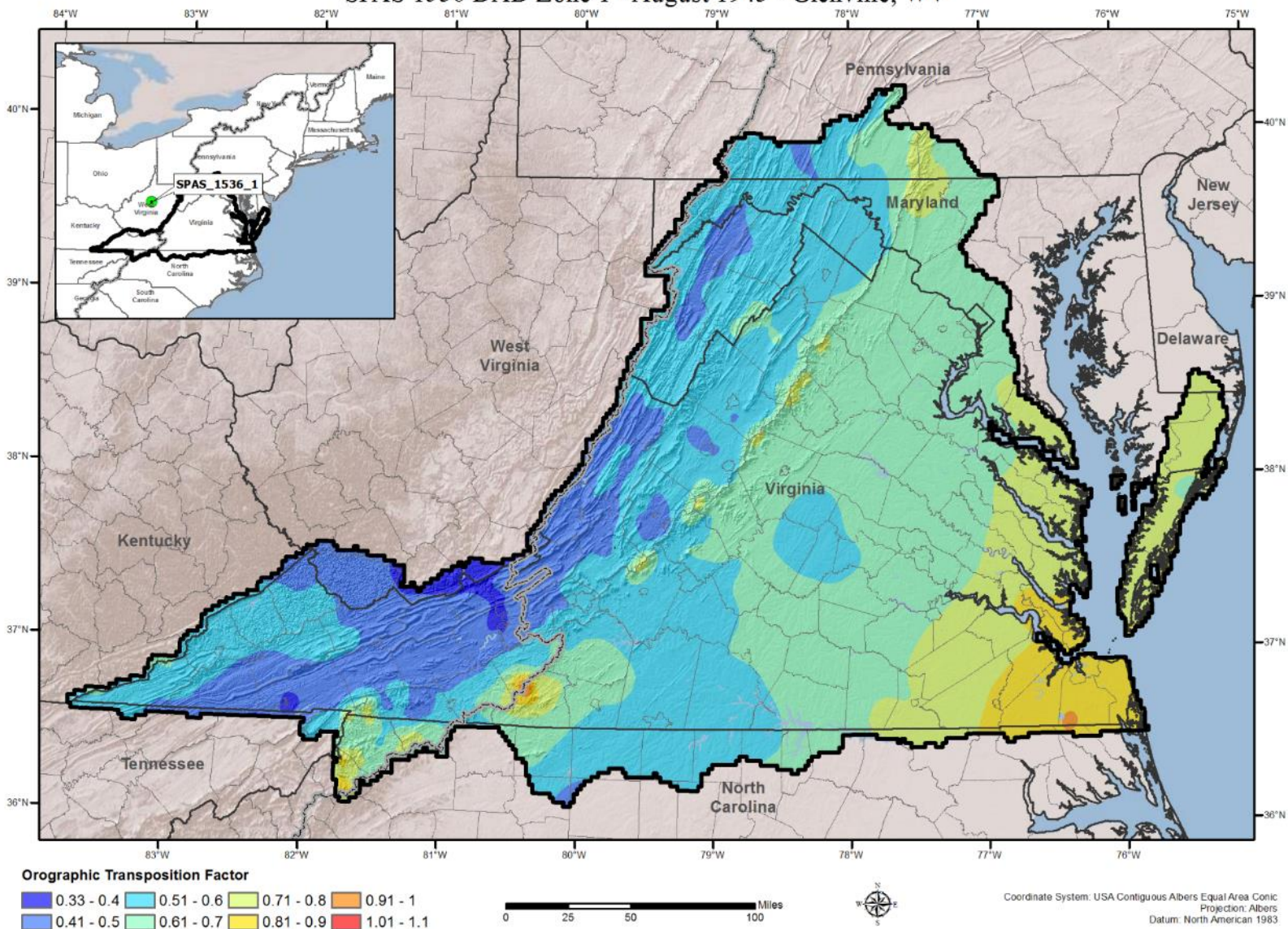
Orographic Transposition Factor (OTF) SPAS 1489 DAD Zone 1 - July 1897 - Jewell, MD



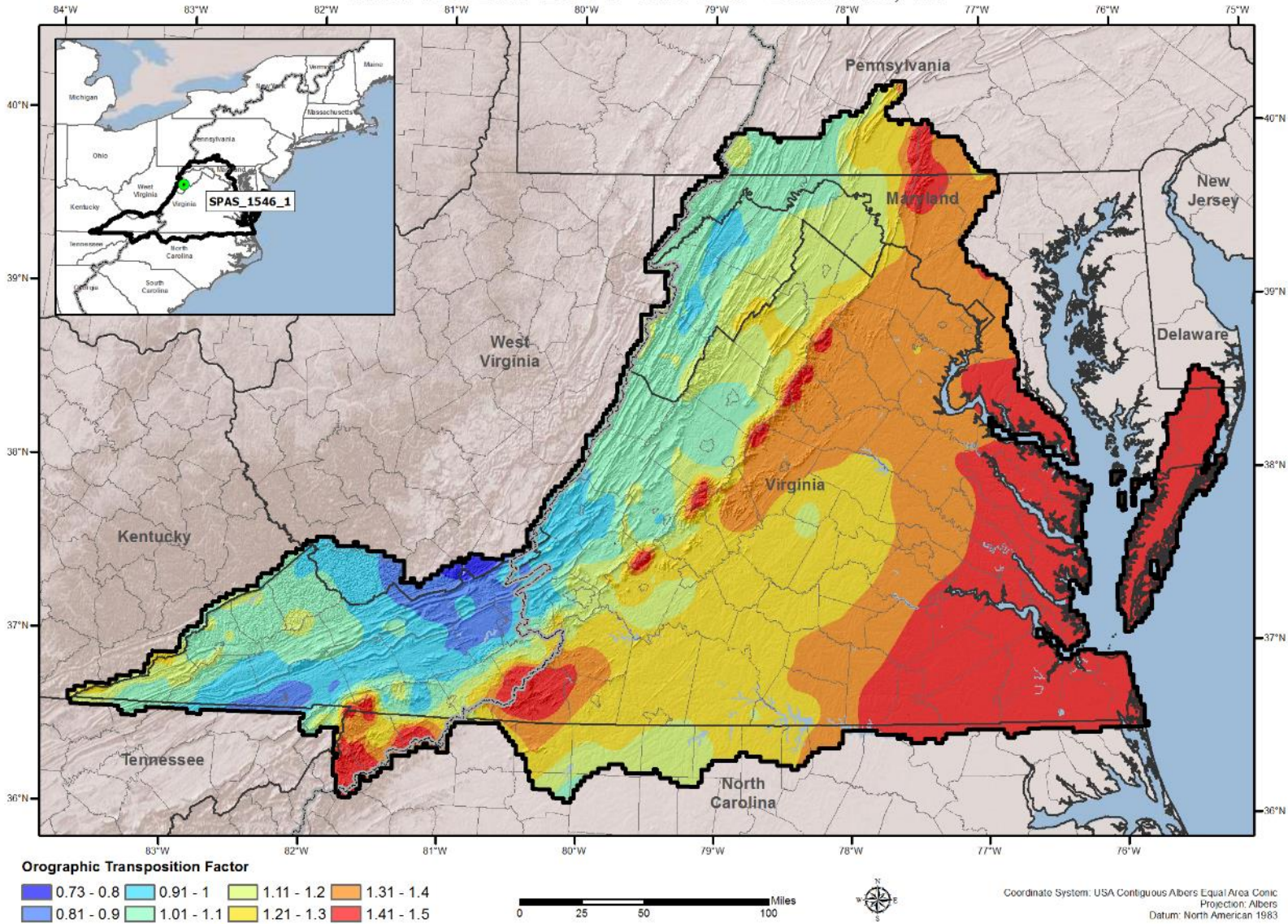
Orographic Transposition Factor (OTF)
 SPAS 1534 DAD Zone 1 - September 1940 - Ewan, NJ



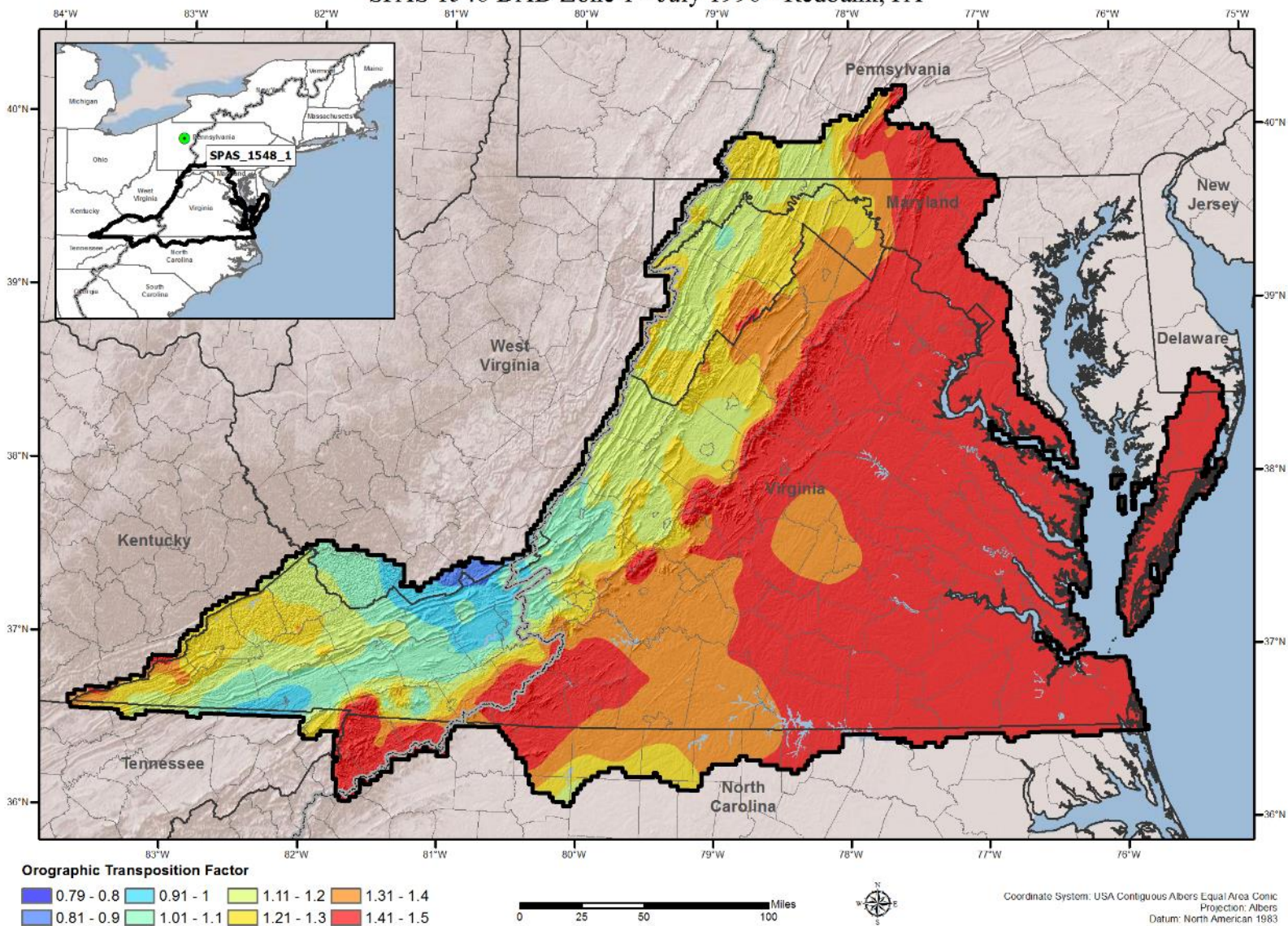
Orographic Transposition Factor (OTF) SPAS 1536 DAD Zone 1 - August 1943 - Glenville, WV



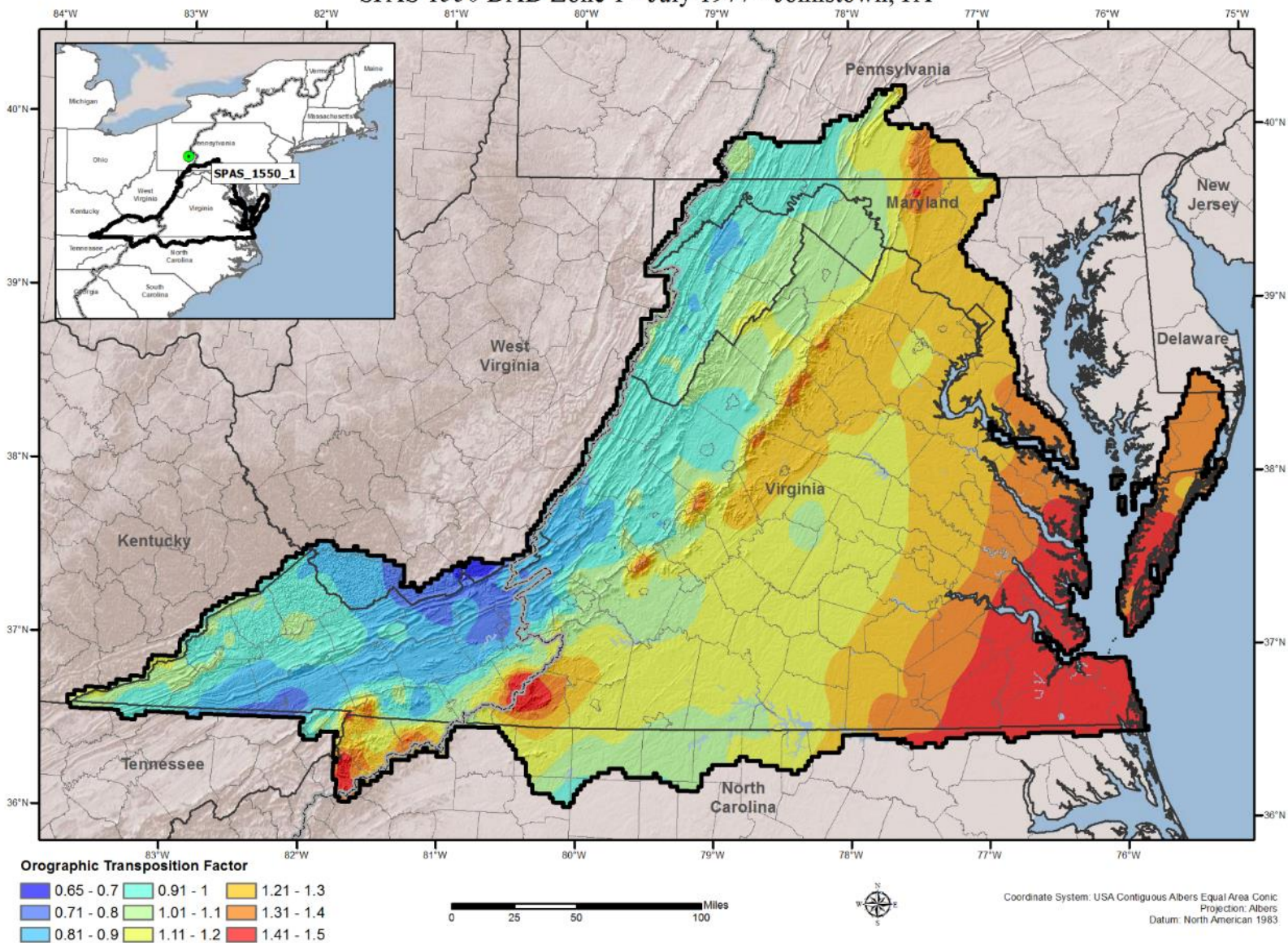
Orographic Transition Factor (OTF) SPAS 1546 DAD Zone 1 - June 1949 - Little River, VA



Orographic Transposition Factor (OTF) SPAS 1548 DAD Zone 1 - July 1996 - Redbank, PA

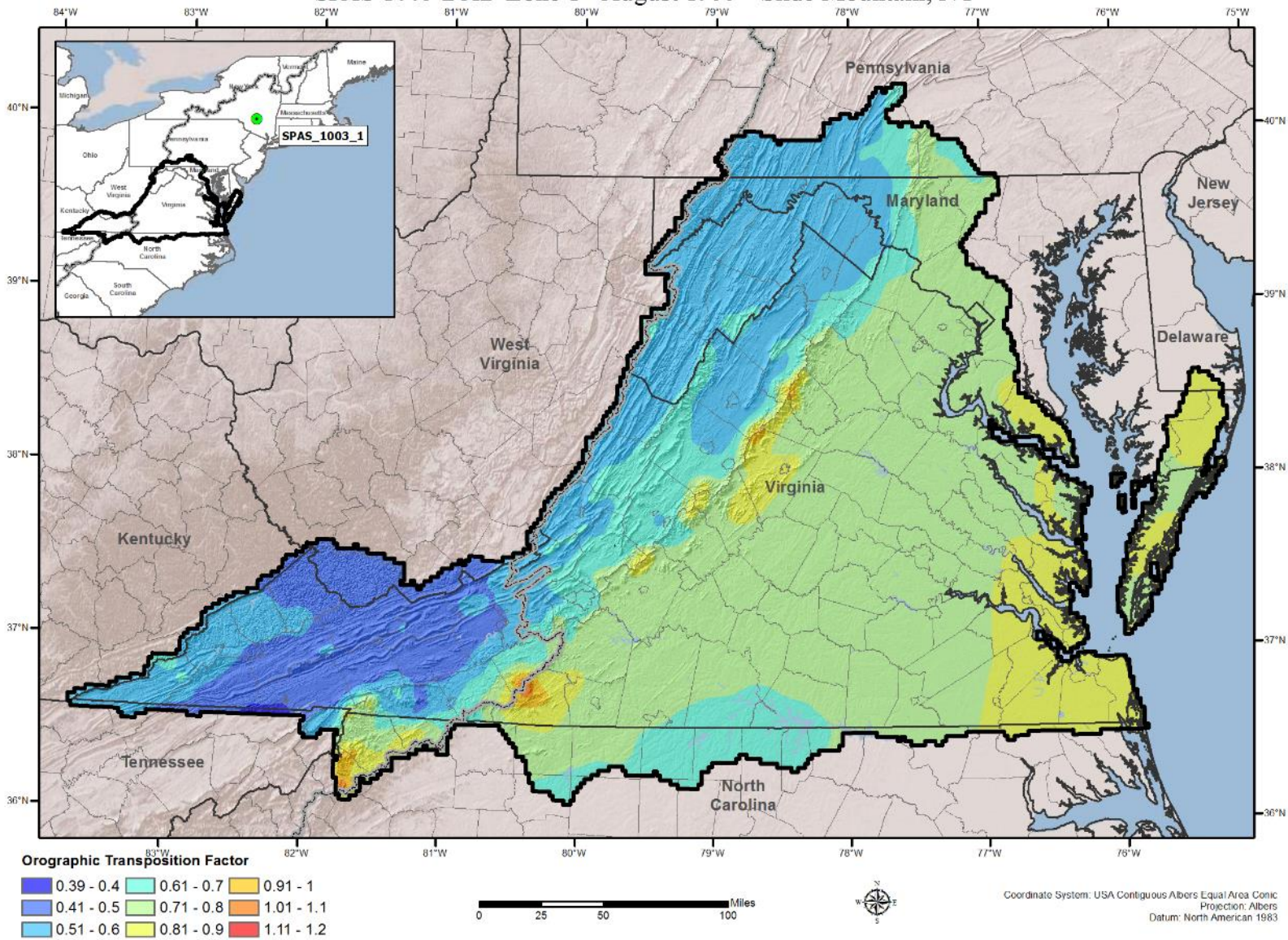


Orographic Transposition Factor (OTF) SPAS 1550 DAD Zone 1 - July 1977 - Johnstown, PA

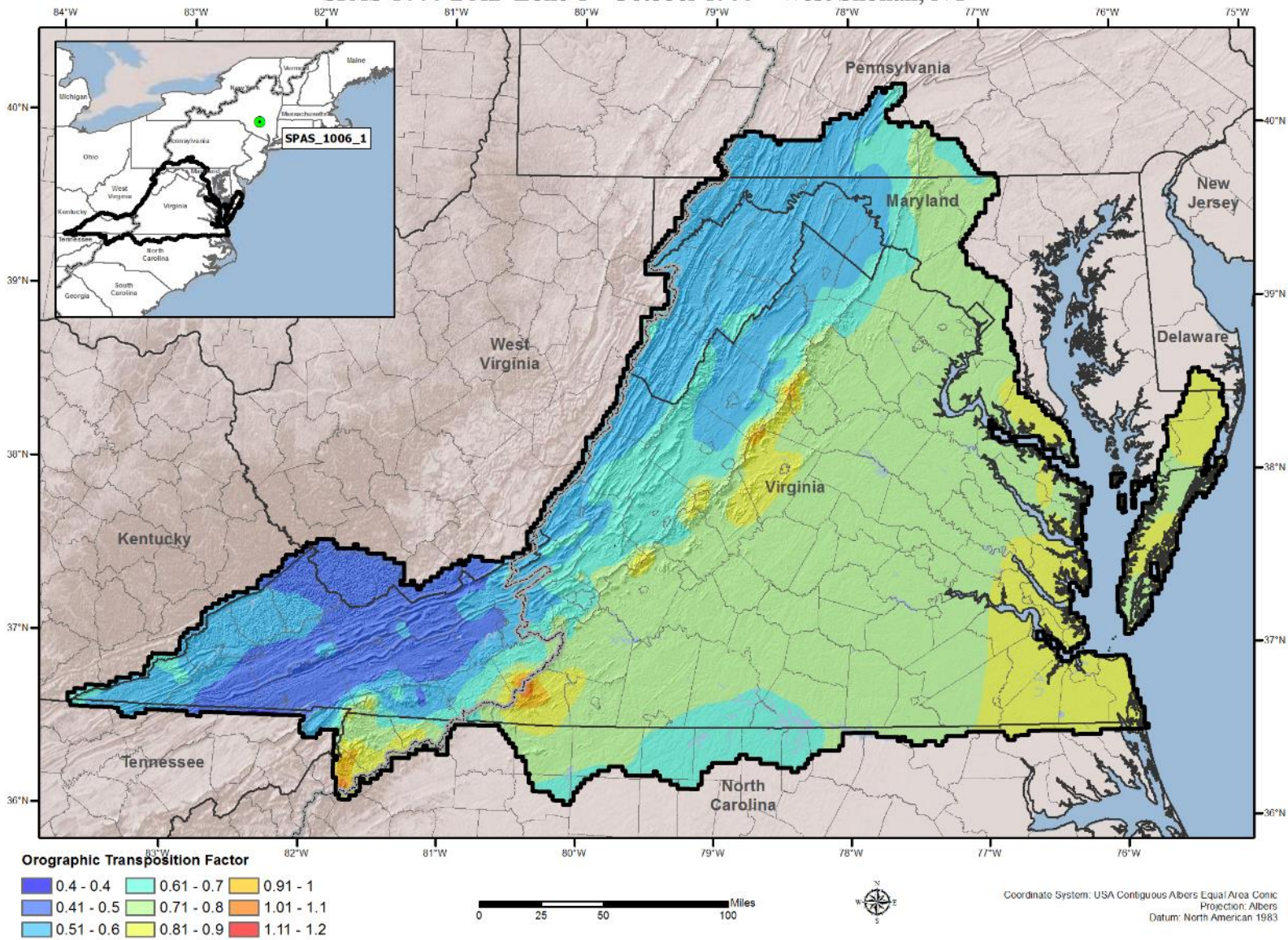


Tropical Storms

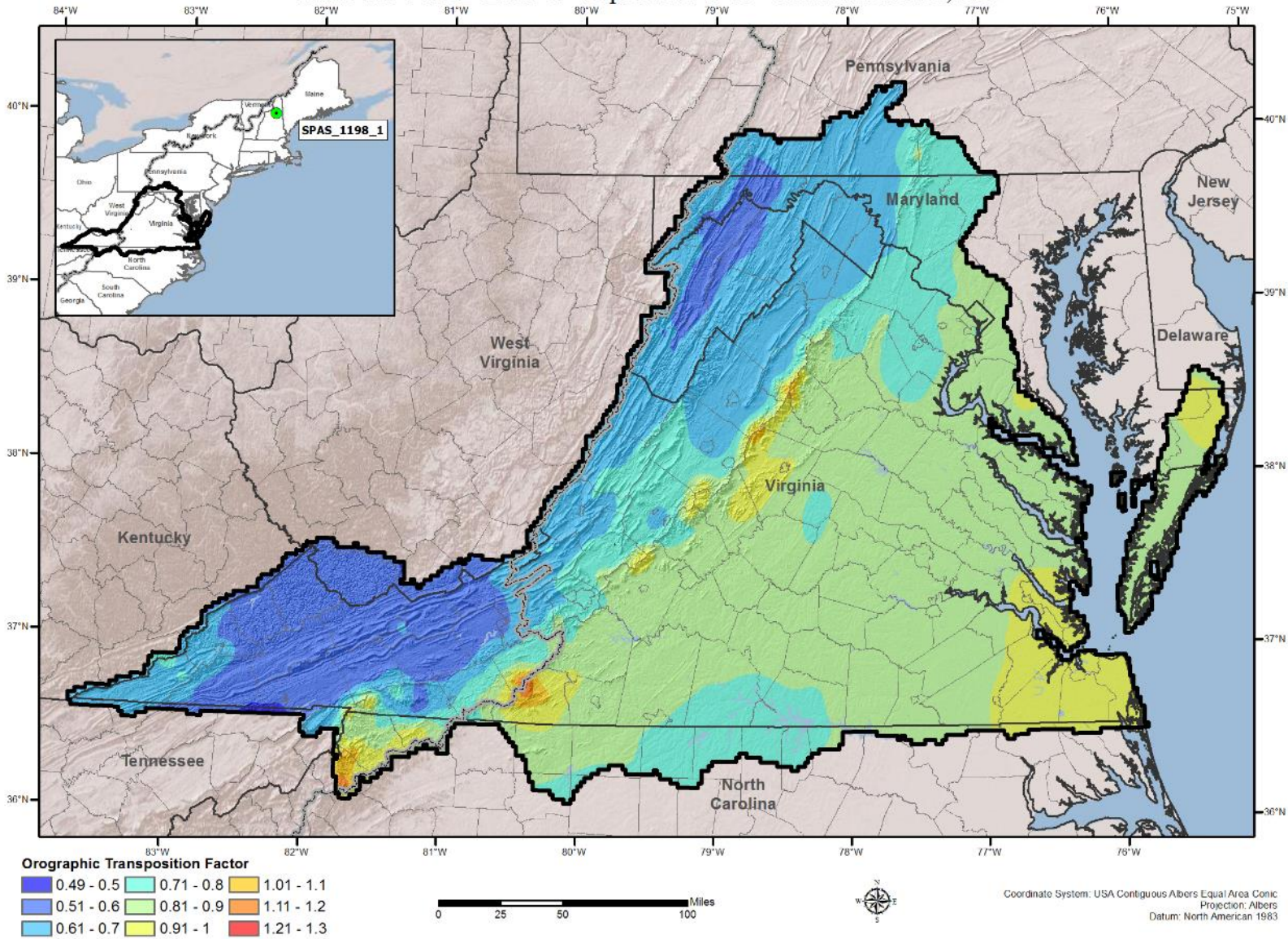
Orographic Transposition Factor (OTF) SPAS 1003 DAD Zone 1 - August 1955 - Slide Mountain, NY



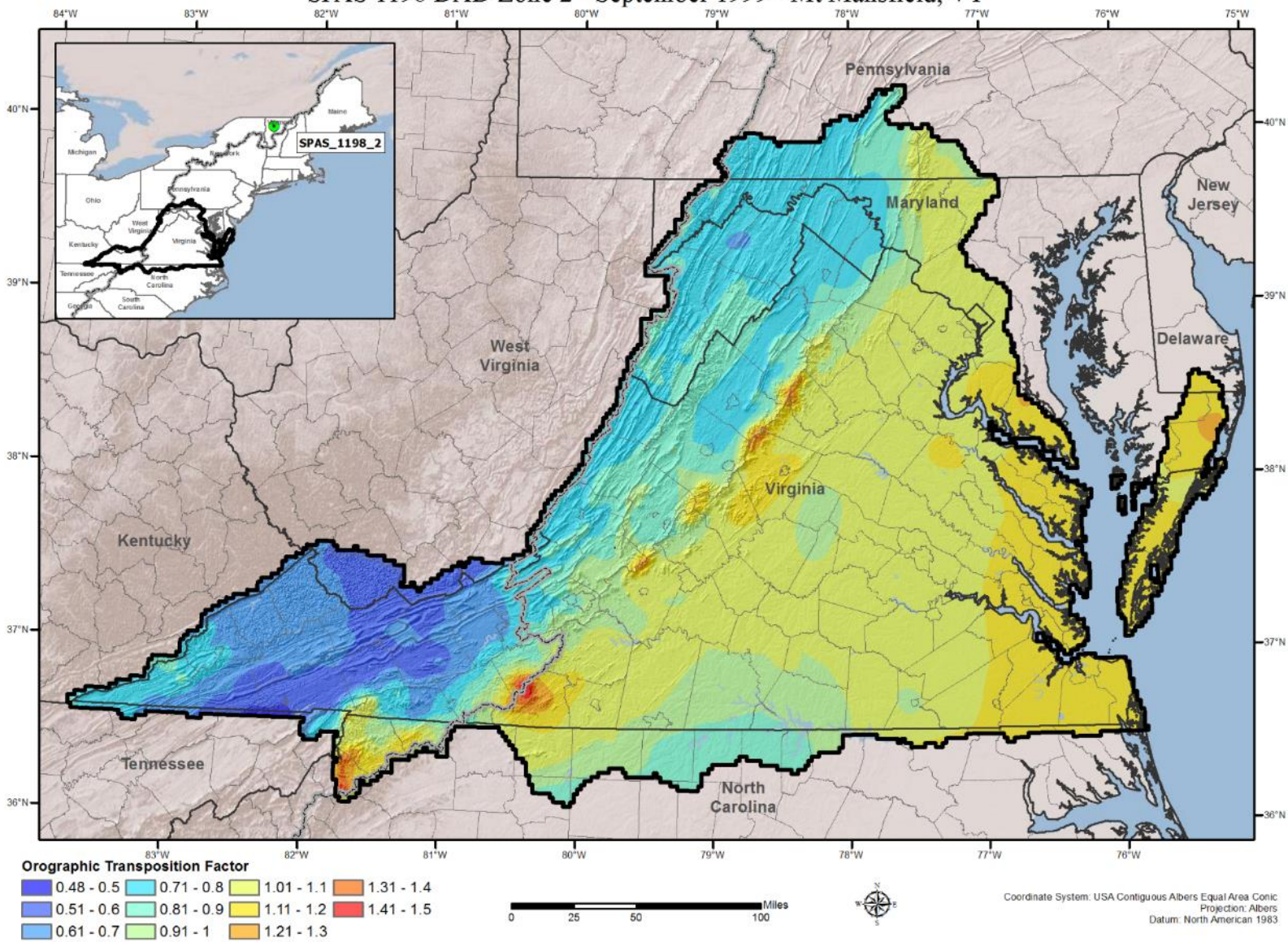
Orographic Transposition Factor (OTF)
 SPAS 1006 DAD Zone 1 - October 1955 - West Shokan, NY



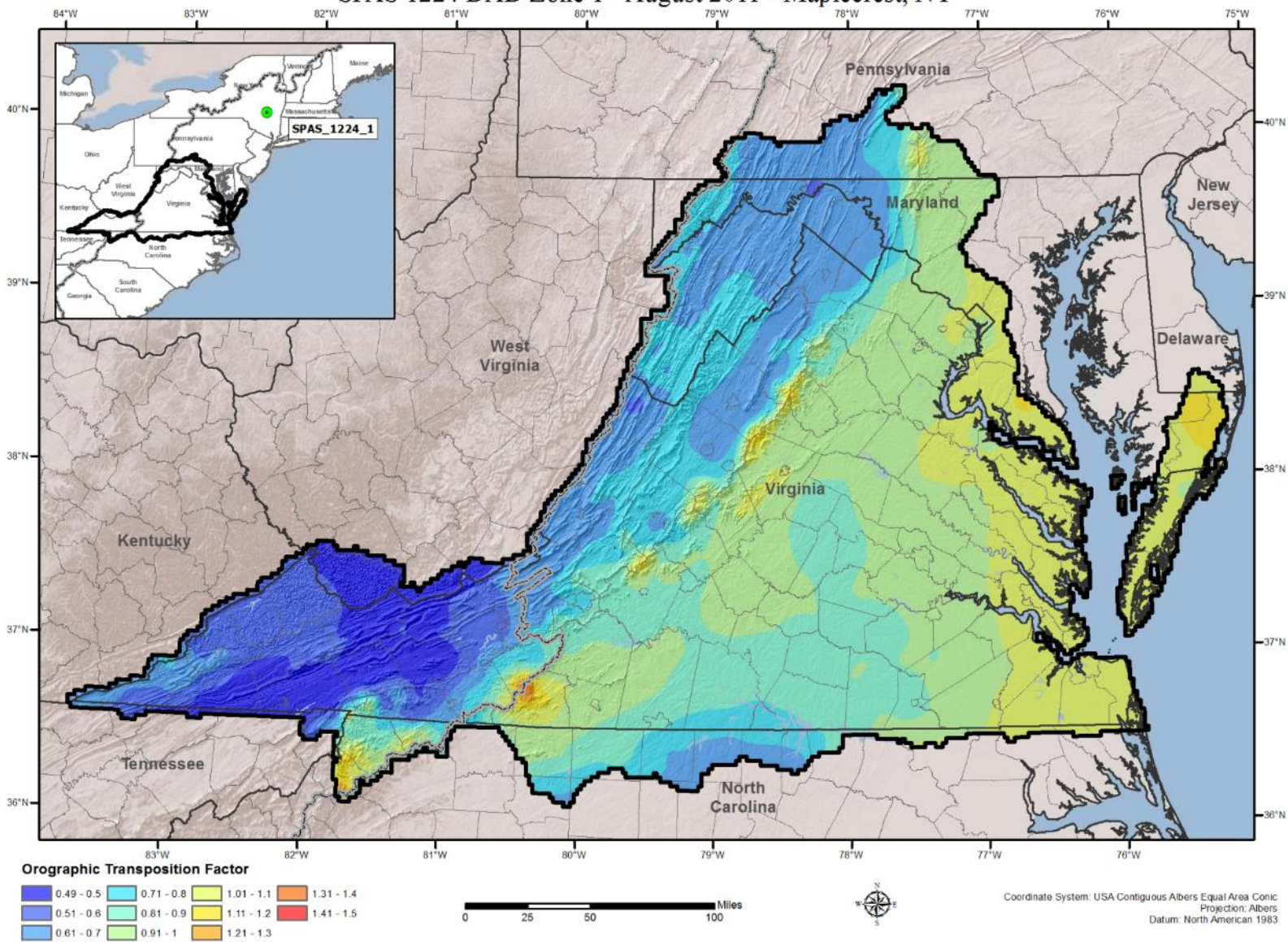
Orographic Transposition Factor (OTF)
 SPAS 1198 DAD Zone 1 - September 1999 - Pinkham Notch, NH



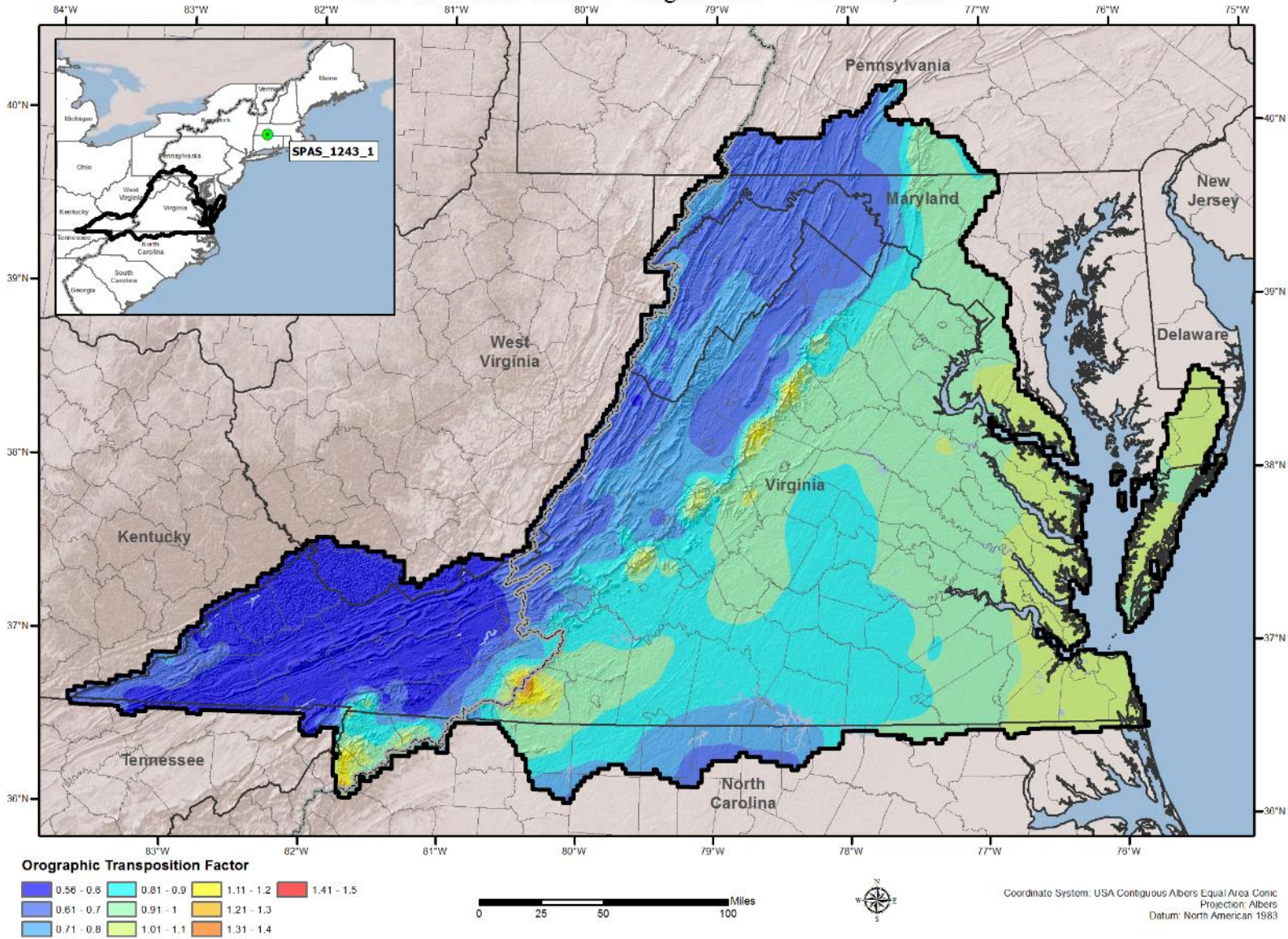
Orographic Transposition Factor (OTF)
 SPAS 1198 DAD Zone 2 - September 1999 - Mt Mansfield, VT



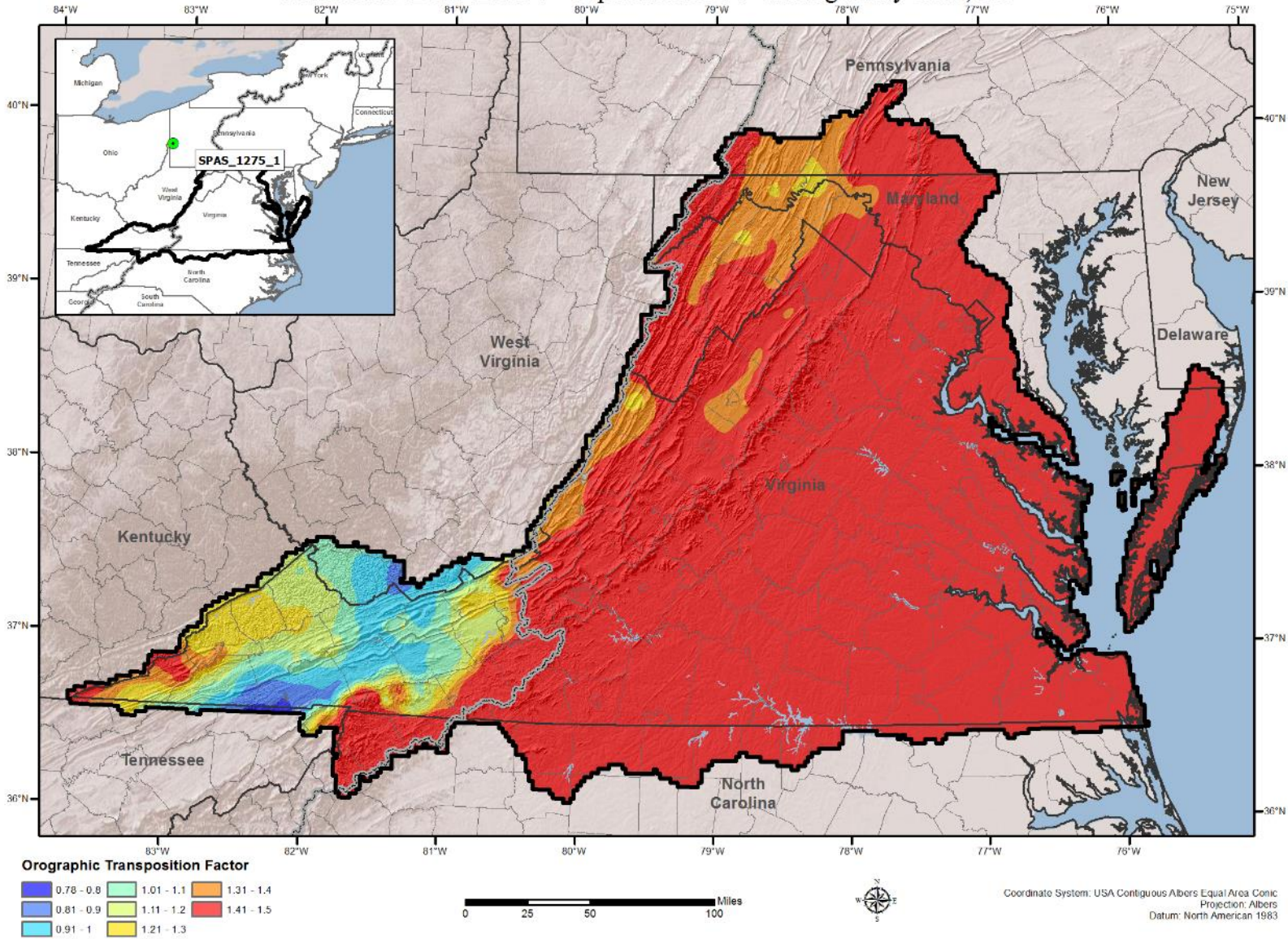
Orographic Transposition Factor (OTF) SPAS 1224 DAD Zone 1 - August 2011 - Maplecrest, NY



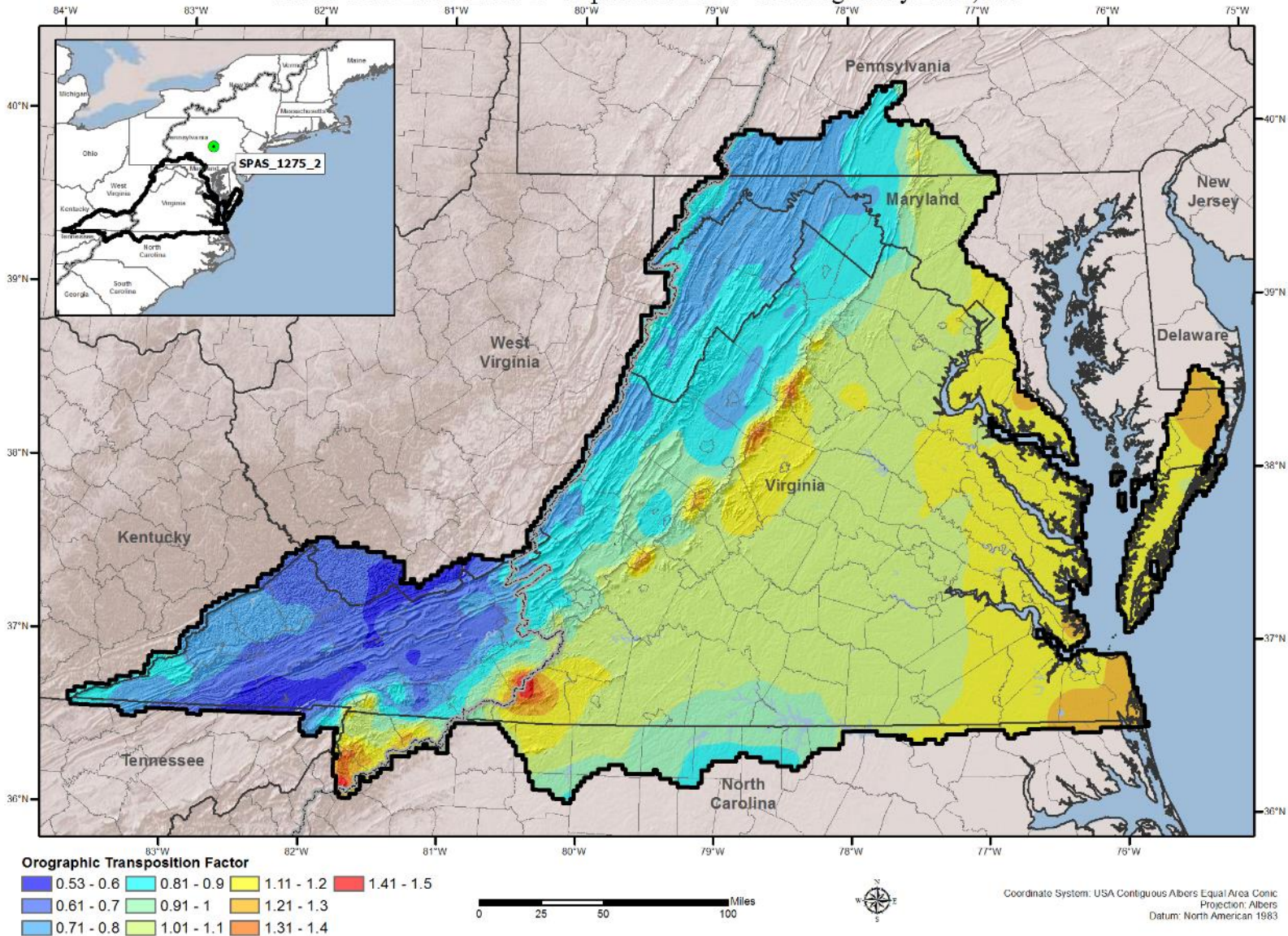
Orographic Transposition Factor (OTF) SPAS 1243 DAD Zone 1 - August 1955 - Westfield, MA



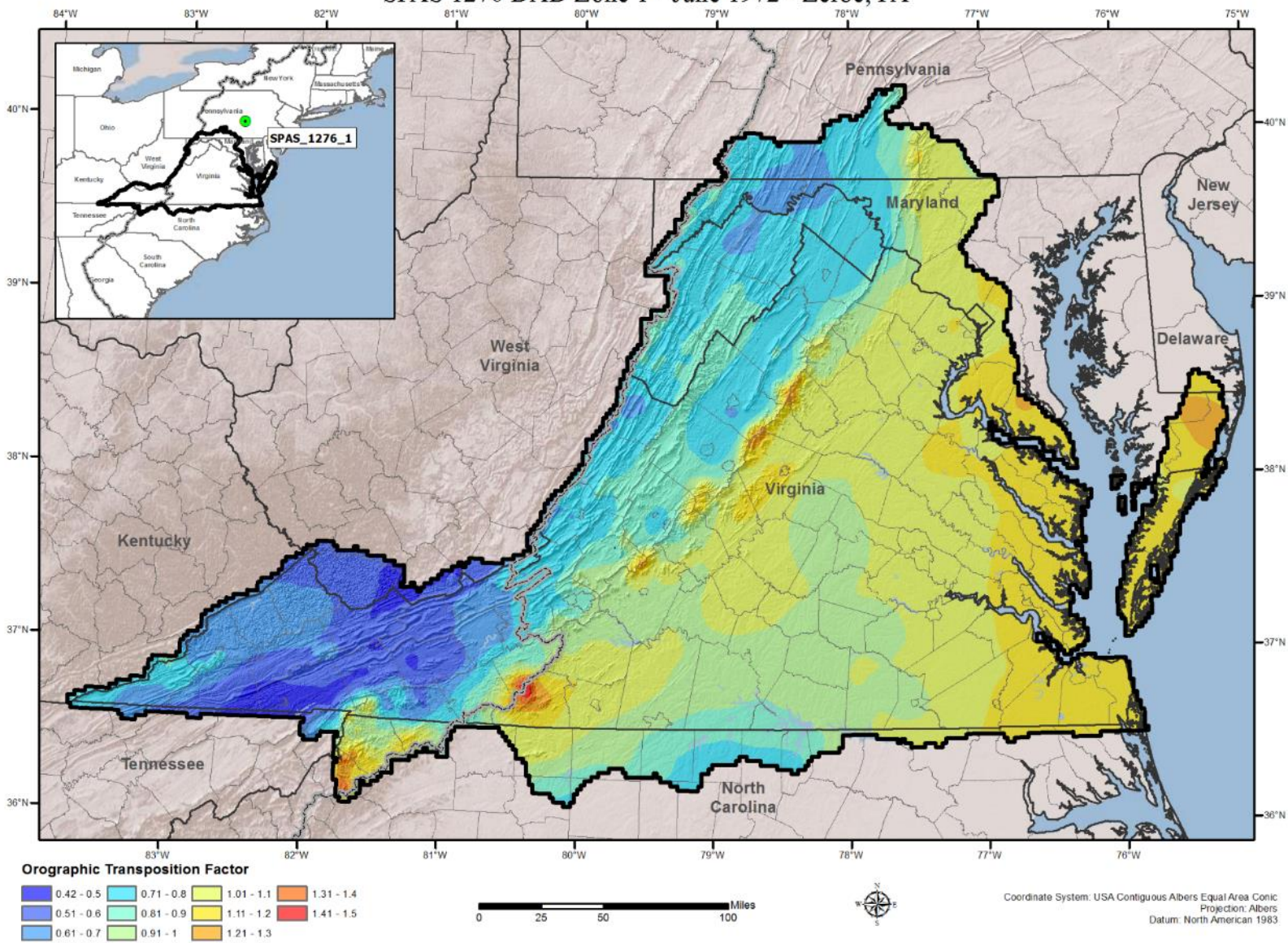
Orographic Transposition Factor (OTF) SPAS 1275 DAD Zone 1 - September 2004 - Montgomery Dam, PA



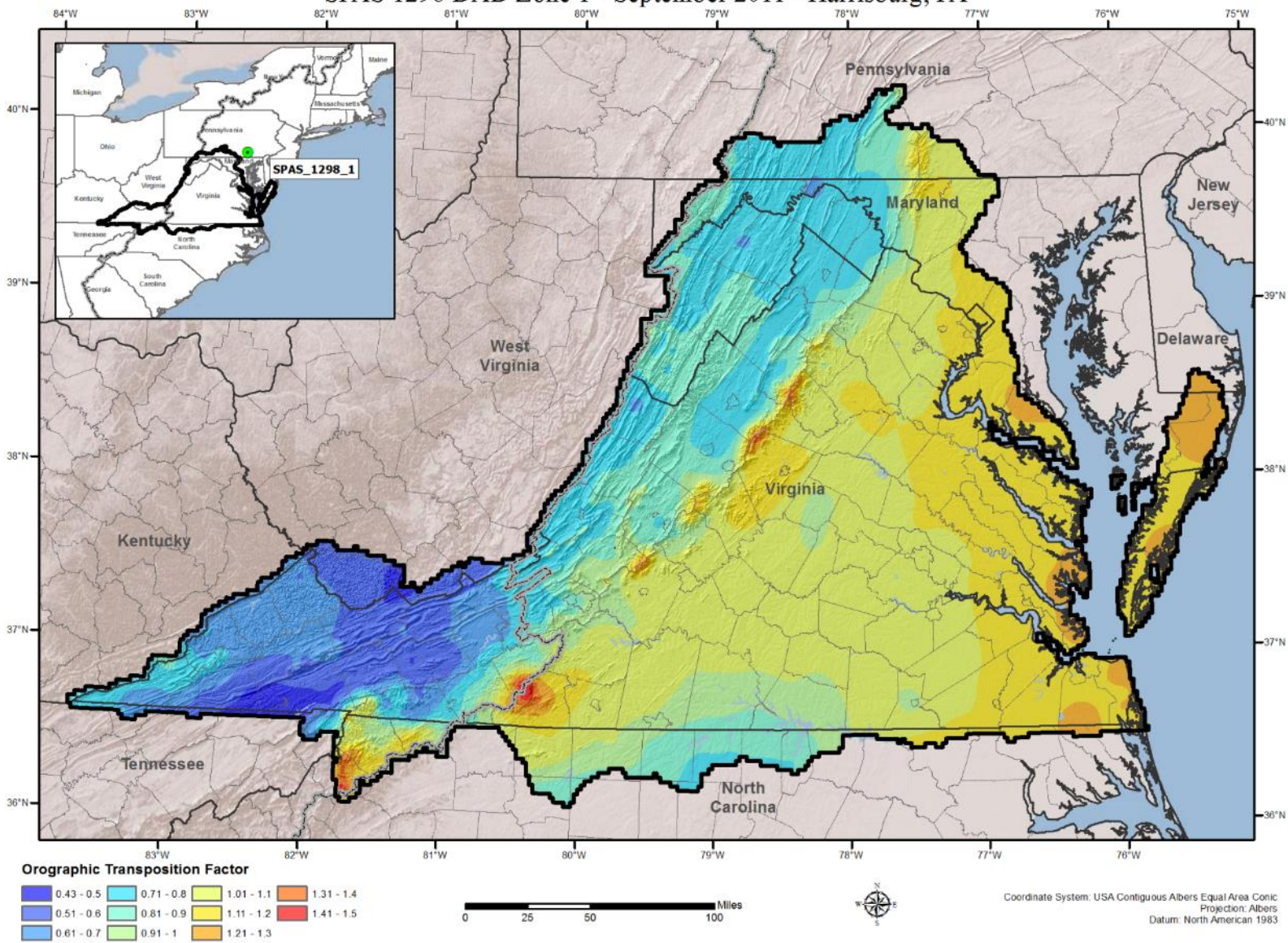
Orographic Transposition Factor (OTF) SPAS 1275 DAD Zone 2 - September 2004 - Mountgomery Dam, PA



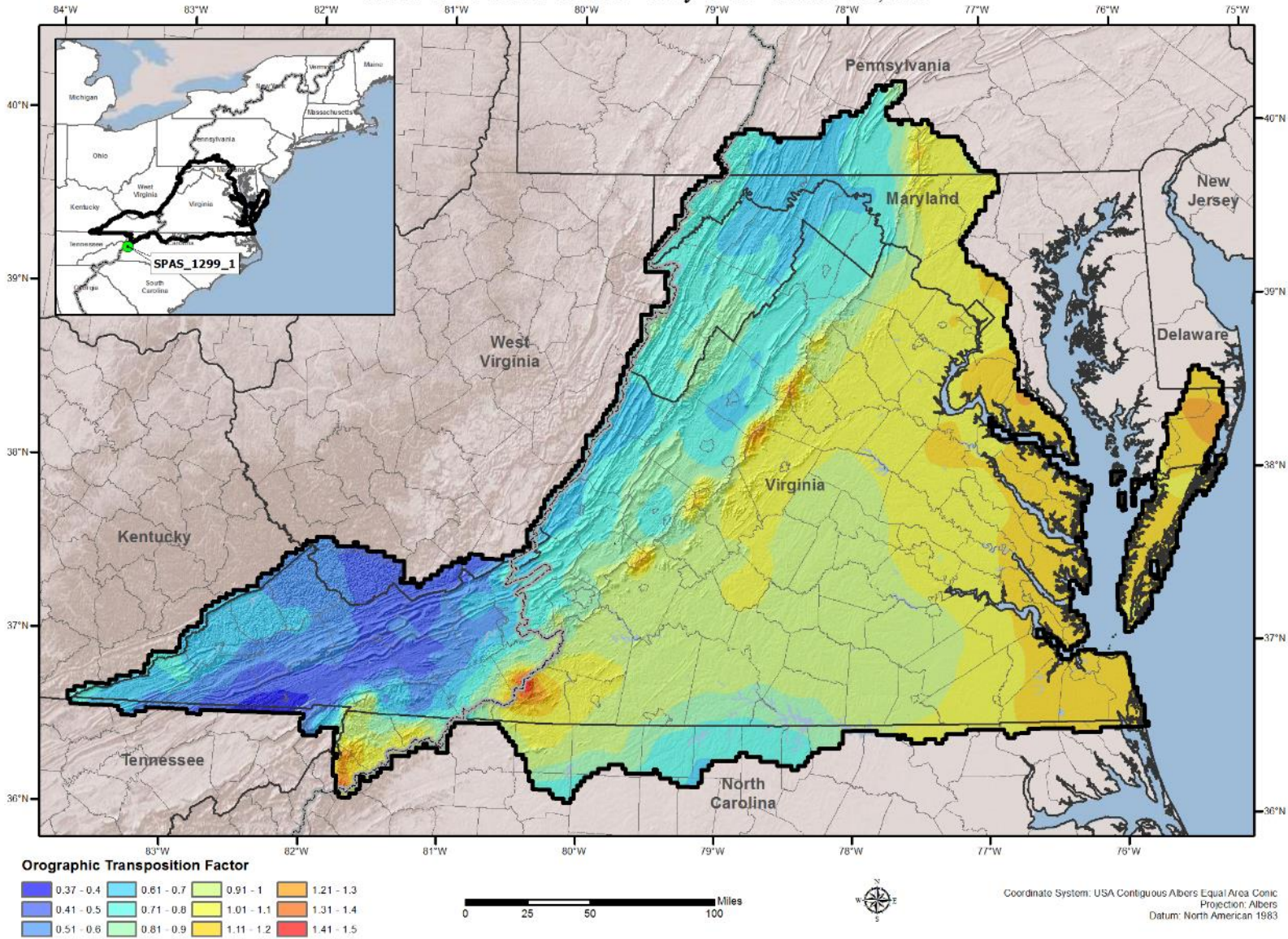
Orographic Transposition Factor (OTF) SPAS 1276 DAD Zone 1 - June 1972 - Zerbe, PA



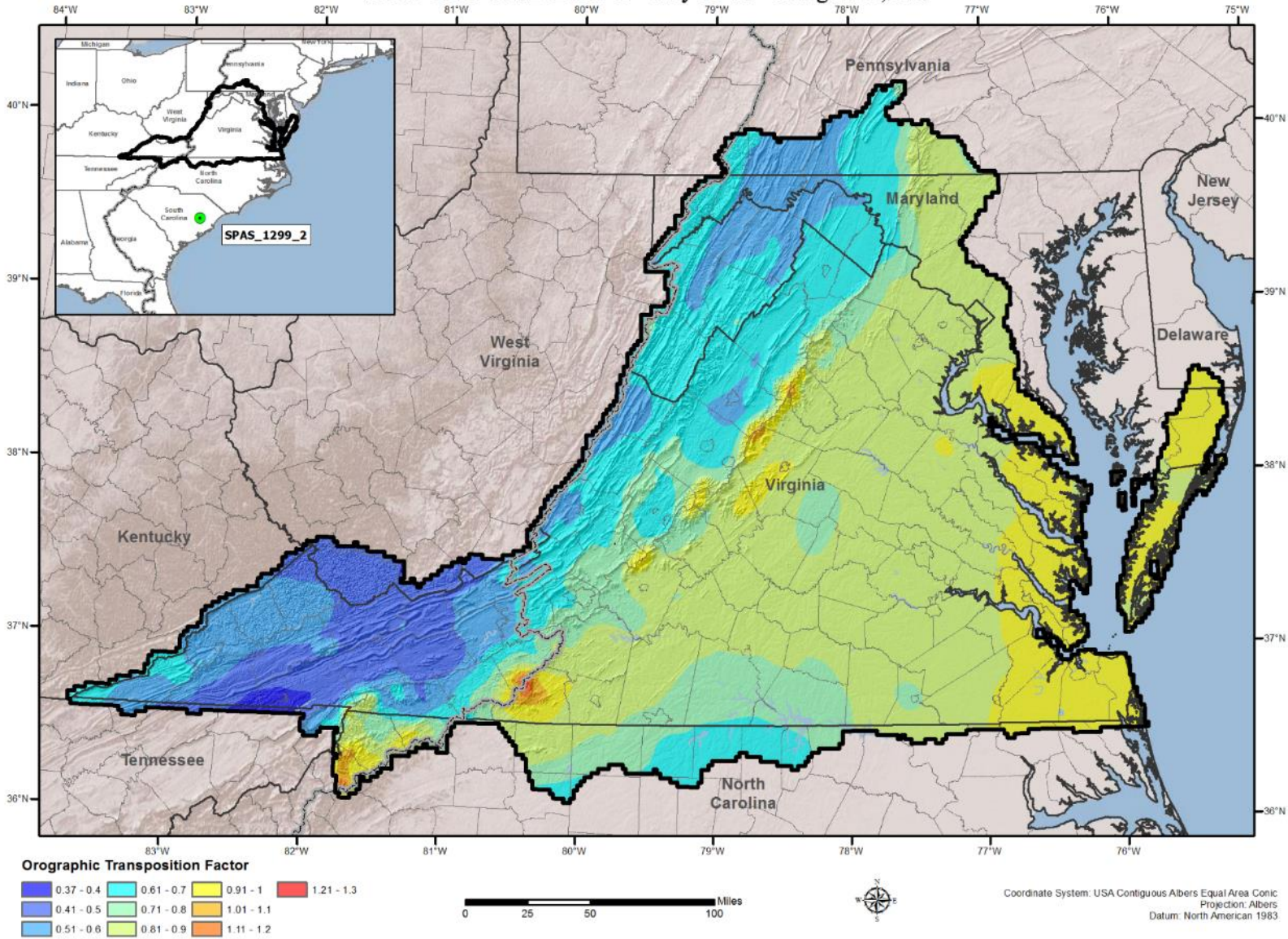
Orographic Transposition Factor (OTF) SPAS 1298 DAD Zone 1 - September 2011 - Harrisburg, PA



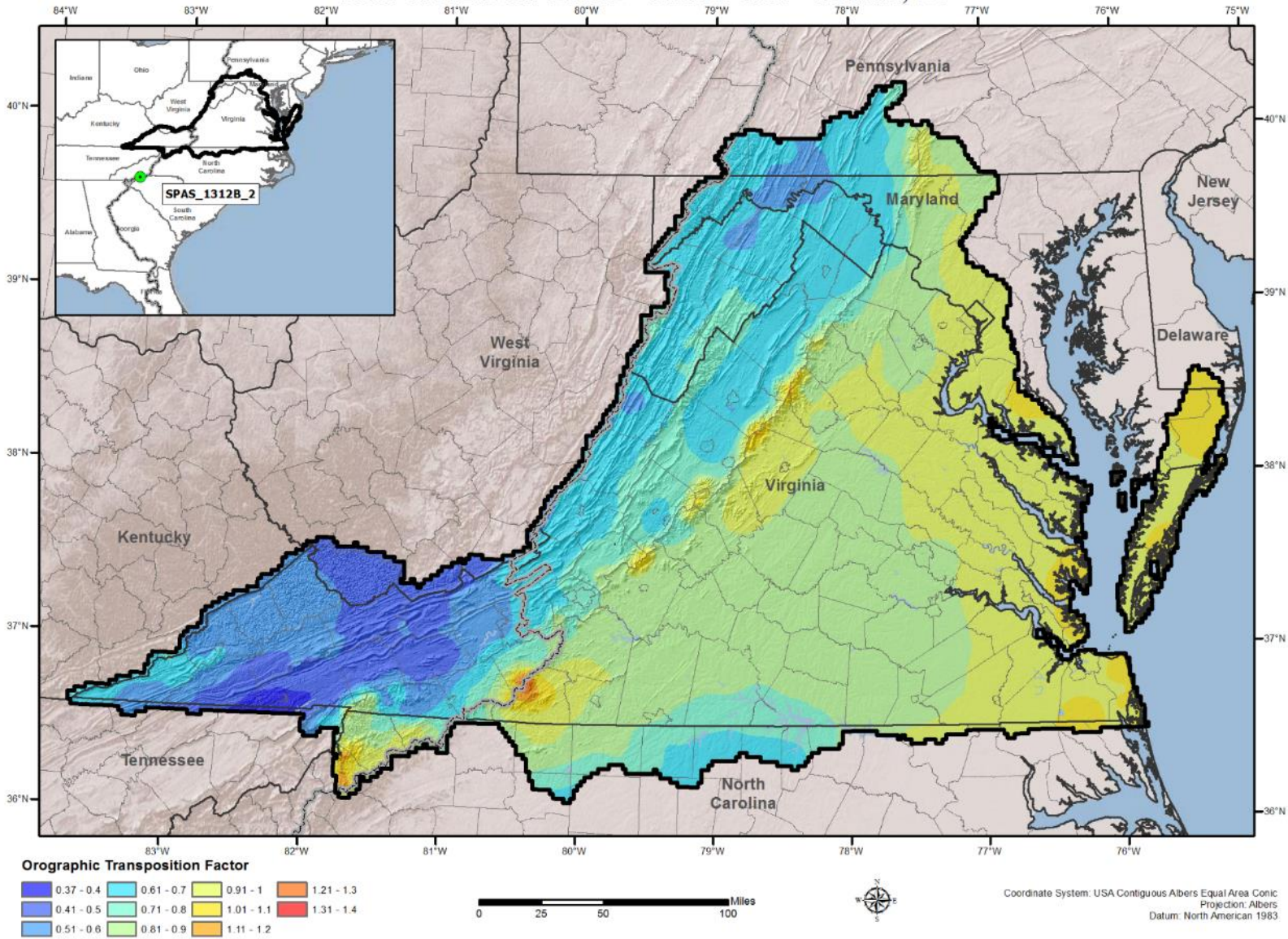
Orographic Transposition Factor (OTF) SPAS 1299 DAD Zone 1 - July 1916 - Alta Pass, NC



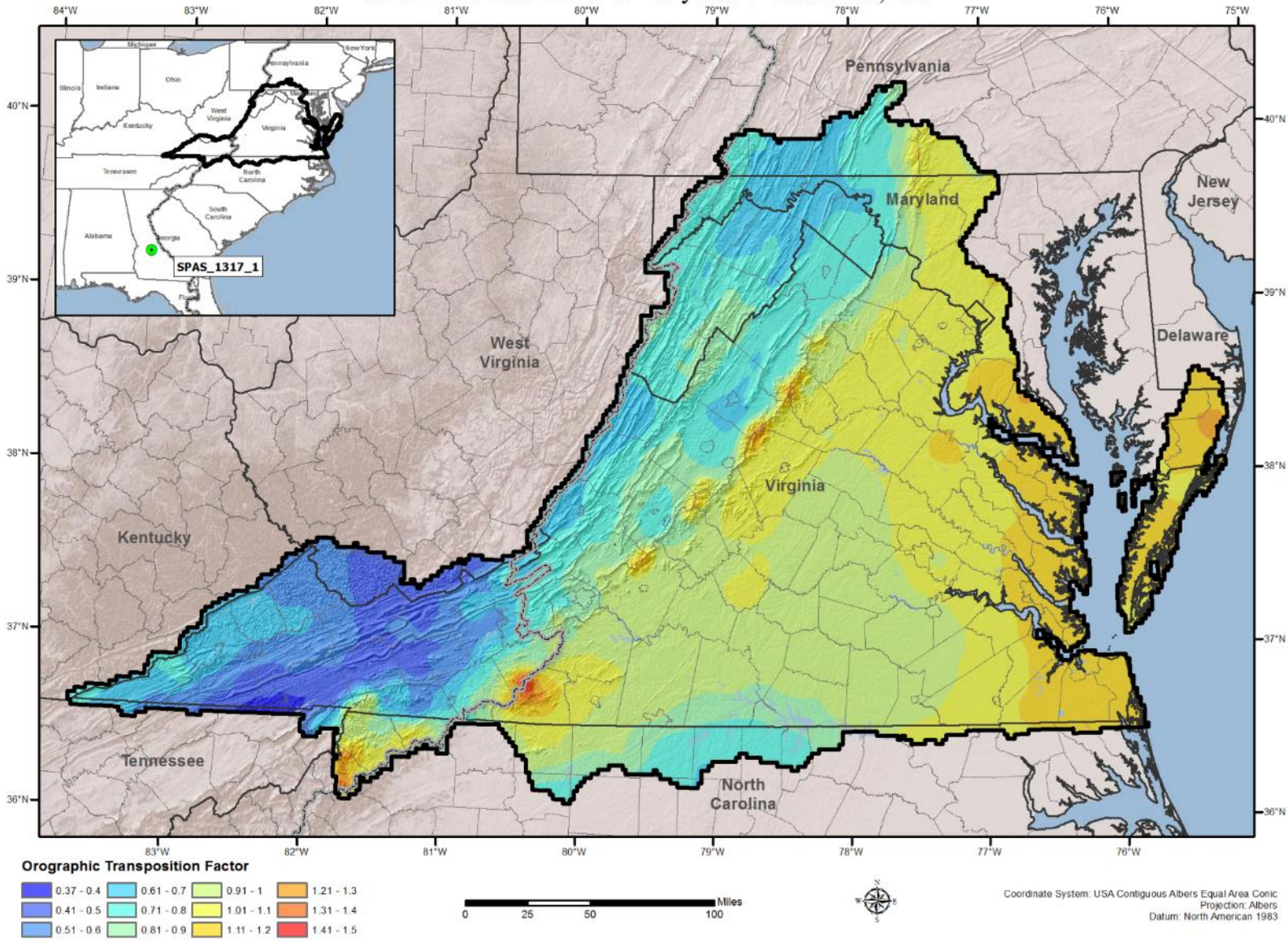
Orographic Transposition Factor (OTF) SPAS 1299 DAD Zone 2 - July 1916 - Kingstree, NC



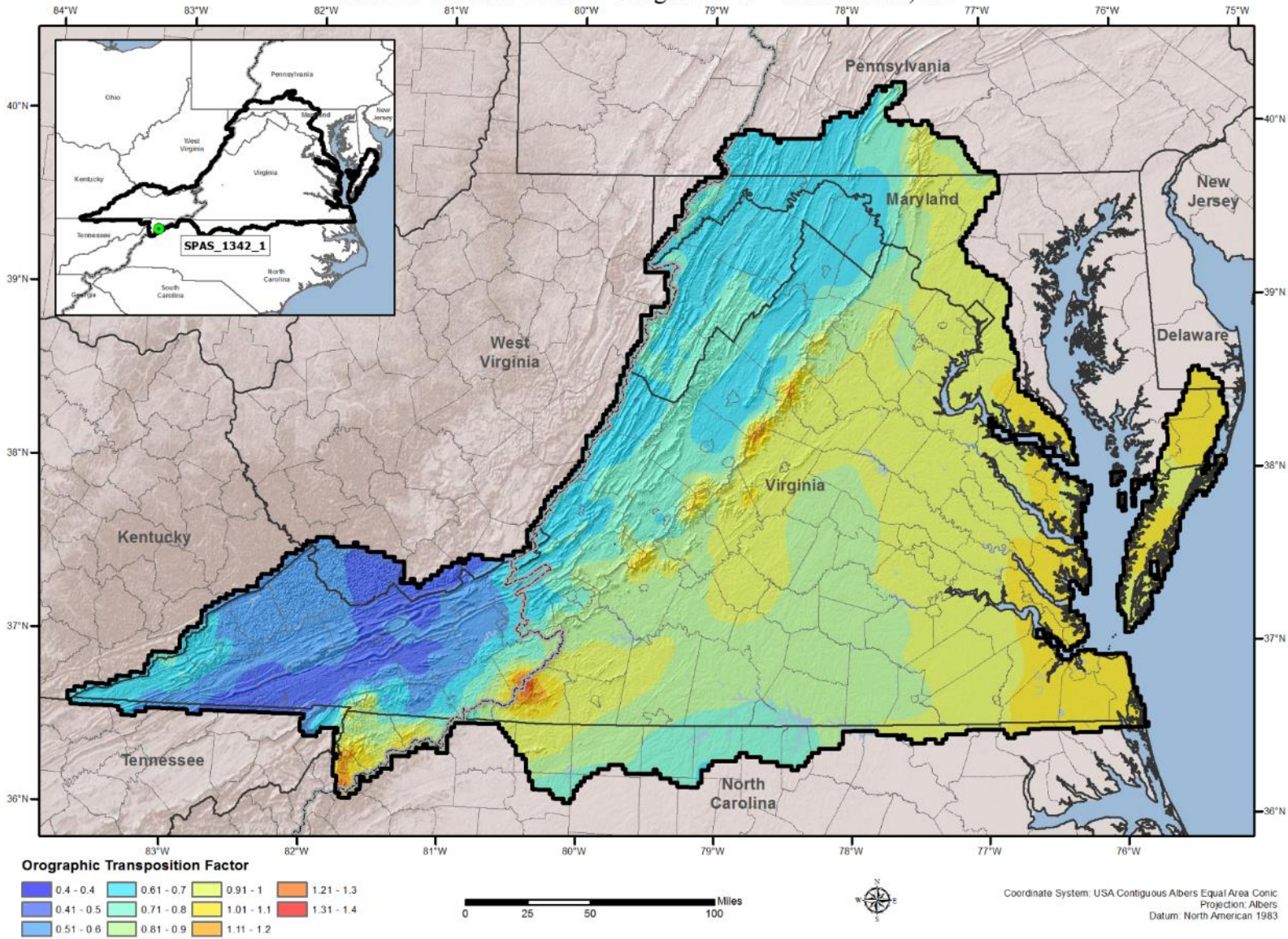
Orographic Transposition Factor (OTF)
 SPAS 1312B DAD Zone 2 - October 1964 - Rosman, NC



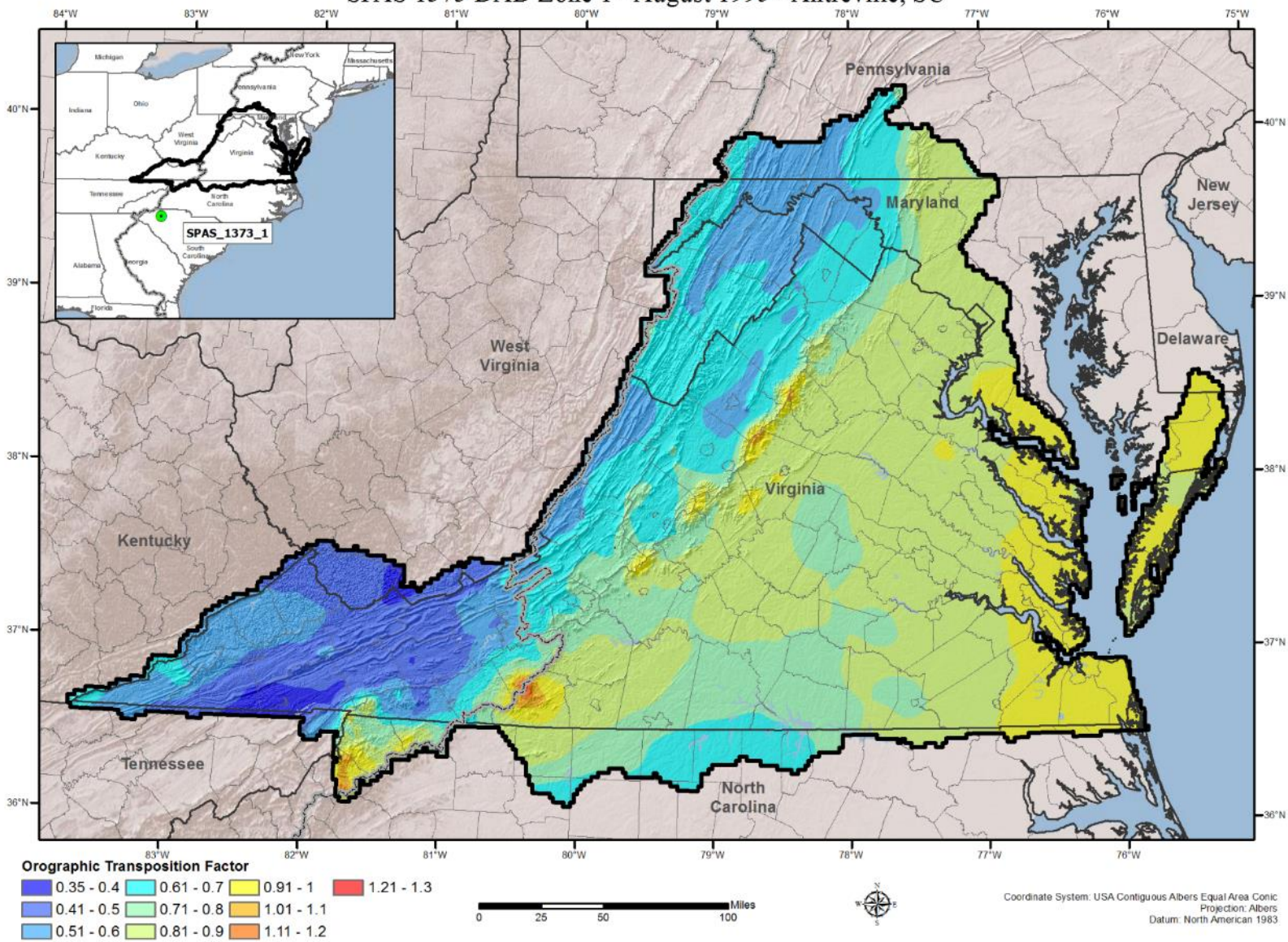
Orographic Transposition Factor (OTF) SPAS 1317 DAD Zone 1 - July 1994 - Americus, GA



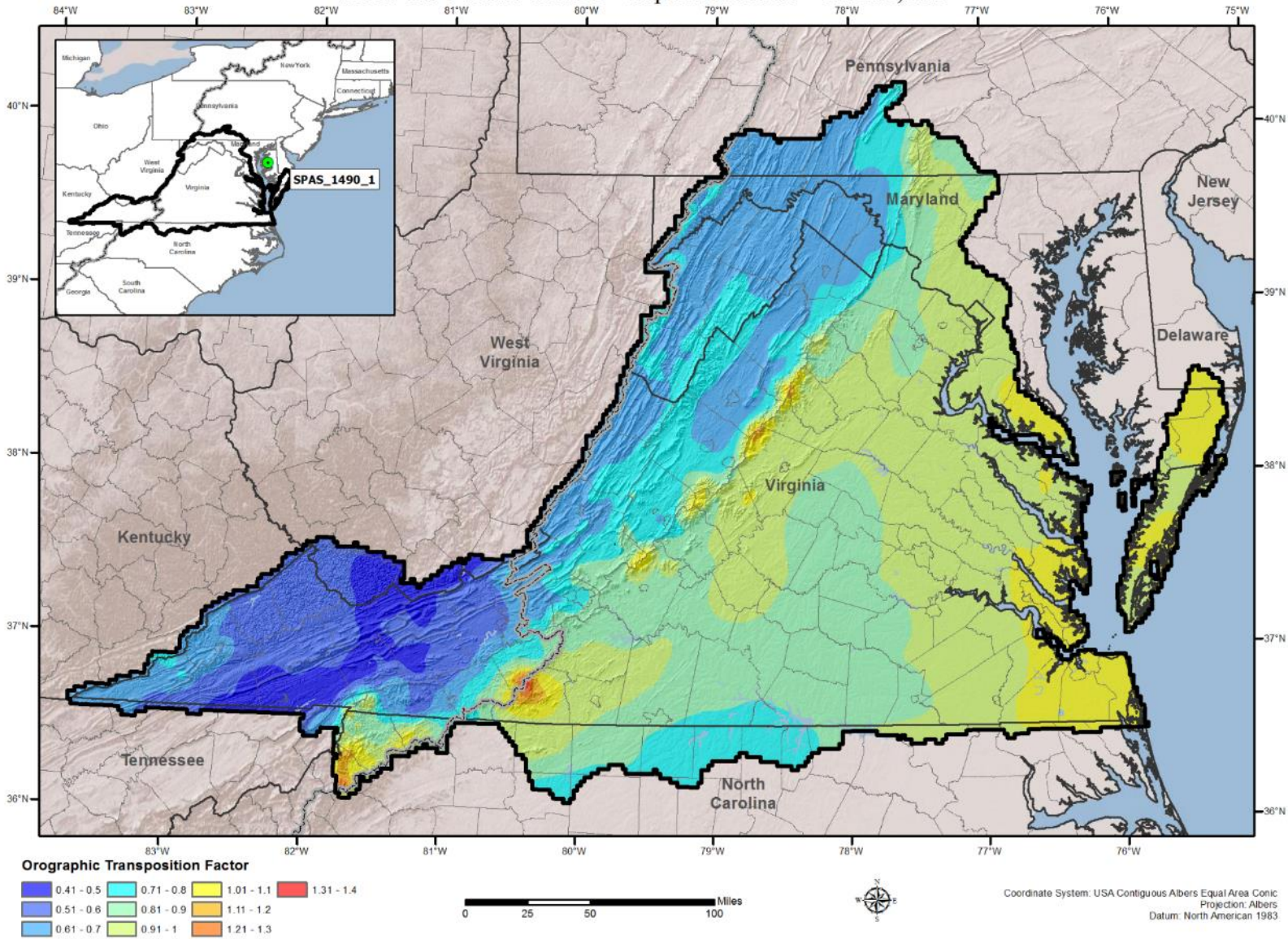
Orographic Transposition Factor (OTF)
 SPAS 1342 DAD Zone 1 - August 1940 - Mt Mitchell, NC



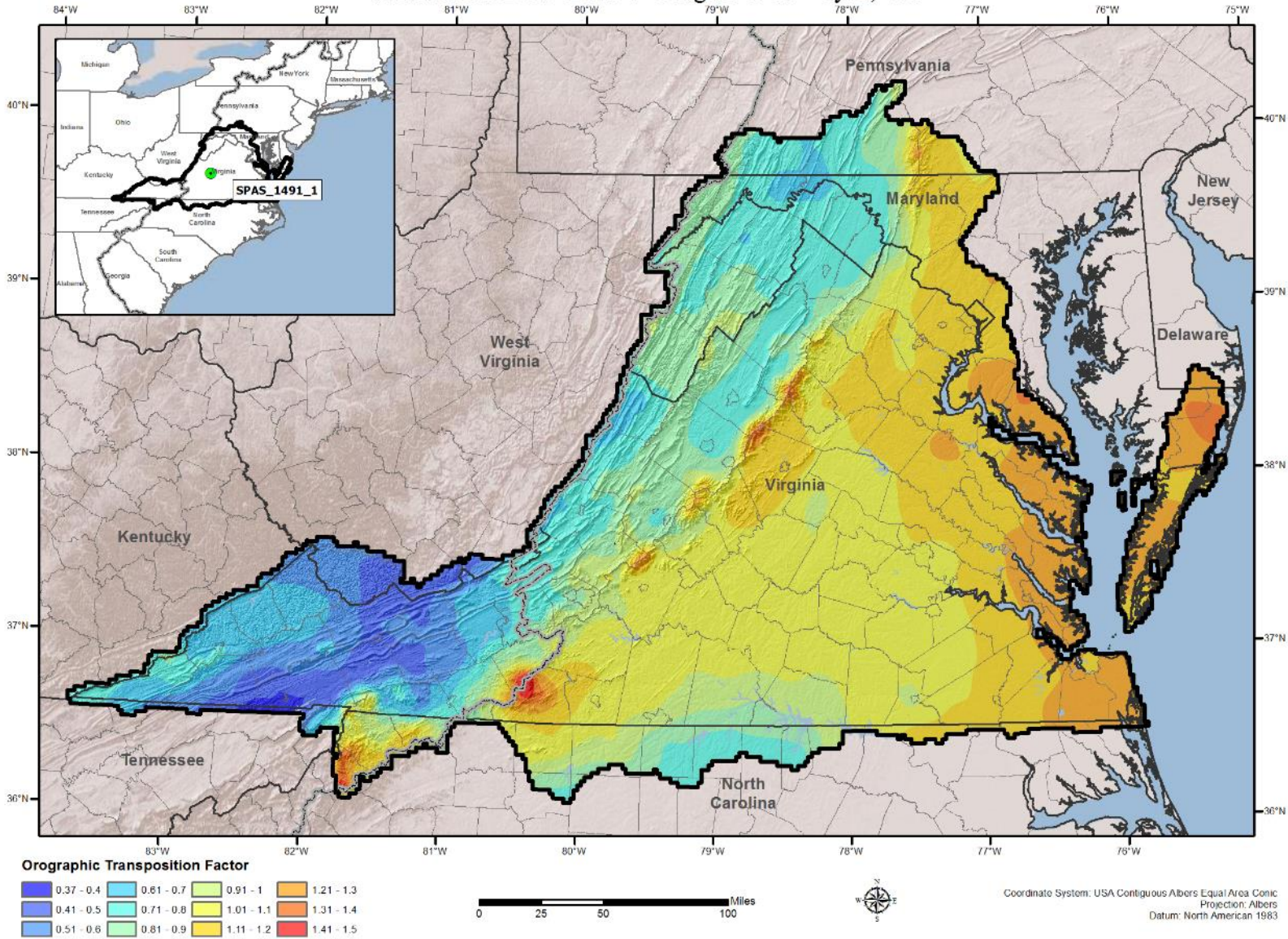
Orographic Transposition Factor (OTF) SPAS 1373 DAD Zone 1 - August 1995 - Antreville, SC



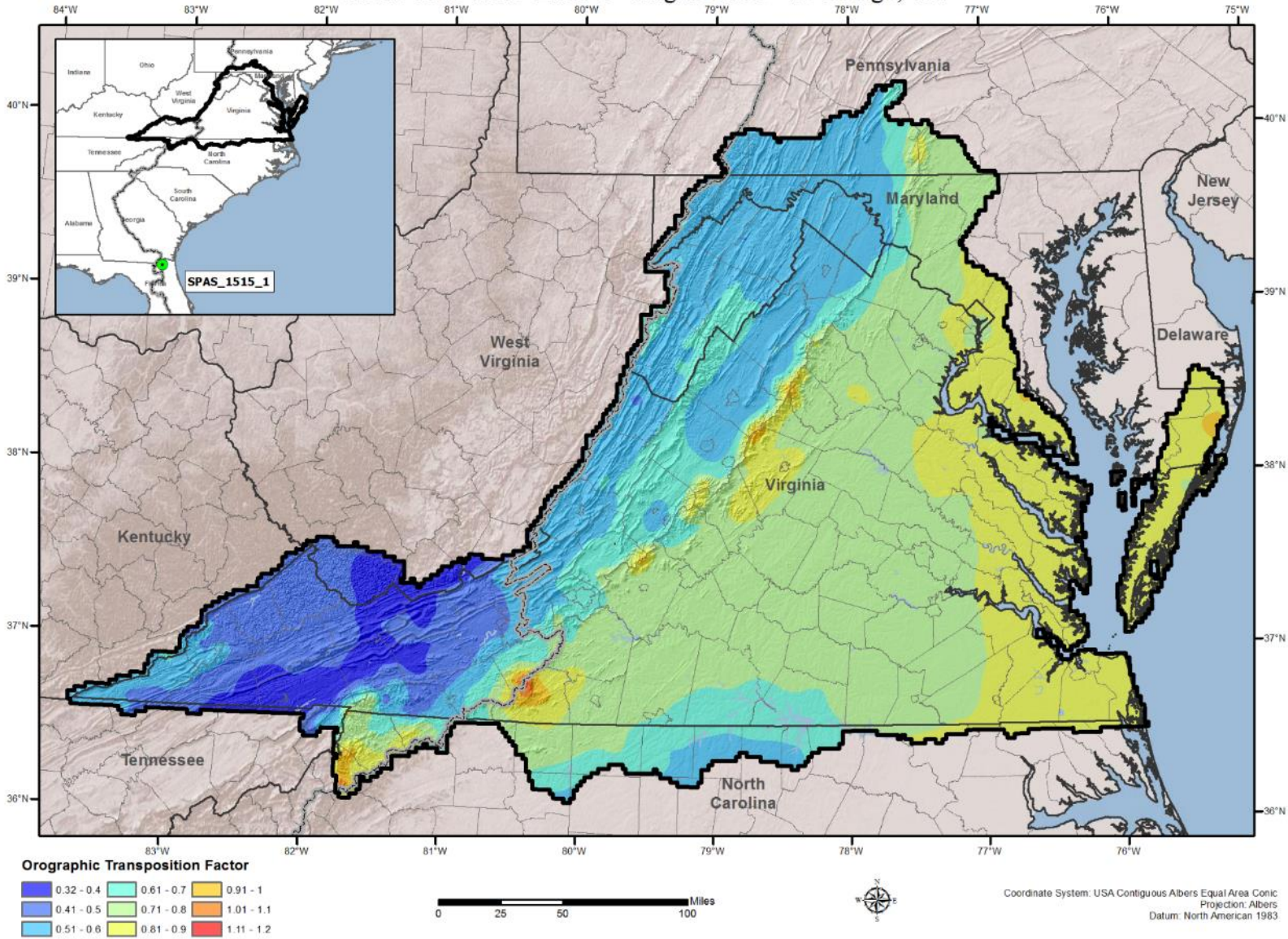
Orographic Transposition Factor (OTF)
 SPAS 1490 DAD Zone 1 - September 1935 - Easton, MD



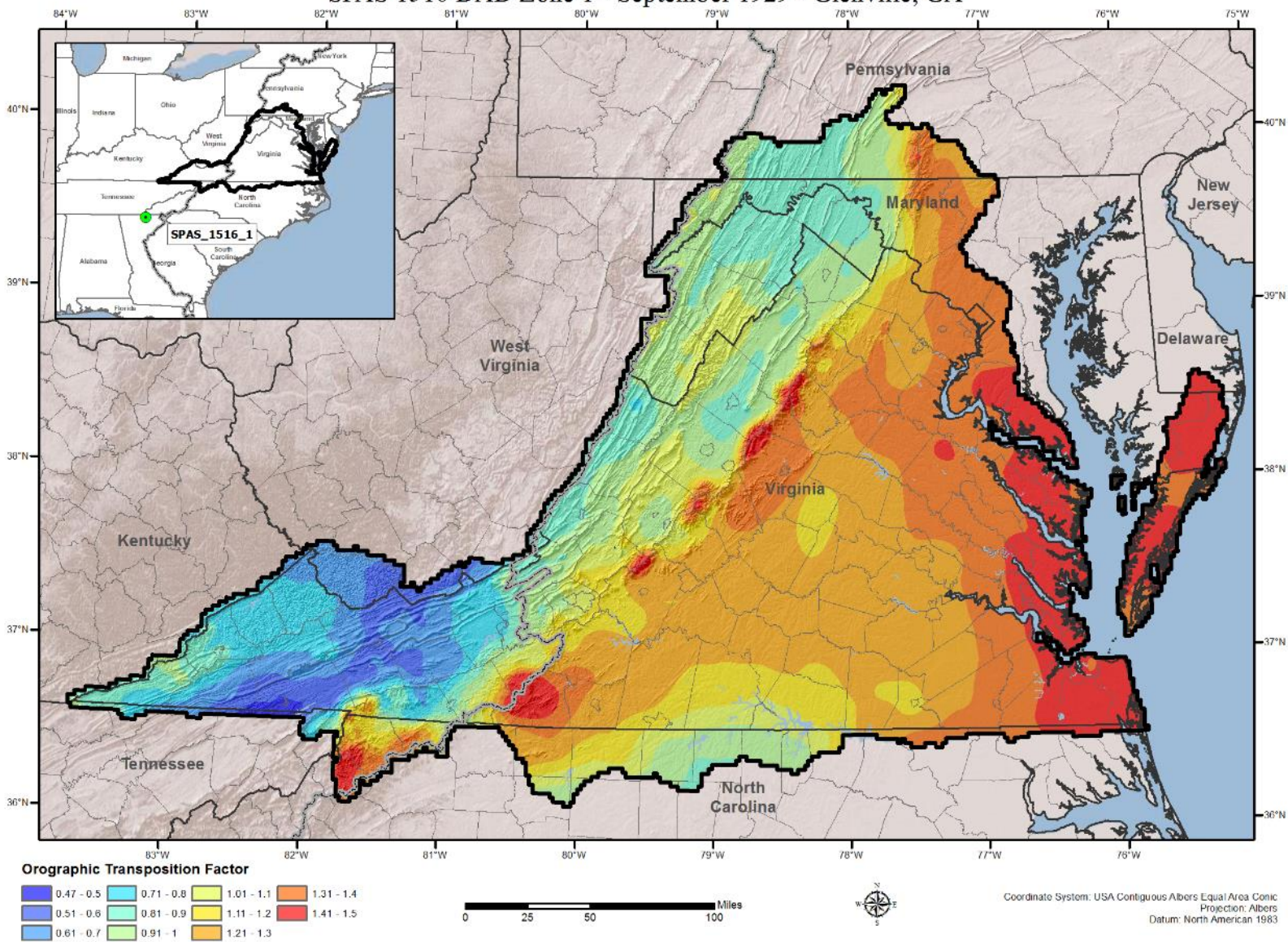
Orographic Transposition Factor (OTF) SPAS 1491 DAD Zone 1 - August 1969 - Tyro, VA



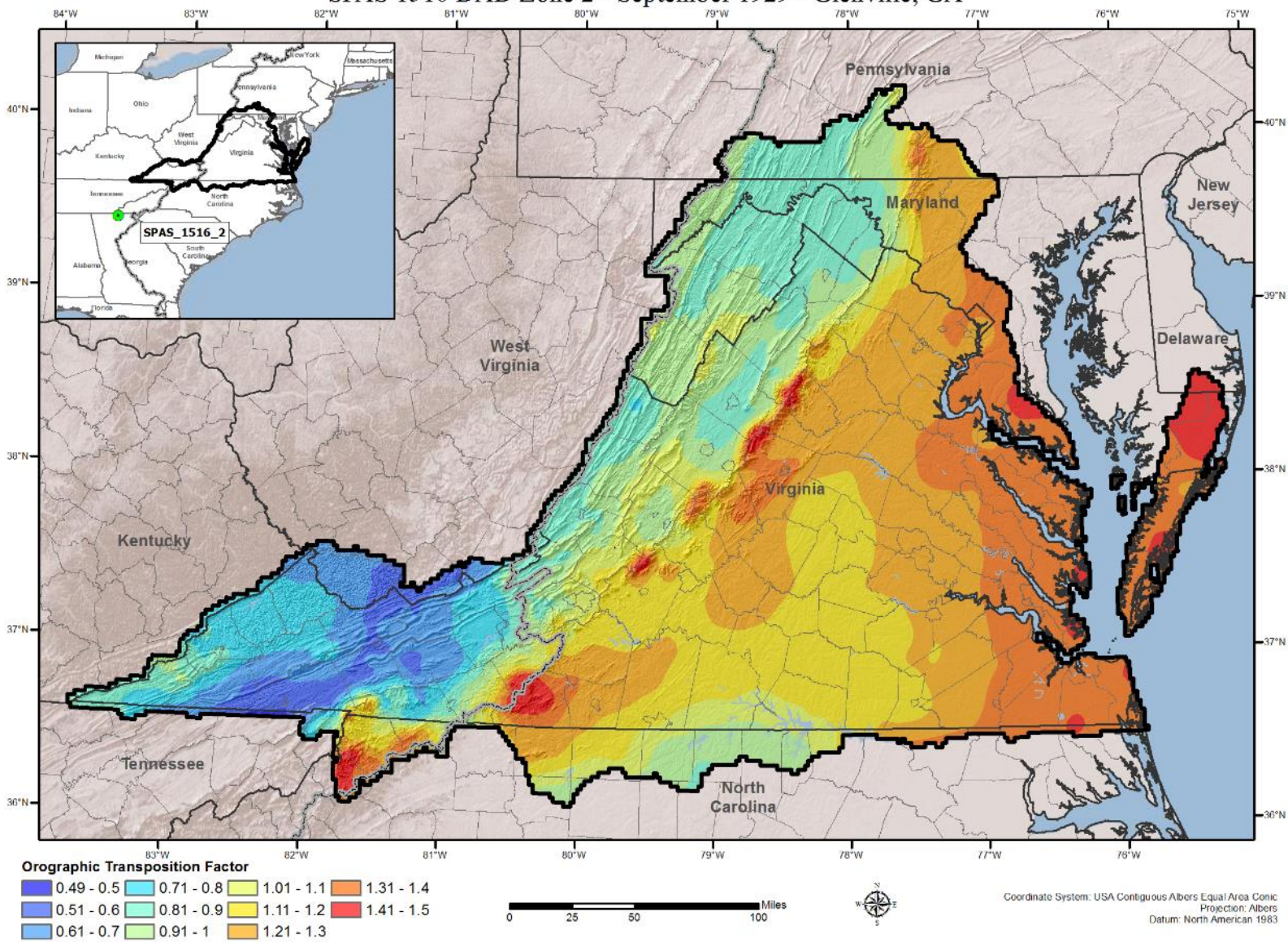
Orographic Transposition Factor (OTF) SPAS 1515 DAD Zone 1 - August 1911 - St George, GA



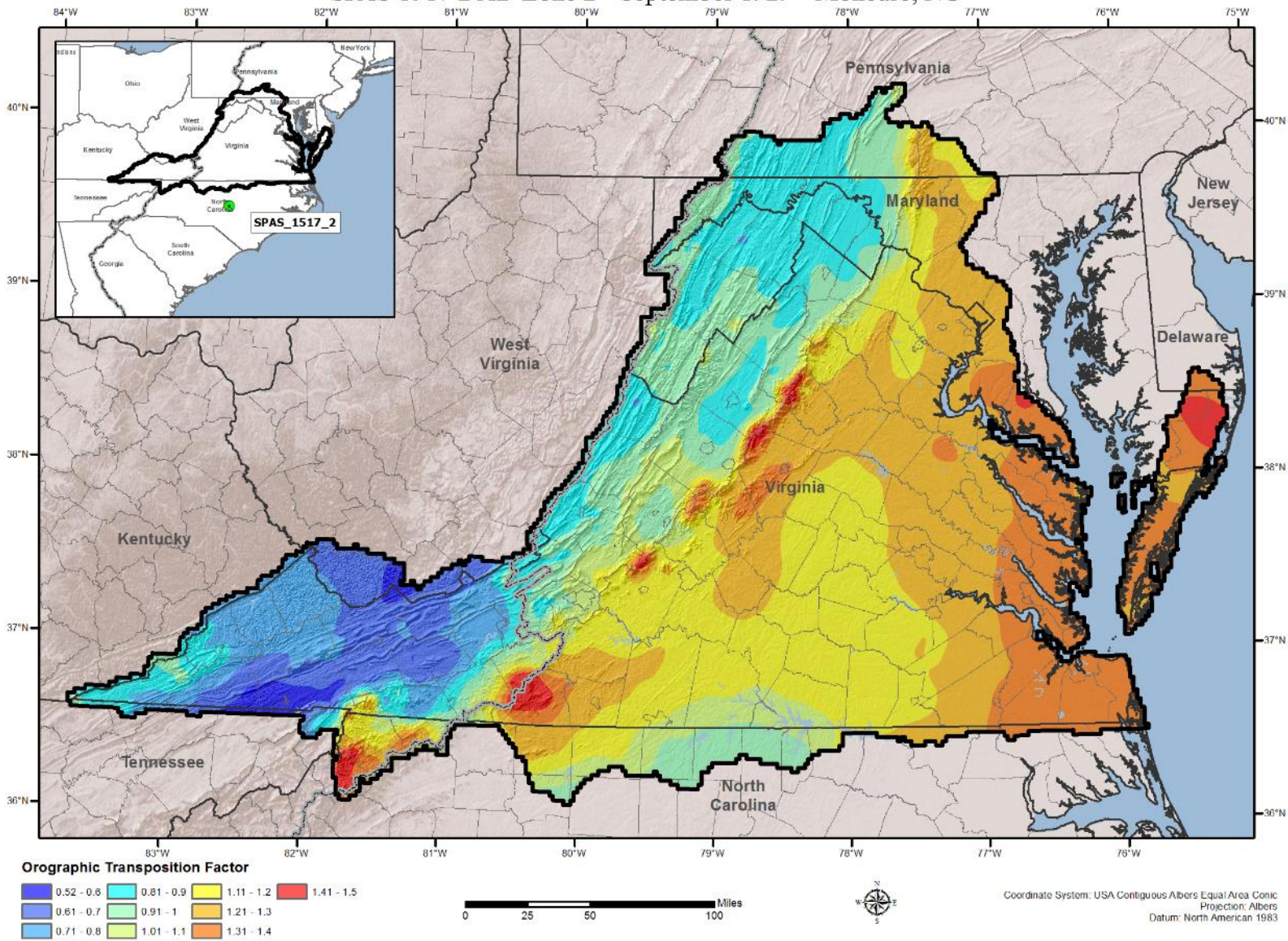
Orographic Transposition Factor (OTF)
 SPAS 1516 DAD Zone 1 - September 1929 - Glenville, GA



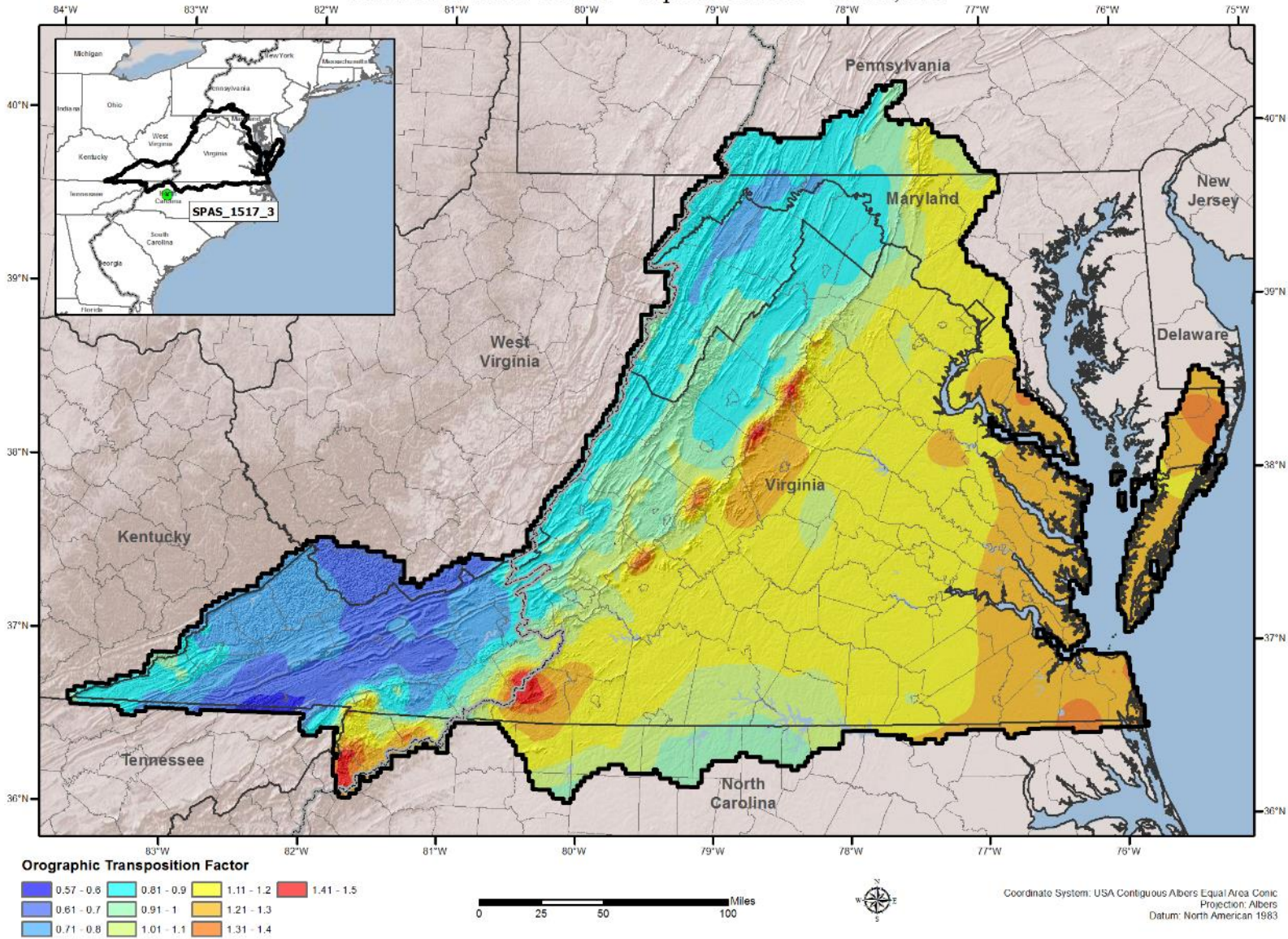
Orographic Transposition Factor (OTF) SPAS 1516 DAD Zone 2 - September 1929 - Glenville, GA



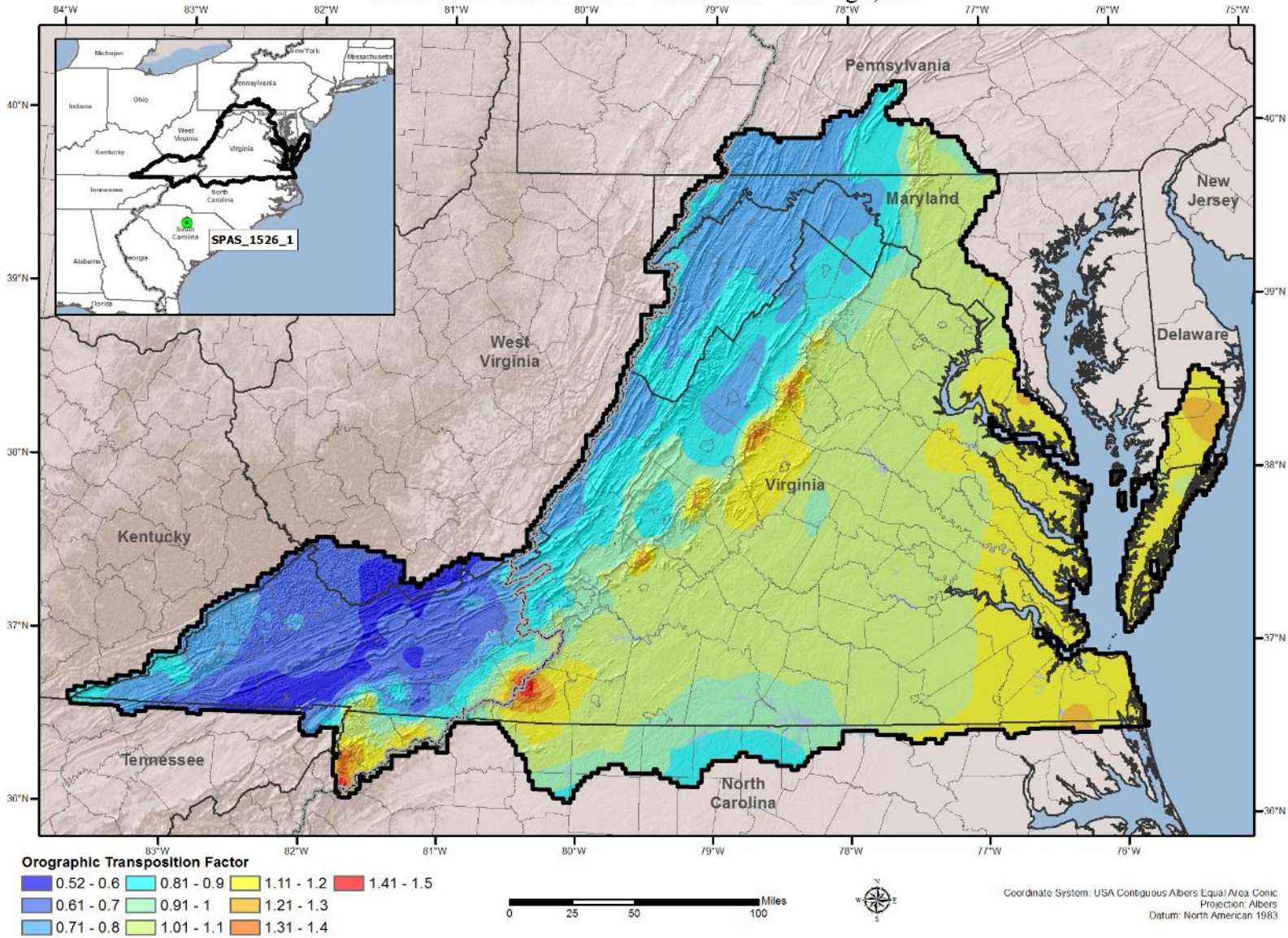
Orographic Transposition Factor (OTF)
 SPAS 1517 DAD Zone 2 - September 1929 - Moncure, NC



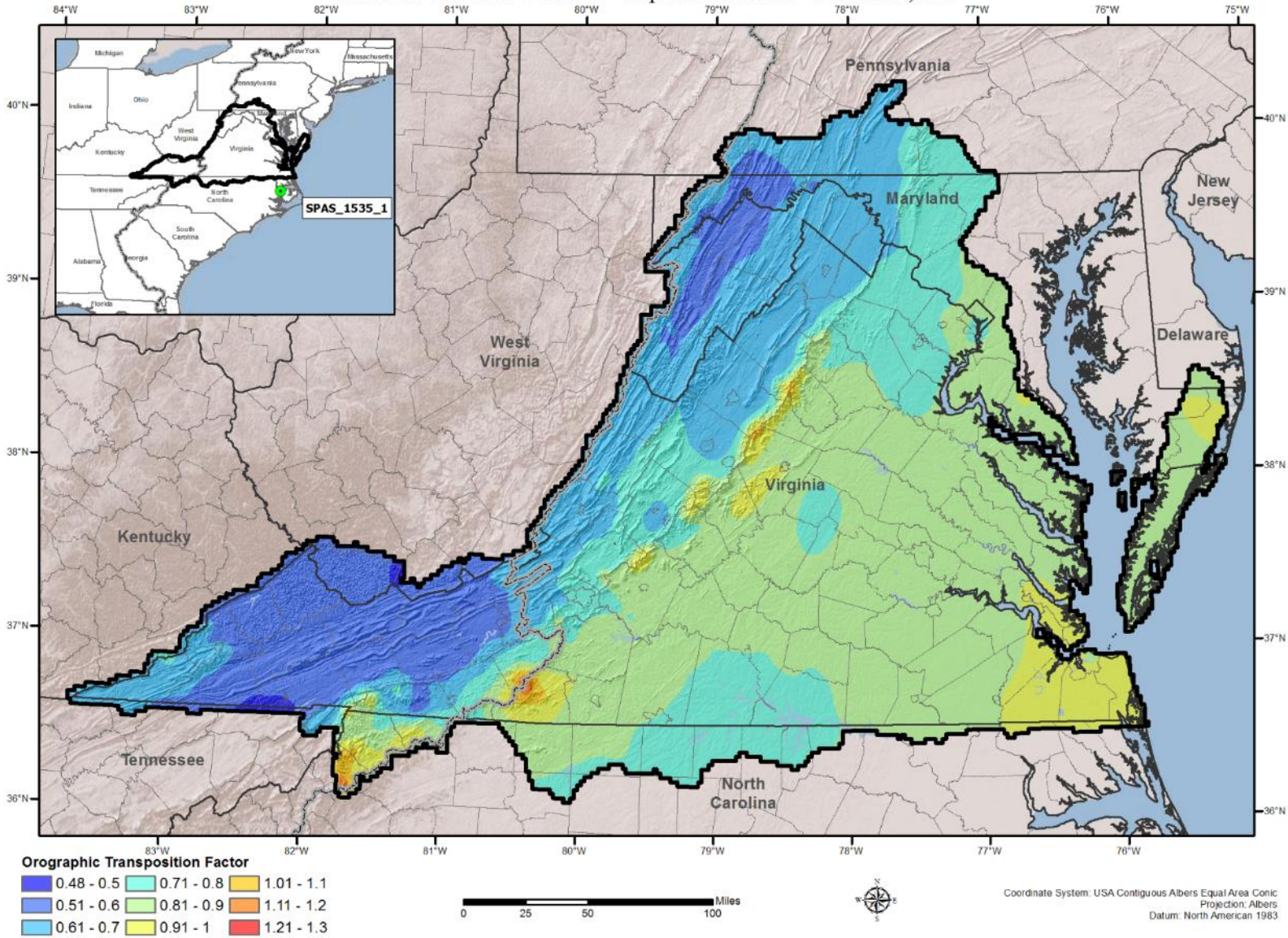
Orographic Transposition Factor (OTF) SPAS 1517 DAD Zone 3 - September 1929 - Settle, NC



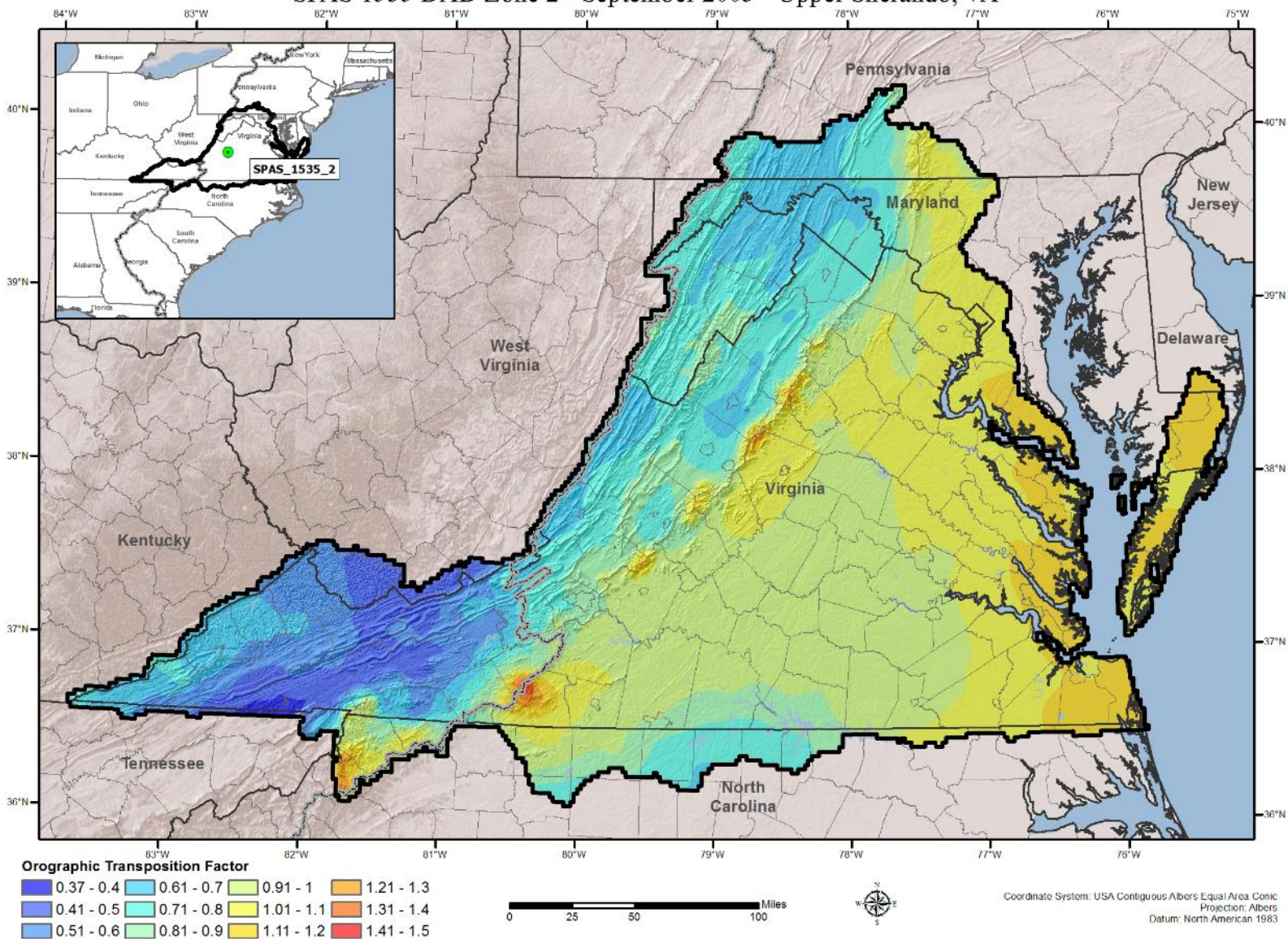
Orographic Transposition Factor (OTF) SPAS 1526 DAD Zone 1 - June 2006 - Raleigh, NC



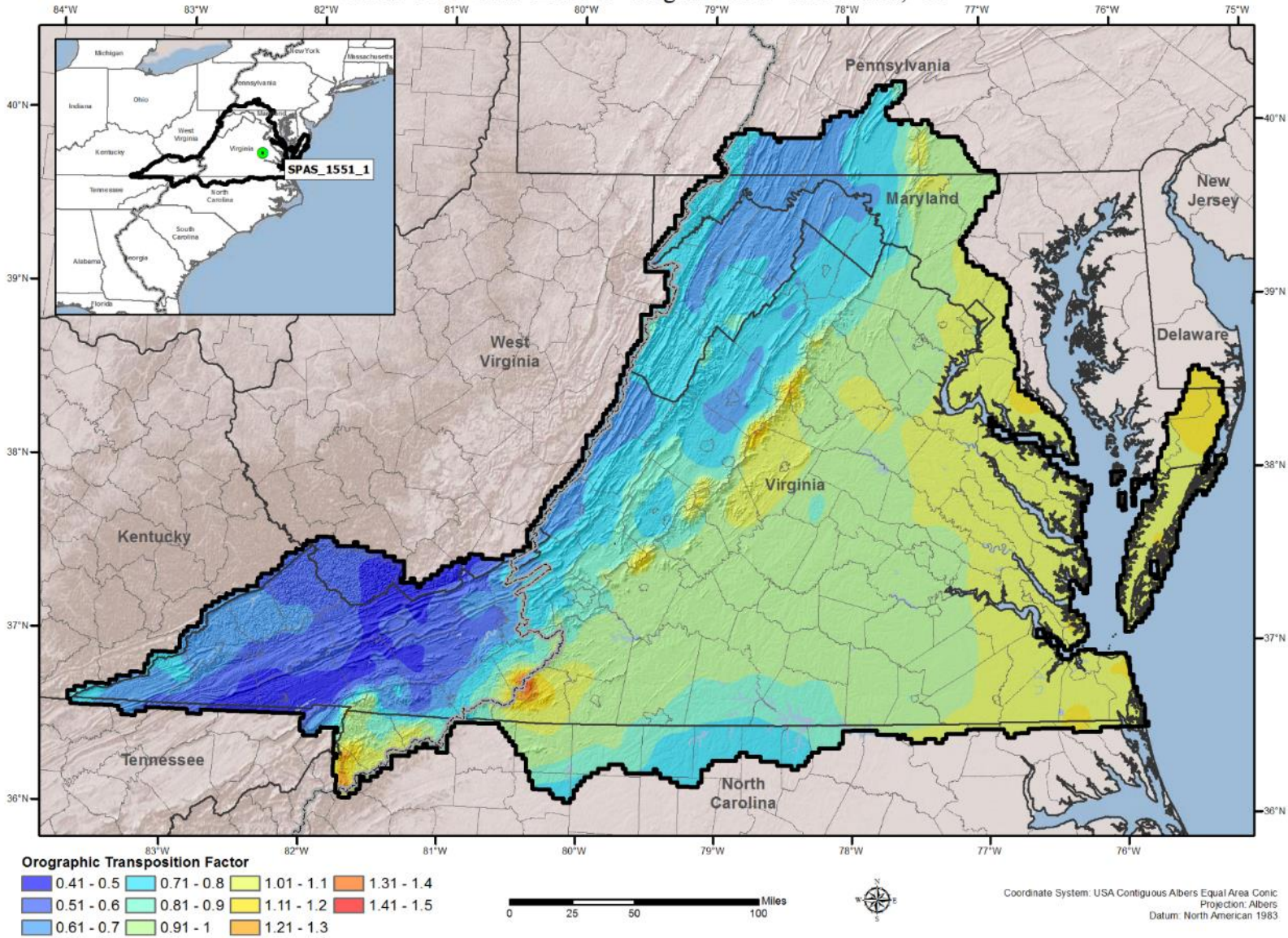
Orographic Transposition Factor (OTF)
 SPAS 1535 DAD Zone 1 - September 2003 - Edenton, NC



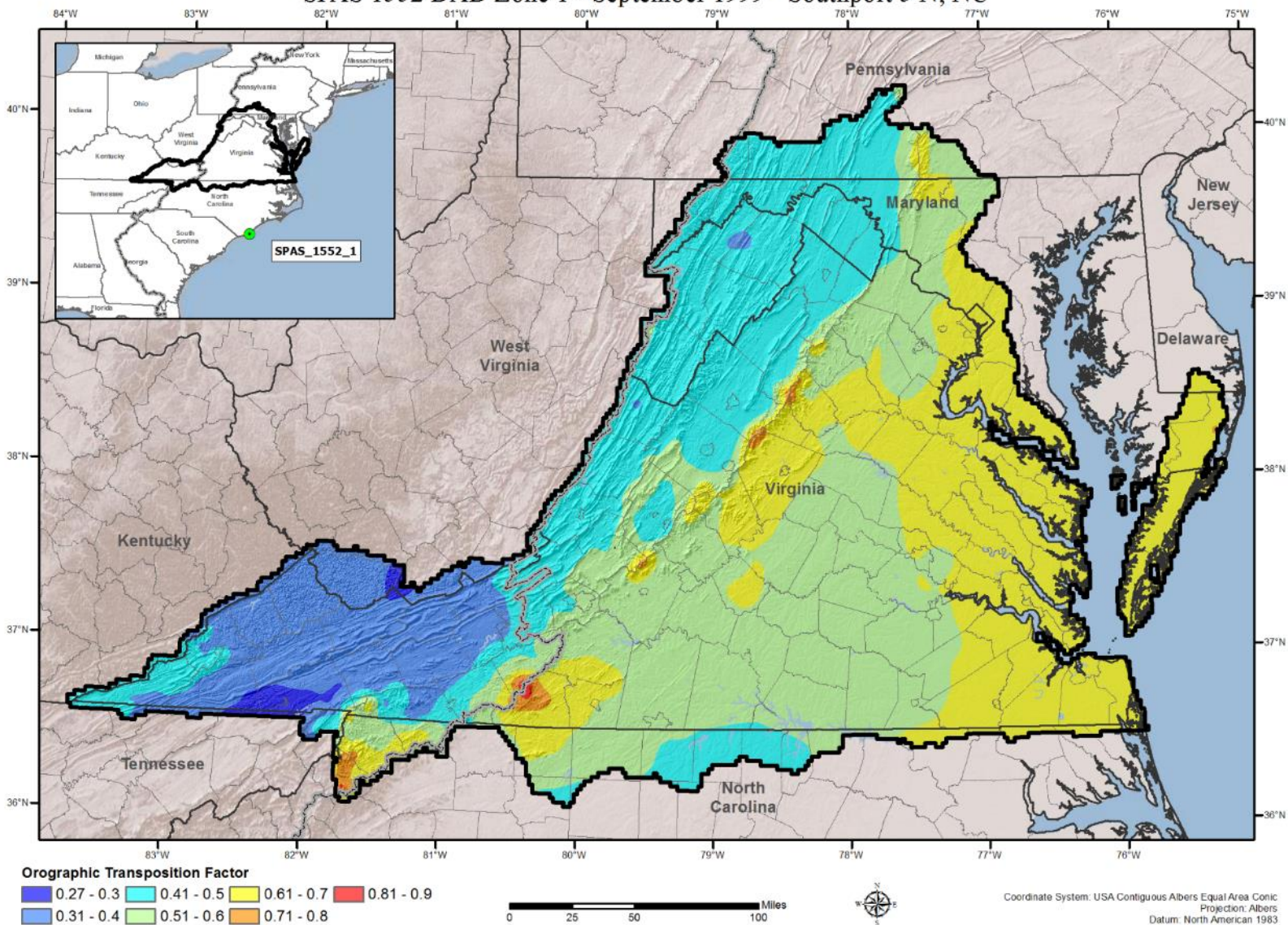
Orographic Transposition Factor (OTF) SPAS 1535 DAD Zone 2 - September 2003 - Upper Sherando, VA



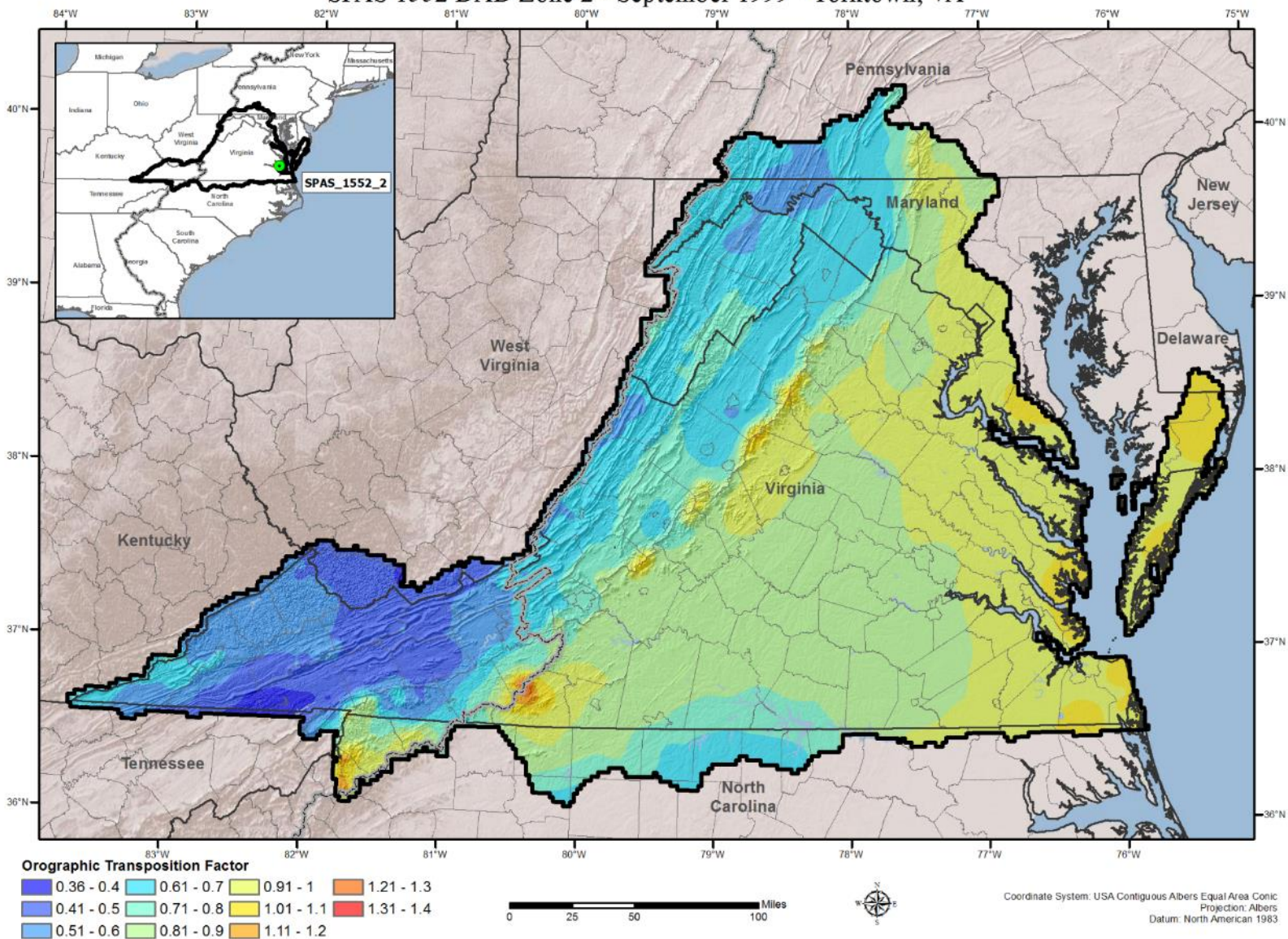
Orographic Transposition Factor (OTF) SPAS 1551 DAD Zone 1 - August 2004 - Richmond, VA



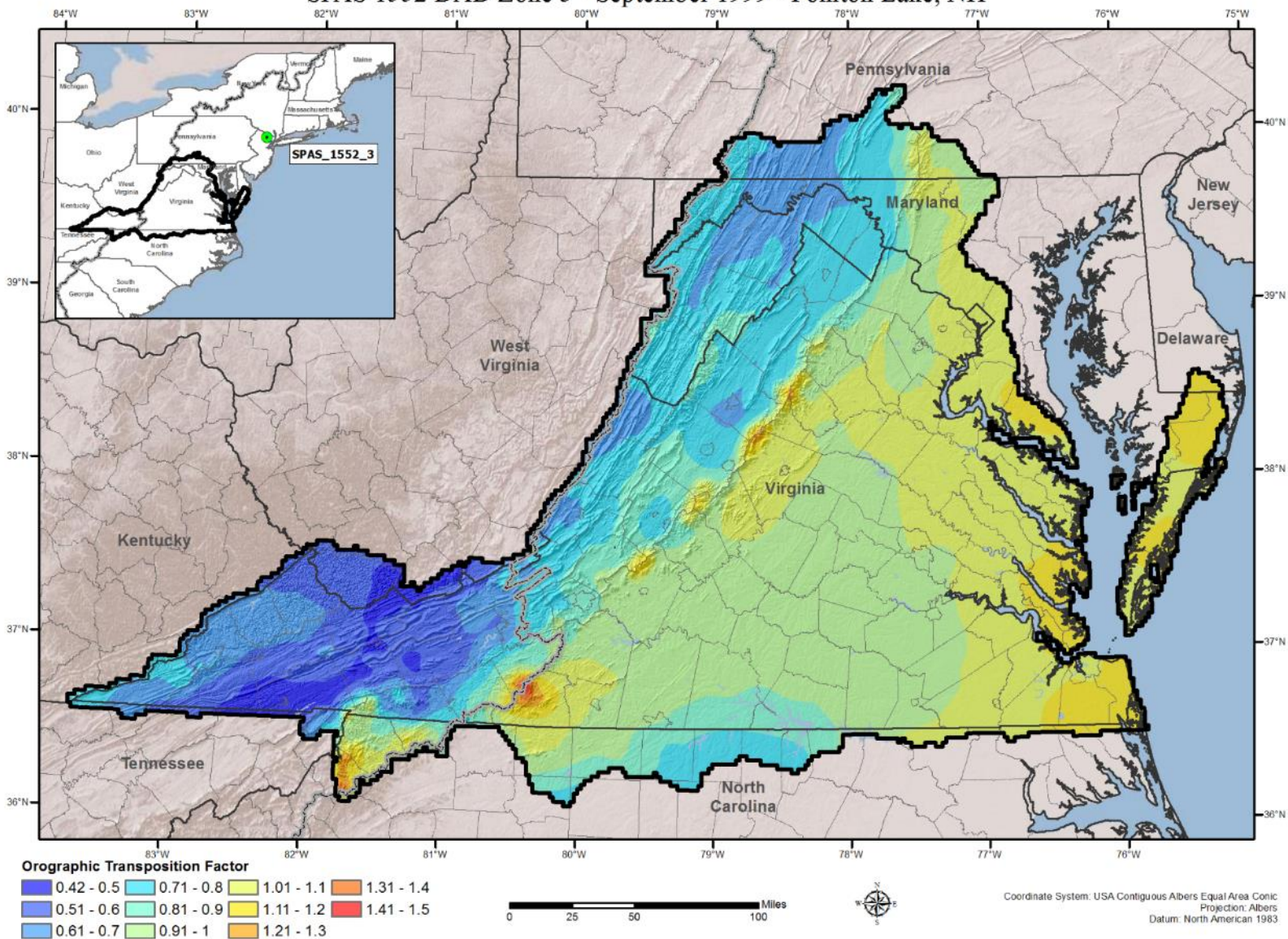
Orographic Transposition Factor (OTF)
 SPAS 1552 DAD Zone 1 - September 1999 - Southport 5 N, NC



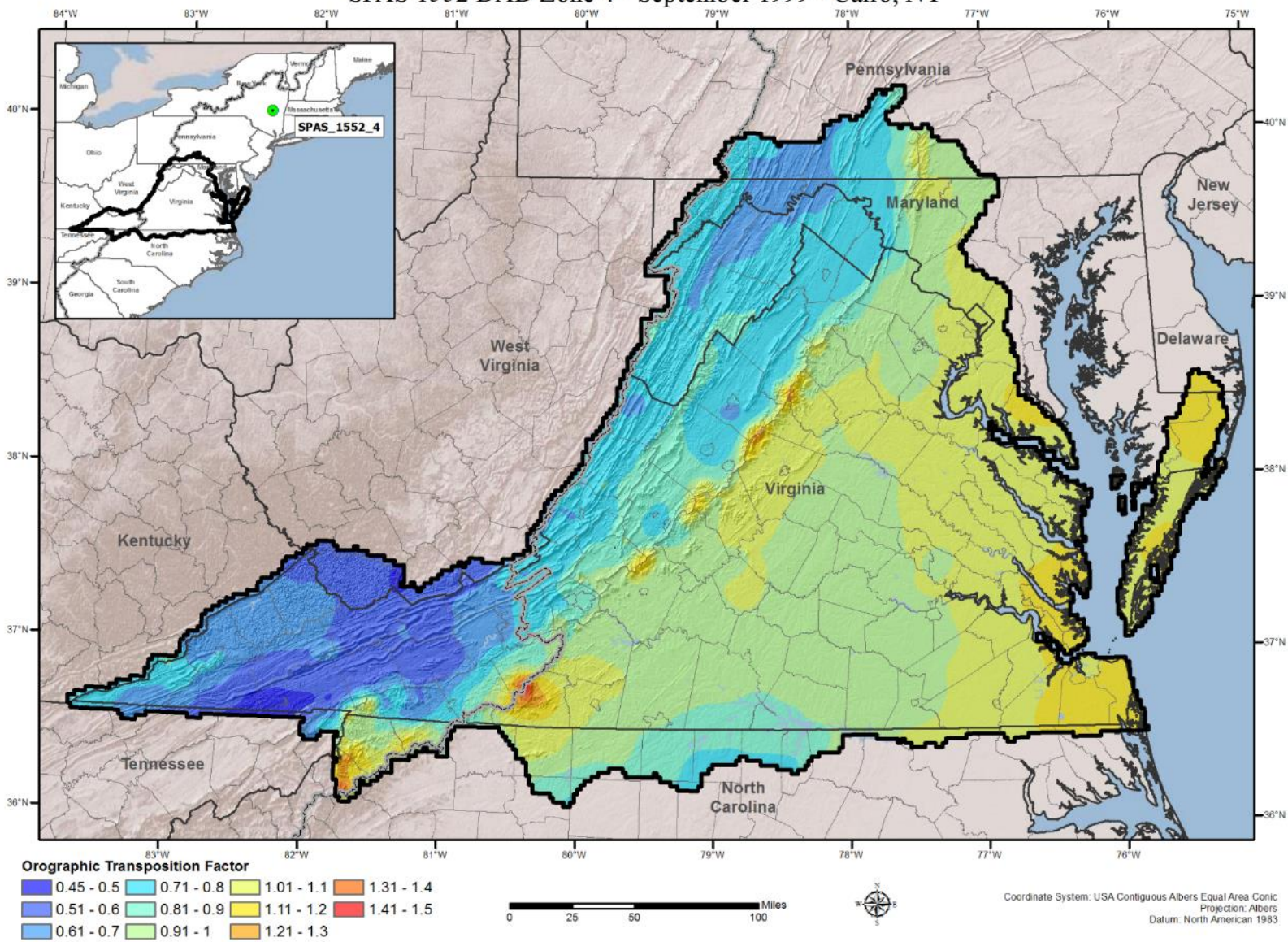
Orographic Transposition Factor (OTF)
 SPAS 1552 DAD Zone 2 - September 1999 - Yorktown, VA



Orographic Transposition Factor (OTF) SPAS 1552 DAD Zone 3 - September 1999 - Pomton Lake, NH



Orographic Transposition Factor (OTF) SPAS 1552 DAD Zone 4 - September 1999 - Cairo, NY



Appendix D

PMP Evaluation Tool Python Script

Name: PMP_Calc.py

Version: 1.00

ArcGIS Version: ArcGIS Desktop 10.2 SP1 (2014)

Author: Applied Weather Associates

Usage: The tool is designed to be executed within an the ArcMap or ArcCatalog desktop environment.

Required Arguments:

- An AOI polygon shapefile or feature class

Description:

This tool calculates PMP depths for a given drainage basin for the specified durations. PMP point values are calculated (in inches) for each grid point (spaced at 90 arc-second intervals) over the project domain. The points are converted to gridded PMP datasets for each duration.

```
----- '''
#####
## import Python modules

import sys
import arcpy
from arcpy import env
import arcpy.management as dm
import arcpy.conversion as con

env.overwriteOutput = True                # Set overwrite option

#####
## get input parameters

basin = arcpy.GetParameter(0)              # get AOI Basin Shapefile
home = arcpy.GetParameterAsText(1)        # get location of 'PMP' Project Folder
outLocation = arcpy.GetParameterAsText(2)
genDurations = arcpy.GetParameter(3)     # get general storm durations (string)
locDurations = arcpy.GetParameter(4)     # get local storm durations (string)
tropDurations = arcpy.GetParameter(5)    # get tropical storm durations (string)

dadGDB = home + "\\Input\\DAD_Tables.gdb" # location of DAD tables
adjFactGDB = home + "\\Input\\Storm_Adj_Factors.gdb" # location of feature datasets
containing total adjustment factors

def pmpAnalysis(aoiBasin, stormType, durList):

#####
## Create PMP Point Feature Class from points within AOI basin and add fields
def createPMPfc():

    arcpy.AddMessage("\nCreating feature class: 'PMP_Points' in Scratch.gdb...")
    dm.MakeFeatureLayer(home + "\\Input\\Non_Storm_Data.gdb\\Vector_Grid", "vgLayer") #
    make a feature layer of vector grid cells
    dm.SelectLayerByLocation("vgLayer", "INTERSECT", aoiBasin) # select the
    vector grid cells that intersect the aoiBasin polygon
```

```

    dm.MakeFeatureLayer(home + "\\Input\Non_Storm_Data.gdb\Grid_Points", "gpLayer")      #
make a feature layer of grid points
    dm.SelectLayerByLocation("gpLayer", "HAVE_THEIR_CENTER_IN", "vgLayer")          #
select the grid points within the vector grid selection
    con.FeatureClassToFeatureClass("gpLayer", env.scratchGDB, "PMP_Points")        # save
feature layer as "PMP_Points" feature class
    arcpy.AddMessage("(" + str(dm.GetCount("gpLayer")) + " grid points will be analyzed)")

# Add PMP Fields
for dur in durList:
    arcpy.AddMessage("\n\t...adding field: PMP_" + str(dur))
    dm.AddField(env.scratchGDB + "\\PMP_Points", "PMP_" + dur, "DOUBLE")

# Add STORM Fields (this string values identifies the driving storm by SPAS ID number)
for dur in durList:
    arcpy.AddMessage("\n\t...adding field: STORM_" + str(dur))
    dm.AddField(env.scratchGDB + "\\PMP_Points", "STORM_" + dur, "TEXT", "", "", 16)

return

#####
## Define getAOIarea() function:
## getAOIarea() calculates the area of AOI (basin outline) input shapefile/
## featureclass. The basin outline shapefile must be projected. The area
## is square miles, converted from the basin layers projected units (feet
## or meters). The aoiBasin feature class should only have a single feature
## (the basin outline). If there are multiple features, the area will be stored
## for the final feature only.

def getAOIarea():
    sr = arcpy.Describe(aoiBasin).SpatialReference      # Determine aoiBasin spatial reference system
    srname = sr.name
    srtype = sr.type
    srunitname = sr.linearUnitName                      # Units
    arcpy.AddMessage("\nAOI Basin Spatial Reference: " + srname + "\nUnit Name: " + srunitname +
"\nSpatial Ref. type: " + srtype)

    aoiArea = 0.0
    rows = arcpy.SearchCursor(aoiBasin)
    for row in rows:
        feat = row.getValue("Shape")
        aoiArea += feat.area
    if srtype == 'Geographic':                          # Must have a surface projection
        arcpy.AddMessage("\nThe basin shapefile's spatial reference '" + srtype + "' is not supported. Please
use a 'Projected' shapefile or feature class.\n")
        raise SystemExit
    elif srtype == 'Projected':
        if srunitname == "Meter":
            aoiArea = aoiArea * 0.000000386102          # Converts square meters to square miles
        elif srunitname == "Foot" or "Foot_US":
            aoiArea = aoiArea * 0.00000003587          # Converts square feet to square miles
        else:
            arcpy.AddMessage("\nThe basin shapefile's unit type '" + srunitname + "' is not supported.")
            sys.exit("Invalid linear units")            # Units must be meters or feet

    aoiArea = round(aoiArea, 3)

```

```

arcpy.AddMessage("\nArea of interest: " + str(aoiArea) + " square miles.")

if arcpy.GetParameter(6) == False:
    aoiArea = arcpy.GetParameter(7) ## Enable a constant area size
    arcpy.AddMessage("\n***Area used for PMP analysis: " + str(aoiArea) + " sqmi***")
    return aoiArea

#####
## Define dadLookup() function:
## The dadLookup() function determines the DAD value for the current storm
## and duration according to the basin area size. The DAD depth is interpolated
## linearly between the two nearest areal values within the DAD table.
def dadLookup(stormLayer, duration, area): ## dadLookup() accepts the current storm layer
name (string), the current duration (string), and AOI area size (float)
    #arcpy.AddMessage("\t\tfunction dadLookup() called.")
    durField = "H_" + duration ## defines the name of the duration field (eg., "H_06" for 6-
hour)
    dadTable = dadGDB + "\\ " + stormLayer
    rows = arcpy.SearchCursor(dadTable)

    try:
        row = rows.next() ## Sets DAD area x1 to the value in the first row of the DAD
table.
        x1 = row.AREASQMI
        y1 = row.getValue(durField)
        xFlag = "FALSE" ## xFlag will remain false for basins that are larger than the
largest DAD area.
    except RuntimeError: ## return if duration does not exist in DAD table
        return

    row = rows.next()
    i = 0
    while row: ## iterates through the DAD table - assigning the bounding values
directly above and below the basin area size
        i += 1
        if row.AREASQMI < area:
            x1 = row.AREASQMI
            y1 = row.getValue(durField)
        else:
            xFlag = "TRUE" ## xFlag is switched to "TRUE" indicating area is within
DAD range
            x2 = row.AREASQMI
            y2 = row.getValue(durField)
            break

        row = rows.next()
    del row, rows, i

    if xFlag == "FALSE":
        x2 = area ## If x2 is equal to the basin area, this means that the largest DAD
area is smaller than the basin and the resulting DAD value must be extrapolated.
        arcpy.AddMessage("\t\tThe basin area size: " + str(area) + " sqmi is greater than the largest DAD
area: " + str(x1) + " sqmi.\n\t\tDAD value is estimated by extrapolation.")
        y = x1 / x2 * y1 ## y (the DAD depth) is estimated by extrapolating the DAD area to
the basin area size.
        return y ## The extrapolated DAD depth (in inches) is returned.

```



```

# arcpy.AddMessage("\nArea = " + str(area) + "\nx1 = " + str(x1) + "\nx2 = " + str(x2) + "\ny1 = " +
str(y1) + "\ny2 = " + str(y2))

x = area                                # If the basin area size is within the DAD table area range, the DAD
depth is interpolated
deltax = x2 - x1                        # to determine the DAD value (y) at area (x) based on next lower
(x1) and next higher (x2) areas.
deltay = y2 - y1
diffx = x - x1

y = y1 + diffx * deltay / deltax

if x < x1:
    arcpy.AddMessage("\t\tThe basin area size: " + str(area) + " sqmi is less than the smallest DAD table
area: " + str(x1) + " sqmi.\n\t\tDAD value is estimated by extrapolation.")

return y                                # The interpolated DAD depth (in inches) is returned.

#####
## Define updatePMP() function:
## This function updates the 'PMP_XX_' and 'STORM_XX' fields of the PMP_Points
## feature class with the largest value from all analyzed storms stored in the
## pmpValues list.
def updatePMP(pmpValues, stormID, duration):                                # Accepts four arguments:
pmpValues - largest adjusted rainfall for current duration (float list); stormID - driver storm ID for each
PMP value (text list); and duration (string)
    pmpfield = "PMP_" + duration
    stormfield = "STORM_" + duration
    gridRows = arcpy.UpdateCursor(env.scratchGDB + "\\PMP_Points")        # iterates
through PMP_Points rows
    i = 0
    for row in gridRows:
        row.setValue(pmpfield, pmpValues[i])                            # Sets the PMP field value equal
to the Max Adj. Rainfall value (if larger than existing value).
        row.setValue(stormfield, stormID[i])                            # Sets the storm ID field to indicate
the driving storm event
        gridRows.updateRow(row)
        i += 1
    del row, gridRows, pmpfield, stormfield
    arcpy.AddMessage("\n\t" + duration + "-hour PMP values update complete. \n")
    return

#####
## The outputPMP() function produces raster GRID files for each of the PMP durations.
## Also, a space-delimited PMP_Distribution.txt file is created in the 'Text_Output' folder.
def outputPMP(type, area, outputPath):

    pmpPoints = env.scratchGDB + "\\PMP_Points"                            # Location of 'PMP_Points' feature class
which will provide data for output
    outType = type[:1]
    outArea = str(int(area)).rjust(5, '0')
    outGDB = "PMP_" + str(int(area)) + ".gdb"                            # Check to see if PMP_XXXXX.gdb
already exists
    if not arcpy.Exists(outPath + "\\" + outGDB):
        arcpy.AddMessage("\nCreating output geodatabase '" + outGDB + "'")

```

```

    dm.CreateFileGDB(outPath, outGDB)
    arcpy.AddMessage("\nCopying PMP_Points feature class to " + outGDB + "...")
    con.FeatureClassToFeatureClass(pmpPoints, outPath + "\\ " + outGDB, type + "_PMP_Points_" +
str(int(area)))

    arcpy.AddMessage("\nBeginning PMP Raster Creation...")

    for dur in durList:                                # This code creates a raster GRID from the current PMP
point layer
        durField = "PMP_" + dur
        outLoc = outPath + outGDB + "\\ " + outType + "_" + dur + "_" + outArea
        arcpy.AddMessage("\n\tInput Path: " + pmpPoints)
        arcpy.AddMessage("\tOutput raster path: " + outPath)
        arcpy.AddMessage("\tField name: " + durField)
        con.FeatureToRaster(pmpPoints, durField, outLoc, "0.025")
        arcpy.AddMessage("\tOutput raster created...")
        del durField, outLoc, dur

    arcpy.AddMessage("\nPMP Raster Creation complete.")

    ##### This section applies the metadata templates to the output GIS files #####
    pointMetaLoc = home + "\\Input\\Metadata_Templates\\PMP_Points_Metadata_FGDC.xml" #
Location of feature class metadata template
    rasMetaLoc = home + "\\Input\\Metadata_Templates\\PMP_Raster_Metadata_FGDC.xml" #
Location of raster file metadata template

    arcpy.AddMessage("\nAdding metadata to output files...")
    ##    arcpy.AddMessage("\n\tPMP_Points feature class")
    ##    con.MetadataImporter(pointMetaLoc, pmpPoints)                                # Applies metadata to
'PMP_Points' feature class
    for dur in durList:                                # Applies metadata to PMP Rasters
        outLoc = outPath + outGDB + "\\ " + outType + "_" + dur + "_" + outArea
        targetPath = outLoc
        con.MetadataImporter(rasMetaLoc, targetPath)
        del dur, outLoc, targetPath
    arcpy.AddMessage("\nOutput metadata import complete.")

    return

#####
## This portion of the code iterates through each storm feature class in the
## 'Storm_Adj_Factors' geodatabase (evaluating the feature class only within
## the Local, Tropical, or general feature dataset). For each duration,
## at each grid point within the aoi basin, the transpositionality is
## confirmed. Then the DAD precip depth is retrieved and applied to the
## total adjustment factor to yield the total adjusted rainfall. This
## value is then sent to the updatePMP() function to update the 'PMP_Points'
## feature class.

##~~~~~
~~~~~##

    desc = arcpy.Describe(basin)                                # Check to ensure AOI input shape is a
Polygon. If not - exit.
    basinShape = desc.shapeType
    if desc.shapeType == "Polygon":

```

```

    arcpy.AddMessage("\nBasin shape type: " + desc.shapeType)
else:
    arcpy.AddMessage("\nBasin shape type: " + desc.shapeType)
    arcpy.AddMessage("\nError: Input shapefile must be a polygon!\n")
    sys.exit()

createPMPfc() # Call the createPMPfc() function to create the
PMP_Points feature class.

env.workspace = adjFactGDB # the workspace environment is set to the
'Storm_Adj_Factors' file geodatabase

aoiSQMI = round(getAOIarea(),2) # Calls the getAOIarea() function to
assign area of AOI shapefile to 'aoiSQMI'

for dur in durList:
    stormList = arcpy.ListFeatureClasses("", "Point", stormType) # List all the total adjustment
factor feature classes within the storm type feature dataset.

arcpy.AddMessage("\n*****\nEvaluating "
+ dur + "-hour duration...")

pmpList = []
driverList = []
gridRows = arcpy.SearchCursor(env.scratchGDB + "\\PMP_Points")
try:
    for row in gridRows:
        pmpList.append(0.0) # creates pmpList of empty float values for
each grid point to store final PMP values
        driverList.append("STORM") # creates driverList of empty text
values for each grid point to store final Driver Storm IDs
    del row, gridRows
except UnboundLocalError:
    arcpy.AddMessage("\n***Error: No data present within basin/AOI area.***\n")
    sys.exit()

for storm in stormList:
    arcpy.AddMessage("\n\tEvaluating storm: " + storm + "...")
    dm.MakeFeatureLayer(storm, "stormLayer") # creates a feature layer for the
current storm
    dm.SelectLayerByLocation("stormLayer", "HAVE_THEIR_CENTER_IN", "vgLayer") # examines
only the grid points that lie within the AOI
    gridRows = arcpy.SearchCursor("stormLayer")
    pmpField = "PMP_" + dur
    i = 0
    try:
        dadPrecip = round(dadLookup(storm, dur, aoiSQMI),3)
        arcpy.AddMessage("\t\t" + dur + "-hour DAD value: " + str(dadPrecip) + chr(34))
    except TypeError: # In no duration exists in the DAD table - move
to the next storm
        arcpy.AddMessage("\t\t***Duration '" + str(dur) + "-hour' is not present for '" + str(storm) +
"'.***\n")
        continue
    arcpy.AddMessage("\t\tComparing " + storm + " adjusted rainfall values against current driver
values...\n")

```

```

    for row in gridRows:
        if row.TRANS == 1:
            # Only continue if grid point is transpositionable ('1'
            is transpositionable, '0' is not).
            try:
                # get total adj. factor if duration exists
                adjRain = round(dadPrecip * row.TAF,1)
                if adjRain > pmpList[i]:
                    pmpList[i] = adjRain
                    driverList[i] = storm
            except RuntimeError:
                arcpy.AddMessage("\t\t *Warning* Total Adjusted Raifnall value falied to set for row " +
str(row.CNT))
                break
            del adjRain
            i += 1
        del row
    del storm, stormList, gridRows, dadPrecip
    updatePMP(pmpList, driverList, dur) # calls function to update "PMP Points" feature class
    del dur, pmpList

    arcpy.AddMessage("\n'PMP_Points' Feature Class 'PMP_XX' fields update complete for all '" +
stormType + "' storms.")

    outputPMP(stormType, aoisQMI, outputPath) # calls outputPMP() function

    del aoisQMI
    return

##~~~~~
~~~~~##

if genDurations:
    type = "General"
    durations = genDurations
    dm.CreateFolder(outLocation, type)
    outputPath = outLocation + "\\General\\"
    arcpy.AddMessage("\nRunning PMP analysis for storm type: " + type)
    pmpAnalysis(basin, type, durations) # Calls the pmpAnalysis() function to calculate the general storm
PMP
    arcpy.AddMessage("\nGeneral Winter storm analysis
complete...\n*****
*****")

if locDurations:
    type = "Local"
    durations = locDurations
    dm.CreateFolder(outLocation, type)
    outputPath = outLocation + "\\Local\\"
    arcpy.AddMessage("\nRunning PMP analysis for storm type: " + type)
    pmpAnalysis(basin, type, durations) # Calls the pmpAnalysis() function to calculate the local storm
PMP
    arcpy.AddMessage("\nLocal storm analysis
complete...\n*****
*****")

if tropDurations:
    type = "Tropical"

```

```

durations = tropDurations
dm.CreateFolder(outLocation, type)
outputPath = outLocation + "\\Tropical\\"
arcpy.AddMessage("\nRunning PMP analysis for storm type: " + type)
pmpAnalysis(basin, type, durations) # Calls the pmpAnalysis() function to calculate the tropical storm
PMP
arcpy.AddMessage("\nTropical storm analysis
complete...\n*****
*****")

```

Appendix E

PMP Version Log: Changes to Storm Database and Adjustment Factors

v.85

- 19 storms included. 7 General, 7 Local, 5 Tropical
- No transposition limits.

v.90

- Added Transposition limits for East or West of the Appalachian Crest. Held storms to side of crest that it occurred.
- Set OTF for SPAS 1345_1 to 1

v.91

- 63 Storms included. 22 General, 19 Local, and 22 Tropical.

v.92

- 68 Storm included. 22 General, 21 Local, and 25 Tropical
- Added Local Storm SPAS 1536_1 (Glennville, WV)
- Added Local Storm SPAS 1546_1 (Little River, VA)
- Created 7 Transposition Zones. 3 west of Appalachian crest and 4 East of crest.
- SPAS 1344_1 – Normalized OTF to Max of 1.00
- SPAS 1345_1 – Normalized OTF to Max of 1.00 – Only allowed Transposable to Zone 4.
- Added Tropical Storm SPAS 1551_1 (Richmond, VA)

General Storms

- Set SPAS 1340_1 to Zone 1, 5, and 6 limited to areas above 1,000 ft elevation.
- Set SPAS 1346_1 to zone 1, 3,4,5,6 limited to areas above 1,000 ft elevation.
- Set SPAS 1357_1 to zone 2 and 3.
- Set SPAS 1380_1 to zone 1, 3,4,5,6 limited to areas over 1,000 ft elevation.
- Set SPAS 1433_1 to zone 2 & 3.
- Set SPAS 1183_1 to Zone 2 & 3.
- SPAS 1305_1 not transposable to Virginia.
- Set SPAS 1435_1 to zone 2 & 3.
- Set SPAS 1430_1 to zone 2 & 3.
- Set SPAS 1311_1 to zone 2 & 3.
- Set SPAS 1195_2 to Zone 1, 5, & 6 above 1,000 ft elevation.
- Set SPAS 1194_1 to zone 1, 5, & 6 limited to areas North of 38° N.
- Set SPAS 1195_1 to zone 1, 5, & 6 limited to areas North of 38° N.
- Set SPAS 1350_1 to zone 6 & 7 with zone 6 limited to below 700 ft.
- Added SPAS 1312A_1. Set to zones 2 & 3
- Set SPAS 1312A_2 to zone 3 & 4.
- Set SPAS 1514_1 to zone 1,5 & 6

- Set SPAS 1431_1 to zone 2 & 3
- Set SPAS 1339_1 to zone 1, 5, & 6

Local Storms

- Set SPAS 1340_1_Loc to zone 1, 5, & 6 limited to areas above 1,000 ft
- Set SPAS 1427_1 to zone 2 & 3
- Set SPAS 1426_1 to zone 2 & 3
- Set SPAS 1376_1 to zone 2 & 3
- Set SPAS 1049_1 to zone 1, 5 & 6 above 1,000 ft
- Set SPAS 1534_1 to zone 6 & 7 limited to areas below 700 ft
- Set SPAS 1429_2 to zone 2 & 3
- Set SPAS 1434_1 to zone 2 & 3
- Set SPAS 1415_1 to zone 6 & 7 below 700 ft
- Set SPAS 1489_1 to zone 6 & 7 below 700 ft
- Set SPAS 1546_1 to zone 1, 5 & 6 limited to areas above 1,000 ft
- Set SPAS 1432_1 to zone 2 & 3
- Set SPAS 1406_1 to Zones 1, 5 & 6 above 1,000 ft or actual location of DAD zone
- Set SPAS 1402_2 to zone 3 & 4
- Set SPAS 1345_1 to zone 4
- Set SPAS 1017_1 to zone 1, 5, & 6
- Set SPAS 1040_1 to zone 1, 5, & 6

Tropical Storms

- Set SPAS 1299_1 to zone 1, 4, 5 & 6 limited to areas above 1,000 ft
- Set SPAS 1490_1 to zone 6 & 7
- Set SPAS 1516_1 to zone 2,3,4,6 & 7
- Added SPAS 1516_2 set to zones 1& 5
- Set SPAS 1299_2 to zone 6 & 7 limited to areas below 1,000 ft
- Set SPAS 1224_1 to zone 1, 5, and 6 limited to areas above 1,000 ft
- Set SPAS 1517_2 to Zones 6 & 7 limited to areas below 1,000 ft
- Added SPAS 1275_2 zone 1, 5, 6, 7
- Set SPAS 1198_2 to zone 1 & 5
- Set SPAS 1342_1 to zone 1, 4, 5, & 6. Zone 1,5,6 above 1000 ft
- Set SPAS 1002_1 to zone 6 & 7 limited to areas below 1,000 ft
- Set SPAS 1198_1 to zone 1, 5 & 6 limited to areas North of 38° N
- Set SPAS 1551_1 set to zone 6 & 7
- Set SPAS 1312B_2 to zone 1,4,5,6. Zones 1,5,6 above 1,000 ft
- Set SPAS 1517_3 to zone 1 & 5
- Set SPAS 1003_1 to zone 1, 5 & 6 limited to areas above 1,000 ft

- Set SPAS 1515_1 to zone 6 & 7 below 700 ft
- Set SPAS 1491_1 to zones 1, 5 & 6 or actual location of DAD zone
- Set SPAS 1006_1 to zone 1, 5 & 6 above 1,000 ft
- Set SPAS 1243_1 to zones 6 & 7
- Set SPAS 1012_2 to zones 6 & 7 below 1000 ft

v.93

- SPAS_1406_1 reduced elevation limit from 1,000 to 500ft
- SPAS_1218_1 removed from Virginia zone 4 but left in for TVA zone 4
- SPAS_1299_1 removed from zone 7, limited zone 5 to below 1,000 ft
- SPAS_1536_1 zone 2, 3 & 4. OTF normalized to a max of 1
- Added SPAS_1550_1. Set to zones 2, 3, and 4
- Replaced SPAS 1002 with SPAS 1552_3 & 4. Same Trans limits
- Replaced SPAS 1012_2 with SPAS 1552_1 & 2. Same Trans limits
- Added SPAS 1535_2 set to zones 1,5 & 6 above 500 ft
- Added SPAS_1373_1. Limited to zone 6
- Added SPAS 1535_1 set to zones 6 & 7
- Set OTF of SPAS 1430_1 to 1. Used target elevation for MTF calculation instead of storm center to match what was done in TVA.
- Added SPAS 1526_1. Set to zones 6 & 7
- Added SPAS 1548_1. Set to zone 4
- Set SPAS 1317_1 to same as TVA south of TSR contour line.
- Added SPAS 1533_1. Set to zones 1, 5 & 6 above 1,000 ft

v.94

- Lowered elevation constraint on 1491_1 to 700 ft
- Manually selected some points in 1406_1 that fell below 500ft in zone 1.
- Reduced OTF of 1534_1. Reclassified range of 1 – 1.5 to 1 – 1.2 in coastal region
- Removed 1198_1 from zone 6
- Removed 1224_1 from zone 7
- Added 1243 to zones 1 & 5
- Set 1299_1 to 1, 4, 5 & 6 above 1,000 ft

v.94a

- Removed elevation constraint for SPAS 1491_1 and set to zones 1, 5, 6 & 7

v.95

- Re-calculated OTF values using NOAA 14 for storms in the NE states that previously used TP 40 data.

v.96

- Limited lower limit of OTF for SPAS 1345 to .50
- Added SPAS 1428_1. Set to zone 2

Appendix F

PMP Storm Data (Separate Binding)

Appendix G

Storm Precipitation Analysis System (SPAS) Description

Table of Contents

Introduction	3
Setup	4
SPAS Analysis Domain	4
SPAS Analysis Time Frame	5
Data	5
Hourly Precipitation Data	6
Daily Precipitation Data	7
Supplemental Precipitation Gauge Data	7
Basemap	8
Radar Data	8
Methodology	11
Daily and Supplemental Precipitation to Hourly	11
Gauge Quality Control	13
Mass Curve Check	13
Gauge Mis-location Check	14
Co-located Gauge QC	14
Spatial Interpolation	15
Basic Approach	15
Basemap Approach	15
Radar Approach	16
Z-R Relationship	16
Radar-aided Hourly Precipitation Grids	18
Radar- and Basemap-Aided Hourly Precipitation Grids	18
SPAS versus Gauge Precipitation	19
Test Cases	22
"Pyramidville" Storm	23
Ritter, Iowa Storm, June 7, 1953	24
Westfield, Massachusetts Storm, August 8, 1955	25
Output	26
Summary	27
References	29

Introduction

The Storm Precipitation Analysis System (SPAS) is grounded on years of scientific research with a demonstrated reliability in hundreds of post-storm precipitation analyses. It has evolved into a trusted hydrometeorological tool that provides accurate precipitation data at a high spatial and temporal resolution for use in a variety of sensitive hydrologic applications (Faulkner et al., 2004, Tomlinson et al., 2003-2012). Applied Weather Associates, LLC and METSTAT, Inc. initially developed SPAS in 2002 for use in producing Depth-Area-Duration values for Probable Maximum Precipitator (PMP) analyses. SPAS utilizes precipitation gauge data, “basemaps” and radar data (when available) to produce gridded precipitation at time intervals as short as 5-minutes, at spatial scales as fine as 1 km² and in a variety of customizable formats. To date (April 2012) SPAS has been used to analyze over 230 storm centers across all types of terrain, among highly varied meteorological settings and some occurring over 100-years ago.

SPAS output has many applications including, but not limited to: hydrologic model calibration/validation, flood event reconstruction, storm water runoff analysis, forensic cases and PMP studies. Detailed SPAS-computed precipitation data allow hydrologists to accurately model runoff from basins, particularly when the precipitation is unevenly distributed over the drainage basin or when rain gauge data is limited or not available. The increased spatial and temporal accuracy of precipitation estimates has eliminated the need for commonly made assumptions about precipitation characteristics (such as uniform precipitation over a watershed), thereby greatly improving the precision and reliability of hydrologic analyses.

In order to instill consistency in SPAS analyses, many of the core methods have remained consistent from beginning. However, SPAS is constantly evolving and improving through new scientific advancements and as new data and improvements are incorporated. This write-up describes the current inter-workings of SPAS, but the reader should realize SPAS can be customized on a case-by-case basis to account for special circumstances; these adaptations are documented and included in the deliverables. The overarching goal of SPAS is to combine the strengths of rain gauge data and radar data (when available) to provide sound, reliable and accurate spatial precipitation data.

Hourly precipitation observations are generally limited to a small number of locations, with many basins lacking observational precipitation data entirely. Meanwhile Next Generation Radar (NEXRAD) data provides valuable spatial and temporal information over data-sparse basins, it has historically lacked reliability for determining precipitation rates and reliable quantitative precipitation estimates (QPE). The improved reliability in SPAS is made possible by hourly calibration of the NEXRAD radar-precipitation relationship, combined with local hourly bias adjustments to force consistency between the final result and “ground truth” precipitation measurements. If NEXRAD radar data is available (generally for storm events since the mid-1990's), precipitation at temporal scales as frequent as 5-minutes is available, otherwise the precipitation data is available hourly. A summary of the general SPAS processes are shown in flow chart in Figure G.1.

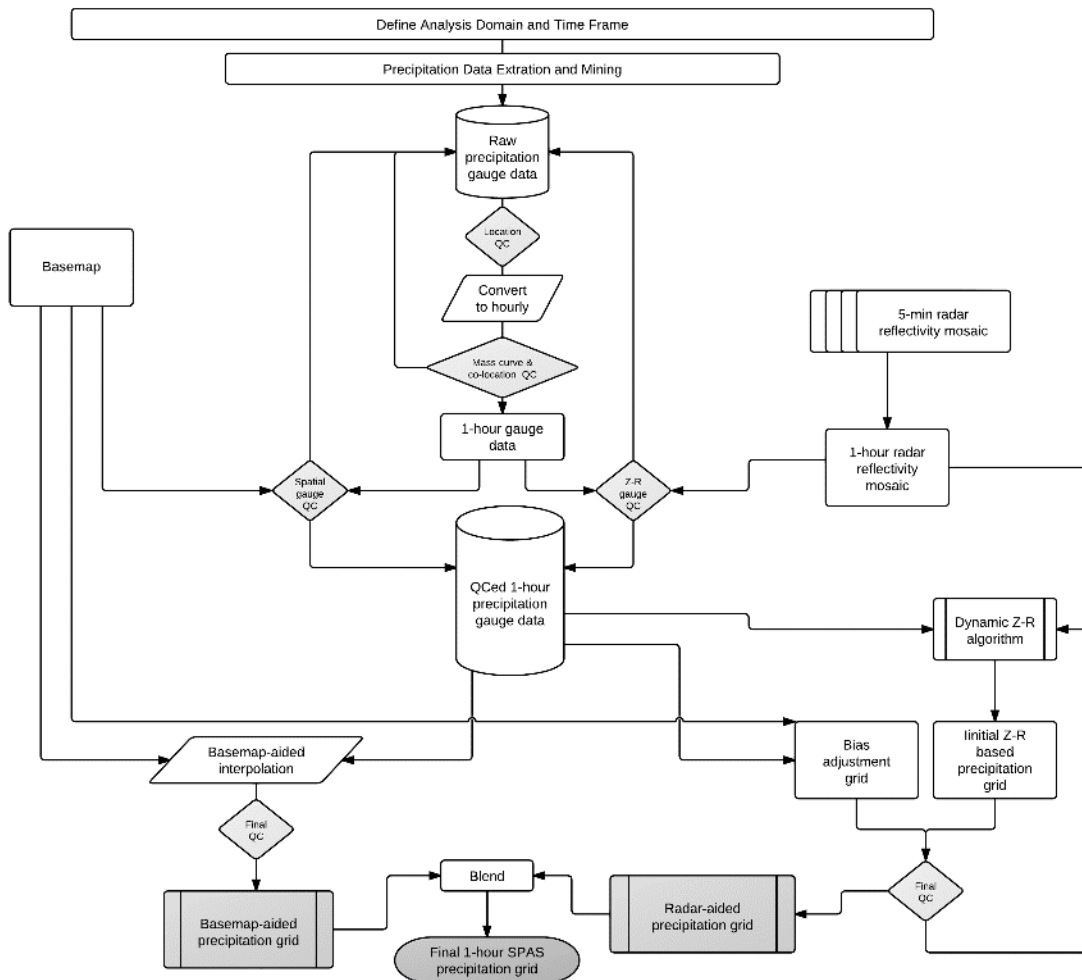


Figure G.1 SPAS flow chart.

Setup

Prior to a SPAS analysis careful definition of the storm analysis domain and time frame to be analyzed is established. Several considerations are made to ensure the domain (longitude-latitude box) and time frame are sufficient for the given application.

SPAS Analysis Domain

For PMP applications it is important to establish an analysis domain that completely encompasses a storm center, meanwhile hydrologic modeling applications are more concerned about a specific basin, watershed or catchment. If radar data is available, then it is also important to establish an area large enough to encompass enough stations (minimum of ~30) to adequately derive reliable radar-precipitation intensity relationships (discussed later). The domain is defined by evaluating existing documentation on the storm as well as plotting and evaluating initial precipitation gauge data on a map. The analysis domain is defined to include as many hourly recording gauges as possible given

their importance in timing. The domain must include enough of a buffer to accurately model the nested domain of interest. The domain is defined as a longitude-latitude (upper left and lower right corner) rectangular region.

SPAS Analysis Time Frame

Ideally, the analysis time frame, also referred to as the Storm Precipitation Period (SPP), will extend from a dry period through the target wet period then back into another dry period. This is to ensure that total storm precipitation amounts can be confidently associated with the storm in question and not contaminated by adjacent wet periods. If this is not possible, a reasonable time period is selected that is bounded by relatively lighter precipitation. The time frame of the hourly data must be sufficient to capture the full range of daily gauge observational periods in order for the daily observations to be disaggregated into estimated incremental hourly values (discussed later). For example, if a daily gauge takes observations at 8:00 AM, then the hourly data must be available from 8:00 AM the day prior. Given the configuration of SPAS, the minimum SPP is 72 hours and aligns midnight to midnight.

The core precipitation period (CPP) is a sub-set of the SPP and represents the time period with the most precipitation and the greatest number of reporting gauges. The CPP represents the time period of interest and where our confidence in the results is highest.

Data

The foundation of a SPAS analysis is the “ground truth” precipitation measurements. In fact, the level of effort involved in “data mining” and quality control represent over half of the total level of effort needed to conduct a complete storm analysis. SPAS operates with three primary data sets: precipitation gauge data, a “basemap” and, if available, radar data. Table G.1 conveys the variety of precipitation gauges usable by SPAS. For each gauge, the following elements are gathered, entered and archived into to SPAS database:

- Station ID
- Station name
- Station type (H=hourly, D=Daily, S=Supplemental, etc.)
- Longitude in decimal degrees
- Latitude in decimal degrees
- Elevation in feet above MSL
- Observed precipitation
- Observation times
- Source
- If unofficial, the measurement equipment and/or method is also noted.

Based on the SPP and analysis domain, hourly and daily precipitation gauge data are extracted from our in-house database as well as the Meteorological Assimilation Data

Ingest System (MADIS). Our in-house database is contains data dating back to the late 1800s, while the MADIS system (described below) contains archived data back to 2002.

Hourly Precipitation Data

Our hourly precipitation database is largely comprised of data from NCDC TD-3240, but also precipitation data from other mesonets and meteorological networks (e.g. ALERT, Flood Control Districts, etc.) that we have collected and archived as part of previous studies. Meanwhile, MADIS provides data from a large number of networks across the U.S., including NOAA’s HADS (Hydrometeorological Automated Data System), numerous mesonets, the Citizen Weather Observers Program (CWOP), departments of transportation, etc. (see http://madis.noaa.gov/mesonet_providers.html for a list of providers). Although our automatic data extraction is fast, cost-effective and efficient, it never captures all of the available precipitation data for a storm event. For this reason, a thorough “data mining” effort is undertaken to acquire all available data from sources such as U.S. Geological Survey (USGS), Remote Automated Weather Stations (RAWS), Community Collaborative Rain, Hail & Snow Network (CoCoRaHS), National Atmospheric Deposition Program (NADP), Clean Air Status and Trends Network (CASTNET), local observer networks, Climate Reference Network (CRN), Global Summary of the Day (GSD) and Soil Climate Analysis Network (SCAN). Unofficial hourly precipitation are gathered to give guidance on either timing or magnitude in areas otherwise void of precipitation data. The WeatherUnderground and MesoWest, two of the largest weather databases on the Internet, contain a good deal of official data, but also unofficial gauges.

Table G.1 Different precipitation gauge types used by SPAS.

Precipitation Gauge Type	Description
Hourly	Hourly gauges with complete, or nearly complete, incremental hourly precipitation data.
Hourly estimated	Hourly gauges with some estimated hourly values, but otherwise reliable.
Hourly pseudo	Hourly gauges with reliable temporal precipitation data, but the magnitude is questionable in relation to co-located daily or supplemental gauge.
Daily	Daily gauge with complete data and known observation times.
Daily estimated	Daily gauges with some or all estimated data.
Supplemental	Gauges with unknown or irregular observation times, but reliable total storm precipitation data. (E.g. public reports, storms reports, “Bucket surveys”, etc.)

Supplemental estimated	Gauges with estimated total storm precipitation values based on other information (e.g. newspaper articles, stream flow discharge, inferences from nearby gauges, pre-existing total storm isohyetal maps, etc.)
-------------------------------	--

Daily Precipitation Data

Our daily database is largely based on NCDC’s TD-3206 (pre-1948) and TD-3200 (1948 through present) as well as SNOTEL data from NRCS. Since the late 1990s, the CoCoRaHS network of more than 15,000 observes in the U.S. has become a very important daily precipitation source. Other daily data is gathered from similar, but smaller gauge networks, for instance the High Spatial Density Precipitation Network in Minnesota.

As part of the daily data extraction process, the time of observation, as indicted in database (if available), accompanies each measured precipitation value. Accurate observation times are necessary for SPAS to disaggregate the daily precipitation into estimated incremental values (discussed later). Knowing the observation time also allows SPAS to maintain precipitation amounts within given time bounds, thereby retaining known precipitation intensities. Given the importance of observation times, efforts are taken to insure the observation times are accurate. Hardcopy reports of “Climatological Data,” scanned observational forms (available on-line) and/or gauge metadata forms have proven to be valuable and accurate resources for validating observation times. Furthermore, erroneous observation times are identified in the mass-curve quality-control procedure (discussed later) and can be corrected at that point in the process.

Supplemental Precipitation Gauge Data

For gauges with unknown or irregular observation times, the gauge is considered a “supplemental” gauge. A supplemental gauge can either be added to the storm database with a storm total and the associated SPP as the temporal bounds or as a gauge with the known, but irregular observation times and associated precipitation amounts. For instance, if all that is known is 3” fell between 0800-0900, then that information can be entered. Gauges or reports with nothing more than a storm total are often abundant, but in order to use them, it is important the precipitation is only from the storm period in question. Therefore, it is ideal to have the analysis time frame bounded by dry periods.

Perhaps the most important source of data, if available, is from “bucket surveys,” which provide comprehensive lists of precipitation measurements collected during a post-storm field exercise. Although some bucket survey amounts are not from conventional precipitation gauges, they provide important information, especially in areas lacking data. Particularly for PMP-storm analysis applications, it is customary to accept extreme, but

valid non-measured precipitation values in order to capture the highest precipitation values.

Basemap

“Basemaps” are independent grids of spatially distributed weather or climate variables that are used to govern the spatial patterns of the hourly precipitation. The basemap also governs the spatial resolution of the final SPAS grids, unless radar data is available/used to govern the spatial resolution. Note that a base map is not required as the hourly precipitation patterns can be based on a station characteristics and an inverse distance weighting technique (discussed later). Basemaps in complex terrain are often based on the PRISM mean monthly precipitation (Figure G.2a) or Hydrometeorological Design Studies Center precipitation frequency grids (Figure G.2b) given they resolve orographic enhancement areas and micro-climates at a spatial resolution of 30-seconds (about 800 m). Basemaps of this nature in flat terrain are not as effective given the small terrain forced precipitation gradients. Therefore, basemaps for SPAS analyses in flat terrain are often developed from pre-existing (hand-drawn) isohyetal patterns (Figure G.2c), composite radar imagery or a blend of both.



Figure G.2 Sample SPAS “basemaps:” (a) A pre-existing (USGS) isohyetal pattern across flat terrain (SPAS #1209), (b) PRISM mean monthly (October) precipitation (SPAS #1192) and (c) A 100-year 24-hour precipitation grid from NOAA Atlas 14 (SPAS #1138).

Radar Data

For storms occurring since approximately the mid-1990's, weather radar data is available to supplement the SPAS analysis. A fundamental requirement for high quality radar-estimated precipitation is a high quality radar mosaic, which is a seamless collection of concurrent weather radar data from individual radar sites, however in some cases a single radar is sufficient (i.e. for a small area size storm event such as a thunderstorm). Weather radar data has been in use by meteorologists since the 1960's to estimate precipitation depths, but it was not until the early 1990's that new, more accurate NEXRAD Doppler radar (WSR88D) was placed into service across the United States. Currently efforts are underway to convert the WSR88D radars to dual polarization (DualPol) radar. Today, NEXRAD radar coverage of the contiguous United States is comprised of 159 operational sites and 30 in Canada. Each U.S. radar covers an approximate 285 mile (460

km) radial extent and while Canadian radars have approximately 256 km (138 nautical miles) radial extent over which the radar can detect precipitation. (see Figure G.3) The primary vendor of NEXRAD weather radar data for SPAS is Weather Decision Technologies, Inc. (WDT), who accesses, mosaics, archives and quality-controls NEXRAD radar data from NOAA and Environment Canada. SPAS utilizes Level II NEXRAD radar reflectivity data in units of dBZ, available every 5-minutes in the U.S. and 10-minutes in Canada.

NEXRAD Coverage Below 10,000 Feet AGL

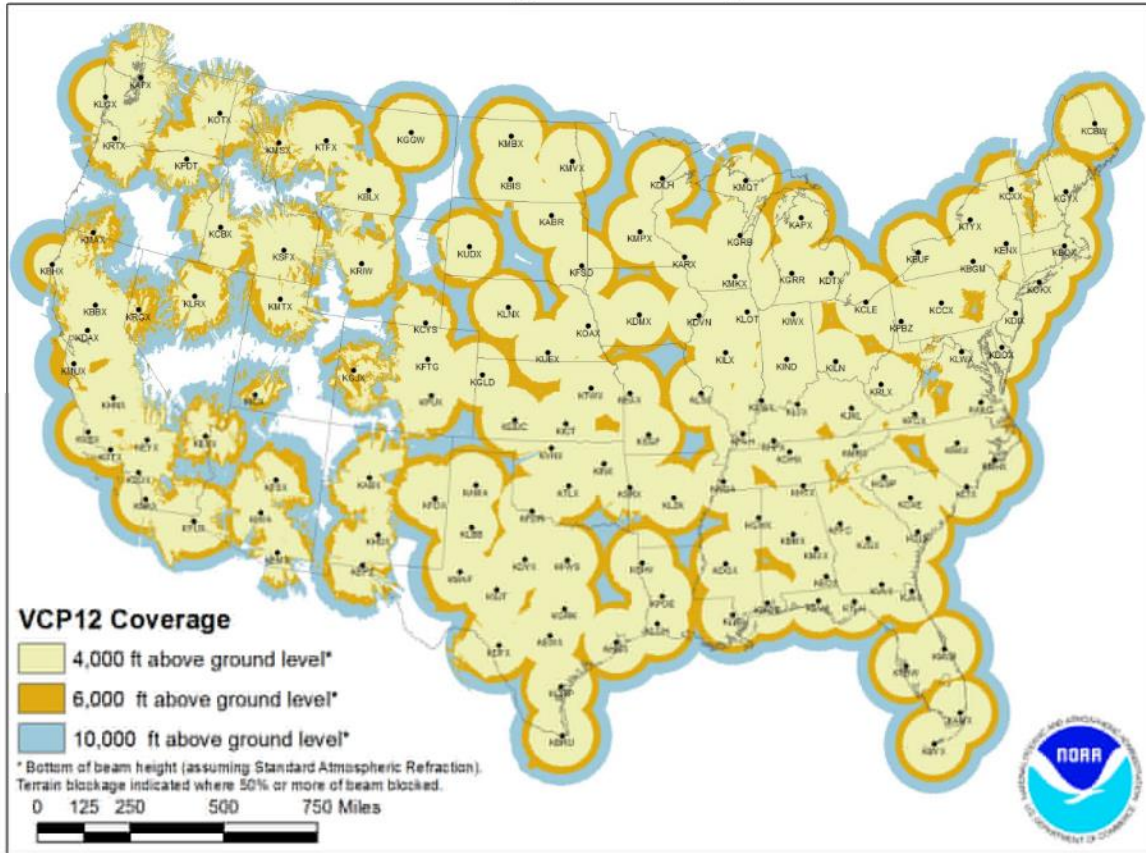
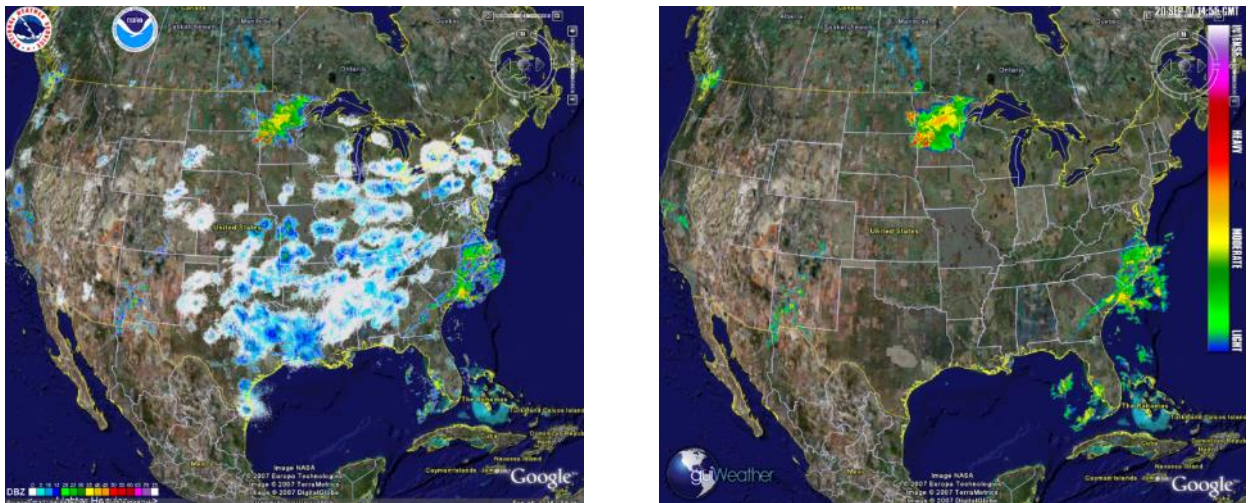


Figure G.3 U.S. radar locations and their radial extents of coverage below 10,000 feet above ground level (AGL). Each U.S. radar covers an approximate 285 mile radial extent over which the radar can detect precipitation.

The WDT and National Severe Storms Lab (NSSL) Radar Data Quality Control Algorithm (RDQC) removes non-precipitation artifacts from base Level-II radar data and remaps the data from polar coordinates to a Cartesian (latitude/longitude) grid. Non-precipitation artifacts include ground clutter, bright banding, sea clutter, anomalous propagation, sun strobes, clear air returns, chaff, biological targets, electronic interference and hardware test patterns. The RDQC algorithm uses sophisticated data processing and a Quality Control Neural Network (QCNN) to delineate the precipitation echoes caused by

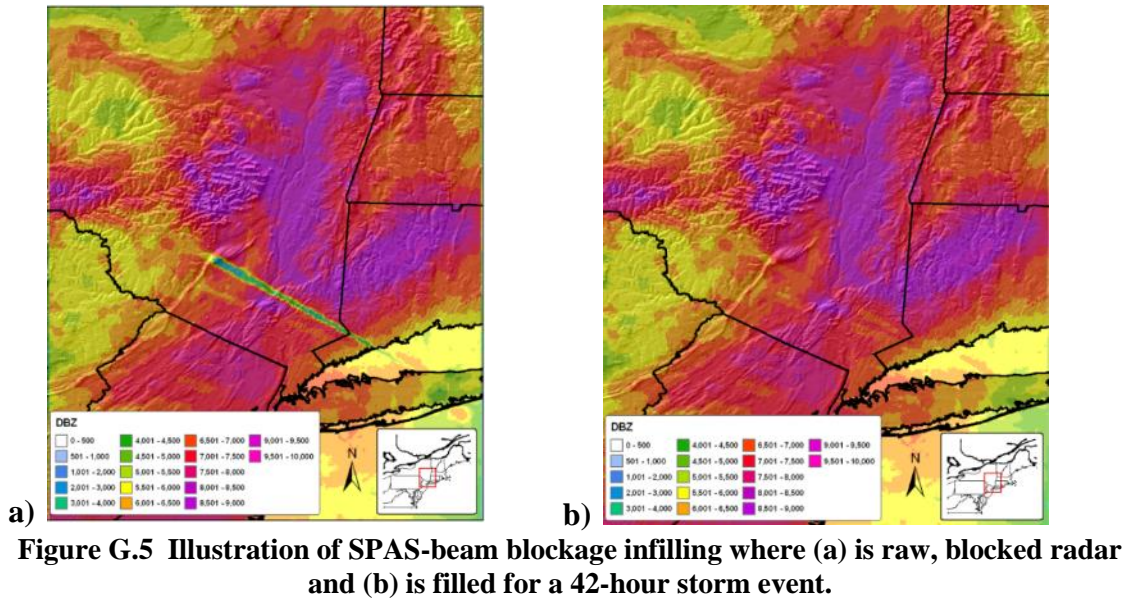
radar artifacts (Lakshmanan and Valente 2004). Beam blockages due to terrain are mitigated by using 30 meter DEM data to compute and then discard data from a radar beam that clears the ground by less than 50 meters and incurs more than 50% power blockage. A clear-air echo removal scheme is applied to radars in clear-air mode when there is no precipitation reported from observation gauges within the vicinity of the radar. In areas of radar coverage overlap, a distance weighting scheme is applied to assign reflectivity to each grid cell, for multiple vertical levels. This scheme is applied to data from the nearest radar that is unblocked by terrain.

Once the data from individual radars have passed through the RDQC, they are merged to create a seamless mosaic for the United States and southern Canada as shown in Figure G.4. A multi-sensor quality control can be applied by post-processing the mosaic to remove any remaining “false echoes”. This technique uses observations of infra-red cloud top temperatures by GOES satellite and surface temperature to create a precipitation/no-precipitation mask. Figure G.4 shows the impact of WDT’s quality control measures. Upon completing all QC, WDT converts the radar data from its native polar coordinate projection (1 degree x 1.0 km) into a longitude-latitude Cartesian grid (based on the WGS84 datum), at a spatial resolution of $\sim 1/3^{\text{rd}}$ -square mile for processing in SPAS.



a) **b)**
Figure G.4 (a) Level-II radar mosaic of CONUS radar with no quality control, (b) WDT quality controlled Level-II radar mosaic.

SPAS conducts further QC on the radar mosaic by infilling areas contaminated by beam blockages. Beam blocked areas are objectively determined by evaluating total storm reflectivity grid which naturally amplifies areas of the SPAS analysis domain suffering from beam blockage as shown in Figure G.5.



Methodology

Daily and Supplemental Precipitation to Hourly

To obtain one hour temporal resolutions and utilize all gauge data, it is necessary to disaggregate the daily and supplemental precipitation observations into estimated hourly amounts. This process has traditionally been accomplished by distributing (temporally) the precipitation at each daily/supplemental gauge in accordance to a single nearby hourly gauge (Thiessen polygon approach). However, this may introduce biases and not correctly represent hourly precipitation at daily/supplemental gauges situated in-between hourly gauges. Instead, SPAS uses a spatial approach by which the estimated hourly precipitation at each daily and supplemental gauge is governed by a distance weighted algorithm of all nearby true hourly gauges.

In order to disaggregate (i.e. distribute) daily/supplemental gauge data into estimate hourly values, the true hourly gauge data is first evaluated and quality controlled using synoptic maps, nearby gauges, orographic effects, gauge history and other documentation on the storm. Any problems with the hourly data are resolved, and when possible/necessary accumulated hourly values are distributed. If an hourly value is missing, the analyst can choose to either estimate it or leave it missing for SPAS to estimate later based on nearby hourly gauges. At this point in the process, pseudo (hourly) gauges can be added to represent precipitation timing in topographically complex locations, areas with limited/no hourly data or to capture localized convection. In order to adequately capture the temporal variations of the precipitation a pseudo hourly gauge is sometimes necessary. A pseudo gauge is created by distributing the precipitation at a co-located daily gauge or by creating a completely new pseudo gauge from other information such as inferences from COOP observation forms, METAR visibility data (if hourly precipitation isn't already available), lightning data, satellite

data, or radar data. Often radar data is the best/only choice for creating pseudo hourly gauges, but this is done cautiously given the potential differences (over-shooting of the radar beam equating to erroneous precipitation) between radar data and precipitation. In any case, the pseudo hourly gauge is flagged so SPAS only uses it for timing and not magnitude. Care is taken to ensure hourly pseudo gauges represent justifiably important physical and meteorological characteristics before being incorporated into the SPAS database. Although pseudo gauges provide a very important role, their use is kept to a minimum. The importance of insuring the reliability of every hourly gauge cannot be over emphasized. All of the final hourly gauge data, including pseudos, are included in the hourly SPAS precipitation database.

Using the hourly SPAS precipitation database, each hourly precipitation value is converted into a percentage that represents the incremental hourly precipitation divided by the total SPP precipitation. The GIS-ready x-y-z file is constructed for each hour that contains the latitude (x), longitude(y) and percent of precipitation (z) for a particular hour. Using the GRASS GIS, an inverse-distance-weighting squared (IDW) interpolation technique is applied to each of the hourly files. The result is a continuous grid with percentage values for the entire analysis domain, keeping the grid cells on which the hourly gauge resides faithful to the observed/actual percentage. Since the percentages typically have a high degree of spatial autocorrelation, the spatial interpolation has skill in determining the percentages between gauges, especially since the percentages are somewhat independent of the precipitation magnitude. The end result is a GIS grid for each hour that represents the percentage of the SPP precipitation that fell during that hour.

After the hourly percentage grids are generated and QC'd for the entire SPP, a program is executed that converts the daily/supplemental gauge data into incremental hourly data. The timing at each of the daily/supplemental gauges is based on (1) the daily/supplemental gauge observation time, (2) daily/supplemental precipitation amount and (3) the series of interpolated hourly percentages extracted from grids (described above).

This procedure is detailed in Figure G.6 below. In this example, a supplemental gauge reported 1.40" of precipitation during the storm event and is located equal distance from the three surrounding hourly recording gauges. The procedure steps are:

- Step 1. For each hour, extract the percent of SPP from the hourly gauge-based percentage at the location of the daily/supplemental gauge. In this example, assume these values are the average of all the hourly gauges.
- Step 2. Multiply the individual hourly percentages by the total storm precipitation at the daily/supplemental gauge to arrive at estimated hourly precipitation at the daily/supplemental gauge. To make the daily/supplemental accumulated precipitation data faithful to the daily/supplemental observations, it is sometimes necessary to adjust the hourly percentages so they add up to 100% and account for 100% of the daily observed precipitation.

	Hour						
Precipitation	1	2	3	4	5	6	Total
Hourly station 1	0.02	0.12	0.42	0.50	0.10	0.00	1.16
Hourly station 2	0.01	0.15	0.48	0.62	0.05	0.01	1.32
Hourly station 3	0.00	0.18	0.38	0.55	0.20	0.05	1.36
	Hour						
Percent of total storm precip.	1	2	3	4	5	6	Total
Hourly station 1	2%	10%	36%	43%	9%	0%	100%
Hourly station 2	1%	11%	36%	47%	4%	1%	100%
Hourly station 3	0%	13%	28%	40%	15%	4%	100%
<i>Average</i>	1%	12%	34%	44%	9%	1%	100%
Storm total precipitation at daily gauge				1.40			
	Hour						
Precipitation (estimated)	1	2	3	4	5	6	Total
Daily station	0.01	0.16	0.47	0.61	0.13	0.02	1.40

Figure G.6 Example of disaggregation of daily precipitation into estimated hourly precipitation based on three (3) surrounding hourly recording gauges.

In cases where the hourly grids do not indicate any precipitation falling during the daily/supplemental gauge observational period, yet the daily/supplemental gauge reported precipitation, the daily/supplemental total precipitation is evenly distributed throughout the hours that make up the observational period; although this does not happen very often, this solution is consistent with NWS procedures. However, the SPAS analyst is notified of these cases in a comprehensive log file, and in most cases they are resolvable, sometimes with a pseudo hourly gauge.

Gauge Quality Control

Exhaustive quality control measures are taken throughout the SPAS analysis. Below are a few of the most significant QC measures taken.

Mass Curve Check

A mass curve-based QC-methodology is used to ensure the timing of precipitation at all gauges is consistent with nearby gauges. SPAS groups each gauge with the nearest four gauges (regardless of type) into a single file. These files are subsequently used in software for graphing and evaluation. Unusual characteristics in the mass curve are investigated and the gauge data corrected, if possible and warranted. See Figure G.7 for an example.

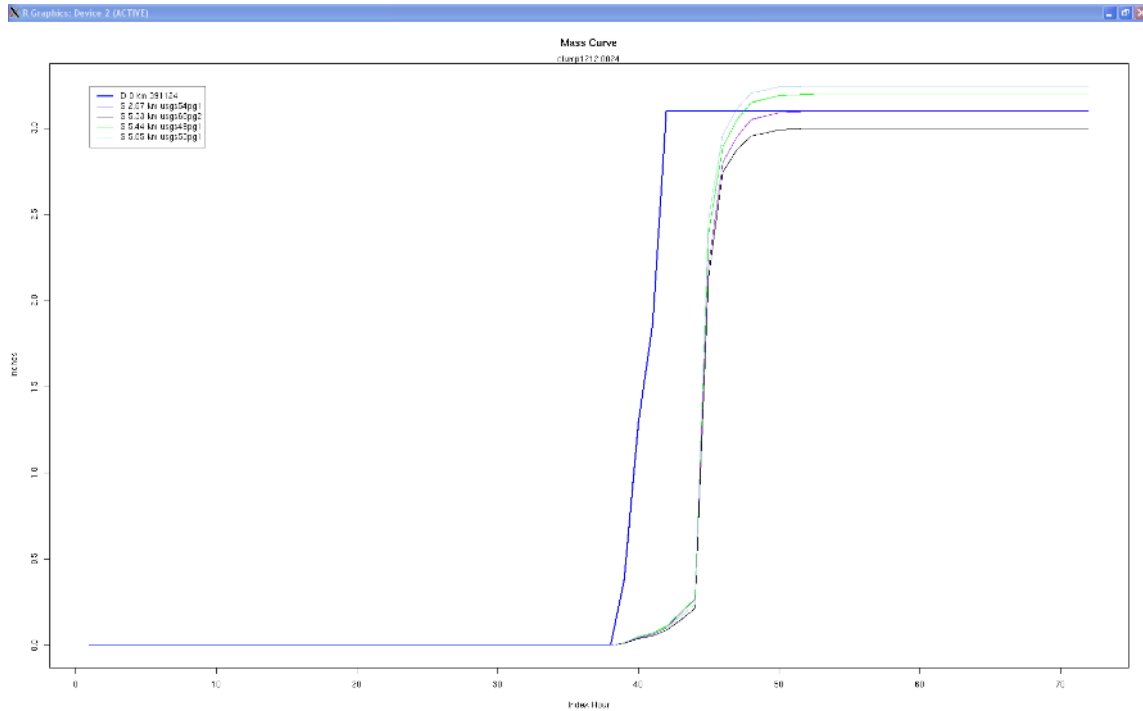


Figure G.7 Sample mass curve plot depicting a precipitation gauge with an erroneous observation time (blue line). X-axis is the SPAS index hour and the y-axis is inches. The statistics in the upper left denote gauge type, distance from target gauge (in km), and gauge ID. In this example, the center gauge (blue line) was found to have an observation error/shift of 1 day.

Gauge Mis-location Check

Although the gauge elevation is not explicitly used in SPAS, it is however used as a means of QCing gauge location. Gauge elevations are compared to a high-resolution 15-second DEM to identify gauges with large differences, which may indicate erroneous longitude and/or latitude values.

Co-located Gauge QC

Care is also taken to establish the most accurate precipitation depths at all co-located gauges. In general, where a co-located gauge pair exists, the highest precipitation is accepted (if accurate). If the hourly gauge reports higher precipitation, then the co-located daily (or supplemental) is removed from the analysis since it would not add anything to the analysis. Often daily (or supplemental) gauges report greater precipitation than a co-located hourly station since hourly tipping bucket gauges tend to suffer from gauge under-catch, particularly during extreme events, due to loss of precipitation during tips. In these cases the daily/supplemental is retained for the magnitude and the hourly used as a pseudo hourly gauge for timing. Large discrepancies between any co-located gauges are investigated and resolved since SPAS can only utilize a single gauge magnitude at each co-located site.

Spatial Interpolation

At this point the QC'd observed hourly and disaggregated daily/supplemental hourly precipitation data are spatially interpolated into hourly precipitation grids. SPAS has three options for conducting the hourly precipitation interpolation, depending on the terrain and availability of radar data, thereby allowing SPAS to be optimized for any particular storm type or location. Figure G.8 depicts the results of each spatial interpolation methodology based on the same precipitation gauge data.

Figure G.8 Depictions of total storm precipitation based on the three SPAS interpolation methodologies for a storm (SPAS #1177, Vanguard, Canada) across flat terrain: (a) no basemap, (b) basemap-aided and (3) radar.

Basic Approach

The basic approach interpolates the hourly precipitation point values to a grid using an inverse distance weighting squared GIS algorithm. This is sometimes the best choice for convective storms over flat terrain when radar data is not available, yet high gauge density instills reliable precipitation patterns. This approach is rarely used.

Basemap Approach

Another option includes the use of a “basemap”, also known as a climatologically-aided interpolation (Hunter 2005). As noted before, the spatial patterns of the basemap govern the interpolation between points of hourly precipitation estimates, while the actual hourly precipitation values govern the magnitude. This approach to interpolating point data across complex terrain is widely used. In fact, it was used extensively by the NWS during their storm analysis era from the 1940s through the 1970s.

In application, the hourly precipitation gauge values are first normalized by the corresponding grid cell value of the basemap before being interpolated. The normalization allows information and knowledge from the basemap to be transferred to the spatial distribution of the hourly precipitation. Using an IDW squared algorithm, the normalized hourly precipitation values are interpolated to a grid. The resulting grid is then multiplied by the basemap grid to produce the hourly precipitation grid. This is repeated each hour of the storm.

Radar Approach

The coupling of SPAS with NEXRAD provides the most accurate method of spatially and temporally distributing precipitation. To increase the accuracy of the results however, quality-controlled precipitation observations are used for calibrating the radar reflectivity to rain rate relationship (Z-R relationship) each hour instead of assuming a default Z-R relationship. Also, spatial variability in the Z-R relationship is accounted for through local bias corrections (described later). The radar approach involves several steps, each briefly described below. The radar approach cannot operate alone – either the basic or basemap approach must be completed before radar data can be incorporated.

Z-R Relationship

SPAS derives high quality precipitation estimates by relating quality controlled level-II NEXRAD radar reflectivity radar data with quality-controlled precipitation gauge data in order to calibrate the Z-R (radar reflectivity, Z, and precipitation, R) relationship. Optimizing the Z-R relationship is essential for capturing temporal changes in the Z-R. Most current radar-derived precipitation techniques rely on a constant relationship between radar reflectivity and precipitation rate for a given storm type (e.g. tropical, convective), vertical structure of reflectivity and/or reflectivity magnitudes. This non-linear relationship is described by the Z-R equation below:

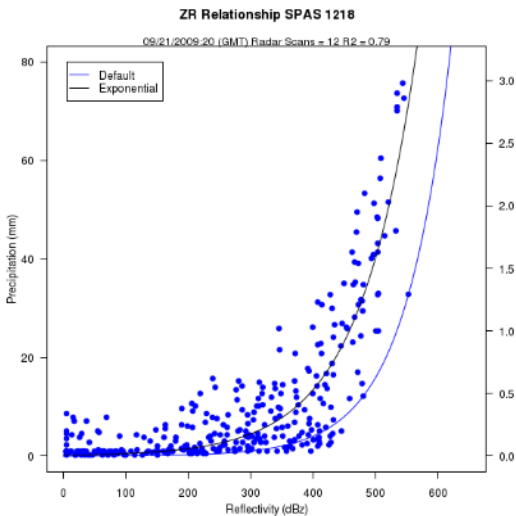


Figure G.9 Example SPAS (denoted as “Exponential”) vs. default Z-R relationship (SPAS #1218, Georgia September 2009).

$$Z = A R^b \quad (1)$$

Where Z is the radar reflectivity (measured in units of dBZ), R is the precipitation (precipitation) rate (millimeters per hour), A is the “multiplicative coefficient” and b is the “power coefficient”. Both A and b are directly related to the rain drop size distribution (DSD) and rain drop number distribution (DND) within a cloud (Martner and Dubovskiy 2005). The variability in the results of Z versus R is a direct result of differing DSD, DND and air mass characteristics (Dickens 2003). The DSD and DND are determined by complex interactions of microphysical processes that fluctuate regionally, seasonally, daily, hourly, and even within the same cloud. For these reasons, SPAS calculates an optimized Z-R relationship across the analysis domain each

hour based on observed precipitation rates and radar reflectivity (see Figure G.9).

The National Weather Service (NWS) utilizes different default Z-R algorithms, depending on the precipitation-causing event, to estimate precipitation through the use of NEXRAD radar reflectivity data across the United States (see Figure G.10) (Baeck and

Smith 1998 and Hunter 1999). A default Z-R relationship of $Z = 300R^{1.4}$ is the primary algorithm used throughout the continental U.S. However, it is widely known that this, compared to unadjusted radar-aided estimates of precipitation, suffers from deficiencies that may lead to significant over or under-estimation of precipitation.

RELATIONSHIP	Optimum for:	Also recommended for:
Marshall-Palmer ($z=200R^{1.6}$)	General stratiform precipitation	
East-Cool Stratiform ($z=130R^{2.0}$)	Winter stratiform precipitation - east of continental divide	Orographic rain - East
West-Cool Stratiform ($z=75R^{2.0}$)	Winter stratiform precipitation - west of continental divide	Orographic rain - West
WSR-88D Convective ($z=300R^{1.4}$)	Summer deep convection	Other non-tropical convection
Rosenfeld Tropical ($z=250R^{1.2}$)	Tropical convective systems	

Figure G.10 Commonly used Z-R algorithms used by the NWS.

Instead of adopting a standard Z-R, SPAS utilizes a least squares fit procedure for optimizing the Z-R relationship each hour of the SPP. The process begins by determining if sufficient (minimum 12) observed hourly precipitation and radar data pairs are available to compute a reliable Z-R. If insufficient (<12) gauge pairs are available, then SPAS adopts the previous hour Z-R relationship, if available, or applies a user-defined default Z-R algorithm from Figure G.10. If sufficient data are available, the one hour sum of NEXRAD reflectivity (Z) is related to the 1-hour precipitation at each gauge. A least-squares-fit exponential function using the data points is computed. The resulting best-fit, one hour-based Z-R is subjected to several tests to determine if the Z-R relationship and its resulting precipitation rates are within a certain tolerance based on the R-squared fit measure and difference between the derived and default Z-R precipitation results. Experience has shown the actual Z-R versus the default Z-R can be significantly different (Figure G.11).

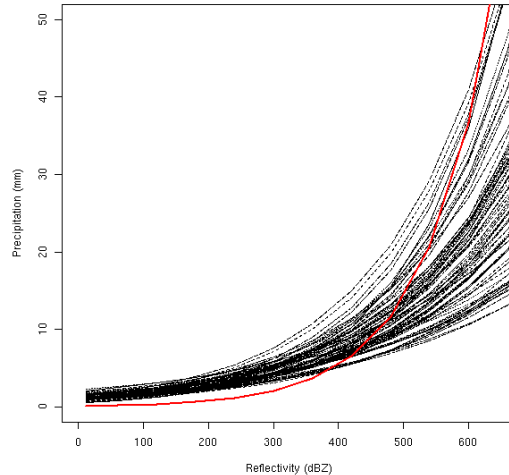


Figure G.11 Comparison of the SPAS optimized hourly Z-R relationships (black lines) versus a default $Z=75R^{2.0}$ Z-R relationship (red line) for a period of 99 hours for a storm over southern California.

Radar-aided Hourly Precipitation Grids

Once a mathematically optimized hourly Z-R relationship is determined, it is applied to the total hourly Z grid to compute an initial precipitation rate (inches/hour) at each grid cell. To account for spatial differences in the Z-R relationship, SPAS computes residuals, the difference between the initial precipitation analysis (via the Z-R equation) and the actual “ground truth” precipitation (observed – initial analysis), at each gauge. The point residuals, also referred to as local biases, are normalized and interpolated to a residual grid using an inverse distance squared weighting algorithm. A radar-based hourly precipitation grid is created by adding the residual grid to the initial grid; this allows the precipitation at the grid cells for which gauges are “on” to be true and faithful to the gauge measurement. The pre-final radar-aided precipitation grid is subject to some final, visual QC checks to ensure the precipitation patterns are consistent with the terrain; these checks are particularly important in areas of complex terrain where even QC’d radar data can be unreliable. The next incremental improvement with SPAS program will come as the NEXRAD radar sites are upgraded to dual-polarimetric capability.

Radar- and Basemap-Aided Hourly Precipitation Grids

At this stage of the radar approach, a radar- and basemap-aided hourly precipitation grid exists for each hour. At locations with precipitation gauges, the grids are equal, however elsewhere the grids can vary for a number of reasons. For instance, the basemap-aided hourly precipitation grid may depict heavy precipitation in an area of complex terrain, blocked by the radar, whereas the radar-aided hourly precipitation grid may suggest little, if any, precipitation fell in the same area. Similarly, the radar-aided hourly precipitation grid may depict an area of heavy precipitation in flat terrain that the basemap-approach missed since the area of heavy precipitation occurred in an area without gauges. SPAS uses an algorithm to compute the hourly precipitation at each pixel given the two results. Areas that are completely blocked from a radar signal are accounted for with the

basemap-aided results (discussed earlier). The precipitation in areas with orographically effective terrain and reliable radar data are governed by a blend of the basemap- and radar-aided precipitation. Elsewhere, the radar-aided precipitation is used exclusively. This blended approach has proven effective for resolving precipitation in complex terrain, yet retaining accurate radar-aided precipitation across areas where radar data is reliable. Figure G.12 illustrates the evolution of final precipitation from radar reflectivity in an area of complex terrain in southern California.

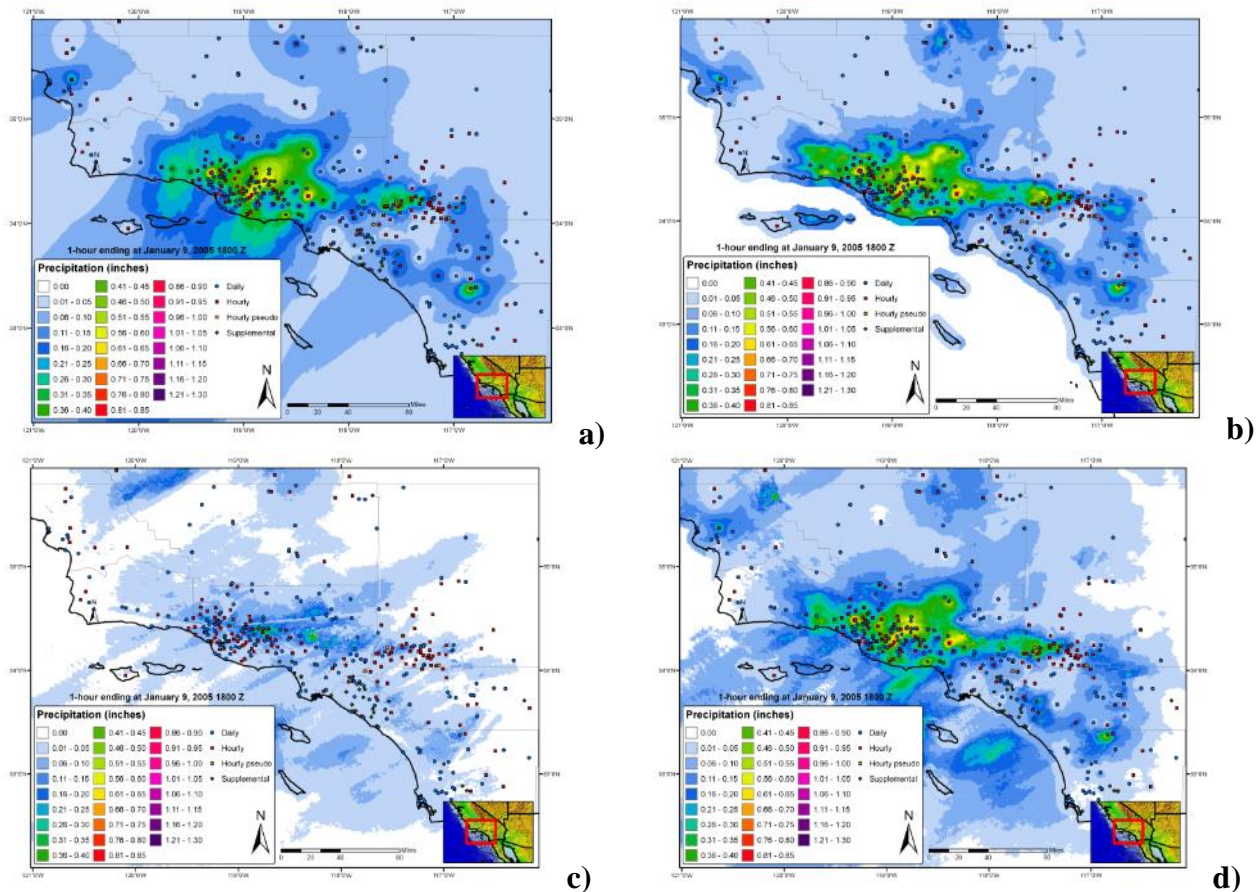


Figure G.12 A series of maps depicting 1-hour of precipitation utilizing (a) inverse distance weighting of gauge precipitation, (b) gauge data together with a climatologically-aided interpolation scheme, (c) default Z-R radar-estimated interpolation (no gauge correction) and (d) SPAS precipitation for a January 2005 storm in southern California, USA.

SPAS versus Gauge Precipitation

Performance measures are computed and evaluated each hour to detect errors and inconsistencies in the analysis. The measures include: hourly Z-R coefficients, observed hourly maximum precipitation, maximum gridded precipitation, hourly bias, hourly mean absolute error (MAE), root mean square error (RMSE), and hourly coefficient of determination (r^2).

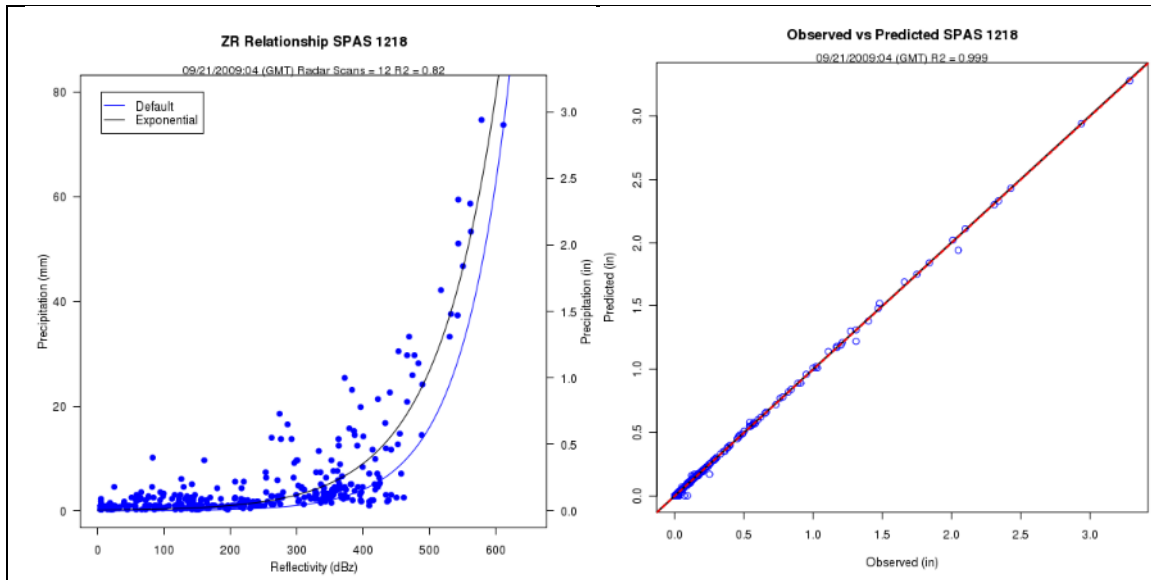


Figure G.13 Z-R plot (a), where the blue line is the SPAS derived Z-R and the black line is the default Z-R, and the (b) associated observed versus SPAS scatter plot at gauge locations.

Comparing SPAS-calculated precipitation (R_{spas}) to observed point precipitation depths at the gauge locations provides an objective measure of the consistency, accuracy and bias. Generally speaking SPAS is usually within 5% of the observed precipitation (see Figure G.13). Less-than-perfect correlations between SPAS precipitation depths and observed precipitation at gauged locations could be the result of any number of issues, including:

- **Point versus area:** A rain gauge observation represents a much smaller area than the area sampled by the radar. The area that the radar is sampling is approximately 1 km^2 , whereas a rain gauge only samples approximately $8.0 \times 10^{-9} \text{ km}^2$. Furthermore, the radar data represents an average reflectivity (Z) over the grid cell, when in fact the reflectivity can vary across the 1 km^2 grid cell. Therefore, comparing a grid cell radar derived precipitation value to a gauge (point) precipitation depth measured may vary.
- **Precipitation gauge under-catch:** Although we consider gauge data “ground truth,” we recognize gauges themselves suffer from inaccuracies. Precipitation gauges, shielded and unshielded, inherently underestimate total precipitation due to local airflow, wind under-catch, wetting, and evaporation. The wind under-catch errors are usually around 5% but can be as large as 40% in high winds (Guo et al., 2001, Duchon and Essenberg 2001, Ciach 2003, Tokay et al., 2010). Tipping buckets miss a small amount of precipitation during each tip of the bucket due to the bucket travel and tip time. As precipitation intensities increase, the volumetric loss of precipitation due to tipping tends to increase. Smaller tipping buckets can have higher volumetric losses due to higher tip frequencies, but on the other hand capture higher precision timing.

- Radar Calibration:** NEXRAD radars calibrate reflectivity every volume scan, using an internally generated test. The test determines changes in internal variables such as beam power and path loss of the receiver signal processor since the last off-line calibration. If this value becomes large, it is likely that there is a radar calibration error that will translate into less reliable precipitation estimates. The calibration test is supposed to maintain a reflectivity precision of 1 dBZ. A 1 dBZ error can result in an error of up to 17% in R_{spas} using the default Z-R relationship $Z=300R^{1.4}$. Higher calibration errors will result in higher R_{spas} errors. However, by performing correlations each hour, the calibration issue is minimized in SPAS.
- Attenuation:** Attenuation is the reduction in power of the radar beams' energy as it travels from the antenna to the target and back. It is caused by the absorption and the scattering of power from the beam by precipitation. Attenuation can result in errors in Z as large as 1 dBZ especially when the radar beam is sampling a large area of heavy precipitation. In some cases, storm precipitation is so intense (>12 inches/hour) that individual storm cells become "opaque" and the radar beam is totally attenuated. Armed with sufficient gauge data however, SPAS will overcome attenuation issues.
- Range effects:** The curvature of the Earth and radar beam refraction result in the radar beam becoming more elevated above the surface with increasing range. With the increased elevation of the radar beam comes a decrease in Z values due to the radar beam not sampling the main precipitation portion of the cloud (i.e. "over topping" the precipitation and/or cloud altogether). Additionally, as the radar beam gets further from the radar, it naturally samples a larger and larger area, therefore amplifying point versus area differences (described above).
- Radar Beam Occultation/Ground Clutter:** Radar occultation (beam blockage) results when the radar beam's energy intersects terrain features as depicted in Figure G.14. The result is an increase in radar reflectivity values that can result in higher than normal precipitation estimates. The WDT processing algorithms account for these issues, but SPAS uses GIS spatial interpolation functions to infill areas suffering from poor or no radar coverage.
- Anomalous Propagation (AP) - AP** is false reflectivity echoes produced by unusual rates of refraction in the atmosphere. WDT algorithms remove most of the AP and false echoes, however in extreme cases the air near the ground may be so cold and dense that a radar beam that starts out moving upward is bent all the way down to the ground. This produces erroneously strong echoes at large distances from the radar. Again, equipped with sufficient gauge data, the SPAS bias corrections will overcome AP issues.

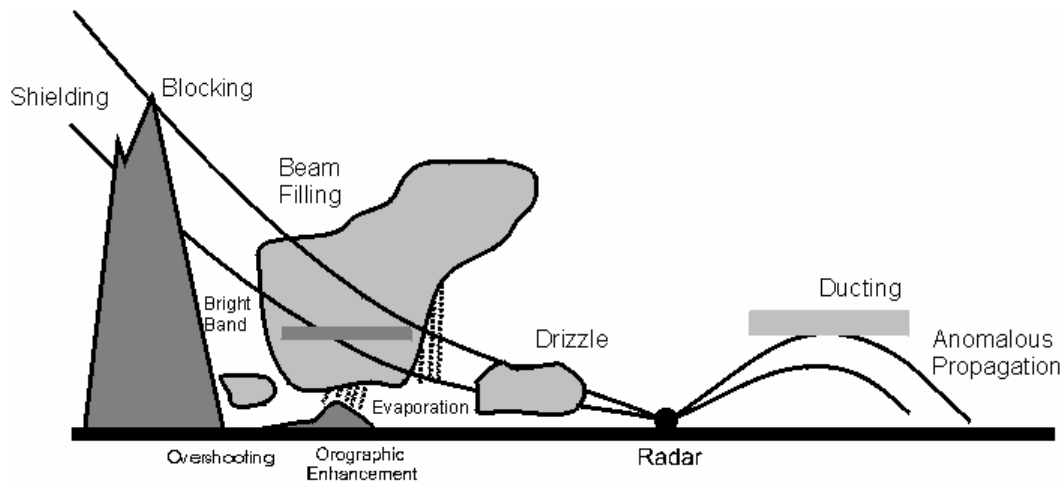


Figure G.14 Depiction of radar artifacts. (Source: Wikipedia)

SPAS is designed to overcome many of these short-comings by carefully using radar data for defining the spatial patterns and relative magnitudes of precipitation, but allowing measured precipitation values (“ground truth”) at gauges to govern the magnitude. When absolutely necessary, the observed precipitation values at gauges are nudged up (or down) to force the SPAS results to be consistent with observed gauge values. Nudging gauge precipitation values helps to promote better consistency between the gauge value and the grid cell value, even though these two values sometimes should not be the same since they are sampling different area sizes. For reasons discussed in the "SPAS versus Gauge Precipitation" section, the gauge value and grid cell value can vary. Plus, SPAS is designed to toss observed individual hourly values that are grossly inconsistent with the radar data, hence driving a difference between the gauge and grid cell. In general, when the gauge and grid cell value differ by more than 15% and/or 0.50 inches, and the gauge data has been validated, then it is justified to nudge (artificially increase or decrease) the observed gauge value to "force" SPAS to derive a grid cell value equal to the observed value. Sometimes simply shifting the gauge location to an adjacent grid cell resolves the problems. Regardless, a large gauge versus grid cell difference is a "red flag" and sometimes the result of an erroneous gauge value or a mis-located gauge, but in some cases the difference can only be resolved by nudging the precipitation value.

Before final results are declared, a precipitation intensity check is conducted to ensure the spatial patterns and magnitudes of the maximum storm intensities at 1-, 6-, 12-, etc. hours are consistent with surrounding gauges and published reports. Any erroneous data are corrected and SPAS re-run. Considering all of the QA/QC checks in SPAS, it typically requires 5-15 basemap SPAS runs and, if radar data is available, another 5-15 radar-aided runs, to arrive at the final output.

Test Cases

To check the accuracy of the DAD software, three test cases were evaluated.

"Pyramidville" Storm

The first test was that of a theoretical storm with a pyramid shaped isohyetal pattern. This case was called the Pyramidville storm. It contained 361 hourly stations, each occupying a single grid cell. The configuration of the Pyramidville storm (see Figure G.15) allowed for uncomplicated and accurate calculation of the analytical DA truth independent of the DAD software. The main motivation of this case was to verify that the DAD software was properly computing the area sizes and average depths.

1. Storm center: 39°N 104°W
2. Duration: 10-hours
3. Maximum grid cell precipitation: 1.00"
4. Grid cell resolution: 0.06 sq.-miles (361 total cells)
5. Total storm size: 23.11 sq-miles
6. Distribution of precipitation:
 - Hour 1: Storm drops 0.10" at center (area 0.06 sq-miles)
 - Hour 2: Storm drops 0.10" over center grid cell AND over one cell width around hour 1 center
 - Hours 3-10:
 1. Storm drops 0.10" per hour at previously wet area, plus one cell width around previously wet area
 2. Area analyzed at every 0.10"
 3. Analysis resolution: 15-sec (~.25 square miles)

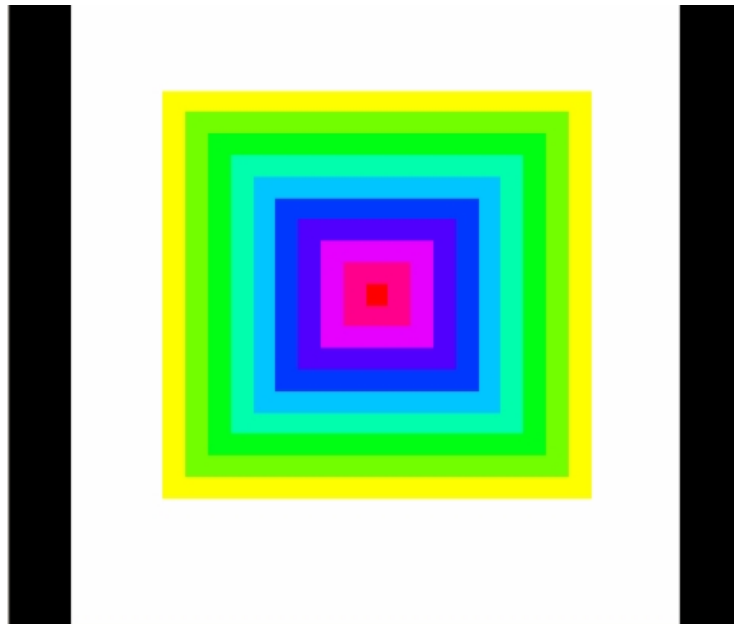


Figure G.15 "Pyramidville" Total precipitation. Center = 1.00", Outside edge = 0.10".

The analytical truth was calculated independent of the DAD software, and then compared to the DAD output. The DAD software results were equal to the truth, thus demonstrating that the DA estimates were properly calculated (Figure G.16).

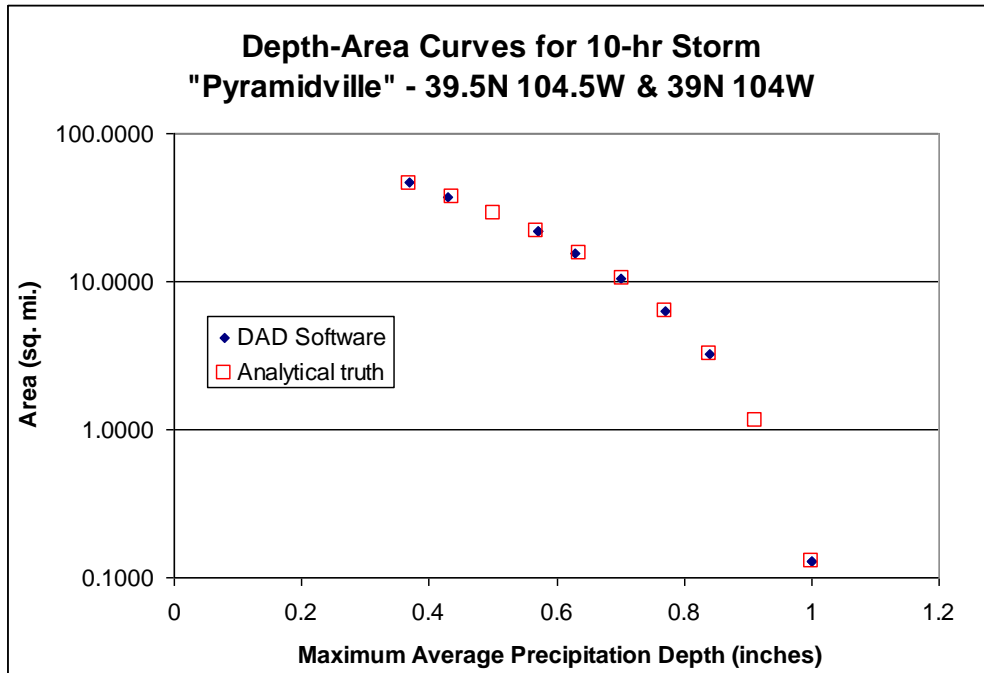


Figure G.16 10-hour DA results for “Pyramidville”; truth vs. output from DAD software.

The Pyramidville storm was then changed such that the mass curve and spatial interpolation methods would be stressed. Test cases included:

- Two-centers, each center with 361 hourly stations
- A single center with 36 hourly stations, 0 daily stations
- A single center with 3 hourly stations and 33 daily stations

As expected, results began shifting from the ‘truth,’ but minimally and within the expected uncertainty.

Ritter, Iowa Storm, June 7, 1953

Ritter, Iowa was chosen as a test case for a number of reasons. The NWS had completed a storm analysis, with available DAD values for comparison. The storm occurred over relatively flat terrain, so orographics was not an issue. An extensive “bucket survey” provided a great number of additional observations from this event. Of the hundreds of additional reports, about 30 of the most accurate reports were included in the DAD analysis.

The DAD software results are very similar to the NWS DAD values (Table G.2).

Table G.2 The percent difference [(AWA-NWS)/NWS] between the AWA DA results and those published by the NWS for the 1953 Ritter, Iowa storm.

%
Difference

Area (sq.mi.)	Duration (hours)				
		6	12	24	total
10		-15%	-7%	2%	2%
100		-7%	-6%	1%	1%
200		2%	0%	9%	9%
1000		-6%	-7%	4%	4%
5000		-13%	-8%	2%	2%
10000		-14%	-6%	0%	0%

Westfield, Massachusetts Storm, August 8, 1955

Westfield, Massachusetts was also chosen as a test case for a number of reasons. It is a probable maximum precipitation (PMP) driver for the northeastern United States. Also, the Westfield storm was analyzed by the NWS and the DAD values are available for comparison. Although this case proved to be more challenging than any of the others, the final results are very similar to those published by the NWS (Table G.3).

Table G.3 The percent difference [(AWA-NWS)/NWS] between the AWA DA results and those published by the NWS for the 1955 Westfield, Massachusetts storm.

%
Difference

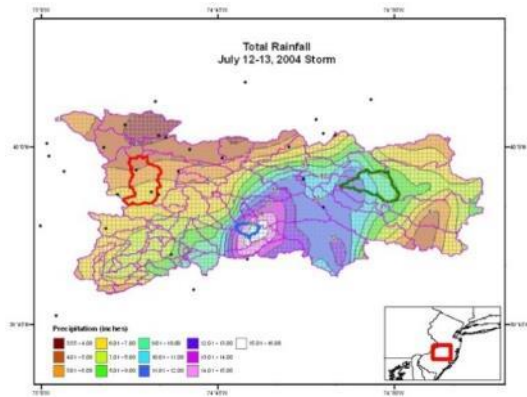
Area (sq. mi.)	Duration (hours)							
		6	12	24	36	48	60	total
10		2%	3%	0%	1%	-1%	0%	2%
100		-5%	2%	4%	-2%	-6%	-4%	-3%
200		-6%	1%	1%	-4%	-7%	-5%	-5%
1000		-4%	-2%	1%	-6%	-7%	-6%	-3%
5000		3%	2%	-3%	-3%	-5%	-5%	0%
10000		4%	9%	-5%	-4%	-7%	-5%	1%
20000		7%	12%	-6%	-3%	-4%	-3%	3%

The principal components of SPAS are: storm search, data extraction, quality control (QC), conversion of daily precipitation data into estimated hourly data, hourly and total storm precipitation grids/maps and a complete storm-centered DAD analysis.

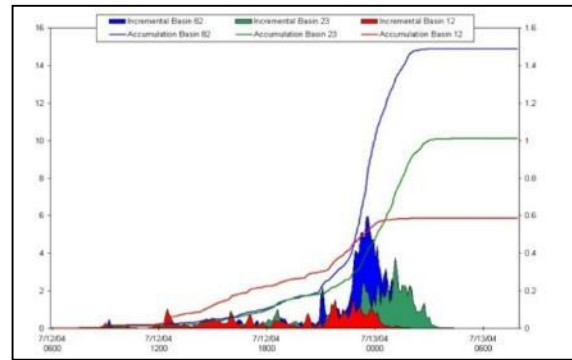
Output

Armed with accurate, high-resolution precipitation grids, a variety of customized output can be created (see Figures G.17a-d). Among the most useful outputs are sub-hourly precipitation grids for input into hydrologic models. Sub-hourly (i.e. 5-minute) precipitation grids are created by applying the appropriate optimized hourly Z-R (scaled down to be applicable for instantaneous Z) to each of the individual 5-minute radar scans; 5-minutes is often the native scan rate of the radar in the US. Once the scaled Z-R is applied to each radar scan, the resulting precipitation is summed up. The proportion of each 5-minute precipitation to the total 1-hour radar-aided precipitation is calculated. Each 5-minute proportion (%) is then applied to the quality controlled, bias corrected 1-hour total precipitation (created above) to arrive at the final 5-minute precipitation for each scan. This technique ensures the sum of 5-minute precipitation equals that of the quality controlled, bias corrected 1-hour total precipitation derived initially.

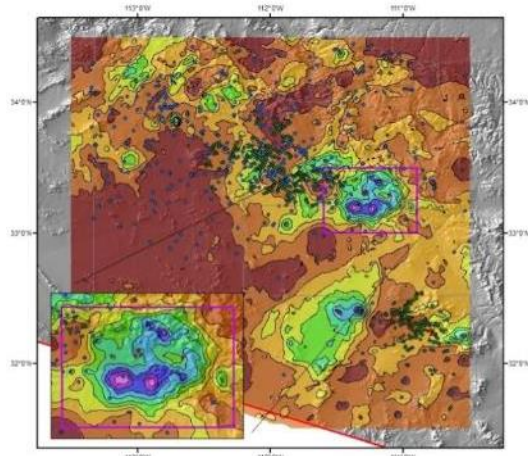
Depth-area-duration (DAD) tables/plots, shown in Figure G.17d, are computed using a highly-computational extension to SPAS. DADs provide an objective three dimensional (magnitude, area size, and duration) perspective of a storms' precipitation. SPAS DADs are computed using the procedures outlined by the NWS Technical Paper 1 (1946). The DAD tables for all analyzed events for this study are shown in Appendix F and are also included as Excel spreadsheets in the digital Appendix M Section VI.



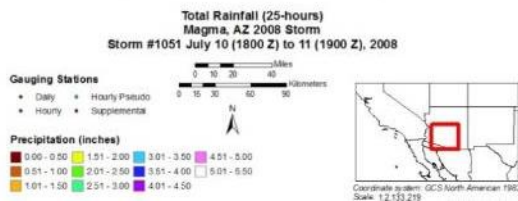
a)



b)



c)



Storm 1048 - Hokah, MN August 18 - August 21, 2007

Area (mi ²)	Duration (hours)									Total
	1	3	6	12	18	24	36	48	72	
0.24	2.45	4.77	7.85	11.89	14.88	17.31	17.55	18.19	18.20	18.20
1	2.12	4.53	7.56	11.64	14.59	17.05	17.31	17.95	18.02	18.02
10	2.12	4.53	7.49	11.10	13.89	15.98	16.31	17.03	17.15	17.17
25	2.12	4.53	6.92	10.42	12.88	14.89	15.34	16.23	16.45	16.46
50	2.11	4.40	6.64	9.65	12.13	14.05	14.46	15.49	15.79	15.79
100	2.09	4.10	6.33	9.37	11.52	13.27	13.63	14.76	15.14	15.14
200	2.03	3.79	6.00	8.87	10.96	12.62	13.37	14.22	14.52	14.52
300	1.95	3.61	5.74	8.55	10.64	12.06	12.99	13.74	14.04	14.04
500	1.79	3.35	5.47	8.13	10.11	11.60	12.27	13.01	13.29	13.30
1,000	1.53	2.99	4.95	7.33	9.17	10.51	11.13	11.94	12.07	12.07
2,000	0.95	2.55	4.36	6.18	8.06	9.30	9.85	10.54	10.75	10.75
5,000	0.87	2.02	3.45	5.19	6.53	7.61	8.18	8.79	8.96	8.98
10,000	0.83	1.54	2.89	4.02	5.39	6.09	6.78	7.31	7.53	7.55
20,000	0.41	0.95	1.84	3.02	3.97	4.53	5.13	5.63	5.87	5.90

d)

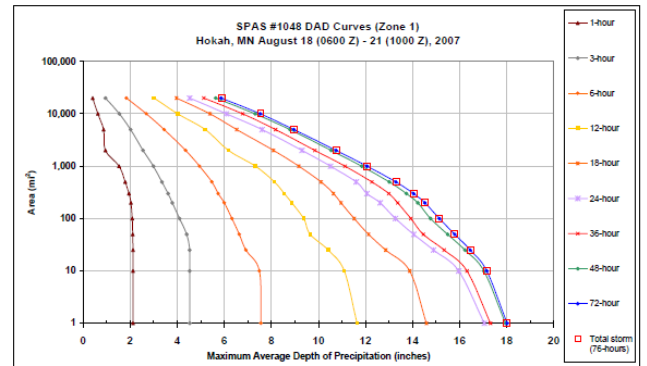


Figure G.17 Various examples of SPAS output, including (a) total storm map and its associated (b) basin average precipitation time series, (c) total storm precipitation map, (d) depth-area-duration (DAD) table and plot, and (e) precipitation gauge catalog with total storm statistics.

Summary

Grounded on years of scientific research with a demonstrated reliability in post-storm analyses, SPAS is a hydro-meteorological tool that provides accurate precipitation analyses for a variety of applications. SPAS has the ability to compute precise and

accurate results by using sophisticated timing algorithms, “basemaps”, a variety of precipitation data and most importantly NEXRAD weather radar data (if available). The approach taken by SPAS relies on hourly, daily and supplemental precipitation gauge observations to provide quantification of the precipitation amounts while relying on basemaps and NEXRAD data (if available) to provide the spatial distribution of precipitation between precipitation gauge sites. By determining the most appropriate coefficients for the Z-R equation on an hourly basis, the approach anchors the precipitation amounts to accepted precipitation gauge data while using the NEXRAD data to distribute precipitation between precipitation gauges for each hour of the storm. Hourly Z-R coefficient computations address changes in the cloud microphysics and storm characteristics as the storm evolves. Areas suffering from limited or no radar coverage, are estimated using the spatial patterns and magnitudes of the independently created basemap precipitation grids. Although largely automated, SPAS is flexible enough to allow hydro-meteorologists to make important adjustments and adapt to any storm situation.

References

- Baeck M.L., Smith J.A., 1998: "Precipitation Estimation by the WSR-88D for Heavy Precipitation Events", *Weather and Forecasting*: Vol. 13, No. 2, pp. 416–436.
- Ciach, G.J., 2003: Local Random Errors in Tipping-Bucket Rain Gauge Measurements. *J. Atmos. Oceanic Technol.*, **20**, 752–759.
- Dickens, J., 2003: "On the Retrieval of Drop Size Distribution by Vertically Pointing Radar", American Meteorological Society 32nd Radar Meteorology Conference, Albuquerque, NM, October 2005.
- Duchon, C.E., and G.R. Essenberg, 2001: Comparative Precipitation Observations from Pit and Above Ground Rain Gauges with and without Wind Shields, *Water Resources Research*, Vol. 37, N. 12, 3253-3263.
- Faulkner, E., T. Hampton, R.M. Rudolph, and Tomlinson, E.M., 2004: Technological Updates for PMP and PMF – Can They Provide Value for Dam Safety Improvements? Association of State Dam Safety Officials Annual Conference, Phoenix, Arizona, September 26-30, 2004.
- Guo, J. C. Y., Urbonas, B., and Stewart, K., 2001: Rain Catch under Wind and Vegetal Effects. *ASCE, Journal of Hydrologic Engineering*, Vol. 6, No. 1.
- Hunter, R.D. and R.K. Meentemeyer, 2005: Climatologically Aided Mapping of Daily Precipitation and Temperature, *Journal of Applied Meteorology*, October 2005, Vol. 44, pp. 1501-1510.
- Hunter, S.M., 1999: Determining WSR-88D Precipitation Algorithm Performance Using The Stage III Precipitation Processing System, Next Generation Weather Radar Program, WSR-88D Operational Support Facility, Norman, OK.
- Lakshmanan, V. and M. Valente, 2004: Quality control of radar reflectivity data using satellite data and surface observations, 20th Int'l Conf. on Inter. Inf. Proc. Sys. (IIPS) for Meteor., Ocean., and Hydr., Amer. Meteor. Soc., Seattle, CD-ROM, 12.2.
- Martner, B.E, and V. Dubovskiy, 2005: Z-R Relations from Raindrop Disdrometers: Sensitivity To Regression Methods And DSD Data Refinements, 32nd Radar Meteorology Conference, Albuquerque, NM, October, 2005
- Tokay, A., P.G. Bashor, and V.L. McDowell, 2010: Comparison of Rain Gauge Measurements in the Mid-Atlantic Region. *J. Hydrometeor.*, **11**, 553-565.
- Tomlinson, E.M., W.D. Kappel, T.W. Parzybok, B. Rappolt, 2006: Use of NEXRAD Weather Radar Data with the Storm Precipitation Analysis System (SPAS) to Provide High Spatial Resolution Hourly Precipitation Analyses for Runoff Model Calibration and Validation, ASDSO Annual Conference, Boston, MA.
- Tomlinson, E.M., and T.W. Parzybok, 2004: Storm Precipitation Analysis System (SPAS), proceedings of Association of Dam Safety Officials Annual Conference, Technical Session II, Phoenix, Arizona.
- Tomlinson, E.M., R.A. Williams, and T.W. Parzybok, September 2003: Site-Specific Probable Maximum Precipitation (PMP) Study for the Great Sacandaga Lake / Stewarts Bridge Drainage Basin, Prepared for Reliant Energy Corporation, Liverpool, New York.

- Tomlinson, E.M., R.A. Williams, and T.W. Parzybok, September 2003: Site-Specific Probable Maximum Precipitation (PMP) Study for the Cherry Creek Drainage Basin, Prepared for the Colorado Water Conservation Board, Denver, CO.
- Tomlinson, E.M., Kappel W.D., Parzybok, T.W., Hultstrand, D., Muhlestein, G., and B. Rappolt, May 2008: Site-Specific Probable Maximum Precipitation (PMP) Study for the Wanahoo Drainage Basin, Prepared for Olsson Associates, Omaha, Nebraska.
- Tomlinson, E.M., Kappel W.D., Parzybok, T.W., Hultstrand, D., Muhlestein, G., and B. Rappolt, June 2008: Site-Specific Probable Maximum Precipitation (PMP) Study for the Blenheim Gilboa Drainage Basin, Prepared for New York Power Authority, White Plains, NY.
- Tomlinson, E.M., Kappel W.D., and T.W. Parzybok, February 2008: Site-Specific Probable Maximum Precipitation (PMP) Study for the Magma FRS Drainage Basin, Prepared for AMEC, Tucson, Arizona.
- Tomlinson, E.M., Kappel W.D., Parzybok, T.W., Hultstrand, D., Muhlestein, G., and P. Sutter, December 2008: Statewide Probable Maximum Precipitation (PMP) Study for the state of Nebraska, Prepared for Nebraska Dam Safety, Omaha, Nebraska.
- Tomlinson, E.M., Kappel, W.D., and Tye W. Parzybok, July 2009: Site-Specific Probable Maximum Precipitation (PMP) Study for the Scoggins Dam Drainage Basin, Oregon.
- Tomlinson, E.M., Kappel, W.D., and Tye W. Parzybok, February 2009: Site-Specific Probable Maximum Precipitation (PMP) Study for the Tuxedo Lake Drainage Basin, New York.
- Tomlinson, E.M., Kappel, W.D., and Tye W. Parzybok, February 2010: Site-Specific Probable Maximum Precipitation (PMP) Study for the Magma FRS Drainage Basin, Arizona.
- Tomlinson, E.M., Kappel W.D., Parzybok, T.W., Hultstrand, D.M., Muhlestein, G.A., March 2011: Site-Specific Probable Maximum Precipitation Study for the Tarrant Regional Water District, Prepared for Tarrant Regional Water District, Fort Worth, Texas.
- Tomlinson, E.M., Kappel, W.D., Hultstrand, D.M., Muhlestein, G.A., and T. W. Parzybok, November 2011: Site-Specific Probable Maximum Precipitation (PMP) Study for the Lewis River basin, Washington State.
- Tomlinson, E.M., Kappel, W.D., Hultstrand, D.M., Muhlestein, G.A., and T. W. Parzybok, December 2011: Site-Specific Probable Maximum Precipitation (PMP) Study for the Brassua Dam basin, Maine.
- U.S. Weather Bureau, 1946: Manual for Depth-Area-Duration analysis of storm precipitation. *Cooperative Studies Technical Paper No. 1*, U.S. Department of Commerce, Weather Bureau, Washington, D.C., 73pp.

Appendix H

Point OTF Evaluation for PMP Calculations – Use of Single Point vs. Areal-Average Precipitation Climatology Values

Background

The calculation of PMP in orographically dynamic areas necessitates accounting for the effect and differences of moisture, topography and elevation on rainfall when transposing a storm. AWA quantifies this effect as the Orographic Transposition Factor (OTF). For a gridded PMP study, the OTF is calculated for each storm at each grid point over a basin domain. The OTF is a ratio of a climatological precipitation depth at a source storm location to the depth at a target grid point within the drainage basin. Typically the precipitation frequency climatology depths, such as NOAA Atlas 14, are used to determine a relationship, or correlation, between the source and target location using the 10 through 1,000-year return frequencies. It is assumed that the difference in the climatological precipitation depths between the storm source location and a transposable target location is primarily due to the effects of elevation and orographics. Therefore, the climatological precipitation relationship between the two locations, when expressed as a factor and applied to a storm's rainfall depth, can be used to determine the adjusted rainfall depth of a storm when transposed to a target location.

Recent approved PMP studies (e.g. Lewis River 2011, Arizona statewide PMP 2013, Susitna-Watana 2014, North Umpqua 2014, Tennessee Valley Authority 2015, Springbank 2015) completed by AWA use a procedure for calculating the OTF for a grid point location by determining the ratio of precipitation frequency values at the SPAS total storm rainfall DAD zone center location to the grid point location. It is assumed that since the rainfall center for a given DAD zone is the location of the greatest total precipitation for an event, that the precipitation climatology data at that same location would *best* represent the orographic rainfall effect attributable to that event. In actuality, the underlying terrain over an area contributes to the orographic effect for a storm event, not only the specific discrete location of the storm center. However, it is assumed that the greater the distance from the storm center, the less representative the underlying precipitation frequency data is to most critical rainfall for that storm event, based on the spatial distribution of the storm analysis. The purpose of this evaluation is to consider the difference in OTF values resulting from applying precipitation climatology values averaged over an area at the storm location versus using the values only at the storm center point, and to discuss which approach is most feasible and appropriate.

Procedure

Fourteen SPAS-analyzed storm centers were assessed to compare OTF values resulting from the use of precipitation climatology values at the storm center point location versus an areal-average of multiple points surrounding the storm center. The storm centers were chosen from events in orographic regions of both the Rocky and the Appalachian Mountain Ranges (Table H.1).

Table H.1 List of storm centers evaluated.

NAME	SPAS	DAD ZONE	STATE	LAT	LON	YEAR	MONTH	DAY	RAINFALL	TYPE
DEER CREEK DAM	1241	2	UT	41.360	-111.910	2010	10	25	4.74	General
COTTONWOOD	1265	1	UT	40.404	-111.638	1982	9	26	10.13	General
COTTONWOOD	1265	2	UT	40.379	-112.204	1982	9	26	10.02	General
COTTONWOOD	1265	3	UT	41.604	-112.013	1982	9	26	9.71	General
ALTA PASS	1299	1	NC	35.879	-81.871	1916	7	13	24.9	General
ELBA	1305	1	AL	31.363	-86.121	1929	3	12	29.73	General
SAVAGETON	1325	1	WY	43.880	-105.930	1923	9	27	17.1	General
BIG THOMPSON CANYON	1231	1	CO	40.479	-105.429	1976	7	31	12.52	Local
MORGAN	1248	1	UT	41.079	-111.654	1958	8	16	7.01	Local
JOHNSON CITY	1343	1	TN	36.304	-82.063	1924	6	13	16.14	Local

ArcGIS and Excel software was used to aid in data extraction and calculations. Figure H.1 shows the location of each analyzed storm center. Centers were deliberately chosen in highly orographic locations or where the precipitation frequency values change rapidly over short distances. These sites were chosen as potentially *worst case* scenarios where the largest difference in point-based OTF vs area-based OTF is likely to occur. Two storms, Savageton, WY and Elba, AL occurred over relatively homogeneous terrain and were included as *typical* scenarios where the point vs areal OTF difference is not likely to be significant.

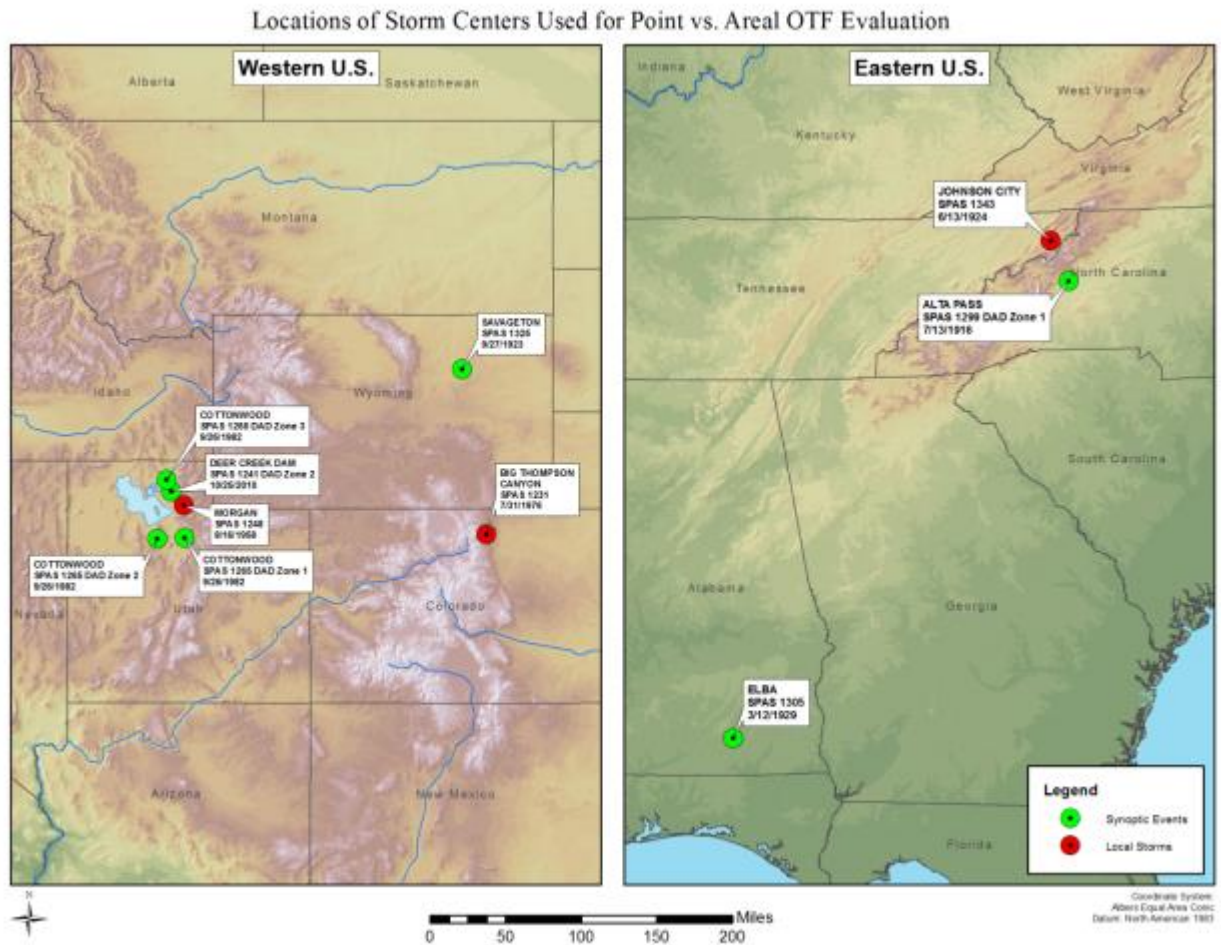


Figure H.1 Locations of analyzed storm centers.

Using ArcGIS, a grid point network was created covering the extent of each SPAS total storm raster. The grid network coincides with the spacing and orientation used for the Wyoming Statewide PMP Study for the Western U.S. storms and the TVA PMP Study for the Eastern U.S. storms. Precipitation frequency climatology depths were extracted to each grid point for the 10, 25, 50, 100, 200, 500, and 1,000-year return frequencies. The 24-hour duration data sets were used for synoptic tropical/general type storms and the 6-hour duration data sets were used for the local storm types.

To calculate the OTF, the ratio of the adjusted precipitation P_a at the target grid cell location to the in-place storm precipitation P_i .

$$OTF = \frac{P_a}{P_i}$$

The in-place storm precipitation is determined by SPAS, 6-hour for local storms, 24-hour for general storms. The adjusted rainfall is predicted from the precipitation climatology datasets using a linear regression best-fit trendline between the precipitation climatology depths (10 through 1000-year) at the source and target locations:

$$P_a = mP_i + b$$

where,

P_o	=	orographically adjusted rainfall (target)
P_i	=	SPAS-analyzed in-place rainfall
m	=	proportionality coefficient (slope)
b	=	error constant (y-intercept)

The location of the target grid cell is not important since this evaluation is only concerned with what values are used at the source location, therefore the target grid cell locations were chosen arbitrarily. The source point location is determined by finding the largest SPAS total storm grid cell and using the centroid. The relationship between the precipitation frequency climatology values at this point and the arbitrary target point is calculated as the OTF as described above, consistent with methods used in past projects.

The OTF is also calculated using a series of incremental area sizes at the storm source location; 10-, 50-, 100-, 250 mi², etc., depending on the storm coverage and type. For a given area size, the grid points are ordered according to the SPAS total storm depth and the extracted values were averaged for the number of grid cells equivalent to the desired area size. For example, if the grid cells are each ~2.5 mi², the precipitation climatology data would be used for the largest four grid points as determined by the SPAS rainfall depth to calculate the 10 mi² areal-average. Depending on the area size and the spatial distribution of the storm, these cells may or may not be contiguous. The cell values are averaged for the 10 through 1,000 year return frequencies. The OTF is calculated as usual, except the areal-average precipitation frequency climatology values are used for the source location, instead of only the values at the maximum SPAS rainfall point.

Example Calculations

EXAMPLE 1

The July 31, 1976 storm over Big Thompson Canyon, CO (SPAS 1231) occurred along the steep and abrupt eastern slopes of the Rocky Mountains. The 6-hour precipitation climatology developed for the Wyoming PMP study was used for this event. At this location, the gradient of precipitation climatology is very high with a large degree of variability over small geographic areas, making a good candidate for a *worst-case* scenario in terms of point vs. areal OTF. Figure H.2 illustrates the SPAS total storm rainfall over the gridded network. Each cell is outlined in a color indicating which areal-average category the cells falls within.

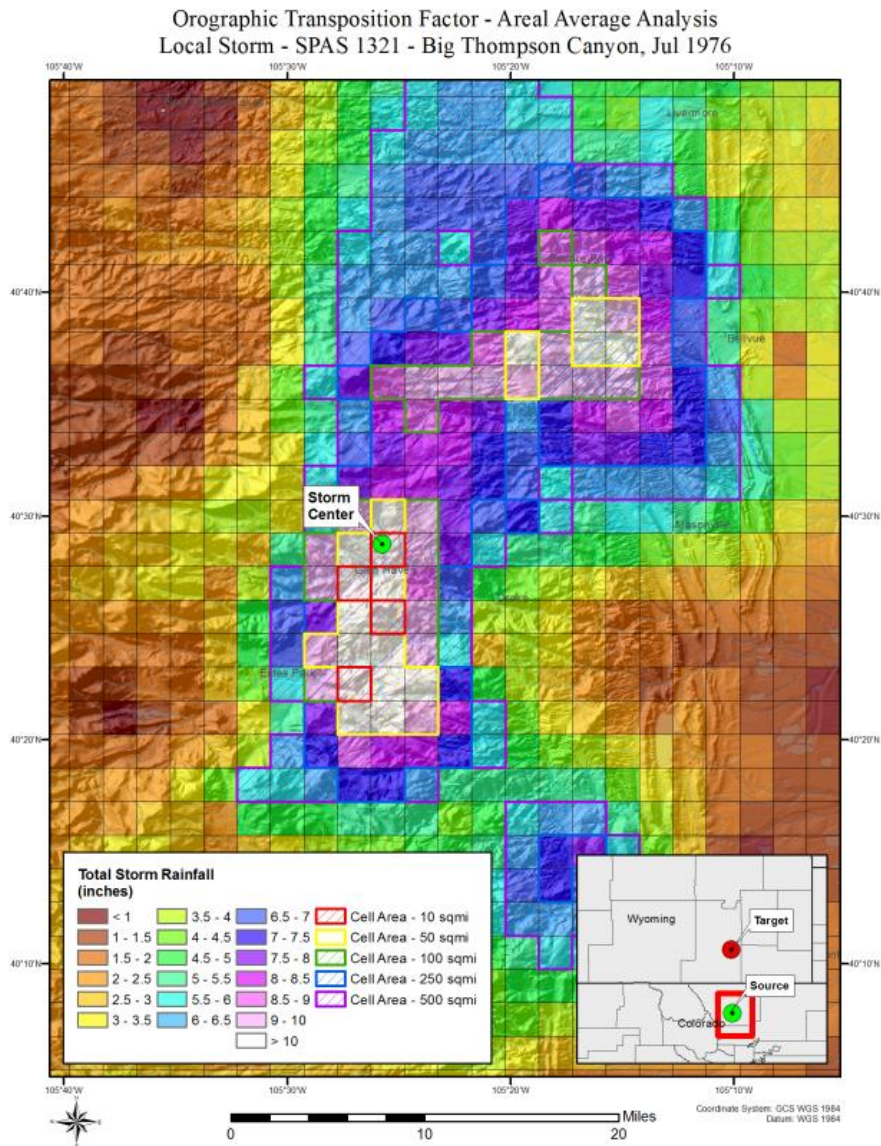


Figure H.2 SPAS 1231 Big Thompson Canyon total storm rainfall by area class.

It is expected that the OTF will vary significantly with the incorporation of data over increased area sizes due to the extreme variation of the precipitation climatology in this area. The OTF values area calculated for using the storm center point location and as an areal-average for each size up to 500 mi² using the relationship between the climatology values at the source and target cells. Figure H.3 shows the best fit trend lines for each of the linear regression relationships. The red line represents the storm center point and each of the other trend lines represents the various areal averages up to 500 mi². The graph visually illustrates the divergence of each areal-average OTF compared to the single-point OTF.

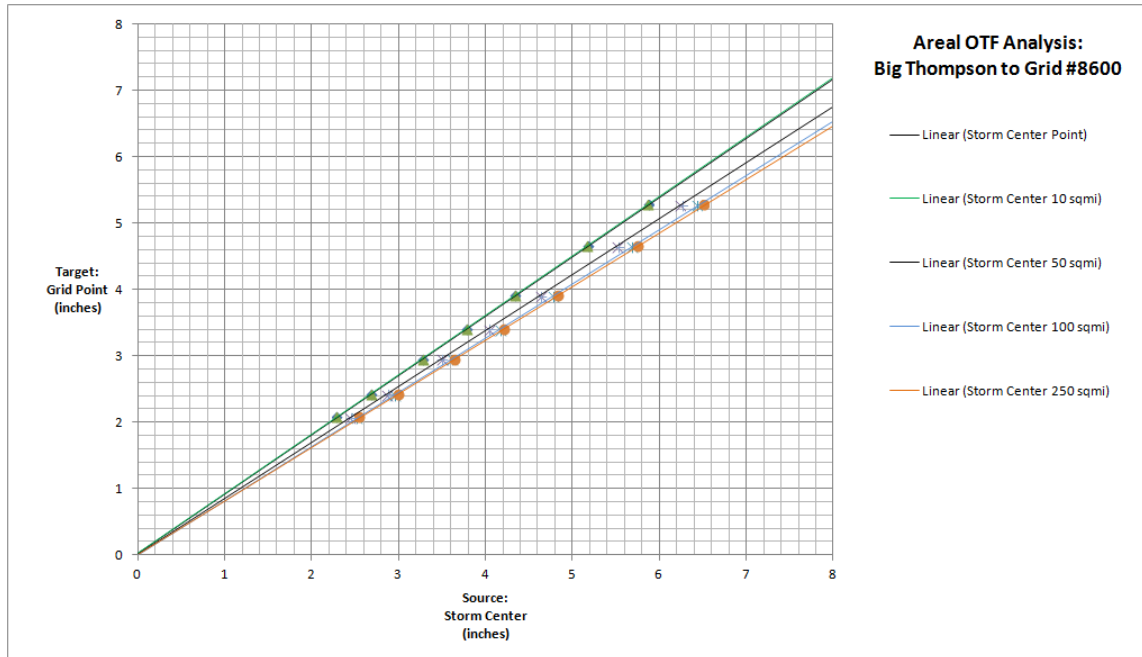


Figure H.3 Linear best fit trend lines for the SPAS 1231 point and areal precipitation climatology relationships.

Table H.2 summarizes the OTF calculated from using the storm center point and each areal-average for each area size and the percent difference of each areal OTF to the point OTF. At 10 mi² there is nearly no difference from using the maximum point only. At 50 mi² the difference increases to a 5% reduction and continues to increase to a 9% reduction at 250 mi², after which it actually reduces to a 6% reduction at 500 mi² where the climatology begins to become smoothed as a regional average.

Table H.2 SPAS 1231 OTF comparison using maximum point and areal averages.

	Target Latitude	Target Longitude	Max 6hr Rainfall	Slope	Y-intercept	Adjusted Rainfall	OTF	% Difference from Point
Point (WY PF)	41.575	-105.450	10.12	0.89	0.03	9.08	0.90	-
10 sqmi	41.575	-105.450	10.12	0.90	0.03	9.09	0.90	0%
50 sqmi	41.575	-105.450	10.12	0.84	0.01	8.54	0.84	-5%
100 sqmi	41.575	-105.450	10.12	0.82	0.00	8.28	0.82	-8%
250 sqmi	41.575	-105.450	10.12	0.81	0.02	8.19	0.81	-9%
500 sqmi	41.575	-105.450	10.12	0.84	0.02	8.51	0.84	-6%

EXAMPLE 2

A similar example is shown for a synoptic storm occurring in a less orographic area. The Savageton, WY synoptic event of September 1923 (SPAS 1325) occurred on the high plains of eastern Wyoming. Although this storm covers a much larger area, the precipitation climatology values and underlying terrain are fairly homogenous in this area. Therefore it is assumed the difference between the point-based OTF and areal-OTF will be much less than what was seen in the Big Thompson Canyon comparison. Figure H.4 shows the SPAS 1325 total storm grid classified by area size.

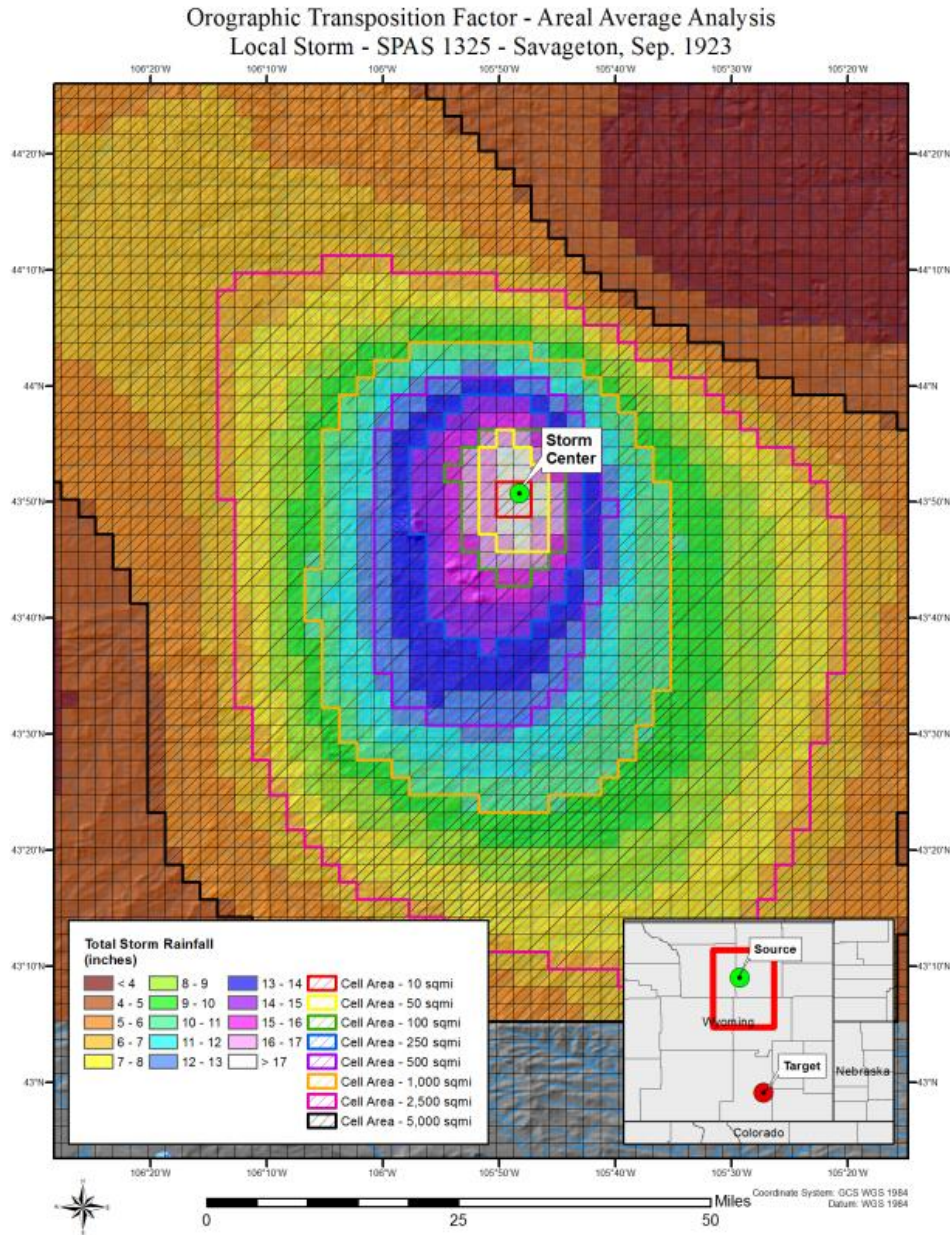


Figure H.4 SPAS 1325 Savageton, WY total storm rainfall by area class.

The best fit trend lines are shown in Figure H.5 for up to 5,000 mi². There is very little divergence from the point to the various areal-average relationships, even over large areas.

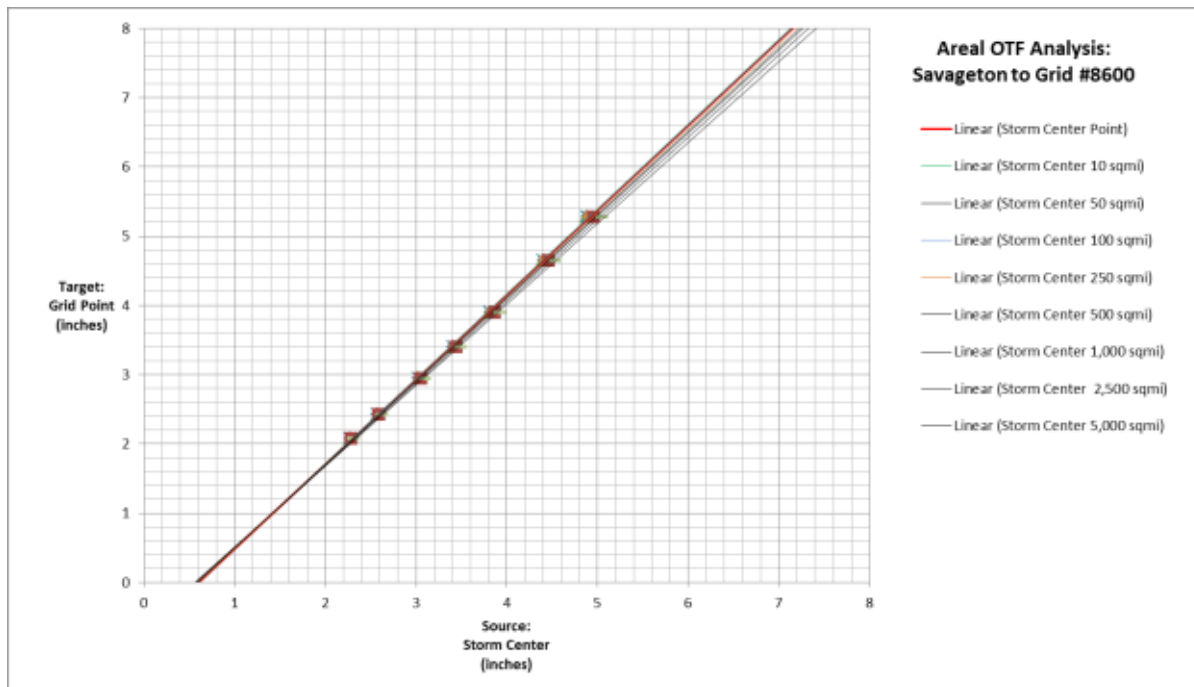


Figure H.5 Linear best fit trend lines for the SPAS 1325 point and areal precipitation climatology relationships.

Table H.3 lists the magnitude and percent differences for the point OTF and areal average OTFs. As expected, the percent difference slowly increases up to a maximum of 5% reduction at 5,000 miles.

Table H.3 SPAS 1325 OTF comparison using maximum point and areal averages.

	Target Latitude	Target Longitude	Max 6hr Rainfall	Slope	Y-intercept	Adjusted Rainfall	OTF	% Difference from Point
Point Location	41.575	-105.450	10.32	1.22	-0.73	11.88	1.15	0%
10 sqmi	41.575	-105.450	10.32	1.23	-0.73	11.91	1.15	0%
50 sqmi	41.575	-105.450	10.32	1.22	-0.73	11.88	1.15	0%
100 sqmi	41.575	-105.450	10.32	1.22	-0.73	11.89	1.15	0%
250 sqmi	41.575	-105.450	10.32	1.21	-0.72	11.80	1.14	-1%
500 sqmi	41.575	-105.450	10.32	1.20	-0.70	11.71	1.13	-2%
1,000 sqmi	41.575	-105.450	10.32	1.20	-0.68	11.65	1.13	-2%
2,500 sqmi	41.575	-105.450	10.32	1.18	-0.67	11.55	1.12	-3%
5,000 sqmi	41.575	-105.450	10.32	1.17	-0.65	11.40	1.10	-5%

Results

Tables H.4 through H.17

Table H.4 SPAS 1241 DAD Zone 2 (Deer Creek Dam, UT) general storm OTF comparison using maximum point and areal averages.

	Target Latitude	Target Longitude	Max 24hr Rainfall	Slope	Y-intercept	Adjusted Rainfall	OTF	% Difference from Point
Point Location	41.575	-105.450	4.54	0.76	-0.79	2.67	0.59	0%
10 sqmi	41.575	-105.450	4.54	0.73	-0.71	2.60	0.57	-2%
50 sqmi	41.575	-105.450	4.54	0.78	-0.69	2.86	0.63	4%
100 sqmi	41.575	-105.450	4.54	0.77	-0.63	2.87	0.63	4%
250 sqmi	41.575	-105.450	4.54	0.83	-0.56	3.22	0.71	12%
500 sqmi	41.575	-105.450	4.54	0.90	-0.52	3.58	0.79	20%
1,000 sqmi	41.575	-105.450	4.54	0.96	-0.49	3.89	0.86	27%
2,500 sqmi	41.575	-105.450	4.54	1.07	-0.47	4.40	0.97	38%

Table H.5 SPAS 1265 DAD Zone 1 (Cottonwood, UT) general storm OTF comparison using maximum point and areal averages.

	Target Latitude	Target Longitude	Max 24hr Rainfall	Slope	Y-intercept	Adjusted Rainfall	OTF	% Difference from Point
Point Location	40.925	-111.050	6.07	0.73	-0.60	3.82	0.63	0%
10 sqmi	40.925	-111.050	6.07	0.84	-0.74	4.39	0.72	9%
50 sqmi	40.925	-111.050	6.07	0.91	-0.72	4.80	0.79	16%
100 sqmi	40.925	-111.050	6.07	0.91	-0.76	4.78	0.79	16%
250 sqmi	40.925	-111.050	6.07	0.95	-0.76	4.99	0.82	19%
500 sqmi	40.925	-111.050	6.07	1.00	-0.75	5.33	0.88	25%
1,000 sqmi	40.925	-111.050	6.07	1.09	-0.77	5.86	0.96	34%

Table H.6 SPAS 1265 DAD Zone 2 (Cottonwood, UT) general storm OTF comparison using maximum point and areal averages.

	Target Latitude	Target Longitude	Max 24hr Rainfall	Slope	Y-intercept	Adjusted Rainfall	OTF	% Difference from Point
Point Location	40.925	-111.050	4.34	0.93	-0.82	3.22	0.74	0%
10 sqmi	40.925	-111.050	4.34	0.95	-0.90	3.22	0.74	0%
50 sqmi	40.925	-111.050	4.34	1.05	-0.91	3.64	0.84	10%
100 sqmi	40.925	-111.050	4.34	1.11	-0.91	3.93	0.90	16%
250 sqmi	40.925	-111.050	4.34	1.27	-0.95	4.58	1.06	31%
500 sqmi	40.925	-111.050	4.34	1.47	-1.00	5.39	1.24	50%
1,000 sqmi	40.925	-111.050	4.34	1.61	-0.97	6.00	1.38	64%

Table H.7 SPAS 1265 DAD Zone 3 (Cottonwood, UT) general storm OTF comparison using maximum point and areal averages.

	Target Latitude	Target Longitude	Max 24hr Rainfall	Slope	Y-intercept	Adjusted Rainfall	OTF	% Difference from Point
Point Location	40.925	-111.050	4.34	0.93	-0.82	3.22	0.74	0%
10 sqmi	40.925	-111.050	4.34	0.95	-0.90	3.22	0.74	0%
50 sqmi	40.925	-111.050	4.34	1.05	-0.91	3.64	0.84	10%
100 sqmi	40.925	-111.050	4.34	1.11	-0.91	3.93	0.90	16%
250 sqmi	40.925	-111.050	4.34	1.27	-0.95	4.58	1.06	31%
500 sqmi	40.925	-111.050	4.34	1.47	-1.00	5.39	1.24	50%
1,000 sqmi	40.925	-111.050	4.34	1.61	-0.97	6.00	1.38	64%

Table H.8 SPAS 1299 (Alta Pass, NC) general storm OTF comparison using maximum point and areal averages.

	Target Latitude	Target Longitude	Max 24hr Rainfall	Slope	Y-intercept	Adjusted Rainfall	OTF	% Difference from Point
Point Location	41.575	-105.450	23.15	0.85	1.47	21.17	0.91	0%
10 sqmi	41.575	-105.450	23.15	0.87	1.46	21.52	0.93	2%
50 sqmi	41.575	-105.450	23.15	0.86	1.46	21.47	0.93	1%
100 sqmi	41.575	-105.450	23.15	0.86	1.48	21.34	0.92	1%
250 sqmi	41.575	-105.450	23.15	0.86	1.46	21.26	0.92	0%
500 sqmi	41.575	-105.450	23.15	0.87	1.27	21.32	0.92	1%
1,000 sqmi	41.575	-105.450	23.15	0.88	1.16	21.47	0.93	1%
2,500 sqmi	41.575	-105.450	23.15	0.90	0.99	21.88	0.95	3%
5,000 sqmi	41.575	-105.450	23.15	0.95	0.92	22.90	0.99	8%

Table H.9 SPAS 1305 (Elba, AL) general storm OTF comparison using maximum point and areal averages.

	Target Latitude	Target Longitude	Max 24hr Rainfall	Slope	Y-intercept	Adjusted Rainfall	OTF	% Difference from Point
Point Location	41.575	-105.450	23.15	0.40	3.58	12.85	0.56	0%
10 sqmi	41.575	-105.450	23.15	0.40	3.56	12.86	0.56	0%
50 sqmi	41.575	-105.450	23.15	0.41	3.54	12.95	0.56	0%
100 sqmi	41.575	-105.450	23.15	0.41	3.55	12.96	0.56	0%
250 sqmi	41.575	-105.450	23.15	0.41	3.55	12.96	0.56	0%
500 sqmi	41.575	-105.450	23.15	0.41	3.56	12.96	0.56	0%
1,000 sqmi	41.575	-105.450	23.15	0.41	3.56	12.94	0.56	0%
2,500 sqmi	41.575	-105.450	23.15	0.41	3.46	12.98	0.56	1%
5,000 sqmi	41.575	-105.450	23.15	0.42	3.38	13.03	0.56	1%

Table H.10 SPAS 1325 (Savageton, WY) general storm OTF comparison using maximum point and areal averages.

	Target Latitude	Target Longitude	Max 6hr Rainfall	Slope	Y-intercept	Adjusted Rainfall	OTF	% Difference from Point
Point Location	41.575	-105.450	10.32	1.22	-0.73	11.88	1.15	0%
10 sqmi	41.575	-105.450	10.32	1.23	-0.73	11.91	1.15	0%
50 sqmi	41.575	-105.450	10.32	1.22	-0.73	11.88	1.15	0%
100 sqmi	41.575	-105.450	10.32	1.22	-0.73	11.89	1.15	0%
250 sqmi	41.575	-105.450	10.32	1.21	-0.72	11.80	1.14	-1%
500 sqmi	41.575	-105.450	10.32	1.20	-0.70	11.71	1.13	-2%
1,000 sqmi	41.575	-105.450	10.32	1.20	-0.68	11.65	1.13	-2%
2,500 sqmi	41.575	-105.450	10.32	1.18	-0.67	11.55	1.12	-3%
5,000 sqmi	41.575	-105.450	10.32	1.17	-0.65	11.40	1.10	-5%

Table H.11 SPAS 1231 (Big Thompson Canyon, CO) local storm OTF comparison using maximum point and areal averages.

	Target Latitude	Target Longitude	Max 6hr Rainfall	Slope	Y-intercept	Adjusted Rainfall	OTF	% Difference from Point
Point Location	41.575	-105.450	10.12	0.89	0.03	9.08	0.90	0%
10 sqmi	41.575	-105.450	10.12	0.90	0.03	9.09	0.90	0%
50 sqmi	41.575	-105.450	10.12	0.84	0.01	8.54	0.84	-5%
100 sqmi	41.575	-105.450	10.12	0.82	0.00	8.28	0.82	-8%
250 sqmi	41.575	-105.450	10.12	0.81	0.02	8.19	0.81	-9%
500 sqmi	41.575	-105.450	10.12	0.84	0.02	8.51	0.84	-6%

Table H.12 SPAS 1248 (Morgan, UT) local storm OTF comparison using maximum point and areal averages.

	Target Latitude	Target Longitude	Max 6hr Rainfall	Slope	Y-intercept	Adjusted Rainfall	OTF	% Difference from Point
Storm Center Point	41.575	-105.450	7.10	0.89	0.05	6.34	0.89	0%
10 sqmi	41.575	-105.450	7.10	0.95	0.09	6.85	0.96	7%
50 sqmi	41.575	-105.450	7.10	0.95	0.09	6.85	0.96	7%
100 sqmi	41.575	-105.450	7.10	0.93	0.08	6.72	0.95	5%
250 sqmi	41.575	-105.450	7.10	0.91	0.06	6.51	0.92	2%
500 sqmi	41.575	-105.450	7.10	0.90	0.05	6.47	0.91	2%

Table H.13 - SPAS 1343 (Johnson City, TN) local storm OTF comparison using maximum point and areal averages.

	Target Latitude	Target Longitude	Max 24hr Rainfall	Slope	Y-intercept	Adjusted Rainfall	OTF	% Difference from Point
Point Location	41.575	-105.450	14.48	1.61	-0.70	22.68	1.57	0%
10 sqmi	41.575	-105.450	14.48	1.61	-0.66	22.69	1.57	0%
50 sqmi	41.575	-105.450	14.48	1.61	-0.64	22.63	1.56	0%
100 sqmi	41.575	-105.450	14.48	1.61	-0.65	22.71	1.57	0%
250 sqmi	41.575	-105.450	14.48	1.61	-0.61	22.67	1.57	0%

Table H.14 - SPAS 1294 (Penrose, CO) hybrid storm OTF comparison using maximum point and areal averages.

	Target Latitude	Target Longitude	Max 6hr Rainfall	Slope	Y-intercept	Adjusted Rainfall	OTF	% Difference from Point
Point (NOAA Atlas 14)	41.575	-105.450	10.52	0.75	0.73	8.58	0.82	-
10 sqmi	41.575	-105.450	10.52	0.78	0.62	8.84	0.84	3%
50 sqmi	41.575	-105.450	10.52	0.79	0.54	8.81	0.84	2%
100 sqmi	41.575	-105.450	10.52	0.78	0.53	8.72	0.83	1%
250 sqmi	41.575	-105.450	10.52	0.77	0.53	8.60	0.82	0%
500 sqmi	41.575	-105.450	10.52	0.77	0.49	8.60	0.82	0%

Table H.15 - SPAS 1302, DAD zone 1 (Boulder, CO) general storm OTF comparison using maximum point and areal averages.

	Target Latitude	Target Longitude	Max 24hr Rainfall	Slope	Y-intercept	Adjusted Rainfall	OTF	% Difference from Point
Point (NOAA Atlas 14)	41.575	-105.450	12.44	0.66	-0.16	7.99	0.64	-
10 sqmi	41.575	-105.450	12.44	0.69	-0.23	8.40	0.67	3%
50 sqmi	41.575	-105.450	12.44	0.66	-0.05	8.17	0.66	1%
100 sqmi	41.575	-105.450	12.44	0.65	0.02	8.11	0.65	1%
250 sqmi	41.575	-105.450	12.44	0.64	0.11	8.06	0.65	1%
500 sqmi	41.575	-105.450	12.44	0.64	0.18	8.19	0.66	2%

Table H.16 - SPAS 1302, DAD zone 3 (Aurora, CO) general storm OTF comparison using maximum point and areal averages.

	Target Latitude	Target Longitude	Max 24hr Rainfall	Slope	Y-intercept	Adjusted Rainfall	OTF	% Difference from Point
Point (NOAA Atlas 14)	41.575	-105.450	10.51	0.82	-0.56	8.08	0.77	-
10 sqmi	41.575	-105.450	10.51	0.82	-0.52	8.07	0.77	0%
50 sqmi	41.575	-105.450	10.51	0.81	-0.48	8.06	0.77	0%
100 sqmi	41.575	-105.450	10.51	0.79	-0.36	7.95	0.76	-1%
250 sqmi	41.575	-105.450	10.51	0.76	-0.23	7.80	0.74	-3%
500 sqmi	41.575	-105.450	10.51	0.77	-0.17	7.96	0.76	-1%

Table H.17 - SPAS 1302, DAD zone 2 (Cheyenne Mtn, CO) general storm OTF comparison using maximum point and areal averages.

	Target Latitude	Target Longitude	Max 6hr Rainfall	Slope	Y-intercept	Adjusted Rainfall	OTF	% Difference from Point
Point (NOAA Atlas 14)	41.575	-105.450	12.46	0.56	0.35	7.30	0.59	-
10 sqmi	41.575	-105.450	12.46	0.56	0.34	7.38	0.59	1%
50 sqmi	41.575	-105.450	12.46	0.56	0.35	7.37	0.59	1%
100 sqmi	41.575	-105.450	12.46	0.56	0.35	7.39	0.59	1%
250 sqmi	41.575	-105.450	12.46	0.57	0.33	7.44	0.60	1%
500 sqmi	41.575	-105.450	12.46	0.60	0.28	7.74	0.62	4%

Discussion

In most cases evaluated, using an areal-average of precipitation climatology values results in different OTF values than using values from a single storm-center point only. The magnitude of the difference varies from storm to storm and generally increases with area size (at least to a certain point), but not always. The two non-orographic region storms, Elba, AL and Savageton, WY, both showed no significant difference between the point and areal-average OTF, as expected in topographically homogeneous areas.

The comparison for the storms over dynamic terrain becomes more complex. None of the three Eastern U.S. storms evaluated showed a significant difference between point or areal-average OTF values, despite two of these events occurring over very dynamic terrain. For the Western U.S. storms occurring over dynamic terrain the results varied somewhat. The Big Thompson Canyon, Deer Creek Dam, and Morgan storms exhibited a small to moderate percent difference between point and areal-average OTF values. The Cottonwood, UT storm centers exhibited very little change at areas less than 50 mi² but the percentages increased rapidly as area size got larger. This is due to the storm centers occurring at peaks or very high elevations among the Wasatch mountains where elevation, and the relating precipitation climatology drops off quite rapidly over relatively short distances. For this reason, the area sizes evaluated probably go far beyond what is representative of the peak rainfall for those storms and the point comparisons with areal averages beyond 10 or 20 mi² may not be particularly applicable to this evaluation, particularly for those storms.

Using areal-average precipitation climatology values may provide somewhat different OTF values than using a single point only in areas with significant topographic variation. The *most* correct approach should apply precipitation climatology values that are the most representative of the most critical precipitation for a given storm event. An areal-average approach introduces terrain beyond the storm center that undoubtedly contributed to the overall rainfall for the event. However, by using an average, the surrounding terrain is given the same “weight” as the terrain under the storm center even though it likely had a lesser contribution to the most extreme rainfall for the event. It can be assumed that farther away from the storm center, the less of an effect the underlying terrain would have on the most extreme rainfall for that event. If an areal-average was used, there would need to be a reasonable areal threshold determined that would strike a balance between too little area not providing a proper representative sample of the underlying terrain and too large of an area introducing terrain that is not applicable to the most extreme rainfall. This threshold would likely be different for every storm and, by necessity, would be highly subjective.

Recommendations

Currently the procedure employed by AWA for calculating OTF involves using only the precipitation climatology values at the storm center point location. Based on this evaluation of ten sample storms, AWA continues to recommend that the single point value be applied rather than an areal-average approach. This study evaluates many of the potentially *worst-case* scenarios, yet for small areas deemed to be the most representative to a storm's extreme rainfall, there is not a significant difference in resulting OTF values when using an areal-average. Furthermore, applying an areal-average approach introduces subjectivity that reduces confidence and technical complexities that reduce the practicality of the OTF analysis overall.

The point-based and areal-average methods both seek to predict the effects of a very complicated relationship between terrain and rainfall using a relatively straightforward approach. Although AWA currently suggests that a point-based approach is *more* appropriate than an areal-average approach for their gridded PMP studies, any new methods, technology, or information should always be considered and applied when appropriate.

Appendix I

HMR Storm Separation Method (SSM)

Applied Weather Associates, LLC (AWA) has reviewed the Storm Separation Method (SSM) as described in detail in HMR 55A and its application in HMR 57 and HMR 59. The SSM is used in hydrometeorological analysis to arrive at an approximation of the non-orographic component of precipitation from storms centered in orographic areas. The SSM was originally developed for HMR 55A (1988) as a standardized procedure to isolate and quantify orographic from non-orographic factors in record setting storms (HMR 59, Section 5.4). HMRs 57 and 59 refer to HMR 55A for details of the development of the SSM. The application of the SSM is described in HMR 57 and HMR 59 with some examples of the maps developed for each publication provided in various figures in Chapter 7 of HMR 57 and Chapter 6 of HMR 59. An attempt was made to acquire copies of the actual maps and data used in the computation of PMP for these publications. AWA visited the Hydrometeorology Design Studies Center (HDSC) December 8-10, 2008 to review archives of maps and working papers for HMRs 55A, 57 and 59. No maps or working papers are available for the SSM applications in those documents. Therefore, the review of the SSM is based entirely on information in HMRs 55A, 57 and 59.

Introduction

The initial review discussion describes the procedure presented in HMR 55A in detail. Maps from HMR 57 were digitized and computations completed based on the discussions in HMR 57. Results from these computations are compared with the HMR 57 PMP maps. Maps in HMR 59 were also digitized but not all maps for the SSM were available. Results from the limited information available are discussed.

The following discussion is extracted from the information provided in HMR 55A for the determination of Free Atmospheric Forced Precipitation (FAFP). The information is condensed to present major discussions. The complete text is available in Sections 6 and 7 of HMR 55A.

HMR 55A Section 6. APPROACHES

1.1 Introduction

HMR 55A states that estimation of PMP in orographic regions is difficult and storm data are limited. This is the result of a low population density that restricts the number of regular observing stations and also limits the effectiveness of supplementary precipitation surveys. In addition, the complicating effects of terrain on storm structure and precipitation must be considered. In HMR 55A, several procedures were investigated, but primary reliance was placed on a procedure that separates the effect of orography from the dynamic effects of the storm.

6.4 Storm Separation Method

It was necessary to find a procedure which would enable the precipitation potential for this diverse terrain to be analyzed in a consistent fashion. The precipitation that results from atmospheric forces (convergence precipitation) involved in the major storms in the region is defined. Convergence precipitation amounts were determined for the 24-hr 10-mi² precipitation amounts for all major storms in the region. These rainfall values were moisture maximized and transposed to locations where similar storms have occurred. The moisture maximized,

transposed values were then analyzed to develop a generalized map of convergence PMP throughout the region.

Values of convergence rainfall were increased for orographic effects that occur over the region. The orographic intensification factor is developed from the 100-yr 24-hr precipitation-frequency amounts of NOAA Atlas 2. Since the dynamic strength of a storm varies from the most intense 1-, 2-, 3-, or 6-hr period through the end of the storm, it is not appropriate to apply the same orographic intensification factor throughout the entire storm. To vary this intensification factor, a storm intensity factor was developed. The storm intensification factor reduced the effect of the orographic factor during the most intense rainfall period of the maximum 24 hours of the storm.

After determining the 24-hr 10-mi² PMP, 6-/24- and 72-/24-hr ratio maps were used to develop PMP values for these two other index durations for the 10-mi² area. Finally, a 1-hr 10-mi² PMP map was developed using a 1-/6-hr ratio map. These four maps provide the key estimates of general-storm PMP for the region.

6.5 Depth-Area Relations

The technique discussed in sections 6.3 and 6.4 provide 10-mi², or point, estimates of general-storm PMP for four index durations. Depth-area relations were developed utilizing data from the important storms of record in and near the study region to permit estimates for larger areas. These relations provide percentages to estimate PMP for areas as large as 5,000 mi². Different depth-area relations are required for disparate regions. Differences also exist between orographic and non-orographic portions of the study region. These differences resulted in a set of depth-area relations.

HMR 55A Section 7. STORM SEPARATION METHOD (SSM)

7.1 Introduction

It was considered necessary to find a property of observed major storm precipitation events that is only minimally affected by terrain so transposition of observed precipitation amounts would not be limited to places where the terrain characteristics are the same as those at the place where the storm occurred. The name given to this idealized property is "free atmospheric forced precipitation" (FAFP) which has been called "convergence only" precipitation in publications such as HMR No. 49. The definition of FAFP is the precipitation not caused by orographic forcing; i.e. it is precipitation caused by the dynamic, thermodynamic, and microphysical processes of the atmosphere. It is all the precipitation from a storm occurring in an area where terrain influence or forcing is negligible, termed a non-orographic area. In areas classified as orographic, it is that part of the total precipitation which remains when amounts attributable to orographic forcing have been removed. Factors involved in the production of FAFP are:

1. Convergence at middle and low tropospheric levels and often, divergence at high levels
2. Buoyancy arising from heating and instability

3. Forcing mesoscale systems, i.e., pseudo fronts, squall lines, bubble highs, etc.
4. Storm structure, especially at the thunderstorm scale involving the interaction of precipitation unloading with the storm sustaining updraft
5. Lastly, condensation efficiency involving the role of hygroscopic nuclei and the heights of the condensation and freezing levels.

It is emphasized that FAFP is an idealized property of precipitation since no experiment has yet been devised to identify in nature which raindrops were formed by orographic forcing and which by atmospheric forcing.

7.2 Glossary of Terms (partial list)

A_o : See P_a . It is the term for the effectiveness of orographic forcing used in module 3.

B_i : It is the term representing the "triggering effects" of orography. It is used in module 2. B_i is a number between 0 and 1.0 representing the degree of FAFP implied by the relative positioning of the 1st through i -th isohyetal maxima with those terrain features (steepest slopes, prominences, converging upslope valleys) generally thought to induce or "stimulate" precipitation. A high positive correlation between terrain features and isohyetal maxima yields a low value for B_i .

BFAC: 0.95 (RCAT). It represents an upper limit for FAFP in modules 2 and 5. See also the definition for PX.

DADRF: The depth-area-duration reduction factor is the ratio of two average depths of precipitation. $DADRF = RCAT/MXVATS$

DADFX: $DADFX = (HIFX)(DADRF)$.

It is used in module 2 to represent the largest amount of non-orographic precipitation caused by the same atmospheric mechanism that produced MXVATS.

F_i : See PCTHIFX: The largest isohyetal value in the non-orographic part of the storm. The same atmospheric forces (storm mechanism) must be the cause of precipitation over the areas covered by the isohyet used to determine HIFX and MXVATS.

I_m : That part of RCAT attributed solely to atmospheric processes and having the dimension of depth. Since it is postulated that FAFP cannot be directly observed in an orographic area, some finite portion of it was caused by forcing other than free atmospheric. The FAFP component of the total depth must always be derived by making one or more assumptions about how the precipitation was caused. The subscript "m" identifies the single assumption or set of assumptions used to derive the amount designated by I. For example, a subscript of 2 will refer to the assumptions used in module 2.

LOFACA: LOFACA is the lowest isohyetal value at which it first becomes clear to the analyst that the topography is influencing the distribution of precipitation depths. Confirmation of this influence is assumed to occur when good correlation is observed between the LOFACA isohyet and one or more elevation contours in the orographic part of the storm. The significance of LOFACA is that precipitation depths at and below this value are assumed to have been produced solely by atmospheric forces without any additional precipitation resulting from topographic effects; i.e., they represent the "minimum level" of FAFP for the storm.

$$\underline{\text{LOFAC}}: \text{LOFAC} = \text{LOFACA} + \frac{\text{AI}}{2} \left(\frac{(\text{AI})}{\text{PB}^2} - 1 \right).$$

It is a refinement to LOFACA based on the concept that AI may prejudice the assigning of a minimum level of FAFF.

MXVATS: The average depth of precipitation for the total storm duration for the smallest area size analyzed, provided that it is not larger than 100 sq mi.

OSL: Orographic Separation Line is a line which separates the region into two distinct regions. In one region, the non-orographic, it is assumed no more than a 5 percent change (in either increasing or decreasing the precipitation amount for any storm or series of storms) results from terrain effect. In contrast, the other region is one where the influence of terrain on the precipitation process is significant. An upper limit of 95 percent and a lower limit of no less than 5 percent is allowed. The line may exist anywhere from a few to 20 miles upwind (where the wind direction is that which is judged to prevail in typical record setting storms).

P_a (and A_a) is a ratio in which the effectiveness of an actual storm in producing precipitation is compared with a conceptualized storm of "perfect" effectiveness.

The SSM was developed because four distinct sets of precipitation were available for record-setting storms.

1. Reported Total storm precipitation, used in Module 1
2. Isohyet and depth-area-duration analyses of total storm precipitation, including Part I and Part II Summaries, used in Module 2
3. Meteorological data and analyses, used in Module 3
4. Topographic charts, used in all modules

It is noted that clearly the SSM depends on the validity of the input information.

The mechanics of the procedure used to arrive at FAFF are accomplished by completing the tasks symbolically represented in a MAIN FLOWCHART for the SSM along with its associated SSM MODULE FLOWCHARTS.

The validity of the techniques in the SSM depends on the validity of the concepts upon which they are based.

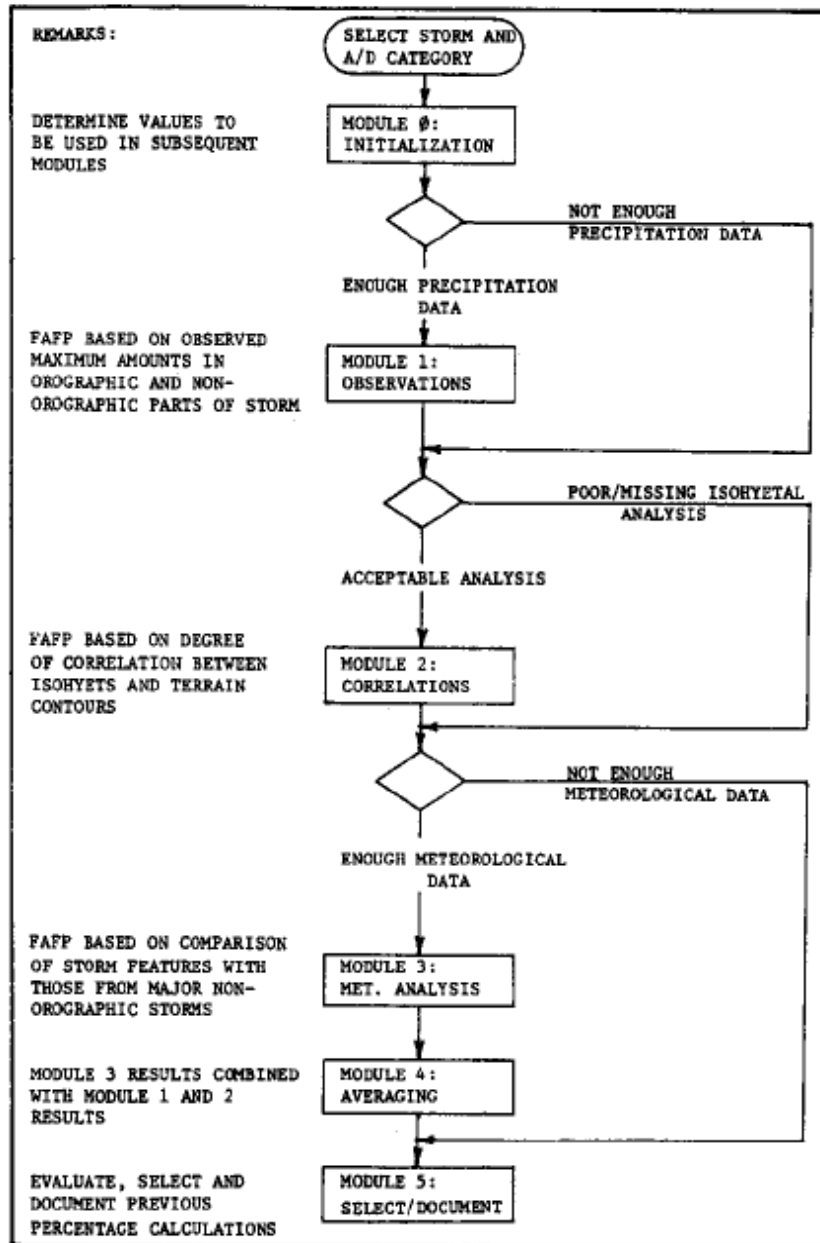


Figure 7.2.—Main flowchart for SSM.

SSM Modules from HMR 55A

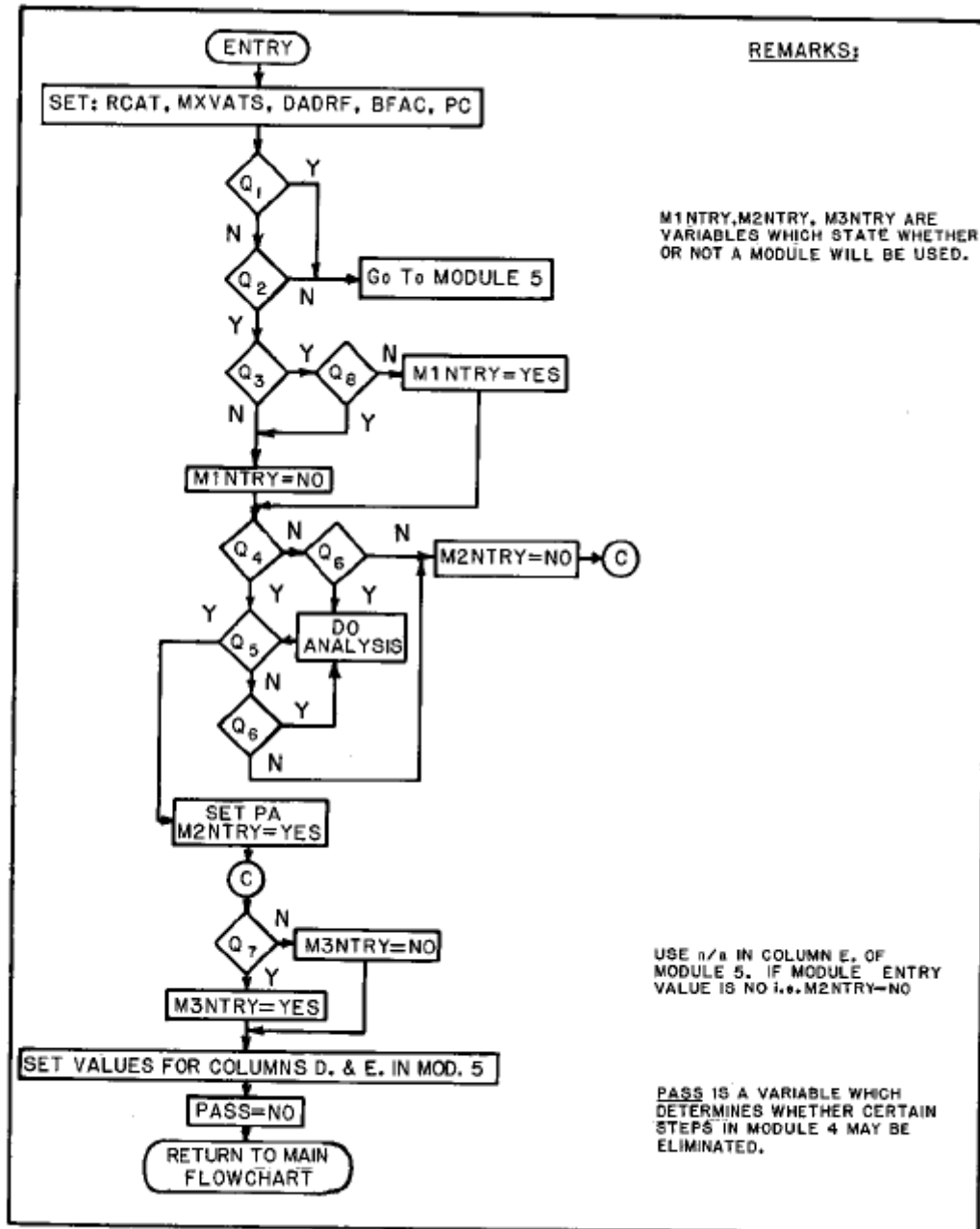


Figure 7.3.—Flowchart for module 0, SSM.

7.4.1.1 Module 0.

Module 0 is used to decide if there is adequate data available. A decision is made by the analyst if there are no data available, if the data are judged to be adequate or if the data are judged to be highly adequate. Values range from 1 for the lowest level to 9 for the highest level.

The analyst assigns the value that is considered most applicable. Questions that are asked include the following:

1. Is the isohyetal analysis reliable?
2. Is there adequate data in non-orographic areas to select a reliable value for non-orographic precipitation?
3. Is the highest observed precipitation in the non-orographic part of the storm equal to zero?
4. Are the data adequate to determine a ratio of the effectiveness of the actual storm in producing precipitation to a conceptual storm of "perfect" effectiveness?

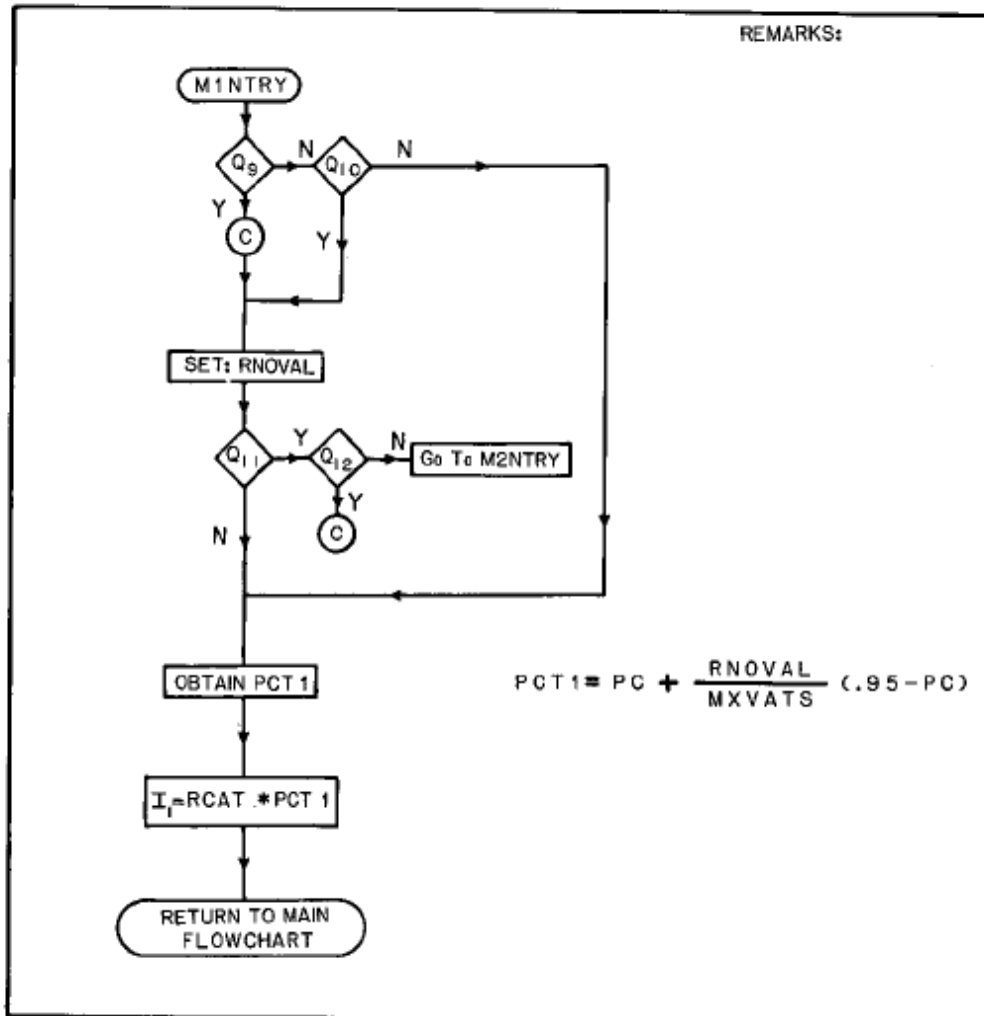


Figure 7.4.—Flowchart for module 1, SSM.

7.4.1.2 Module 1.

An analytical judgment must be made concerning the storm mechanism that resulted in the maximum precipitation over orographic regions and over non orographic regions. Questions asked include the following:

1. Is a review of the data needed?
2. Is the precipitation in the non-orographic region equal to the precipitation in the orographic region?

The reliability of the result of this module depends on the density of good precipitation observations on the date the storm occurred.

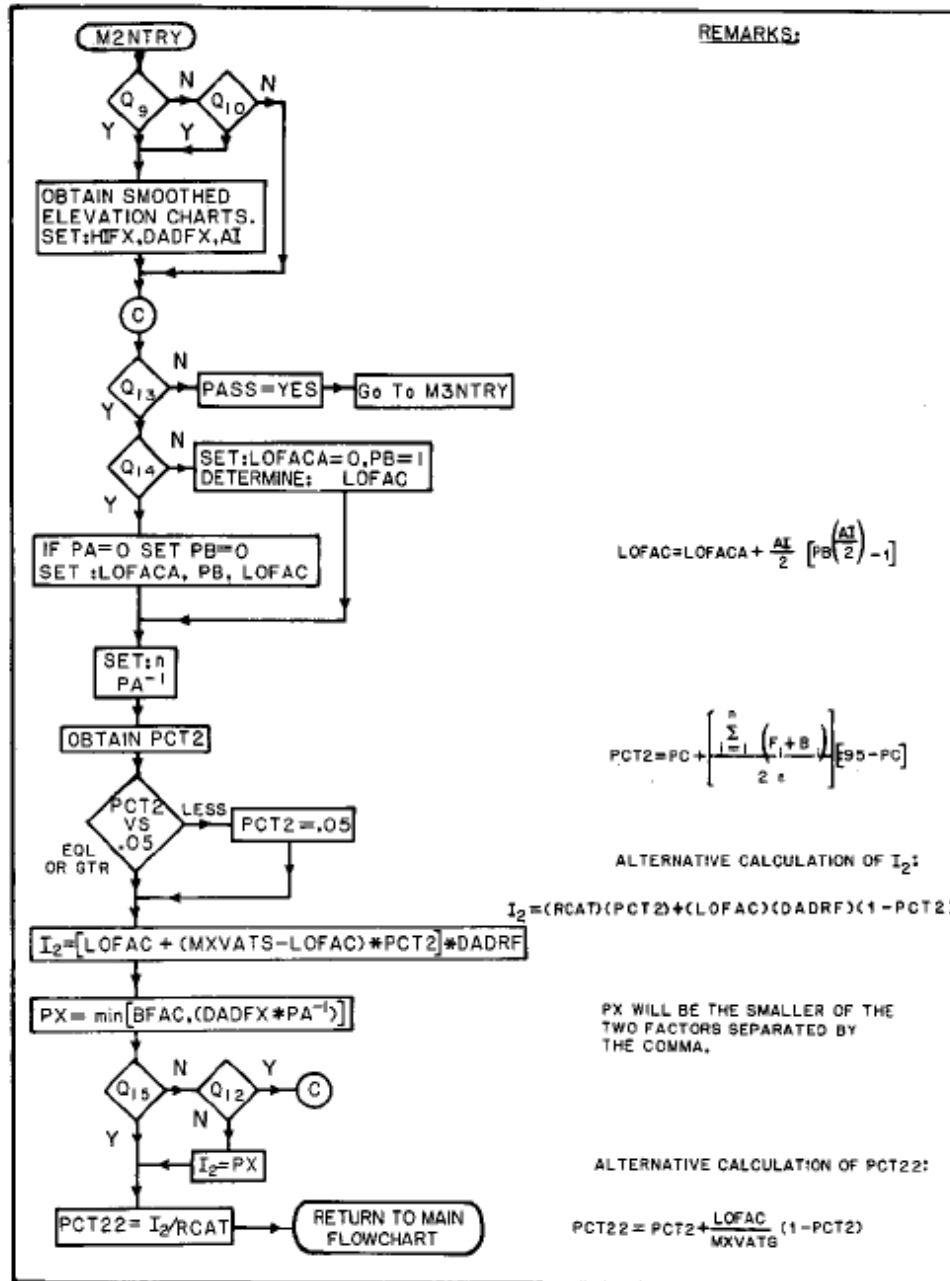


Figure 7.5.--Flowchart for module 2, SSM.

7.4.1.2 Module 2.

In this module, the average depth of precipitation is conceived of a column of water comprised of top and bottom sections. The limit to the top of the bottom section is set by the lowest isohyetal value at which it first becomes clear to the analyst that the topography is influencing the distribution of precipitation depths. The bottom section is conceived to contain only a minimum level of FAFP. The top section contains precipitation that results from orographic forcing or perhaps additional atmospheric forcing. A complex set of judgment

questions are asked to evaluate each section. As in module 1, an analytical judgment must be made. Some of questions asked are as follows:

1. Is a review of the data needed?
2. Can it be determined which isohyetal maxima controls the average depth?
3. Is there a good correlation between some isohyet and the elevation contours in the orographic part of the storm?
4. Is the average depth of precipitation that is FAFP less than or equal to the smaller of either the upper limit for FAFP in module 2 or the largest amount of non-orographic precipitation caused by the same atmospheric mechanism that produced the average depth of precipitation for the total storm duration for the smallest area size analyzed, provided that it is no larger than 100 square miles?

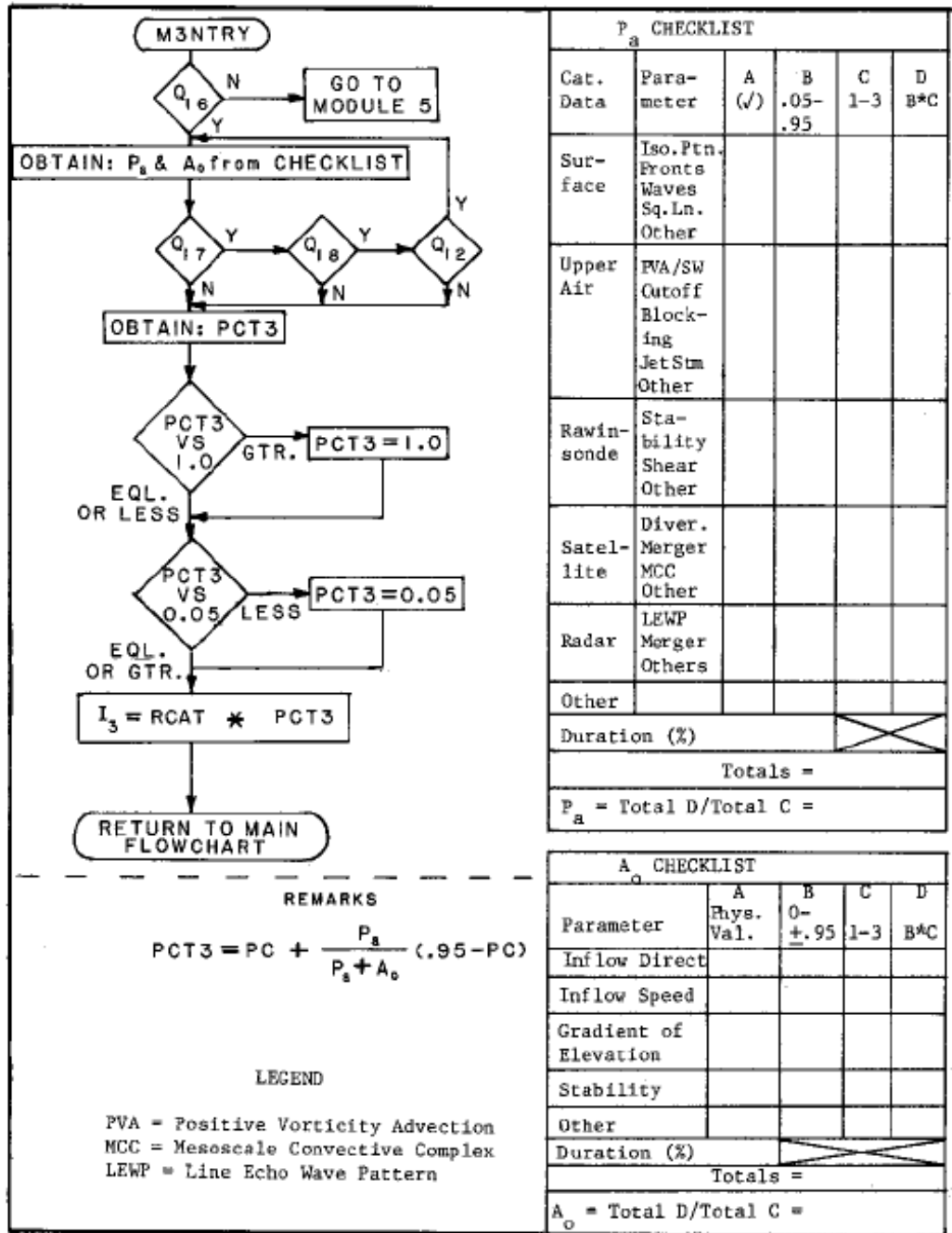


Figure 7.6.—Flowchart for module 3, SSM.

7.4.1.2 Module 3.

This module uses meteorological and terrain information to evaluate an appropriate level of FAFP. This is accomplished through evaluation of the ratio in which the effectiveness of an actual storm in producing precipitation is compared with a conceptualized storm of “perfect” effectiveness. In such a conceptual model, features known by experience to be highly correlated with positive vertical motions, or an efficient storm structure, would be numerous and exist at an

optimum (not always the largest or strongest) intensity level. The presence of one or more features that infer positive vertical motion, or which may contribute toward an efficient storm structure are identified. Then take as a basis for comparison an idealized storm which contains the same features or phenomena and indicate by selecting a number between 0.05 and 0.95, the degree to which the effectiveness of the selected actual storm features/phenomena approaches the effectiveness of the same features/phenomena in the idealized storm. If the quality and quantity of the information permits, the degree of convective-scale forcing may be distinguished from forcing due to larger scale mechanisms. Features may be assigned a weighted value in relationship to others. Meteorological data categories, for which there is not sufficient information from a particular storm, are disregarded in the ratio calculations.

The effectiveness of orographic forcing effects is determined. A vertical displacement parameter is determined using the component of the wind perpendicular to terrain slopes and the slope. The effectiveness is then compared with an idealized value representing 100 percent effectiveness. A stability effectiveness is assigned and combined with the vertical displacement parameter to determine a combined effect. The “model” in module 3 follows the concept that FAFP is directly proportional to the effectiveness of atmospheric forcing and inversely proportional to the effectiveness of the orographic forcing mechanisms.

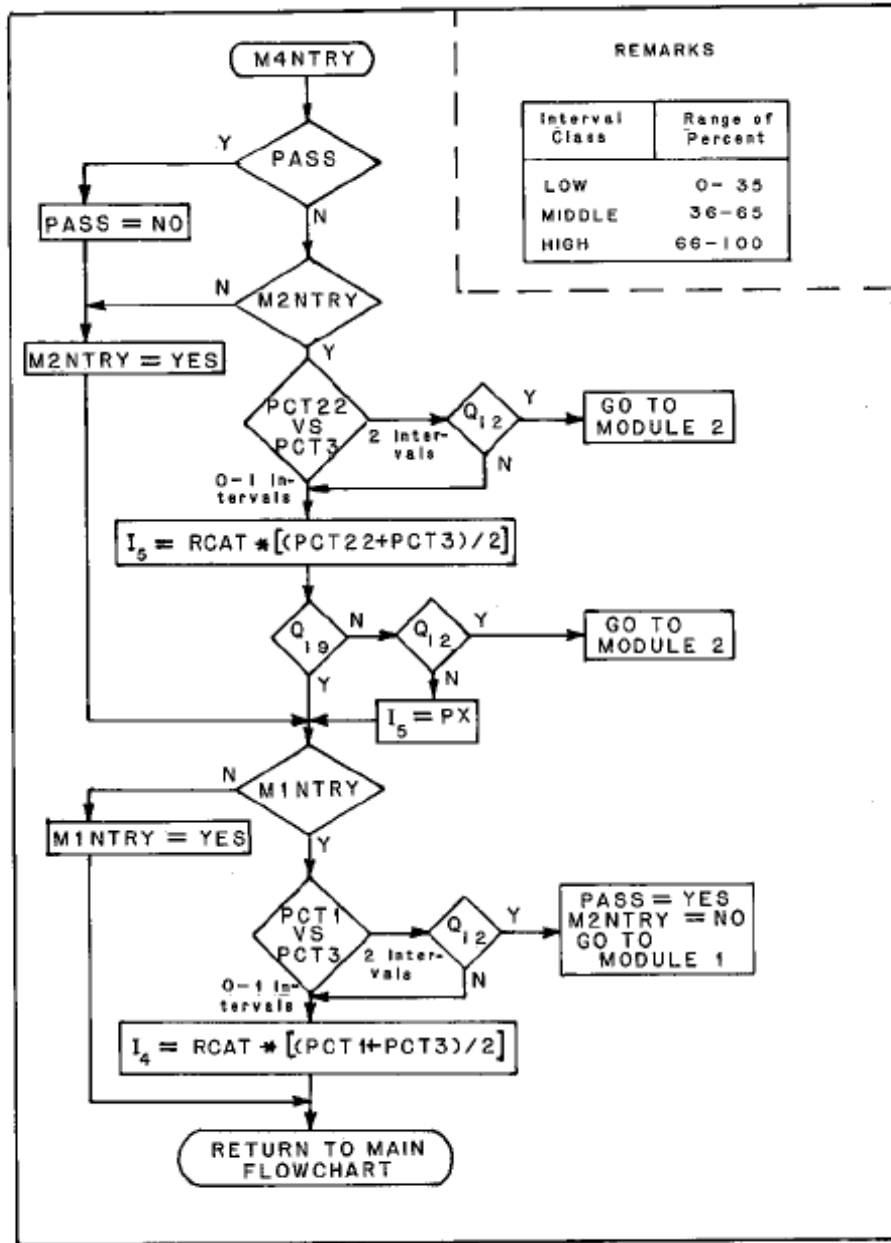


Figure 7.7.—Flowchart for module 4, SSM.

7.4.1.5 Module 4.

A basic assumption underlying the use of module 4 is that better results can be obtained by combining information; i.e., averaging the percentages obtained from the isohyetal analysis with the meteorological analysis and those obtained from analysis of the precipitation observations with the meteorological analysis. Better estimates are produced by averaging when there is little difference in the expressed preference for any one of the techniques or sources of information and, also, when the calculated percentage of FAFP from each of the modules exhibits wide differences.

Little is to be gained from use of the averaging technique over estimates produced by one of the individual analyses of modules 1, 2, or 3 when:

1. There are large differences in the expressed preference for the techniques of one module
2. The sources of information for one of the individual modules is definitely superior
3. The calculated percentages among the modules are in close agreement

DOCUMENTATION AND INDEX SELECTION						
STORM ID/DATE, REMARKS:						
MODULE	PARAMETER	VALUE	EVALUATION SCALE: COL.D 0-9; COL.E 1-9 MODULES 1-3; COL.F: IS THE SUM OF COLS. D&E. COL.D: HOW ADEQUATE IS THE INPUT INFORMATION FOR THE REQUIREMENTS SET BY MODULE'S TECHNIQUE. COL.E: HOW LIKELY IT IS THAT THIS TECHNIQUE WILL ESTIMATE THE CORRECT INDEX VALUE BASED ON ITS ASSUMPTIONS? FOR MODULE 4 SEE SELECTION RULE. OVERALL RULE: SELECT INDEX VALUE WITH LARGEST COL. F SCORE. LARGEST SUBSCRIPT BREAKS TIES.			
			REMARKS	D	E	F
∅	RCAT BFAC MXVATS DADRF PA PC					
1	RNOVAL PCT1 I_1					
2	AI LOFACA PB LOFAC HIFX DADFX PA^{-1} PX n $\sum(F_1 + B_1)$ PCT2 I_2 PCT22					
3	COLUMN	A	B	C		
	INFLOW DIR.	---				
	INFLOW SPD.	---				
	GRAD. ELEV.	---				
	w_0					
	STABILITY					
	A_0					
	SURFACE					
	UPPER AIR					
	RAOB					
	SATELLITE					
	RADAR					
	P_a					
	PCT3					
	I_3					
4	$(PCT22 + PCT3)/2$					
	I_5					
	$(PCT11 + PCT3)/2$					
	I_4					
RETURN TO MAIN FLOWCHART						

Figure 7.8.--Documentation form for SSM, module 5.

7.4.1.6 Module 5.

Module 5 is used for documentation. Values from the other modules are entered into the module 5 sheet. Assigning values involves subjectivity which must be the case because the “correct” value cannot be known and, hence, there is no way to know which of the various techniques used produces “correct” results most frequently. After a storm has been evaluated in each of the modules, all information is available to assign a value to the question “How likely is it that this technique will estimate the correct value based on the assumptions?” If confidence is high, assign a value of either 7, 8 or 9. If confidence is lower, assign a lower number. The scheme is designed to permit selection of one of the module results when there is a strong preference of one of them. The analyst must make a decision as to which module is to be preferred.

The final value selected for FAFP is determined by the largest value in module 5.

AWA Discussion on HMR 55A Modules

After reviewing the information provided above from Sections 6 and 7 of HMR 55A, several observations and conclusions have been made.

1. The procedures presented in HMR 55A are very detailed and following the procedures is at best very difficult since many of the parameters used are not standard meteorological parameters and their physical meaning is rarely intuitive.
2. The definition of terms in most cases includes other terms unique to this procedure and the relationship among parameters, even when a mathematical formula is provided, is not obvious when trying to associate physical characteristics to the combinations of parameters.
3. The formulas provided appear to have been subjectively derived with no obvious physical parameter associations connected through physical meteorological processes. In some cases, the process can be completed but other than a number to plug into a module, there is no meaning to the numbers that can be associated with the physical processes associated with extreme precipitation.
4. There are numerous places in the procedures where subjective evaluations are quantified with some explicit number where the number is no more than the opinion of the analyst. Then that number is used later in the procedure. In the final module, one of the critical inputs is, in the opinion of the analyst, how likely is it that the technique will estimate the correct value based on the assumptions? Examples of subjective decisions are as follows:
 - 1) B_i is the “triggering effect” of orography. It is a number between 0.0 and 1.0 representing the degree of FAFP implied by the relative positioning of isohyetal maxima lines with terrain features.
 - 2) I_m is that part of the average depth of precipitation solely attributed to atmospheric processes
 - 3) LOFACA is the lowest isohyetal value where it first becomes clear to the analyst that topography is influencing the distribution of rainfall depths.
 - 4) P_a and A_a are ratios in which the effectiveness of an actual storm in producing precipitation is compared with a conceptual storm of “perfect” effectiveness.

This is a very interesting subjective decision since if the analyst knew the effectiveness of the conceptual storm of “perfect” effectiveness, then one of the major unknowns in PMP determination is no longer an unknown.

- 5) The statement is made that the validity of the techniques in the SSM depends on the validity of the concepts upon which they are based. Since the concepts involve many subjective judgments, the SSM procedure is only as valid as those subjective judgments. Unfortunately the validity of those judgments vary from analyst to analyst with no way of objectively evaluating their reliability.
- 6) Module 4 makes seemingly contradicting statements. A basic assumption underlying the use of module 4 is that *better results can be obtained by combining information*; i.e., averaging the percentages obtained from the isohyetal analysis with the meteorological analysis and those obtained from analysis of the precipitation observations with the meteorological analysis. *Better estimates are produced by averaging when there is little difference* in the expressed preference for any one of the techniques or sources of information and, *also*, when the calculated percentage of FAFP from each of the modules exhibits *wide differences*.

Little is to be gained from use of the averaging technique over estimates produced by one of the individual analyses of modules 1, 2, or 3 when:

- There are large differences in the expressed preference for the techniques of one module*
- The sources of information for one of the individual modules is definitely superior*
- The calculated percentages among the modules are in close agreement*

The following discussion is extracted from the information provided in HMR 55A for the determination of the orographic factor. The information is condensed to present major discussions. The complete text is available in Section 9 of HMR 55A.

HMR 55A Section 9.2 Orographic Factor, T/C

Maps of 100-yr 24-hr precipitation from NOAA Atlas 2 were used to form a ratio of total 100-yr to convergence component 100-yr rainfall, T/C, and it was assumed that this ratio related to a ratio of similar parameters for PMP. The ratio of T/C can be used as a representative index of orographic effects.

The availability of the 100-yr 24-hr maps provides only part of the needed ratio, the total rainfall or numerator in the fraction, and it remains to determine how to obtain the convergence component, C. The rationale followed was that isopleths of the convergence component would exhibit a smooth, gradually varying geographic pattern. The gradients and general geographic variation would be somewhat similar to the FAFP component. HMR 51 has smooth PMP lines east of the 105th meridian and is assumed to be convergence only PMP, so NOAA Atlas 2 isopluvials for this region are also assumed to be convergence only.

The approach taken to determine C is to look at the 100-yr precipitation analysis for zones of least topographic effect. These zones would be tied together in some form of smooth analysis. A rough pattern of smooth contours was sketched. This provides a map of C. Using NOAA Atlas 2 and the map of C, T/C can be computed.

HMR 55A Section 9.3 Storm Intensity Factor, M

A storm intensity factor adjustment, M, was developed to relate the amount of precipitation that could be expected during the most intense precipitation period to the total amount of precipitation for a period. M varies with storm type.

The 6-hr interval was determined as the duration of the most intense precipitation period with the base period being the 24-hr duration. The storm intensity factor was defined as the ratio of rainfall in the maximum 6-hr period to the rainfall in the basic 24-hr period. M is obtained by dividing the FAFP for 6 hours by the FAFP for 24 hours.

By combining the results of the FAFP, T/C and M evaluations, then PMP can be computed using the FAFP and an orographic influence parameter, K. K is a function of the orographic factor, T/C. PMP is represented as the sum of two parts representing the core period and the remaining period. Through some mathematical combinations,
$$\text{PMP} = (\text{FAFP}) (K) = (\text{FAFP})(M^2 (1-T/C) + T/C)$$

AWA Discussion on HMR 55A Section 9

After reviewing the information provided above from Section 9 of HMR 55A, several observations and conclusions have been made.

1. NOAA Atlas 2 is based on statistical analyses of precipitation data observed within the NOAA Atlas 2 domain. Although NOAA Atlas 2 is being updated for various regions in the United States, it is the current return frequency analysis for this region and is based on evaluation of rainfall data, and hence has a basis for being objectively derived from rainfall observations.
2. C is the 100-year 24-hour convergence only component of rainfall. It is assumed that for regions where there is least orographic influence, NOAA Atlas 2 values approximate C. For regions where there is significant orographic influences, C is subjectively estimated since there are no observational data that provide only the convergence component of observed rainfall. Hence, C much like FAFP, is derived using very limited data and subjective analyses over regions where orographic influences are significant.
3. The M factor also has subjective decisions incorporated into its determination. The duration of the core rainfall period seems to be subjectively derived. For locations where a core period cannot be identified, $M = 0$.
4. For storms without large core precipitation periods, i.e. where M is small or 0, PMP is primarily dependent on FAFP, T and C. While T has basis for being objectively derived, FAFP and C are largely subjective determined. Hence PMP values computed using the SSM provide highly subjective PMP values.

HMR 57 SSM Application

Section 6 Storm Separation Method

The technique for developing FAFP used in HMR 55A is complex and involves the analyst tracking through a set of modules in which knowledge of observed conditions and experience are used to arrive at estimates of FAFP. The estimates are in turn weighted, based on the analyst's judgment of the amount and quality of overall information to obtain a result.

The SSM has undergone minor refinements since its development in HMR 55A. A decision about the level of FAFP for a storm may have to accommodate a fair amount of uncertainty. The questions asked in the SSM modules are formulated in such a way that analysts with different levels of experience could estimate different amounts of FAFP. Under such circumstances a consensus among analysts often leads to the best FAFP estimate for a storm, but the consensus process is not a necessary part of the SSM.

The SSM technique was considered most appropriate for the present study (HMR 57). The technique was applied directly according to original guidance, subject to modifications. A discussion is provided in HMR 57 with the comment that the discussion covers specific changes in details that may be beyond the casual reader's interest. Module 2 was not used to analyze any of the storms but the other modules were used to determine FAFP.

A map of C was constructed using regions of relative minima in the 100-year return frequency map. This was used together with the 100-year return frequency map to compute T/C. For some locations, the T/C maps were subjectively adjusted. The M-Factor for western Washington was determined to be zero so the K factors became T/C.

AWA Discussion on HMR 57 SSM Application

After reviewing the information provided above from Sections 6, 7 and 8 of HMR 57, several observations and conclusions have been made.

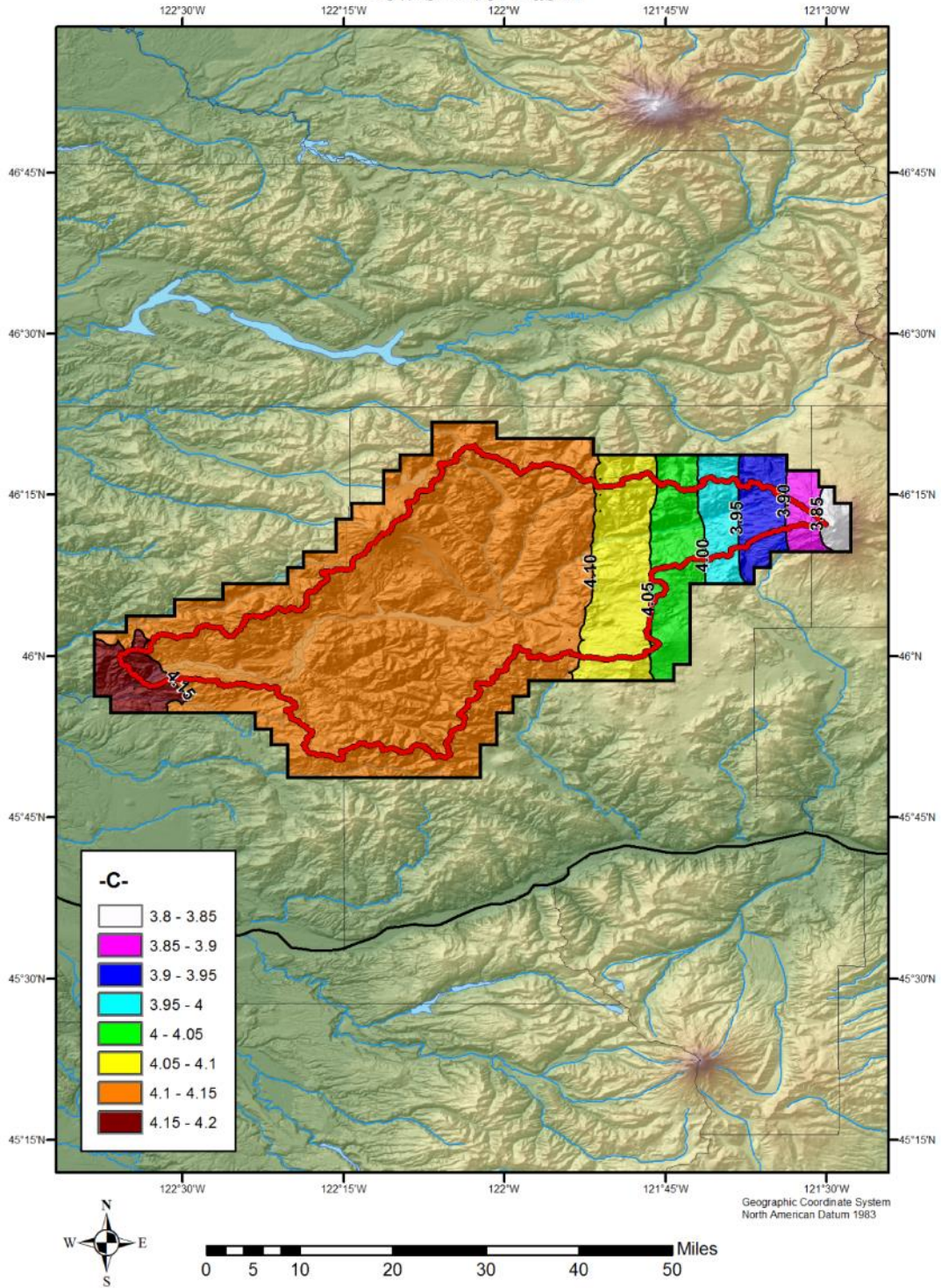
1. The discussion in Section 6 emphasizes that the SSM is complex, involves tracking through a set of modules in which knowledge of observed conditions and experience are used to arrive at estimates of FAFP, estimates are based on the analyst's judgment, and that there is a fair amount of uncertainty indicating that the authors of HMR 57 recognized major issues with the SSM. However, it was applied directly according to the original guidance in HMR 57.
2. The T/C maps were adjusted subjectively with no documentation on what adjustments were made or why.

As discussed earlier, the maps used for FAFP, C and M for computation of PMP in HMR 57 are not available from the HSDC. However, low resolution example maps are published in HMR 57 for these parameters that cover western Washington. Figure 8.1 shows the C map, Figure 8.2 shows the T/C map, Figure 8.3 shows the M factor map and Figure 8.4 shows the orographic factor K map for the Lewis River basin in southern Cascades of Washington state. These maps were digitized in GIS for analysis. Using the formulas in HMR 57 Chapter 8, maps

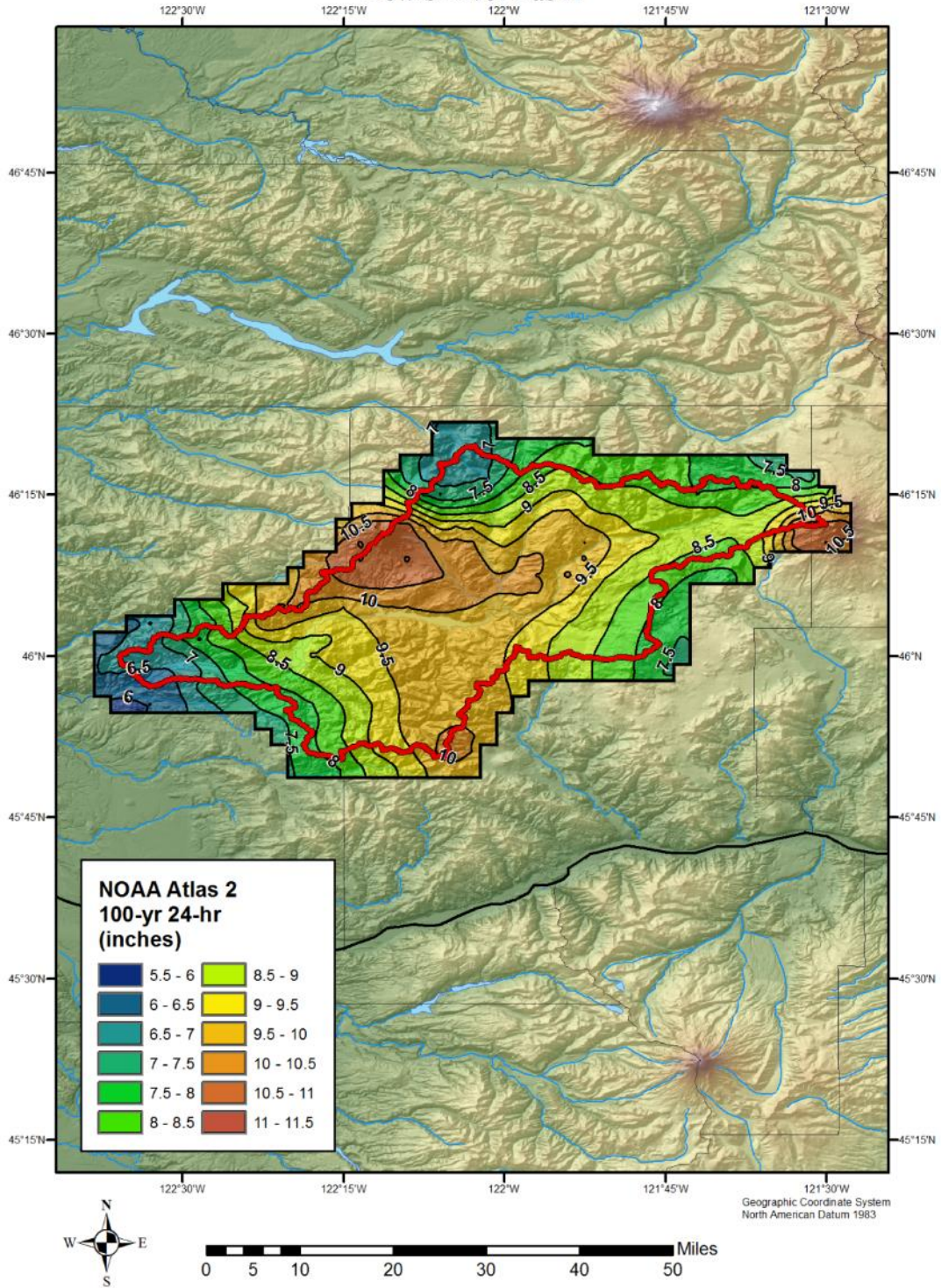
were produced from the digitized figure maps to compare with the maps shown in HMR 57. The Lewis River drainage basin in southern Washington was the domain used for the comparisons.

NOAA Atlas 2 provides the map for the 100-year 24-hour T values. Using the map of C from HMR 57 Figure 8.1, a map of T/C was computed. Since HMR 57 Figure 8.3 shows that $M=0$ for the Lewis River Basin, $K=T/C$. The computed T/C map was compared with HMR 57 Figure 8.4 (HMR 57 K). The NOAA Atlas 2 map, the HMR 57 maps for C and K, and the computed maps for K are shown below. The HMR 57 K map was compared with the computed K map and a percentage difference map is shown.

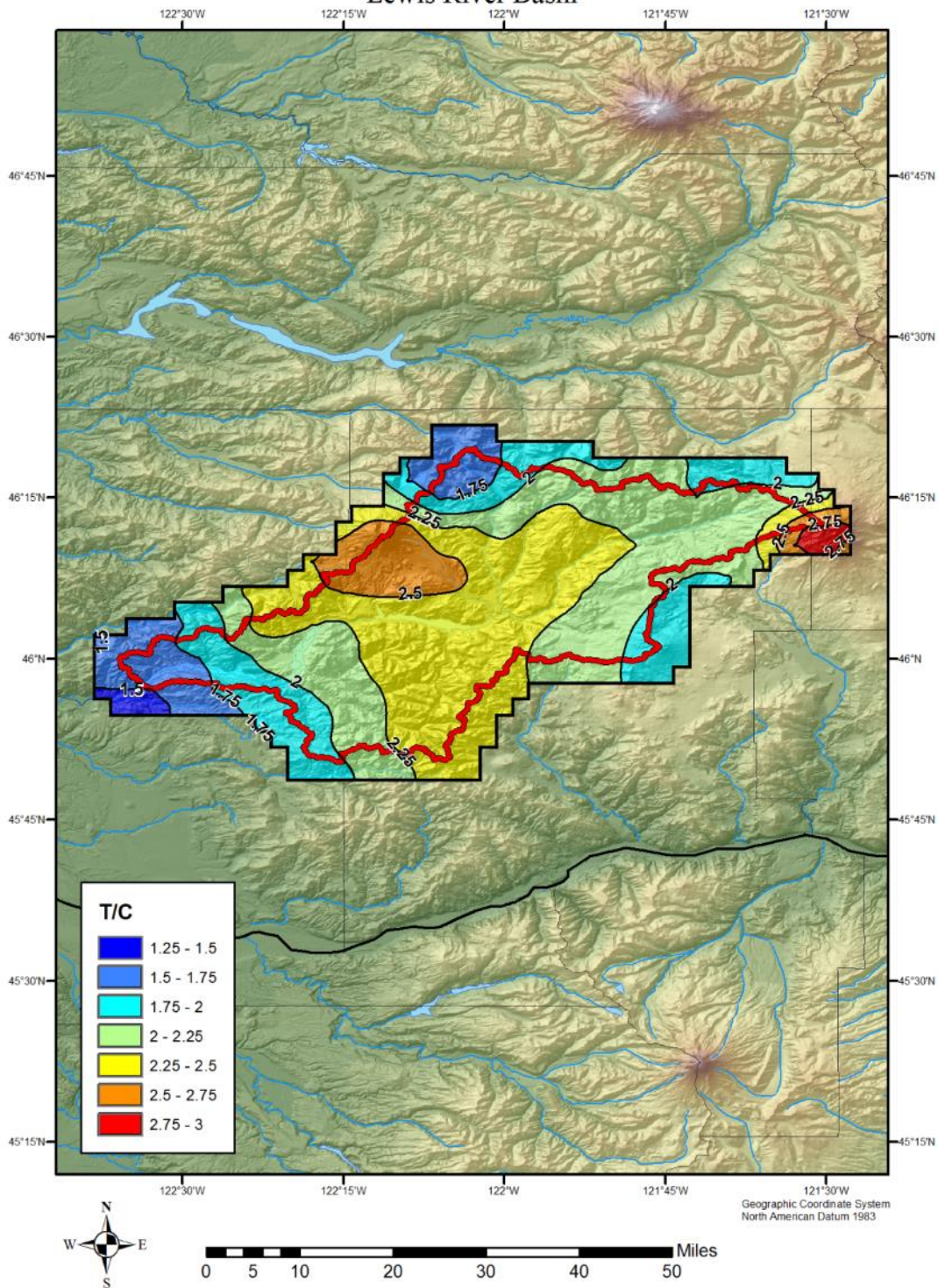
HMR-57 C (from fig 8.1)
Lewis River Basin



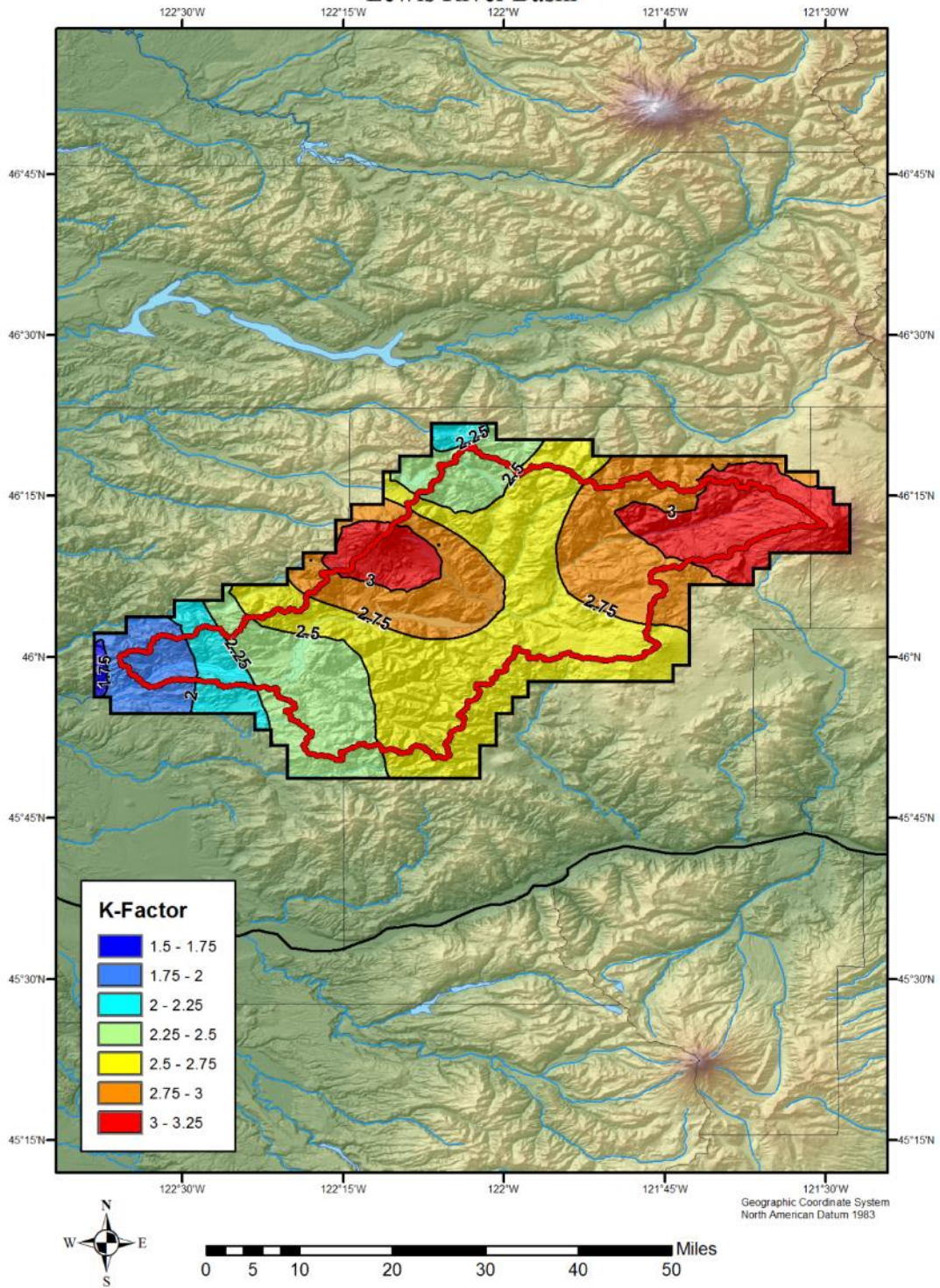
NOAA Atlas 2 100-year 24-hour Precipitation Lewis River Basin



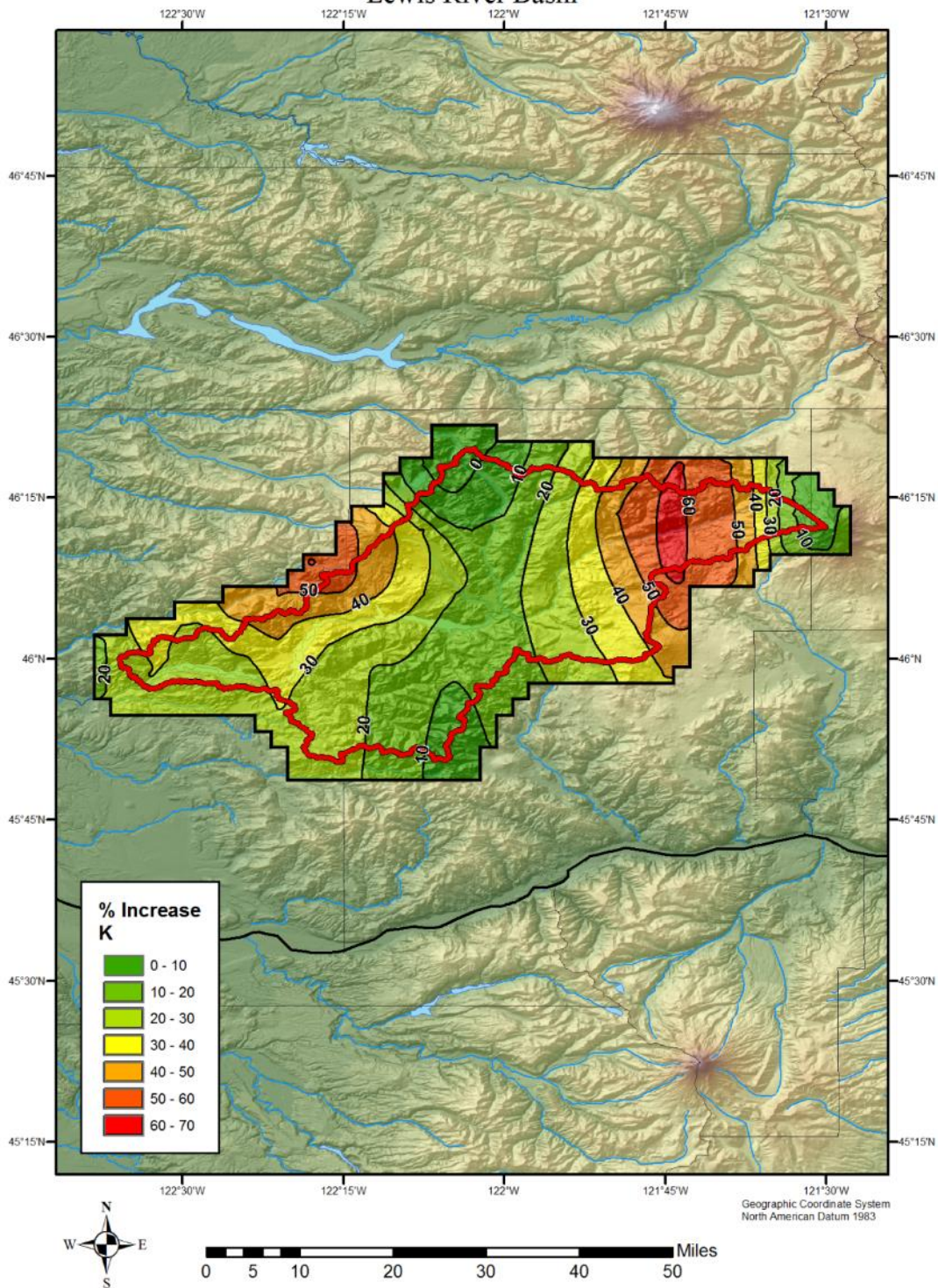
T/C - (NOAA Atlas 2 100-year 24-hour Precipitation ÷ HMR 57 C)
 Lewis River Basin



HMR-57 K-Factor (from fig 8.4)
Lewis River Basin



Percent Increase of HMR 57 K Values from T/C Values Lewis River Basin

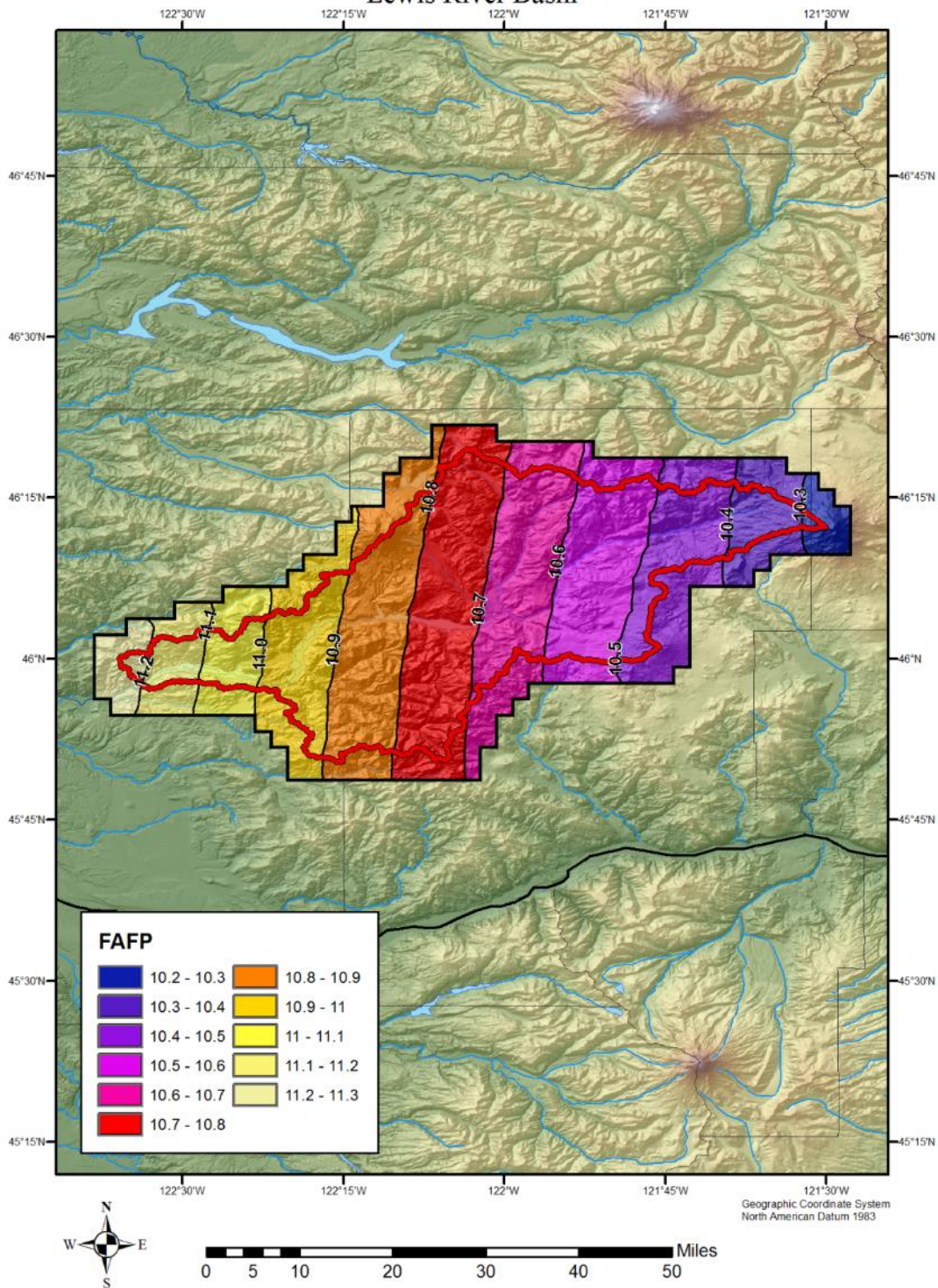


The comparison between the computed K map and the HMR 57 K map shows significant differences. Overall the computed K values are significantly smaller than the K values from HMR 57. The differences range from about 10% to over 60% with the HMR 57 values being consistently larger.

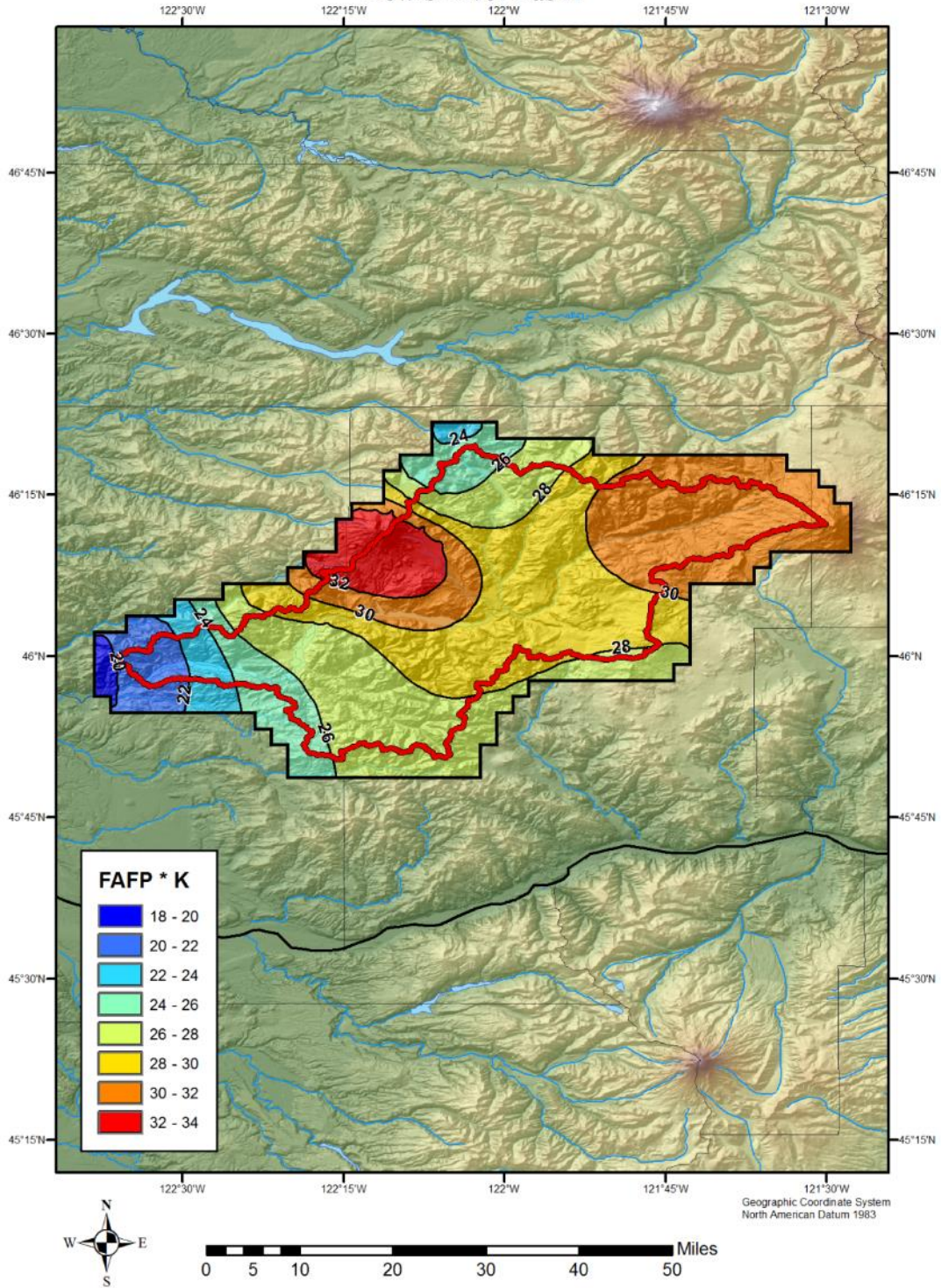
Having values for FAFP from HMR 57 Figure 7.2 and values for K from Figure 8.4, a map of PMP can be constructed using $PMP = (FAFP)(K)$. Figures showing these values are show below along with HMR 24-hour 10-mi² PMP values.

HMR-57 FAFP (from fig 7.2)

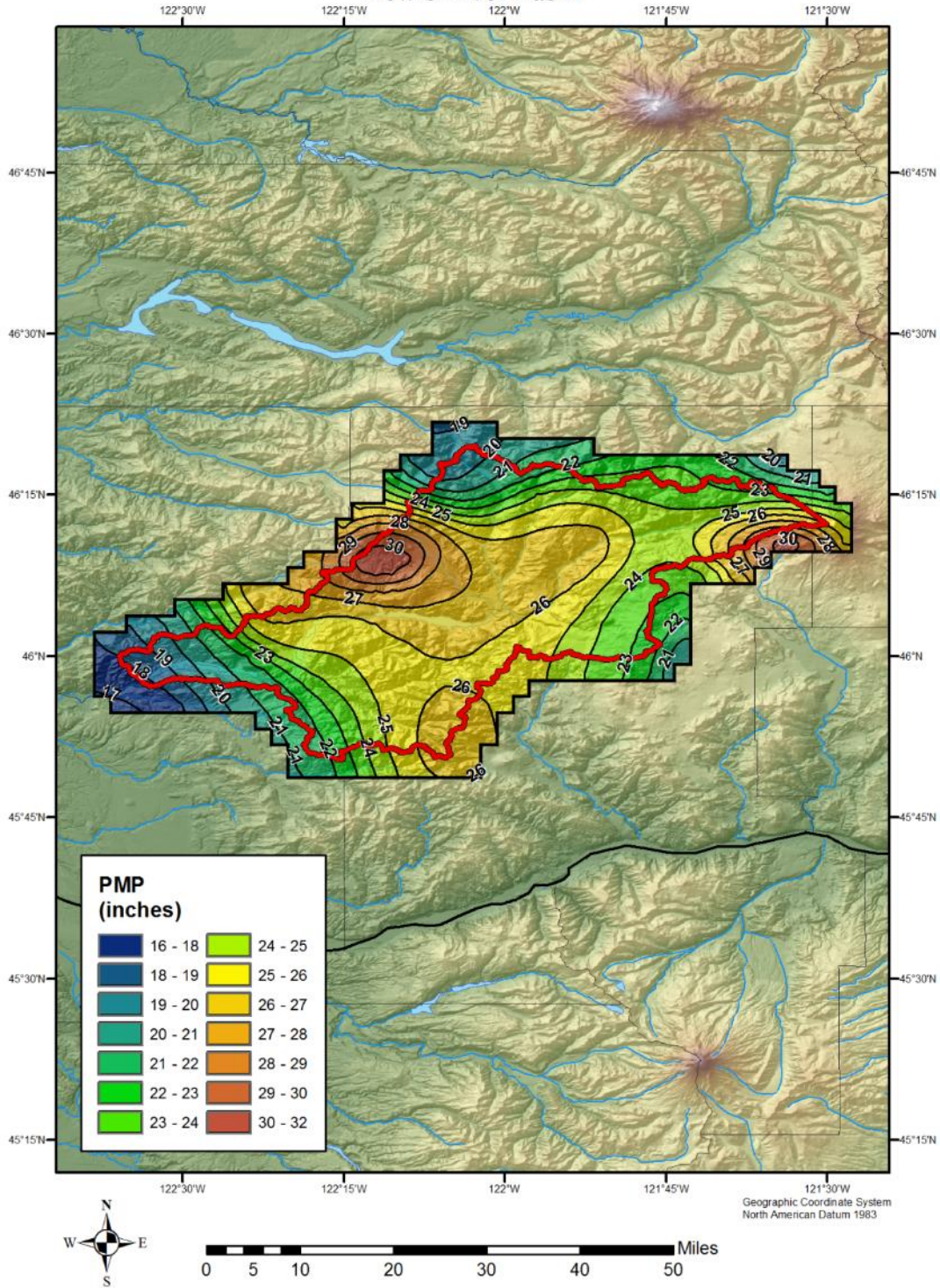
Lewis River Basin



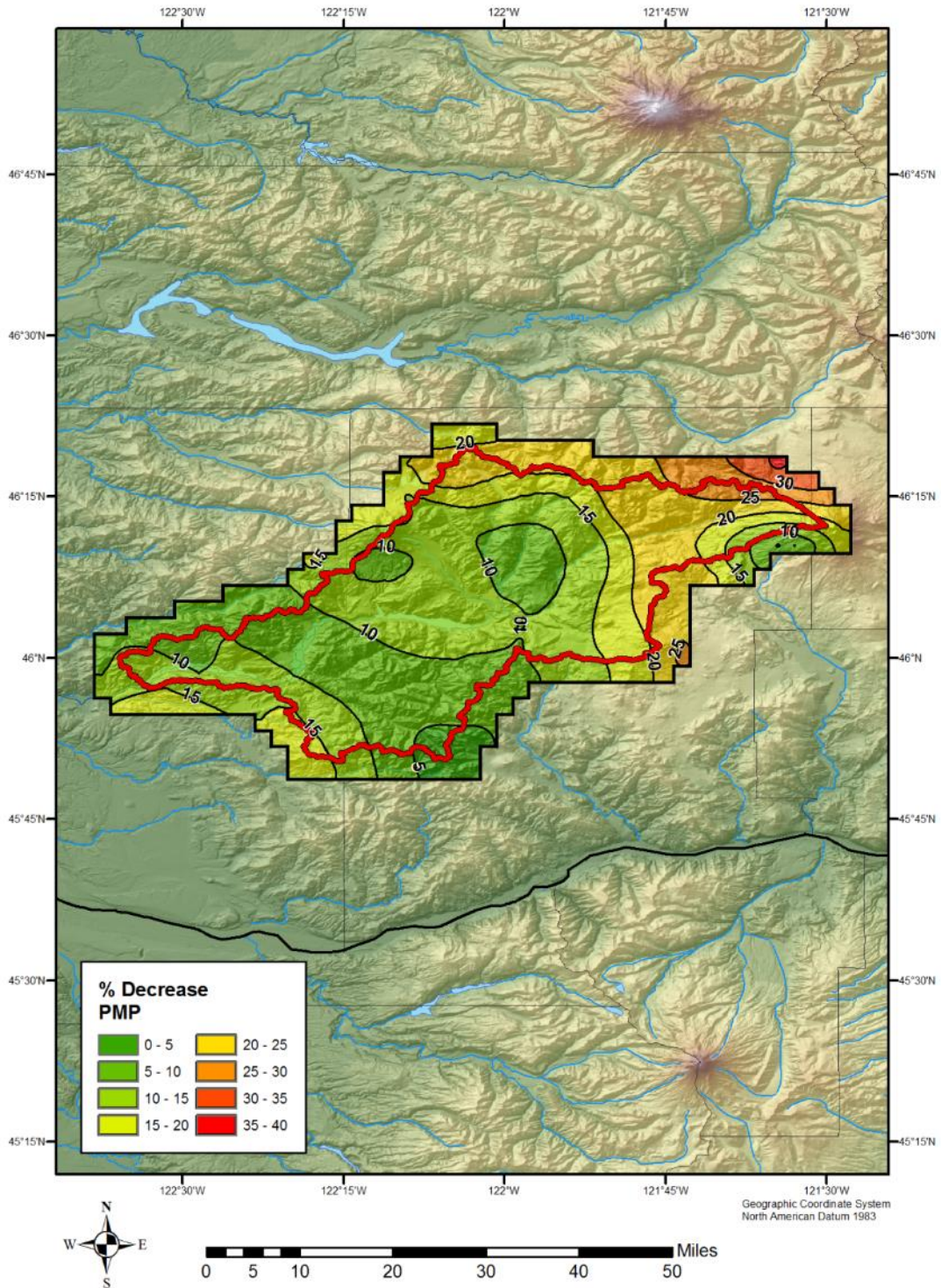
[HMR 57 FAFP] * [HMR 57 K]
Lewis River Basin



HMR-57 24-hour PMP Lewis River Basin



Percent Decrease in HMR 57 24-hr PMP Values from HMR 57 (FAFP * K) Values
Lewis River Basin



The comparison between the computed PMP map and the HMR 57 PMP map also shows significant differences. Overall the computed PMP values are larger than the PMP values from

HMR 57. The differences range from about 7% to over 25% with the HMR 57 values being consistently smaller.

The reasons for these differences are not known. It appears that after the highly subjective SSM procedure is followed, significant changes are manually made to the SSM maps and to the resulting maps of PMP produced using the SSM maps. The conclusion is made that for the Lewis River drainage basin domain, the SSM maps published in HMR 57 cannot be objectively duplicated and using the HMR 57 maps of SSM parameters, the HMR 57 PMP values cannot be objective duplicated.

HMR 59 SSM Application

A similar exercise was completed in the HMR 59 domain in and around the Piru Creek region and the Piru Creek drainage basin in southern California was used as the domain to compare computed maps with HMR 59 maps. Again none of the HMR 59 maps used to compute PMP was available from HDSC. Example low resolution maps for T/C (Figure 6.4), M-factor (Figure 6.5), and the K factor (Figure 6.6) for southern California are included in HMR 59. Unfortunately, the example map for FAFP (Figure 6.3) was for northern California and no example map of C is included in HMR 59. Therefore comparisons of computed maps with HMR 59 maps are limited.

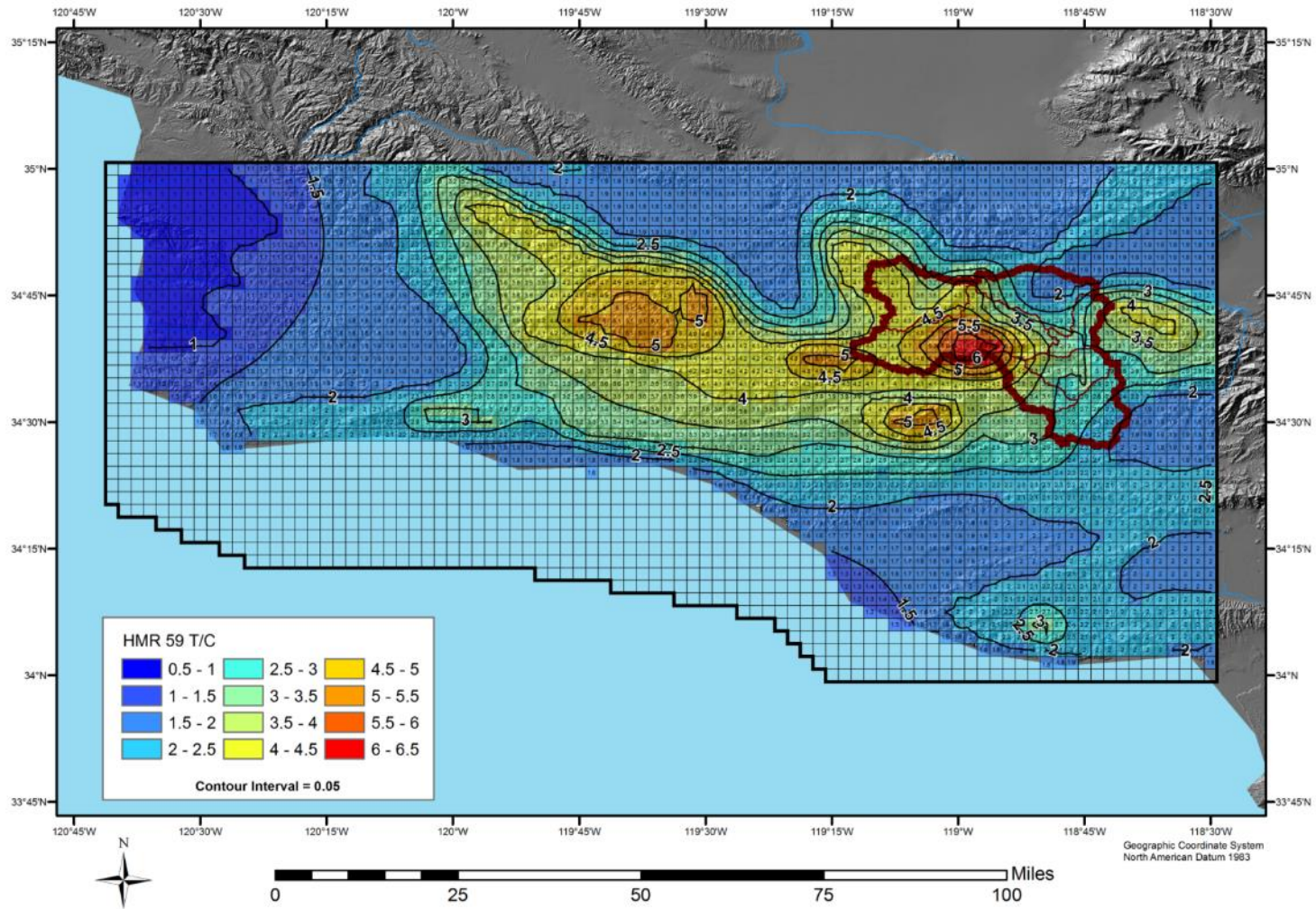
Using the example maps in HMR 59, maps for C and FAFP can be constructed. Unfortunately by constructing these maps, independent comparisons with HMR 59 maps is not possible. Figure 6.4 provides a map of T/C. By inverting the values on this map, a map of C/T was produced. That map is then multiplied by the NOAA Atlas 2 map (T) to produce a map of C. The M-factors for the Piru Creek drainage basin can be determined from Figure 6.5 and of course the PMP values for the Piru Creek domain are available from the HMR 59 PMP maps. Using Equation 6-5 from HMR 59,

$$K = M^2 (1 - (T/C)) + T/C$$

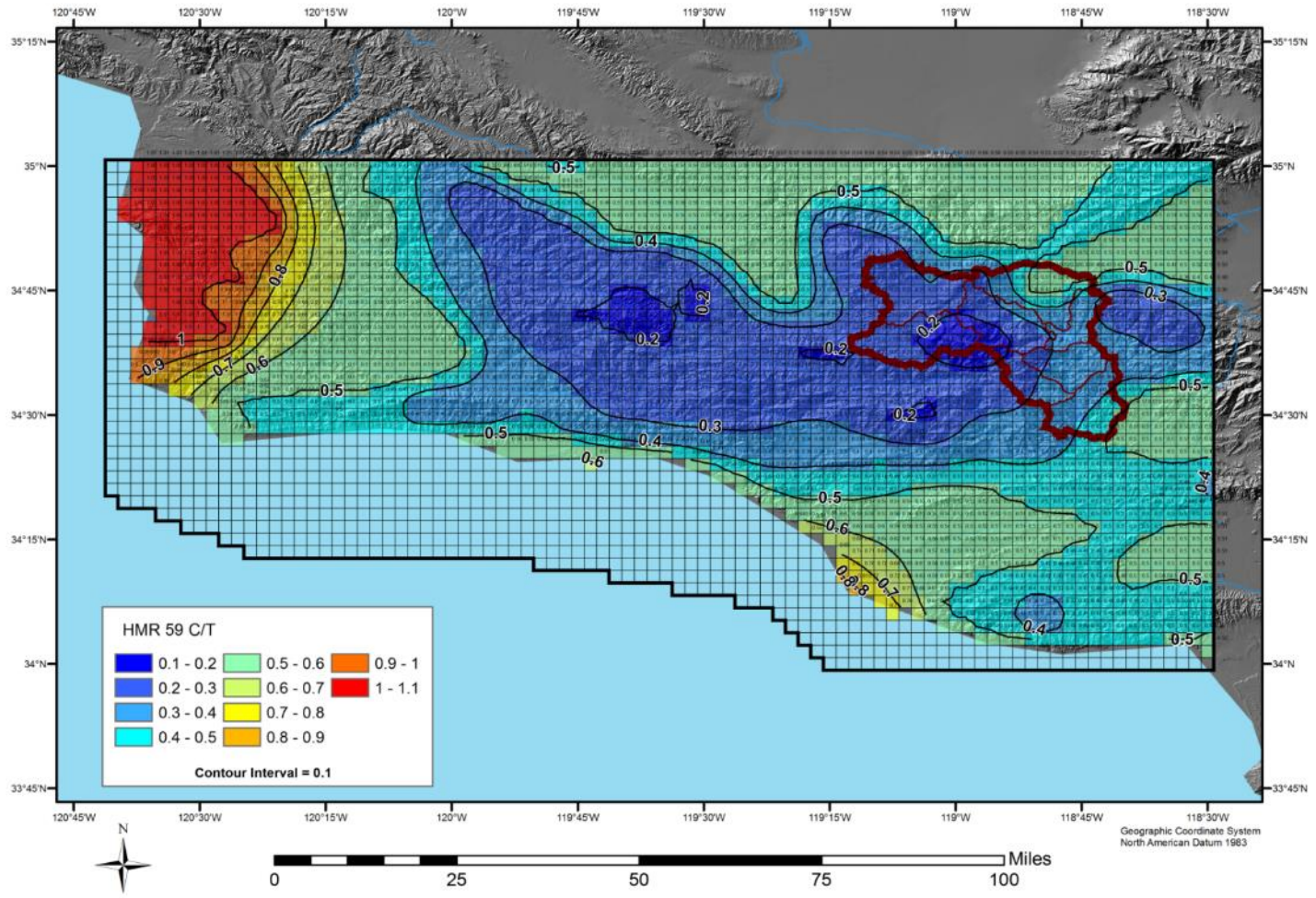
a computed map of K can be constructed.

HMR 59 maps and computed maps are shown below:

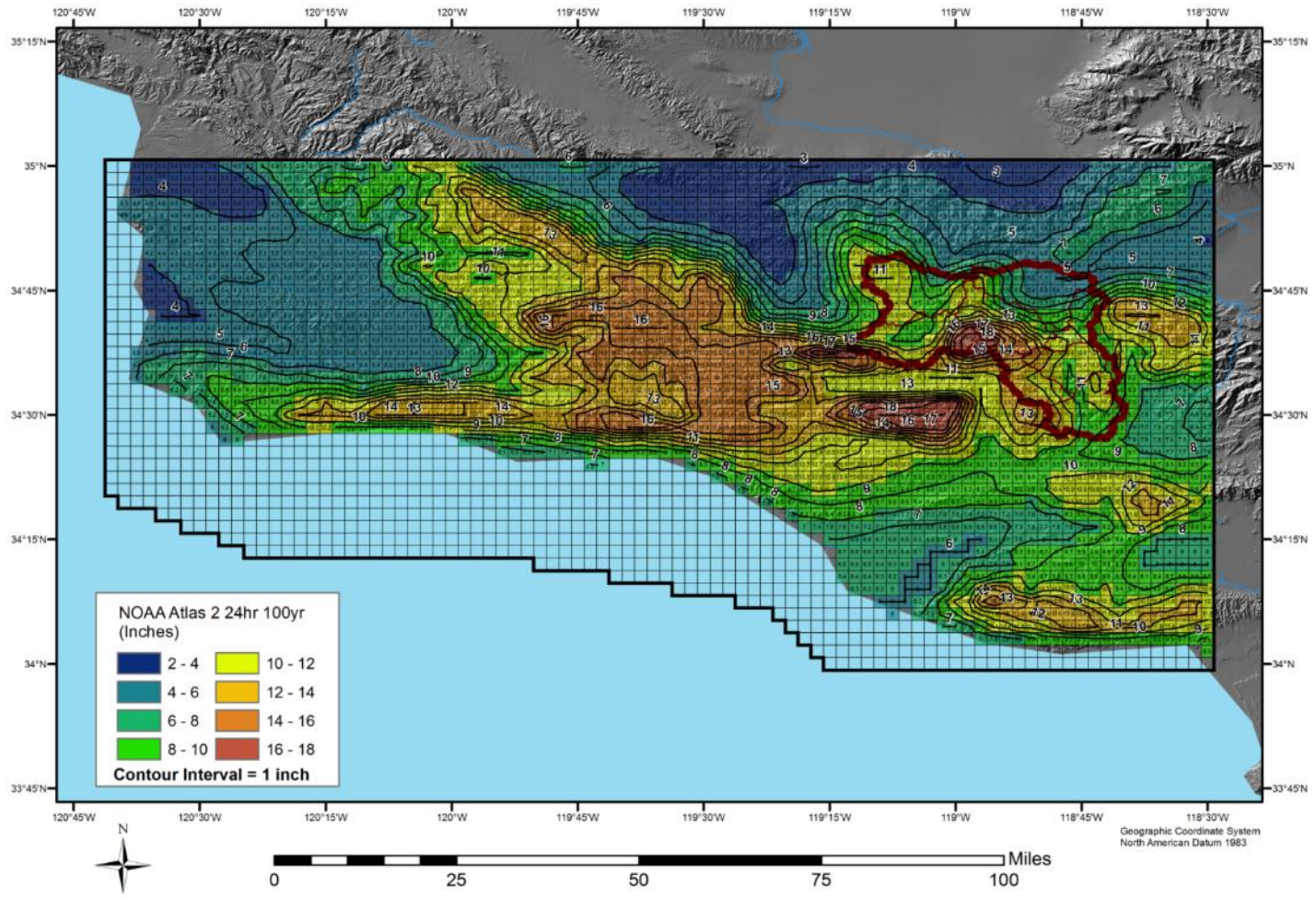
HMR 59 T/C



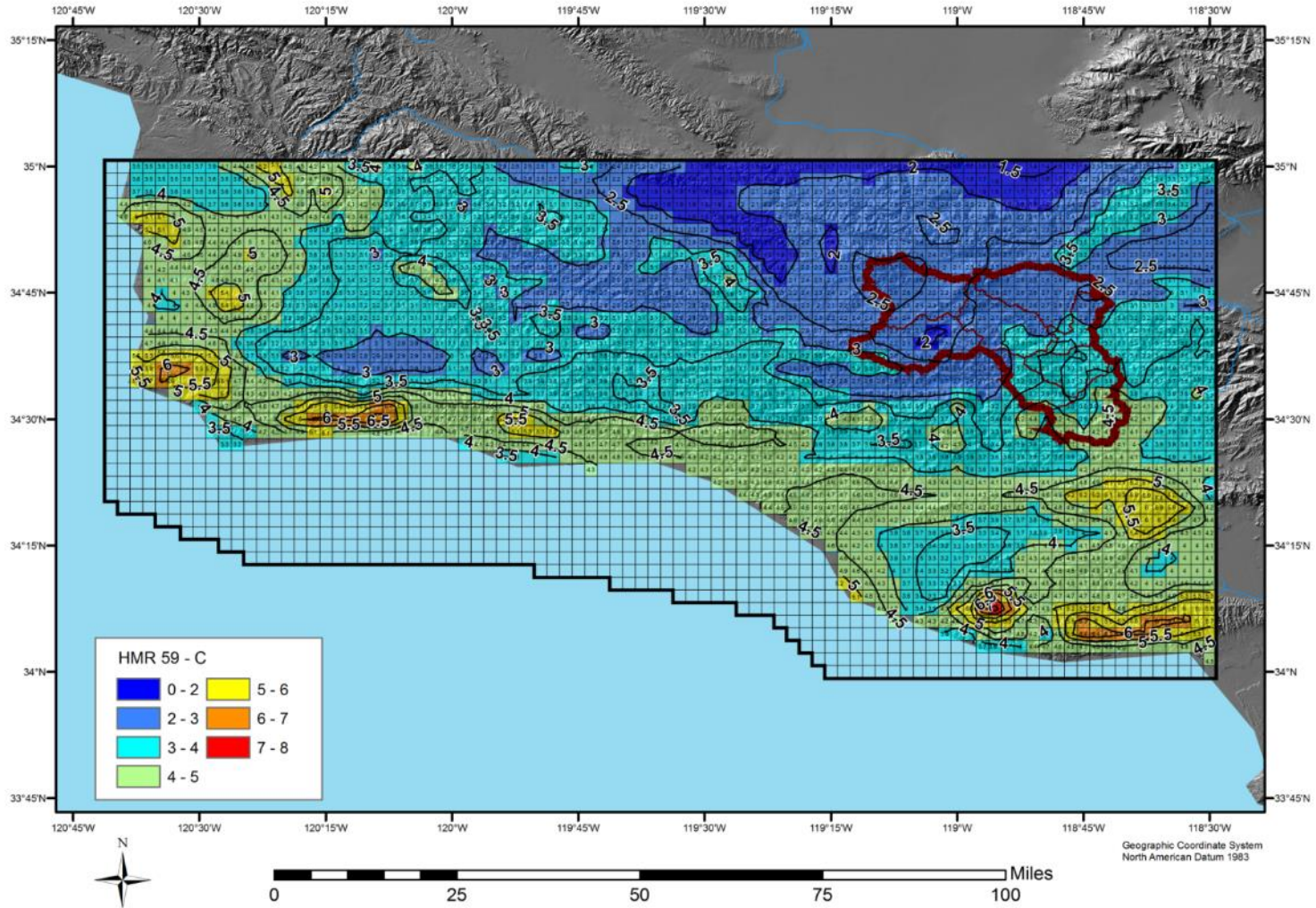
HMR 59 C/T



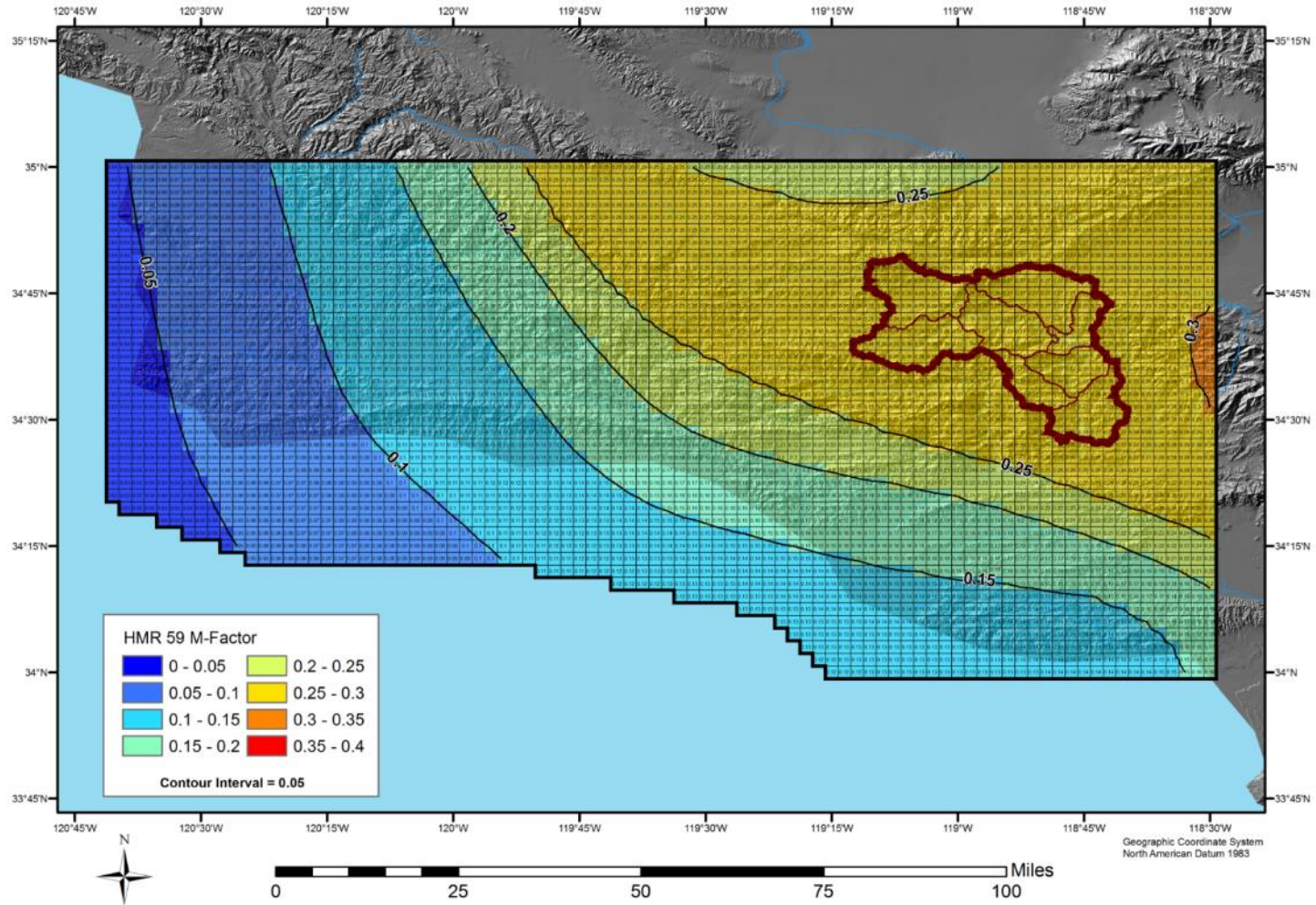
NOAA Atlas 2 - 24-hour 100-year Precipitation Frequency Estimates



HMR 59 100-year Convergence Component "C"

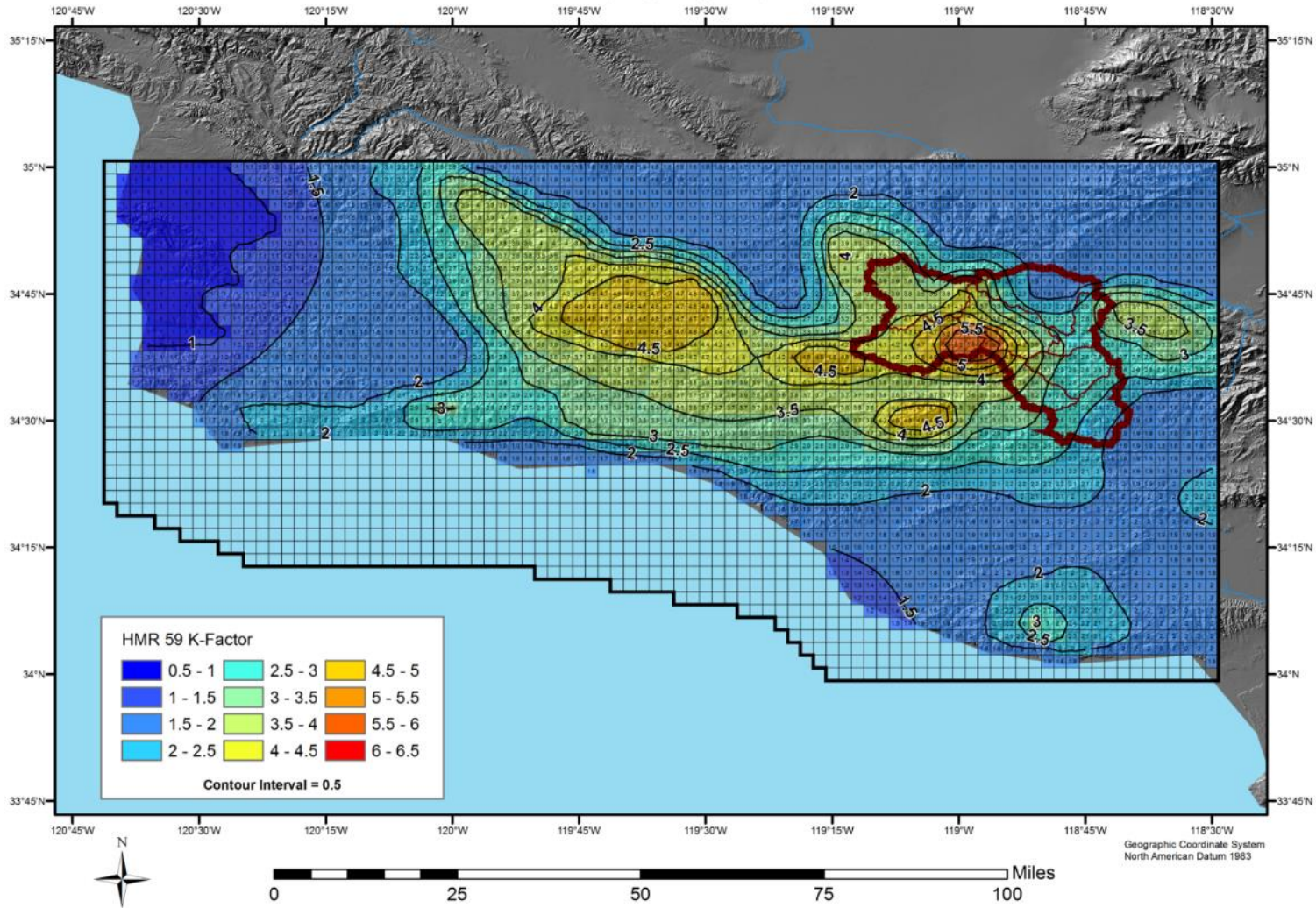


HMR 59 M-Factor

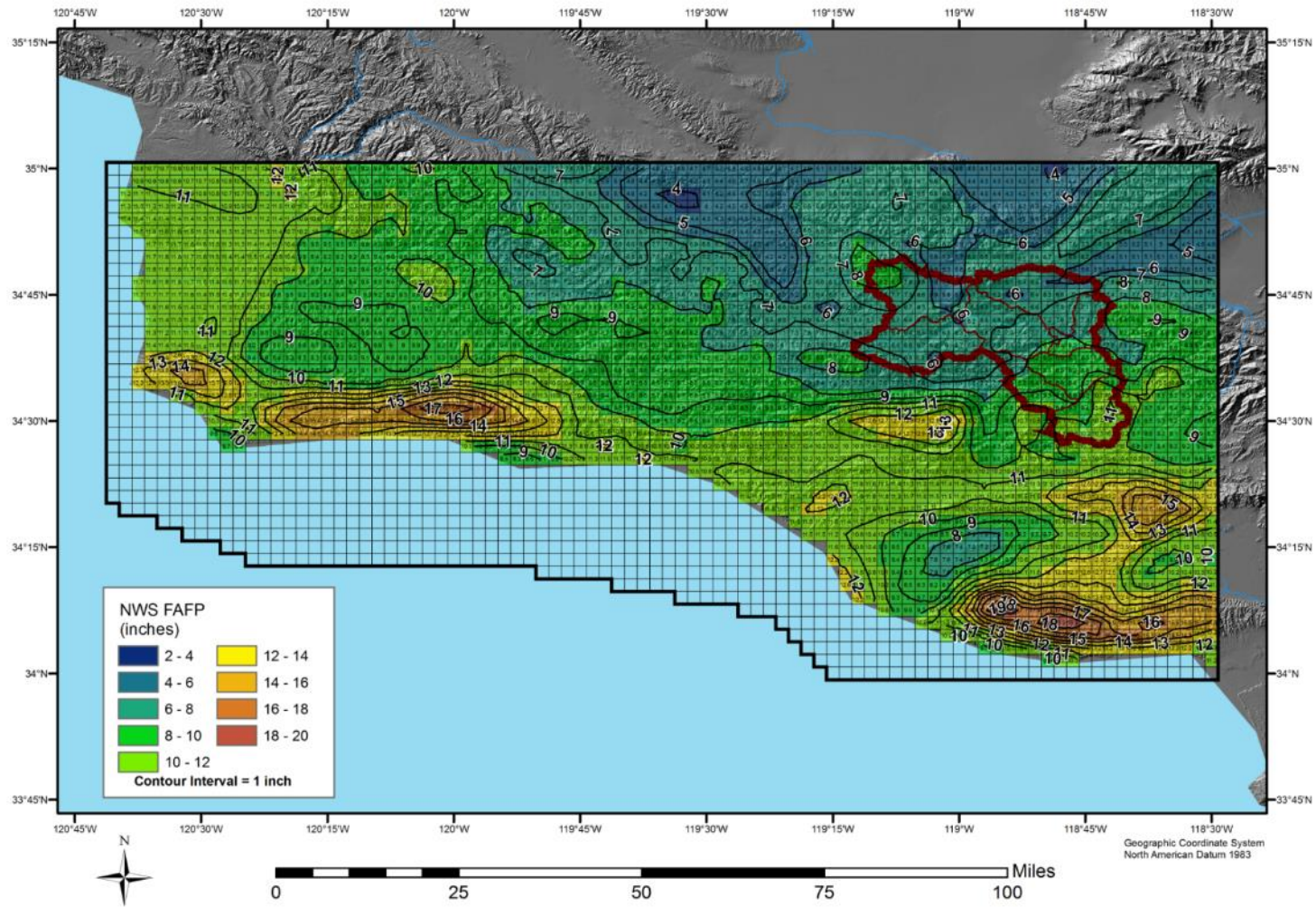


AWA Produced K-Factor

$$K = M^2 (1 - (T/C)) + (T/C)$$



$$\text{NWS FAFP} = \text{PMP} \div K$$



There are several significant observations from these maps. The 100-year C map has been constructed using the HMR 59 T/C map and the NOAA Atlas 2 map for T. Since this map is the 100-year rainfall produced from storm dynamics without any influence from underlying terrain, the gradients of rainfall should be relatively smooth. The C map from HMR 57 shown previously shows a relatively smooth analysis. The constructed C map from the HMR 59 data shows areas of large gradients, especially for coastal regions. Since this map is subjectively constructed in the SSM procedure, the large gradient areas were manually introduced into the analysis for unknown reasons.

A similar observation is made for the constructed FAFP map. FAFP is the rainfall produced by a storm from atmospheric dynamics without the influence of the underlying topography. The FAFP map from HMR 57 shown previously shows a relatively smooth analysis. The large rainfall gradient areas in the FAFP map (HMR 59 Figure 6.3-see below) indicate that subjective adjustments were made to the FAFP map which introduced artificial gradients from the coast through the Central Valley and into the Sierra Nevada.

The K factor map in HMR 59 was compared to the computed K factor map using values for M, C and T from HMR 59 and from NOAA Atlas 2. The comparison resulted in good agreement for the region surrounding the Piru Creek drainage basin.

An interesting region to look at is the relatively non-orographic region between Lompoc and Santa Maria, approximately 120.5W and 34.75N. Both the HMR 59 K factor map and the computed K factor map identify values of M to be approximately 0 and K to be approximately 1. Hence for this area PMP is approximately equal to FAFP.

According to the discussions related to the SSM, the FAFP map is constructed using storm data for regions where K is approximately equal to 1, i.e. regions where orographic influences are at a minimum. This region seems appropriate for K to be approximately 1. The FAFP values in this region are between 11 inches and 12 inches, consistent with the HMR 59 PMP values of approximately 12 inches. However, the largest maximized storm rainfall from storms analyzed for the Piru Creek site-specific PMP study for this region is 4.5 inches from the January 1943 storm. It is not obvious how the largest maximized storm rainfall was increased from 4.5 inches to 11.5 inches resulting significantly larger FAFP values than those from maximized storm rainfall values. It can only be assumed that use of the various subject producers and decisions was applied. These subjective changes drastically affect the final PMP values developed for HMR 59 and of course or not reproducible.

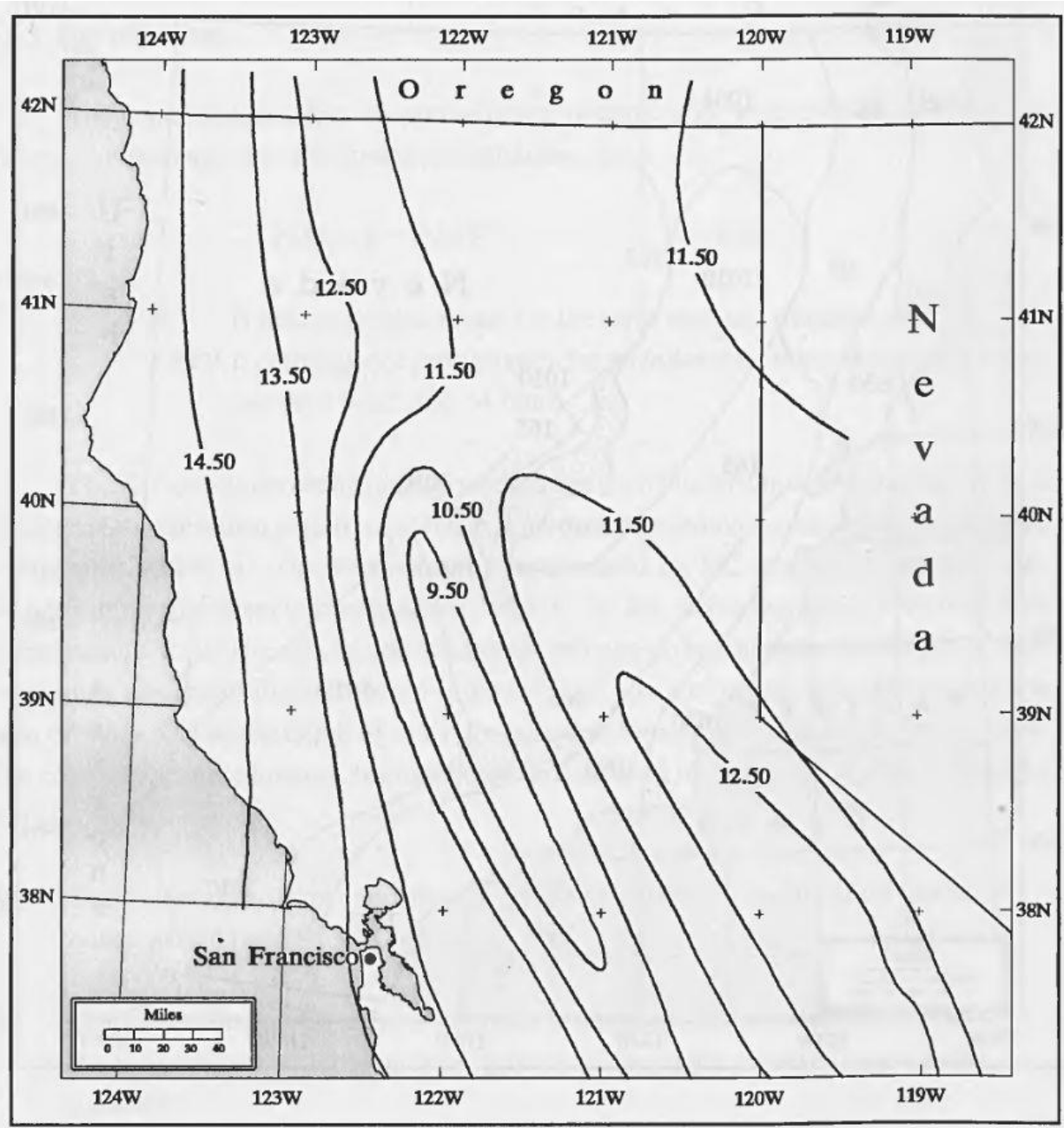


Figure 6.3. *Non-orographic PMP (FAFP) at 1000 mb (inches of rainfall).*

HMR 59 Figure 6.3 FAFP map for northern California

Summary

Discussions on the development of the SSM from HMR 55A have been provided which show the subjectivity associated with the SSM, especially with the development of FAFP and C in the computations. Example maps from HMR 57 and HMR 59 have been compared with computed maps using information in the HMRs. Significant differences between the HMR maps and the computed maps have been shown for HMR 57 in the K factor maps and the PMP maps. For HMR 59, example maps were not available for all parameters so independent comparisons could not be made. However, the FAFP values for the region where K is approximately equal to one shows that the FAFP values for that region are significantly larger than available storm data indicate. Additionally there are large rainfall gradient areas in the HMR 59 FAFP and C maps that are not generally expected and do not show up in the HMR 57 FAFP and C maps. Because of this, serious questions are raised as to the validity of the treatment of orographic influence on rainfall in HMRs 55A, 57, and 59 and the resulting PMP values. Specifically, any values for PMP given in those documents in areas that are orographically influenced should at the very least be re-evaluated to verify their accuracy.

Appendix J
Supplemental Digital Data DVD

Appendix K

Review Board Letters

Robert, Bill and Panel Members:

All recommendations provided to AWA by the Technical Review Panel throughout development of this study have been incorporated into the AWA Final Report dated November 2015. As a result, Art Miller as a Panel Member accepts AWA's estimates for probable maximum precipitation (PMP) for Virginia. These results are applicable to Virginia and should not be used in other States.

The following are some of my comments on the draft report:

Page 2: Last paragraph. Recent sit-specific {PMP studies of the past were limited to data availability and yesterday's technology -- may want to tone down a couple of those sentences).

Page 4: Similar comment may want to rewrite the last sentence.

Page 18: Fourth paragraph Many of the storms ... much better tone

Page 24: First paragraph last sentence. Therefore, the 6-hour I don't know if this is quite right but I don't know what else to recommend. Seems reasonable way to approach OTF.

Page 25 and 26: Last paragraph and top of page 26. A good justification presented. □

Page 28 General comment: The robustness of this study lies in the fact that there were a lot of storms available to use in the development of the PMP.

Section 6 Storm Maximization – No Comment

Page 57 Third paragraph: I am not sure that everyone on the Panel agrees with the statement "However, during this study, further evaluation and discussion showed the MTF is not being "double counted" in the PMP calculation process." It still may be an open issue. I have gone over the calculations and I don't believe the process double accounts. However, for the Virginia study I don't think it has that much of an effect.

You are using the atlas 14 frequency data to determine the best fit trend line and then determine the target adjusted rainfall using the SPAS data for the source. This becomes the new baseline. You then make a correction for the maximization for orographic effect using the OTF. This is my understanding and I don't think it is double accounting.

I really don't have any other comments. I enjoyed Appendix E (SPAS), it is really a powerful tool. Nice study.

Regards,

Art Miller
AECOM
art.miller@aecom.com
814-235-1379

As a member of the Technical Review Panel, I believe that all recommendations provided to AWA by the review panel throughout development of this study have been satisfactorily addressed by AWA and incorporated into the (draft) AWA Final Report dated November 2015. Consequently, I accept AWA's estimates for probable maximum precipitation (PMP) for Virginia. I agree with other panel members that these results are applicable to Virginia and should not be used in other states.

AWA should be commended for their efforts to develop a very complicated study and explain the exact method of analysis through the use of description, examples, and graphics. In my opinion as a member of the review panel, the AWA PMP study for Virginia was performed in accordance with scientifically sound and generally-accepted practices utilizing appropriate data and analysis techniques, and the results are appropriate for use in Virginia.

I am satisfied that the MTF/OTF double-counting question is not an overriding concern, at least in Virginia, and that the methodology used by AWA is appropriate in this study. For OTF, the PRISM modeling system seems to be widely accepted as a highly effective tool with much credibility.

The storm search process was quite exhaustive and indeed makes the study even more robust due to the high number of storms available for analysis.

Following are my specific comments on the draft final report. I have a couple of suggestions (for clarification purposes) in the final report, but in my opinion none are essential and the document is acceptable as is.

In section 5.2 (“**Data Sources**”), I would suggest adding a couple of very brief parenthetical references or descriptions to help clarify the terminology. Specifically, you might want to say what the NCDC Recovery Disk (no. 3) actually is (I don't know that it is referenced elsewhere in the report).

It also may be worth indicating that “Hydrometeorological Reports” (item no. 4) refers to the NOAA/NWS standard HMR series publications (unless you intended a broader interpretation). While familiar to us, some potential readers of this document may be unfamiliar with some of these terms.

Also, in no. 7 (if applicable) I suggest including Regional Climate Centers (RCC) along with state climate offices (some state climate offices are barely funded, if at all, so the RCCs are very important). The generic term “climate center reports” also appears in the first paragraph of section 5.3 (“**Storm Search Method**”). Presumably, that would include reports from NCDC and the RCCs.

Stephen Rich, CCM
Southeast Weather Consulting, LLC
weathercon@bellsouth.net
843-302-1693
November 12, 2015

As a member of the Technical Review Panel, except as noted below, I believe that all recommendations provided to AWA by the review panel throughout development of this study have been satisfactorily addressed by AWA and incorporated into the (draft) AWA Final Report dated November 2015.

The Draft report cites Paragraph 3.1.4 of the WMO's Manual on Estimation of Probable Maximum Precipitation (PMP) regarding the use of precipitation-frequency meteorology in development of the OTF. An excerpt from that WMO's paragraph follows:

Ratios of precipitation-frequency values between those at a storm location and those over an individual basin have been used to adjust rainfall amounts when storms have been transposed in mountainous regions. Since precipitation-frequency values represent equal probability, they can also be used as an indicator of the effects of topography over limited regions. If storm frequency, moisture availability, and other precipitation-producing factors do not vary, or vary only slightly, over an orographic region, differences in precipitation-frequency values should be directly related to variations in orographic effects.

This paragraph raises a number of questions.

WMO notes that precipitation-frequency values have been used previously in mountainous regions. The Virginia PMP Study uses the precipitation-frequency OTF method throughout the state, half of which may be considered non-orographic. I was anticipating that there would be references in the report that indicate where OTF methodology has been used in non-orographic areas. Besides previous AWA studies, is there precedent for this methodology, particularly in non-orographic areas, and if so, cite in the Report.

The WMO reference indicates that use of precipitation-frequency method of orographic adjustment should be used where storm frequency and moisture availability do not vary, or vary only slightly. This implies that similar storm frequency and moisture availability of the storm and target basins is the means by which orographic effects can be isolated and directly inferred from the precipitation-frequency data. Assuming the OTF process is valid in non-orographic areas, the high OTF (up to 1.5) for the SPAS Storm 1534 Ewan, NJ seems excessive when both storm and highest OTF value (Southeast Virginia) are in the Coastal Plain. It appears that the increase in OTF is influenced by higher storm frequency and/or moisture availability, which seems to violate the WMO guideline and indicate double-counting.

The report notes that the OTF process is reproducible and less subjective. I agree with this statement; the process is much more straightforward than the SSM.

The report notes that the OTF is a much more significant adjustment factor than the MTF. And based on comparison, it routinely results in adjustments as low as 0.5 and as high as 1.5. The OTF, as applied in this study, is typically larger than both the MTF and IPMF (for controlling storms). The adjustments for IPMF and MTF are based on a larger/longer basis of previous studies and methodology, while the OTF, as applied in this study, appears to have limited basis of application outside of previous AWA studies. If there are other studies that apply similar OTF methodology, please reference in the report. In the absence of these supporting documents, because of the significant effect of the OTF on PMP values throughout the state, I believe it

would be prudent for AWA's OTF methodology as applied to Virginia be reviewed in a peer-reviewed meteorological journal.

It would be helpful if the OTF plots for all short-list storms be included in an appendix. The appendix fly sheet should preface the limitations in the application of the OTFs (eg, maximum values, transposition zones).

I agree with Art Miller's statements regarding choice of language in reference to past studies.

Page 57, third paragraph: as Art noted, you may want to reword regarding the double-counting issue.

I believe the process, analyses and report were extremely thorough and well-supported with figures and graphics. Well done.

John Harrison
Schnabel Engineering
JOHNH@schnabel-eng.com
November 13, 2015